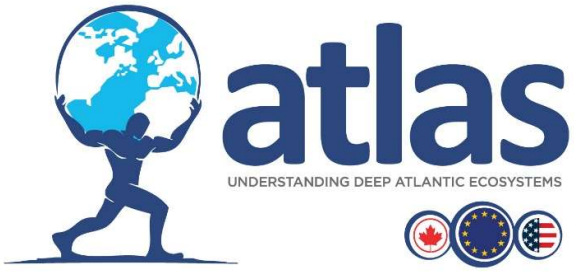

D3.3 Biodiversity, biogeography and GOODS classification system under current climate conditions and future IPCC scenarios

Project acronym:	ATLAS
Grant Agreement:	678760
Deliverable number:	D3.3
Deliverable title:	Biodiversity, biogeography and GOODS classification system under current climate conditions and future IPCC scenarios
Work Package:	WP3
Date of completion:	31st May 2019
Author:	See next page

This project has received funding from the European Union's Horizon 2020 research and innovation programme under grant agreement No 678760 (ATLAS). This output reflects only the author's view and the European Union cannot be held responsible for any use that may be made of the information contained therein.

D3.3 Biodiversity, biogeography and GOODS classification system under current climate conditions and future IPCC scenarios

Telmo Morato[1,2], José-Manuel González-Irusta[1,2], Carlos Dominguez-Carrió[1,2], Chih-Lin Wei[3], Andrew Davies[4], Andrew K. Sweetman[5], Gerald H. Taranto[1,2], Lindsay Beazley[6], Ana García-Alegre[7], Anthony Grehan[8], Pascal Laffargue[9], F. Javier Murillo[6], Mar Sacau[7], Sandrine Vaz[10], Ellen Kenchington[6], Sophie Arnaud-Haond[10], Oisin Callery[8], Giovanni Chimienti[11,12], Erik Cordes[13], Hronn Egilsdottir[14], André Freiwald[15], Ryan Gasbarro[13], Matt Gianni[16]; Kent Gilkinson[17], Vonda E. Wareham Hayes[17], Dierk Hebbeln[18], Kevin Hedges[19], Lea-Anne Henry[20], Georgios Kazanidis[20], Mariano Koen-Alonso[17], Cam Lirette[6], Francesco Mastrototaro[11,12], Lénaick Menot[9], Tina Molodtsova[21], Pablo Durán Muñoz[7], Bramley Murton[22], Covadonga Orejas[23], Maria Grazia Pennino[7], Patricia Puerta[23], Stefán Á. Ragnarsson[14], Berta Ramiro-Sánchez[20], Jake Rice[24], Jesús Rivera[25], Murray Roberts[20], Luís Rodrigues[1,2], Steve W. Ross[26], José L. Rueda[27], Paul Snelgrove[28], David Stirling[29], Margaret Treble[19], Javier Urra[27], Johanne Vad[20], Les Watling[30], Wojciech Walkusz[19], Zeliang Wang[6], Claudia Wienberg[18], Mathieu Woillez[9], Lisa A. Levin[31], Francis Neat[29], Diya Das[1,2], Laurence Fauconnet[1,2], Claudia Viegas[1,2], Pedro Afonso[1,2], Gui Menezes[1,2,32], Mario Rui Pinho[1,2,32], Helder Silva[1,2,32], Alexandra Rosa[1,2], Diana Catarino[1,2], Eva Giacomello[1,2], Javi Guijarro[6], Jason Cleland[20], Isobel Yeo[33], Joana R. Xavier[34,35], Íris Sampaio[2,36], Jeremy Spearman[37], Lissette Victorero[33,38,39,40], Charles G. Messing[41], Meri Bilan[1,2], Jordi Blasco-Ferre[1,2], Jean-François Bourillet[3], Laurent de Chambure[4], Jaime S. Davies[5], Norbert Frank[9], Brigitte Guillaumont[42], Konstantinos Georgoulas[43], Barbara Berx[29], Karine Olu[42], Manuela Ramos[1,2], Laís Ramalho[27], Olga Reñones[23], José Antonio Caballero[27], Fernando Tempera[44], Julie Tourolle[42], Olga Utrilla[27], Inge van den Beld[42], Igor Yashayaev[6], Alberto Serrano[45], Manfred Grasshoff[15], Sébastien Rochette[44], Christopher K. Pham[1,2], Marina Carreiro-Silva[1,2]

1- Okeanos Research Centre, Universidade dos Açores, Horta, Portugal
2- IMAR Instituto do Mar, Universidade dos Açores, Horta, Portugal
3- Institute of Oceanography, National Taiwan University, Taipei, Taiwan
4- Department of Biological Sciences, University of Rhode Island, Kingston, Rhode Island, USA
5- Marine Benthic Ecology, Biogeochemistry and In situ Technology Research Group, The Lyell Centre for Earth and Marine Science and Technology, Heriot-Watt University, Edinburgh, United Kingdom
6- Bedford Institute of Oceanography, Fisheries and Oceans Canada, Dartmouth, NS, Canada
7- Instituto Español de Oceanografía (IEO), Centro Oceanográfico de Vigo, Vigo, Pontevedra, Spain.
8- Earth and Ocean Sciences, NUI Galway, Ireland
9- IFREMER, Centre Atlantique, Nantes, France
10- MARBEC, IFREMER, Univ. Montpellier, IRD, CNRS, France
11- Department of Biology, University of Bari Aldo Moro, Bari, Italy
12- CoNISMa, Rome, Italy
13- Department of Biology, Temple University, Philadelphia, USA
14- Marine and Freshwater Research Institute, Reykjavík, Iceland
15- Senckenberg am Meer, Marine Research Department, Wilhelmshaven, Germany
16- Gianni Consultancy, Amsterdam, Netherlands
17- Northwest Atlantic Fisheries Centre, Fisheries and Ocean Canada, St. John's, NL, Canada
18- MARUM - Center for Marine Environmental Sciences, University of Bremen, Germany
19- Fisheries and Oceans Canada, Winnipeg, MB, Canada
20- School of GeoSciences, Grant Institute, University of Edinburgh, United Kingdom
21- P.P. Shirshov Institute of Oceanology, Moscow, Russia
22- National Oceanography Centre, Southampton, United Kingdom

23- Instituto Español de Oceanografía, Centro Oceanográfico de Baleares, Palma, Spain
24- Fisheries and Ocean Canada, Ottawa, ON, Canada
25- Instituto Español de Oceanografía, Madrid, Spain
26- Center for Marine Science, University of North Carolina at Wilmington, Wilmington, NC, USA
27- Instituto Español de Oceanografía, Centro Oceanográfico de Málaga, Málaga, Spain
28- Department of Ocean Sciences, Memorial University, St Johns, Newfoundland, Canada
29- Marine Laboratory, Marine Scotland Science, Aberdeen, Scotland, UK
30- School of Marine Sciences, University of Maine, Orono, Maine, USA
31- Center for Marine Biodiversity and Conservation and Integrative Oceanography Division, Scripps Institution of Oceanography, UC San Diego, La Jolla, CA, USA
32- Universidade dos Açores, Departamento de Oceanografia e Pescas, 9901-862 Horta, Portugal
33- National Oceanography Centre, Southampton SO14 3ZH, United Kingdom
34- CIIMAR – Interdisciplinary Centre of Marine and Environmental Research of the University of Porto, Matosinhos, Portugal
35- University of Bergen, Department of Biological Sciences and KG Jebsen Centre for Deep-Sea Research, Bergen, Norway
36- Senckenberg am Meer, Abteilung Meeresforschung, Wilhelmshaven, Germany
37- HR Wallingford Ltd, Wallingford OX10 8BA, United Kingdom
38- Institut de Systématique, Évolution, Biodiversité (ISYEB), CNRS, Muséum National d'Histoire Naturelle, Sorbonne Université, École Pratique des Hautes Études, Paris, France
39- Biologie des Organismes et Ecosystèmes Aquatiques (BOREA), CNRS, Muséum national d'Histoire naturelle, Sorbonne Université, Université de Caen Normandie, Université des Antilles, IRD, Paris, France
40- Centre d'Écologie et des Sciences de la Conservation (CESCO), CNRS, Muséum national d'Histoire naturelle, Sorbonne Université, Paris, France
41- Nova Southeastern University, Department of Marine and Environmental Sciences, Dania Beach, Florida, United States
42- IFREMER, UMR MARBEC, Station de Sète, Sète, France
43- Heidelberger Akademie der Wissenschaften, D-69120 Heidelberg, Germany
44- Laboratoire Environnement Profond, IFREMER, France

Contents

Executive summary

Major knowledge gaps and a lack of refined models and cost-effective tools to monitor and predict biodiversity delay agreement and implementation of biodiversity management policies at the highest levels. These delays will be reduced through cross-sectoral, multi-stakeholder trans-Atlantic data-sharing and integration of ocean mixing and food supply into biodiversity maps. The main vision of WP3 Biodiversity and Biogeography is to conduct pilot studies to validate robust and cost-effective techniques to minimise uncertainty in deep ocean biodiversity and biogeography assessment.

At international levels, the Global Open Oceans and Deep Seabed (GOODS) classification scheme is a decision-support tool to help safeguard marine biodiversity, support the ecosystem approach, marine spatial management and the design of MPA networks in national waters and in the international High Seas, thereby helping nations implement global policies enshrined by UNCLOS (e.g. ABNJs), the FAO (e.g. VMEs) and the CBD (e.g. EBSAs). GOODS integrates layers of physical and biological information to delineate biogeographic provinces as entities of flora, fauna and environmental settings. It was later adapted for ABNJ waters >800 m deep, delineating a “Northern Atlantic boreal” and a “North Atlantic” province based on distinct patterns of particulate organic carbon flux and water temperatures. However, the adapted scheme now needs further refinement in light of policy drivers such as the VMEs and EBSAs as it lacks input from structurally complex seabed environments such as CWC reefs, sponge grounds and hydrothermal vents that may also meet EBSA and VME criteria. It could also be substantially improved with input from the latest ocean models integrating horizontal and vertical mixing as water mass characteristics are critical for GOODS boundaries and for species distribution models (SDMs) to predict occurrences of cold-water corals, sponges and fish. Yet even SDMs that integrate larval tracking are still overly simplistic and inaccurate, and at best they use coarse estimates of surface primary production to proxy seafloor food supply.

In this deliverable, ATLAS used a combination of techniques, along with the best available information along with knowledge developments made by WP1 and WP2 and new data gathered by WP3 to improve the understanding of deep-sea the biodiversity and biogeographic patterns of sensitive deep-water ecosystems and deep-sea fish in the North Atlantic and forecast changes under IPCC 21st century scenarios of water mass structure and ocean currents.

CHAPTER 1 - Improve the understanding of biodiversity in the deep North Atlantic

Mapping biodiversity of Vulnerable Marine Ecosystems (VME) indicator taxa, deep-sea fish and habitats across the North Atlantic requires good baseline geo-referenced knowledge of species

diversity and habitats. The ATLAS project provided an unique opportunity to gather information on the distribution and composition of benthic communities across latitude and longitude in the North Atlantic spanning from the Cape Lookout (CS12) in the west, to Faroe-Shetland Channel (CS2) in the east (76° W to 3° E), and from Greenland (CS10) in the north to the Tropic Seamount (CS13) in the south Atlantic (from about 60° to 23° N) (Figure 1). More than 30 benthic communities, including cold-water coral (CWC) reefs and gardens, deep-sea sponge aggregations and hydrothermal vents have been described. In addition, ATLAS partners have contributed to the identification of at least 20 new or putative new species to science.

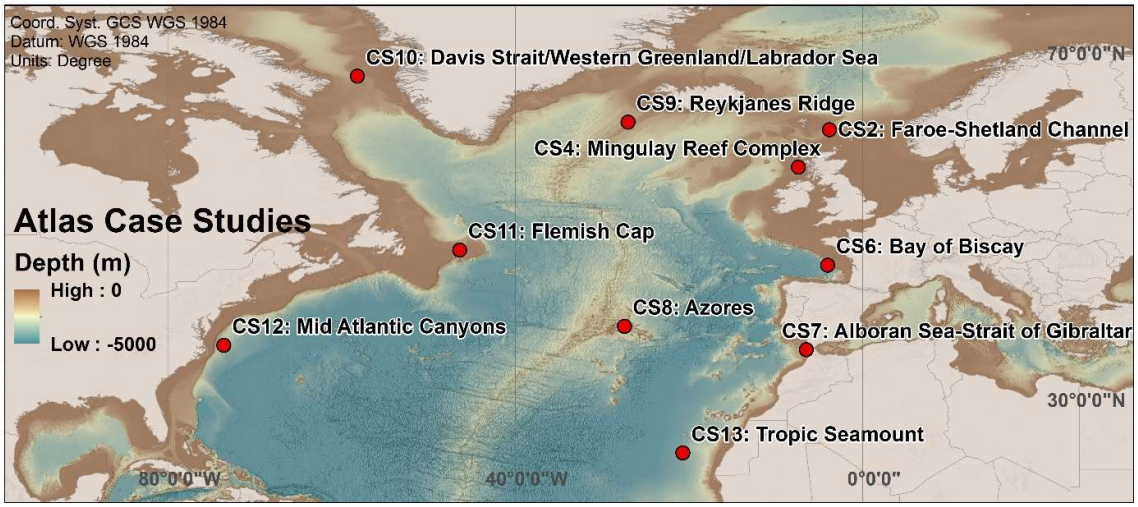

Figure 1. Location of the different study cases of the ATLAS project for which the benthic communities were described within this chapter.

One of the most important benthic community discoveries in the western North Atlantic was the discovery of a *Lophelia pertusa* reef in Greenlandic waters off the SW coast of Greenland (CS10, Kenchington et al., 2017). This discovery extended the known distribution of this species to the northern NW Atlantic and has enabled new interpretations of connectivity with the *L. pertusa* reefs from the Northeast Atlantic. This also represents the northern most record of *L. pertusa* in the NW Atlantic so far. Although it was not possible to extensively sample the area, a diversified associated fauna was described and included species common in the area, as well as rare species, species new to Greenland, and species new to science (see section 1.3.3). *Lophelia pertusa* reefs were also found to be quite extensive further down the northwestern coast of the Atlantic off Cape Lookout, North Carolina (CS12, south of Cape Hatteras, Hourigan et al., 2017). These coral habitats showed great diversity of associated mega- and macrofauna, particularly for fish species, representing the highest fish diversity recorded in association to any other CWC habitat to date, some of them showing existence of a primary (obligate) deep reef ichthyofauna (CSA et al., 2017). The important role of

structural complexity associated with *L. pertusa* reef habitats in supporting high biodiversity has also been demonstrated for Mingulay Reef Complex in the Northeast Atlantic (CS4), improving our understanding the drivers shaping biodiversity patterns. For example, ATLAS analyses revealed that up to 40 taxonomic groups performed a habitat-provisioning role for >40 other species including a diverse community of invertebrates and as attachment substrate for shark egg cases.

Coral gardens dominated by octocorals, particularly *Paragorgia arborea*, are also important habitats in the southeastern US (CS12, north of Cape Hatteras, Packer et al., 2017). Mid-Atlantic canyons in this region were found to harbor different types of coral garden communities occurring in an area that spans only about 500 km of latitude, likely related to the availability of different substrate types and oceanographic conditions (Brooke et al., 2017). This same trend with diverse habitats types associated with submarine canyons has also been observed for the Bay of Biscay (CS6), where 11 coral habitats were mapped and described (van den Beld et al., 2019). Together these case studies provide evidence of the importance of canyon features in providing suitable habitat for CWC communities naturally protected from the impact of bottom trawling fishing.

In the central North Atlantic, the Azores region was found to harbour particularly diverse coral gardens, forming at least seven distinct coral garden communities dominated by different species of octocorals discovered only during ATLAS cruises (CS8, section 1.2.5). Black coral forests of long-lived *Leiopathes* spp. and dendrophylid coral reefs were other CWC habitats found in the region (section 1.2.5). Indeed, with an EEZ of 1-million km^2, the Azores has been one of the most underexplored regions in the Atlantic, with studies reported here showing the great potential for new discoveries in the deep sea. Both historical and new knowledge generated during ATLAS have demonstrated the Azores as a hotspot of CWC diversity, representing the highest species richness known of Octocorallia in Europe and in any of the North Atlantic archipelagos (see section 1.3.2, Sampaio et al., 2019). This has also contributed to the identification of several new species to science associated to these CWC habitats (Carreiro-Silva et al., 2017) and continued work in the identification of new CWC species, especially for the understudied octocoral family Plexauridae (see section 1.3.2).

Coral garden communities were also reported for the Gulf of Cadiz and the Alboran Sea in the Mediterranean (CS7, section 1.2.4) but the biomass and diversity appeared to be lower than that found in the Azores. However, the diversity of associated fauna to sedimentary areas in the region seems to be high with the identification of 10 new species of molluscs, bryozans and echinoderms (section 1.3.1). Patterns in CWC diversity among CS7 areas and the Formigas Seamount in the Azores are being studied in relation to the Mediterranean Outflow Water pathway in the Atlantic (see D3.2 for detailed analyses). Studies so far show the Azores as having mixed zoographic affinities with a

greater affinity to the Lusitanian-Mediterranean biogeographic region and to a lesser extent to the western North Atlantic. However, new data gathered during ATLAS to the west of the Mid-Atlantic Ridge in the Azores (e.g. Gigante Seamount, section 1.2.5) may change this pattern.

Although sponge aggregations were found in several of the CS, their biomass, diversity and community composition varied with latitude. Sponge aggregations constitute the major benthic communities both in terms of biomass and diversity along the continental slopes in the in the eastern Canadian Arctic (northwest Atlantic, Murillo et al., 2018, section 2.1.7). The high productivity of these waters and the meeting of the arctic and boreal astrophorid sponge faunas in this region may explain the high diversity found there. Sponge aggregations composed by *Geodia* spp. and flabellate sponges were also identified as important benthic communities in the Faroe-Shetland Channel but in the latter case aggregations appeared to have lower biomass and occurred within a narrow zone between 450 and 530 m depth, within relatively warm and saline water masses (CS2, Kazanidis et al., 2019, section 1.2.1). At intermediate latitude areas, such as the Azores, Gulf of Cadiz and Alboran Sea in the Mediterranean, sponge aggregations were mainly composed of hexactinellids and lithistid *sensu lato* sponges (CS7-8, sections 1.2.4, 1.2.5). Further south in the Irving Seamount (part of the Atlantis-Meteor Seamount Complex, section 1.2.5.6) and in the Tropic Seamount (northwestern African continental margin, section 1.2.10), the glass sponge *Poliopogon amadou* formed extensive monospecific sponge grounds below 2500 m depth (Ramiro-Sánchez et al., 2019).

During ATLAS, we also had the opportunity to visit sections of the Mid-Atlantic Ridge (MAR) in the Azores region and in the Reykjanes Ridge in the southwest of Iceland (CS8-9, sections 1.2.5, 1.2.6). An important discovery in the Azores was a new hydrothermal vent field, the “Luso” vent field, on the slopes of the Gigante Seamount, further demonstrating the discovery potential of new habitats in deep-sea environments (CS8, section 1.2.5). This vent system differs from other vent fields along the MAR, by being characterized by fluids of low temperature mainly composed of iron and carbon dioxide, with no sulphur and little methane, with a likely important role in enhancing primary productivity for megafauna in an oligotrophic region as the Azores. Studies on associated fauna to Steinahóll hydrothermal vent at Reykjanes Ridge have revealed a strong zonation of the vent and non-vent fauna, with the presence of *L. pertusa* reefs and sponge grounds in the vicinity of the vent field.

Overall, these studies identified several areas with high density of bioengineering species (e.g. CWCs, sponges) characterized by slow-growing, long-lived and late-maturity, traits that limit their potential for resilience and recovery from human disturbances such as bottom fishing, oil and gas extraction and, in the future, deep-sea mining. As such the habitats they form may meet the criteria of both VMEs (Vulnerable Marine Ecosystems; FAO) and EBSAs (Ecologically or Biologically Significant Marine

Areas; CBD). Indeed the information reported here has already contributed to the management and conservation measures to protect some of these habitats. Examples are the protection of sponge aggregations in the "Faroe-Shetland Channel Nature Conservation Marine Protected Area" (FSC NCMPA, see CS2) or the protection of coral habitats in submarine canyons on the Bay of Biscay under the Nature 2000 Habitats directive (CS6, section 1.2.3). In the Azores, the Condor Seamount has been protected from fishing since 2010 and has been included in the Azores Marine Park since 2016, showing signs of fish stock recovery for some species during the 6 years closure (CS8, section 1.2.5).

In the northwestern Atlantic, the identification of coral, sponge and sea pens from the trawl surveys has been used to establish marine refuges in the Eastern Canadian Arctic bioregion and to identify Canadian Ecologically and Biologically Significant Areas (CS10, section 1.2.7). In the Eastern US, the discovery of important Vulnerable Marine Ecosystems have been used as the main tool by management agencies to evaluate, describe, map, and finally approve very large marine protected areas that target deep-sea corals, submarine canyons, and methane seeps (CS12, section 1.2.9). Work developed in the Flemish Cap has contributed to defining biological traits for deep-sea corals which best describe the VMEs in this region, to investigate the possibility to apply these modeling techniques for the assessment of Significant Adverse Impacts in the NAFO Regulatory Area (CS11, section 1.2.8).

Discoveries reported here have also contributed towards ongoing Biodiversity Beyond National Jurisdiction (BBNJ) treaty negotiation discussions and to build a case to nominate Tropic Seamount as a candidate EBSA in Areas Beyond National Jurisdiction for the Convention on Biological Diversity, based on the discovery of sponge aggregations and coral gardens on this seamount in areas of deep-sea mining interest (CS13, section 1.2.10).

However, in many instances, such as the case of the Azores, new potential VMEs have been identified only recently during the course of ATLAS and will serve as the basis to inform management and conservation policies in the near future (CS8, section 1.2.5). For example, new knowledge on coral garden communities in Mar da Prata Ridge collected in ATLAS, is being used to inform the Regional Government of the Azores on potential fisheries closed areas in this ridge. Plans are also being developed together with the Azores Government to protect the new hydrothermal vent field "Luso" located in an important fishing ground in the Azores.

Another important aspect of the studies reported here is the new knowledge gathered on the species biodiversity in different geographic regions of the North Atlantic, in many instances in the format of image catalogues crossed referenced with vouchered specimens and taxonomists (e.g. CS2, 8, 10, 12). These will serve as baselines to monitor the impact of human activities, including climate change, and to understand biogeographic patterns across the Atlantic. Overall, these studies contributed to a

better understanding of the biogeographic affinities and provinces in the North Atlantic as reported in Chapter 2 of this report.

CHAPTER 2 - Biogeography of the deep North Atlantic: Evaluating the 'Global Open Oceans and Deep Seabed' and the 'Ecological Marine Units' biogeographic classification systems

Understanding patterns of marine biogeography is essential for the adequate management of deep-sea ecosystems under increasing multiple pressures such as climate change, oil and gas activities, bottom trawling, and potentially in the future, deep-sea mining and deep-sea tourism. Being able to identify and delineate ocean regions that harbour unique, endemic and rare species is important because these regions need to be accounted for and given adequate spatial management, e.g., as a criterion for the designation of an area as an Ecological or Biologically Significant marine Area (EBSA), or as part of a High Seas Marine Protected Area (MPA) network. If the full range of biogeographic regions is not considered in management decisions, we risk losing species and not adhering to the Convention on Biological Diversity (CBD) obligations to conserve biological diversity.

Unlike many Exclusive Economic Zones (EEZs), the limited records of species occurrence in Areas Beyond National Jurisdiction (ABNJs) have often restricted more comprehensive studies of the biogeography of deep-sea species. Environmental, historical and biological factors are known to be driving factors of species distribution, with biogeographic classifications being used to analyse patterns of marine biodiversity and advancing knowledge of evolutionary and ecosystem processes, even with this lack of information (e.g. Costello et al., 2017). It was recognised that biogeography of complex deep-sea habitats such as those created by some Vulnerable Marine Ecosystem (VMEs) indicator taxa is especially poorly known, an issue that must be addressed as VMEs have international conservation and management significance through this designation.

Attempting to rectify the lack of biogeographic data for Earth's largest biome, the deep sea, must also be complemented by alternative approaches to understanding biogeographic patterns, and for this reason, several classification systems based purely on physiognomic proxies (seafloor bathymetry, oceanographic variables) have recently been promoted. This task in ATLAS focuses on (1) validating two existing biogeographical classification systems for complex habitats in the deep North Atlantic: the Global Open Oceans and Deep Seabed (GOODS; UNESCO, 2009) classification system and the Ecological Marine Units (EMUs), created by ESRI; and (2) looking at the drivers of bioregionalisation in the North Atlantic. In a later chapter in this Deliverable, we will also evaluate climate-induced changes in GOODS biogeographic provinces in the North Atlantic. Species-assemblage structure of several taxa

across a range of localities in the North Atlantic were tested against marine provinces proposed by the GOODS and EMUs classifications. The whole dataset of available VME taxa in the North Atlantic, together with the Subclasses Hexacorallia and Octocorallia failed to show any significant differences in their distribution for any of the classifications, possibly indicating a widespread distribution. However, the biogeographical analysis to understand the drivers of bioregionalisation produced 36 clusters in the North Atlantic, which highlighted there is structure in the species composition of the basin. The main environmental predictor driving differences between areas was temperature followed by food supply and speed of currents. Together, these results point to a further division of the GOODS bathyal provinces in an eastern and western separation and, to some extent, a differentiation north and south of the Azores. Understanding the drivers of these regions in conjunction with forecasts of key VME species distribution models provides an outlook of how the GOODS provinces will change in future climate conditions and what regions acting as refugia might be potentially included in an MPA network. In particular, the bathyal depths will likely be the most affected with a general northwards extension, however the abyssal province will be impacted to a lesser extent. These results should be taken with caution as the available baseline data were heterogeneous and records were not well represented across the ocean basin. The study also highlighted the need for data collection and collaboration to ensure biogeographical analyses are robust and useful for the management of marine ecosystems.

CHAPTER 3 - Predicted spatial distribution of biodiversity in the deep North Atlantic under current environmental conditions

More than any other biome on earth existing knowledge of deep-sea ecosystems advances slowly leaving many biological and ecological questions unanswered (Danovaro et al., 2017). Namely, *in situ* observations are still sparsely collected and data on faunal biodiversity distributions remains limited. ATLAS WP3, has significantly contributed to the increased knowledge on the biodiversity (Chapter 1) and biogeography (Chapter 2) of the North Atlantic but large areas of this ocean-basin still remain poorly sampled and known. The vast expanse and high cost and difficulty of directly observing the deep-sea floor over large areas means that we will rarely be able to document the full distribution of species; making habitat suitability modelling tools of paramount importance for evaluating the distribution of deep-water species. Environmental niche modelling, also called species distribution models (SDMs), habitat suitability models (HSM) or climate envelope models (CEM), are powerful tools to predict the distribution of species along wide geographical areas and forecast changes under

future climatic scenarios (Pearson & Dawson, 2003; Hijmans & Graham, 2006; Wiens et al., 2009; Hattab et al., 2014).

The use of species distribution modeling has grown enormously in recent years with the accumulation of appropriate response and predictor data sets often global in scope. At the same time, exploitation of the deep sea is increasing and diversifying both within and beyond national jurisdictions while knowledge of the actual distribution of deep-sea biodiversity is still poor due to the limited spatial footprint of sampling to date. Therefore, there is now a great need for robust species distribution modelling that can inform decision making and anticipate global change. In particular, to support spatial planning and implementation of EU and other international directives such as the Voluntary Specific Workplan on Biodiversity in Cold-water Areas within the Jurisdictional Scope of the Convention on Biological Diversity, as adopted at CBD COP13 (EEC, 1992; EC, 2008; 2014; FAO, 2009; CBD 2013). In this chapter, ATLAS used the best available information along with knowledge developments made by WP1 and WP2 and a combination of modelling techniques to improve our understanding on the distribution of sensitive deep-water ecosystems and deep-sea fish, to predict the regional and basin scale occurrence of quality assured VME indicator taxa and deep-sea fish species, and inform analyses of the biogeographic patterns in the North Atlantic.

Habitat suitability models of vulnerable marine ecosystem indicator taxa and commercially important deep-sea fish were developed at the ocean-basin scale and in 9 ATLAS case studies across the North Atlantic (Figure 2); from the Florida-Haterras slopes, Flemish Cap, and Davis Strait in the western Atlantic, to the Icelandic and Azores waters in the central Atlantic, and to the Rockall Bank, Porcupine Seabight, the Bay of Biscay, and the Tropic Seamount in the Eastern Atlantic.

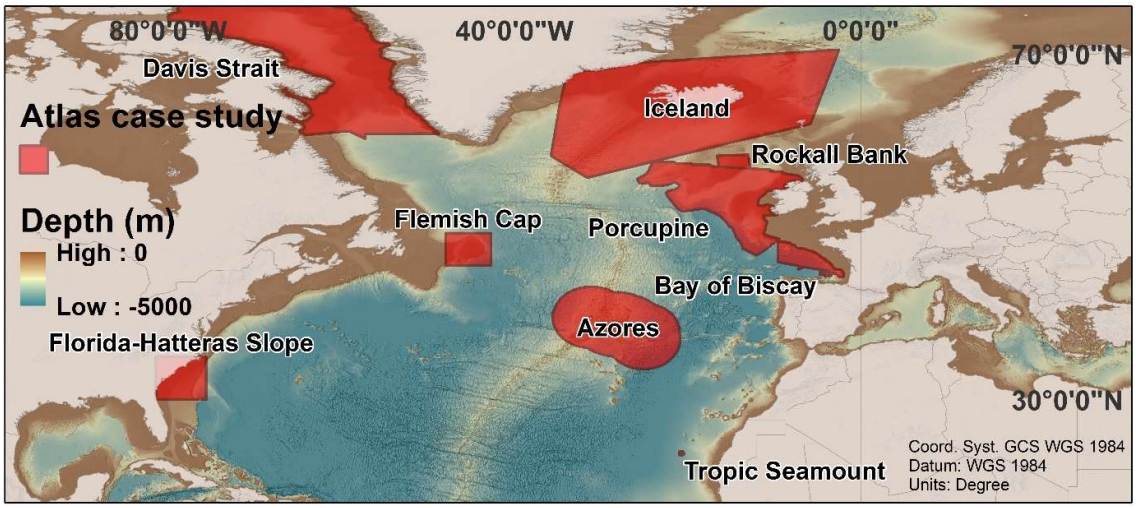

Figure 2. Habitat suitability models were developed at regional case study and ocean-basin scales.

Ocean-basin scale habitat suitability models have proved to be valuable tools for evaluating the potential distribution of deep-sea benthic species at large scale, and to identify broad areas of conservation (Ardron et al., 2014; Reiss et al., 2014) or blue growth importance. However, our results also demonstrated that after identifying those broad areas in the North Atlantic, regional habitat suitability models with higher spatial resolution will help the implementation of area based management tools at a finer scale. This is well illustrated in a comparison of the outputs of the ocean-basin scale model with the regional model outputs for *Lophelia pertusa*.

For example, the *L. pertusa* ocean-basin scale model, successfully identifies canyons in the Bay of Biscay as the most suitable area for this species. However, the regional model is actually able to identify what specific canyons in that region seemed to be the most suitable for *L. pertusa*. In the Florida-Hatteras of the NW Atlantic case study, the habitat suitability index of *L. pertusa* seemed to be similar between the regional and the ocean-basin scale models, but the ocean-basin scale model seemed to produce more plausible results; highlighting the importance of having a good spatial coverage of the species occurrence data. On the contrary, both in the Porcupine Bank in the Irish shelf and in the Rockall Bank, the ocean-basin scale model significantly over-predict the suitable habitat of *L. pertusa* when compared to the regional models.

There are multiples reasons for the inconsistencies between models at different scales including the spatial resolution and quality of the terrain and environmental data, the volume, the quality and the spatial coverage of the occurrence data, the availability of absence records, model selection,

assumptions and parametrization, among others (Robinson et al., 2017). The ocean-basin scale model suffers from a number of common and well-known limitations that may be more pronounced when modelling deep-sea taxa. It is known that cold-water coral distributions respond to small-scale fluctuations of different terrain attributes, such as substrate type and seabed rugosity (De Clippele et al., 2017), and oceanographic conditions (Bennecke & Metaxas, 2017). However, both terrain and environmental information was derived from global datasets and not from detailed deep-sea in situ measurements which does not discriminate between areas with high small-scale heterogeneity. Furthermore, regional scale models are constrained to the regional distribution of presence records and therefore are able to account for changes in species distribution caused by anthropogenic disturbances, something especially relevant in areas exposed to high levels of trawling such as the NE Atlantic (Eigaard et al., 2017).

The quantity and the spatial distribution of available occurrence data, and to some degree of uncertainty on deep-sea species identification (mostly for VME indicator taxa) and geo-location of occurrence data, also generates increased uncertainty in the model outputs. Finally, the use of presence-only records (as opposed to abundance data) with no true absence data, also generates increased uncertainty and usually over predict habitat suitability (Zaniewski et al., 2002). The deep sea is still one of the least studied and sampled areas on the planet and therefore many species are still unknown or the taxonomy still has to be resolved and the real spatial distribution is also undetermined (mostly for VME indicator taxa). This source of uncertainty will only be reduced with extensive exploration of the deep-sea environment.

Habitat suitability projections as those presented here, can be used to develop research agendas that confirm and advance the model outputs and clarify the roles of predictor variables in determining distributions. Incorporating these needs into global observing efforts (e.g., Deep Ocean Observing Strategy) can help identify data gaps, designate spatial locations for collection of physical and biogeochemical data from moorings, floats, ship tracks, or observatories, and advance technologies such as imaging and eDNA that can improve species detection.

Once habitat suitability models are sufficiently ground-truthed they can become a valuable tool to inform environmental management and conservation policy (Robinson et al., 2017), including taking climate change into consideration. Protected areas in the deep sea take the form of Vulnerable Marine Ecosystem designation by the Regional Fisheries Management Organizations and Arrangements to regulate fishing, Areas of Particular Environmental Interest by the International Seabed Authority (ISA) to regulate seabed mining, Ecologically and Biologically Significant Areas (EBSAs) by the contracting parties to the Convention on Biological Diversity to highlight biodiversity, National Marine Monuments

by the USA, etc. Similar protections are under discussion at the UN as part of a new biodiversity treaty to apply to areas beyond national jurisdiction. Each of these area-based management tools can benefit from the habitat suitability modeling approaches developed here. Within the fishing industries, accurate knowledge of VME distributions in relation to climate change parameters can be used to regulate fishing gear, locations and timing both within and beyond national jurisdiction.

CHAPTER 4 - Changes in biodiversity, GOODS and GES under IPCC scenarios

The deep sea plays a critical role in global climate regulation through uptake and storage of heat and carbon dioxide. But this uptake causes warming, acidification, and deoxygenation of deep waters, leading to decreased food availability. These changes and their forecasted projections are likely to severely affect productivity, biodiversity, and distributions of deep-sea fauna, especially Vulnerable Marine Ecosystems and their indicator species, and commercially important deep-sea fishes, thereby compromising key ecosystem services. Understanding how climate change can lead to shifts in deep-sea species distributions is critically important in developing management measures that consider such changes; especially those aimed to preserving refugia areas to aid conservation of cold-water corals or secure food, income and livelihoods from fisheries.

Climate-induced changes in deep-sea biodiversity distribution

We used environmental niche modelling along with the best available species occurrence data and a set of environmental parameters to model the habitat suitability for key cold-water coral and commercially important deep-sea fish species under present-day (1951-2000) environmental conditions and to forecast changes under future (2081-2100) climate projections (RCP8.5 or a business-as-usual scenario) for the entire North Atlantic Ocean. Our results show a marked decrease of 30% to 100% in suitable habitat for cold-water corals and a marked shift in the suitable habitat of deep-sea fishes from 2.0° to 9.9° towards higher latitudes. Our projections forecast the largest reductions in suitable habitat for the scleractinian coral *Lophelia pertusa* and the octocoral *Paragorgia arborea*, with declines of at least 79% and 99%, respectively. We predict expansion of suitable habitat by 2100 only for the fishes *Helicolenus dactylopterus* and *Sebastes mentella* by about 20 to 30%, mostly through northern latitudinal range expansion. Our modelling results forecasted limited climate refugia locations in the North Atlantic by 2100 for scleractinian corals (between 29% and 44% of North Atlantic present-day habitat), even smaller refugia locations for the octocorals *Acanella arbuscula* and *Acanthogorgia armata* (1.9-14.8% of present-day suitable habitat), and almost no refugia locations for *Paragorgia arborea*. Our results highlight the need to understand how anticipated climate change

will affect the distribution of deep-sea species, and highlight the importance to identify and preserve of climate refugia for Vulnerable Marine Ecosystems and commercially important deep-sea fishes.

Climate-induced changes in biogeography and biogeographic regions

With such forecasted changes in species suitable habitat, it is likely that species biogeography will change under future climate conditions. Our work also suggested that the existing Global Open Oceans and Deep Seabed (GOODS) provinces might change under future climate conditions. The bathyal province BY4 around the Mid-Atlantic Ridge will suffer environmental changes mostly related to decreased food supply that may affect the distribution of vulnerable marine ecosystem indicator taxa. The cluster corresponding to the New England and Corner Seamounts is likely to be a refugia for some scleractinian species. The northern cluster coinciding with GOODS bathyal northern North Atlantic (BY2) will possibly suffer the strongest changes. Octocorals are forecast to lose habitat in an extensive measure in the Reykjanes Ridge, the continental shelf west of this ridge (Davis Strait and Labrador Sea), and east towards Rockall. This is likely the result of changes in temperature across a latitudinal gradient with this province probably moving northwards in the future. It is possible that this area will become available for other scleractinian taxa found at southern latitudes and hence GOODS bathyal province BY4 extending its limit up to the Davis Strait. Finally, GOODS suggests one homogeneous abyssal province for the North Atlantic. Even with inconclusive evidence of an eastern and western separation as results vary depending on taxa, future climate changes are unlikely to make any spatial differentiation or major latitudinal shift in this province.

Climate-induced changes in Good Environment Status

The remarkable reduction of scleractinian and octocoral suitable habitat predicted towards 2100, may imply the loss of an important part of the cold-water coral reefs and gardens. A decrease in the suitable habitat for cold-water corals, may produce a significant loss in biodiversity as well as negative effects in ecosystem functioning, and on the goods and services it provides. Therefore, the occurrence of Vulnerable Marine Ecosystems has been suggested as one indicator for assessing the Good Environmental Status (GES) in the deep sea (ATLAS D3.1 Deliverable). It can thus be anticipated that the reduction of the suitable habitat of some indicator taxa and, consequently, their associated fauna will have a negative effect in the GES of certain areas of the deep North Atlantic. The likely shifts of deep-water fish species towards higher latitudes may also have a direct impact on the GES of certain areas of the North Atlantic. Although, the ‘empty’ niche generated by the northward movement of one species may promote the replacement by another (usually southern) fish species. Therefore, without a broad understanding of the climate-induced changes in the distribution of deep-sea fishes, it will be difficult to predict and measure fish stock indicators of Good Environmental Status.

In summary, climate change will definitely affect the GES of the North Atlantic but predicting GES future trends will be challenging. Habitat suitability models may become a useful tool to produce insights into the future GES; especially in the deep sea due to the difficulties to get access to this remote realm. Due to limited data availability (over space and time), difficulties in setting baselines, lack of standardisations (and a whole series of issues summarised in ATLAS Deliverable 3.1), makes the assessment of deep-sea good environmental status under current and future environmental conditions a huge challenge. Knowledge gained in the ATLAS exercise of assessing GES in the deep-sea in combination with the outputs of the models in future climate scenarios, as well as the increasing knowledge on performance of key organisms under different environmental conditions, will be extremely useful tools for assessing environmental status of deep-sea ecosystems under the future climatic scenarios predicted by the IPCC, and for management purposes.

Conclusions

Habitat suitability models that are sufficiently ground-truthed, become a valuable tool to inform environmental management and conservation policy and provide a basis for taking climate change into consideration, as demonstrated here. However, more than any other biome on earth, the deep sea suffers from a lack of *in situ* observations and data on faunal biodiversity and distributions; which brings some additional uncertainties to modeling exercises. The vast expanse and high cost and difficulty of directly observing the deep-sea floor over large areas means that we will rarely be able to document the full distribution of species. This makes habitat suitability modelling tools of paramount importance for evaluating the distribution of data-poor deep-water species and to understand how current biogeography may alter. Habitat suitability projections under current and future climate scenarios, can be used to develop research agendas that confirm and advance the model outputs and clarify the roles of predictor variables in determining species distributions. Incorporating these needs into global observing efforts (e.g., the Deep Ocean Observing Strategy) can help fill data gaps, determine spatial locations for the collection of key physical and biogeochemical data using moorings, floats, ship tracks, or observatories, and advance technologies such as imaging and eDNA that can improve species detection. Further integration of species-level biogeochemical and physical data, as well as results of the ecophysiological performance of deep-sea organisms from *ex situ* experimental work, will improve suitability and distribution mapping, but additional mechanistic (experimentally derived) understanding is needed of how climate drivers elicit ecological responses. The United Nations' Decade for Ocean Science, the Global Ocean Observing System (GOOS) and the Regular Process for Global Reporting and Assessment of the State of the Marine Environment (a.k.a. World Ocean Assessment) are forward-looking international entities that can help set such science agendas.

In summary, we have showed that despite all the caveats, habitat suitability models are useful tools for predicting potential future changes in the distribution of deep-water species and may be used to inform management decisions. This is especially the case when such dramatic changes as shown here are forecasted. Such models will improve in concert with climate change predictions. We hope the present study can provide a suitable template for and will stimulate similar analyses conducted for other taxa or regions.

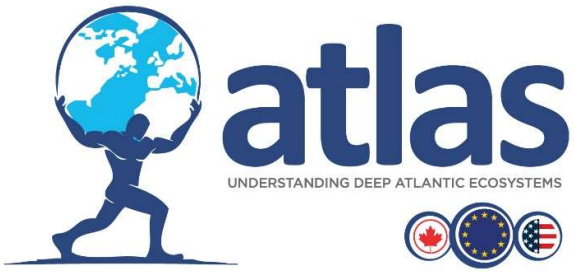

CHAPTER 1 - Improve the understanding of biodiversity in the deep North Atlantic

Project acronym:	ATLAS
Grant Agreement:	678760
Deliverable number:	D3.3
Deliverable title:	Biodiversity, biogeography and GOODS classification system under current climate conditions and future IPCC scenarios
Work Package:	3
Date of completion:	31/05/2019
Author:	See next page

This project has received funding from the European Union's Horizon 2020 research and innovation programme under grant agreement No 678760 (ATLAS). This output reflects only the author's view and the European Union cannot be held responsible for any use that may be made of the information contained therein.

1 Chapter 1: Improve the understanding of biodiversity in the deep North Atlantic

Marina Carreiro-Silva[1], Carlos Dominguez-Carrió[1], Sophie Arnaud-Haond[2,3], Meri Bilan[1], Jordi Blasco-Ferre[1], Jean-François Bourillet[3], José Antonio Caballero[4,] Laurent de Chambure[5], Jaime S. Davies[6], Pablo Durán Muñoz[7], Hrönn Egilsdóttir[8], André Freiwald[9], Norbert Frank[10], Brigitte Guillaumont[3], Ana Garcia-Alegre[7] , Konstantinos Georgoulas[10], Manfred Grasshoff[9], Dierk Hebbeln[12], Lea-Anne Henry[11], Georgios Kazanidis[11], Ellen Kenchington[13], Cam Lirette[13], Lénaïck Menot[2], Francis Neat[14], F. Javier Murillo[13], Barbara Berx[14], Karine Olu[3], Covadonga Orejas[15], Patricia Puerta[15], Stefán Áki Ragnarsson[8], Berta Ramiro-Sánchez[11], Manuela Ramos[1], Laís Ramalho[4], Olga Reñones[15], Jesús Rivera[16], Murray Roberts[11], Steve W. Ross[17], José Luis Rueda[4], , Íris Sampaio[1], Mar Sacau[7], Alberto Serrano[18], Gerald Taranto[1] , Fernando Tempera[2], Julie Tourolle[3], Johanne Vad[11], Inge van den Beld[3], Claudia Wienberg[12], Javier Urra[4], Olga Utrilla[4], Igor Yashayaev[13], Telmo Morato[1]

[1]IMAR-University of Azores, Portugal carreirosilvamarina@gmail.com
[2]Laboratoire Environnement Profond, IFREMER, France
[3]Ifremer, UMR MARBEC, Station de Sète, Sète, France
4Instituto Español de Oceanografía, Centro Oceanográfico de Málaga, Málaga, Spain
[5]LDC_CONSULT, Bayonne, France[6]Department of Biological Sciences, University of Rhode Island, Kingston, Rhode Island, USA
[7]Instituto Español de Oceanografía (IEO), Centro Oceanográfico de Vigo, Vigo, Pontevedra, Spain
[8]Marine and Freshwater Research Institute, Reykjavík, Iceland
[9]Senckenberg am Meer, Marine Research Department, Wilhelmshaven, Germany
[10]Heidelberger Akademie der Wissenschaften, D-69120 Heidelberg, Germany
[11]School of GeoSciences, The University of Edinburgh, UK
[12]MARUM - Center for Marine Environmental Sciences, University of Bremen, Germany
[13]Bedford Institute of Oceanography, Department of Fisheries and Oceans, Canada
[14]Marine Scotland, Marine Laboratory, Aberdeen, United Kingdom
[15]Instituto Español de Oceanografía, Centro Oceanográfico de Baleares, Palma, Spain
[16]Instituto Español de Oceanografía, Madrid, Spain
[17]Center for Marine Science, University of North Carolina-Wilmington, US
[18]Instituto Español de Oceanografía (IEO). Centro Oceanográfioc de Santander, Spain

Contents

1.1 Executive summary

Mapping biodiversity of Vulnerable Marine Ecosystems (VME) indicator taxa, deep-sea fish and habitats across the North Atlantic requires good baseline geo-referenced knowledge of species diversity and habitats. The ATLAS project provided an unique opportunity to gather information on the distribution and composition of benthic communities across latitude and longitude in the North Atlantic spanning from the Cape Lookout (CS12) in the west, to Faroe-Shetland Channel (CS2) in the east (76°W to 3°E), and from Greenland (CS10) in the north to the Tropic Seamount (CS13) in the South Atlantic (from about 60° to 23°N). More than 30 benthic communities, including cold-water coral (CWC) reefs and gardens, deep-sea sponge aggregations and hydrothermal vents have been described. In addition, ATLAS partners have contributed to the identification of at least 20 new or putative new species to science.

One of the most important benthic community discoveries in the western North Atlantic was the discovery of a *Lophelia pertusa* reef in Greenlandic waters off the SW coast of Greenland (CS10, Kenchington et al. 2017). This discovery extended the known distribution of this species to the northern NW Atlantic and has enabled new interpretations of connectivity with the *L. pertusa* reefs from the NE Atlantic. This also represents the northern most record of *L. pertusa* in the NW Atlantic so far. Although it was not possible to extensively sample the area, a diversified associated fauna was described and included species common in the area, as well as rare species, species new to Greenland, and species new to science (see section 2.3.3). An ATLAS cruise visited this reef site in 2018. *Lophelia pertusa* reefs were also found to be quite extensive further down the northwestern coast of the Atlantic off Cape Lookout, North Carolina (CS12, south of Cape Hatteras, Hourigan et al., 2017). These coral habitats showed great diversity of associated mega- and macrofauna, particularly for fish species, representing the highest fish diversity recorded in association to any other CWC habitat to date; some of them showing existence of a primary (obligate) deep-reef ichthyofauna (CSA et al., 2017). The important role of structural complexity associated with *L. pertusa* reef habitats in supporting high biodiversity has also been demonstrated for the Mingulay Reef Complex in the Northeast Atlantic (CS4), improving our understanding of the drivers shaping biodiversity patterns.

Coral gardens dominated by octocorals, particularly *Paragorgia arborea*, are also important habitats in the southeastern US (CS12, north of Cape Hatteras, Packer et al., 2017). Mid-Atlantic canyons in this region were found to harbour different types of coral garden communities occurring in an area that spans only about 500 km of latitude, likely related to the availability of different substrate types and oceanographic conditions (Brooke et al., 2017). This same trend with diverse habitats types associated with submarine canyons has also been observed for the Bay of Biscay (CS6), where 11 coral habitats

were mapped and described (van den Beld et al., 2019). Together these case studies provide evidence of the importance of canyon features in providing suitable habitat for CWC communities naturally protected from the impact of bottom trawling fishing.

In the central North Atlantic, the Azores region was found to harbor particularly diverse coral gardens, forming at least seven distinct coral garden communities dominated by different species of octocorals discovered only during ATLAS cruises (CS8, section 2.2.5). Black coral forests of long-lived *Leiopathes* spp. and dendrophylid coral reefs were other CWC habitats found in the region (section 2.2.5). Indeed, with an EEZ of 1-million km^2, the Azores has been one of the most underexplored regions in the Atlantic, with studies reported here showing the great potential for new discoveries in the deep sea. Both historical and new knowledge generated during ATLAS have demonstrated the Azores as a hotspot of CWC diversity, representing the highest species richness known of Octocorallia in Europe and in any of the North Atlantic archipelagos (see section 2.3.2, Sampaio et al., 2019). This has also contributed to the identification of several new species to science associated with these CWC habitats (Carreiro-Silva et al., 2017) and continued work in the identification of new CWC species, especially for the understudied octocoral family Plexauridae (see section 2.3.2).

Coral garden communities were also reported for the Gulf of Cadiz and the Alboran Sea in the Mediterranean (CS7, section 2.2.4) but the biomass and diversity appeared to be lower than that found in the Azores. However, the diversity of associated fauna in sedimentary areas in the region seems to be high with the identification of 10 new species of molluscs, bryozans and echinoderms (section 2.3.1). Patterns in CWC diversity among CS7 areas and the Formigas Seamount in the Azores are being studied in relation to the Mediterranean Outflow Water pathway in the Atlantic (see D3.2 for detailed analyses). Studies so far show the Azores as having mixed zoogeographic affinities with a greater affinity to the Lusitanian-Mediterranean biogeographic region and to a lesser extent to the western North Atlantic. However, new data gathered during ATLAS to the west of the Mid-Atlantic Ridge in the Azores (e.g. Gigante Seamount, section 2.2.5) may change this pattern.

Although sponge aggregations were found in several of the CS, their biomass, diversity and community composition varied with latitude. Sponge aggregations constitute the major benthic communities both in terms of biomass and diversity along the continental slopes in the in the eastern Canadian Arctic (NW Atlantic, Murillo et al., 2018, section 2.1.7). The high productivity of these waters and the meeting of the arctic and boreal astrophorid sponge faunas in this region may explain the high diversity found there. Sponge aggregations composed by *Geodia* spp. and flabellate sponges were also identified as important benthic communities in the Faroe-Shetland Channel but in the latter case aggregations appeared to have lower biomass and occurred within a narrow zone between 450 and 530 m depth,

within relatively warm and saline water masses (CS2, Kazanidis et al., 2019, section 2.2.1). At intermediate latitude areas, such as the Azores, Gulf of Cadiz and Alboran Sea in the Mediterranean, sponge aggregations were mainly composed of hexactinellids and lithistid *sensu lato* sponges (CS7-8, sections 1.2.4, 1.2.5). Further south in the Irving Seamount (part of the Atlantis-Meteor Seamount Complex, section 2.2.5) and in the Tropic Seamount (northwestern African continental margin, section 2.2.10), the glass sponge *Poliopogon amadou* formed extensive monospecific sponge grounds below 2500 m depth (Ramiro-Sánchez et al., 2019).

During ATLAS, we also had the opportunity to visit sections of the Mid-Atlantic Ridge (MAR) in the Azores region and in the Reykjanes Ridge to the southwest of Iceland (CS8-9, sections 2.2.5, 2.2.6). An important discovery in the Azores was a new hydrothermal vent field, the "Luso" vent field, on the slopes of the Gigante Seamount, further demonstrating the discovery potential of new habitats in deep-sea environments (CS8, section 2.2.5). This vent system differs from other vent fields along the MAR, by being characterized by fluids of low temperature mainly composed of iron and carbon dioxide, with no sulphur and little methane, likely with an important role in enhancing primary productivity for megafauna in an oligotrophic region as the Azores. Studies on fauna associated with the Steinahóll hydrothermal vent at Reykjanes Ridge have revealed a strong zonation of the vent and non-vent fauna, with the presence of *L. pertusa* reefs and sponge grounds in the vicinity of the vent field.

Overall, these studies identified several areas with high density of bioengineering species (e.g., CWCs, sponges) characterized by slow-growing, long-lived and late-maturity, traits that limit their potential for resilience and recovery from human disturbances such as bottom fishing, oil and gas extraction and, in the future, deep-sea mining. As such the habitats they form may meet the criteria of both VMEs (FAO) and EBSAs (CBD). Indeed, the information reported here has already contributed to the management and conservation measures to protect some of these habitats. Examples are the protection of sponge aggregations in the "Faroe-Shetland Channel Nature Conservation Marine Protected Area" (FSC NCMPA, see CS2) or the protection of coral habitats in submarine canyons on the Bay of Biscay under the Nature 2000 network and Habitats directive canyons represents a step forward in the protection of deep-sea habitats in the French Atlantic (CS6, section 2.2.3). In the Azores, the Condor Seamount has been protected from fishing since 2010 and has been included in the Azores Marine Park since 2016, showing signs of fish stock recovery for some species during the 6 years' closure (CS8, section 2.2.5).

In the NW Atlantic, the identification of coral, sponge and sea pens from the trawl surveys has been used to establish marine refuges in the Eastern Canadian Arctic bioregion and to identify Canadian

EBSAs (CS10, section 2.2.7). In the Eastern US, the discovery of important VMEs have been used as the main tool by management agencies to evaluate, describe, map, and finally approve very large marine protected areas that target deep-sea corals, submarine canyons, and methane seeps (CS12, section 2.2.9). Work developed in the Flemish Cap has contributed to defining biological traits for deep-sea corals, which will inform ecosystem-level assessments of significant adverse impacts in the NAFO Regulatory Area (CS11, section 2.2.8).

Discoveries reported here have also contributed to ongoing Biodiversity Beyond National Jurisdiction (BBNJ) treaty negotiations and to building a case to nominate Tropic Seamount as a candidate EBSA in Areas Beyond National Jurisdiction for the Convention on Biological Diversity, based on the discovery of sponge aggregations and coral gardens in this seamount in areas with deep-sea mining interest (CS13, section 2.2.10).

However, in many instances, such as the case of the Azores, new potential VMEs have been identified only recently during the course of ATLAS and will serve as the basis to inform management and conservation policies in the near future (CS8, section 2.2.5). For example, new knowledge on coral garden communities in Mar da Prata Ridge collected in ATLAS, is being used to inform the Regional Government of the Azores on potential fisheries closed areas in this ridge. Plans are also being developed together with the Azores Government to protect the new hydrothermal vent field “Luso” located in an important fishing ground in the Azores. Results of work done in CS3 feed into a proposal of a Natura 2000 network in the Bay of Biscay to define sectors to protect reef habitats under the Habitats Directive (MNHN-SPN and GIS-Posidonie 2014). The designation of a Natura 2000 network comprising submarine canyons represents a step forward in the protection of deep-sea habitats in the French Atlantic (van den Beld et al., 2017).

Another important aspect of the studies reported here is the new knowledge gathered on the species biodiversity in different geographic regions of the North Atlantic, in many instances in the format of images catalogues crossed referenced with vouchered specimens and reviewed by taxonomists (e.g., CS2, 8, 10, 12). These will serve as baselines to monitor the impact of human activities, including climate change and to understand biogeographic patterns across the Atlantic. Overall, the species list built within these studies contributed to a better understanding of the biogeographic affinities and provinces in the North Atlantic as reported in Chapter 2 of this report.

1.2 Description of new deep-sea benthic communities

A major component of the ATLAS project has been the collection of new data on biodiversity and benthic communities through dedicated cruises using different technological means including ROV video surveys, submersibles and drop-down camera systems, and the collection of biological samples. In this section, we provide a summary description of benthic communities within each of the ATLAS case studies, with the exception of CS 1, 3 and 5 where no new information on benthic communities has been collected (Figure 1). This information was based on 20 new cruises conducted within the framework of ATLAS (both ATLAS lead and external, see MS 9). Historical data collected during cruises prior to ATLAS were also used in some CS for the characterization of new benthic habitats, species and species associations. For detailed information on the cruises contributing to this section please consult the cruise reports made available in Open Access through the ATLAS community page at Zenodo (https://zenodo.org/communities/atlas).

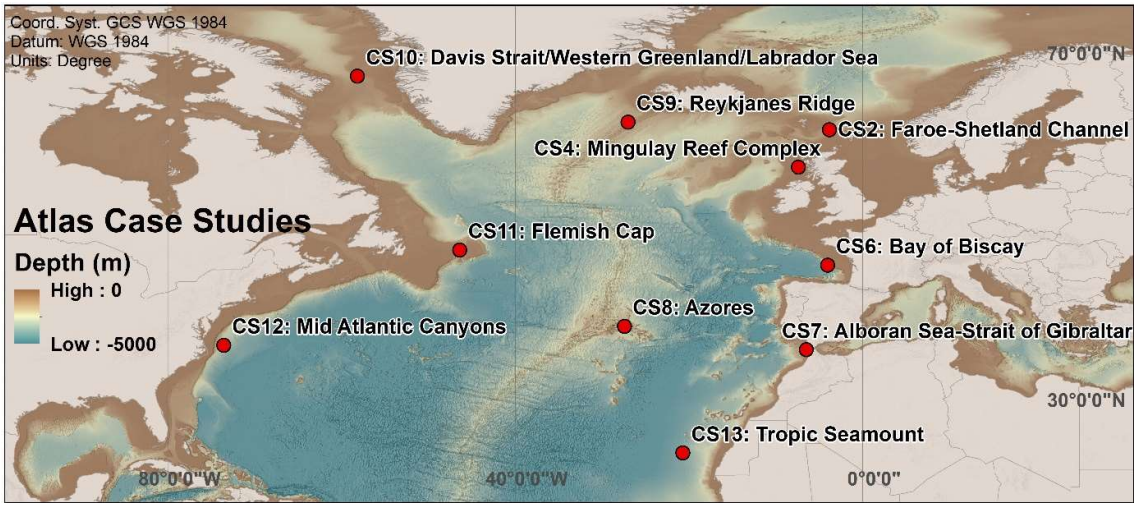

Figure 3. Location of the different study cases of the ATLAS project for which the benthic communities were described within this chapter.

1.2.1 Case Study 2: Distribution and structure of deep-sea sponge aggregations in the Faroe-Shetland Channel Nature Conservation Marine Protected Area

Authors: Georgios Kazanidis, Johanne Vad, Lea-Anne Henry, Francis Neat, Barbara Berx, , Konstantinos Georgoulasand John Murray Roberts

Study area and environmental setting The Faroe-Shetland Channel (FSC), NE Atlantic (Figure 4), is characterized by complex hydrography as five water masses flow through it: North Atlantic Water (NAW), Modified North Atlantic Water (MNAW), Modified East Icelandic Water (MEIW), Norwegian Sea Arctic Intermediate Water (NSAIW), and Norwegian Sea Deep Water (NSDW) (Hansen & Østerhus, 2000). The channel has many different sedimentary habitat types including iceberg ploughmarks, a contourite band, North Sea Fan, the Norwegian Basin and the floor of the Faroe-Shetland Channel (Masson, 2001). This area is particularly interesting for studies on biodiversity as it hosts diverse faunal communities including dense sponge aggregations at ~500 m water depth. Interestingly, Hátún et al. (2017) have shown a decline over the last 25 years in silicate concentrations in North Atlantic including the FSC. Changes in the temperature and salinity profiles over the last two decades, have also been shown (McKenna et al., 2016 and references therein). On top of that the FSC hosts multisectoral human activities including demersal fisheries, oil & gas installations and shipping (see Kazanidis et al., 2019 for details).

In this study, we focused in areas inside and outside the FSC Nature Conservation Marine Protected Area (FSC NC MPA, hereafter) (Figure 4). According to the Joint Nature Conservation Committee (JNCC) website (http://jncc.defra.gov.uk) the FSC NCMPA has a size of 23,682 km^2. The site ranges from 330 m below sea level at the edge of the Faroe-Shetland Channel continental slope, extending down the slope into the deep and cooler arctic influenced waters 2420 m below sea level. In areas inside and outside the FSC NC MPA different type of substrates have been observed like cobble, cobble with boulders, soft sediments and soft sediments with boulders (see Kazanidis et al., 2019 for details).

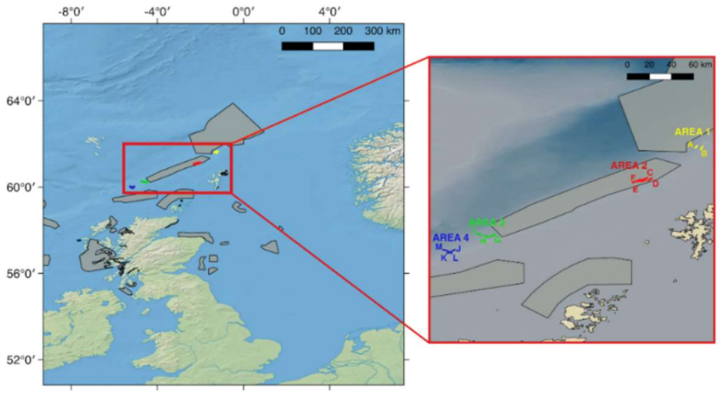

Figure 4. Faroe-Shetland Channel wider area highlighting the Nature Conservation Marine Protected Area (red rectangle) (left panel) and camera tows inside (area 2) and outside the NCMPA (areas 1, 3 and 4) (right panel) (from Kazanidis et al., 2019).

Description of benthic communities The FSC NCMPA is a key area for studying the role of water mass characteristics (McKenna et al. ,2016 and references therein) and human activities (Bullough et al., 1998; Vad et al., 2018) on vulnerable marine ecosystems (VMEs) like deep-sea sponge aggregations.

Taking into account the unique suite of features existing in the FSC NCMPA we studied the role of depth, type of substratum, temperature, salinity and demersal fisheries on the distribution and structure of deep-sea sponge aggregations inside (Area 2) and outside (Areas 1, 3, 4) the FSC NCMPA (Figure 4). Examination of sponge aggregations was based on the collection of images from 13 towed-camera transects that were carried out in areas inside and outside the FSC NC MPA (Figure 4). We also developed a sponge morphotype catalogue (Figure 5) taking into account sponges seen in the camera transects and available scientific literature (Boury-Esnault & Rützler, 1997; Klitgaard & Tendal 2004; Cárdenas et al., 2013; Henry & Roberts, 2014). Results of this study have been published in Kazanidis et al. (2019).

The study revealed higher sponge morphotype diversity, density as well as a higher number of body-size cohorts inside than outside the NCMPA. Statistical analysis provided evidence that demersal fisheries, substratum, salinity and temperature explained a statistically-significant amount of variation of sponge morphotype density across the studied area.

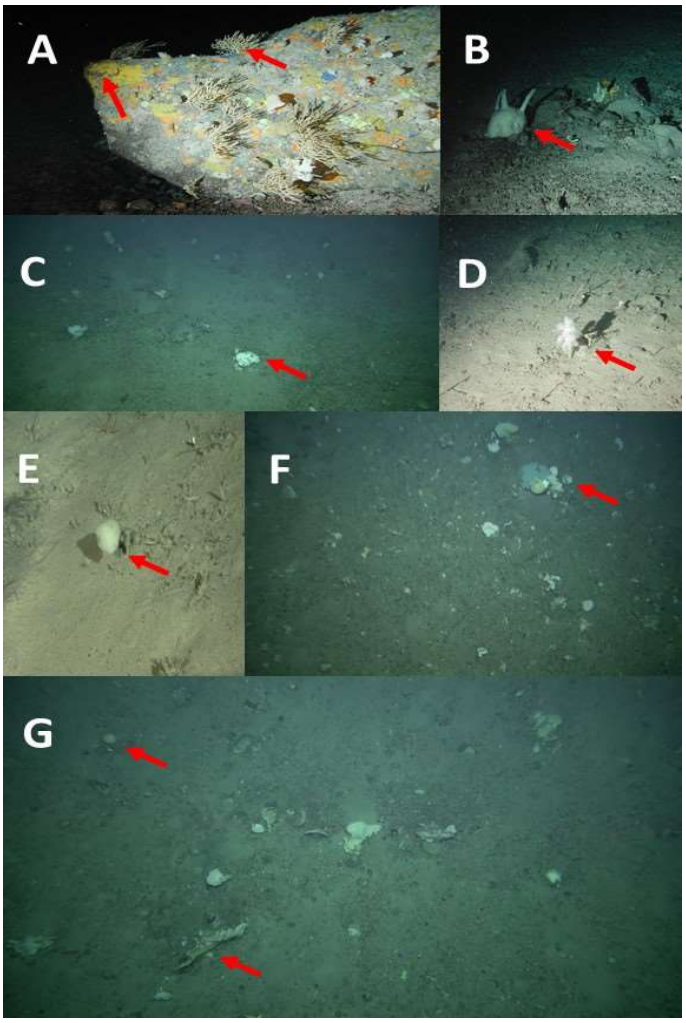

Figure 5. Categories of sponge morphotypes from the Faroe-Shetland Channel. Category 1: 1126 encrusting (A), Category 2: arborescent ("tree-like")(A), Category 3: massive (C), spherical (G) 1127 and papillate (B). Category 4: flabellate ("fan-shaped")(G) and caliculate ("cup-shaped")(F). 1128 Category 5: stipitate ("stalked")(E) and clavate ("club-shaped")(D).

The present work (Kazanidis et al., 2019) highlights the vulnerability of the FSC deep-sea sponge aggregations to both demersal fisheries and changes in oceanic conditions. This work, also, made a substantial contribution to the monitoring of deep-sea sponge aggregations in FSC NCMPA, which is crucial in this era of industrial activities' encroachment and long-term changes in oceanic conditions (Hátún et al., 2017).

1.2.2 Case Study 4: One on top of the other: investigating habitat supply by macrobenthos in Mingulay Reef Complex

Authors: Georgios Kazanidis, Lea-Anne Henry, John Murray Roberts

Study area and environmental setting The Mingulay Reef Complex (MRC, hereafter) is an inshore seascape of reef mounds in east Mingulay (Outer Hebrides Sea) in western Scotland (Figure 6). It is found in a topographically complex deep-water channel connecting south to the Scottish continental shelf and Atlantic Ocean and is restricted to areas of full salinity Atlantic waters (35 psu) (Roberts et al., 2005; 2009). MRC is one of the most-studied cold-water coral reefs in terms of acoustic seabed mapping, hydrographic circulation and biodiversity (Roberts et al., 2005; 2009; Henry et al., 2010; 2013; Findlay et al., 2013; Navas et al., 2014; De Clippele et al., 2017). A detailed characterization of oceanographic conditions is given in D3.2.

Figure 6. Mingulay Reef Complex in the Outer Hebrides Sea (NE Atlantic).

Description of benthic communities Studies on the structure and functioning of the Mingulay Reef Complex benthic communities have revealed a mosaic of habitats including framework of live *L. pertusa*, fine to coarse sediments, coarse substrates, coral rubble and dead coral framework with the latter being colonized by a species-rich community dominated by suspension- and filter-feeders in terms of species richness and biomass (Roberts et al., 2005; 2009; Henry et al,. 2010; 2013; Duineveld et al., 2012; Kazanidis et al., 2016). Interestingly, a recent study unraveled that the massive sponge *Spongosorites coralliophaga* had higher species richness, diversity, density and biomass of macrobenthos living attached on its surfaces than the surrounding fragments of dead *Lophelia pertusa*

(Kazanidis et al., 2016). However, apart from the *L. pertusa* fragments and sponges, almost nothing is known about habitat supply from other organisms in Mingulay Reef Complex, e.g., bivalves, bryozoans and ascidians. Investigating habitat supply by Mingulay macrobenthos can have multiple benefits like: a) unravelling unknown aspects around the 3D structure of CWCRs (Roberts et al., 2009); b) distinguishing species-specific associations [e.g. possible preferential colonisation on a (biogenic) habitat by a taxonomic group] (Klitgaard, 1995); and c) improving our knowledge about the resilience of CWCR biodiversity under future oceanic conditions (e.g., ocean acidification and its impact on calcified ecosystem engineers) (Hennige et al., 2015). Working on these aspects can advance our understanding about the structure and the function of CWCRs under current and future scenarios.

In order to unravel the habitat-supplying macrobenthos as well as the species living attached to those ecosystem engineers at Mingulay Reef Complex, Van-Veen grab samples were collected over 44 stations in 2009 (Van-Veen grab samples *n*=10), 2010 (*n*=15) and 2011 (*n*=19). Collection depth ranged from 108-190 m water depth. Samples were sieved on board (1-mm mesh size), with specimens being sorted, identified at the highest possible taxonomic level (i.e., mostly at the species level) and their associations were recorded. The examination revealed 40 habitat-providing taxonomic groups and 43 epifaunal taxonomic groups (Figure 7). Habitat-providing species, i.e. the hosts, comprised a wide group including mainly sessile (e.g., the bivalve *Pododesmus squama,* the bivalve *Heteranomia squamula*) (Figure 8) as well as mobile fauna (e.g., the gastropod *Emarginula fissura*), calcified (e.g., the bryozoan *Omalosecosa ramulosa,* the brachiopod *Novocrania anomala,* Figure 8) and non-calcifed organisms (e.g., the ascidian *Polycarpa pomaria*), shark eggs as well as the parchment-like tubes of Eunicidae polychaetes (Figure 8). In addition there were cases where an epifaunal specimen attached to a host was later colonised by another species (e.g., the cirripedian *Verruca stroemia* was found attached on the bivalve *Heteranomia squamula* which in turn was attached on a parchment-like Eunicidae tube).

Bryozoans had the highest number of habitat-providing species (n=14), followed by molluscs (n=7) and polychaetes (n=5) (Figure 7). Habitat-providing specimens were mainly colonised by one or two species; however there were cases where up to five species were recorded on a single specimen (e.g., the bryozoans *Schizomavella linearis*, *Tubulipora* sp., *Oncousoecia dilatans*, the ascidian *Polycarpa pomaria* and the cirripedian *Verruca stroemia* were all hosted on a single specimen of the bivalve *Pododesmus squama*). Bryozoans were the group with the highest number of epifaunal species (n=26) followed by molluscs (n=5) (Figure 7). Hydrozoans were also found to act as hosts and epifauna; their identification at species level was under progress during the development of this document and thus they were not included in the present analysis.

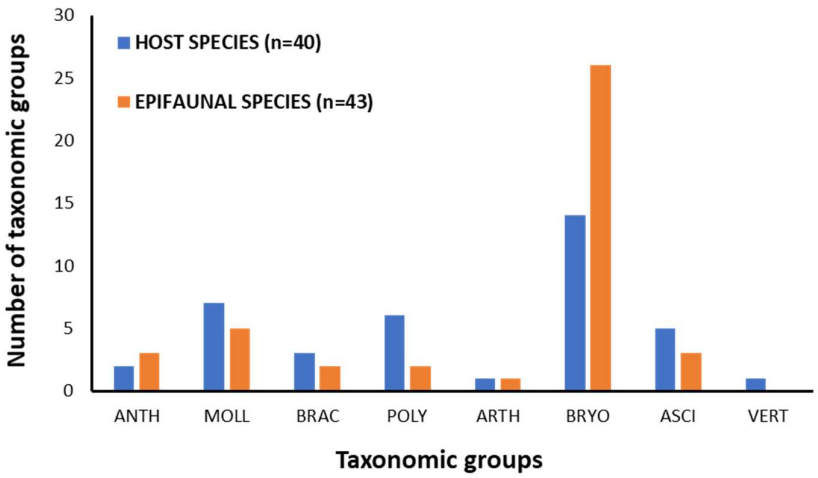

Figure 7. Number of taxonomic groups providing habitat (i.e. the hosts) to macrobenthic species (i.e. the epifauna) at Mingulay Reef Complex. ANTH: Anthozoans; MOLL: Molluscs; BRAC: Brachiopods; POLY: Polychaetes; ARTH: Arthropods; BRYO: Bryozoans; ASCI: Ascidians; VERT: Vertebrates.

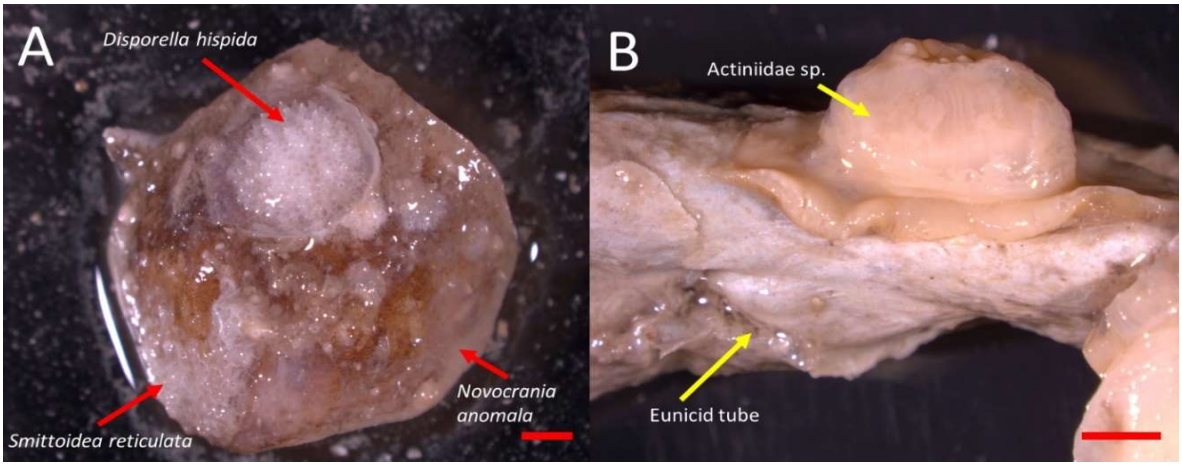

Figure 8. ***A:*** *The brachiopod* Novocrania anomala *hosting the bryozoans* Disporella hispida *and* Smittoidea reticulata*. Scale bar 1mm.* ***B:*** *Actiniidae specimen attached on an empty parchment-like tube of Eunicidae polychaete. Scale bar 2mm. Images credits: Georgios Kazanidis – ATLAS project.*

This study has advanced our knowledge about the role of structural complexity in supporting high biodiversity in Mingulay Reef Complex. Understanding the drivers shaping biodiversity patterns is important for the implementation of efficient conservation strategies protecting Vulnerable Marine Ecosystems in the deep sea.

1.2.3 Case Study 6: Distribution and diversity of coral habitats in canyons of the Bay of Biscay

Authors: Inge M. J. van den Beld, Jean-François Bourillet, Sophie Arnaud-Haond, Laurent de Chambure, Jaime S. Davies, Brigitte Guillaumont, Karine Olu, Julie Tourolle, Lénaïck Menot

Study area and environmental setting The continental margin of the Bay of Biscay, located west of France and north of Spain, is incised by over a hundred submarine canyons (Figure 9). Oceanographic conditions in the area are influenced by several water masses with different origins and densities and small scale processes such as tidal currents and internal waves (van Aken et al., 2000a,b) which may influence the occurrence of benthic communities. Results of the study presented here have been partly published in van den Beld et al. (2017). For more information on the geomorphology and oceanography of the area please refer to this publication.

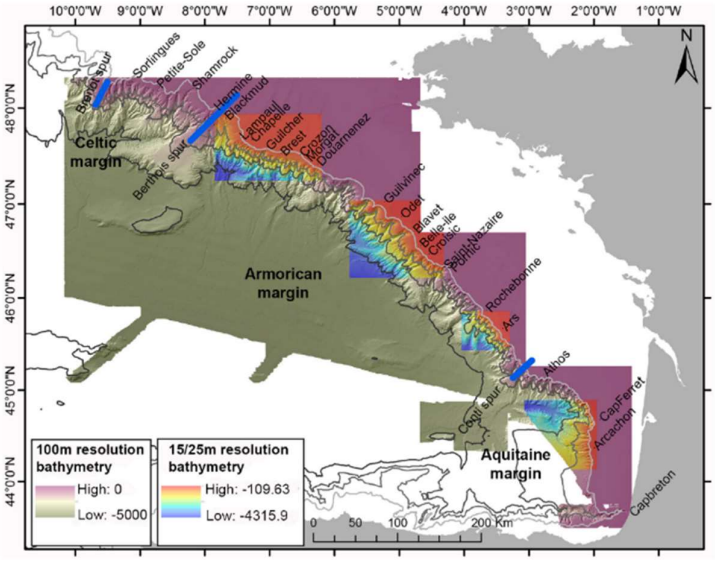

Figure 9. Map of the submarine canyons incising the continental slope of the Bay of Biscay (from van den Beld et al., 2017)

Description of benthic communities Cold-water coral reefs in the Bay of Biscay are known since the end of the 19th century (Le Danois, 1948) but a systematic exploration aiming at characterizing and mapping CWC habitats was carried out only in 2009-2012. A total of 24 canyons were explored during 48 dives of a ROV and a towed camera. Using the CoralFish habitat classification (Davies et al., 2017), 11 coral habitats were mapped, totalizing a linear of 46 km out of the 180 km surveyed. Coral rubbles (18 km) and coral reefs (11 km) were the most common coral habitats. Some examples of coral habitat types found in the study are shown in Figure 10.

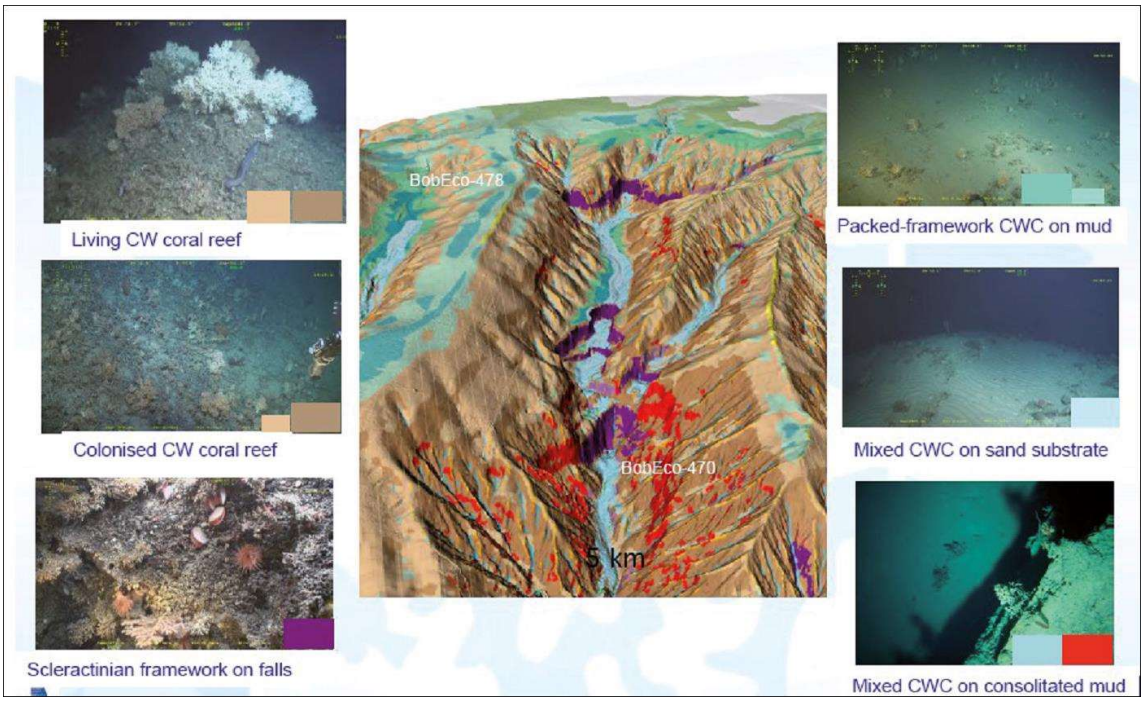

Figure 10. Habitat types and spatial distribution at Lampaul Canyon, one of the canyons with largest diversity of habitat types recorded during the study.

The image-based census of coral assemblages yielded 6,287 specimens or colonies belonging to 59 coral morphotypes, while non-coral megafaunal assemblages summed up 32,500 individuals belonging to more than 160 morphotypes (van den Beld et al., 2017). The inventory provided an update of the deep-sea species catalogue of the NE Atlantic (Howell et al., 2017).

The community structure and composition analysis of both coral and non-coral assemblages showed that coral habitat cluster into three groups (van den Beld et al., 2017; Figure 11): 1) aggregations of the two reef-building corals *Lophelia pertusa* and *Madrepora oculata*, whose common feature is to offer biogenic substrate for colonisation; 2) aggregations of antipatharians, alcyonaceans and scleractinians on hard substrates; and 3) aggregations of gorgonians or pennatulids on soft substrates.

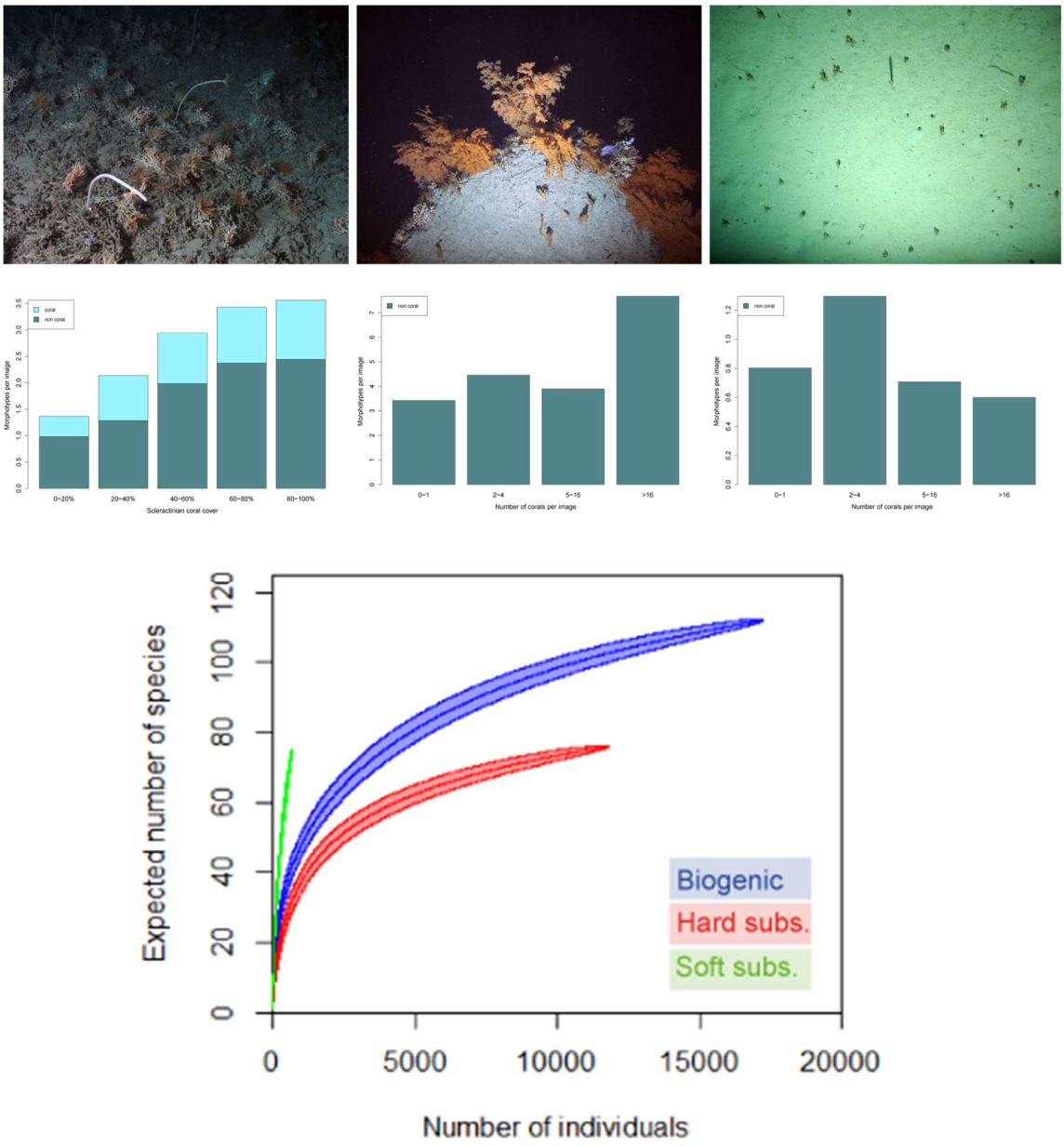

Figure 11. The diversity of coral habitats associated with biogenic, hard and soft substrates in the Bay of Biscay. The upper panel shows illustrations of the three categories of habitats (see text). The middle panel shows the mean number of species per image of the fauna as a function of coral coverage or density. The lower panel shows the individual-based rarefaction curves of the non-coral fauna for each of three categories of coral habitats.

The coral habitats on soft sediments are characterized by aggregations of the alcyonacean *Acanella* sp. or the two pennatulids *Kophobelemnon* cf. *stelliferum* and *Distichoptilum gracile*. These aggregations are mostly monospecific although *K. stelliferum* can co-occur with *Acanella* sp. as was already observed in the submarine canyons of the South West Approaches in the northern Bay of Biscay (Davies et al., 2014; Howell et al., 2010). Overall, megafaunal assemblages associated with coral habitats on soft sediments show the lowest densities of individuals and morphotypes at local scale.

Three morphotypes are most characteristics of coral habitats on soft sediments: Cerianthidae sp1, *Bolocera* sp1 and *Pentametrocrinus atlanticus*.

Coral habitats on hard substrates include diverse aggregations of antipatharians, alcyonaceans, and colonial scleractinians on bed rocks and consolidated muds. Coral and non-coral assemblages showed the highest densities and alpha diversity compared to biogenic and soft-substrate habitats (van den Beld et al., 2017). This is particularly so for coral aggregations mixing scleractinians, antipatharians and gorgonians. The distribution of this habitat was skewed towards the steeper slopes (> 20°) in canyons (van den Beld et al., 2017), and share some resemblance with the coral cliff habitat described in the Whittard Canyon (Huvenne et al., 2011). A striking characteristic of the coral habitats on hard substrates is the overwhelming dominance of brachiopods, which contribute to 73% of the abundance of the non-coral fauna.

Biogenic habitats are created by aggregations of the two scleractinian corals *Lophelia pertusa* and *Madrepora oculata*. The two species are syntopic in the Bay of Biscay (Arnaud-Haond et al., 2017). The bathymetric range of the coral rubbles is wider than the bathymetric range of living corals. The shallower coral rubbles could be the fossils of ancient reefs dating back to the last glacial age (De Mol et al., 2011). But the distribution of coral rubbles is also skewed towards topographically less complex and slopping areas than living corals, which may suggest that living corals preferably occurred in non-trawlable areas (van den Beld et al., 2017). Beta-diversity was high among patches of biogenic habitats, which is due to the fact that those habitats offer suitable niches for the fauna characteristics of both soft-sediments and hard-substrates. The crinoid *Koehlermetra porrecta* and the echinoid *Cidaris cidaris* are among the most characteristics species of the non-coral megafauna, locally aggregating in large numbers in biogenic habitats. Beyond the elevated position in the benthic boundary layer that the coral framework may offer, the biotic relationships with *K. porrecta* are unknown while it has been shown that *C. cidaris* is feeding on the reef-building corals (Stevenson & Rocha, 2013).

In order to assess the engineering role of corals, the relationship between coral cover or coral density and the abundance and the diversity of the associated fauna has been tested. In biogenic habitats, the abundance and diversity of the megafauna linearly increases with coral cover, providing evidence for the ecological role of coral reefs (Figure 11). In habitats dominated by antipatharians and alcyonaceans on hard substrates or dominated by pennatulids on soft substrates, higher abundance and diversity of the megafauna is only found associated with the highest densities of corals (i. e., over 16 colonies

per image). The occurrence of such high densities however is quite rare, representing 2% to 3% of images where those habitats have been recorded.

Results of this study feed into a proposal of a Natura 2000 network in the Bay of Biscay to define sectors to protect reef habitats under the Habitats Directive (MNHN-SPN and GIS-Posidonie, 2014). The designation of a Natura 2000 network comprising submarine canyons represents a step forward in the protection of deep-sea habitats in the French Atlantic (van den Beld et al., 2017).

1.2.4 Case Study 7: Gulf of Cádiz, Strait of Gibraltar and Alborán Sea

The Strait of Gibraltar (SG) and the surrounding areas, Gulf of Cádiz (GoC) in the Atlantic, and Alboran Sea (AS) in the Mediterranean, are key areas to understand the distribution and connectivity of marine communities (Patarnello et al., 2007). Within this setting, the SG represents an oceanographic transition area, connecting the Atlantic Ocean and the Mediterranean Sea, which circulation is characterised by a two-layer system: a surface eastward Atlantic water inflow and the deep westward outflow of saline Mediterranean water (MOW), with variable interface depth at around 100 m (Lacombe & Richez, 1982).

In this section, we focus of the major findings of the multidisciplinary deep-sea campaign MEDWAVES exploring and sampling seamounts, banks and the shelf from the Alboran Sea in the Mediterranean to the Azores on the Mid-Atlantic Ridge, including Chella Bank, Gulf of Cadiz, Ormonde Seamount and Formigas Bank (Figure 12). The aim of this campaign was to measure the influence of the MOW export on the Atlantic Ocean's circulation and ecosystems including genetic connectivity and biogeography. This section describes the benthic communities found in two key areas visited during the campaign, the Gazul Mud Volcano in the Gulf of Cadiz and Seco de los Olivos (Chella Bank) in the Alborán Sea. Benthic communities found at Formigas Bank are described as part of CS8.

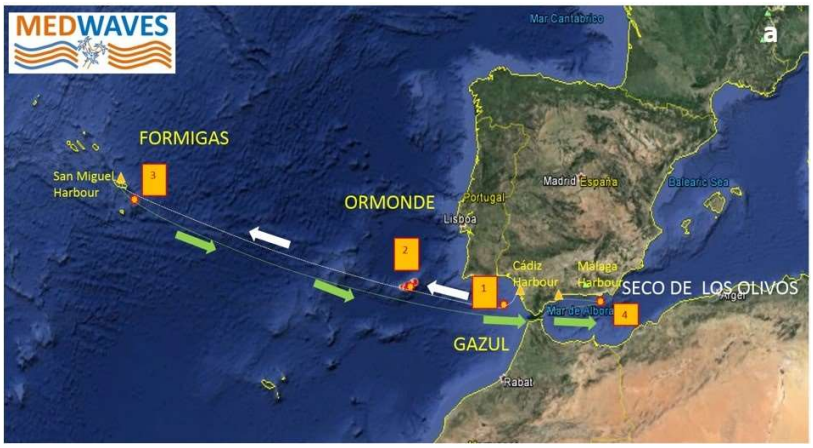

Figure 12. Route of the MEDWAVES cruise, number 1 indicates the location of the Gazul Mud Volcano in the Gulf of Cadiz and number 4 indicates the location of Seco de los Olvios (Chella Bank) in the Alborán Sea.

Benthic communities of Gazul Mud Volcano (Gulf of Cádiz)

Authors: Covadonga Orejas, Patricia Puerta, José Luis Rueda, Javier Urra, Jesús Rivera

Study area and environmental setting Gazul is a mud volcano located in the northeastern part of the Gulf of Cádiz (Figure 12). Mud vulcanos consist in cone-shaped edifices built up by successive episodes of mud flows as a result of degassing processes in deep diapiric marls bodies, evidenced in Gazul by the presence of methane-derived authigenic carbonates such as large chimneys and slabs. Gazul shape is sculpt by intense bottom currents produced by the Mediterranean Outflow Water (MOW), carving two depressions at both sides of the volcano cone downstream (Figure 13). Oceanographic conditions at Gazul were characterized by a two-layer flow, with Atlantic waters on the upper layer and waters of Mediterranean influence near the bottom. Details of the geomorphological and oceanographic characteristics were included in Orejas et al. (2017) and ATLAS deliverable D 3.2.

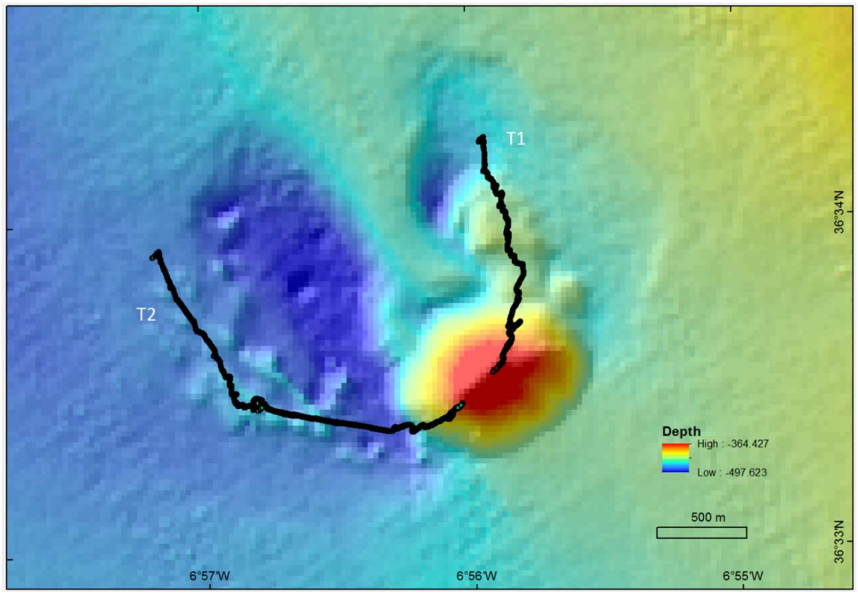

Figure 13. Multibeam bathymetry of Gazul Mud Volcano with the locations of the two ROV transects (T1 and T2) conducted during the MEDWAVES cruise.

Description of benthic communities The characterization of the megabenthic fauna in Gazul was based on still images extracted from two ROV video transects conducted in the area (Figure 13) (details on the methodology have been included in ATLAS deliverable 3.2). A total of 39, including species and morphospecies of megabenthic invertebrates belonging to 8 Phyla were identified in the study. Cnidarians (10 Anthozoans and 2 Hydrozoan including species and morphotypes) and Porifera (13 including species and morphotypes) were the most representative groups. For many taxa, the identification of specimens could only be made to morphotype categories (e.g. Porifera) or family level, with the number of species potentially increasing after revision by specialized taxonomists.

Overall, the abundances of megabenthic species were low, but higher in the north flank of the mud volcano (T1, Figure 13) characterised by higher substrate heterogeneity, in comparison with the west flank of the mud vulcano (T2, Figure 13), mostly dominated by soft bottoms (Figure 14).

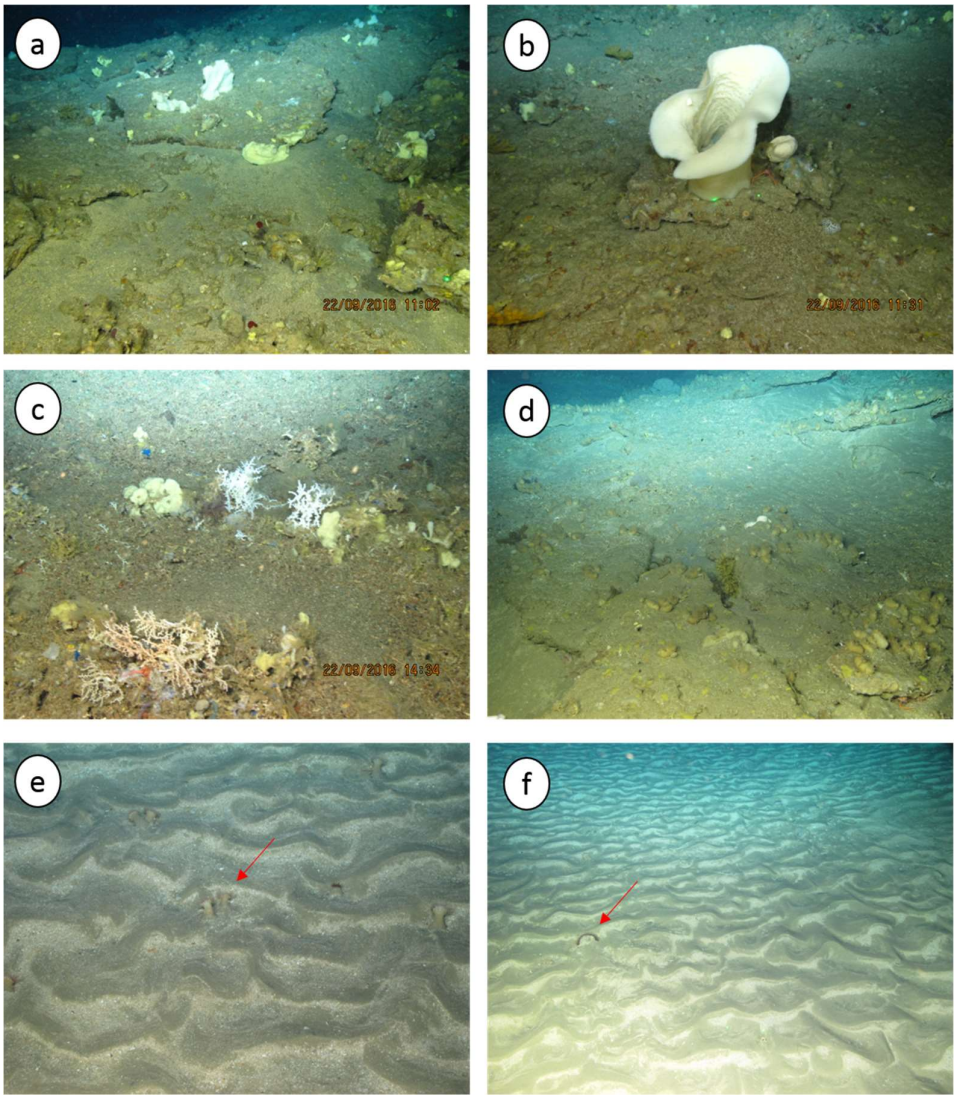

Figure 14. Benthic habitats and communities of Gazul Mud Volcano (from ca. 470 to ca. 400 m depth). a) Sponge field colonising areas in hard authigenic carbonates (slabs), b) specimen of the sponge Asconema setubalense*, c) patches of small colonies of the scleractinian coral* Madrepora oculata *with sponges, d) specimens of the ascidian* Polycarpa *sp. in hard authigenic carbonates (slabs), e) sandy bottom with ripples and the actinia* Actinauge richardi *(indicated by the red arrows) f) sandy substrate with presence of the solitary corals* Flabellum chunii *(indicated by the red arrows).*

Five types of benthic communities were identified in association with different substrate types and bathymetric ranges; some of those are displayed in Figure 14. Deepest areas of the north flank (ca 460 to 448 m depth) characterized by detritic and hard authigenic carbonates (slabs) interspersed with

sand were dominated by gorgonians of the genus *Acanthogorgia*, different porifera morphotypes, namely the sponge *Asconema setubalense* (Figure 14a,b), and patchy occurrence of crinoids. Low densities of the solitary scleractinian *Flabellum chunii* dominated detritric substrates at 450m depth. Shallowest areas of this flank (443 to 385 m depth) characterized by rocky substrates were colonized by different morphotypes of Porifera and the scattered presence of *Acanthogorgia* spp. The presence of white coral colonies, largely dominated by *Madrepora oculata* mixed with a few *Lophelia pertusa,* was also noted in this area (Figure 14c).

The deepest areas of the west flank of Gazul (ca 473 to 464m depth) displayed a quasi-monospecific community of the actinia *Actinauge richardi,* with occasional occurrence of the solitary scleractinian *Flabellum chunii* (Figure 14e,f). Areas with mixed substrate with soft sediment and rocky boulders in this flank (ca 464m depth) were dominated by the gorgonians *Acanthogorgia* spp. and high abundances of the ascidian *Polycarpa* sp. on rocky bolders (Figure 14d). Shallower areas of this flank (482 to 408 m) characterized by detritic bottoms, were dominated by a mixed assemblage of poriferans and lower abundance of *Acanthogorgia* spp. Small white colonies (*Lophelia pertusa* and *Madrepora oculata*) were present in patches of rocky substrate.

Several of the identified benthic communities may fit the FAO of the United Nations criteria for defining what constitutes a VME (FAO, 2009). These were soft bottom sponge aggregations dominated by *Leiodermatium* sp. and in some areas with the presence of *Asconema setubalenense*; hard bottom coral gardens dominated by *Acantogorgia* spp, in some cases with the presence of large colonies of the gorgonian *Callogorgia verticillata*; hard bottom gorgonian coral garden dominated by Plexauridae octocorals. Soft bottom coral gardens formed by the solitary scleractinian coral *Flabellum chunii* and soft bottom anemone aggregations of *Actinauge richardi* were also noted in some areas. The gastropod *Charonia lampas* is a protected species found occasionally in the area. It is classified as vulnerable in the Spanish Red-list (although not listed under IUCN) and protected by the Annex II of the Barcelona Convention.

Benthic communities of Seco de los Olivos (Alboran Sea)

Authors: Covadonga Orejas, Olga Reñones, Patricia Puerta, José Luis Rueda, Javier Urra, Jesús Rivera

Study area and environmental setting Seco de los Olivos also called Chella Bank (Figure 12) is located in a very active tectonic area in the NE Alboran Sea (Western Mediterranean) resulting from two transpressive fault zones. The seamount has a volcanic nature denoted by the rocky outcrops around the vertices and top of the seamount and a flat summit characteristic of a guyot. Oceanographic

patterns in the seamount are characterized by Atlantic-origin warmer and fresher surface waters overlying cooler, saltier deeper waters, with a salinity maximum about 400-500 m depth corresponding to the core of the Levantine Intermediate Water, the main contributor to the characteristics of the Mediterranean Outflow Water. Details of the geomorphological and oceanographic characterization were included in Orejas et al. (2017) and ATLAS deliverable 3.2.

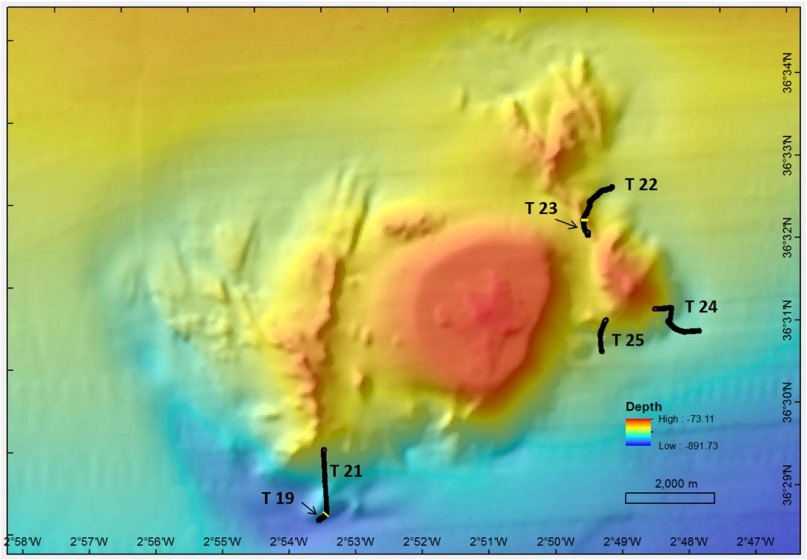

Figure 15. Multibeam bathymetry of Seco de los Olivos (Chella Bank), showing the locations of the ROV transects conducted during the MEDWAVES cruise.

Description of benthic communities The characterization of the megabenthic fauna was based on still images extracted from six ROV video transects (T) conducted in the east and northeast (T 22- T 25) and southwest (T 19, T 21) sides of the guyot (Figure 15, detailed methods in D3.2). A total of 62 species and morphospecies of megabenthic invertebrates belonging to 6 Phyla were identified in the study. Cnidarians (13 species and morphotypes) and poriferans (18 species and morphotypes) were the most representative groups. For many taxa, the identification of specimens could only be made to morphotype categories (e.g., Porifera) or Family level, with the number of species potentially increasing after revision by specialized taxonomists.

Two types of benthic communities, associated respectively with muddy substrates and soft detritic substrates with patched occurrence of rocky substrates, dominated the studied area across the bathymetric gradient (from 790 to 220 m depth). Muddy substrates generally displayed low occurrence of megabenthic organisms, with the exception of some isolated sponges. However, sea pens (*Kophobelemon* spp., *Pennatula aculeata*), different species of ceriantharians and holothurians (*Parantichopus* spp. and *Mesothuria intestinalis)* were found in southwest and northeast slopes of the

seamount (T19, 21, 24; Figure 16). The asteroidea *Brisingella* sp. was also observed in high densities in the NW slope of the seamount in association with a large population of the fish *Gadiculus argenteus* (T21, Figure 16).

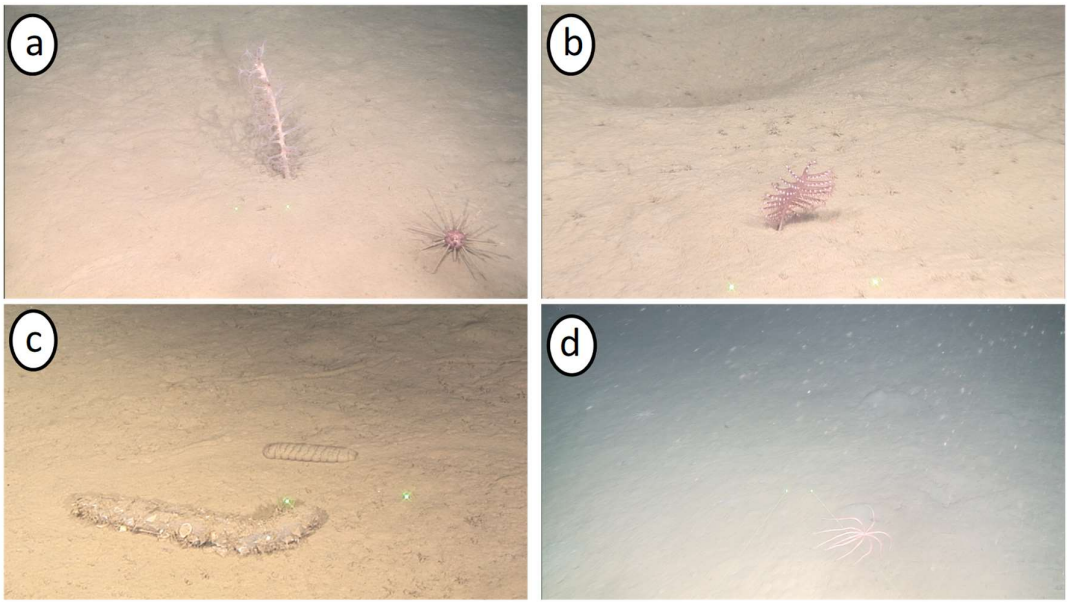

Figure 16. Megabenthic species observed in the muddy bottoms of Seco de los Olivos gullot. a) Kophobelemon *sp. (770-420 m depth), b) sea pen, probably a* Pennatula aculeata *(750 - 630 m depth), c) the holothuroidea* Mesothuria intestinalis *(640-570 m depth), d) the asteroidean* Brisingella *sp. (650-550 m depth).*

A diverse assemblage of sponges, including encrusting, pedunculate, massive and lamellate morphotypes dominated soft detritic substrates with patched occurrence of rocky substrates (Figure 17). Only four sponges were identified to genus level: *Cladocroce, Rhizaxinella, Asconema* and *Phakellia.* Although abundances were overall low, *Cladocroce*, together with encrusting sponges, dominated some areas of the NE slope of the seamount (T 22, Figure 17), with lower occurrence of *Asconema* and *Phakellia*. Encrusting sponges dominated in the eastern slope of the seamount (T25, Figure 17). Sporadic occurrences of different cnidarian species (i.e., alcyonaceans and some specimens of the black coral *Paranthipathes)* were observed in areas where hard substrates were present in the SW and NE slopes of the seamount (T21, 22, Figure 17b,c) in association with the fish *Hoplostethus mediterraneus* (Figure 17b) and *Helicolenus dactylopterus*. Cnidarians were mostly represented by *Acanthogorgia* spp. which occurred in the NE slope of the seamount (T23, Figure 17d); other frequent cnidarian species were the scleractinian coral *Dendrophyllia cornigera* and the black coral *Parantipathes* sp.

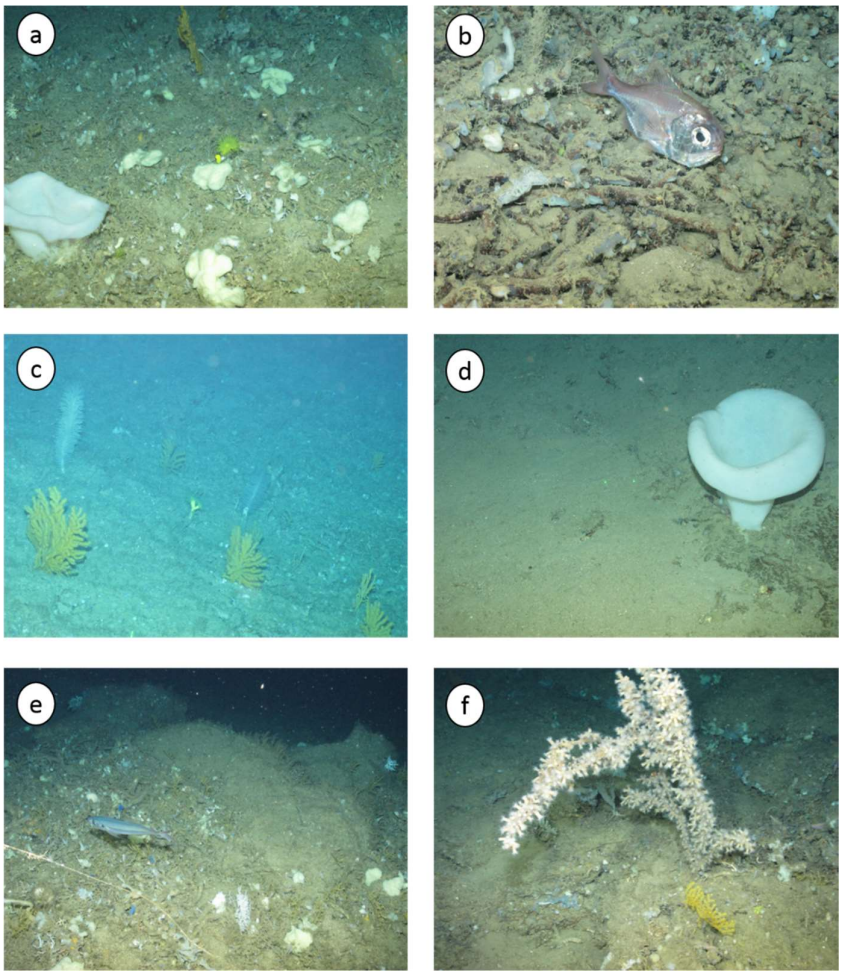

Figure 17. Benthic habitats and communities of Seco de los Olivos gullot a) Sponge field (200-250 m depth), b) specimen of Hoplostethus mediterraneus *lying in the seafloor covered by coral rubble (690 m depth), c) coral garden dominated by* Acanthogorgia *spp. (200-250 m depth), d) large specimen of the deep-sea sponge* Asconema setubalense *in soft substrate (ca. 600 m depth), e) a promontory covered by sponges and some cnidarians, as well as an specimen of* Trachurus trachurus *and long-line remains (200-250 m depth), f) Zoanthidae and* Acanthogorgia *sp. colonies (200-250 m depth).*

Several of the identified benthic communities may fit the FAOof the United Nations criteria for defining what constitutes a VME(FAO, 2009), as applied in the "Mediterranean VME indicator features, habitats and taxa" proposed by the VMEs working group from GFCM adopted by the Scientific Advisory Committee (Report WGVME, 2018). These are deep-sea sponge aggregations with mixed assemblages of encrusting, pedunculate, massive and lamellate morphotypes; hard bottom coral gardens dominated by *Acantogorgia* spp. and soft bottom coral gardens presenting a mixed community of gorgonians and black coral (*Parantipathes* sp.) and sea pen fields composed by different species (e.g., *Kophobelemon* sp., *Pennatula* spp.).

1.2.5 Case study 8: Azores region

Authors: Carlos Dominguez-Carrió, Marina Carreiro-Silva, Gerald H. Taranto, Manuela Ramos, Jordi Blasco-Ferre, Meri Bilan, Fernando Tempera, Cova Orejas, Patricia Puerta, Norbert Frank, André Freiwald, Dierk Hebbeln, Claudia Wienberg, Telmo Morato

The Azores is a volcanic archipelago located in the northeast Atlantic, above a tectonically active triple junction between the North American, Eurasian and African plates. Portugal's sovereignty in the Azores covers about 1 million square kilometres, and a claimed extended continental platform that expands this area to the double of this size, including the Great Meteor Complex, south of the Azores (Figure 18).

Oceanography in the region is influenced by two eastward currents branching from the Gulf Stream, the North Atlantic Current in the north and the Azores Current to the south (Klein & Siedler, 1989). Mediterranean water eddies (meddies) are also an important feature in the region, present as distinct lenses of warm and salty Mediterranean water at 800-1200 m deep (Bashmachnikov et al., 2009). In general, productivity is low, but localized upwelling associated with island slopes and seamounts can enhance local production (Bashmachnikov et al., 2004; Morato et al., 2008). The water current patterns result in a complex circulation, high salinity and temperature, and a low nutrient regime that typifies the Azores (Santos et al., 1995; Bashmachnikov et al., 2004; Palma et al., 2012).

The rough seafloor topography comprises island slopes, seamounts, deep fracture zones, trenches, and abyssal plains exceeding 5,000m depth. Seamounts are prominent topographic features in the Azores, with 460 seamount-like features identified to date that may occupy 37% of the total area of the EEZ (Morato et al., 2008; 2013). These geomorphological features favor the occurrence of different deep-sea ecosystems in the region comprising deep-sea hydrothermal vents, CWC gardens and reefs, and sponge aggregations. Despite some knowledge on the prominent ecosystems in the Azores, the area explored corresponds to only a small fraction of the EEZ. Thus, oceanographic cruises conducted within the framework of ATLAS have contributed to the identification of numerous new benthic communities, which are briefly characterized below.

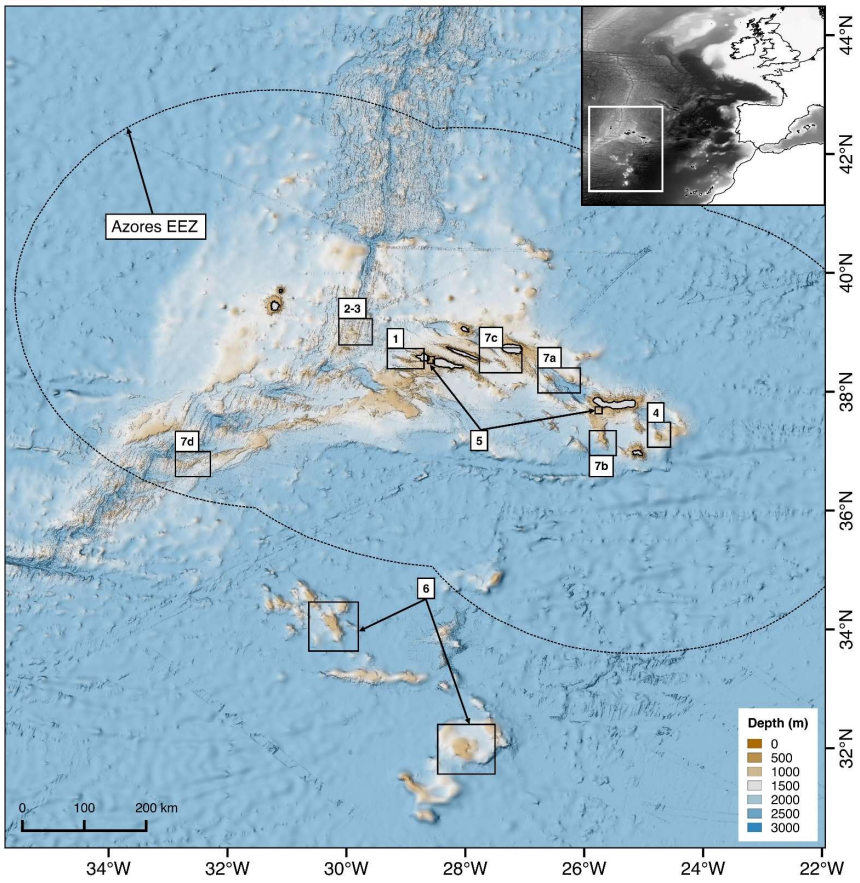

Figure 18. Map of the Azores region showing the location of the different study areas targeted during ATLAS oceanographic cruises: (1) Condor Seamount; (2) Gigante Seamount; (3) Luso hydrothermal vent field; (4) Formigas Bank; (5) Eguchipsammia cf. cornucopia *reefs; (6) Atlantis and Irving Seamounts (Great Meteor Complex); (7) other areas of interest.*

The benthic communities of Condor Seamount

Study area and environmental setting Condor is an elongated volcanic seamount located 17 km southwest of Faial Island (Figure 19). Its ridge extends NW-SE for 39 km, with its shallowest point on its flat summit at 185 m depth, and its flanks extending with gentle slopes down to 2000 m depth (Tempera, 2013). The oceanographic conditions over Condor are mainly characterized by an enclosed circulation around the seamount and pronounced mixing most probably due to semidiurnal tidal effects (Bashmachnikov et al., 2013). This influences the sedimentation processes and organic matter distribution, which appear to follow the seamount model (more organic matter on the seamount than adjacent areas; Zeppilli et al., 2013). The temperature ranges between 12-16 °C throughout the year, whereas salinity is stable at 36 psu.

Due to its proximity to land, this seamount has been targeted by local demersal fisheries (bottom longline and handline) since the 1990s, with fish catches accounted for almost 2% of the total fish

landings of the Azorean region until 2008 (Menezes et al., 2013). However, since 2010 an area of 242 km^2 surrounding the seamount has been closed to fisheries for research purposes (Morato et al., 2010) and set as a scientific underwater "observatory" within the Condor project (EEA grant; Giacomello et al., 2013). Since then, Condor has been an important focus of scientific activity, with several studies carried out regarding its geomorphology (Tempera, 2013), ocean circulation patterns (Bashmachnikov et al., 2013), phytoplankton communities (Santos et al., 2013) and demersal fish assemblages (Porteiro et al., 2013; Menezes et al., 2013), among others. The Condor Seamount has been included in the Azores Marine Park since 2016.

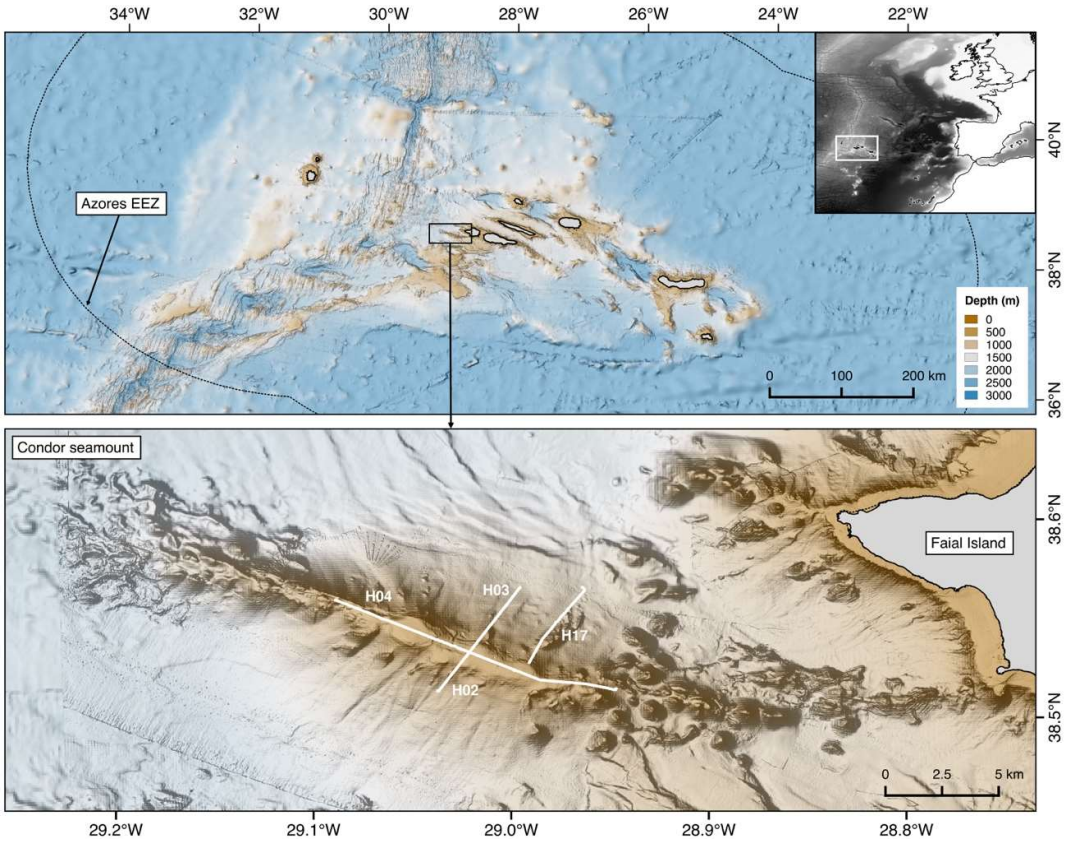

Figure 19. Location of the 4 tow-cam video transects performed on the summit (H04) and the flanks of Condor Seamount (H02-03-04-17).

Description of benthic communities Throughout the CONDOR and FP7 CoralFISH and MIDAS projects, explorations carried out using small ROVs provided some insights about the composition of the invertebrate communities that structure its benthic habitats (e.g., Tempera et al., 2012), but the ATLAS project has given the possibility to further quantify the abundance of the megabenthic species. The objective of these analyses is to better understand the structure of its main benthic assemblages and the environmental drivers of their distribution. The work was based on 4 tow-cam video transects

performed between 200 and 1150 m depth, on both flanks and the summit of the seamount (Figure 19). The amount of video footage recorded in those dives sums up to more than 33 hours of bottom time, which corresponds to more than 25 linear km of seabed. The megabenthic fauna of Condor Seamount resembles that of other seamounts of the Azorean region, with a clear dominance of octocorals as the main habitat forming species. Overall, more than 95 different species of invertebrates and 45 species of fish were identified in the images. Porifera (48%) and Cnidaria (29%) were the best represented phyla, accounting for almost 80% of the species identified so far, leaving the remaining phyla relatively underrepresented.

Condor Seamount shows a very clear zonation pattern strongly linked to depth, with the composition of the assemblages located on the summit displaying significant differences from those found on the seamount flanks. Coral gardens formed by the octocorals *Viminella flagellum* (Figure 20a), *Dentomuricea* aff. *meteor* (Figure 20b) and *Callogorgia verticillata* (Figure 20c), together with the large hydrozoan cf. *Lytocarpia myriophyllum* dominate the summit of Condor. The three gorgonian species are found forming a mixed assemblage both in consolidated and unconsolidated substrates, with the dominance of one species over the others changing throughout the summit. Further analyses are currently being underway to identify the environmental factors that determine the observed changes in their relative abundances. Also at the summit, particularly on the hard substrates of the eastern edge of the seamount, a dense aggregation of the hexactinellid sponge *Asconema* sp. has been found (Figure 20d), with densities above 6 ind/m^2. A small area of the summit also holds a patch of the scleractinian coral genus *Eguchipsammia*, composed mainly of coral rubble with a few living colonies over an area of 100 meters in length (Figure 20e).

The flanks of the seamount are characterised by a greater proportion of unconsolidated substrates compared to the summit, with sandy and gravelly areas more common towards its deeper part. This type of substrate diminishes the abundance of sessile organisms, with sandy patches generally colonized by the foraminifera *Syringammina fragillissima* (Figure 20f), which can be accompanied by cerianthids and the solitary scleractinian *Flabellum chunii*. Coarser substrate areas on both flanks are dominated by lithistid sponge species, replacing gorgonian corals in most areas of both flanks. Some frequent sponge species include *Leiodermatium pffeiferae*, *Neophrissospongia nolitangere*, *Macandrewia azorica* and *Petrosia crassa*, among many others (Figure 20g). Although sponges may dominate the flanks, two coral assemblages can be found on the flanks. On the southern side, gorgonians of the genus *Acanthogorgia* are found in combination with the laminate sponge *Pachastrella monilifera*, whilst coral gardens formed by the white gorgonian *Candidella imbricata* can be observed in the deepest part of the seamount (Figure 20i), in most cases accompanied by the

yellow cup coral *Leptopsammia formosa*. Many of the benthic communities described for this area may fit the FAO's VME criteria and thus may need conservation measures to protect these habitats from human pressures.

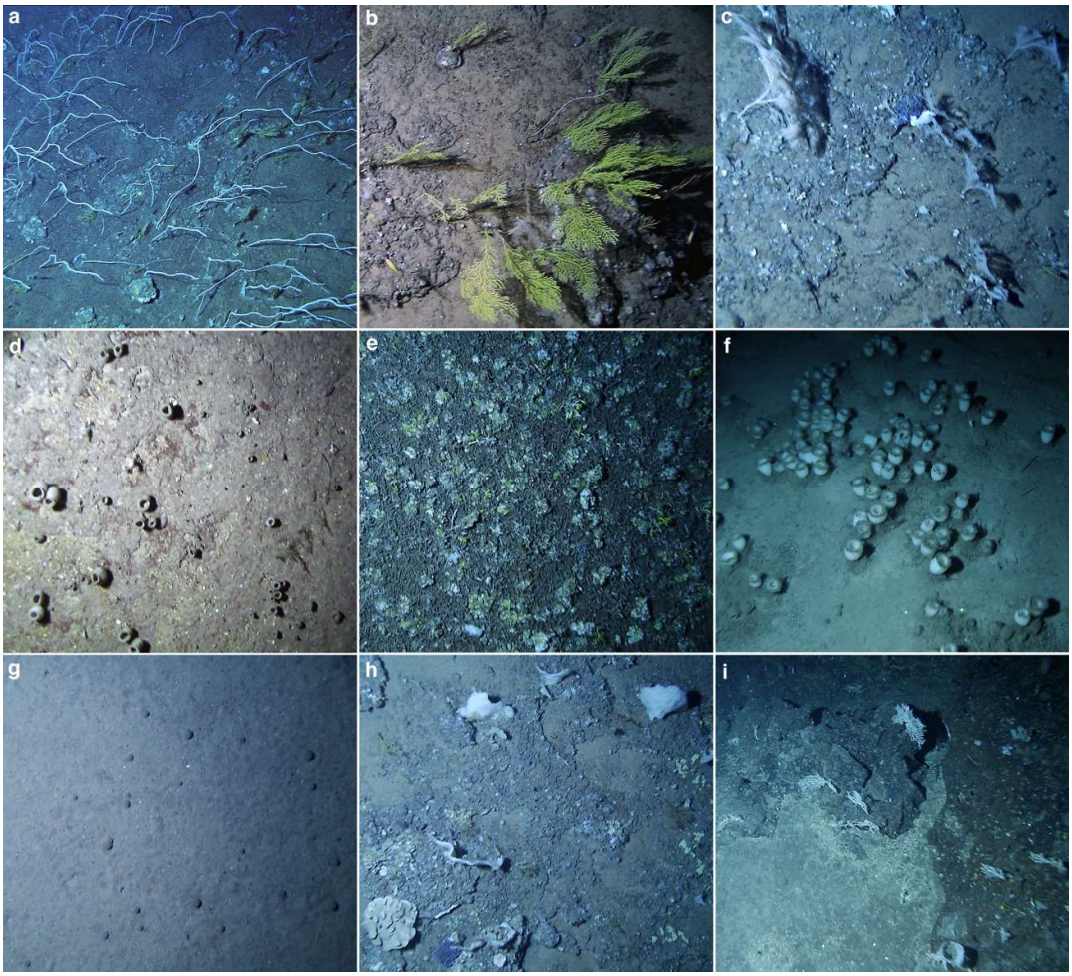

Figure 20. Images of the main benthic communities found in Condor Seamount. (a) One of the variations of the mixed coral garden found on the summit, with a dominance of of the whip coral Viminella flagellum. *(b) Another variation of the coral garden, in this case characterised by the large densities of the yellow arborescent octocoral* Dentomuricea *cf.* meteor. *(c) Areas with high densities of the primnoid* Callogorgia verticillata*, with individuals reaching heights above 1 m. (d) Aspect of the community dominated by the glass sponge* Asconema *sp., mostly found on the summit. (e) Patch of coral rubble formed by the skeletons of the scleractinian coral* Eguchipsammia*, with a few live colonies. (f) Aggregation of the hexactinellid sponge* Pheronema carpenter *on the flanks of the seamount. (g) Sparse colonies of the foraminifera* Syringammina fragillissima *on the soft-bottom areas of the flanks. (h) Sponge diversity found on the seamount flanks. (i) The deepest areas explored host a community dominated by the white gorgonian coral* Candidella imbricata.

Deep-sea epibenthic faunal assemblages of the Gigante Complex Area

Study area and environmental setting

The Gigante Complex Area (GCA) is located between the islands of Flores and Faial (Figure 21). It sits over the Mid-Atlantic Ridge, extremely close to the triple junction of the African, European and North

American plates. Gigante is a ridge-like seamount (~10 x 6 km), that rises 800 m from the seafloor to water depths of ~150 m. It follows the main trend of the Azores volcanic emplacement direction (~110-120º) and is crossed by lineaments parallel to the Mid-Atlantic Ridge (MAR) (Lourenço et al., 1998). Moreover, it is located in the southern edge of the diffuse boundary between the Nubia and Eurasia lithospheric plates, whose intersection with the MAR defines the locus of the Azores triple junction (Luis & Miranda, 2008; Marques et al., 2013). The combination of Azores magmatic processes with their contiguity to the MAR makes the Gigante Seamount a place of interest to assess on-going volcanic-tectonic and hydrothermal processes, in the context of a large-scale plume-ridge interaction, affecting the Azores Platform between Hayes and Maxwell fracture zones. Overall this area has been poorly studied in the past. It is known to represents an important ground for visiting pelagic species and an area of enhanced micronekton abundance. Although it is a common fishing ground for local fishermen, very little is known about local benthic communities.

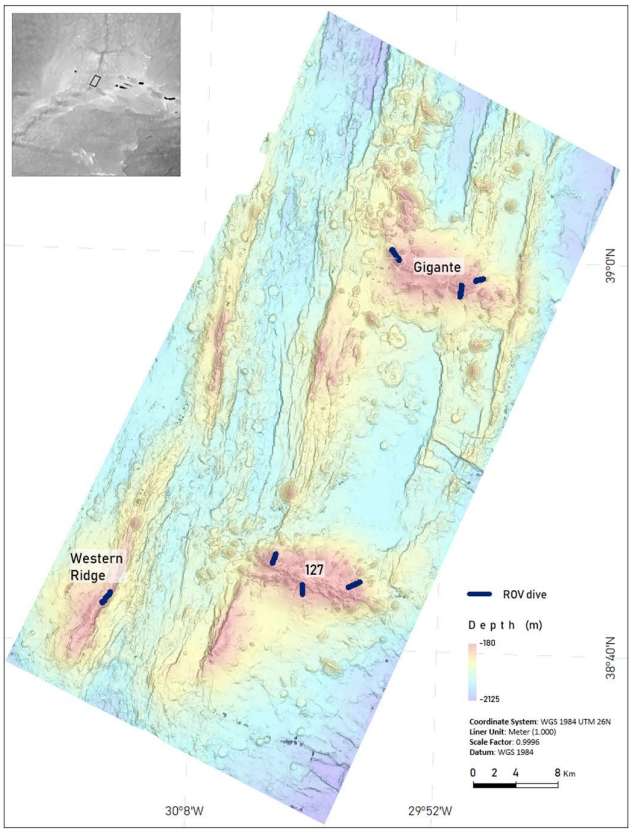

Figure 21. Gigante Complex Area with the three peaks explored during the Blue Azores 2018 expedition: Gigante, 127 and Western Ridge.

Description of benthic communities

A preliminary characterization of predominant sessile fauna and of fish and shark aggregations was based on seven video transects recorded by the ROV LUSO in 2018 (Figure 21), during the expedition Blue Azores 2018. The ROV dives occurred at depths of about 250-800 m on flanks and summits of three peaks of the GCA: Gigante, 127 and Western Peak. To date about 200 morphospecies were identified, mostly belonging to the taxonomic groups Cnidaria (80), Porifera (60) and Actinopterygii (34).

Preliminary analysis suggested that substratum type and stability, sediment deposition and bathymetric changes shaped local communities. At the considered depth range and on similar substrata, aggregations gradually faded into each other with a slow turnover of species and a progressive change in relative abundance. Soft bottoms were the most common substratum on lower slopes (~500-800m) and were mostly colonized by several species of solitary corals of the genera *Flabellum* and *Deltocyathus* (Figure 22a). Other distinctive, but rarer, assemblages on soft bottoms were dense aggregations of the fish Berycidae *Hoplostethus mediterraneus* on the 127 (NW flank) (Figure 22b) and aggregations of the glass sponge *Pheronema carpenteri* on the Gigante (SE flank) (Figure 22c). At similar depths, faunal assemblages on hard substrata appeared to depend on the dimension and stability of the hard patches and on the levels of sediment deposition. As deposition rates and sediment instability increased, average organism size decreased. Small Porifera were the predominant group on high deposition sites (Figure 22d), occasionally in association with small colonies of Octocorallia (mostly families Acanthogorgiidae, Paramuriceidae and Plexauridae) and Antipatharia (mostly Aphanipathidae) (Figure 22e). Larger areas of hard substrata, especially lithic rocks, hosted a wider variety of organisms which could form isolated aggregations as for example: the octocoral *Narella*, the soft coral *Anthomastus*, and unidentified Nidaliidae species (below ~650m) (Figure 22f); the large octocoral *Callogorgia verticillata* (Figure 22g); massive and tubular sponges (Figure 22h); and octocoral *Anthothela* sp. dominated facies (Figure 22i). Intact basaltic balloons hosted two main assemblages. One dominated by the flabellate sponge cf. *Poecillastra compressa* and the coralliid *Pleurocorallium* cf. *johnsoni*, often in association with colonies of *Anthomastus*, smaller sponges and, more rarely, octocorals of the families Acanthogorgiidae, Nidaliidae and Plexauridae (Figure 22j). The other dominated by a high density and diversity of encrusting sponges. Crumbled lava balloons normally exhibited a lower diversity and abundance with visible resident organisms limited to small Porifera and black corals (*Parantipathes hirondelle* and *Stichopathes gravieri*) (Figure 22k). On the Gigante (NW flank), lava balloons were also associated with the shallowest hydrothermal vent field identified on the Mid-Atlantic Ridge (the Luso hydrothermal vent field, see section 1.2.5).

The gorgonian species *Paragorgia arborea* and *Paragorgia johnsoni* formed distinctive assemblages both on basaltic and lithic rocks, with some coral colonies reaching sizes over 1m in height. These octocorals were found in association with vent cirripeds (alive on basaltic rocks, dead on lithic rocks) suggesting a potential relation with vent sites (Figure 22l). Moving toward shallower areas (~500-300m), Scleraxonia octocorals (Coralliidae and Paragorgiidae) became progressively rarer. On the contrary, the whip coral *Viminella flagellum* was ubiquitous on hard patches within this depth range.

On the deeper end of the range, *V. flagellum* colonies were smaller and sparse, mostly mixed with Coralliidae, Acanthogorgiidae and Porifera (Figure 22m). Toward the shallower end of the range coral and sponge diversity tended to increase, especially on the peak area of the Gigante, where *V. flagellum* colonies were found in association with large sponges (e.g., *Leiodermatium lynceus*, cf. *Characella pachastrelloides*, cf. *Neophrissospongia nolitangere*) and at least four families of gorgonians (Plexauridae, Primnoidae, Ellisellidae and Acanthogorgiidae) (Figure 22n) including, among others, the following species: *Callogorgia verticillata*, *Candidella* cf. *imbricata*; *Dentomuricea* cf. *meteor*, *Muriceides* spp., *Acanthogorgia* cf. *hirsuta*. On hard substrate, stony corals of the order scleractinia were rare with the exception of *Enallopsammia rostrata* (on shallower areas of the Gigante) and cf. *Leptopsammia formosa* (very abundant on all the explored area of the western ridge). Finally, multiple sightings of likely pregnant sharks (*Dalatias licha*), generally in association with little valleys on seamounts' flanks, suggest that this area might be important for deep-sea sharks (Figure 22o).

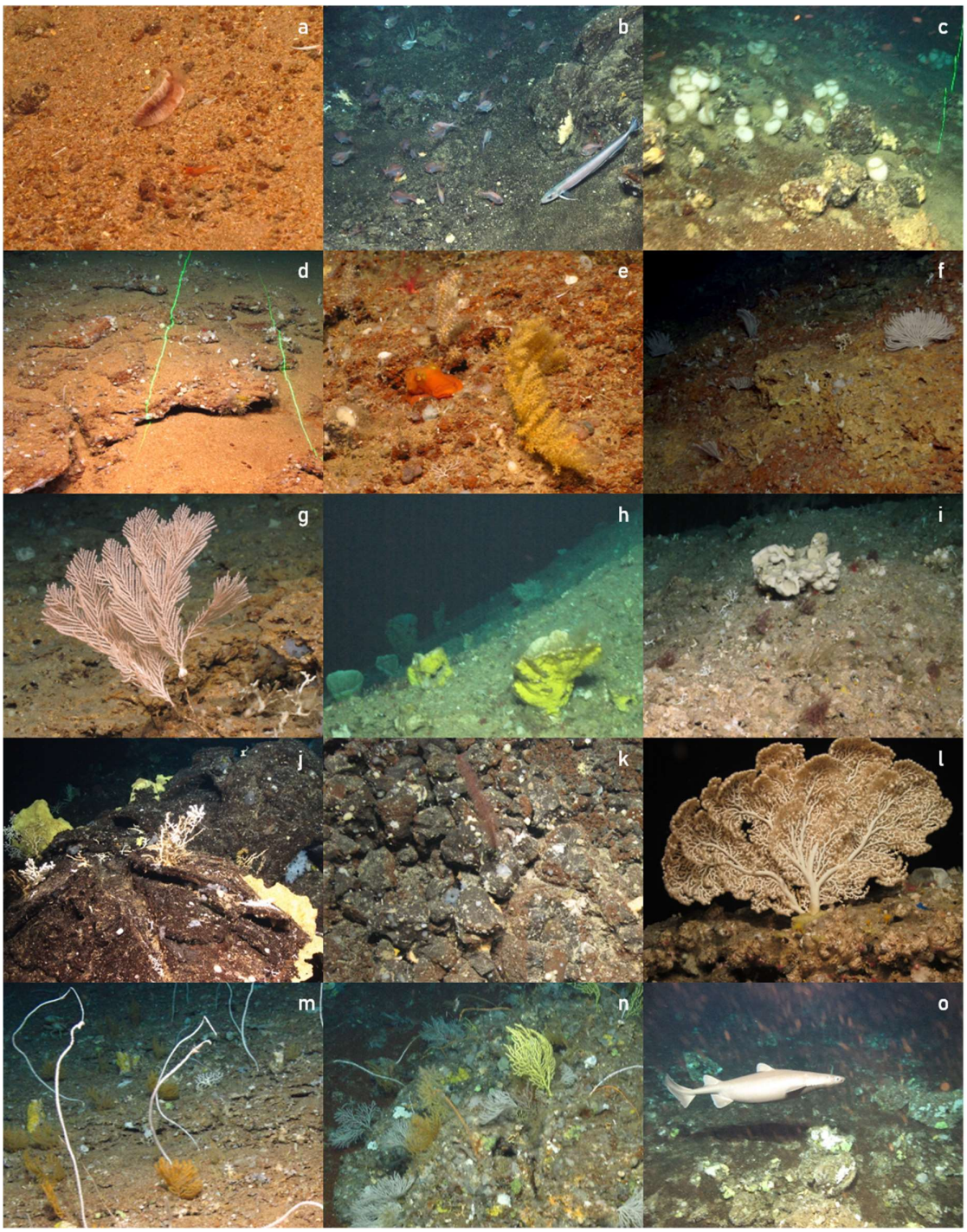

Figure 22. Some of the benthic assemblages of the GCA. (a) Flabellum *cf.* chuni*. (b)* Molva macrophthalma *and aggregation of* Hoplostethus mediterraneus*. (c)* Pheronema carpenteri*. (d) Encrusting and small globular sponges on rocky outcrops in high sedimentation areas. (e)* Acanthogorgia armata*, another species of Acanthogorgiidae and the cephalopoda* Pteroctopus tetracirrhus*. (f)* Narella *cf.* bellissima *assemblage. (g)* Callogorgia verticillata*. (h) tubular sponge aggregation (cf.* Characella pachastrelloides*). (i)* Anthothela *dominated facies with cf.* Neophrissospongia nolitangere*, Coralliidae and Plumulariidae species. (j) cf.* Poecillastra compressa *and* Pleurocorallium *cf.* johnsoni*. (k)* Parantipathes hirondelle *on crumbled basaltic rock. (l)* Paragorgia johnsoni*, dead cirripeds, Alcyoniidae and Dendrophylliidae species. (m)* Viminella flagellum*,* Acanthogorgia *cf.* hirsuta*, cf.* Characella pachastrelloides*, cf.* Hemicorallium *sp. (n)* V. flagellum, Candidella *cf.* imbricata*;* Dentomuricea *cf.* meteor *and encrusting sponges. (o) Deep water shark* Dalatias licha*.*

Overall, the dives performed in GCA revealed a series of benthic habitats of ecological significance, which should be considered when designing and implementing management policies: (1) The summits of the 3 seamounts hosted very dense and diverse coral gardens, where large octocorals (*Viminella flagellum*, *Dentomuricea* aff. *meteor* and *Acanthogorgia* cf. *hirsuta*) and large sponges generate complex three-dimensional structures that provide a suitable habitat for a wide range of associated species; (2) Areas of large basaltic lava ballons located on the deep slopes of Gigante and 127 Seamounts, where a specific association of the sponge *Poecillastra compressa* and the octocoral *Pleurocorallium* cf. *johnsoni* can be observed; (3) The northern flank of Gigante Seamount, which hosts dense patches of various coral species, as well as aggregations of large tubular, flabellate and massive sponges; (4) Areas of the 127 Seamount, which are home to deep-sea sharks, and its soft-bottom areas on the deepest slope, which hosts very dense aggregations of the Silver roughy *Hoplostethus mediterraneus*; (5) The slopes of the western ridge are colonized by large specimens of the gorgonian coral *Paragorgia johnsoni*, creating the one of the best-preserved aggregations of this species identified in the Azores EEZ so far, with colonies reaching heights of over 1.5 m.

A new hydrothermal vent field discovered on the slopes of Gigante Seamount (Mid-Atlantic Ridge, Azores)

Study area and environmental setting A new hydrothermal vent field was discovered on June 16th 2018 on the slopes of Gigante (Figure 23), a seamount located on the Mid-Atlantic Ridge (MAR), half way between Pico and Kurchatov fracture zones (see section 2.2.5.2 for more details on Gigante geomorphology). The “Luso” hydrothermal vent field was uncovered at 570 m depth during the Blue Azores 2018 Expedition with the ROV LUSO on board NRP Gago Coutinho. Following this discovery, and taking advantage of an ongoing collaboration between IMAR-UAz and Nadine Le Bris from the Sorbonne Université, the Luso vent field was revisited on the 4th of August 2018 with the ROV VICTOR6000 onboard the RV L'Atalante to perform additional observations and sampling to initiate the multidisciplinary characterization of the discovered vent field.

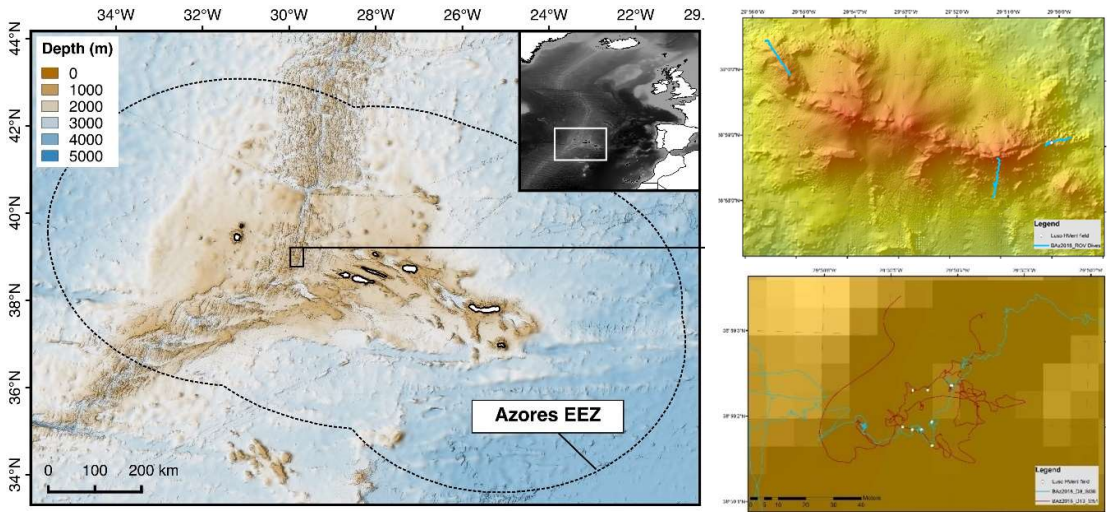

Figure 23. Map of the location of the large Gigante Seamount Complex (left) and the Gigante Seamount (right) with the "LUSO" hydrothermal vent field (white dot in top right panel). Known chimney-like structures are also shown (white dots in bottom right panel). Blue and red lines show ROV dives conducted during the Blue Azores Expedition 2018.

Description of benthic communities Luso hydrothermal vent field occupies an area of about 400 m^2 and is composed of at least 26 chimney-like structures of different sizes; with orifices up to about 30 cm in diameter (Figure 24). Active and inactive vent chimneys are distributed preferentially along the ENE-WSW fractures. Chimneys were composed by loose and fragile material, displaying a concentric composition reflected in different colours and textures. In general, three compositional zones can be recognized: i) the innermost zone, which is in contact with the hydrothermal fluid, composed of white, loose and low-density precipitates, with rare green clays, with a mineralogical composition characterized by a dominance of amorphous Si (Opal A); ii) the middle zone shows brownish to yellowish precipitates, intermixed with olive-green clays scattered locally, with a mineralogical composition characterized by an intermixed clay composition with amorphous Si and oxyhydroxides; iii) the outermost zone is composed by brownish ochre material, dominated by Fe-Mn oxyhydroxides. Inactive chimneys do not present a clear zonation and are dominated by a darker material, showing an enrichment in Fe-oxyhydroxides crosscut by fine and dark glassy veinlets with a deep purple tint (identified as amorphous silica) and an unclear zone I, well-defined in the active chimneys.

Hydrothermal fluids are transparent but well noticeable from a distance. They are moderately warm reaching a stable maximum temperature of 62°C when measured *ca.* 10 cm inside the outer rim of the main chimney conduit. Fluids are moderately acidic (pH 5.6-5.7), iron-rich (from 226.3 to 336.7 µM total HNO3-leachable iron), CO_2 rich, hydrogen rich (up to 357 µM), with moderate methane contents (up to 4.9), but contain no sulphides.

This system thus differs considerably from other hydrothermal fields along the MAR, characterized by fluids of high temperature, high concentrations of methane, sulphur and metals, supporting high biomass of specialized chemosynthetic fauna (Van Dover, 2000). The geological and physical-chemical nature (low temperature, high CO_2) of this vent system resembles the low-temperature hydrothermal vents (Pele's vents) at Loihi Seamount in Hawaii (Karl et al., 1988), and elsewhere in the Pacific (e.g., Kennedy et al., 2003) dominated by extensive deposits of Fe oxides of microbial origin.

Figure 24. Examples of chimney like structures in the "LUSO" hydrothermal vent field

Biological observations on the vents showed no typical hydrothermal vent macrofaunal, as opposed to other hydrothermal vent fields along the MAR. However, a total of 28 taxa were identified from the LUSO vent field, corresponding to 8 phyla. None of the observed taxa are considered vent specific; Crustacea being the largest group collected, both in terms of number of organisms and species. For many taxa, the identification of specimens could only be made to Family level, with the number of species potentially increasing after revision by specialized taxonomists. Dense aggregations of the tubiculous amphipods of the Family Ischyroceridae (c.f. genus *Nopotomus*) dominated the external surfaces of the active and inactive vent chimneys but appeared more abundant in active vent chimneys (Figure 25). This is a putative new species to science, which requires further verification. Amphipods of the Family Cappellidae were commonly observed together with the tubiculous amphipods, and the presence of the gastropod *Calliostoma lithocolletum* was also noted in the large active chimney of the primary venting area. Conspicuous faunal elements in the secondary venting

areas dominated by small active chimney area were the large balonomorph barnacle *Pachylasma* cf. *giganteum* with signs of iron precipitation on its exoskeleton and the zoanthid *Parazoanthus aliceae* (Figure 25). The crustacean *Paromola cuvieri* was also commonly observed in the vicinity of the small active chimneys but were also common outside the vent field. Chimney walls were also densely populated by hydrarians of the genus *Sertularella* and *Lafoe dumosa*. Inactive vent chimneys were characteristically covered by tubiculous amphipods, the hydrarian *Ectopleura larynx* and small recruits of the balanomorph barnacle *P. giganteum*. As the vent field area ends, the abundance of balonomorph barnacles is progressively reduced and diverse coral gardens composed by the gorgonians *Paragorgia aborea*, *P. johnsoni*, *Pleurocorallium johnsoni* and soft coral *Anthomastus* cf. *agaricus* among other species dominate outcrops of pillow basalts (Figure 25).

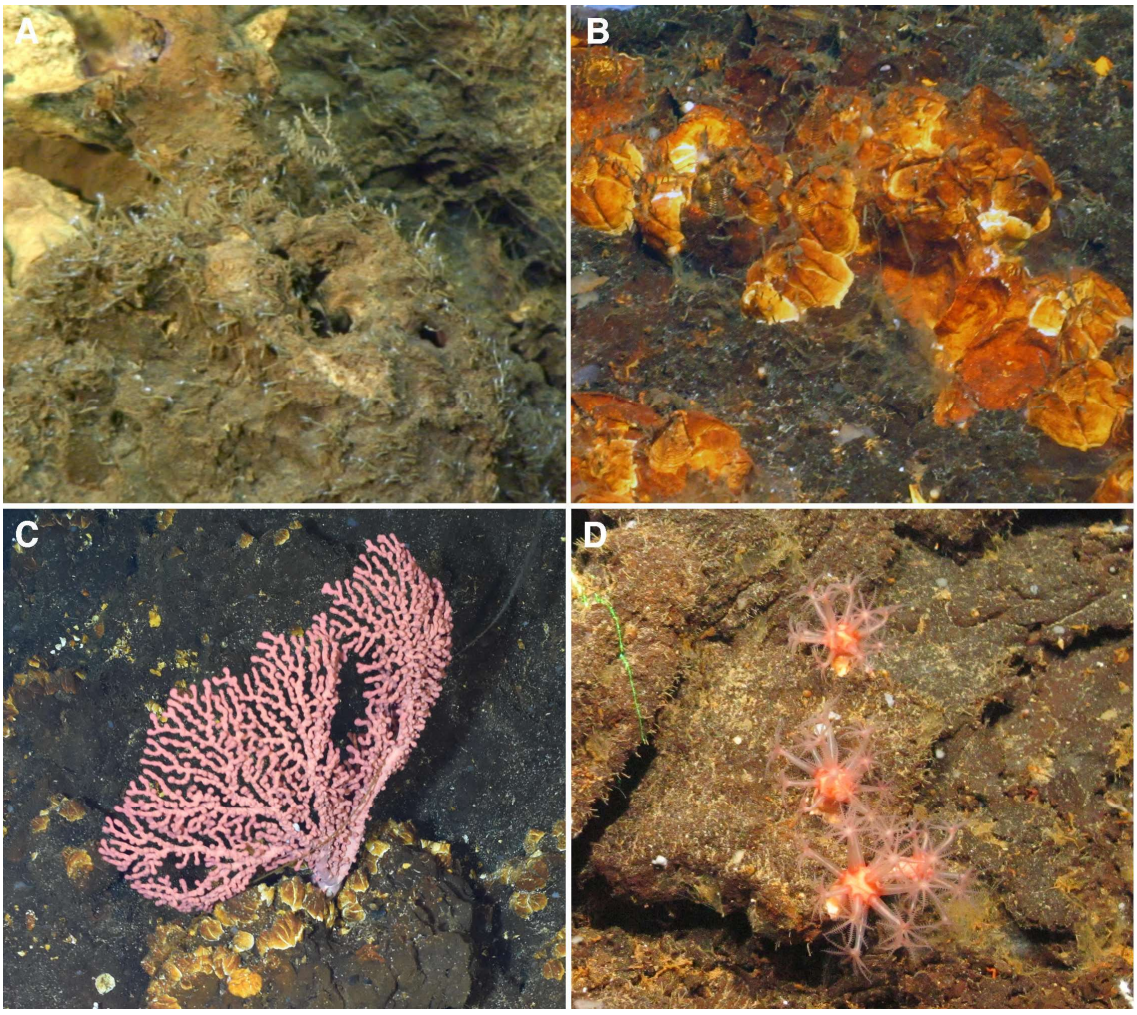

Figure 25. Examples of the benthic macrofauna found on Luso hydrothermal vent field. a) tubiculous amphipods of the Family Ischyroceridae (cf. genus Nopotomus*), b) balonomorph barnacle* Pachylasma *cf.* giganteum *with signs of iron precipitation on its exoskeleton, c)* Paragorgia arborea *and d)* Anthomastus *cf.* agaricus*.*

This new exciting discovery has the particularity of being located in an important fishing ground, close to the shores of the Azores and highlighting once again how little we know about the deep sea, even when the deep sea is our backyard. At a time when the UN is developing a new international agreement on the conservation and sustainable use of biodiversity in areas beyond national jurisdiction (BBNJ), it needs to be highlighted that individual countries must develop science-based management strategies for deep-sea exploration in their own waters as a basis for conservation and sustainable management of the deep sea in national jurisdictions. Such strategies should translate in real efforts to develop consistent field work activities for mapping VMEs and defining baseline conditions. The European Union, and nations like Portugal in particular, are taking great strides to develop trans-Atlantic collaborations to map the deep sea. It would be a costly mistake to neglect what needs to be discovered and protected in the deep-ocean waters close to our shores, much of which remains to be discovered.

The benthic communities of Formigas Seamount

Study area and environmental setting The Formigas Bank is located 34 miles southwest of São Miguel Island, in the easternmost part of the Terceira Rift, at the western end of the Eurasian–Nubian plate boundary (Figure 26). The Terceira Rift is characterized by a succession of rift basins and bathymetric highs, in some cases reaching the surface and forming islands, such as Graciosa, Terceira and São Miguel, as well as the Formigas Islets (Weiß et al., 2015a). The bathymetric highs evolved due to the strong volcanism of the area, which led to a high number of volcanic cones of variable high, especially northeast of the Formigas Islets (Weiß et al., 2015b). The Formigas Bank, which was formed 4 MYA (Abdel-Monem et al., 1975), has a trapezoidal shape delimited by curved scarps that trend westward, with faults that dissect the volcanic edifice in the directions NNE-SSW and NNW-SSE (Quartau et al., 2018). The Digital Elevation Model (DEM) of Formigas Bank developed during the MedWaves cruise shows that this tectonically active area has two main fracture directions, with a flat abyssal plain at 1,800 m on the western sector (see Deliverable 3.2). The location of Formigas Seamount in the westernmost part of the Azores archipelago exerts a strong influence in the oceanographic conditions, with strong stratification on water masses in the same area: the North Atlantic Central Water (NACW, 150-500 m depth), the Antarctic Intermediate Waters (AAIW, 500-700 m), the Mediterranean Outflow Water (MOW, 700-1300 m) and the North Atlantic Deep water (NADW, below 1300 m). Further details are provided in Deliverable 3.2.

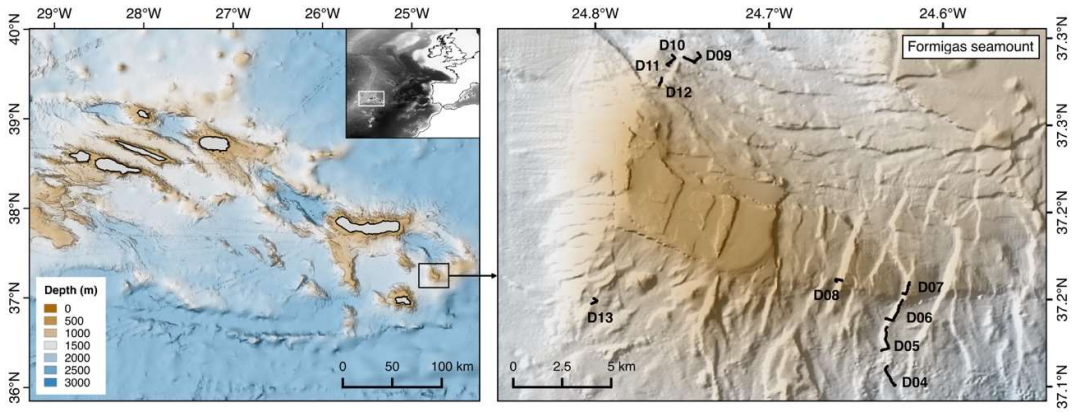

Figure 26. (Left) Black box identifies Formigas Bank, south-east of Sao Miguel Island. (Right) Location of the 10 ROV transects (D04-D13) performed on the NW, SE and SW flanks of Formigas Seamount.

The Formigas Bank was declared a Nature Reserve by the Azorean Regional Assembly in 1988, protecting 523.93 km^2 including the emerged area to depths of more than 1,700 m. Most types of fishing activities are prohibited, including those that use hooks and lines, as well as gillnets, with the exception of registered artisanal fishermen that use boats smaller than 14 m (Decreto Legislativo Regional Nº11/88/A). The area is also considered a European Site of Community Importance as part of the Natura 2000 Network.

Description of benthic communities As part of the MedWaves cruise, 10 ROV dives were performed on the different flanks of the Formigas Bank, at depths between 480 m and 1580 m (Figure 26). Over 36 hours of video images were acquired, covering over 14 km of seabed. Almost 25,000 invertebrate organisms were identified and annotated from the video footage, which corresponded to more than 160 morphospecies. The largest part of the identified taxa corresponded to Cnidaria (75) and Porifera (55), with less representatives for the remaining phyla. Due to the large diversity of taxa found in Formigas, a great taxonomical effort is still being carried out to identify as many organisms as possible to species level. Although Cnidaria was the most diverse phylum, the most abundant was Porifera, with almost 60% of the organisms identified belonging to this phylum. This was particularly so in the case of small encrusting and digitate Porifera, which were very abundant in the shallowest dives, dominating a large part of the hard substrates. Besides these small sponge species, the most abundant invertebrates were the octocorals of the family Primnoidae *Narella versluysi* and *Narella bellissima* and the Isididae octocoral *Acanella arbuscula*.

Regarding the composition of the invertebrate community, a very clear pattern was observed along the slopes, with a dominance of sponge species in the shallowest areas explored (400-800 m), which were substituted by Cnidaria species with increasing depths (Figure 27). The highest number of coral

species was observed between 1200 and 1400 m depth, with almost 60 taxa identified, including several species of scleractinians, gorgonians, black corals and bamboo corals.

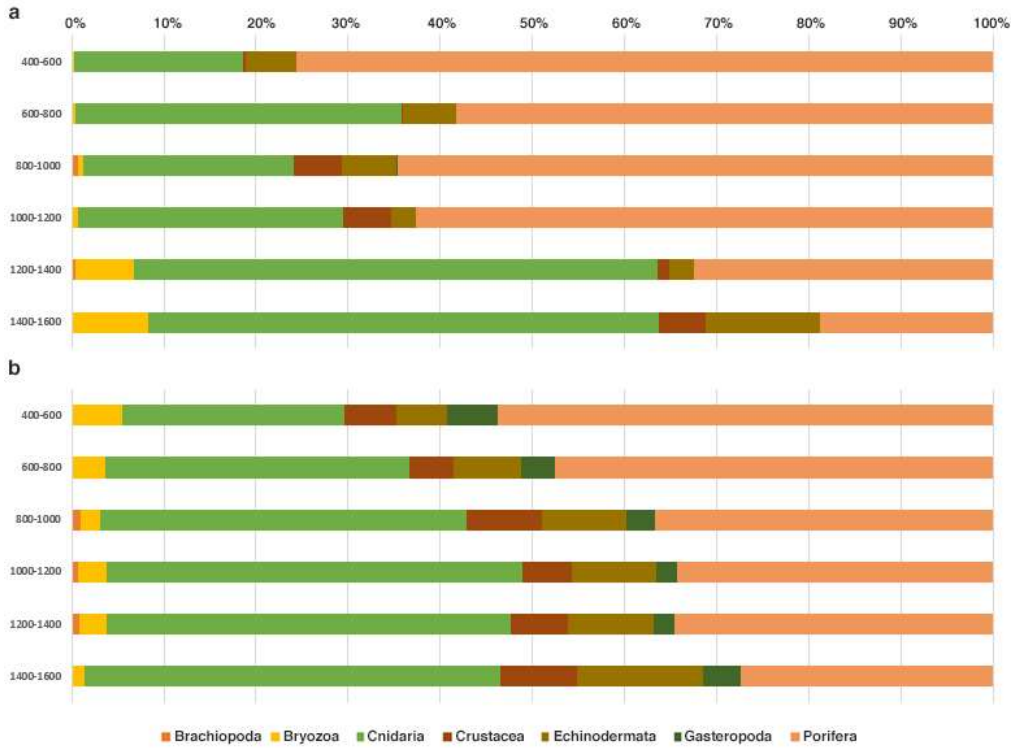

Figure 27. (a) Percentage of organisms of each phylum and (b) percentage of species of each phylum identified along the bathymetric gradient.

Quantitative analyses are currently being carried out to determine the species associations that can be found in Formigas Bank. Preliminary analyses have identified more than 10 megabenthic communities, distributed at different depths along the slope of Formigas Bank. The shallowest areas explored, on the SE flank, were colonized by the octocoral cf. *Nicella granifera* and the lithistid sponge *Macandrewia azorica*, together with other encrusting and digitate Porifera. This flank also hosted communities of the gorgonians *Narella versluysi* and *N. bellissima*, together with the gorgonian *Acanthogorgia* sp. and the sponge *Poecillastra compressa* (Figure 28g), generating dense patches between 700 and 1000 m depth. Also in this same bathymetric range, areas with the scleractinians *Solenosmilia variabilis*, *Lophelia pertusa* and *Madrepora oculata* could also be observed (Figure 28e), in general with low numbers. More common were the octocorals *Acanella arbuscula* and *Chrysogorgia agassizi* (Figure 28h), which distributed together in low densities from 700 m all the way to 1400 m depth. In the vertical walls of the SE flank, at around 900 m depth, the 'living-fossil community' of the cyrtocrinid *Cyathidium foresti* could also be identified (Figure 28i), together with Brachiopoda, encrusting and hexactinellid sponges attached to the rock.

On this same SE flank, around 1000 m depth, aggregations of the lollipop sponge *Stylocordila pellita* (Figure 28b) and the white gorgonian *Candidella imbricata* (Figure 28d) could also be observed. In the deepest areas explored, between 900 and 1400 m, a mixed community of corals and sponges was observed, especially in colonizing outcropping rocks. In these areas, highly species-rich patches were observed (Figure 28f), where a variety of coral and sponge species was annotated, including the octocorals *Candidella imbricate* and *Acanella arbuscula*, the scleractinians *Lophelia pertusa* and *Desmophyllum dianthus*, the black corals *Anthipathes* cf. *erinaceus* and *Leiopathes expansa* and the yellow sponge *Poecillastra compressa*, among others.

Figure 28. Examples of the benthic fauna observed in Formigas Bank. (a) The hexactinellid sponge Pheronema carpenteri*. (b) The lollipop sponge* Stylocordila pellita *and the gorgonian* Chrysogorgia agassizi*. (c) A solitary individual of the crustacea* Aristaeopsis edwardsiana*, always found on soft substrates below 1000 m. (d) Coral garden dominated by the octocoral* Candidella imbricata *and an unidentified orange gorgonian. (e) A solitary colony of the cold-water coral* Lophelia pertusa*. (f) Mixed coral garden with a wide variety of coral and sponge species, such as* Candidella imbricata, Acanella arbuscula, Lophelia pertusa, Desmophyllum dianthus, Anthipathes *cf.* erinaceus, Leiopathes expansa *and* Poecillastra compressa*, among others. (g) Coral garden found between 700 and 1400 m, dominated by the white primnoid species* Narella bellissima *and* Narella versluysi*, together with the yellow gorgonian* Acanthogorgia *sp. (h) Hard bottoms with* Acanella arbuscula*. (i) Vertical walls colonized by the ancient crinoid* Cyathidium foresti*.*

Regarding the fish fauna, almost 500 individuals were identified in the video images, belonging to 30 species. The most common fishes were *Neocyttus helgae* (30%) and *Synaphobranchus* sp. (23%), with a global dominance of eel like fishes (36% of the total number of individuals). Other relevant fishes were Macrouridae, with 68 individuals belonging to 9 different species.

The very dense and highly diverse coral gardens and sponge aggregations found in this seamount likely fit FAO VME criteria. Although this seamount is already designated a Special Area of Conservation, an OSPAR Marine Protected Area and a Nature Reserve, this protection is based on the presence of sublittoral biotopes of high conservation interest (e.g., Cystoseira and Laminaria beds), and importance as feeding grounds, spawning and nursery areas for many marine species, including fish, cetaceans and turtles. The new knowledge on deep-sea megafaunal communities provided here further emphasises the importance of this seamount as an area of high conservation interest.

Eguchipsammia c.f. *cornucopia* coral reefs in the Azores: refugia from the geological past?

Study area and environmental setting Mont'Ana is a 2km-wide volcanic cone located on the southern flank of the Faial-Pico Passage (Figure 29a). Its geomorphology is marked by a partial collapse running southwestwards that removed the original cone top and left some prominent rims. The edifice rises from depths of ~430m on the northeast and ~650m on the southwest, culminating at 280 m on a small rejuvenated peak located at the centre of the edifice. The oceanographic conditions in this underwater volcano are largely influenced by the enhanced hydrodynamics generated by the funneling of tidal currents through the passage separating the islands of Faial and Pico (Simões et al., 1999).

The José Gaspar Seamount is a submarine volcano with a near conical shape and a diameter of ~1.6 km (Figure 29b). It arises from 646 m depth up to a central peak at 291 m, perpendicular to its eastern flank, where a small elongated spur is developed. The seamount is located about 10 nm southwest of Ponta Delgada, São Miguel. The oceanographic conditions at José Gaspar are typical for seamounts with tidal amplification and internal wave formation. The mixed volcano-bioclastic sand found at the base of José Gaspard Seamount is structured with active and sharp-crested ripple marks most likely induced by the tidal-driven internal waves. Higher upslope, the basaltic rocks form isolated ridges and boulder accumulations above the sediment surface as a sign of steadily decreasing loose sediment cover and increasing bottom current energy at the top of the seamount spur. An enhanced food supply and attenuated sedimentation regime promoted by stronger currents could favor the occurrence of benthic assemblages at these sites.

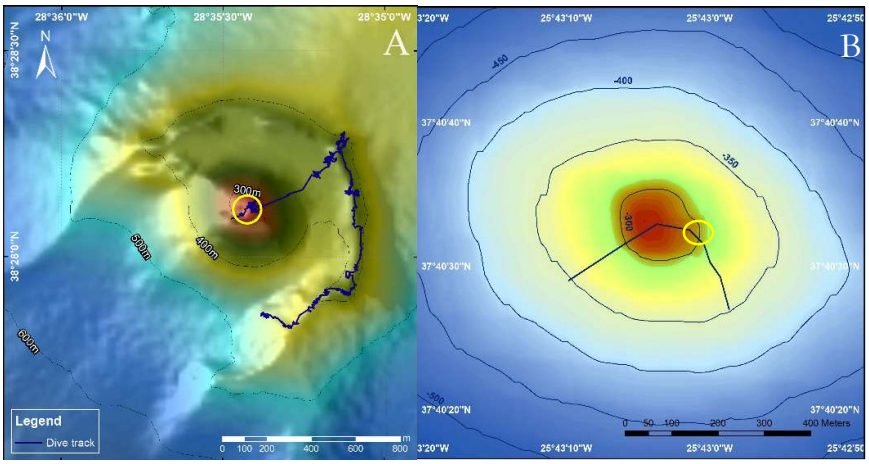

Figure 29. A. Map of Mont'Ana in the Faial-Pico Channel (from Tempera et al., 2015). B. Map of José Gaspar Seamount close to São Miguel Island (yellow circle delineates reef area). See Figure 18 for general location of study areas within the Azores region.

Description of benthic communities The characterization of benthic communities was based on two 2-2.5 km long video transects undertaken at Mont'Ana with the submersible Lula 1000 (Rebikoff-Niggeler Foundation) in July 2013 and August 2014; and one 0.5 km long transect undertaken with the ROV Squid (MARUM) at José Gaspar Seamount in October 2019 during the ATHENA cruise (Universität Heidelberg, MARUM Universität Bremen, and Senckenberg am Meer).

These explorations resulted in the discovery of the first extant reef formed by the azooxanthellate scleractinian *Eguchipsammia* cf. *cornucopia* Cairns, 1994 (Dendrophylliidae) in the Azores. The first record of this reef was made at 280-300m depth on Mont'Ana in the Faial-Pico Channel (Figure 29a, Tempera et al., 2015). The central denser area of this reef occupied an estimated area of 1,000 m^2 on the very top of the volcanic cone. The underlying substrate was partially visible underneath the dead framework, suggesting that the reef is less than 1 m thick (Figure 30a,c). A second *E. cornucopia* reef was recently recorded at the summit of José Gaspar underwater volcano at 300 m depth and occupied an estimated area of 400 m^2 (Figure 29b). The reef at this location was not as developed as in Mont'Ana, with large areas of dead coral framework and only small patches of visible living coral veneer (Figure 30b).

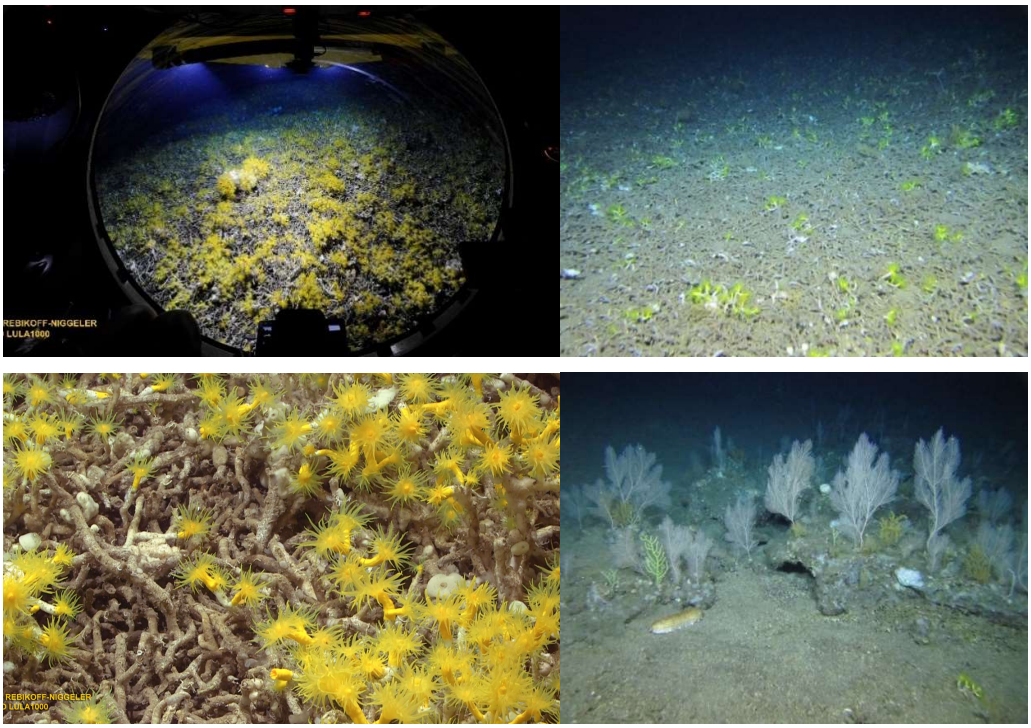

Figure 30. A. Eguchipsammia *cf* cornucopia *reef at Mont'Ana photographed from inside the Lula 1000. B.* E. cornucopia *reef at José Gaspar Seamount C. Close up of living reef framework. D. Octocorals* Callogorgia verticillata*,* Acanthogorgia *sp. and* Dentomuricea *cf.* meteor *colonizing large boulders in José Gaspar Seamount.*

Although the reef in Mont'Ana was firstly identified prior to ATLAS, the characterization of associated fauna based on the collected video transects has been conducted only recently within the ATLAS project. Associated fauna at both locations included 48 (morpho) species belonging to 7 phyla. Porifera was the most diverse group with 17 morphospecies. At José Gaspar Seamount, octocorals of the species *Callogorgia verticillata*, *Dentomuricea* cf. *meteor* and *Acanthogorgia* sp. were commonly observed on rocky boulders interspersed in the *E. cornucopia* framework (Figure 30d). Fish, namely *Helicolenus dactylopterus* were also commonly observed particularly at Mon't Ana Reef where the overall diversity of associated fauna was also higher. However, corals of the genus *Eguchipsammia* are not solidly attached to a hard substrate but are instead free-lying on the seabed (Zibrowius, 1980; Cairns, 2000). This means that with time coral branches intertwine with adjacent colonies to form a semi-rigid network with a wide variety of microhabitats: (1) the exposed surfaces of live or dead corals; (2) the internal coral skeleton, utilized by endolithic borers; (3) the porous areas within the colonies network; and (4) the sand or rock habitat underneath the reef framework. Therefore, the diversity of associated fauna estimated here using video analysis might underestimate the real diversity of fauna associated with these reefs.

The distribution range of the genus *Eguchipsammia* in the Atlantic Ocean, based on both recent and fossil records, included several locations in the Gulf of Mexico and Caribbean, at depths between 9

and 300 m, and in the northwestern Atlantic, from the Coral Patch Seamount to the Celtic Sea at depths ranging between 330 to 960 m (Cairns, 2000; Wienberg et al., 2013). The record of *Eguchipsammia* in the Azores, attests the presence of the genus in the central North Atlantic, filling the gap within its amphi-Atlantic distribution (Tempera et al., 2015).

The discovery of *E. cornucopia* forming reef-like structures suggests that the bioengineering role of this genus may be undervalued (Tempera et al., 2015). Similar to some formerly congeneric *Dendrophyllia* species in the geological record (e.g., Lauridsen et al., 2012), *E.* cf. *cornucopia* may be an important upper-slope, cold-water, reef-building coral in the Azores that presently does not form reefs elsewhere in the Atlantic. The occurrence of *E. cornucopia* as reef-forming habitat support the hypothesis that seamounts in the Azores may constitute refugia for ancient deep-sea fauna. The particular nature of this reef habitat and singularity in the North Atlantic calls for conservation measures to protect this habitat from human pressures.

Deep-sea epibenthic faunal assemblages on two open ocean guyots: the Atlantis and Irving (Atlantis-Meteor Seamount Complex, NE Atlantic)

Study area and environmental setting The Atlantis-Meteor Seamount Complex (AMSC) is an isolated group of open-ocean guyots in the Portuguese extended continental shelf (Figure 31), also named South Azores Seamount Chain. Here, we present the results of a baseline study carried out on the western flanks of two poorly studied seamounts from the northern and central part of the complex: the Atlantis and Irving Seamounts. The Atlantis is the northern and largest seamount of the AMSC Chain (Figure 31B). It has a complex structure with a NW-SE trend, reaching about 65 km in length and rising from about 2500 depth. It contains two large guyots with oval-shaped and flat-topped surfaces. The sampling site was in the southern Atlantis guyot at the western flank at 34° 05'N / 30° 10'W, which has the top at 250 m.

The Irving Seamount is located close to the midpoint of the AMSC (Figure 31C), at about 32°N / 28°W and rises from 3400 m depth from the edge of a broad plateau. The seamount has an oval shape structure, reaching about 100 km in length and with a NW-SE direction. Its summit is also typical of a guyot and it has an equivalent radius of 8 km flat surface, with the top at nearly 260 m below sea level. The general circulation of the upper water masses (0-700 m) in the Great Meteor region is influenced by the North Atlantic Central Water (NACW). The Atlantis Seamount located in the upper north section of the AMSC is also under the direct influenced by the Azores Current (AzC), whereas Irving to the

south is more influenced by the Subtropical Mode Water (StrMW). Comparatively to the AzC, the StrMW is characterised by its elevated temperature, salinity, lower oxygen, higher nutrient contents.

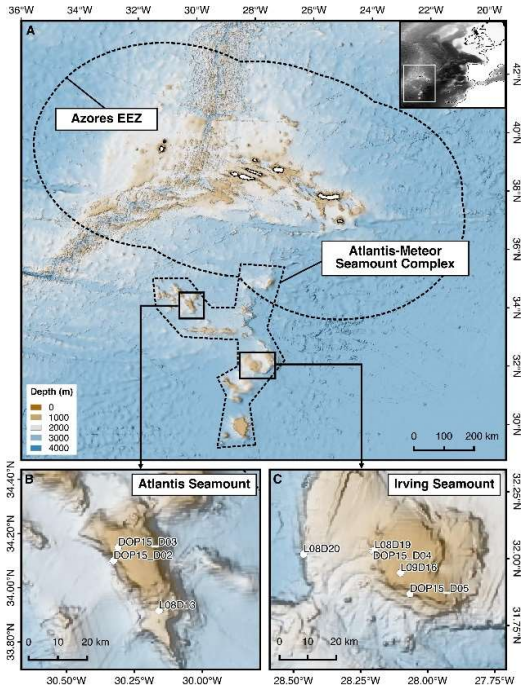

Figure 31. A. Map of the Atlantis Meteor Seamount Chain located 600 Km south the Azores Archipelago. B. Map of the Atlantis Seamount. White dots indicate ROV transects carried out during BIOMETORE 2015 (DOP15D02 and DOP15D03) and EMEPC 2008 (L08D13) expeditions. C. Map of the Irving Seamount. White dots indicate ROV transects carried out during BIOMETORE 2015 (DOP15D04 and DOP15D05) and EMEPC 2008 (L08D20 and L08D19) and 2009 (L09D16) expeditions.

Description of benthic communities The characterisation of benthic fauna was based on 8 Remotely Operated Vehicle (ROV) video transects conducted at depths between 300 and 2600 m during the years 2008-09 and 2015. A total record of 6041 organisms belonging to 144 morphospecies of megabenthic invertebrates (>2 cm) were identified on the slopes and bathyal areas of Atlantis and Irving Seamounts. Cnidarians (40 Anthozoans and 6 Hydrozoans morphotypes) and poriferans (50 Demosponges and 9 Hexactinellids) were the most representative taxonomic groups in all depth strata analysed (Figure 32). These bioengineering species represented nearly 65% of the species of the community in both seamounts, accompanied in many instances by other invertebrates, such as crustaceans, echinoderms and molluscs (16%). Fishes represented 19% of all species identified.

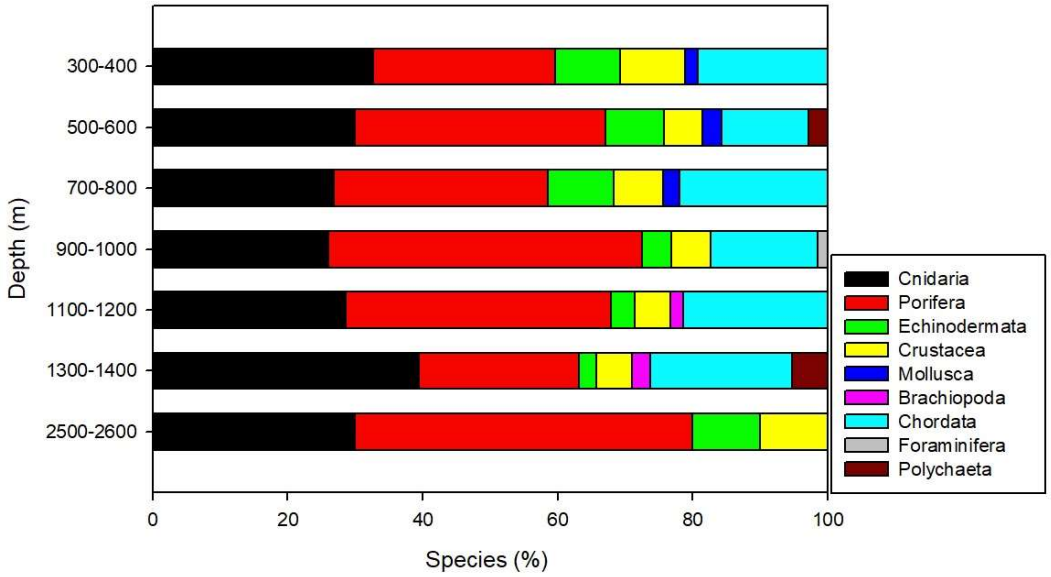

Figure 32. Percentage of species per phylum in the different depth ranges explored.

Although the general trend along both study areas was a low number of organisms, certain habitat-forming species were recorded displaying a highly patchy distribution. The distribution of seven epibenthic assemblages was markedly explained by depth, followed by the availability of sand/rock sediments and the structure of the water masses. The flattened summit of Irving Seamount covered with sand is colonized by two different communities (Figure 33): an aggregation of the echinoderms *Coelopleuros floridanus* and *Luidia ciliaris* (assemblage A) and the cup-coral *Flabellum chunii* together with the black coral *Parantipathes hirondelle* (assemblage B), which were very frequent in large sedimentary areas. The rocky outcrops of the upper slope (200-700 m) of both seamounts were characterized by species representative of the Macaronesian Region (assemblage C): *Viminella flagellum*, colonial dendrophyllids, *Leptosammia formosa*, *Villogorgia bebrycoides*, *Stylaster* sp. and lithistids e.g., *Neophrissospongia nolitangere*. These areas are under the influence of the Northeast Atlantic Central Water (NACW), and the seasonal influence of the Azores Current (AzC) in the Atlantis, and the Subtropical Mode Water (StrMW) in Irving.

At depths between 700-1500 m (upper to mid bathyal) of the Irving Seamount, coincident with intermediate water masses, the Mediterranean Outflow Water (MOW) and the modified Antarctic Intermediate Water (mAAIW), two assemblages with distinct sponge fauna and sparse solitary corals were depicted: assemblage D, with Rosselidae*, Aphrocallistes beatrix*, *Pheronema carpenteri* and *Craniella longipilis* with *P. hirondelle* and assemblage E, found in mixed substrates with a sparse

presence of hexactinellids (*Farrea* sp. and *Regadrella phoenix*) and stylasterids (*Pliobothrus* sp. and *Stylaster* sp.).

In the transition zone to the mid-bathyal boundary layer (lower than 1100 m), slightly influenced by the North Atlantic Deep Water (NADW), we found occurrences of widely distributed species (such as *Acanella arbuscula*) and scattered occurrences of *Iridogorgia* sp. and *Hyalonema* sp. (assemblage F). These species were present in both seamounts, specifically in rocky outcrops immersed in sandy areas. The lower bathyal (2500-2600 m) strata at Irving, strongly influenced by NADW, was characterized by the assemblage G dominated by the sponge *Poliopogon amadou* colonizing hard substrates, and *Euplectella suberea* in soft bottom areas.

Some of the identified assemblages may fit the FAO definition of VMEs (FAO, 2009). However, large densities of coral gardens and sponge grounds seem to be scarce in the western flanks of both seamounts. This situation might respond to the asymmetric sedimentary depositional trend of the seamounts, the low productivity of the area over the North Atlantic subtropical gyre and the high degree of isolation of this geological complex.

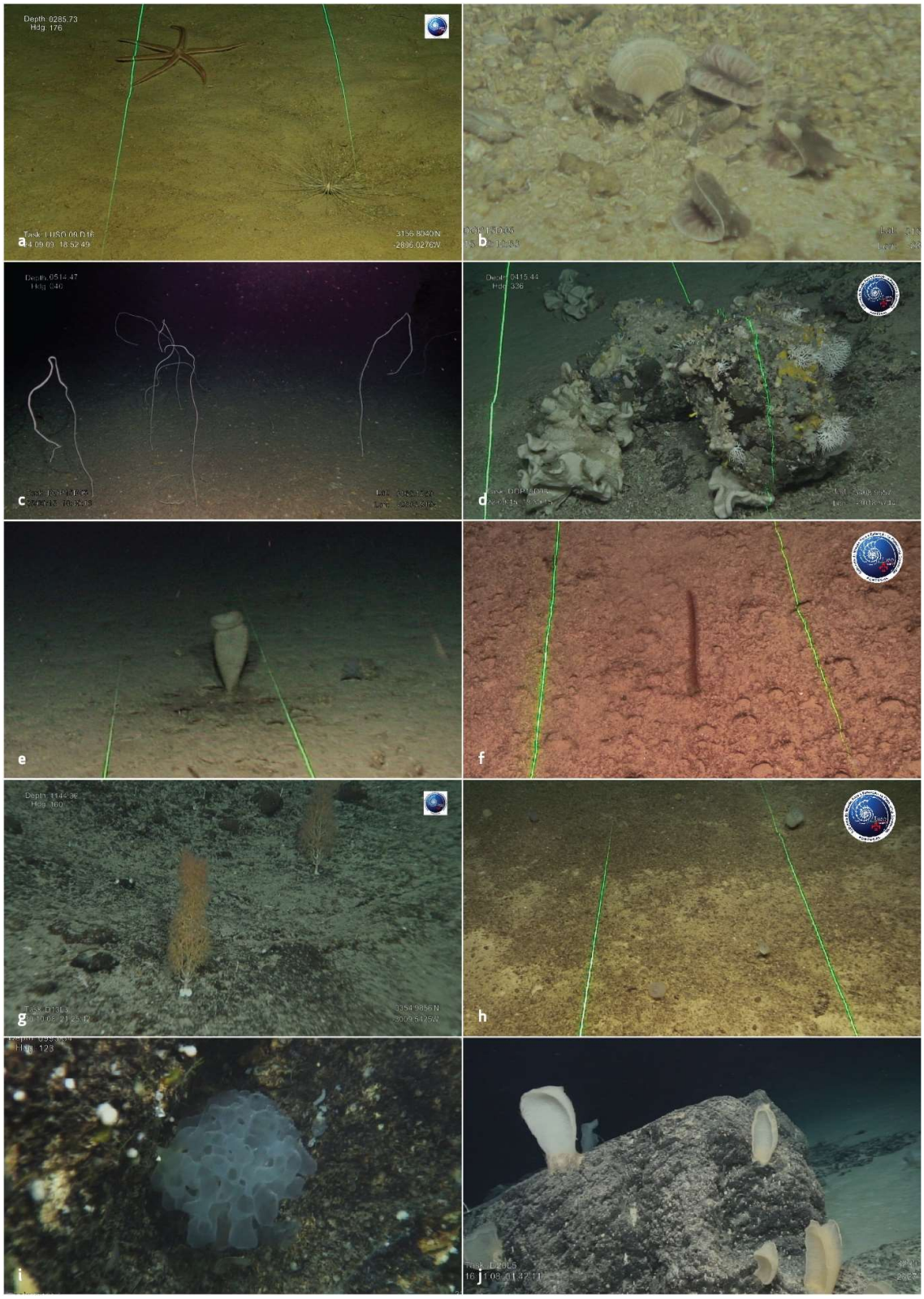

Figure 33. Examples of the most representative habitat-forming species. a) Coelopleurus floridanus and Luidia *cf.* ciliaris. *Assemblage A; b)* Flabellum chunii, *Assemblage B; c)* Viminella flagellum *and d)* Neophrissospongia nolitangere, *Assemblage C ; e) Rossellidae and f)* Parantipathes hirondelle, *Assemblage D; g)* Acanella arbuscula *and h)* Hyalonema *sp. Assemblage E; h)* Farrea occa, *Assemblage F; i)* Poliopogon amadou, *Assemblage G.*

Benthic communities in other seamounts of the Azores EEZ

Last year, some other seamounts have also been prospected by means of visual methods, mostly drop-down camera systems. These surveys have provided new and relevant information on the diversity and species composition of less known and unexplored seamounts, which will help towards better understanding the diversity of benthic habitats of the Azores deep-sea ecosystem.

The benthic communities of Dom João de Castro Seamount

Dom João de Castro is a volcanic seamount located between the islands of Terceira and São Miguel (Figure 18, box 7a). The seamount was formed after a volcanic eruption that occurred in 1720, generating a small island of 150 m height. Erosional processes made the island disappear, and the top of the seamount is currently found below sea surface, at 13 m depth. Cardigos et al. (2005) found several hydrothermal orifices at only 20 m depth, with gas discharging from the vents dominated by CO_2 (90%), with lesser H_2S, H_2 and CH_4. There was no typical hydrothermal vent fauna associated with these vents. The authors also found evidence of further vents in deeper areas of the seamount flanks, between 150 and 400 m. Dom João Castro has historically been an important demersal fishing ground, with target species including the blackspot seabream *Pagellus bogaraveo* and the bluemouth rockfish *Helicolenus dactylopterus*. The area is included in the Natura 2000 Network.

During the MapGES cruise in 2018, five deployments of the drop-cam system were carried out in Dom João de Castro Seamount to evaluate the composition of the benthic communities found between 300 and 500 m depth. In most cases, the benthic communities identified were dominated by the gorgonian *Callorgorgia verticillata*, which formed relatively dense aggregations, with some very large colonies (Figure 34). The whip coral *Viminella flagellum* and the large hydrozoan cf. *Lytocarpia myriophyllum* were also observed as accompanying species, but never seen forming dense patches. These areas may fit the FAO definition of VMEs due to the size, density and fragility of its main structuring species (FAO, 2009). Not many colonies showed signs of fishing impacts, although there was a considerable number of small fishing lines laying over the seabed or entangled around rocks. Further deep, around 500 m depth, rocky outcrops were dominated by the white octocoral *Pleurocorallium johnsoni,* accompanied by the soft coral *Anthomastus* sp. The most commonly identified fish species in Dom João de Castro were the bluemouth rockfish *Helicolenus dactylopterus*, the offshore rockfish *Pontinus kuhlii,* the Atlantic wreckfish *Polyprion americanus* and the European conger *Conger conger*.

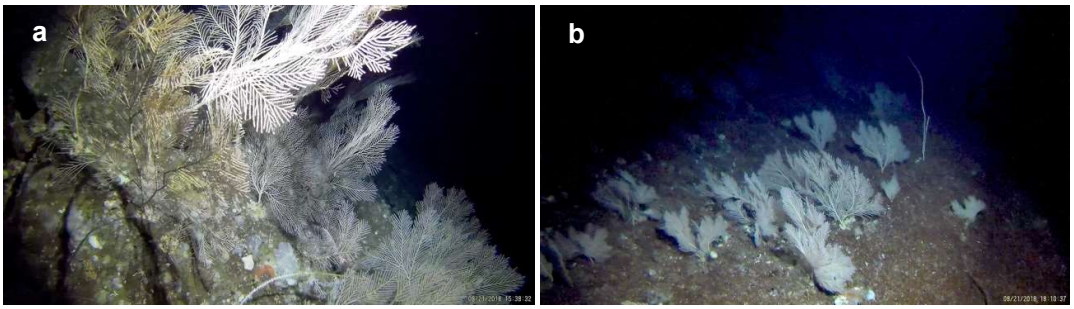

Figure 34. Images of the dense aggregations of Callogorgia verticillata *found in Dom João de Castro Seamount.*

The benthic communities of Alcatraz Seamount

Alcatraz is a relatively deep seamount located only 18 nm east of Dom João de Castro, with the shallowest point of its elongated summit at 360 m depth (Figure 18, box 7a). There was no previous information about the composition of its benthic communities besides some by-catch data obtained from the fishing fleet. During the 2018 MapGES cruise, four drop-down deployments were carried out on the northern side of the seamount, exploring depths between 400 and 600 m depth.

Several large sponge species were observed on the rocky outcrops, in which to include the litisthids *Leiodermatium pfeifferae*, *Leiodermatium lynceus,* cf. *Neophrissospongia nolitangere* and cf. *Petrosia*, as well as the giant sponge cf. *Characella pachastrelloides* (Figure 35a). Sparse colonies of the whip coral *Viminella flagellum* were observed among the sponges, some of them reaching very large sizes. Monospecific patches of this whip coral were also spotted on the shallowest part of the seamount (Figure 35b). It is relevant to point out the high number of fishing lines that were observed in all deployments, some of which seemed to be abandoned in recent times.

Figure 35. Images of the benthic communities observed in Alcatraz Seamount, (a) including a wide variety of giant sponges and (b) aggregations of the whip coral Viminella flagellum.

The benthic communities of Mar da Prata

Mar da Prata is an elongated ridge located between the islands of São Miguel and Santa Maria (Figure 18, box 7b). It is one of the largest seamount areas in the Azores, connected in its northern side to the island of São Miguel, and has steep slopes on all other sides. Its summit reaches depths of 200 m, with three main peaks located along the seamount. It has historically been an important fishing target for the fishermen based on the islands of São Miguel and Santa Maria due to its proximity, although its relevance has declined in recent years due to stock reductions.

During the 2018 MapGES cruise, three deployments of the drop-cam system were fulfilled on the southern tip of Mar da Prata Seamount, between 200 and 300 m depth. Whilst most of the large rocky outcrops observed were characterized by lithistid sponges and gorgonian corals of the species *Viminella flagellum* (Figure 36a), a very dense patch of the yellow gorgonian *Dentomuricea* cf. *meteor* was found (Figure 36b). This area may fit the FAO definition of a VME.

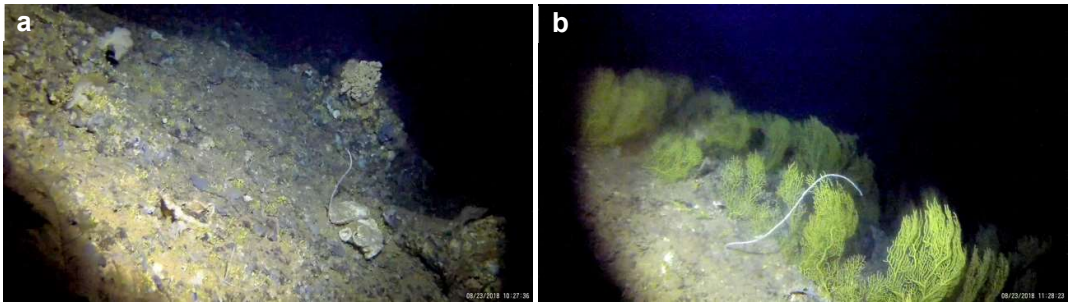

Figure 36. (a) Area dominated by lithistid sponges on hard substrates. (b) Dense aggregation of the octocoral Dentomuricea *aff.* meteor *in the southernmost sector of Mar da Prata Seamount.*

The benthic communities of South Terceira and São Jorge de Fora

The southern slope of Terceira Island, as well as the elongated seamount São Jorge de Fora, located 20 km south of Terceira, were explored during the 2018 Nico Expedition on board of the R/V Pelagia (Figure 18, box 7c). Two tow-cam video transects were carried out on the southern slopes of Terceira, exploring almost 2 km of seabed between 830 and 500 m depth. The deepest sections of those dives were characterized by soft substrates (mostly muds and fine sands) with some small scattered boulders. These areas seem to hold very low species diversity, with few megafauna species of large sizes observed. The soft substrates were mainly colonized by the foraminifera cf. *Syringammina fragilissima* and the boulders had only some sponges attached to them, such as the hydrarian cf. *Leiodermatium pfeifferae*. Moving upwards, the rocky outcrops started to be colonized by the yellow solitary coral *Leptopsammia formosa*, which reached relatively high densities, together with other

coral species such as the soft coral *Anthomastus* cf. *agaricus*, the octocoral *Corallium johnsoni* and small sponge species, always in very low numbers. The shallowest areas explored held two distinct benthic communities, one dominated by the whip coral *Viminella flagellum*, which became the most abundant coral species (Figure 37a), and the presence of some large gorgonians of the species *Paragorgia johnsoni* (Figure 37b), some of which showed signs of being affected by the fishing activity.

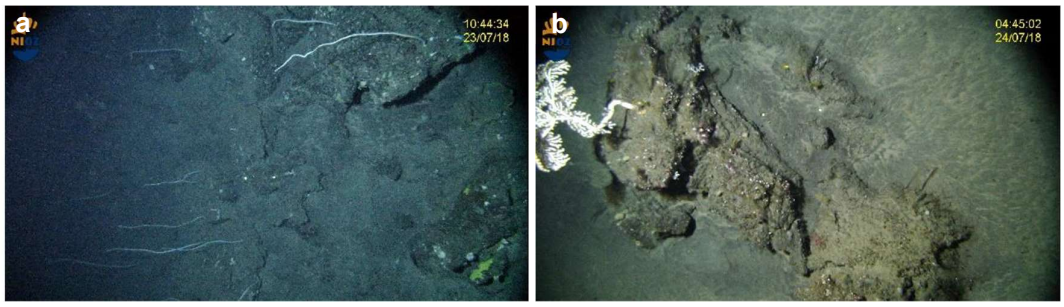

Figure 37. Images of the benthic habitats found on the southern slope of Terceira Island. (a) Area dominated by the whip coral Viminella flagellum*, at 500 m depth. (b) Large* Paragorgia johnsoni *on a rocky outcrop, accompanied by the soft-coral* Anthomastus *cf.* agaricus *at 600 m depth*.

São Jorge de Fora Seamount was explored by performing one long dive of almost 6 km, which crossed the whole seamount from one side to the other. The dive started at depths of 1300 m, it reached the summit at 500 m and ended at 1000 m on the other side of the seamount, providing a very nice cross section of its benthic habitats. A very clear zonation pattern could be observed regarding the composition of the benthic communities, with very well-defined species compositions along the depth gradient. The deepest areas were characterised by the presence of muds and fine sands, with the foraminifera cf. *Syringammina fragilissima*. Not many megafauna species could be identified besides some sea urchins (cf. *Cidaris cidaris*) and sparse *Acanella arbuscula* corals, together with some large crustaceans of the species *Aristaeopsis edwardsiana*. Aggregations of the gorgonians *Narella bellissima* and *N. verluysi* could be observed on both sides of the seamount (Figure 38a), accompanied by the sea urchins *Cidaris cidaris* and *Echinus melo*, the yellow solitary coral *Leptopsammia formosa* and the large sponge *Pheronema carpenteri*. At around 600 m depth, an aggregation of large gorgonians of *Callogorgia verticillata* was observed (Figure 38b), with relatively high densities in some areas and a distribution that lasted several tens of meters. On the summit, at around 50 m depth, the hard substrates were colonized by gorgonians of the species *Viminella flagellum*, accompanied by other corals such as the black coral *Paranthipathes larix*, the soft coral *Anthomastus* cf. *agaricus* and the gorgonian *Acanthogorgia* sp., the white sea urchin *Echinus melo* and many encrusting sponges.

Figure 38. Images of São Jorge de Fora Seamount. (a) Aggregation of the primnoid Narella verluysi *on hard susbtrates. (b) Aggergation of the large coral* Callogorgia verticillate *at around 600 m depth on the southern flank of the seamount.*

The benthic communities of Cavalo Seamount

Cavalo Seamount is found very close to the Mid-Atlantic Ridge, on the European plate (Figure 18, box 7d). From all the seamounts explored, Cavalo is the furthest away from the islands within the EEZ of the Azores, more than 300 km away from Faial Island. One tow-cam transect of 2 km in length was carried out in Cavalo during the 2018 Nico Expedition, at depths of 600-675 m. Most of the dive was performed on hard substrates dominated by the gorgonians *Narella bellissima* and *Narella versluysi*, both found in rather high densities (Figure 39a). Those two species were accompanied by a wide range of other large gorgonian species, such as *Paragorgia johnsoni*, *Corallium* cf. *johnsoni* and *Callogorgia verticillata*, together with a few massive and laminate sponges. The soft coral *Anthomastus* cf. *agaricus* and the sea urchins *Cidaris cidaris* and *Echinus* sp. were also commonly observed. This species association lasted a few hundred meters, and may fit the FAO definition of VME. In the shallowest part of the summit, the community changed and was dominated by the yellow gorgonian *Acanthogorgia* sp. and very large colonies of the gorgonian species *Callogorgia verticilata*, with some small *Paragorgia* spp. also found as accompanying species.

Figure 39. Images recorded on Cavalo Seamount. (a) Very dense aggregation of the primnoid corals Narella verluysi *and* Narella bellissima*, accompanied by a wide variety of other coral and sponge species. (b) Large specimen of the coral* Paragorgia johnsoni*.*

1.2.6 Case Study 9: Reykjanes Ridge: Comparing vent system to non-vent system communities

Authors: Hrönn Egilsdóttir, Stefán Áki Ragnarsson

Study area and environmental settings The Reykjanes Ridge is a section of the Mid-Atlantic Ridge and is strongly shaped by volcanic processes (Figure 40). The seafloor around the middle of the ridge is comprised mostly of highly rugose seafloor with hard substrates but with softer sediments accumulating where there are depressions (Pałgan et al., 2017). Soft sediments prevail off the ridge flanks to the southwest and northeast, i.e., the Irminger- and Iceland Basins, respectively.

South and southwest of Iceland, Atlantic water dominates in the upper 800 m layer which ranges in temperature from 6 to 11°C, depending on the depth and season. The salinity is typically between 35.0 and 35.2 ‰. Below 1000 m depth the seafloor is exposed to 2-4°C overflow water that flows southwards across the Greenland-Iceland-Faroe Ridge and along the Icelandic Slope and Reykjanes Ridge.

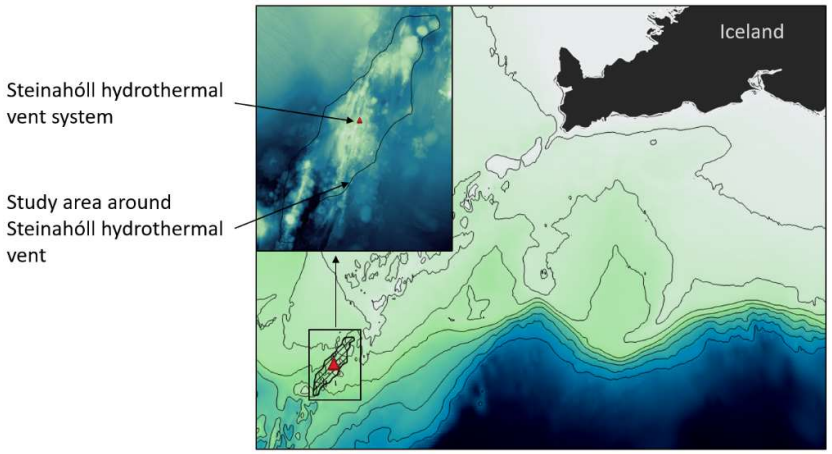

Figure 40. The Reykjanes Ridge and the location of the Steinahóll hydrothermal vent site.

Description of benthic communities A region on the Reykjanes Ridge that is of special interest is a hydrothermal vent site, Steinahóll (Figure 40). It is located at 200-300 meters, at the boundary between what is defined as shallow and deep hydrothermal vent systems (Tarasov et al., 2005). The Steinahóll hydrothermal vent site may harbour biological resources suitable for bioprospecting (Omarsdottir et al., 2013) and it is thus important to advance knowledge of benthic communities to inform marine spatial planning in the region.

Underwater video footages and photographs (ROV and Campod) have been obtained to describe the fauna and habitats on the Reykjanes Ridge in four surveys (2004, 2010, 2012 and 2018). Most of the data collection has been confined within the shallower northern part of the ridge, including the Steinahóll area.

At the vent site, white bacterial mats cover many hard and some soft substrates, but the species richness and abundance of the megabenthic fauna at the actual vent sites were very low (Figure 41).

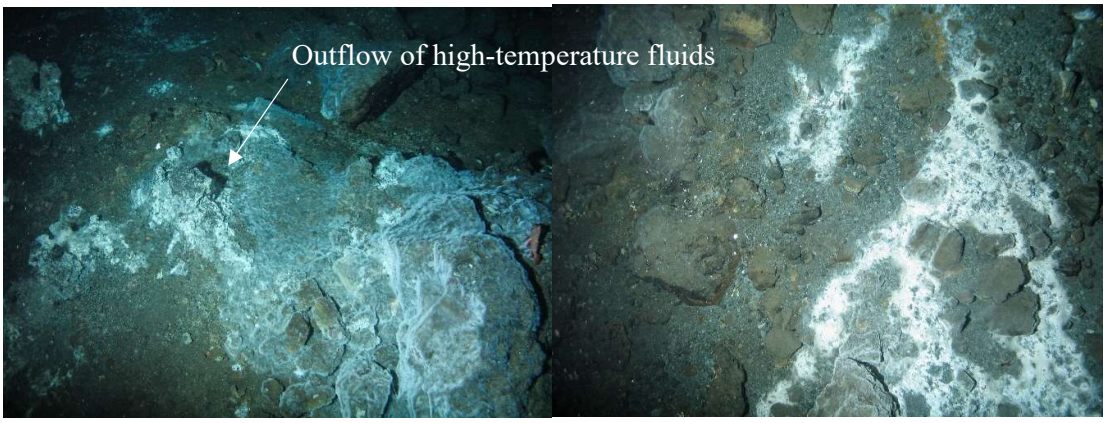

Figure 41. Outflow of high-temperature fluids and bacterial mats at the Steinahóll hydrothermal vent field.

Moving further away from the hydrothermal vent sites, there is a notable increase in benthic biodiversity. This includes reef-forming CWC species, *Lophelia pertusa and Madrepora oculata* (Figure 42a,b) and a wide range of sponge species such as *Mycale lingua*, *Asconema foliatum* and various other sponge species (Figure 42c,d). The presence of dead frameworks of *L. pertusa* (sometimes covered partly by lava) and coral rubble suggest that their cover may have been greater in the past, and some may have been killed by the onset of volcanic activity. Other coral species observed on the ridge were, for example, the octocorals *Paragorgia arborea*, *Primnoa resedaeformis* and species belonging to the families Anthothelidae and Nephtheidae. A comparison between soft and hard substrates near the vent system showed marked differences in the biodiversity of megabenthic communities, with hard substrates acting as a habitat harbouring more diverse communities, such as diverse sponge communities (Figure 42c,d).

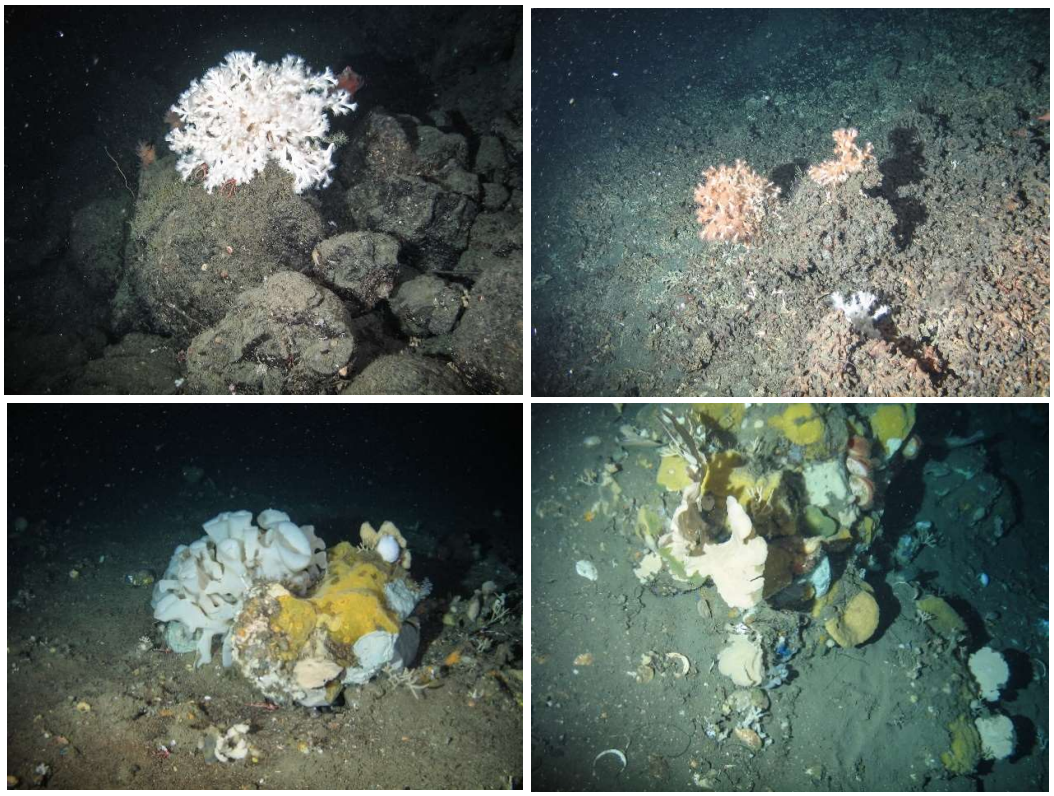

Figure 42. Examples of benthic communities in the vicinity of the Steinahóll hydrothermal vent field. (a) Lophelia pertusa *colonizing basaltic outcrops; (b) rubble and scattered colonies of live* L. pertusa *and (c, d) diverse sponge communities on hard substrates.*

Fishing gear remains, mostly longlines, were commonly observed on and around the Steinahóll vent site. Steinahóll hydrothermal vent system and surrounding benthic communities fit the fit the FAO of the United Nations criteria for defining what constitutes a VME (FAO, 2009) sensitive to disturbances, such as fishing and may need conservation management measures.

1.2.7 Case Study 10: Davis Strait, Eastern Arctic

Authors: Ellen Kenchington, Igor Yashayaev, F. Javier Murillo, Cam Lirette

Study area and environmental setting The Davis Strait joins two oceanic basins, Baffin Bay and the Labrador Sea, and separates southwestern Greenland and south-eastern Baffin Island, the latter constituting the largest island in the Canadian Arctic Archipelago. It connects to the Arctic Ocean in the north via Baffin Bay and to the Atlantic Ocean in the south via the Labrador Sea. It is considered the world's largest strait and is renowned for exceptionally strong tides, which range from 9 to 18 m, and a complex hydrography. The slopes at the Labrador Sea flank of the ridge drop to 2500 m or more (Figure 43).

The Labrador Sea is the key basin of the Atlantic Ocean with respect to receiving and mixing the Arctic and Atlantic waters, Greenland freshwater flux and continental runoff (Yashayaev et al., 2015), and recurrent production gas and freshwater enriched cold and dense intermediate water masses ventilating the deep and abyssal layers of the North Atlantic (Yashayaev & Loder, 2016; 2017; Rhein et al., 2017) and meridional overturning circulation (Thornalley et al., 2018). These processes administer climate and ecosystem of the subpolar region, shaping and maintaining its deep-sea communities from top (Fragoso et al., 2016a; 2016b; 2018) to bottom (Kenchington et al., 2017). In particular, we observe a massive spring bloom in the northern Labrador Sea south of Davis Strait which the strongest manifestation of primary productivity in the North Atlantic. At the same geographical location, we report high abundance of benthic fauna presenting species unique to the area and the western subpolar North Atlantic as a whole (see below). The oceanographic conditions (physical properties, chemical tracers and composition of lower tropic levels) in Labrador Sea are regularly monitored through an ATLAS partner – the Atlantic Zone Off-Shelf Monitoring Program (AZOMP) - visiting the area on its multidisciplinary missions every spring. The monitored processes and features of key relevance to the ATLAS objective include deep convection, distribution and mixing of Arctic and Greenland fresh water, carbon sequestration and primary production, zooplankton communities, boundary processes and fluxes, circulation and inflow of Atlantic Waters (warmer than 4°C), so vital for the unique coral and sponge colonies recently discovered and documented at various locations along the sea margin, and even wildlife (birds and sea mammals).

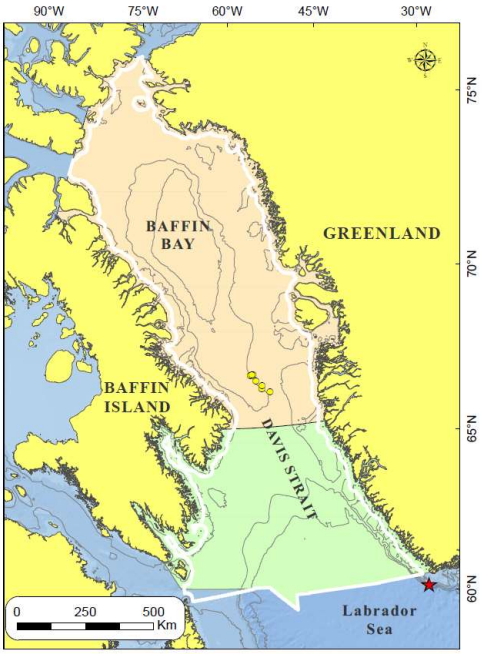

Figure 43. Location of the Davis Strait/Baffin Bay case study area showing place names, the spatial extent used for species distribution modeling (white outline), the marine spatial planning areas (green and tan), the location of the Circumpolar Biodiversity Monitoring Program monitoring sites established for the Council of Arctic Flora and Fauna (CAFF) (yellow circles), and the location of the Lophelia pertusa *reef discovery (red star). Depth contours at 200m, 1000m and 2000m are shown.*

Description of benthic communities The first reported *Lophelia pertusa* reef from Greenlandic waters was found at 886-932 m depth on a steep continental slope off southwest Greenland (Kenchington et al., 2017, Figure 44). Analyses of hydrographic data showed that the reef was located in a layer of Atlantic Water of stable temperature (3.5-4.5°C) and salinity (34.88-34.94) with water density slightly higher (27.63 – 27.75 kg m^{-3}) than reported for the northeast Atlantic, and exceptionally high currents of >15 cm s^{-1} at 1000 m. The intermediate salinity maximum, in the near-bottom water mass characteristics, was found in the depth range where the corals were found. We discovered signals of consistent vertical and horizontal transport at 700 - 900 m over the reef area. Although this area is not directly influenced by intermediate and deep convection in the Labrador Sea, the seasonal evolution of near-bottom temperature, salinity and density for the 700-900 m depth range revealed strong seasonal patterns with both temperature and salinity reducing to their annual minimal values at the end of March and staying low for one month with an indication of a second minimum in June, 3 months later. The occurrence and temporal extent of these minima likely arises through a combination of local convection from the surface and advection of cooled and freshened waters at depth from the Irminger Sea.

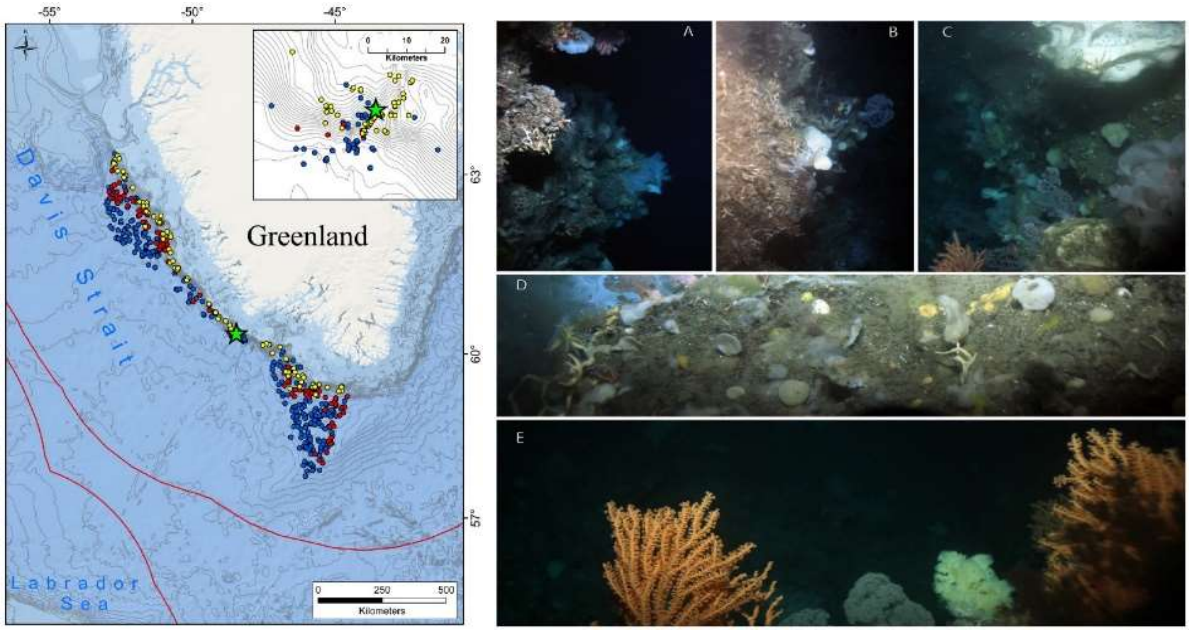

Figure 44. Map showing the position of CTD profiles (colored dots) used to summarize temperature, salinity and density in the vicinity of the Lophelia pertusa reef (green star) off southwest Greenland. In situ photographs of the L. pertusa reef and other associated octocoral fauna and sponges from the vicinity of the reef: A, B Living L. pertusa on the steep slope with underlying bioherm; C, D non-reef habitat on the same transect line that is dominated by sponges; E Primnoa resedaeformis and smaller soft corals (Nephtheidae) (from Kenchington et al., 2017).

Baker et al. (2018a) provide baseline documentation of the epibenthic megafauna in the Disko Fan Conservation Area in Canadian waters in Davis Strait. Photo transects were established as long-term biodiversity monitoring sites to monitor the impact of human activity, including climate change, on the region's benthic marine biota in accordance with the protocols of the Circumpolar Biodiversity Monitoring Program established by the Council of Arctic Flora and Fauna (CAFF). A total of 480 taxa were found, 280 of which were identified as belonging to one of the following phyla: Annelida, Arthropoda, Brachiopoda, Bryozoa, Chordata, Cnidaria, Echinodermata, Mollusca, Nemertea, and Porifera. Following the same CAFF protocols, macrofauna from grab samples sieved at 0.5 mm and 1 mm have been identified and 90 foraminiferal taxa were identified in meiofaunal samples.

In the northwest Atlantic, along the continental slopes, sponges can make up the majority of the benthic biomass, and in the eastern Canadian Arctic, sponges and sponge grounds occur in both Davis Strait and Baffin Bay (Murillo et al., 2018; Figure 45). Sponge communities include arctic and boreal astrophorid grounds and at least 112 species have been identified from the region (Brøndsted, 1933). Murillo et al. (2018) have identified 93 sponges from trawl catches and produced predictive maps of sponge community distributions in this region. Kenchington et al. (2016) have identified significant concentrations of VME indicators (sponges, large and small gorgonian corals and sea pens) in the

Canadian portion of the study area and Beazley et al. (2016) have produced predictive species distributions for the same taxa using Random Forest models.

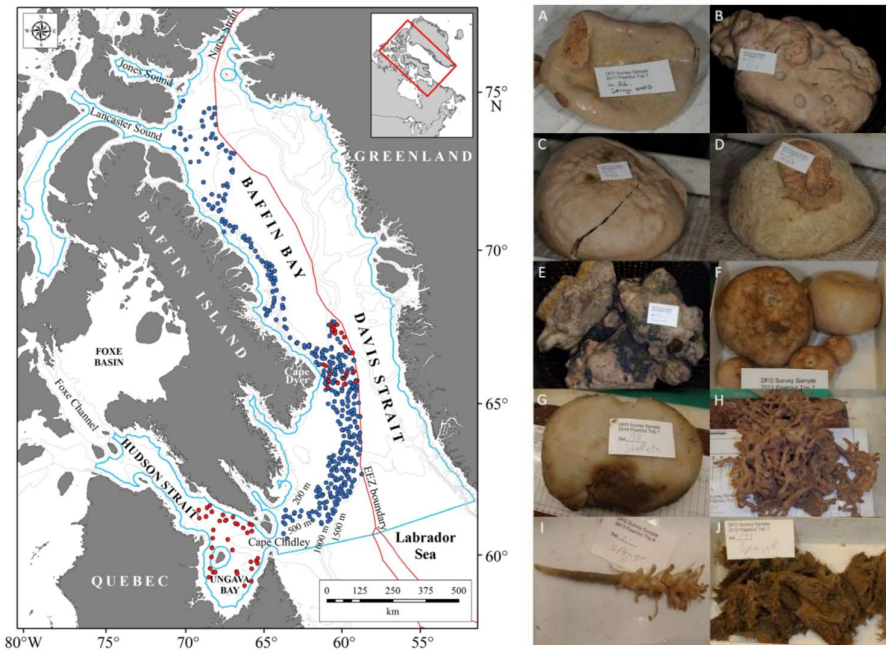

Figure 45. Study area in the eastern Arctic showing the position of the 456 depth-stratified random trawl locations used to sample the sponges are indicated by the blue (Alfredo gear) and red (Cosmos gear) circles (from Murillo et al., 2018). Selected indicator species of eastern Canadian Arctic sponge assemblages (from Murillo et al., 2018). A) Geodia atlantica*; B)* G. barretti*; C)* G. macandrewii*; D)* Stelletta normani; *E)* Stryphnus fortis*; F)* G. hentscheli*, G)* Stelletta raphidiophora*; H)* Bathydorus *sp. nov; I)* Chondrocladia (Chondrocladia) grandis*; J)* Lissodendoryx (Lissodendoryx) complicata. *(A) to (E) are indicator species of the boreal sponge grounds dominated by astrophorids in the North Atlantic; (F) and (G) are indicator species of the Arctic sponge grounds; and (H) to (J) indicators of the Arctic slope sponge communities.*

The establishment of the benthic monitoring sites (Baker et al., 2018a) in the Disko Fan Conservation Area (https://www.dfo-mpo.gc.ca/oceans/oeabcm-amcepz/refuges/diskofan-eng.html) was done in response to the call for standardized monitoring of marine benthic communities in the Arctic by the Conservation of Arctic Flora and Fauna (CAFF), the biodiversity working group of the Arctic Council. Similarly, the identification of the trawl-caught sponge species in this region (Murillo et al., 2018) will be used to monitor trends in sponge biodiversity. These publications will be considered in the next State of the Arctic Marine Biodiversity Report (SAMBR) which synthesises the state of knowledge about biodiversity in Arctic marine ecosystems, including trends in biodiversity across six focal ecosystem components (FECs): marine mammals, seabirds, marine fishes, benthos, plankton, and sea ice biota. The indicator species identified by Murillo et al. (2018) will be used for future monitoring of this area.

Within the Canadian portion of the Case Study Area, the identification of coral, sponge and sea pens from the trawl surveys (Kenchington et al., 2016) was used to establish 3 marine refuges in the Eastern Canadian Arctic (Nunavut) bioregion. The Disko Fan Conservation Area is 7,485 km^2 and was

delineated on the basis of narwhal distribution and the identification of significant concentrations of large gorgonian corals, including large tracts of globally unique, high-density bamboo corals (https://www.dfo-mpo.gc.ca/oceans/oeabcm-amcepz/refuges/diskofan-eng.html). This area was also identified as a Canadian Ecologically and Biologically Significant Area in 2011 based on oceanographic characteristics, its function as an overwintering habitat for narwhal, and the presence of several species ofCWC. The Davis Strait Conservation Area (https://www.dfo-mpo.gc.ca/oceans/oeabcm-amcepz/refuges/davisstrait-detroitdavis-eng.html) protects 17,298 km^2 and was established to protect significant concentrations of small gorgonian corals, large gorgonian corals, sea pens and sponges based on the identification and analyses of these taxa from trawl catches. Lastly, our analyses were used to identify an area that crossed two biogregions: the Eastern Arctic and Newfoundland-Labrador Shelves Bioregions (Nunavut and Newfoundland and Labrador). The Hatton Basin Conservation Area (https://www.dfo-mpo.gc.ca/oceans/oeabcm-amcepz/refuges/hattonbasin-bassinhatton-eng.html) is a large area protecting 42,459 km^2 established to protect CWCs and sponges. The scientific advice that went into these designations is summarized by DFO (2017). All 3 areas contribute to Canada's approach to identifying other effective area-based conservation measures in support of the achievement of Canada's marine conservation targets under the CBD.

1.2.8 Case study 11: Trait-based approach on deep-sea corals in the high-seas of the Flemish Cap and Flemish Pass (northwest Atlantic)

Authors: Ana García-Alegre, F. Javier Murillo, Mar Sacau, Ellen Kenchington, Alberto Serrano, Pablo Durán Muñoz

Study area and environmental setting The Flemish Cap and Pass are located in the NW Atlantic, in an Area Beyond National Jurisdiction (ABNJ), within the Northwest Atlantic Fisheries Organization (NAFO) Regulatory Area (Figure 46). The study area includes the Flemish Cap -an isolated plateau of approximately 200 km, located about 600 km to the east of Newfoundland, the Flemish Pass, a channel of ~1,200 m deep which separates Flemish Cap and the Grand Banks of Newfoundland, and the NE part of the Grand Bank of Newfoundland.

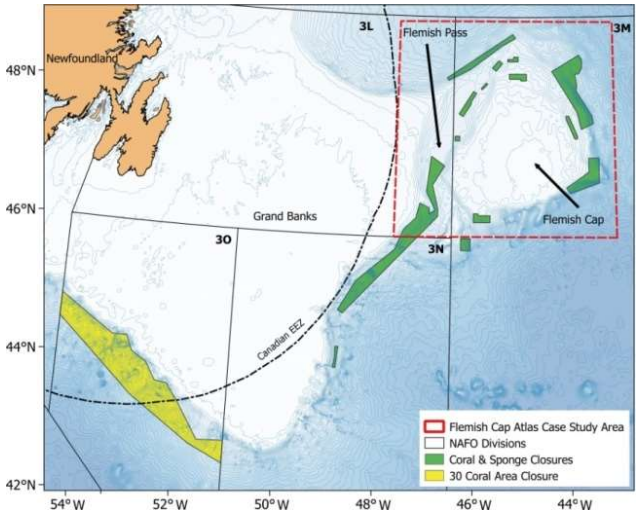

Figure 46. Location of the Flemish Cap Case Study area showing the NAFO divisions and closures

This area is within a transition zone between cold subpolar waters, influenced by fluctuations in the Labrador Current and in the North Atlantic Current (Gil et al., 2004). The Grand Banks Shelf is separated from the Flemish Cap by the cold southward flow of the Labrador Current (Colbourne & Footek, 2000). Different types of valuable habitats and ecosystems, such as deep-water corals and deep-sea sponge grounds were described (see Murillo et al., 2011; 2012) and therefore some areas have been closed to bottom fisheries by NAFO (Figure 46). We focus our study on deep-sea coral aggregations which represent important ecosystems in this area with the objective to perform a revision on deep-sea coral traits in this area. This ongoing work (García-Alegre et al., 2018) analyzes which biological traits are useful to classify corals in the study area, prioritizing traits where information is available and that capture variation for a range of biological or ecological processes.

Description of benthic communities Fourty taxa of corals were identified in the area from bottom trawl research vessel surveys (2007-2017) and rock dredges (2009-2010). They included 22 Alcyonacea, 11 Pennatulacea, 3 Antipatharia and 4 Scleractinia (Figure 47). Taxa were grouped in 32 taxa-traits (Table 1) although eight taxa-traits were not included in the final analysis due to different reasons.

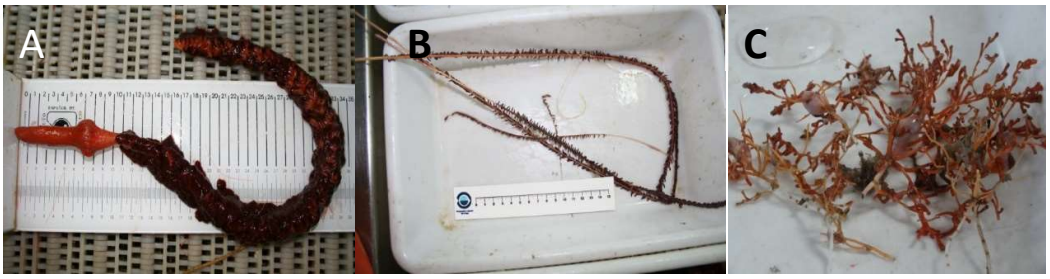

Figure 47. Main cold-water coral species of the study: (a) Anthoptilum grandriflorum*; (b)* Funiculina quarangularis*; (c)* Acanella arbuscula*. Photo credits IEO-Vigo.*

Table 1. Corals identified in the study area and grouped for the traits analysis in taxa traits. Taxa in blue was excluded because it was found just in two trawls where the identification is not yet confirmed and taxa in red were excluded because there were only found in rock dredge samples.

TAXA-TRAITS	ORDER
Acanella arbuscula *Acanthogorgia armata* *Anthomastus spp.* *Anthothela grandiflora* *Clavulariidae* *Nephtheidae (Drifa/Duva)* *Gersemia sp.* *Heteropolypus sol* *Keratoisis spp.* *Paragorgia spp. (arborea/johnsoni)* *Paramuricea spp.* *Parastenella atlantica* *Placogorgia sp.* *Primnoa resedaeformis* *Radicipes gracilis* *Swiftia sp.* *Telestula septentrionalis*	**Alcyonacea**
Anthoptilum grandiflorum *Distichoptilum gracile* *Funiculina quadrangularis* *Halipteris spp. (finmarchica/christii)* *Kophobelemnon stelliferum* *Pennatula spp. (aculeata/grandis)* *Protoptilum carpenteri* *Umbellula lindahli* *Virgularia mirabilis*	**Pennatulacea**
Leiopathes sp. *Stauropathes arctica* *Stichopathes sp.*	**Antipatharia**
Desmophyllum dianthus *Flabellum alabastrum* *Caryophyllidae (Caryophyllia/Vaughanella)*	**Scleractinea**

Twenty-one biological traits were identified as suitable to define deep-sea corals in the Flemish Cap and Flemish Pass prioritizing traits where information is available and that capture variation for a range of biological or ecological processes. Three of the aforementioned traits (longevity, living habitat, living location) were not used in the analysis as they were invariant with current knowledge in all taxa studied, but that information is suitable for other studies that take into account a wider range of taxa or community traits (Table 2).

Table 2. Traits identified as suitable to define deep-sea corals in the study area. Traits in red were not used in the analysis.

CATEGORY	TRAIT
Distribution and Habitat	Living habitat
	Living location
	Exposure potential (related to body form)
	Attachment degree
	Attachment strenght
	Movement type
	Mobility
	Preferred substrate
General Biology	Maximum size
	Body design
	Degree of flexibility
	Resource capture method
	Food type
	Defence mechanisms
	Intra-specific sociability
	Fragility
	Growth form
	Body hardness
Reproduction/Life Cycle	Longevity (years)
	Reproductive method
	Reproductive type/Sexual system

Categories for each trait were defined and scored by each taxon based on literature review and personal observation. Then a fuzzy coded matrix was constructed based on the information gathered for each taxon. Each trait was broken down in different categories or modalities which included all the attributes for each taxa and classified for each affinity to each category. Fuzzy coding allows including the different degree that taxa reveal of the different categories of a variable (Chevenet et al., 1994). It also allows recording for a taxon that exhibits affinity for more than one category of each trait variable (Bremmer et al., 2003). In this study we used a scale of 0-3 where 0 is no affinity to a category and 3 is high affinity, and where no information for a trait was available a score of zero was applied (other studies used this scale: Bremmer et al., 2003; Kenchington et al., 2007)

In conclusion, 19 traits were found appropriate to classify deep-sea corals in the study area and 24 taxa were selected as suitable for Fuzzy Correspondence Analysis (FCA). This work contributes to defining biological traits for deep-sea corals which best describe the VMEs in the Flemish Cap and Flemish Pass, as a first step to improve the understanding of CWC ecosystems and study the possibility to apply species distribution modeling techniques on taxa classified by the trait analysis (in case their EVs response were similar). Moreover, the study was presented to the NAFO and will contribute to the advice on the assessment of significant adverse impacts in the NAFO Regulatory Area.

1.2.9 Case Study 12: Recent deep-sea discoveries off the eastern US

Authors: Steve W. Ross

Study area and environmental setting The Case Study 12 area includes three sub-areas that have been particularly well studied. From south to north the sub-areas are the deep-sea coral banks off Cape Lookout, North Carolina (NC) (Ross & Nizinski, 2007), the Hatteras Middle Slope (HMS, Ross et al., 2001), and two Mid-Atlantic Canyons (Norfolk and Baltimore) and surroundings (CSA et al., 2017) (Figure 48). They straddle or are adjacent to the well-known biogeographic boundary around Cape Hatteras, which separates warm temperate from cool temperate regions (Briggs, 1974). Their benthic communities are generally different from each other, even though this area spans only about 500 km of latitude. All three sub-areas exhibit complex habitats and soft substrata, and all are variously influenced by the Gulf Stream.

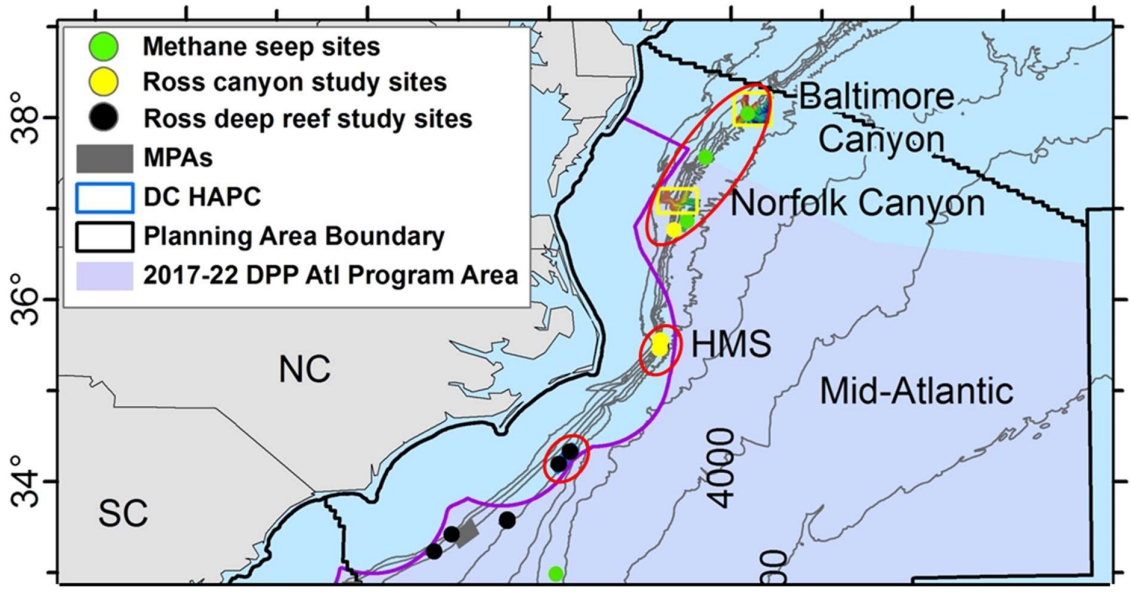

Figure 48. Three sub-areas circled in red comprise the ATLAS Case Study 12 area in the western North Atlantic Ocean. The southernmost are the Cape Lookout Lophelia pertusa *bioherms, HMS represents the Hatteras Middle Slope and Norfolk and Baltimore Canyons and surroundings are the northernmost area.*

The slope off Cape Lookout is subject to wide swings in water properties, especially currents and temperature, mediated by meanders of the Gulf Stream (Bane & Brooks, 1979). Bottom slope is fairly gradual with carbonate sediments punctuated by a few areas of large *Lophelia pertusa* coral bioherms. Biologically and physically, the most unusual and unique area is the HMS. The oceanography of this small area is so complex and different from other areas that it seems very likely to have mediated observed ecological differences. Here, the Gulf Stream turns northeastward and is met on its inshore side by the upper water column, south-flowing Virginia Current and on its offshore side by the deep, south-flowing Western Boundary Undercurrent. These (and other) current interactions result in an

area below 200 m depth of high turbidity exhibiting little or no net motion (see reviews in Diaz et al., 1994; Sulak & Ross, 1996; Bauer et al., 2002 and references therein). The HMS slope exhibits some of the highest carbon deposition rates of any area of the US Atlantic (Thomas et al., 2002). The bottom topography here is rugged, comprised of a series of small steep sided mini-canyons made of consolidated mud. The Middle Atlantic Slope is characterized by numerous submarine canyons, and two of the best studied are Baltimore and Norfolk Canyons (Figure 48, Obelcz et al., 2014). Although these two canyons are influenced by similar, large scale hydrographic conditions, mostly driven by the shelf-slope front, these large canyons influence local oceanography as well as organic deposition patterns. Differences in canyon size, shape and orientation can cause differences in oceanographic influences (CSA et al., 2017), and year-long near-bottom measurements revealed differences between the two canyons (e.g., greater bottom current speeds in Norfolk Canyon) (CSA et al., 2017). Western North Atlantic Central Water (WNACW) and Western Atlantic Sub-Arctic Intermediate Water (WASIW) were observed below the shelf-slope front. Both canyons exhibit persistent, mid-water nepheloid layers.

Description of benthic communities

New deep-sea coral habitats were discovered within the region, which occur as large bioherms as well as smaller colonies associated with submarine canyons. Deep-sea coral biodiversity is high, but species zoogeography differs north and south of Cape Hatteras, NC. Seventy-eight species of corals were recently listed off the northeastern US (NEUS, north of Cape Hatteras, Packer et al., 2017), while 201 species were documented off the southeastern US (SEUS, south of Cape Hatteras, Hourigan et al., 2017). Ecosystems are dominated by *L. pertusa* and other scleractinians (e.g., *Enallopsammia* spp. and *Madrepora oculata*) south of Cape Hatteras, while octocorals, particularly *Paragorgia arborea*, in some instances associated with P*rimnoa resedaeformis* and *Anthothela grandiflora* dominate north of Cape Hatteras (Figure 49). For details, see Ross & Nizinski (2007), Brooke & Ross (2014), Brooke et al. (2017), Hourigan et al. (2017), Packer et al. (2017). Reasons for the different benthic coral communities in the northeastern versus southeastern Atlantic are not fully understood, but the relative rarity of *L. pertusa* in the northeastern Atlantic may be due to a combination of infrequent larval delivery, specific habitat requirements (i.e., steep, rocky, current-swept walls with clefts or overhangs) and loss of older colonies (Brooke et al., 2014; 2017).

Many invertebrates collected around SEUS deep coral banks and NEUS Canyons are new to the area (Ross & Nizinski, 2007; CSA et al., 2017). New species have been discovered, such as a file shell (*Acesta cryptadelphe*, Gagnon et al., 2015) and starfishes (Mah et al., 2010), and several others are still being described. In addition, about 20% of the galatheoid type squat lobsters collected in this region, most

around deep coral and canyon habitats, may be new species or are otherwise poorly documented (see Coykendall et al., 2017 and CSA et al., 2017). Past studies have also demonstrated that about 57% of the hydroid fauna identified so far are new records to the SEUS either latitudinally and/or bathymetrically (Henry et al., 2008). These studies in a whole demonstrate the high diversity not only of the bioengineering coral species, but also the invertebrate fauna associated with these habitats.

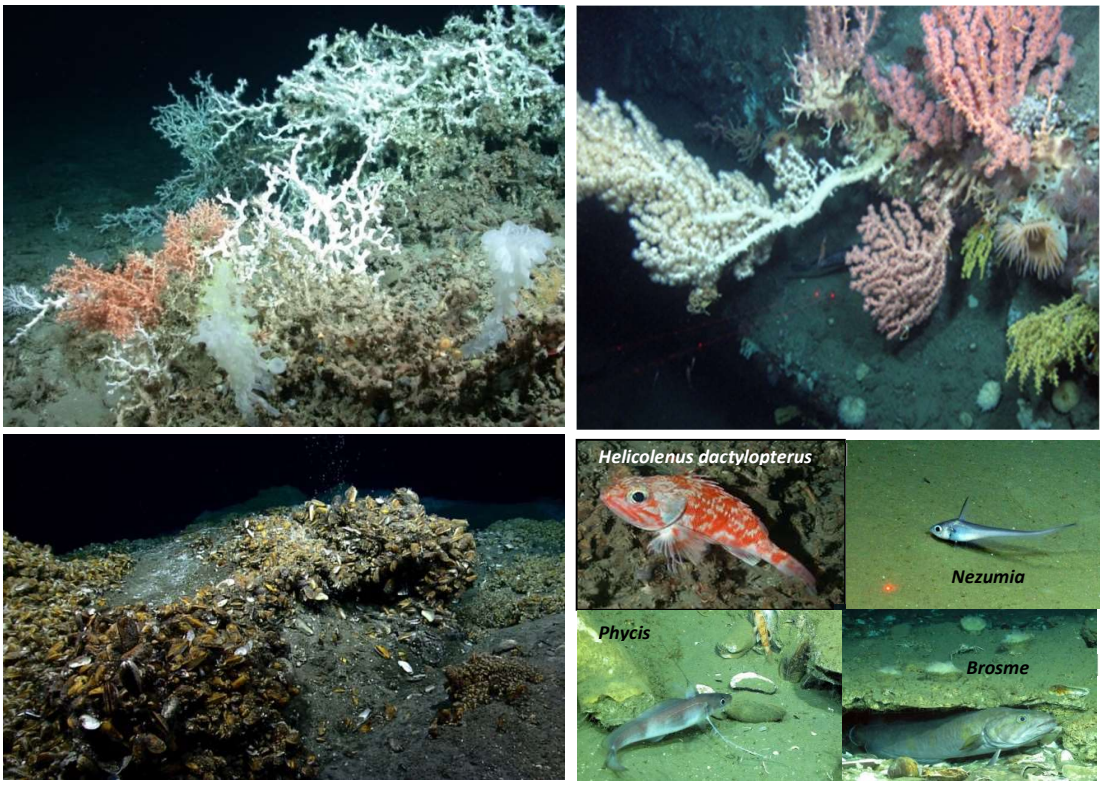

Figure 49. Examples of deep-sea habitats found off the Eastern USA. A: Lophelia pertusa *bioherms off the southeastern US; B: Coral gardens dominated by the octocoral* Paragorgia arborea *off the northeastern US; C: Methane seep community near Norfolk Canyon; D. Examples of fish species associated with coral, canyon, and seep habitats.*

In a region where methane seeps were unknown, within the last few years, hundreds of cold seeps have been reported on the northeastern US slope, including two well documented ones near Baltimore Canyon and Norfolk Canyon (Skarke et al., 2014; CSA et al., 2017). These support extensive chemosynthetic communities and promote hard bottom habitat via authigenic carbonates and mussel beds. These are extensively used by fishes (Ross et al., 2015) and other fauna (CSA et al., 2017).

New species of fishes have been discovered in association with these habitats including: *Psednos rossi* (Chernova & Stein, 2004), *Ophichthus brevirostris* (McCosker & Ross, 2007), *Etaptretus lopheliae* (Fernholm & Quattrini, 2008), *Bellottia cryptica* and *Bellottia robusta* (Nielsen et al., 2009) and a potential new species of *Conger* under evaluation (Quattrini et al., *in prep.*).

Coral habitats in the SEUS region are important for fishes, with 99 fish species documented on and around deep (>300 m) coral habitat from Cape Lookout to about Cape Canaveral, more than any other area of deep corals to date, of which about 20% were new to the SEUS Region (Ross & Quattrini, 2007; 2009). Several of these fish species were discovered to be closely tied to the reef habitat, with the existence of a primary (obligate) deep reef ichthyofauna (Ross & Quattrini, 2007; Quattrini, 2012). Fishes also form unique assemblages within submarine canyon ecosystems off the northeastern US. An unusual community was documented off Cape Hatteras, which expressed smaller body sizes than elsewhere, lower activity, adaptation to low dissolved oxygen, lower species richness but higher biomass than other areas (Sulak & Ross, 1996; Moser et al., 1996). This assemblage appeared to be responding to distinctive oceanographic and environmental conditions. At least 123 fish species were documented around Norfolk and Baltimore Canyons (230 to 1600 m depths), more than previously reported from this slope region (Ross et al., 2015). In shallower waters (ca. 120 m) nearby, shipwrecks harboured a different but diverse fauna (38 species), and the wrecks provided habitat extensively used by chain dogfish (*S. retifer*) as spawning substrate (Ross et al., 2016)

The benthic habitats described here fit the FAOcriteria of VME (FAO, 2009). This is supported by several studies on the life history traits of corals demonstrating that black corals and bamboo corals from SEUS can grow slowly and live longer than 2,500 years (e.g., Williams et al., 2006; 2007; Sinclair et al., 2011), making these organisms particularly slow to recover from disturbances such as fishing impacts. Genetic data for *Lophelia pertusa* from the Gulf of Mexico through the SEUS and across the Atlantic reveals unexpected population isolation and heterogeneity, suggesting that an effective management scheme for *L. pertusa* involves regional reserve networks (Morrison et al., 2011). Overall, data from the multi-disciplinary studies reported here have been used as the main tool by management agencies to evaluate, describe, map, and finally approve very large marine protected areas that target deep-sea corals, submarine canyons, and methane seeps. Examples are the enactment of large Coral Habitat Area of Particular Concern (CHAPC) off the southeastern US, that includes the Cape Lookout Coral Banks, designated by the South Atlantic Fishery Management Council where fishery related bottom disturbing activities are not allowed (Martin, 2014; Hourigan et al., 2017). Other examples are the designation of HMS as an Essential Fish Habitats by the South Atlantic Fishery Management Council; and the designation of one of the largest (38,000 sq. mi) marine protected areas off the US East Coast - the Frank R. Lautenberg Deep-Sea Coral Protection Area, that includes deep-sea coral habitats in submarine canyons, including the deep-sea coral habitats in Norfolk and Baltimore Canyons described here.

1.2.10 Case Study 13: Summary of Biodiversity and Biogeography Discoveries on the Tropic Seamount (High Seas, eastern central Atlantic)

Authors: Berta Ramiro-Sánchez, Lea-Anne Henry

Much of the ATLAS project relies on availability of data. However, biodiversity records from the deep and High Seas areas of the North Atlantic are sparse, even after data compilations from various databases have been exhausted. A unique opportunity to add more data to the High Seas biodiversity database (which would later be interrogated for the biogeography and GOODS analyses) arose just after the ATLAS project was launched, wherein a collaboration between ATLAS and the MarineE-Tech project was established to record VMEs from the Tropic Seamount, off the Canary Islands.

Study area and environmental setting The Tropic Seamount (Figure 50) (23°55' N, 20°45'W) is a four-armed, star-shaped guyot dated to 91.1 ± 0.2 Ma (van den Bogaard, 2013), that lies within the Western Sahara Seamount Province, along the northwestern African continental margin of the northeast Atlantic. With a flat-topped summit (slope of 0.5°- 4°) sitting at approximately 1000 m water depth with its base rooted at approximately 4200 m depth, the seamount presents a truncated cone slightly elongated along a north-south axis, measuring about 42 km in length and 37 km in width (Palomino et al., 2016). The flanks of the seamount are divided by four ridges 10-13 km in length with slopes ranging from 5° to 45°. Radiating from the summit, the flanks also exhibit gullies measuring 3-10 km in length (Palomino et al., 2016). The seamount is thought to have once been an oceanic island that eroded and subsided to its present depth at 1000 m (Schmincke & Graf, 2000).

Oceanographic conditions in Tropic Seamount are influenced by the seasonally productive waters off the NW African coast and the more oligotrophic waters of the North Atlantic subtropical gyre (Henderiks, 2001). The surface waters above are fed by the Canary Current (CC), which flows south-westward along the African coast and it turns west to join the North Equatorial Current at 20°-25° N. Below the seasonal thermocline and waters influenced by coastal upwelling (< 100 m), the North Atlantic Central Water (NACW) and South Atlantic Central Water (SACW) lie above ~700 m. Detailed information on oceanographic conditions can be found in Hernández-Guerra et al. (2001); Knoll et al. (2002); Hernández-Guerra et al. (2005); Pastor et al. (2012); Bashmachnikov et al. (2015) and Pastor et al. (2015).

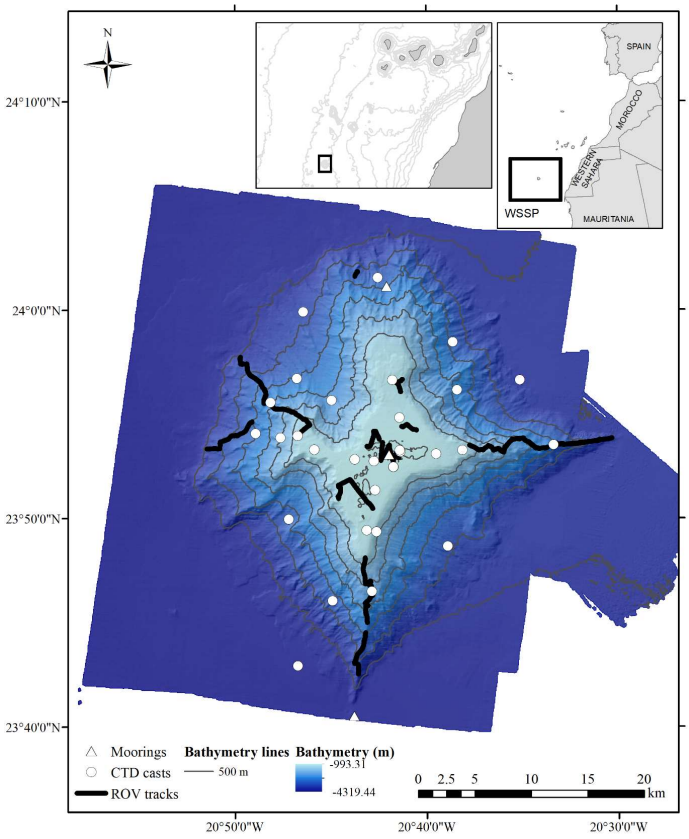

Figure 50. Location of the Tropic Seamount in the northeast tropical Atlantic with the different sampling operations: ROV tracks (thick black lines), CTD casts (white circles) and moorings (white triangles). Inset images show the location of the study area in relation to northwest Africa and the Western Sahara Seamount Province (WSSP).

Description of benthic communities

Although its composition and volcanic origin is well studied (Schmincke & Graf, 2000; van den Bogaard, 2013), little is known about the seamount fauna here, apart from a few reports of deep-sea corals (Schmincke & Graf, 2000; Vázquez et al., 2011). Preliminary video analysis revealed the existence of a diverse set of VME indicator taxa, as found and described from other seamount ecosystems (e.g., Rowden et al., 2010; Serrano et al., 2017). However, one of the most distinctive observations was the occurrence of dense aggregations of the hexactinellid sponge *Poliopogon amadou* Thomson, 1878, which formed extensive areas of sponge grounds in the deeper flanks of the seamount.

A recent dedicated exploration mission and geological survey, led by the National Oceanographic Centre (NOC) (Southampton, UK) on the RRV *James Cook* (Cruise JC142) as part of the Marine E-tech project, focused on assessing controls on the formation, distribution and composition of seafloor ferromanganese crust deposits on the Tropic Seamount and impacts of their future potential exploitation by the deep seabed mining industry. The mission was conducted from 29 October 2016 - 08 December 2016, wherein part of the exploration mission was to survey using a remotely operated

vehicle (ROV) to characterise the biological communities on Tropic Seamount, both by providing video and stills imagery and by sampling organisms for taxonomy using both molecular and classical morphological-based classifications. Results of this study have been published in Ramiro-Sánchez et al. (2019) and data are being prepared to submit as a database into PANGAEA.

The result of our collaboration was the discovery of multiple VME types on the seamount, including high-density octocoral gardens*, Solenosmilia variabilis* patch reefs, xenophyophores, crinoid fields and a relatively rare and biogeographically restricted type of deep-sea sponge ground formed by the glass sponge *Poliopogon amadou* (Figure 51). Egg-laying grounds for a deep-sea squid species were also found on octocoral gardens. Within this study an ensemble species distribution model predicting distribution of *P. amadou* was also constructed, as is reported in chapter 3 of this deliverable.

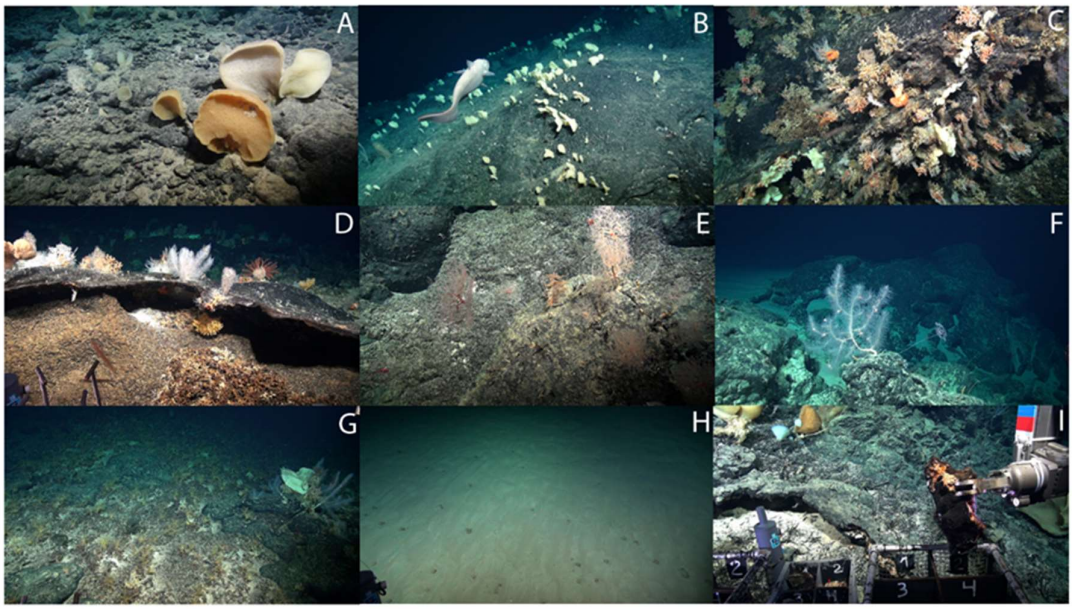

Figure 51. Seabed photographs showing some of the VME indicator taxa observed on the Tropic Seamount. A. Specimens of Poliopogon amadou*. B. Sponge ground of* Poliopogon amadou*. C. Coral garden on a ledge with diverse octocorals and patches of* Solenosmilia variabilis*. D. Octocoral garden and coral rubble. E. Antipatharian species,* Metallogorgia melanotrichos *and* Chrysogorgia *sp. F. Unidentified black coral. G. A crinoid field of possibly* Thalassometra lusitanica*. H. Field of xenophyophores. I. The ROV Isis sampling ferromanganese crust. (from Ramiro-Sanchez et al., 2019).*

Many international taxonomists helped to verify species identities from >18,000 stills images, and some molecular genetic sequencing (COI and 18S) was performed to confirm some species identifications as well. This resulted in the identification of at least 30 megafaunal species including 17 species of CWCs (scleractinians, octocorals and antipatharians), 10 species of sponges, 5 species of crinoids, xenophyophores. This number is conservative and may grow and potentially include new species to science as taxonomical and molecular analyses of the collected specimens progresses. Notably, many of the VMEs co-occurred in areas with mineral resources that would be of great interest to the deep seabed mining sector, including tellurium and FeMn deposits. However, the thickness of

FeMn crusts and their metal composition probably means that extraction is unlikely to be viable in the near future (Yeo et al., 2018). Discoveries reported here have direct relevance for ongoing Biodiversity Beyond National Jurisdiction (BBNJ) treaty negotiations and as the ATLAS team prepares to submit an EBSA template to nominate the Tropic Seamount as an EBSA in Areas Beyond National Jurisdiction for the Convention on Biological Diversity, in time for the next Intergovernmental Conference on BBNJ early in 2019.

1.3 New species and species range extensions in the deep sea

The deep ocean is the largest and least explored biome on Earth, with the highest potential for the discovery of new species to science. During the ATLAS project numerous biological samples have been collected with the objective of not only characterizing deep-sea biodiversity, but also to produce vouchered specimen records that can be used to validate species identification based on video analysis, an essential step towards the characterization of new habitats and identify emergent ecosystem properties such as taxonomic distinctness across the North Atlantic. In this section, we present an overview of the new species that have been identified so far within the ATLAS framework and others that are under current description. Species geographic and bathymetric range extensions are also given for different CS in an effort to improve our understanding on species biogeographical boundaries in the North Atlantic and potential changes related to climate change.

1.3.1 Case Study 7: Gulf of Cádiz-Strait of Gibraltar-Alboran Sea

Authors: José L. Rueda, Javier Urra, Laís V. Ramalho, Olga Utrilla, José Antonio Caballero

Under the framework of the ATLAS project, studies on the biodiversity of different habitats occurring in geomorphological features (mud volcanoes of the Gulf of Cádiz and seamounts of the Alboran Sea) have resulted so far on the finding and description of 10 new species to science. These new species mainly belong to the groups of molluscs (4 spp.), bryozoans (5 spp.) and echinoderms (1 sp.). Further studies of the material may highlight the presence of other potential new species and records of polychaetes and peracarid crustaceans which are still under anatomical and morphological study. The report will focus on the species that have been described so far or are under description and will be published in the coming months.

Molluscs

This group has been studied in collaboration with Dr. Serge Gofas and Carmen Salas from Universidad de Málaga (Spain) and under the framework of two Masters Theses by Olga Utrilla and José Antonio Caballero, both of them students of the Universidad de Málaga (Spain). The material was collected in the MEDWAVES expedition, but also in previous expeditions (INDEMARES, MONCARAL, MEDITS expeditions) which increased the spatial coverage of the study. The studied material was collected in mud volcanoes (MV) of the Gulf of Cádiz (MEDWAVES-Gazul MV, INDEMARES-several MVs of the Spanish Margin) and at Seco de los Olivos Seamount in the Alboran Sea (MEDWAVES-cold-water coral related habitats, MONCARAL-summit of Seco de los Olivos, MEDITS-adjacent bottoms).

In the Gulf of Cádiz, the best studied area was Gazul MV (using samples from MEDWAVES and INDEMARES), which represents a biodiversity hotspot for the Gulf of Cádiz. Under the framework of the Masters Thesis defended by Olga Utrilla, a total of 266 species of molluscs were found so far at Gazul MV, of which 47 are new records for the Spanish waters of the Gulf of Cádiz, with six of them representing new records for Spanish waters, and another three species are new to science. The new records for the Spanish waters are the monoplacophoran *Veleropilina* sp., the gastropods *Akritogyra conspicua*, *Narrimania concinna*, *Ringicula* cf. *blanchardi*, *Ringicula pirulina*, and the bivalve *Draculamya porobranchiata*. One of the new species is a small marginellid gastropod that is similar to *Dentimargo auratus* or to the one erroneously assigned to *D. bojadorensis* by Cossignani (2006) and that was collected in northern African margin. Another of the species is a small rissoid gastropod assigned to the *Onoba* genus that is similar to previously known species such as *O. dimassai, O. oliverioi* and *O. gianninii*. The last species is a bivalve from the Cuspidariidae family, probably belonging to the genera *Myonera*, due to the high similarities with *M. sulcifera* from the Porcupine Abyssal Plain.

No further details or pictures can be included in the report because the manuscript is in the final stage to be submitted to the journal *Scientia Marina*.

The high species richness of molluscs observed in Gazul MV could be mainly related to the combination of different sampling methods, the study of the thanatocoenosis, the high habitat heterogeneity of this MV and its geographical location between different biogeographical regions (Lusitanian, Mediterranean, Mauritanian). The best represented species were *Bathyarca philippiana* and *Asperarca nodulosa*, in both the taxocoenosis and thanatocoenosis, followed by *Leptochiton* sp., *Astarte sulcata* and *Limopsis angusta*. This thanatocoenosisalso harbours low frequent species that are nowadays typical of northern latitudes (e.g., *Nuculana pernula, Chlamys islandica*), indicators of past fluid venting at MVs (e.g., *Lucinoma asapheus*), or very restrictive to specific hosts such as cold-water corals (e.g., *Iphitus tuberatus*).

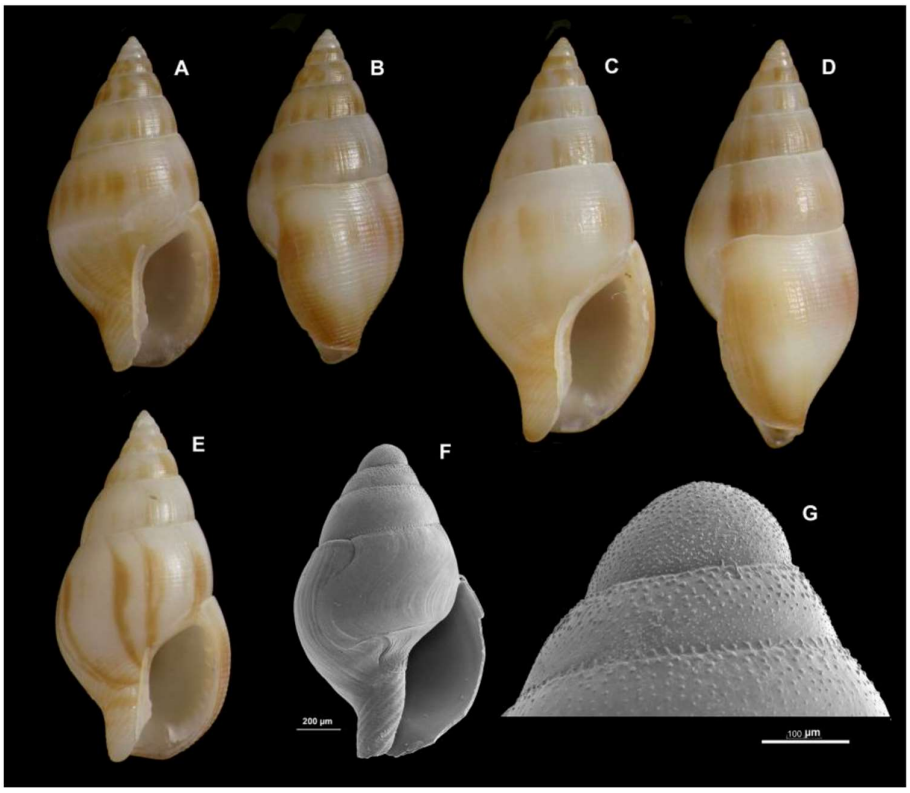

Figure 52. Mitrella templadoi *n. sp. A, B. Specimen from Seco de los Olivos, 250 m, MEDWAVES VV39, 250 m (8.7 mm). C,D. Same locality, MEDWAVES VV38, 250 m (10.2 mm). E. Same locality (9.1 mm). F. Scanning electron micrograph of a juvenile specimen from Seco de los Olivos, MEDWAVES VV35, 320 m, showing the protoconch-teleoconch limit (scale bar 200 µm). G. Detail of first protoconch whorls of the same specimen (scale bar 100 µm).*

At Seco de los Olivos, the molluscs are being studied in detail under the framework of a current Masters Thesis by the student José Antonio Caballero from the University of Málaga. More than 150 species have been found in the samples so far, including one new species to science assigned to the *Mitrella* genus (Figure 52). This species was previously figured by Bouchet & Warén (1985) who

reported on a single worn shell collected off the Azores in 843-900 m. They suggested some resemblance to *Mitrella profundi*, described from two localities, off Cuba (805 fathoms) and off Cape Hatteras (107 fathoms), and figured for comparison a type specimen from the United States National Museum collection. An immature shell from Galicia Bank was also figured by Rolán Mosquera (1983) as "*Columbella* sp.". The manuscript by Gofas et al. (2019) has been accepted with minor changes in Bulletin of Marine Science with the title "*Planktotrophic Columbellidae (Gastropoda) in the Northeast Atlantic and the Mediterranean, with description of a new species in the genus* Mitrella".

Bryozoans

This group has been studied in collaboration with Dr. Laís V. Ramalho from Museu Nacional, Universidade Federal do Rio de Janeiro (Brazil) and Instituto de Pesquisas Jardim Botânico do Rio de Janeiro using material collected in the MEDWAVES expedition, but also in previous ones (INDEMARES, CADHYS, MONCARAL, MEDITS expeditions) for increasing the spatial coverage of the studies as it was also done for the molluscs. The studied material was collected in mud volcanoes (MV) and diapirs of the Gulf of Cádiz (MEDWAVES-Gazul MV, INDEMARES-several MVs of the Spanish Margin, CADHYS-diapirs) and at Seco de los Olivos Seamount in the Alboran Sea (MEDWAVES-cold-water coral related habitats, MONCARAL-summit of Seco de los Olivos, MEDITS-adjacent bottoms).

In the MVs of the Gulf of Cádiz, samples were collected with different sampling methods (Van Veen, Shipek, Box-corer, benthic dredge, beam-trawl). Forty taxa belonging to 26 families and 31 genera have been identified, dominating those of the Class Gymnolaemata followed by Stenolaemata. Most taxa were found in a single MV (Gazul) and others in several MVs, including the taxa *Adeonellopsis*, *Palmicellaria*, *Tessaradoma*, *Reteporellina*, and *Schizomavella* sp. 2. Gazul MV displayed the highest number of taxa, followed by Tarsis, Chica, Pipoca, Almazán and Aveiro MVs. Most of the species identified here have a wide distribution, occurring from north Atlantic to Mediterranean including records to Portugal Shelf, but some few species had a more restricted distribution such as: *Jubella enucleata* (Galicia and north of Portugal), *Schizomavella linearis profunda* (Portugal and Gulf of Cádiz), and *Herentia thalassae* (Northern Spain and Portugal) and *Palmiskenea gautieri*, here recorded for the first time out of the Mediterranean Sea. Several factors may influence the observed bryozoan biodiversity such as the type and heterogeneity of substrates, and habitats as well as the depth.

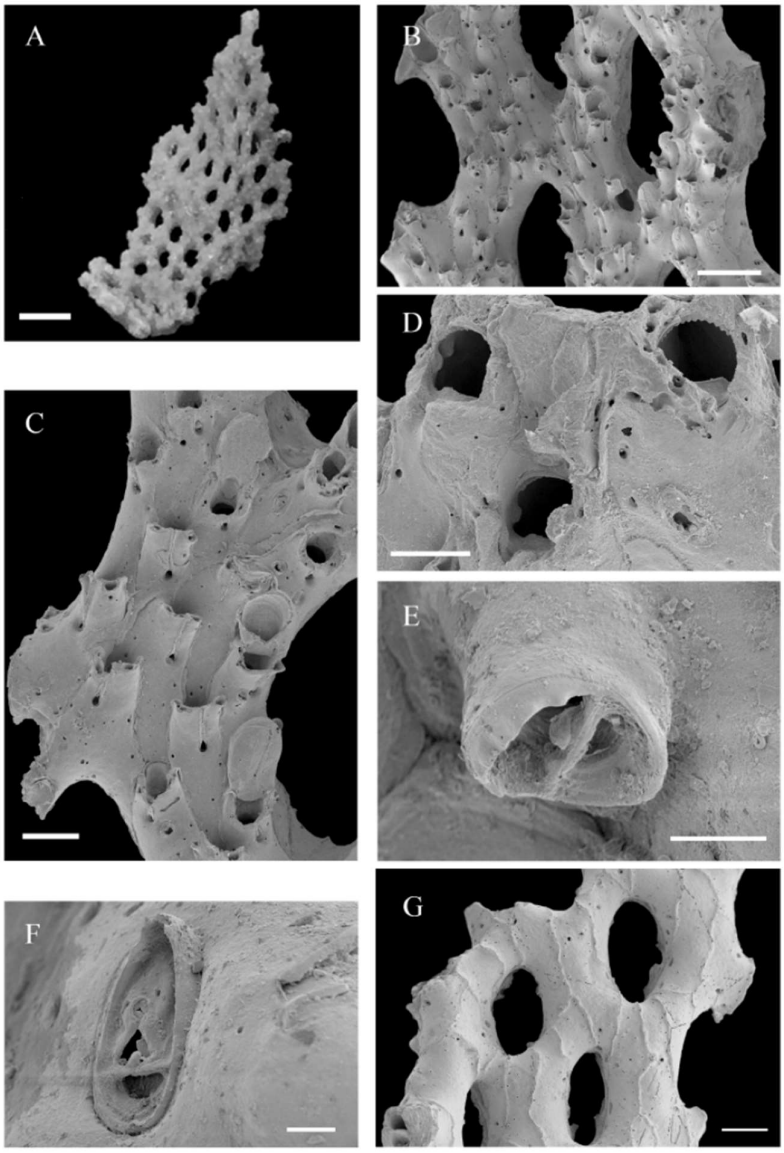

Figure 53. Reteporella victori *n. sp. MNCN 25.03/4001. A, general view of the colony fragment; B, general view of a part of the colony showing frontal surface and fenestrulae; C, detail of a branch with fertile and infertile zooids. Note the ong fissure ending in a pseudospiramen; D, close-up of the primary orifice with beaded anter; E, close-up of an oval avicularium with serrated rostrum and small columella on a short cystid; F, triangular avicularium with a trifoliate palate and slightly raised rostrum; G, dorsal side with fenestrulae, sutures and avicularia. Scale bars: A, 4 mm; B, 500 µm; C, 200 µm; D, 100 µm; E–F, 25 µm, G, 300 µm.*

The identification to species level of the bryozoan material has detected 4 new species to science and several records for the area. An article published in *Zootaxa* by Ramalho et al. (2018) dealt with the *Reteporella* genus in a diapiric and MV field of the Gulf of Cádiz, with the description of *Reteporella victori* n. sp. (Figure 53). The new species can be distinguished from *R. mediterranea* and *R. pelecanus* mainly by the presence of circular, peristomial avicularia with a serrated rostrum, raised by a short cystid. The colonies of *R. victori* were collected at the base of Gazul MV on massive authigenic carbonates (mainly slabs) colonized by small sponges (*Haliclona*), serpulid polychaetes (*Filograna*),

hydrozoans (*Polyplumaria*), and echinoids (*Cidaris cidaris, Gracilechinus acutus*). In that study, two species assigned to *Reteporella* were recorded for the first time in the Atlantic (*R. mediterranea* and *R. pelecanus*) and redescribed. Previous records of those species are from shelf bottoms of the Mediterranean, but the occurrence of these two species on MVs of the Spanish Margin may be linked to the strong influence of the Mediterranean Outflow Water (MOW) bottom current in this area. The MOW promotes the presence of a typical Mediterranean fauna in some regions of the northeastern part of the Gulf of Cádiz (e.g., *Leptometra phalangium* in the Pipoca MV) (Palomino et al., 2016a; Rueda et al., 2016). Another 3 bryozoan species belonging to the genera *Antropora*, *Porella* and *Microporella* are new to science but no further details or pictures can be included in the report because the manuscript is in the final stage to be submitted to the journal *Zootaxa*.

At Seco de los Olivos Seamount, samples were collected with a Van Veen grab in MEDWAVES, MONCARAL and MEDITS expeditions and ROV in MEDWAVES. A total of 25 specimens have been identified so far, including 19 Cheilostomatas and 6 Cyclostomatas. Among them, one species are described as new to science (*Buskea*) and three species are reported for the first time in the Mediterranean Sea (*Terminoflustra baleei*, *Marguetta pulchra*, and *Schizomavella linearis profunda*) (Figure 54). Some species showed a high frequency of occurrence in the samples, such as in the case of *Reteporella pelecanus* that was found in most Van Veen samples analyzed so far and in samples collected by ROV, *Adeonellopsis distoma* that occurred in seven samples and the new species of *Buskea* that was collected in six samples. Besides a high frequency, these species together with *Tervia irregularis* showed high abundance values in the samples. No further details or pictures of the new species to science can be included in the report because the manuscript is in preparation and some results will be presented at the 18th International Bryozoology Association Conference in 2019 in Liberec (Czech Republic).

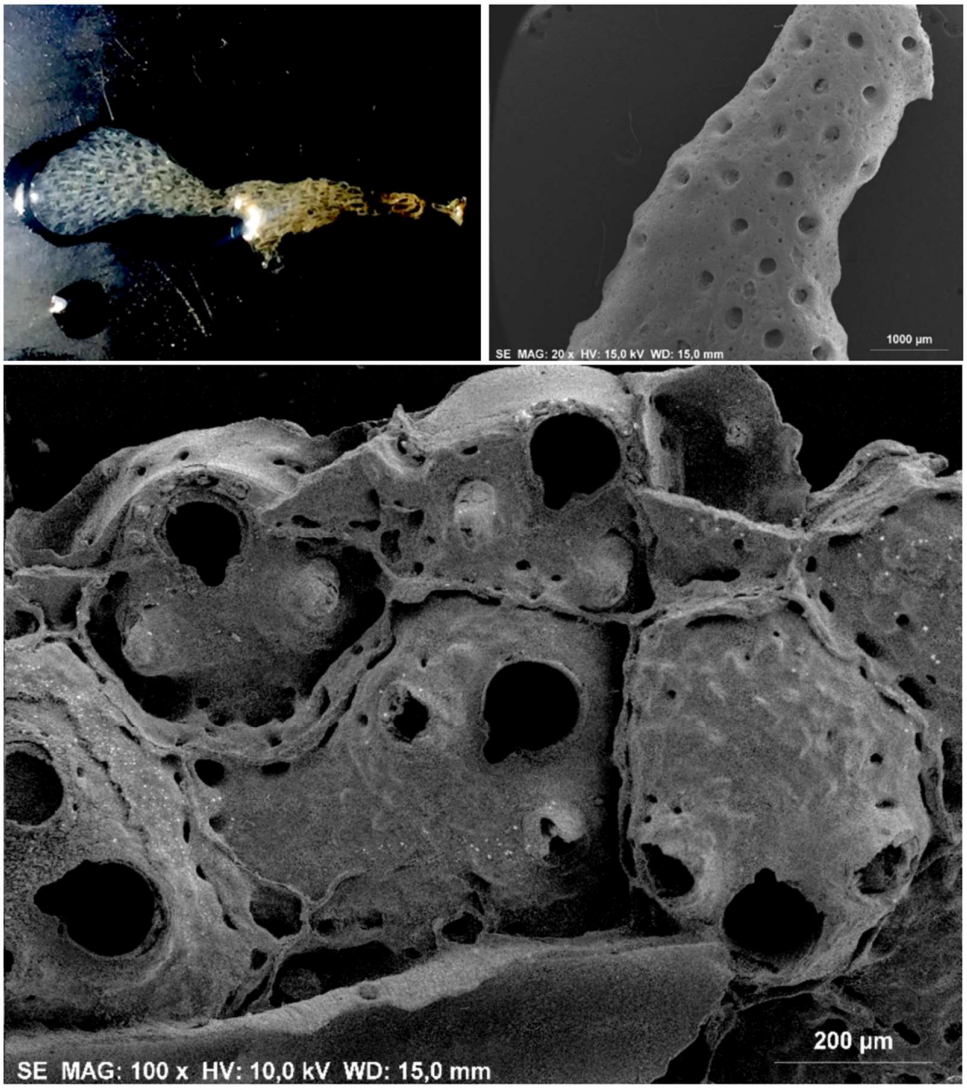

Figure 54. Bryozoan species reported for the first time in the Mediterranean Sea and collected during the MEDWAVES expedition at Seco de los Olivos: Terminoflustra baleei *(above),* Marguetta pulchra *(center) and* Schizomavella linearis profunda *(below).*

Echinoderms

The study of echinoderms collected in MEDWAVES and other previous expeditions (INDEMARES, MEDITS, MONCARAL) that explored the Gulf of Cádiz and Alboran Sea has been carried out in collaboration with Dr. Maria Eugenia Manjón-Cabeza from the University of Málaga and Francina Moya from Instituto Español de Oceanografía. More than 45 species have been found so far, including new records for the area and one new species to science. The new species has been assigned to the *Ophiothrix* genus from material collected at Gazul MV and Seco de los Olivos Seamount (Figure 55). The species can be abundant on coral rubble bottoms of both Gazul MV and Seco de los Olivos Seamount. No further details or pictures of the new species to science can be included in the report because the manuscript is still in preparation.

Figure 55. Samples of coral rubble from Seco de los Olivos Seamount where the Ophiothrix species was collected during MEDWAVES expedition (left) and detail of the aboral part of one individual (right).

1.3.2 Case study 8: Azores region

Authors: Marina Carreiro-Silva, Íris Sampaio, André Freiwald, Manfred Grasshoff, Telmo Morato

Revision of Octorallia taxonomic knowledge: nomenclature checklist, new records and range extensions

The Azores region in the Central North Atlantic is located in a strategic area to understand patterns of biodiversity, connectivity and biogeographic affinities across the Atlantic Ocean. Past studies have suggested the Azores as a hotspot of CWC biodiversity (Braga-Henriques et al., 2013). In an effort to increase the knowledge on cold-water octocoral diversity in the Azores, the zoological nomenclature of octocorals of the Azores was reviewed within a PhD thesis on the framework of the ATLAS project (see Sampaio et al., 2019). This subclass of the Cnidaria phylum includes gorgonians, sea pens, soft corals and precious corals with a morphology that varies from an encrusting stolon to an arborescent or feather-like animal (Bayer, 1956; Kükenthal, 1915).

A list of 98 names of octocorals was compiled for the region representing the highest species richness known of Octocorallia in Europe and in any of the North Atlantic archipelagos (Figure 56). In relation to other lists of species given to the Azores, this checklist includes for the first time species names of Pennatulacea, the sea pens gathering for the first time all the octocorals known to exist in this area (Figure 56). However, 3 nomenclatural errors were also noticed and are now in need of taxonomic clarification that may result in future synonyms or chresonyms (Sampaio et al., 2019). Additionally, further taxonomic work will result in new species descriptions.

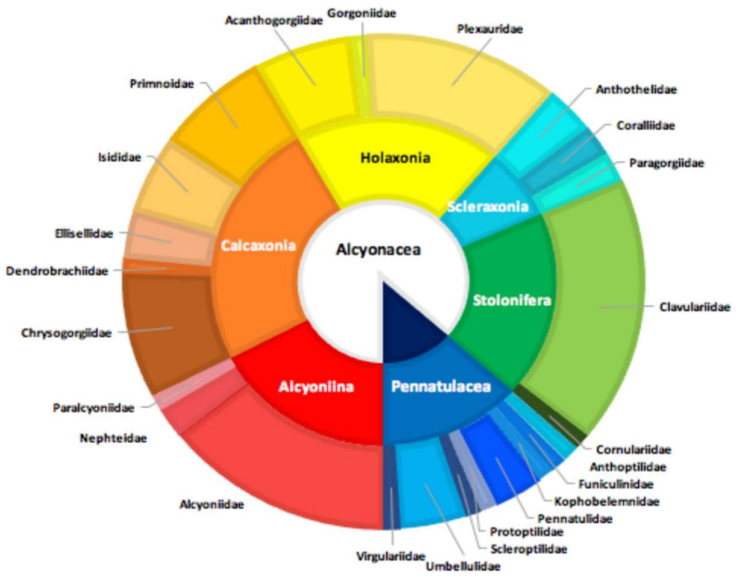

Figure 56. Species richness of Octocorallia of the Azores within taxonomic literature at three levels: orders, sub-orders and families (from Sampaio et al., *2019).*

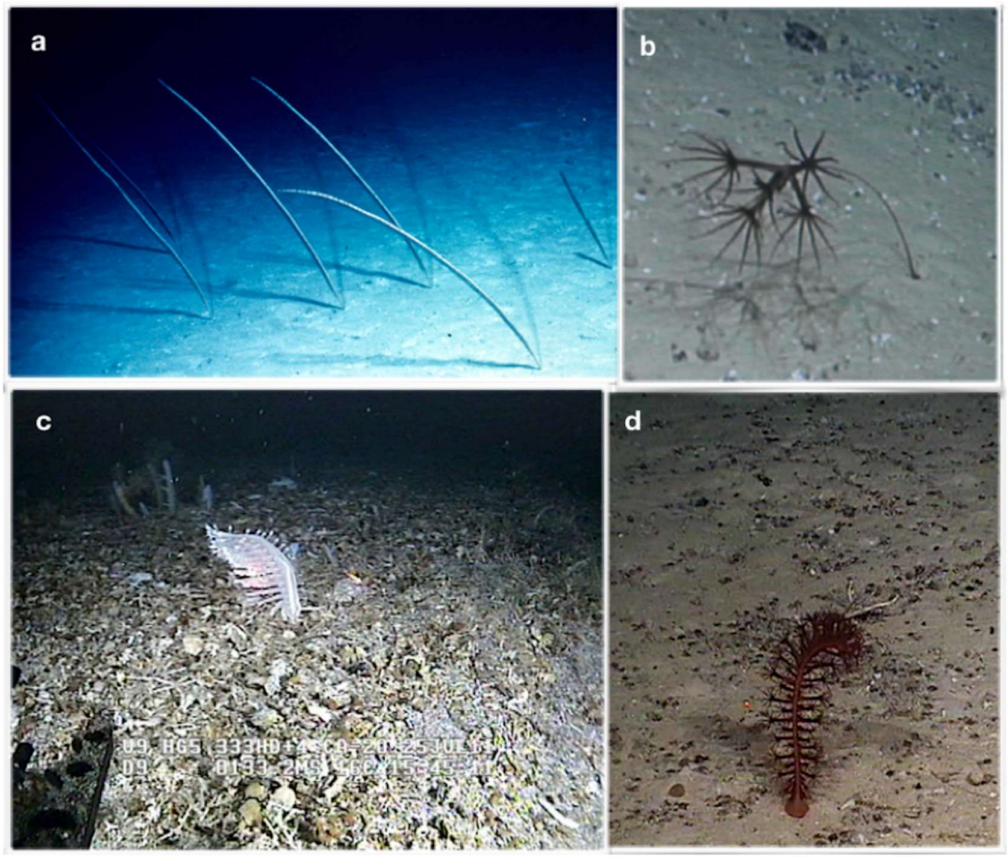

Figure 57. Underwater images of Pennatulacea of the Azores: a) Sea pen field b) Umbellula *cf.* pallida*, c)* Pennatula *cf.* phosphorea *and d) cf.* Anthoptilum murrayi*. Copyright: French bathyscape Archimède Expedition Azores 1969/Station Marine d' Endoume, (a), EMEPC2019/Iris Sampaio (b), Project CoralFish/ ImagDOP (c) and Dr. Odd Aksel Bergstad, Project MARECO, Institute of Marine Research, Bergen (d) (from Sampaio et al., 2019).*

While taxonomic literature is an essential source on biodiversity data, museum collections are often a source of new discoveries in what regards new species or new distributional records of species for a region and depth (Sampaio et al., *submitted*). The Naturalis Biodiversity Center (NBC) in Leiden harbours a collection gathered during several years on the southern NE Atlantic Ocean during the CANCAP project and Mauritania II Dutch expeditions (1976-1988) which took place in several Macaronesia archipelagos including the Azores, Madeira and Cape Verde. Octocorals from those projects were mostly identified by Dr. Manfred Grasshoff, the leading expert on NE Atlantic octocorals. However, octocoral records collected during these expeditions remained mostly unpublished. The exception being the genera *Alcyonium* (Stokvis & van Ofwegen, 2006; Sampaio et al., 2016), some Alcyonacea of the Azores (Braga-Henriques et al., 2013) and *Spinimuricea atlantica* (Johnson, 1862) (Grasshoff, 1992). A visit to the Naturalis Biodiversity Center in 2018 resulted in a reference list of Plexauridae records for the NE Atlantic Ocean (Sampaio et al., *submitted*). In all the sampling locations of the Dutch expeditions, twenty-four Plexauridae species were found, of which six species are putatively new to science (Sampaio et al., *submitted*). Moreover, seven species have now its

distribution increased in the different Macaronesia archipelagos. In addition, five species had its bathymetric distribution increased on a basin scale, while at a regional scale, there were fourteen species with its bathymetric range increased based on CANCAP and Mauritania II records (Sampaio et al., *submitted*).

The Azores archipelago was the second archipelago with higher species richness recorded during these Dutch expeditions after the tropical Cape Verde Archipelago. In the Azores, CANCAP recorded 8 species and the higher number of genera of Plexauridae (6) (Sampaio et al*., submitted*). Moreover, *Paramuricea biscaya* Grasshoff, 1977 was discovered for the first time at the Azorean marine waters and at Selvagens Islands, extending its Atlantic distribution to the south (Figure 57, Grasshoff, 1977) and increasing the total number of octocoral species names for the Azorean marine waters from 79 to 99 species.

No further details or pictures can be included in the report because the manuscript Sampaio et al. is being edited for publication in *Zookeys* (Sampaio Í, Carreiro-Silva M, Freiwald A, Menezes G, Grasshoff M (*submitted*) Natural history reference collections as a basis for sound biodiversity assessments – the Naturalis CANCAP and Mauritania II octocoral (Holaxonia, Plexauridae) collection).

1.3.2.1 New species to science

The octocoral genus *Swiftia* (family Plexauridae)

The octocoral family Plexauridae (Order Alcyonacea) is one of the most abundant but least studied families of gorgonians of the NE Atlantic Ocean. Within this family the genus *Swiftia* shows ample geographic distribution with variations in the form and color of the morphospecies found but high uncertainty on the species assignment. With the objective of investigating the species diversity an phylogenetic relationship in *Swiftia* from the NE Atlantic, a reference database with samples of *Swiftia* from the NE Atlantic and Mediterranean Sea was built form specimens stored at European Natural History Museum Collections. Type specimens of *Swiftia borealis* and *Swiftia rosea* were borrowed from the Zoology Museum of the University of Copenhagen while reference specimens of *Swiftia dubia* were borrowed from Senckenberg Museum and Naturalis Biodiversity Center (Figure 58). The three species hypotheses which form part of the last revision of this genus in Grasshoff (1977) were tested by integrating morphology with molecular biology and zoogeography in species delimitation. About 100 specimens of *Swiftia* recently collected from Scandinavia to Mauritania during several cruises (e.g. ATLAS MEDWAVES, FATE and M128) and stored at collections like COLETA and Senckenberg am Meer, were measured and sequenced. Morphological

analyses have considered three dimensional scales when describing the morphology of a gorgonian: the colony, the polyps and coenenchyme, and the sclerome (Figure 58, Figure 59, Figure 60). Moreover, a DNA barcode based in three molecular markers (COI + igr1 + mtMutS) and the nuclear ribosomal – DNA Internal Transcribed Spacer 2 (ITS2) was obtained for some specimens in Piran, Slovenia under the support of an ASSEMBLE Plus project (DeepSwit). This dataset is being analysed with the new species hypotheses foreseen. This work lays the foundations for further research in shifts of distribution ranges, biogeography, discovery of biodiversity hotspots, evolution and conservation of octocorals in the NE Atlantic.

Figure 58. Colonies of the three species known to inhabit the NE Atlantic Ocean and Mediterranean Sea and species hypotheses currently being tested: a) Swiftia borealis *from the Zoological Museum of the University of Copenhagen, b)* Swiftia rosea pallida *from the Zoological Museum of the University of Copenhagen, c)* Swiftia dubia *(as* S. pallida*) from the Senckenberg Museum; d)* Swiftia rosea *from Naturalis, e)* Swiftia *sp. from the MSM 16/3 cruise to Mauritania,* Swiftia *sp., from MEDWAVES cruise at the Azores.*

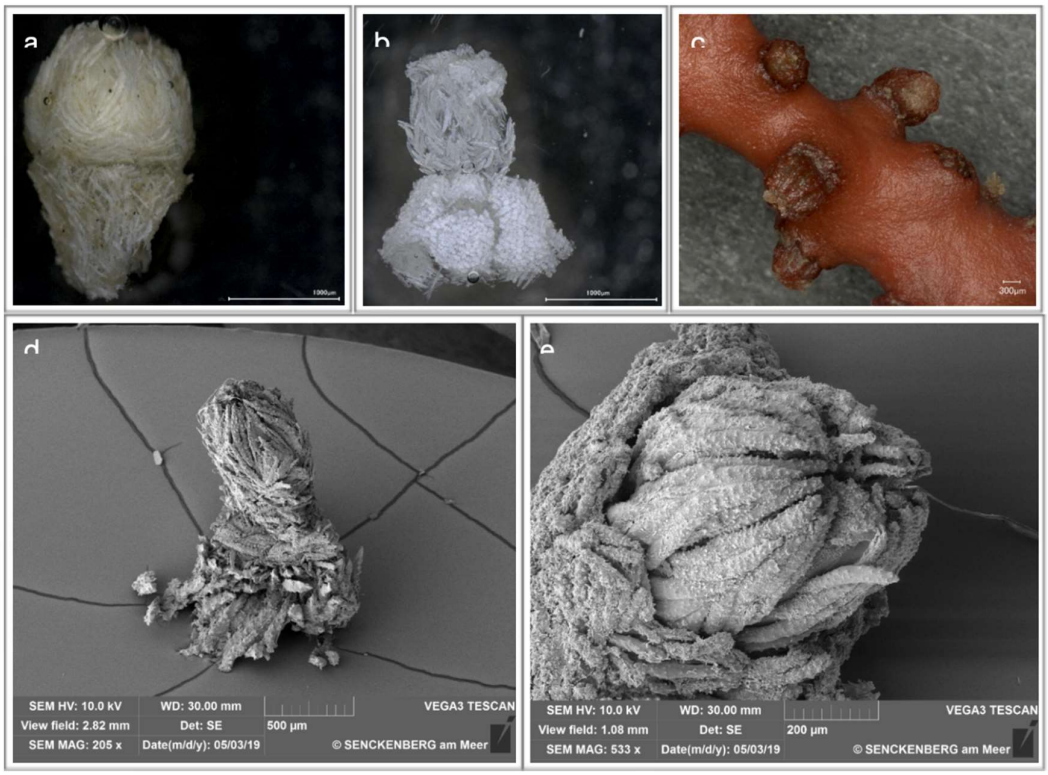

Figure 59. Polyps of Swiftia taken with Keyence digital microscope a) Swiftia borealis, b) Swiftia rosea c) Swiftia sp. and SEM d) Swiftia borealis and Swiftia dubia.

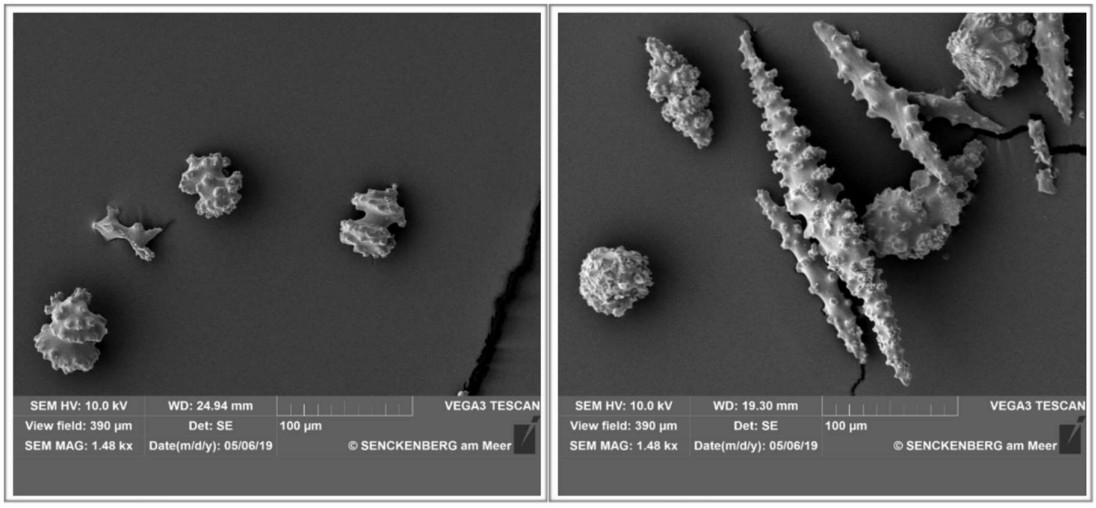

Figure 60. Swiftia *sclerome photographed with SEM: a) capstans of the outer layer of the calyx and b) spindles from the inner layer of the coenenchyme.*

Zoantharians associated with cold-water corals

One important group of associated sessile fauna to cold-water corals are zoantharians, a group of cnidarians often found in association with marine invertebrates, including corals, in shallow and deep-sea environments. Using analyses of molecular data (mtDNA COI, 16S, and 12S rDNA) coupled with ecological and morphological characteristics, four new species and a new combination of zoantharians associated with stylasterids, antipatharians and octocorals in the Azores at depths between 110 and 800m (see Figure 61 for details on the new species and Carreiro-Silva et al., 2017). Among these new species, the zoantharians associated with octocorals revealed evidence of a parasitic relationship where the zoantharian progressively eliminates gorgonian tissue and uses the gorgonian axis for structure and support, and coral sclerites for protection. In contrast, zoantharians associated with stylasterids and antipatharians seem to use corals as support without damage to their host. Phylogenic reconstructions suggest coevolution of zoantharian and cold-water coral species associating a unique type of host (or typology of substrate) to each of the monophyletic clade of zoantharians with long evolutionary histories in association with their hosts. The greatest incidence of zoantharians were found to occur on the octocorals *Callogorgia verticillata* and *Paracalyptrophora josephinae*, two species that are most often captured or damaged during longline fishing operations in the Azores (Sampaio et al., 2012), raising the hypothesis that removal of coral tissue caused by fishing line abrasion can increase the area of bare skeleton available for colonization by zoantharians. Given the parasitic behavior displayed by zoantharians, a better knowledge on the effect of fishing and climate change on the severity of parasitic association is required to predict changes in octocoral populations in the future.

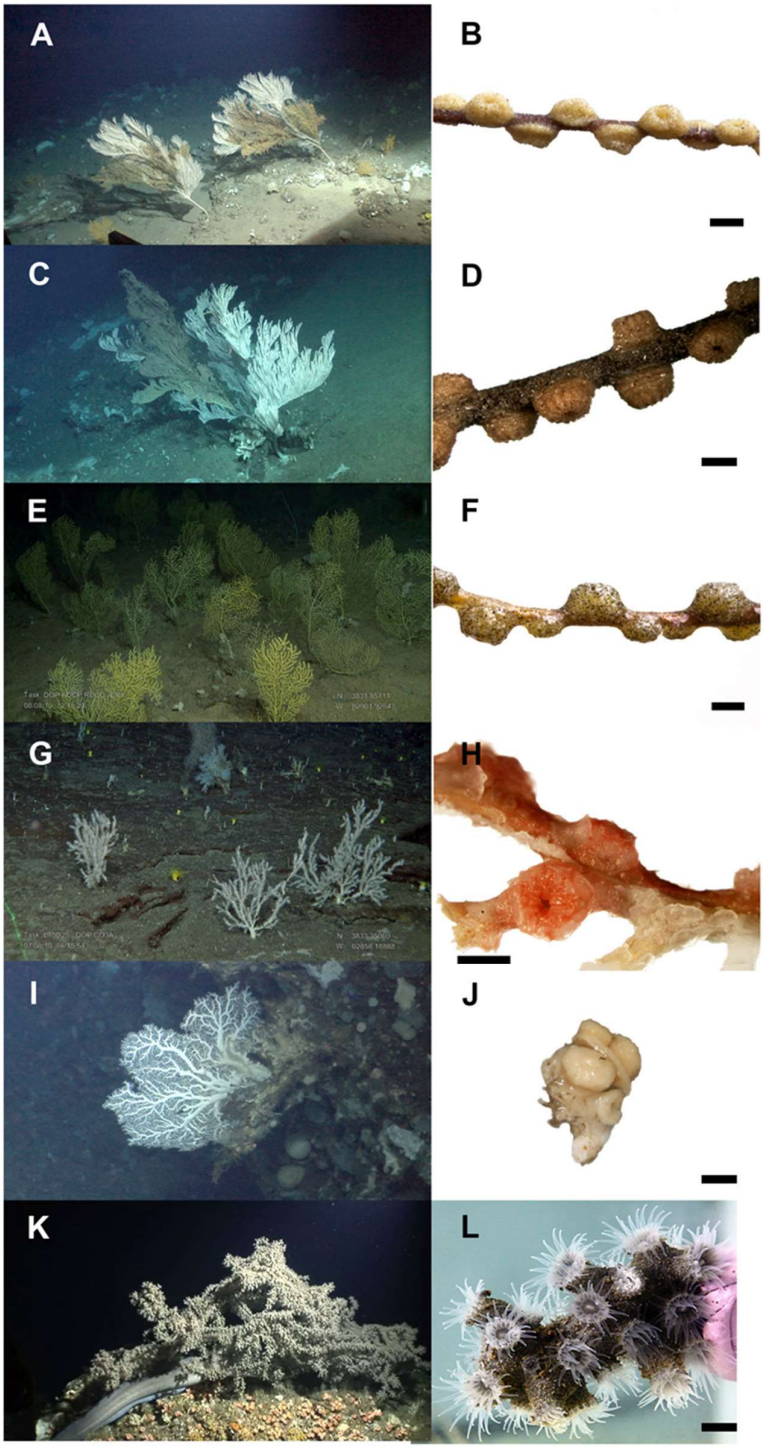

Figure 61. Photographs of zoantharians and respective cold-water coral hosts in the Azores. (A) octocoral Callogorgia verticillata*; and (B) associated zoantharian* Zibrowius primnoidus *comb. nov.; (C) octocoral* Paracalyptrophora josephinae*; and (D) associated zoantharian* Zibrowius alberti *sp. n.; (E) octocoral* Dentomuricea *aff.* meteor*, and (F) associated zoantharian* Zibrowius alberti *sp. n.; (G) octocoral* Candidella imbricata *and (H) associated zoantharian* Hurlizoanthus hirondelleae *sp. n.; (I) stylasterid* Errina dabneyi *and (J) associated zoantharian* Parazoanthus aliceae *sp. n. ; (K) antipatharian* Leiopathes *sp. and (L) associated zoantharian* Epizoanthus martinsae *sp. n.. Scale bar = 2mm for (B,D,F,H) and 4 mm for (L). Photo credits: CORAZON project/Rebikoff-Niggeler Foundation (A,C,I,K); CoralFISH/CONDOR projects (E,G). (from Carreiro-Silva et al., 2017).*

1.3.3 Case Study 10: Davis Strait, Eastern Arctic

Authors: Ellen Kenchington

To date two new bryozoan species have been described from the Case Study Area: *Turbicellepora hansenae* sp. n. Denisenko, 2016 and *Turbicellepora greenlandica* Denisenko, 2016 both described by Denisenko (2016) from material described in Kenchington et al. (2017). Denisenko (2016) notes the importance of this area for bryozoan fauna and the need for further collections to better understand the bryozoan fauna of the region. We are also aware of two new species of sponge that have been reported (Murillo et al., 2018) and are currently being described. These are the glass sponge *Bathydorus* Schulze, 1886 sp. n. in the family Rossellidae and *Calthropella* Sollas, 1888 sp. n. of the family Calthropellidae.

In addition, 13 new records for the Case Study Area were documented (Table 1), including Cnidarians and Bryozoans documented from samples collected at the Lophelia pertusa reef (see above; Kenchington et al., 2017). However by far the greatest number of new records for the study area come from the Porifera and the work of Tompkins and Baker in identifying the many sponge taxa in this region (Tompkins et al., 2017; Baker et al., 2018b,c) which were used by Murillo et al. (2018) to describe and predict sponge assemblages. Another 16 sponges from 10 families (Table 3) are new records for the northwest Atlantic, having largely been reported from the northeast Atlantic. One species of sponge, *Mycale* (*Mycale*) cf. *toporoki* Koltun, 1958, is a North Pacific species having been described from South Sakhalin and the South Kurile Island region. The designation cf. was applied to 6 of these species as the size of the spicules or other diagnostic characters did not exactly match the original description of the species. This is not surprising given the geographic location of the study area and the associated environmental variables (Beazley et al., 2018).

Table 3. New range extensions reported for Case Study Area 10. The designation cf. is short for conferre*, which means "compare to" and is used to denote species names where the size range of the spicules or other diagnostic characters did not exactly match the species descriptions which is not unusual given the geographic location of the study area.*

Phylum	Family	Species	Reference
New Records for the Case Study Area			
Cnidaria	Caryophylliidae	*Lophelia pertusa* (Linnaeus, 1758)	Kenchington et al. (2017)
Bryozoa	Tubuliporidae	*Exidmonea atlantica* (Forbes in Johnston, 1847)	Kenchington et al. (2017)
	Celleporidae	*Turbicellepora boreale* Hayward & Hansen, 1999	Denisenko (2016); Kenchington et al. (2017)
Porifera	Polymastiidae	*Polymastia grimaldii* (Topsent, 1913)	Murillo et al. (2018)
		Polymastia thielei Koltun, 1964	Murillo et al. (2018)
		Polymastia mamillaris (Müller, 1806)	Murillo et al. (2018)
		Polymastia andrica de Laubenfels, 1949	Murillo et al. (2018)
		Spinularia sarsi (Ridley & Dendy, 1886)	Murillo et al. (2018)
		Sphaerotylus capitatus (Vosmaer, 1885)	Murillo et al. (2018)
	Ancorinidae	*Stelletta normani* Sollas, 1880	Murillo et al. (2018)
		Stryphnus fortis (Vosmaer, 1885)	Murillo et al. (2018)
	Euretidae	*Chonelasma choanoides* Schulze & Kirkpatrick, 1910	Murillo et al. (2018)
	Mycalidae	*Mycale (Mycale) loveni* (Fristedt, 1887)	Murillo et al. (2018)

New Records for the Northwest Atlantic			
Porifera	Coelosphaeridae	*Forcepia (Forcepia) forcipis* (Bowerbank, 1866)	Kenchington et al. (2017); Tompkins et al. (2017); Murillo et al. (2018)
		Forcepia (Forcepia) thielei Lundbeck, 1905	Tompkins et al. (2017); Murillo et al. (2018)
		Forcepia (Forcepia) fabricans (Schmidt, 1874)	Tompkins et al. (2017); Murillo et al. (2018)
		Lissodendoryx (Lissodendoryx) lundbecki Topsent, 1913	Tompkins et al. (2017); Murillo et al. (2018)
		Lissodendoryx (Ectyodoryx) cf. *multiformis* (Brøndsted, 1932)	Tompkins et al. (2017); Murillo et al. (2018)
		Lissodendoryx (Lissodendoryx) stipitata (Arnesen, 1903)	Tompkins et al. (2017); Murillo et al. (2018)
	Dendoricellidae	*Dendoricella flabelliformis* (Hansen, 1885)	Baker et al. (2018a); Murillo et al. (2018)
	Polymastiidae	*Sphaerotylus borealis* (Swartschewsky, 1906)	Murillo et al. (2018)
		Polymastia cf. *nivea* (Hansen, 1885)	Murillo et al. (2018)
	Mycalidae	*Mycale (Mycale)* cf. *arctica* (Fristedt, 1887)	Murillo et al. (2018)
	Microcionidae	*Clathria (Clathria) barleei* (Bowerbank, 1866)	Murillo et al. (2018)
	Myxillidae	*Melonanchora* cf. *emphysema* (Schmidt, 1875)	Baker et al. (2018b); Murillo et al. (2018)
	Tethyidae	*Tethya norvegica* Bowerbank, 1872	Murillo et al. (2018)
	Chalinidae	*Haliclona (Gellius) varia* (Bowerbank, 1875)	Murillo et al. (2018)
	Niphatidae	*Hemigellius* cf. *pumiceus* (Fristedt, 1885)	Murillo et al. (2018)
	Desmacellidae	*Desmacella inornata* (Bowerbank, 1866)	Murillo et al. (2018)
New Records for the North Atlantic			
Porifera	Mycalidae	*Mycale (Mycale)* cf. *toporoki* Koltun, 1958	Murillo et al. (2018)

1.4 References

Abdel-Monem, A. A., Fernandez, L. A., & Boone, G.M. (1975). K-Ar ages from the eastern Azores group (Santa Maria, São Miguel and the Formigas Islands). *Lithos*, 8 (4), 247-254.

Arnaud-Haond, S., Van den Beld, I. M. J., Becheler, R., Orejas, C., Menot, L., Frank, N., Grehan, A., & Bourillet, J. F. (2017). Two "pillars" of cold-water coral reefs along Atlantic European margins: Prevalent association of Madrepora oculata with Lophelia pertusa, from reef to colony scale. *Deep Sea Research Part II: Topical Studies in Oceanography, 145*, 110-119.

Baker, E., Beazley, L., McMillan, A., Rowsell, J., & Kenchington, E. (2018a). Epibenthic Megafauna of the Disko Fan Conservation Area in the Davis Strait (Eastern Arctic) Identified from *In Situ* Benthic Image Transects. *CanadianTechnical Report of Fisheries and Aquatic Sciences,* 3272, vi + 391 p.

Baker, E., Odenthal, B., Tompkins, G., Walkusz, W., Siferd, T., & Kenchington, E. (2018b). Sponges from the 2010-2014 Paamiut Multispecies Trawl Surveys, Eastern Arctic and Subarctic: Class Demospongiae, Subclass Heteroscleromorpha, Order Poecilosclerida, Families Crellidae and Myxillidae. *Canadian Technical Report of Fisheries and Aquatic Sciences, 3253*, iv + 52 p.

Baker, E., Odenthal, B., Walkusz, W., Siferd, T., Rios, P., Tompkins, G., & Kenchington, E. (2018c). Sponges from the 2010-2014 Paamiut Multispecies Trawl Surveys, Eastern Arctic and Subarctic: Class Demospongiae, Subclass Heteroscleromorpha, Order Poecilosclerida, Families Dendoricellidae and Tedaniidae. *Canadian Technical Report of Fisheries and Aquatic Sciences, 3282,* v + 46pp.

Bane, J., & Brooks, D. (1979). Gulf Stream meanders along the Continental Margin from the Florida Straits to Cape Hatteras. *Geophysical Research Letters*, 6, 280–282.

Bashmachnikov, I., Lafon, V. & Martins, A. (2004) SST stationary anomalies in the Azores region. *Proc SPIE,* 5569,148–155.

Bashmachnikov, I., Mohn, C., Pelegri, J.L., Martins, A., Jose, F., Machín, F. & White, M. (2009) Interaction of Mediterranean water eddies with Sedlo and Seine Seamounts, Subtropical Northeast Atlantic. *Deep Sea Research Part II: Topical Studies in Oceanography,* 56(25), 2,593–2,605.

Bashmachnikov, I., Loureiro, C. M., & Martins, A. (2013). Topographically induced circulation patterns and mixing over Condor seamount. *Deep Sea Research Part II: Topical Studies in Oceanography,* 98, 38–51.

Bashmachnikov, I., Nascimento, Â., Neves, F., Menezes, T., & Koldunov, N. V. (2015). Distribution of intermediate water masses in the subtropical northeast Atlantic. *Ocean Science,* 11, 803–827. doi:10.5194/os-11-803-2015.

Bauer, J. E., DeMaster, D. J., Repeta, D. J., & Verity, P.G.(eds.) (2002). Biogeochemistry and cycling of carbon in the northwest Atlantic continental margin: findings of the Ocean Margin Program. *Deep-Sea Research Part II: Topical Studies in Oceanography*, 49 (20).

Bayer, F. M. (1956). *Octocorallia*. Treatise on invertebrate paleontology, 166-231.

Beazley, L., Murillo, F.J., Kenchington, E., Guijarro, J., Lirette, C., Siferd, T., Treble, M., Baker, E., Bouchard Marmen, M., & Tompkins MacDonald, G. (2016). Species Distribution Modelling of Corals and Sponges in the Eastern Arctic for Use in the Identification of Significant Benthic Areas. *CanadianTechnical Report of Fisheries and Aquatic Sciences,* 3175, vii + 210p.

Bouchet, P., & Warén, A. (1985). Revision of the northeast Atlantic bathyal and abyssal Neogastropoda excluding Turridae (Mollusca, Gastropoda). *Bollettino Malacologico Supplement, 1*, 120–296.

Boury-Esnault, N., & Rützler, K. (1997). Thesaurus of sponge morphology. *Smithsonian Contributions in Zoology,* 596, 55 pages.

Braga-Henriques, A., Porteiro, F.M., Ribeiro, P.A., de Matos, V., Sampaio, I., Ocana, O. & Santos, R.S. (2013). Diversity, distribution and spatial structure of the cold-water coral fauna of the Azores (NE Atlantic). *Biogeosciences*, 10, 529–590.

Bremner, J., Frid, C. L. J., & Rogers, S. I. (2003). Assessing marine ecosystem health: the long-term effects of fishing on functional biodiversity in North Sea benthos. *Aquatic Ecosystem Health & Management*, 6(2), 131-137.

Briggs, J.C. (1974). *Marine Zoogeography*. McGraw-Hill.

Brøndsted, H.V. (1933). The Godthaab Expedition 1928. Porifera. *Medd. Gronl.,* 79, 1–25.

Brooke, S. D., Watts, M. W., Heil, A. D., Rhode, M., Mienis, F., Duineveld, G.C .A., Davies, A. J., & Ross, S.W. (2017). Distributions and habitat associations of deep water corals in Norfolk and Baltimore canyons, Mid-Atlantic Bight, USA. *Deep-Sea Research Part II: Topical Studies in Oceanography,* 137, 131-147.

Brooke, S., & Ross, S. W. (2014). First observations of the cold-water coral *Lophelia pertusa* in mid-Atlantic canyons of the USA. *Deep-Sea Research Part II: Topical Studies in Oceanography*, 104, 245-251.

Bullough, L. W., Turrell, W. R., Buchan, P., & Priede, I. G. (1998). Commercial deep water trawling at sub-zero temperatures - Observations from the Faroe-Shetland channel. *Fisheries Research*, 39, 33-41. doi:10.1016/S0165-7836(98)00170-2.

Cairns, S. D. (2000). A revision of the shallow-water azooxanthellate Scleractinia of the western Atlantic. *Studies of the Natural History of the Caribbean Region*, 75, 1–321.

Cárdenas, P., Rapp, H. T., Klitgaard, A. B., Best, M., Thollesson, M., & Tendal, O. S. (2013). 745 Taxonomy, biogeography and DNA barcodes of Geodia species (Porifera, Demospongiae, 746

Tetractinellida) in the Atlantic boreo-arctic region. *Zoological Journal of the Linnean Society*, 169, 251–311. 747 https://doi.org/10.1111/zoj.12056.

Cardigos, F., Colaço, A., Dando, P.R., Ávila, S.P., Sarradin, P.M., Tempera, F., Conceição, P., Pascoal, A. & Serrão Santos, R. (2005) Shallow water hydrothermal vent field fluids and communities of the D. João de Castro Seamount (Azores). *Chemical Geology, 224*, 153–168.

Carreiro-Silva, M., Ocaña, O. V., Stanković, D., Sampaio, I., Porteiro,, F., Fabri M-C., & Stefanni, S. (2017). Zoanthids associated with cold-water corals in the Azores Region: hidden diversity in the deep-sea in the deep-sea. *Frontiers in Marine Science*, 4, 88.

Chernova, N.V., & Stein, D.L. (2004). A remarkable new species of *Psednos* (Teleostei: Liparidae) from the western North Atlantic *Ocean. Fishery Bulletin*, 102(2), 245-250.

Chevenet, F., Doledec, S., & Chessel, D. (1994). A fuzzy coding approach for the analysis of long-term ecological data. *Freshwater Biology*, 31, 295–309.

Coykendall, D. K., Nizinski, M. S., & Morrison, C. L. (2017). A phylogenetic perspective on diversity of Galatheoidea (*Munida, Munidopsis*) from cold-water coral and cold seep communities in the western North Atlantic Ocean. *Deep-Sea Research Part II: Topical Studies in Oceanography*, 137, 258-272.

CSA Ocean Sciences Inc., Ross, S., Brooke, S., Baird, E., Coykendall, E., Davies, A., Demopoulos, A., France, S., Kellogg, C., Mather, R., Mienis, F., Morrison, C., Prouty, N., Roark, B., & Robertson, C. (2017). *Exploration and Research of Mid-Atlantic Deepwater hard Bottom Habitats and Shipwrecks with Emphasis on Canyons and Coral Communities: Atlantic Deepwater Canyons Study*. Vol I. Final Technical Rept., Vol. II: Final Appendices. U.S. Dept. of the Interior, Bureau of Ocean Energy Management, Atlantic OCS Region. OCS Study BOEM, 2017-060 (Vol. I) & 061 (Vol. II), 1000 p + appendices.

Davies, J. S., Guillaumont, B., Tempera, F., Vertino, A., Beuck, L., Ólafsdóttir, S. H., Smith, C. J., Fosså, J. H., van den Beld, I. M. J., Savini, A., Rengstorf, A., Bayle, C., Bourillet, J. F., Arnaud-Haond, S., & Grehan, A. (2017). A new classification scheme of European cold-water coral habitats: Implications for ecosystem-based management of the deep sea. *Deep Sea Research Part II: Topical Studies in Oceanography, 145* (Supplement C), 102-109.

Davies, J. S., Howell, K. L., Stewart, H. A., Guinan, J., & Golding, N. (2014). Defining biological assemblages (biotopes) of conservation interest in the submarine canyons of the South West Approaches (offshore United Kingdom) for use in marine habitat mapping. *Deep Sea Research Part II: Topical Studies in Oceanography, 104,* 208-229.

De Mol, L., Van Rooij, D., Pirlet, H., Greinert, J., Frank, N., Quemmerais, F., & Henriet, J.-P. (2011). Cold-water coral habitats in the Penmarc'h and Guilvinec Canyons (Bay of Biscay): Deep-water versus shallow-water settings. *Marine Geology, 282* (1-2), 40-52.

De Clippele L, Gafeira J, Robert K, Hennige S, Lavaleye MS, Duineveld GCA, HUvenne VAI, Roberts JM (2017) Using novel acoustic and visual mapping tools to predict the small-scale spatial distribution of live biogenic reef framework in cold-water coral habitats. Coral Reefs 36:255-268

Denisenko, N.V. (2016). Two new species of the genus *Turbicellepoa* Ryland, 1963 (Bryozoa: Celleporidae) found on *Lophelia* coral from the Greenland slope. *Zootaxa,* 4066, 177–182.

DFO (2017) *Delineation of Significant Areas of Coldwater Corals and Sponge-Dominated Communities in Canada's Atlantic and Eastern Arctic Marine Waters and their Overlap with Fishing Activity.* DFO Canadian Science Advisory Secretariat Science Advisory Report 2017/007.

Diaz, R.J., Blake, J.A., & Cutter, G.R. (1994). Input, accumulation and cycling of materials on the continental slope oV Cape Hatteras. *Deep-Sea Research Part II: Topical Studies in Oceanography*, 41, 707–710.

Duineveld, G. C. A., Jeffreys, R. M., Lavaleye, M. S. S., Davies, A. J., Bergman, M. J. N., Watmough, T., & Witbaard, R, (2012). Spatial and tidal variation in food supply to shallow cold-water coral reefs of the Mingulay Reef complex (Outer Hebrides, Scotland). *Marine Ecology Progress Series*, 444, 97-115.

FAO (2009) *International Guidelines for the Management of Deep-sea Fisheries in the High Seas*. Rome. Pp 73.

Fernholm B., & Quattrini A. M. (2008). A new species of Hagfish (Myxinidae: *Eptatretus*) associated with deep-sea coral habitat in the Western North Atlantic. *Copeia,* 2008 (1), 126–132.

Findlay, H., Artioli, Y., Moreno Navas, J., Hennige, S.J., Wicks, L.C., Huvenne, V.A.I., Woodward, E.M.S. & Roberts, J.M. (2013) Tidal downwelling and implications for the carbon biogeochemistry of cold-water corals in relation to future ocean acidification and warming. *Global Change Biology, 19*, 2708-2719.

Fragoso, G. M., Poulton, A. J., Yashayaev, I. M., Head, E. J. H., Johnsen, G., & Purdie, D. A. (2018). Diatom biogeography from the Labrador Sea revealed through a trait-based approach. *Frontiers in Marine Science*, 5, 297.

Fragoso, G., Poulton, A., Yashayaev, I., Head, E. & Purdie, D., (2016a). Spring phytoplankton communities of the Labrador Sea (2005–2014): pigment signatures, photophysiology and elemental ratios, *Biogeosciences Discussions*, doi: 10.5194/bg-2016-295.

Fragoso, G., Poulton, A., Yashayaev, I., Head, E., Stinchcombe, M. & Purdie, D. (2016b) Biogeographical patterns and environmental controls of phytoplankton communities from contrasting hydrographical zones of the Labrador Sea, *Progress in Oceanography*, V, 141, 212–226. doi: 10.1016/j.pocean.2015.12.007.

Gagnon, J. -M., Kenchington, E., Port, A., Anstey, L.J., & Murillo, F.J. (2015). Morphological and genetic variation in North Atlantic giant file clams, *Acesta* spp. (Bivalvia: Limidae), with description of a new cryptic species in the north-west Atlantic. *Zootaxa*, 4007(2), 151-180.

García-Alegre, A., Murillo, F.J., Sacau, M., Kenchington, E., Serrano, A. & Durán Muñoz, P. (2018). Trait-based approach on deep-sea corals in the high-seas of the Flemish Cap and Flemish Pass (northwest Atlantic). *4th World Conference on Marine Biodiversity*, 13-16, May 2018. Montréal, Canada.

Giacomello, E., Menezes, G. M., & Bergstad, O. A. (2013). An integrated approach for studying seamounts: CONDOR observatory. *Deep Sea Research Part II: Topical Studies in Oceanography*, 98, 1–6.

Gil, J., Sánchez R., Cerviño, S., & Garabana, D. (2004). Geostrophic circulation and heat flux across the Flemish Cap, 1988-2000, *Journal of Northwest Atlantic Fishery Science*, 34, 61-81.

Gofas, S., Luque Ángel, L., & Urra, J. *accepted.* Planktotrophic Columbellidae (Gastropoda) in the Northeast Atlantic and the Mediterranean. *Bulletin of Marine Science.*

Grasshoff, M. (1977). Die Gorgonarien des östlichen Nordatlantik und des Mittelmeeres: III. Die Familie Paramuriceidae (Cnidaria: Anthozoa). "*Meteor - Forschungs - Ergebnisse, D*, 27, 5–76.

Grasshoff, M. (1992). Die Flachwasser-Gorgonarien von Europa und Westafrika (Cnidaria, Anthozoa). *Courier Forschungsinstitut Senckenberg*, 149, 1–135.

Hansen, B., & Østerhus, S. (2000). North atlantic–nordic seas exchanges. *Progress in Oceanography*, 45, 109–208. doi: 10.1016/S0079-6611(99)00052-X.

Hátún, H., Azetsu-Scott, K., Somavilla, R., Rey, F., Johnson, C., Mathis, M., Mikolajewicz, U., Coupel, P., Tremblay, J.- **É**., Hartman, S., Pacariz, S. V., Salter, I., & Ólafsson, J. (2017). The subpolar gyre regulates silicate concentrations in the North Atlantic. *Scientific Reports*, 7, 14576.

Henderiks, J. (2001). *Coccolith studies in the Canary Basin: Glacial-Interglacial paleoceanography of the Eastern Boundary Current System*. Available at: http://www.academia.edu/28505222/Coccolith_studies_in_the_Canary_Basin [Accessed September 28, 2018].

Hennige, S. J., Wicks, L. C., Kamenos, N. A., Perna, G., Findlay, H. S., & Roberts, J. M. (2015). Hidden impacts of ocean acidification to live and dead coral framework. *Proceedings of the Royal Society B: Biological Sciences*, 282, 20150990.

Henry, L. -A., & Roberts, J. M. (2014). Applying the OSPAR habitat definition of deep-sea sponge aggregations to verify suspected records of the habitat in UK waters, *JNCC Report* No, 508, 41.

Henry, L. -A., Nizinski, M. S., & Ross, S. W. (2008). Occurrence and biogeography of hydroids (Cnidaria: Hydrozoa) from deep-water coral habitats off the southeastern United States. *Deep-Sea Research Part I: Oceanographic Research Papers*, 55(6), 788-800.

Henry, L., Davies, A. J., & Roberts, J. M. (2010). Beta diversity of cold-water coral reef communities off western Scotland. *Coral Reefs*, 29, 427-436.

Henry, L-A, Moreno, N, J., & Roberts, J. M. (2013). Multi-scale interactions between local hydrography, seabed topography, and community assembly on cold-water coral reefs. *Biogeosciences*, 10, 2737-2746.

Hernández-Guerra, A., Fraile-Nuez, E., López-Laatzen, F., Martínez, A., Parrilla, G., & Vélez-Belchí, P. (2005). Canary Current and North Equatorial Current from an inverse box model. *Journal of Geophysical Research: Oceans,* 110, 1–16. doi:10.1029/2005JC003032.

Hernández-Guerra, A., López-Laatzen, F., Machín, F., De Armas, D., & Pelegrí, J. L. (2001). Water masses, circulation and transport in the eastern boundary current of the North Atlantic subtropical gyre. *Scientia Marina,* 65, 177–186.

Hourigan, T.F., Reed, J., Pomponi, S., Ross, S. W., David, A. W., & Harter, S. (2017). State of Deep-Sea Coral and Sponge Ecosystems of the Southeast United States. In: Hourigan, T.F., P.J. Etnoyer, S.D. Cairns (eds.). *The State of Deep-Sea Coral and Sponge Ecosystems of the United States.* NOAA Technical Memorandum NMFS-OHC-4, Silver Spring, MD, 60.

Howell, K. L., Davies, A. J., & van den Beld, I. (2017). *Deep-sea species image catalogue.* University of Plymouth, Ifremer, NOAA. http://www.deepseacatalogue.fr/ On-line version 3.

Howell, K. L., Davies, J. S., & Narayanaswamy, B. E. (2010). Identifying deep-sea megafaunal epibenthic assemblages for use in habitat mapping and marine protected area network design. *Journal of the Marine Biological Association of the United Kingdom, 90* (1), 33-68.

Huvenne, V. A. I., Tyler, P. A., Masson, D. G., Fisher, E. H., Hauton, C., Hühnerbach, V., Le Bas, T. P., & Wolff, G. A. (2011). A Picture on the Wall: Innovative Mapping Reveals Cold-Water Coral Refuge in Submarine Canyon. *PloS One, 6* (12), e28755.

Johnson, J. Y. (1862). Descriptions of some New Corals from Madeira. *Proceedings of the Zoological Society of London*, 30 (1), 194-197. https://doi.org/10.1111/j.1469-7998.1862.tb06497.x.

Karl, D.M., Brittain, A.M. & Tilbrook, B.D. (1989). Hydrothermal and microbial processes at Loihi Seamount, a mid-plate hot-spot volcano. *Deep Sea Research Part II: Topical Studies in Oceanography*, 36, 1655–1673.

Kazanidis, G., Henry, L. A., Roberts, J. M., & Witte, U. F. M. (2016). Biodiversity of *Spongosorites coralliophaga* (Stephens, 1915) on coral rubble at two contrasting cold-water coral reef settings. *Coral Reefs*, 35, 193-208.

Kazanidis, G., Vad, J., Henry, L, -A., Neat, F., Berx, B., Georgoulas, K., & Roberts, J. M. (2019). Distribution of deep-sea sponge aggregations in an area of multisectoral activities and changing oceanic conditions. *Frontiers in Marine Science*, 6, 163. doi: 10.3389/fmars.2019.00163

.

Kenchington, E., Yashayaev, I., Tendal, O. S., & Jørgensbye, H. (2017). Water mass characteristics and associated fauna of a recently discovered *Lophelia pertusa* (Scleractinia: Anthozoa) reef in Greenlandic waters. *Polar Biology,* 40, 321-337.

Kennedy, C.B., Scott, S.D., & Ferris, F.G. (2003) Characterization of bacteriogenic iron oxide deposits from Axial Volcano, Juan de Fuca Ridge, Northeast Pacific Ocean. *Geomicrobiology Journal*, *20*, 199–214.

Klein, B. & Siedler, G. (1989) On the origin of the Azores current. *Journal of Geophysical Research B, 94*, 6159–6168.

Klitgaard, A. B. (1995). The fauna associated with outer shelf and upper slope sponges (Porifera, Demospongiae) at the Faroe Islands, Northeastern Atlantic. *Sarsia*, *80*, 1-22.

Klitgaard, A. B., & Tendal, O.S. (2004). Distribution and species composition of mass occurrences of large-sized sponges in the northeast Atlantic. *Progress in Oceanography*, *61*, 57–98.

Kükenthal, W. V. (1915). *Pennatularia*. Das Tierreich. Volume 43. R. Friedländer und Sohn, Berlin, 132.

Lacombe, H., & Richez, C. (1982). The regime of the Strait of Gibraltar. Elsevier, *Oceanography Series*, 34, 13-73.

Lauridsen, B. W., Bjerager, M., & Surlyk, F. (2012). The middle Danian Faxe Formation—new lithostratigraphic unit and a rare taphonomic window into the Danian of Denmark. *Bulletin of the Geological Society of Denmark*, *60*, 47–60.

Le Danois, E. (1948). *Les Profondeurs de la Mer.* Payot, Paris.

Lourenço, N. L. J. F., Miranda, J. M., Luis, J. F., Ribeiro, A., Victor, L. M., Madeira, J., & Needham, H. D. (1998). Morpho-tectonic analysis of the Azores Volcanic Plateau from a new bathymetric compilation of the area. *Marine Geophysical Research, 20*(3), 141-156.

Luis, J. F., & Miranda, J. M. (2008). Reevaluation of magnetic chrons in the North Atlantic between 35 N and 47 N: Implications for the formation of the Azores Triple Junction and associated plateau. *Journal of Geophysical Research: Solid Earth, 113*(B10).

Mah, C., Nizinski, M., & Lundsten, L. (2010). Phylogenetic revision of the Hippasterinae (Goniasteridae; Asteroidea): systematics of deep sea corallivores, including one new genus and three new species. *Zoological Journal of the Linnean Society*, 160, 266-301.

Marques, F. O., Catalão, J. C., DeMets, C., Costa, A. C. G., & Hildenbrand, A. (2013). GPS and tectonic evidence for a diffuse plate boundary at the Azores Triple Junction. *Earth and Planetary Science Letters, 381*, 177-187.

Martin, A. (2014). Implementation of Coral Habitat Areas of Particular Concern (CHAPCs): South Atlantic Fishery Management Council process. In: Bortone, S.A. (ed.) *Interrelationships between corals and fisheries*. CRC Marine Biol Ser No. 16. CRC Press, Boca Raton, 39–50.

Masson D. G. (2001). Sedimentary processes shaping the eastern slope of the Faroe-Shetland Channel. *Continental Shelf Research*, 21, 825–857.

McCosker, J. E., & Ross, S. W. (2007). A new deepwater species of the snake eel genus *Ophichthus* (Anguilliformes: Ophicthidae), from North Carolina. *Copeia*, 2007(4), 783-787.

McKenna, C., Berx, B., & Austin, W. E. N. (2016). The decomposition of the Faroe-Shetland Channel water masses using Parametric Optimum Multi-Parameter analysis. *Deep-Sea Research Part I: Oceanographic Research Papers*, 107, 9-21.

Menezes, G. M., Diogo, H., & Giacomello, E. (2013). Reconstruction of demersal fisheries history on the Condor seamount, Azores archipelago (Northeast Atlantic). *Deep Sea Research Part II: Topical Studies in Oceanography*, 98, 190–203.

MNHN-SPN & GIS-Posidonie (2014). *Méthodologie et Recommandations pour l'Extension du Réseau Natura 2000 Au-delà de la mer Territoriale pour l'Habitat récifs* (1170): Région Biogéographique Marine Atlantique. Rapport SPN 2014.

Morato, T., Kvile, K.Ø., Taranto, G.H., Tempera, F., Narayanaswamy, B.E., Hebbeln, D., Menezes, G.M., Wienberg, C., Santos, R.S. & Pitcher, T.J. (2013) Seamount physiography and biology in the north-east Atlantic and Mediterranean Sea. *Biogeosciences*, 10, 3039–3054.

Morato, T., Machete, M., Kitchingman, A., Tempera, F., Lai, S., Menezes, G., Pitcher, T.J. & Santos, R.S. (2008) Abundance and distribution of seamounts in the Azores. *Marine Ecology Progress Series*, 357, 17–21.

Morato, T., Pitcher, T. J., Clark, M. R., Menezes, G. M., Tempera, F., Porteiro, F. M., Giacomello, E., & Santos, R. S. (2010). Can We Protect Seamounts for Research? A Call for Conservation. *Oceanography*, 23, 190–199.

Morrison, C.L., Ross, S. W., Nizinski, M. S., Brooke, S., Järnegren, J., Waller, R. G., Johnson, R. L., & King, T. L. (2011). Genetic discontinuity among regional populations of *Lophelia pertusa* in the North Atlantic Ocean. *Conservation Genetics*, 12, 713-729.

Moser, M. L., Ross, S. W., & Sulak, K. J. (1996). Metabolic responses to hypoxia of *Lycenchelys verrillii* (wolf eelpout) and *Glyptocephalus cynoglossus* (witch flounder): sedentary bottom fishes of the Hatteras/Virginia Middle Slope. *Marine Ecology Progress Series*, 144, 57-61.

Murillo F. J., Durán Muñoz, P., Cristobo J., Ríos P., González C., Kenchington E., Serrano, A. (2012). Deep-sea sponge grounds of the Flemish Cap, Flemish Pass and the Grand Banks of Newfoundland (Northwest Atlantic Ocean): distribution and species composition. *Marine Biology Research*, 8, 842-854.

Murillo, F. J., Durán Muñoz, P., Altuna, A., & Serrano, A. (2011). Distribution of deep-water corals of the Flemish Cap, Flemish Pass, and the Grand Banks of Newfoundland (Northwest Atlantic Ocean): interaction with fishing activities. *ICES Journal of Marine Science*, 68, 319-332.

Murillo, F. J., Kenchington, E., Tompkins, G., Beazley, L., Baker, E., Knudby, A., & Walkusz, W. (2018). Sponge assemblages and predicted archetypes in the eastern Canadian Arctic. *Marine Ecology Progress Series,* 597, 115-135.

Navas, J.M., Miller, P.L., Henry, L.-A., Hennige, S.J. & Roberts, J.M. (2014) Ecohydrodynamics of cold-water coral reefs: a case study of the Mingulay Reef Complex (Western Scotland). *PLoS ONE*, 9 [doi: 10.1371/journal.pone.0098218].

Nielsen, J. G., Ross, S. W., & Cohen, D. M. (2009). Atlantic occurrence of the genus *Bellottia* (Teleostei, Bythitidae) with two new species from the Western North Atlantic. *Zootaxa*, 2018, 45-57.

Obelcz, J., Brothers, D., Chaytor, J., ten Brink, U., Ross, S. W., & Brooke, S. (2014). Geomorphic characterization of four shelf-sourced submarine canyons along the U.S Mid-Atlantic continental margin. *Deep-Sea Research Part II: Topical Studies in Oceanography*, 104, 106-119.

Omarsdottir, S., Einarsdottir, E., Ögmundsdottir, H., Freysdottir, J., Olafsdottir, E., Molinski, T., *et al.* (2013). Biodiversity of benthic invertebrates and bioprospecting in Icelandic waters. *Phytochemistry Reviews,* 12(3)**,** 517-529. doi: 10.1007/s11101-012-9243-7.

Orejas, C., Addamo, A., Álvarez, M., Aparicio, A., Alcoverro, D., Arnaud-Haond, S., *et al.* (2017). *Cruise report MEDWAVES survey. (MEDiterranean out flow WAter and Vulnerable EcosystemS)* ATLAS Project H2020, 211 & Appendixes.

Packer, D. B., Nizinski, M. S., Bachman, M. S., Drohan, A. F., Potti, M., & Kinlan, B. P. (2017). State of Deep-Sea Coral and Sponge Ecosystems of the Northeast United States. In: Hourigan, T. F., Etnoyer, P. J., Cairns, S. D. (eds.). *The State of Deep-Sea Coral and Sponge Ecosystems of the United States.* NOAA Technical Memorandum NMFS-OHC-4, Silver Spring, MD., 60.

Pałgan, D., Devey, C.W., & Yeo, I.A. (2017). Volcanism and hydrothermalism on a hotspot–influenced ridge: Comparing Reykjanes Peninsula and Reykjanes Ridge, Iceland. *Journal of Volcanology and Geothermal Research,* 348**,** 62-81.

Palma, C., Lillebø, A.I., Borges, C., Souto., M., Pereira, E., Duarte, A.C. & Abreu, M.P. (2012). Water column characterisation on the Azores platform and at the seamounts south of the archipelago. *Marine Pollution Bulletin*, 64, 1884–1894.

Palomino, D., López-González, N., Vázquez, J. T., Fernández-Salas, L. M., Rueda, J. L. et al. (2016a). Multidisciplinary study of mud volcanoes and diapirs and their relationship to seepages and bottom currents in the Gulf of Cádiz continental slope (northeastern sector). *Marine Geology*, 378, 196–212.

Palomino, D., Vázquez, J.-T., Somoza, L., León, R., López-González, N., Medialdea, T., et al. (2016b). Geomorphological features in the southern Canary Island Volcanic Province: The importance of volcanic processes and massive slope instabilities associated with seamounts. *Geomorphology*, 255, 125–139.

Pastor, M., Peña-Izquierdo, J., Pelegrí, J., & Marrero-Díaz, Á. (2012). Meridional changes in water mass distributions off NW Africa during November 2007/2008. *Ciencias Marina,* 38, 223–244.

Pastor, M., Vélez-Belchí, P., & Hernández-Guerra, A. (2015). Water Masses in the Canary Current Large Marine Ecosystem. *IOC Technical Series,* 15, 733–79.

Patarnello, T., Volckaert, F.A.M.J., & Castilho, R. (2007). Pillars of Hercules: is the Atlantic-Mediterranean transition a phylogeographical break? *Molecular Ecology*, 16, 4426-4444.

Porteiro, F.M., Gomes-Pereira, J.N., Pham, C.K., Tempera, F. & Santos, R.S. (2013). Distribution and habitat association of benthic fish on the Condor seamount (NE Atlantic, Azores) from in situ observations. *Deep-Sea Research Part II: Topical Studies in Oceanography,* 98, Part A, 114-128.Quartau, R., Ramalho, R., Rivera, J., Orejas, C., Tempera, F., Afonso, P., & Ricchi, A. (2018). The morphology of the Formigas Bank and its significance to the onset of Terceira Rift. *Geophysical Research Abstracts*, Vol. 20, EGU2018-8879.

Quattrini, A. M., Ross, S. W., Carlson, M. C. T., & Nizinski, M. S. (2012). Megafaunal-habitat associations at a deep-sea coral mound off North Carolina, USA. *Marine Biology*, 159, 1079-1094.

Ramalho, L. V., López-Fé, C, M., & Rueda, J. L. (2018). Three species of *Reteporella* (Bryozoa: Cheilostomata) in a diapiric and mud volcano field of the Gulf of Cádiz, with the description of *Reteporella victori* n. sp. *Zootaxa*, 4375(1), 090–104.

Ramiro-Sánchez B., Gonzalez I, J., Henry, L. A., Cleland, J., Yeo, I., Xavier, J.R., Carreiro-Silva, M., Sampaio, I., Spearman, J., Victorero, L., Messing, C., Kazanidis, G., Roberts, J.M., & Murton, B (2019, in press). Characterization and mapping of a deep-sea sponge ground on the Tropic Seamount (Northeast tropical Atlantic): implications for spatial management in the High Seas. *Frontiers in Marine Science, 6*, 278.

Rhein, M., Steinfeldt, R., Kieke, D., Stendardo, I., & Yashayaev, I. (2017). Ventilation variability of Labrador Sea Water and its impact on oxygen and anthropogenic carbon: a review. *Philosophical Transactions of the Royal Society A: Mathematical, Physical and Engineering Sciences*, 375 (2102). 20160321. doi:10.1098/rsta.2016.0321.

Roberts, J. M., Brown, C. J., Long, D., & Bates, C. R. (2005). Acoustic mapping using a multibeam echosounder reveals cold-water coral reefs and surrounding habitats. *Coral Reefs*, 24, 654-669.

Roberts, J. M., Davies, A. J., Henry, L., Dodds, L. A., Duineveld, G. C. A., Lavaleye, M. S. S., Maier, C., van Soest, R.W.M., Bergman, M.J.N., Huhnerbach, V., Huvenne, V.A.I., Sinclair, D. J., Watmough, T., Long, D., Green, S. L., & van Haren, H. (2009). Mingulay reef complex: an interdisciplinary study of cold-water coral habitat, hydrography and biodiversity. *Marine Ecology Progress Series*, 397, 139-151.

Rolán, M. E. (1983). Moluscos de la ria de Vigo 1. Gasteropodes. *Thalassas*, 1 (1) Anexo 1, 1-383.

Ross, S. W., & M.S. Nizinski. (2007). State of Deep Coral Ecosystems in the U.S. Southeast Region: Cape Hatteras to southeastern Florida. p. 233-270, Ch 6 In: Lumsden, S. E., Hourigan, T. F., Bruckner, A. W. & Dorr,G. (eds.). *The State of Deep Coral Ecosystems of the United States*. NOAA Tech. Memo. CRCP-3. Silver Spring, MD., 365.

Ross, S. W., & Quattrini, A. M. (2007). The Fish Fauna Associated with Deep Coral Banks off the Southeastern United States. *Deep-Sea Research Part I: Oceanographic Research Papers,* 54(6), 975-1007.

Ross, S. W., & Quattrini, A. M. (2009). Deep-sea reef fish assemblage patterns on the Blake Plateau (Western North Atlantic Ocean). *Marine Ecology*, 30, 74-92.

Ross, S. W., Aschenbach E. F., III & J. Ott. (2001). *Literature and data inventory related to the Hatteras Middle Slope ("The Point") Area Off North Carolina.* Occasional Papers of the NC State Museum of Natural Sciences and the NC Biol. Surv. No. 13. Raleigh, NC, 352 p + appendix.

Ross, S. W., Rhode, M. & Quattrini, A. M. (2015). Demersal fish distribution and habitat use within and near Baltimore and Norfolk Canyons, U.S. middle Atlantic slope. *Deep-Sea Research Part I: Oceanographic Research Papers,* 103, 137-154.

Ross, S. W., Rhode, M., Viada, S. T., & Mather, R. (2016). Fish species associated with shipwreck and natural hard- bottom habitats from the middle to outer continental shelf of the Middle Atlantic Bight near Norfolk Canyon. *Fishery Bulletin,* 114, 45-57.

Rowden, A. A., Schlacher, T. A., Williams, A., Clark, M. R., Stewart, R., Althaus, F., et al. (2010). A test of the seamount oasis hypothesis: seamounts support higher epibenthic megafaunal biomass than adjacent slopes. *Marine Ecology*, 31, 95–106.

Rueda, J. L., González-García, E., Krutzky, C., López-Rodríguez, F. J., Bruque, G., et al (2016). From chemosynthesis-based communities to cold-water corals: Vulnerable deep-sea habitats of the Gulf of Cádiz. *Marine Biodiversity*, 46(2), 473-482.

Sampaio, Í., Freiwald, A., Porteiro, F. M., Menezes, G., & Carreiro-Silva, M. (2019). Census of Octocorallia (Cnidaria: Anthozoa) of the Azores (NE Atlantic): a nomenclature update. *Zootaxa*, 4550 (4), 451–498. http://dx.doi.org/10.11646/zootaxa.4550.4.1.

Sampaio, Í., Stokvis, F.R., & Ofwegen, L. P. V. (2016). New name for the soft coral Alcyonium rubrum Stokvis & van Ofwegen, (2006) (Alcyonacea, Alcyoniidae): Alcyonium burmedju nom. n. *Zookeys*, 619, 163–165. https://doi.org/10.3897/zookeys.619.10086.

Sampaio, I., Braga-Henriques, A., Pham, C., Ocana, O., De Matos, V., Morato, T. & Porteiro, F.M. (2012) Cold-water corals landed by bottom longline fisheries in the Azores (north-eastern Atlantic). *Journal of the Marine Biological Association of the U.K,* 92,1547-1555.Santos, R.S., Hawkins, S., Monteiro, L.R., Alves, M. & Isidro, E.J. (1995). Marine research, resources and conservation in the Azores. *Aquatic Conservation: Marine and Freshwater Ecosystems,* 5, 311–354.

Schmincke, H. -U., & Graf, G. (2000). *DECOS / OMEX II, Cruise No., 43*, 25 November 1998 - 14 January 1999. Hamburg: Leitstelle METEOR, Institut für Meereskunde der Universität Hamburg doi:10.2312/cr_m43.

Scientific Advisory Committee on Fisheries (SAC). *Report of the second meeting of the Working Group on Vulnerable Marine Ecosystems (WGVME).* FAO headquarters, Rome, Italy, 26 – 28 February 2018. 57p.

Serrano, A., González-Irusta, J. M., Punzón, A., García-Alegre, A., Lourido, A., Ríos, P., et al. (2017). Deep-sea benthic habitats modeling and mapping in a NE Atlantic seamount (Galicia Bank). *Deep-Sea Research Part I: Oceanographic Research Papers*, 126, 115–127.

Simões, A., Duarte, R., & Alves, M. (1997). A pilot ocean monitoring site at Azores islands. pp. 444-454. In J. H. Stel, H. W. A. Behrens, J. C. Borst, L. J. Droppert & J. P. van der Meulen (eds.). Operational Oceanography: The Challenge for European Co-Operation. Proceedings of the First International Conference on EUROGOOS. Elsevier Science Ltd, The Hague.

Sinclair, D. J., Williams, B., Allard, G., Ghaleb, B., Fallon, S., Ross, S. W., & Risk, M. (2011). Reproducibility of trace element profiles in a specimen of the deep-water bamboo coral *Keratoisis* spp. *Geochimica et Cosmochimica Acta*, 75, 5101-5121.

Skarke, A., Ruppel, C., Kodis, M., Brothers, D., & Lobecker, E. (2014). Widespread methane leakage from the seafloor on the northern US Atlantic margin. *Nature Geosciences*, 7, 657–661.

Stevenson, A., & Rocha, C. (2013). Evidence for the bioerosion of deep-water corals by echinoids in the Northeast Atlantic. *Deep Sea Research Part I: Oceanographic Research Papers, 71, 73-78.*

Stokvis, F. R., & Ofwegen, L. P. V. (2006). New and redescribed encrusting species of Alcyonium from the Atlantic Ocean (Octocorallia: Alcyonacea: Alcyoniidae). *Zoologische Mededelingen*, 80 (4), 165–183.

Sulak, K. J., & Ross, S. W. (1996). Lilliputian bottom fish fauna of the Hatteras upper middle continental slope. *Journal of Fish Biology*, 49 (Suppl. A), 91-113.

Tarasov, V., Gebruk, A., Mironov, A., & Moskalev, L. (2005). Deep-sea and shallow-water hydrothermal vent communities: two different phenomena? *Chemical Geology,* 224(1-3)**,** 5-39.

Tempera, F., Carreiro-Silva, M., Jakobsen, K., Porteiro, F., Braga-Henriques, A. & Jakobsen, J. (2015). An Eguchipsammia (Dendrophylliidae) topping on the cone. *Marine Biodiversity, 45,* DOI 10.1007/s12526-014-0220-9

Tempera, F., Giacomello, E., Mitchell, N., Campos, A.S., et al. (2012) Mapping the Condor seamount seafloor environment and associated biological assemblages (Azores, NE Atlantic). In: Baker E, Harris P (eds) *Seafloor Geomorphology as Benthic Habitat: Geohab Atlas of Seafloor Geomorphic Features and Benthic Habitats.* Elsevier, New York, p 807-818Tempera, F., Atchoi, E., Amorim, P., Gomes-Pereira, J. & Gonçalves, J. (2013). *Atlantic Area Marine Habitats. Adding new Macaronesian habitat types from the Azores to the EUNIS Habitat Classification*. Technical Report No. 4/2013 - MeshAtlantic, IMAR/DOP-UAç, Horta, 126pp.

Thomas, C. J., Blair, N. E., Alperin, M. J., DeMaster, D. J., Jahnke, R. A., Martens, C. S., & L. Mayer (2002). Organic carbon deposition on the North Carolina continental slope off Cape Hatteras (USA). p. 4687-4709. In: Bauer, J. E., DeMaster, D. J., Repeta, D. J., & Verity, P.G. (eds.). Biogeochemistry and cycling of carbon in the northwest Atlantic continental margin: findings of the Ocean Margin Program. *Deep-Sea Research Part II: Topical Studies in Oceanography*, 49 (20).

Thornalley, D. J. R., Oppo, D. W., Ortega, P., Robson, J. I., Brierley, C. M., Davis, R., Hall, I. R., Moffa-Sanchez, P., Rose, N. L., Spooner, P. T., Yashayaev, I., & Keigwin, L.D. (2018). Anomalously weak Labrador Sea convection and Atlantic overturning during the past 150 years, *Nature*, 556, 227-230.

Tompkins, G., Baker, E., Anstey, L., Walkusz, W., Siferd, T. & Kenchington, E. (2017). Sponges from the 2010-2014 Paamiut Multispecies Trawl Surveys, Eastern Arctic and Subarctic: Class Demospongiae, Subclass Heteroscleromorpha, Order Poecilosclerida, Family Coelosphaeridae, Genera Forcepia and Lissodendoryx. *Canadian Technical Report of Fisheries and Aquatic Sciences, 3224,* v + 129pp. Vad J., Kazanidis G., Henry L, -A., Jones D. O. B., Tendal O. S., Christiansen S., Henry, T. B., & Roberts, J. M. (2018). Potential impacts of offshore oil and gas activities on deep-sea sponges and the habitats they form. *Advances in Marine Biology*, 79, 33-60.

van Aken, H. M. (2000a). The hydrography of the mid-latitude Northeast Atlantic Ocean I: the deep water masses. *Deep Sea Research Part I: Oceanographic Research Papers, 47*, 757–788.

van Aken, H. M. (2000b). The hydrography of the mid-latitude Northeast Atlantic Ocean II: the intermediate water masses. *Deep Sea Research Part I: Oceanographic Research Papers, 47,* 789–824.

van den Beld, I. M. J., Bourillet, J. -F., Arnaud-Haond, S., de Chambure, L., Davies, J. S., Guillaumont, B., Olu, K., & Menot, L. (2017). Cold-Water Coral Habitats in Submarine Canyons of the Bay of Biscay. *Frontiers in Marine Science, 4* (118).

van den Bogaard, P. (2013). The origin of the Canary Island Seamount Province - New ages of old seamounts. *Scientific Reports*, 3, 2107.

Van Dover, C.L. (2000) *The Ecology of Deep-sea Hydrothermal Vents.* Princeton University Press, Princeton, New Jersey. 424 pp.

Vázquez, J. T., Somoza, L., Rengel, J. A., Medialdea, T., Millán, A., Alcalá, C., et al. (2011). *Informe científico-técnico de la campaña oceanográfica DRAGO 0511. Ampliación de la plataforma continental de España al oeste de las islas Canarias.* Available at: http://www.repositorio.ieo.es/e-ieo/handle/10508/451 [Accessed October 10, 2018].

Weiß, B. J., Hübscher, C., & Lüdmann, T. (2015a). The tectonic evolution of the southeastern Terceira Rift/São Miguel region (Azores). *Tectonophysics*, 654, 75–95.

Weiß, B. J., Hübscher, C., Wolf, D., & Lüdmann, T. (2015b). Submarine explosive volcanism in the southeastern Terceira Rift/São Miguel region (Azores). *Journal of Volcanology and Geothermal Research*, 303, 79–91.

Wienberg, C., Wintersteller, P., Beuck, L. & Hebbeln, D. (2013). Coral Patch seamount (NE Atlantic)—a sedimentological and megafaunal reconnaissance based on video and hydroacoustic surveys. *Biogeosciences*, 10, 3421–3443.

Williams, B., Risk, M. J., Ross, S. W., & Sulak, K. J. (2006). Deep-water Antipatharians: proxies of environmental change. *Geology*, 34(9), 773-776.

Williams, B., Risk, M. J., Ross, S. W., & Sulak, K. J. (2007). Stable isotope data from deep-water Antipatharians: 400-year records from the southeastern coast of the United States of America. *Bulletin of Marine Science*, 81(3), 437-447.

Yashayaev, I., & Loder, J. W. (2016). Recurrent replenishment of Labrador Sea Water and associated decadal-scale variability, *Journal of Geophysical Research: Oceans*, *121*(11), 8095-8114, doi:10.1002/2016JC012046.

Yashayaev, I., & Loder, J. W. (2017). Further intensification of deep convection in the Labrador Sea in 2016, *Geophysical Research Letters,* 44, 1429–1438. doi:10.1002/2016GL071668.

Yashayaev, I., Seidov, D., & Demirov, E. (2015). A new collective view of oceanography of the Arctic and North Atlantic basins, *Progress in Oceanography*, 132, 1–21.

Yeo, I. A., Dobson, K., Josso, P., Pearce, R. B., Howarth, S. A., Lusty, P. A. J., Le Bas, T. P., & Murton, B. J. (2018) Assessment of the mineral resource potential of Atlantic ferromanganese crusts based on their growth history, microstructure, and texture. *Mineral*, 8, 327.

Zeppilli, D., Bongiorni, L., Cattaneo, A., Danovaro, R. & Santos, R.S. (2013). Meiofauna assemblages of the Condor Seamount (North-East Atlantic Ocean) and adjacent deep-sea sediments. *Deep Sea Research Part II: Topical Studies in Oceanography, 98,* 87-100Zibrowius, H. (1980). Les Scleractiniares de la Méditerranée et de l'Atlantique nord-oriental. *Bulletin du Musée océanographique de Monaco*, 11, 1–284.

CHAPTER 2 - Biogeography of the deep North Atlantic: Evaluating the 'Global Open Oceans and Deep Seabed' and the 'Ecological Marine Units' biogeographic classification systems

Project acronym:	ATLAS
Grant Agreement:	678760
Deliverable number:	D3.3
Deliverable title:	D3.3 Biodiversity, biogeography and GOODS classification system under current climate conditions and future IPCC scenarios
Work Package:	WP3
Date of completion:	31st May 2019
Author:	Berta Ramiro-Sánchez, Lea-Anne Henry, Telmo Morato, Gerald Taranto, Johanne Vad, Marina Carreiro-Silva, José Manuel González-Irusta,, Pablo Durán Muñoz, Mar Sacau, Ana García-Alegre, Carlos Dominguez-Carrió, Covadonga Orejas, Ellen Kenchington, Jake Rice, Zeliang Wang, Steve Ross, Lenaick Menot, Dierk Hebbeln, Bramley Murton, J. Murray Roberts

This project has received funding from the European Union's Horizon 2020 research and innovation programme under grant agreement No 678760 (ATLAS). This output reflects only the author's view and the European Union cannot be held responsible for any use that may be made of the information contained therein.

2 Chapter 2: Biogeography of the deep North Atlantic: Evaluating the 'Global Open Oceans and Deep Seabed' and the 'Ecological Marine Units' biogeographic classification systems in the deep North Atlantic

Berta Ramiro-Sánchez[1], Lea-Anne Henry[1], Telmo Morato[2], Gerald Taranto[2], Johanne Vad[1], Marina Carreiro-Silva[2], José Manuel González-Irusta[2,3], Pablo Durán Muñoz[3], Mar Sacau[3], Ana García-Alegre[3], Carlos Dominguez-Carrió[2], Covadonga Orejas[3], Ellen Kenchington[4], Jake Rice[4], Zeliang Wang[4], Steve Ross[5], Lenaick Menot[6], Dierk Hebbeln[7], Bramley Murton[8], J. Murray Roberts[1]

1- School of GeoSciences, The University of Edinburgh, UK, berta.ramiro@ed.ac.uk
2- IMAR-University of Azores, Portugal
3- Spanish Institute of Oceanography, Spain
4- Bedford Institute of Oceanography, Department of Fisheries and Oceans, Canada
5- Center for Marine Science, University of North Carolina-Wilmington, US
6- Laboratoire Environnement Profond, IFREMER, France
7- Center for Marine Environmental Sciences, University of Bremen, Germany
8- National Oceanography Centre, Southampton, United Kingdom

Contents

2.1 Executive summary

Understanding patterns of marine biogeography is essential for the adequate management of deep-sea ecosystems under increasing multiple pressures such as climate change, oil and gas activities, bottom trawling, and potentially in the future, deep-sea mining. Being able to identify and delineate ocean regions that harbour unique, endemic and rare species is important because these regions need to be accounted for and given adequate spatial management, e.g., as a criterion for the designation of an area as an Ecological or Biologically Significant marine Area (EBSA), or as part of a High Seas Marine Protected Area (MPA) network. If the full range of biogeographic regions is not considered in management decisions, we risk losing species and not adhering to the Convention on Biological Diversity (CBD) obligations to conserve biological diversity.

Unlike many Exclusive Economic Zones (EEZs), the limited records of species occurrence in Areas Beyond National Jurisdiction (ABNJs) have often restricted more comprehensive studies of the biogeography of deep-sea species. Environmental, historical and biological factors are known to be driving factors of species distribution, with biogeographic classifications being used to analyse patterns of marine biodiversity and advancing knowledge of evolutionary and ecosystem processes, even with this lack of information (e.g. Costello et al., 2017). It was recognised that biogeography of complex deep-sea habitats such as those created by some vulnerable marine ecosystem (VMEs) indicator taxa is especially poorly known, an issue that must be addressed as VMEs have international conservation and management significance through this designation.

Attempting to rectify the lack of biogeographic data for Earth's largest biome, the deep sea, must also be complemented by alternative approaches to understanding biogeographic patterns, and for this reason, several classification systems based purely on physiognomic proxies (seafloor bathymetry, oceanographic variables) have recently been promoted. This task in ATLAS focuses on (1) validating two existing biogeographical classification systems for complex habitats in the deep North Atlantic: the Global Open Oceans and Deep Seabed (GOODS; UNESCO, 2009) classification system and the Ecological Marine Units (EMUs), created by ESRI; and (2) looking at the drivers of bioregionalisation in the North Atlantic. In a later chapter in this Deliverable, we will also evaluate climate-induced changes in GOODS biogeographic provinces in the North Atlantic. Species-assemblage structure of several taxa across a range of localities in the North Atlantic were tested against marine provinces proposed by the GOODS and EMUs classifications. The whole dataset of available VME taxa in the North Atlantic, together with the Subclasses Hexacorallia and Octocorallia failed to show any significant differences in their distribution for any of the classifications, possibly indicating a widespread distribution. However, the biogeographical analysis to understand the drivers of bioregionalisation produced 36

clusters in the North Atlantic, which highlighted there is structure in the species composition of the basin. The main environmental predictor driving differences between areas was temperature followed by food supply and speed of currents. Together, these results point to a further division of the GOODS bathyal provinces in an eastern and western separation and, to some extent, a differentiation north and south of the Azores. Understanding the drivers of these regions in conjunction with forecasts of key VME species distribution models provides an outlook of how the GOODS provinces will change in future climate conditions and what regions acting as refugia might be potentially included in an MPA network. In particular, the bathyal depths will likely be the most affected with a general northwards extension, however the abyssal province will be impacted to a lesser extent. These results should be taken with caution as the available baseline data were heterogeneous and records were not well represented across the ocean basin. The study also highlighted the need for data collection and collaboration to ensure biogeographical analyses are robust and useful for the management of marine ecosystems.

2.2 Introduction

Biogeography is the study of the patterns and processes that govern the distribution of species in geographic space and through time. Often, marine biogeography seeks to partition the ocean into distinct regions or provinces based on species distributions. Defining these boundaries is however challenging because in the marine realm faunal discontinuities are not abrupt and vary with ocean basin and latitude (Watling et al., 2013). Indeed, there are only a few attempts to classify the deep-sea floor beyond the depths of the continental shelf (Watling et al., 2013). Even the mesopelagic zone (200 – 1000 m depth) has only been recently classified into biogeographical units using a semi-objective workflow based on expert knowledge on environmental drivers and faunal distributions (Sutton et al., 2017). Despite being highly under sampled, general patterns in the deep sea can still be described based on observations (McClain & Hardy, 2010). However, most of the deep seabed lies in ABNJs where the biogeography of VMEs has received relatively little attention and where governance is limited. Such ecosystems are often characterised by slow-growing, long-lived and late-maturing species, traits that limit their potential for resilience and recovery from human disturbances such as bottom-contact fishing and, potentially in the future, deep-sea mining (Ramirez-Llodra et al., 2011). Nevertheless, the distribution and driving factors of occurrence of most VMEs remain poorly understood mainly due to the difficulties of collecting benthic data from deep-water environments - especially in large areas far from land—and the costs associated with these explorations. Therefore, an improved understanding of VME marine biogeography can lead to better ocean governance in a

future ocean challenged by rapid rates of climate change and the exploitation of living and non-living resources in the deep ocean.

Biogeographic studies have focused on small groups of well-known species at regional scales to just a few more broad spatial scale studies (Costello et al., 2017). Main proposed regional boundaries were based on the distribution of model deep-sea benthic fauna, with most of them recognising that distribution patterns of faunal groups are defined by factors such as temperature and food supply (McClain et al., 2009, McClain & Schlacher, 2015). These groups included isopods (Kussakin, 1973; Menzies et al., 1973), tunicates (Monniot, 1979), asteroids (Sibuet, 1979), brachiopods (Zezina, 1997), bivalves and gastropods (Linse et al., 2006). Specialised habitats with distinct evolutionary history and ecological factors such as hydrothermal vents (Van Dover, 2000; Bachraty et al., 2009) and cold seeps (Sibuet & Oly, 1998; Levin, 2005) have also been classified. Because the bathyal (300 – 3,500 m depth) is characterized by a complex topography and heterogeneous habitat, classifications have mostly focused on the abyssal (Menzies et al., 1973; Kussakin, 1973; Vinogradova, 1979) and hadal (Belyaev, 1989) depth zones, much more homogenous and accessible at the times when deep-sea exploration started. Focus on the bathyal included the study of specific areas such the Nazca and Sala y Gomez Ridges (Parin et al., 1997) and the Southern Ocean (Linse et al., 2006). Zezina (1997) reviewed all available bathyal studies until then and summarised the classifications but mainly based it on brachiopods. Cairns & Chapman (2001) investigated the distribution of deep-sea scleractinian corals across 38 geographic regions in the North Atlantic using cluster analysis and found three superclusters: western Atlantic, eastern Atlantic and a cold-temperate Atlantic. Russian scientists have prolifically sampled the bathyal of the Mid-Atlantic Ridge between the Azores and the Reykjanes Ridge (Gebruk et al., 2010) and suggested their biogeographic origins (Mironov & Gebruk, 2006; Mironov & Krylova, 2006).

Many biogeographic classifications are based on limited biological datasets and many exhibit a high level of endemism in many deep-sea habitats. As a result, this limited data may not be easily generalized because different taxa will show different biogeographies as a reflection of their evolutionary history and environmental adaptations (Costello et al., 2017). In addition, new information on a species may invalidate previously observed patterns by altering the importance of responsible factors or by highlighting the limitedness of the data creating artefacts in the data (Costello et al., 2017). In order to tackle data limited situations, biogeographic classifications have been based on oceanographic proxies to predict areas likely to have different faunal compositions (Watling et al., 2013).

The latest deep seabed classification systems are the Global Open Oceans and Deep Seabed (GOODS) (UNESCO, 2009; Watling, 2013) and the Ecological Marine Units (Sayre et al., 2017). The GOODS classification is an expert opinion- and hypotheses- driven approach that divides the ocean into pelagic and benthic biogeographic provinces based on environmental variables (UNESCO, 2009; Watling, 2013). The environmental variables used thought to be good indicators of species distribution were depth (ETOPO2 and Srtm30 bathymetric data); temperature, salinity and oxygen from the 2009 World Ocean Atlas (WOA) dataset; and particulate organic flux (POC) from Lutz et al. (2007). The pelagic zone was divided into 30 biogeographic provinces mostly based on oceanographic and bathymetric information. The benthic zone was divided into three main depth layers: the bathyal (800 – 3,500 m), the abyssal (3,500 – 6,500 m) and the hadal (>6,500 m). The start of the classification at 800 m attempts to address the lack of knowledge pertaining to ABNJs as, with a few exceptions, the upper bathyal (300 – 800 m) is within national EEZs (Watling et al., 2013). Provinces were initially hypothesized based on environmental and biological data by scientists at a workshop using expert knowledge, and later reviewed. The proposed benthic biogeographic provinces were 14 for the bathyal, 13 for the abyssal and 10 for the hadal zone. GOODS divides the North Atlantic lower bathyal into three provinces: the Arctic (BY1), Northern Atlantic Boreal (BY2) and North Atlantic (BY4). The Arctic province shows very cold temperatures (mean of -0.7°C) and a POC flux of 5.2 $g \cdot m^{-2} \cdot yr^{-1}$. The Northern Atlantic Boreal is characterised by an average temperature of 3°C, an average salinity of 34.9 psu, and reduced POC flux, but with spring bloom pulses. The North Atlantic province has a higher average temperature (5.58°C) and variable POC flux. On the other hand, the abyssal zone shows only one province (AB2) characterized by the influence of the North Atlantic Deep Water and a POC flux with a latitudinal gradient. The extent of these provinces is shown in Figure 62.

In contrast, Sayre et al. (2017) followed a quantitative, unsupervised approach to produce the EMUs, which partitions the global oceans using k-means clustering. Similarly to GOODs, EMUs are based on physical and chemical environmental data, have a global extent and a three-dimensional application representing the whole water column. Environmental data for EMUs were derived from the 2013 World Ocean Atlas dataset, and included temperature, salinity, oxygen, nitrate, phosphate, and silicate. The optimal cluster number indicated the presence of 37 three-dimensional mutually exclusive EMUs across the world's oceans. These units are not to be confused with water masses because of their unknown geographic origin, but rather as volumetric regions with a homogeneous composition (Sayre et al., 2017). In the deep North Atlantic, EMU classification predicts five provinces. The provinces are numbered and their technical name concatenates the water column depth with the province specific environmental values. These correspond to province 29 (deep, very cold, normal salinity, moderate oxygen, medium nitrate, low phosphate and silicate); 36 (bathypelagic, very cold,

euhaline, oxic, medium nitrate, low phosphate and silicate); 37 (bathypelagic, very cold, euhaline, oxic, high nitrate, low phosphate, medium silicate); 13 (bathypelagic, very cold, euhaline, hypoxic, high nitrate, medium phosphate, high silicate); 14 (bathypelagic, very cold, euhaline, oxic, high nitrate, low phosphate, high silicate). The extent of the EMUs provinces are shown in Figure 63. See also Table 4 for a summary of environmental values from both biogeographic classification systems.

Understanding connectivity is critical to the interpretation of any spatial or temporal changes in the High Seas (UNESCO, 2009), which is of particular relevance to protecting VMEs, given the limited knowledge on distribution patterns. Despite its coarse resolution, the GOODS system might offer the potential to delineate EBSAs required by the CBD (2009), as it provides data on basin-scale processes and geographic boundaries (Gregr et al., 2012). Nevertheless, the GOODS classification still requires to be validated with species distribution data, particularly for the lower bathyal, as many of the provinces in this realm have few data (Watling et al., 2013) and also to account for projected climate change scenarios. The GOODS provinces should be considered as centres of distribution of deep-sea fauna, as province boundaries are uncertain and they are most likely to be transition zones rather than absolute boundaries (Watling et al., 2013).

Biogeographic classifications have been used to analyse patterns of biodiversity and advancing knowledge in understanding evolutionary and ecosystem processes (e.g. Spalding et al., 2007; Briggs & Bowen, 2012), even when this information is limited in certain regions (Rice et al., 2011). Based on environmental variables or biological information, or a combination of both, biogeographic classifications are hypotheses-driven exercises that 'reflect biological units with a degree of common history and coherent response to perturbations and management actions' (UNESCO, 2009). These units are relatively unique at a chosen scale (UNEP-WCMC, 2007) and have several potential uses in marine policy and management. Rice et al. (2011) summarised their value for identifying: (1) units for monitoring and assessing status, trends and threats (e.g. environmental reporting); (2) units for ecosystem-based management of human activities (e.g. implementation of area-based management measures such as MPAs, fisheries conservation measures and identification of VMEs); and (3) units used to research responses to climate change scenarios (e.g. habitat predictive modelling, research planning). The information fed into these policy-making processes and management initiatives needs to be based on comprehensive biogeographic data (Rice et al., 2011), but after years of mapping global marine regions, there are still no robust biogeographic boundaries delineated in the ocean (Costello et al., 2017), namely in the deep sea.

The aim of this task was to validate the existing biogeographical classifications GOODS (UNESCO, 2009; Watling et al., 2013) and EMUs (Sayre et al., 2017) for VME indicator species in the deep North Atlantic;

to propose a new biogeography classification below 200 m in the North Atlantic that could better explain deep-sea biogeography. The specific objectives of this work were to design a hierarchical classification system for VME indicator taxa and evaluate the performance with the GOODS and EMUs classification tools to document the relationship between environmental proxy classifications and species diversity. In particular, to test whether the existing classifications are suitable for all VME taxa and for taxon groups individually. By comparing these classifications with new biogeographic realms resulting from a data-driven approach we aimed to pinpoint important factors in biogeography. Due to the international conservation and management significance of VMEs, the results of addressing VME biogeography can help in understanding patterns in taxonomic richness and provide a tool for spatial management of the deep-seabed. Additionally, we used the outputs of the habitat suitability models for key cold-water coral species under future (2081-2100) climate projections (RCP8.5 or a business-as-usual scenario) to evaluate the climate-induced changes in GOODS biogeographic provinces in the North Atlantic.

2.3 Methodology

2.3.1 Data

GOODS and EMUs biogeographic provinces

The GOODS provinces were obtained from Watling et al. (2013). The original EMUs created by Sayre et al. (2017) were downloaded from the ESRI website for the Atlantic Ocean (EMUs V1. Atlantic Ocean) and for the Arctic Ocean (EMUs V1. Arctic Ocean). Data were available in the format of a point mesh at 0.25° cell grid resolution at different depth levels. The layer corresponding to the bottom depth was selected and initially filtered to obtain records beyond 200 m depth. These data were then converted into polygons for the bottom depth level. The EMUS were re-sampled to generate EMUs at 1° cell grid resolution following preliminary observations of the sparse distribution of the species data. Geoprocessing of the data was performed using ArcGIS 10.6.1.

VME indicator species

Occurrence data from VME species were compiled in an effort from partners of the EU-ATLAS project, literature and the publicly available OBIS, ICES, and NOAA databases. We focused on species-level biogeography because a rigorous assessment of benthic biogeography of the deep sea is still lacking

and, given the threats of climate change and deep-sea exploration, it should be addressed. The queried taxa comprised the classes Hexacorallia, Octocoralia, Hydrozoa, the molluscs class Bivalvia, the order Decapoda (Crustacea), the class Crinoidea (Phylum Echinodermata) and the Phylum Porifera. Georeferenced presence-only records were obtained from public databases such as the Ocean Biogeographic Information System portal (OBIS), the NOAA Deep Sea Coral Data Portal, and the ICES VMEs data portal. Additional data was obtained from institutional databases of ATLAS partners participating in this work to include more recent species records of information held by research institutes. The species required were *Acanthogorgia armata*, *Acanella arbuscula*, *Lophelia pertusa*, *Madrepora oculata*, *Paragorgia arborea* and *Desmophyllum dianthus*. Data were obtained from the Department of Fisheries and Oceans (DFO; Canada), Spanish Institute of Oceanography (IEO, Spain), IFREMER, (France), University of Edinburgh (UK), University of Bremen-Marum (Germany), and the University of North Carolina Wilmington (US). The point species records encompassed areas along the east coast of US and Canada, the Bay of Biscay, Bermuda, the Logachev Mounds and the Tropic Seamount (Ramiro-Sánchez et al., in press).

A literature search provided records of deep-sea corals and sponges, mainly (Tabachnick & Menshenina, 2002; Cairns, 2006; Cairns & Bayer, 2006; Cairns, 2007; Carvalho et al., 2015; Molodtsova, 2006; Molodtsova, 2011; Molodtsova et al., 2008; Simpson & Watling, 2011; Tabachnick & Collins, 2008; Pante & Watling, 2012; Hestetun et al., 2015; Watling, 2015; Xavier et al., 2015; Howell et al., 2016; Cárdenas et al., 2017).

The species names were manually matched to the World Register of Marine Species and inspected for errors to identify misspellings and synonyms. Taxonomic errors are also possible in the data, but we have used the best available data. We excluded records with land locations and those located in areas shallower than 200 m based on GEBCO bathymetry. The depth entries in OBIS contain errors therefore the GEBCO and EMODnet bathymetric maps were used to assess the likely depth of occurrences. Species that only appeared once in the dataset were also removed to account for sampling bias. This resulted in 741 species names in the dataset. To test whether the biogeographic classifications represent different taxonomic groups, we categorised the VME indicator taxa into the following classes: stony corals; generic sponges; gorgonians; lace corals; sea pens; soft corals; black corals and stalked crinoids.

2.3.2 Validation of GOODS and EMUs

Since the GOODS classification system starts at 800 m water depth, only records below this depth level were retained from the original database to test biogeography with this system. In contrast, for the

EMUs analysis, all species records below 200 m were retained. A prerequisite of the comparison of community composition among biogeographic provinces is that species occurrence data were aggregated into study areas (Costello et al., 2017) and assigned to corresponding GOODS and EMUs provinces. This allowed investigation of what regions in the North Atlantic drive the differences between biogeographic provinces. Data were therefore aggregated into areas that generally followed large-scale seafloor or ocean features such as seamount chains, fracture zones, abyssal plains and oceanic ridges, but that also included the most data records. In such a manner, the study areas were thought to portray a coherent representation of historical events that might have led to evolutionary processes of the present species. Study areas were defined as: northern Mid-Atlantic Ridge north of the Azores, Mid-Atlantic Ridge south of the Azores, and southernmost Mid-Atlantic Ridge; Reykjanes Ridge; the New England abyssal plain and New England Seamounts; the Corner Seamounts, Rockall Bank, the Labrador Sea, the Flemish Cap, Canary Basin, Romanche Fracture and the South Azores Seamount Chain. The list of a priori study areas can be found in Table 4 and shown in Figure 62, Figure 63, and Figure 64. Data aggregation and delineation of study areas was conducted in ArcGIS v10.2.1. To assign a GOODS and EMUs' biogeographic province to each study area, the areas were overlaid with each classification system and the province that geographically corresponded to that study area was assigned. If a study area fell within two provinces, species records were assigned individually to the province they fell into. For instance: records found in the study area Tropic Seamount would be classified into province level bathyal (800 - 3,500) or abyssal (>3,500 m) in the GOODS classification. Equally, when testing against the EMUs classification, the records within the Tropic Seamount would be classified into levels according to the EMUs provinces found in the study area. Only areas that had three or more species were retained after removing species that occurred only once in the species-by-site matrix. This produced a total of 22 nested study areas for GOODS. For EMUs, 34 nested study areas were used for the biogeography of all VME indicator species; 22 nested study areas for the analysis of octocorals, and 17 nested study areas for the analysis of hexacorals.

Data were grouped by VME indicator groups into black corals, hydroids, stony corals, sponges, gorgonians and chemosynthetic taxa. Mapping of these groups revealed that there was insufficient data across taxa to conduct individual analyses for several coarser taxonomic levels, therefore we performed biogeographical analyses for all indicator species together for the GOODS and EMUs validation. Additionally, we also used the Subclasses Hexacorallia and Octocorallia to test the EMUs classification. Data were particularly limited for black corals and hydroids, while stony corals, sponges, gorgonians and chemosynthetic taxa included more species and records.

Table 4. List of a priori study areas created to aggregate species records as a pre-requisite for analysis to compare communities under the GOODS and EMUs biogeographic classification systems.

Study areas	
Canary Basin	New England Seamounts (NE Seamounts)
Condor Seamount (MOW Seamounts)	North Cape
Corner Seamounts	Norwegian Sea
Eastern North Atlantic	Reykjanes Ridge
Flemish Cap	Rockall Bank North
Labrador Sea	Rockall Bank South
Mid-Atlantic Ridge North (MAR N)	Romanche Fracture Zone
Mid-Atlantic Ridge South of the Azores (MAR S)	Sierra Leone Fracture Zone
Southernmost Mid-Atlantic Ridge (MAR S S)	South Azores Seamount Chain
New England Abyssal Plain (NE Basin)	Tropic Seamount

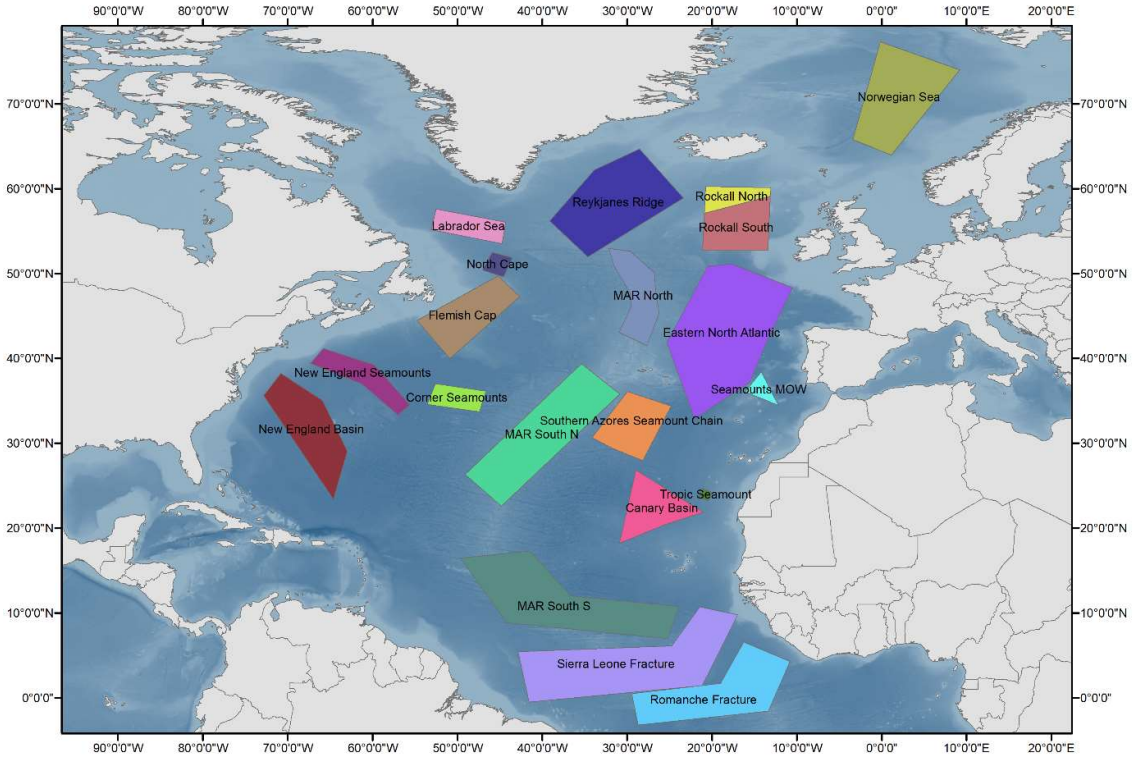

Figure 62. A priori study areas created to aggregate species records as a pre-requisite for analysis to compare communities under the GOODS and EMUs biogeographic classification systems.

We transformed the species occurrence dataset into a species/grid cell contingency table of presence and absence. We further removed species that appeared only once and retained those study areas that had three or more species. We used Jaccard's coefficient to compare the number of species common to a pair of geographic areas in proportion to the unique and total number of samples in both areas. This coefficient is: (C)/(A+B+C),

where C is the number of species present in both areas and A and B are the total number of species that only occur in each area. This coefficient gives more weight to the number of species' occurrence between the two areas than the joint absences. Jaccard's coefficient is one of the most widely used indices in biogeography for species' turnover and produces very similar results to other similarity indices (Costello et al., 2017). Hierarchical clustering with unweighted group-averaged linking (UPGMA) was then performed using this similarity matrix for all VME biogeography. We conducted a similarity profile test (SIMPROF) using the R package 'clustsig' to determine which clusters of areas are significant different ($p < 0.05$). A similarity percentage (SIMPER) analysis was applied to identify the species contributing most to differences between significant clusters. To test whether there was a significant relationship between the study areas and the biogeographical provinces we used permutational multivariate analysis of variance (permanova) using the R package 'vegan'. This test uses the results of a cluster analysis using a similarity index of preference and compares it with what groupings would arise randomly by permutation. All analyses were performed with the R software (R Core Development, 2018).

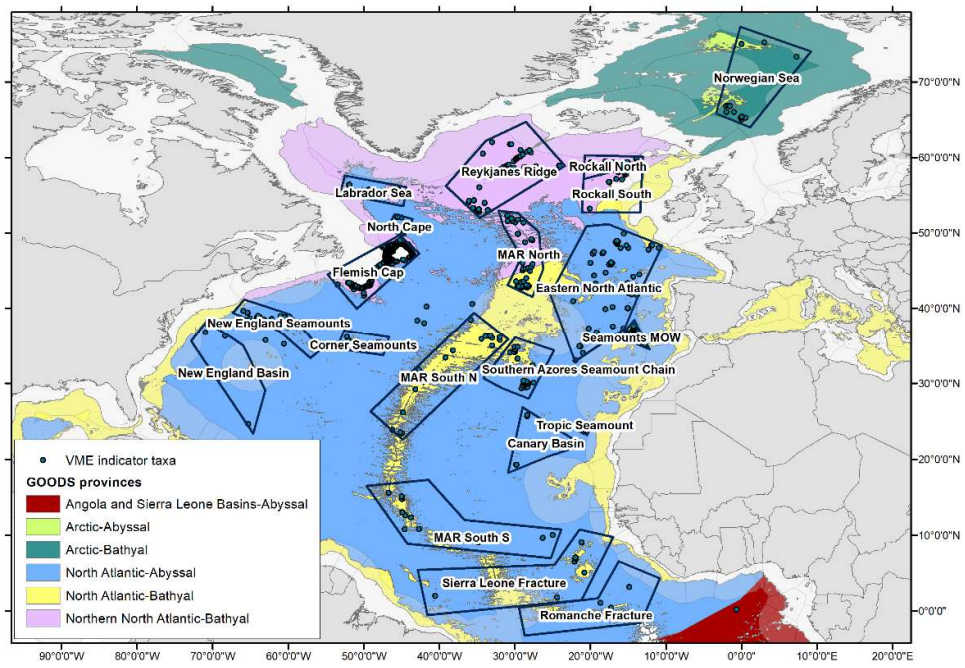

Figure 63. GOODS provinces in the North Atlantic. The High Seas are delimited by each country's EEZ. Only VME records below 800 m water depth and present in international waters were analysed (yellow dots). Data were aggregated into study areas shown as grey polygons and assigned to the GOODS province they overlapped.

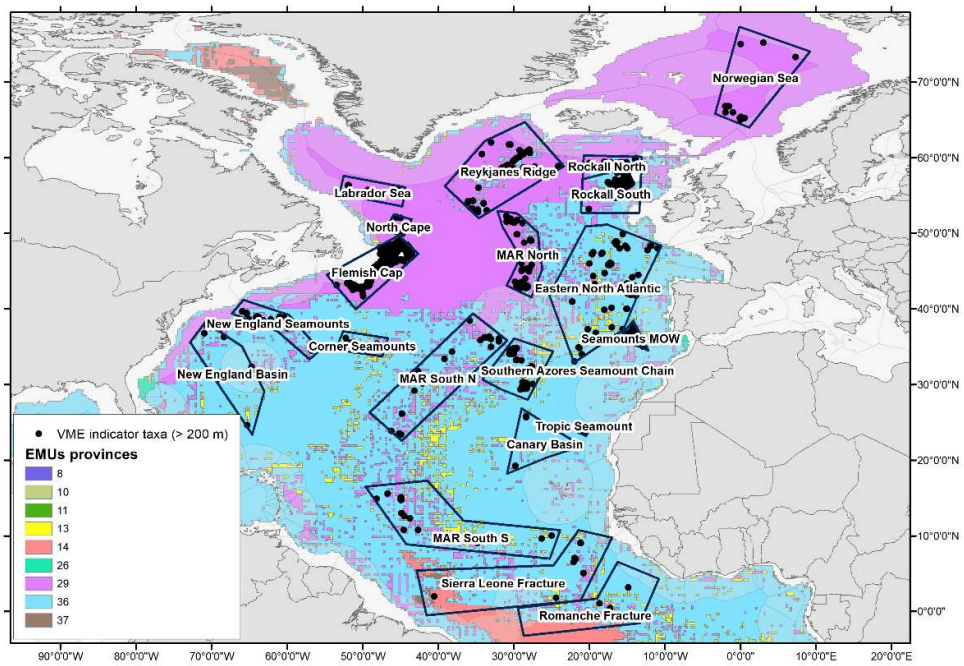

Figure 64. EMUs provinces, and their corresponding EMU number, in the North Atlantic. The High Seas are delimited by each country EEZ waters. Only VME records below 200 m water depth and present in international waters were analysed (black points). Data were aggregated into areas shown as grey polygons and assigned to the EMU province they overlapped.

2.3.3 Environmental drivers

Abiotic parameters

In order to test what environmental parameters drive VME biogeography in the North Atlantic, environmental data included a global bathymetry model (GEBCO 2014 Grid) downloaded at a resolution of 0.008° and the 2018 European digital terrain model (EMODnet) at a resolution of 1/16 arc minutes. The EMODnet bathymetric model was resampled using bilinear interpolation to the GEBCO bathymetry and both merged to obtain the highest resolution available at the North Atlantic basin-scale. A set of additional seafloor variables was derived from the bathymetric data, as quantitative seabed predictors, using the Benthic Terrain Model tool in ArcGIS 10.1 (ESRI, 2015). The variables were fine (3/25 radius) and broad-scale (25/250 radius) Bathymetric Position Index (BPI) and slope.

Environmental variables of present-day conditions were downloaded from the Earth System Grid Federation (ESGF) Peer-to-Peer (P2P) enterprise system (https://esgf-node.llnl.gov). These included particulate organic carbon (POC) flux at 100 m depth (epc100, mg $C \cdot m^{-2} \cdot d^{-1}$), dissolved oxygen concentration at seafloor ($mL \cdot L^{-1}$), pH at seafloor, potential temperature at seafloor (°C), carbonate

ion concentration ($CO3^{-2}$ mol·m^{-3}) at seafloor, and carbonate ion concentration (mol·m^{-3}) for seawater in equilibrium with pure aragonite and calcite at seafloor. The epc100 was converted to export POC flux (epc) at the seafloor using the Martin curve (Martin et al., 1987) following the equation: epc = epc100*(water depth/export depth)$^{-0.858}$, where the export depth was set to 100 m. Aragonite and calcite saturation state at seafloor were computed by dividing carbonate ion concentration (mol·m^{-3}) at seafloor by the carbonate ion concentration (mol·m^{-3}) for seawater in equilibrium with pure aragonite and calcite at seafloor. Other variables included were speed, direction and salinity from the period 1990 to 2015 at a resolution ~1/12 degree obtained from Wang et al. (2016). We downloaded additional environmental variables from the Bio-Oracle v2.0 dataset (Assis et al., 2017; Tyberghein et al., 2012) that represented conditions between 2000 and 2014. The variables included maximum currents velocity (m·s^{-1}) and maximum silicate concentration (mol·m^{-3}) at the seafloor. All abiotic variables were gridded and re-scaled to 2° grid cells by bilinear interpolation to match the species records spatial scale. The environmental characteristic properties of the North Atlantic provinces of the GOODS and EMUs are shown in Table 5.

To limit the effect of collinear variables and avoid Type I errors, we determined the correlation between the environmental predictors using the R package 'corrplot' (Wei & Simko, 2017). Known causal relationships (e.g. the determination of dissolved oxygen by water temperature) aided the identification of variables to exclude. Calcite, broad and fine BPI, pH and depth were removed from analysis as these variables showed strong correlation ($\rho \geq 0.7$) with aragonite, dissolved O_2, temperature and silicate (Figure 65). Furthermore, a forward stepwise selection step on consecutive RDA models further determined the significant environmental variables to be used in the statistical analysis. In total, seven environmental variables were used in the statistical analysis (Table 6).

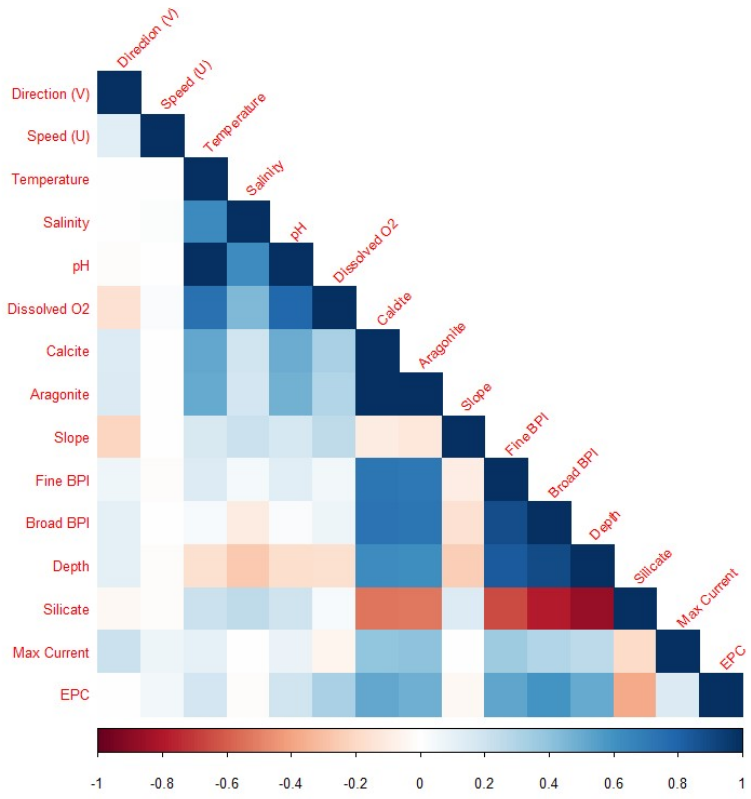

Figure 65. Correlation plot of available environmental variables. Variables showing strong correlation (ρ ≥ 0.7) with other factors were removed from the analysis.

Table 5. Environmental characteristic properties of the North Atlantic provinces of the GOODS and EMUs existing biogeographic classifications.

Classification	Province	Temperature (°C)	Salinity	Dissolved O2 (µmol/l)	Nitrate (µmol/l)	Phosphate (µmol/l)	Silicate µmol/l)	POC flux (g m-2 yr-1)
GOODS	Arctic (BY1)	-0.69	34.9		---	---	---	5.2
	Northern Atlantic Boreal (BY2)	3	34.9		---	---	---	
	North Atlantic (BY4)	5.58	35.6		---	---	---	
	Abyssal (AB2)	3	34.8		---	---	---	
EMUs	29	0.69	34.89	6.71	13.83	0.96	9.87	---
	36	4.58	34.76	5.27	22.74	1.53	27.13	---
	37	3.13	34.52	4.25	32.7	2.26	62.6	---
	13	1.93	34.67	3.26	37.03	2.6	138.03	---
	14	0.88	34.7	4.74	32.71	2.27	115.2	---

Table 6. Environmental variables considered in the redundancy analysis (RDA) models. Variables used in the final RDA are highlighted in bold.

Environmental variables	
Aragonite (Ωar)	**Maximum speed current ($m \cdot s^{-1}$)**
Calcite (Ωcal)	pH
Depth (m)	**Salinity (psu)**
Direction (V)	**Silicate ($mol \cdot m^{-3}$)**
Dissolved O2 ($ml \cdot l^{-1}$)	**Slope (degrees)**
Exported Particulate Carbon (EPC) ($mg\ C \cdot m^{-2} \cdot d^{-1}$)	**Speed (U)**
Fine BPI	**Temperature (°C)**

Biogeography classification for VME indicator taxa in the North Atlantic

We further demarcated deep-sea benthic clusters in the North Atlantic based on VME indicator data and assessed the association of these clusters with a variety of environmental parameters to understand the present biogeography of VMEs and extract their environmental drivers. To do this, we aggregated the species occurrence data to 2° latitude-longitude grid cells. We chose this spatial scale balancing a coherent representation of spatial community composition and the retention of geographical cells with low number of species records. Similarly to the GOODS and EMUs assessment analyses, we transformed the occurrence dataset into a species/grid cell contingency table of presence and absence. We further removed any species that appeared only once across the presence/absence matrix and only retained those grid cells with five or more species. This aimed to account for sampling bias in some measure. The final matrix resulted in 254 cells, each cell covering 2° latitude-longitude (~ 12,309 km^2 at the equator), and 528 species.

The similarity of community composition between grid cells across the North Atlantic was evaluated through hierarchical clustering with un-weighted group-averaged linking (UPGMA). We conducted a similarity profile analysis (SIMPROF) using the R package 'clustsig' (Whitaker & Christman, 2014) on the Jaccard dissimilarity matrix to test for significant differences between grid cells. We used the default parameters of 1,000 permutations to create the mean expected similarity profile of the data and 999 permutations to create the simulated profile for use in comparing with its null distribution at a significance level of 0.05 and 0.01 to evaluate clusters at different tolerance thresholds. We also applied a 10 % dissimilarity cut-off to the hierarchical clustering to produce clusters and compare these with the clusters produced by the SIMPROF tests.

To evaluate the role of environmental parameters in explaining the differences between clusters, a linear redundancy analysis (RDA) on the environmental variables was performed followed by a stepwise selection procedure. RDA is an extension of principal component analysis (PCA) in which the response variables (here community data matrix) can be modelled as a function of multiple explanatory variables (Zuur et al., 2007). Here nine explanatory variables were retained for further analysis due to their significant effect on the distribution of VME indicator taxa. These included: aragonite, direction of currents, maximum speed of currents, currents speed, slope, exported particulate carbon, temperature, salinity, and silicate (Table 6). A final matrix with 254 grid cells and 528 species was used for the RDA model and the Hellinger standardisation was applied to reduce the weight of rare species (present in fewer grid cells) and to maintain linear relationships between the community data matrix and environmental variables (Legendre & Gallagher, 2001). In the Hellinger standardisation, each measurement (here presence/absence of a species) is divided by the corresponding row sum (the grid cells) of the community data matrix before a square root transformation is applied (Borcard et al., 2018). The RDA was conducted with R package vegan (Oksanen et al., 2017). All statistical analyses were performed using R v3.2.4 (R Development Core Team 2017).

2.4 Results

2.4.1 Validation of GOODS and EMUs

GOODS

Analysis of biogeographical structure of all available VME indicator species by areas in the North Atlantic revealed five significant groups ($p < 0.05$) in the data based on Jaccard similarity: (1) Labrador Sea, Eastern North Atlantic and the New England Basin Seamount; (2) the MAR south of the Azores; (3) the Corner and New England Seamounts; (4) the Sierra Leone Fracture, the northern MAR, Reykjanes Ridge, Flemish Cap and the southern part of Rockall; (5) the Tropic Seamount, Seamounts of the Mediterranean Outflow Water (MOW) and the Southern Azores Seamount Chain (Figure 66). The areas North Cape, Canary Basin, Norwegian Sea and Romanche Fracture were excluded from analysis as they contained less than three species after cleaning the database from unique species. Analysis of similarity percentage showed the species discriminating between the resulting clusters from the SIMPROF analysis (Table 7). The ordered cumulative contribution of the first five species between clusters is also presented in Table 7. When doing the same analysis for VME records

aggregated by GOODS province level and area, five clusters were also found with slight variations to the general clusters by areas (Figure 67). The main difference is that the Tropic Seamount becomes a cluster on its own. The southern part of the Mid-Atlantic Ridge clusters together at abyssal and bathyal levels. The abyssal plains of the Labrador Sea, Eastern North Atlantic and New England form one group. The South Azores Seamount Chain clusters with the Condor Seamounts area. Finally, all the bathyal records of the Corner and New England Seamounts, the north Mid-Atlantic Ridge, the Reykjanes Ridge, Flemish Cap and Rockall form one significant cluster (Figure 67).

The permutational multivariate analysis of variance did not detect significant differences ($p > 0.05$) however between the species composition of the subareas across the different GOODS provinces (Table 8).

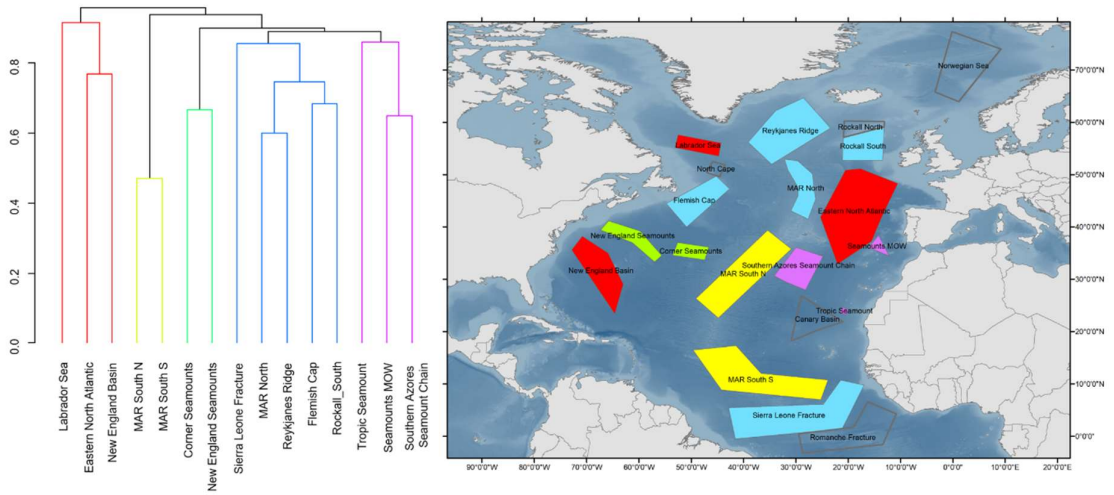

Figure 66. Study sites showing five significant species groups ($p < 0.05$) in the North Atlantic identified from a similarity profile test (SIMPROF) analysis. Data occurrences are from depths below 800 m. On the right, map with the areas used to aggregate the data. Colours correspond to the five statistically significant clusters in the graph on the left. Areas not included in the analysis because they had less than three species are shown in grey.

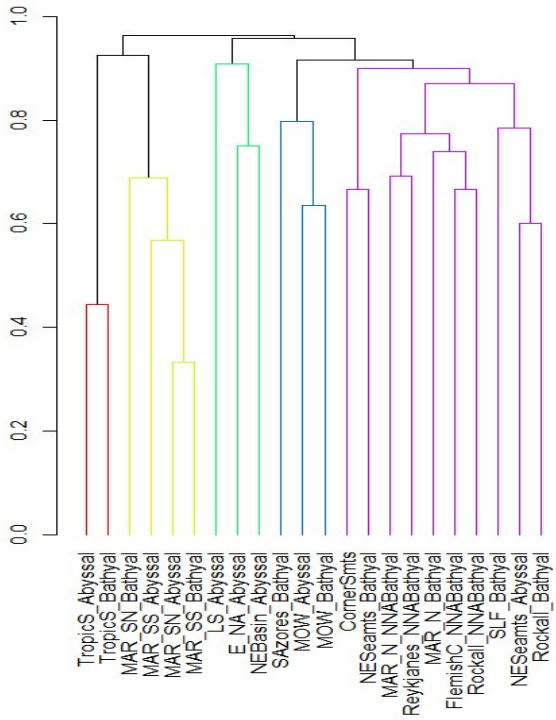

Figure 67. Study sites aggregated by GOODS provinces showing five significant species groups ($p < 0.05$) in the North Atlantic identified from a similarity profile test (SIMPROF) analysis. The available GOODS provinces in the North Atlantic are bathyal (Bathyal), abyssal (Abyssal), bathyal northern North Atlantic (NNA_Bathyal) and abyssal northern North Atlantic (NNA_Abyssal). Areas are defined as: TropicS: Tropic Seamount; MAR_SN: northern part of the southern Mid-Atlantic Ridge; MAR_SS: southern part of the southern Mid-Atlantic Ridge; LS: Labrador Sea; E_NA: Eastern North Atlantic; NEBasin: New England Basin; SAzores: South Azores Seamount Chain; MOW: Condor Seamount; CornerSmts: Corner Seamounts; NESeamts: New England Seamounts; MAR_N: north part of the Mid-Atlantic Ridge; Reykjanes: Reykjanes Ridge; FlemishC: Flemish Cap; Rockall: Rockall; SLF: Sierra Leone Fracture.

Table 7. Discriminating species between the significant clusters obtained by the SIMPROF test for species found in waters below 800 m. In parenthesis are ordered cumulative contribution of the first five species between clusters.

	Cluster 1	**Cluster 2**	**Cluster 3**	**Cluster 4**	**Cluster 5**
Cluster 1	---	Alvinocaris markensis (0.06) Bathymodiolus puteoserpentis (0.11) Chaceon affinis (0.17) Maractis rimicarivora (0.23) Mirocaris fortunata (0.29)	Calyptrophora microdentata (0.05) Candidella imbricata (0.10) Chrysogorgia abludo (0.15) Chrysogorgia artospira (0.20) Chrysogorgia tricaulis (0.25)	Lophelia pertusa (0.06) Funiculina quadrangularis (0.12) Madrepora oculata (0.17) Munidopsis antonii (0.21) Fungiacyathus (Bathyactis) marenzelleri (0.25)	Metallogorgia melanotrichos (0.07) Solenosmilia variabilis (0.12) Poliopogon amadou (0.16) Fungiacyathus (Bathyactis) marenzelleri (0.21) Munidopsis antonii (0.26)
Cluster 2	---	---	Alvinocaris markensis (0.04) Bathymodiolus puteoserpentis (0.07) Chrysogorgia abludo (0.11) Chrysogorgia artospira (0.15) Chrysogorgia tricaulis (0.18)	Alvinocaris markensis (0.04) Bathymodiolus puteoserpentis (0.09) Chaceon affinis (0.13) Lophelia pertusa (0.17) Maractis rimicarivora (0.22)	Alvinocaris markensis (0.05) Bathymodiolus puteoserpentis (0.10) Chaceon affinis (0.15) Maractis rimicarivora (0.20) Metallogorgia melanotrichos (0.25)
Cluster 3	---	---	---	Calyptrophora microdentata (0.04) Candidella imbricata (0.08) Chrysogorgia abludo (0.13) Chrysogorgia artospira (0.17) Chrysogorgia tricaulis (0.21)	Calyptrophora microdentata (0.04) Candidella imbricate (0.09) Chrysogorgia abludo (0.13) Chrysogorgia artospira (0.18) Chrysogorgia tricaulis (0.22)
Cluster 4	---	---	---	---	Metallogorgia melanotrichos (0.05) Funiculina quadrangularis (0.10) Lophelia pertusa (0.14) Poliopogon amadou (0.17) Madrepora oculata (0.20)

EMUs

Analysis of geographical structure in the biogeography of all available VME indicator species below 200 m water depth aggregated by study areas revealed 7 significant groups ($p < 0.05$). These are shown in Figure 68. The northern North Atlantic study areas cluster together, as well as the southern study areas formed southern clusters. The eastern and western basins are grouped in the same cluster. The most striking result was the study area Sierra Leone Fracture clustering with the northern Rockall North study area. The areas Labrador Sea, North Cape, Canary Basin, Norwegian Sea and Romanche Fracture were excluded from analysis as they contained less than three species after cleaning the database from unique species. Analysis of similarity percentage showed the species discriminating between the resulting clusters from the SIMPROF analysis (Table 9). The ordered cumulative contribution of the first five species between clusters is also presented in Table 9.

Testing differences between subareas assigned to EMUs provinces, the permutational multivariate analysis of variance did not detect significant differences ($p > 0.05$) between the species composition of the subareas across the different EMUs provinces (Table 8). Equally, no significant differences were found for octocorals and hexacorals ($p > 0.05$) (Table 8).

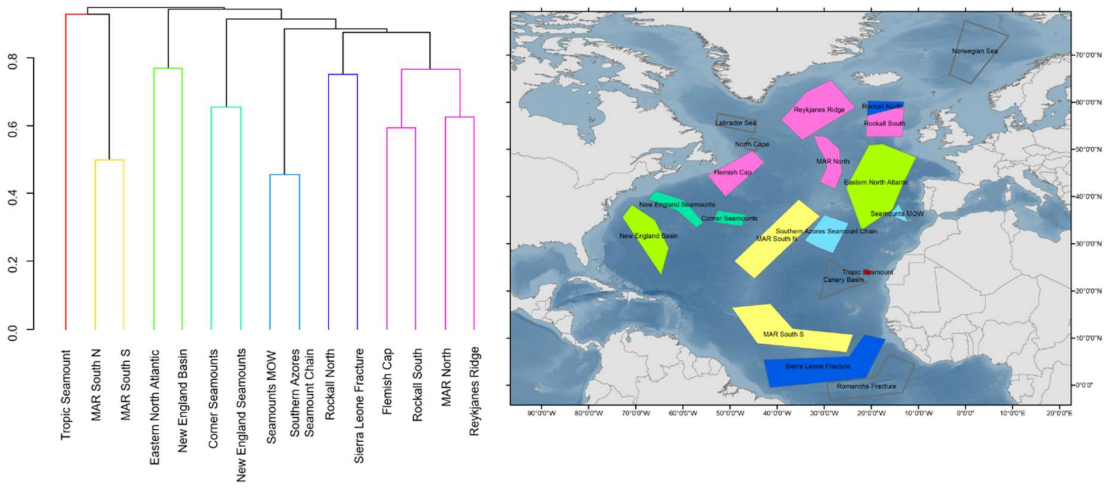

Figure 68. Study sites showing seven significant species groups ($p < 0.05$) in the North Atlantic identified from a similarity profile test (SIMPROF) analysis. Data occurrences are from depths below 200 m. On the right, map with the areas used to aggregate the data. Colours correspond to the five statistically significant clusters in the graph on the left. Areas not included in the analysis because they had less than three species are shown in grey.

Table 8. Permanova results comparing species-assemblage structure between study areas grouped by biogeographic provinces. Neither GOODS nor EMUs showed significant differences between the provinces at the p < 0.05 level.

	R^2		*p < 0.05*	
	GOODS	**EMUs**	**GOODS**	**EMUs**
All VME taxa	0.122	0.138	0.07	0.669
Hexacorallia	--	0.107	--	0.887
Octocorallia	--	0.140	--	0.641

Table 9. Discriminating species between the significant clusters obtained by the SIMPROF test for species found in waters below 200 m.

	Cluster 1	**Cluster 2**	**Cluster 3**	**Cluster 4**	**Cluster 5**	**Cluster 6**	**Cluster 7**
Cluster 1	---	Acanella arbuscula (0.05) Alvinocaris markensis (0.11) Bathymodiolus puteoserpentis (0.16) Chaceon affinis (0.22) Hemicorallium niobe (0.27)	*Abyssopathes lyra* (0.07) *Epizoanthus abyssorum* (0.15) *Hemicorallium niobe* (0.22) *Hemicorallium tricolor* (0.30) *Hertwigia falcifera* (0.37)	*Calyptrophora microdentata* (0.05) *Candidella imbricata* (0.09) *Chrysogorgia abludo* (0.14) *Chrysogorgia artospira* (0.19) *Chrysogorgia tricaulis* (0.24)	Aglaophenia tubulifera (0.03) Anomocora fecunda (0.07) Balanophyllia (Balanophyllia) cellulosa (0.10) Callogorgia verticillata (0.14) Calyptrophora josephinae (0.17)	Acanella arbuscula (0.08) Hemicorallium Niobe (0.16) Hemicorallium tricolor (0.24) Hertwigia falcifera (0.32) Lophelia pertusa (0.39)	Desmophyllum dianthus (0.04) Flabellum (Ulocyathus) alabastrum (0.08) *Hemicorallium niobe* (0.12) *Hemicorallium tricolor* (0.16) Lophelia pertusa (0.20)
Cluster 2	---	---	*Abyssopathes lyra* (0.05) *Alvinocaris markensis* (0.10) *Bathymodiolus puteoserpentis* (0.15) *Chaceon affinis* (0.20) *Epizoanthus abyssorum* (0.25)	*Alvinocaris markensis* (0.03) *Bathymodiolus puteoserpentis* (0.07) *Calyptrophora microdentata* (0.10) *Candidella imbricata* (0.14) *Chaceon affinis* (0.17)	Aglaophenia tubulifera (0.03) Alvinocaris markensis (0.06) Anomocora fecunda (0.09) Balanophyllia (Balanophyllia) cellulosa (0.12) Bathymodiolus puteoserpentis (0.14)	Alvinocaris markensis (0.06) Bathymodiolus puteoserpentis (0.12) Chaceon affinis (0.18) Lophelia pertusa (0.25) Maractis rimicarivora (0.31)	Alvinocaris markensis (0.03) Bathymodiolus puteoserpentis (0.07) Chaceon affinis (0.10) Flabellum (Ulocyathus) alabastrum (0.13) Lophelia pertusa (0.17)
Cluster 3	---	---	---	*Abyssopathes lyra* (0.04) *Calyptrophora microdentata* (0.09) *Candidella imbricata* (0.13) *Chrysogorgia abludo* (0.17) *Chrysogorgia artospira* (0.22)	*Abyssopathes lyra* (0.03) *Aglaophenia tubulifera* (0.06) *Anomocora fecunda* (0.10) *Balanophyllia (Balanophyllia) cellulosa* (0.13) *Callogorgia verticillata* (0.16)	*Abyssopathes lyra* (0.09) *Epizoanthus abyssorum* (0.18) *Lophelia pertusa* (0.28) *Madrepora oculata* (0.37) *Munidopsis crassa* (0.46)	*Abyssopathes lyra* (0.04) *Epizoanthus abyssorum* (0.09) *Lophelia pertusa* (0.13) *Munidopsis crassa* (0.17) *Geodia atlantica* (0.20)

Cluster 4	---	---	---	---	*Aglaophenia tubulifera* (0.03) *Anomocora fecunda* (0.05) *Balanophyllia (Balanophyllia) cellulose* (0.08) *Callogorgia verticillata* (0.11) *Calyptrophora josephinae* (0.13)	*Calyptrophora microdentata* (0.05) *Candidella imbricata* (0.10) *Chrysogorgia abludo* (0.15) *Chrysogorgia artospira* (0.20) *Chrysogorgia tricaulis* (0.26)	*Calyptrophora microdentata* (0.03) *Candidella imbricata* (0.07) *Chrysogorgia abludo* (0.10) *Chrysogorgia artospira* (0.13) *Chrysogorgia tricaulis* (0.16)
Cluster 5	---	---	---	---	---	Aglaophenia tubulifera (0.04) Anomocora fecunda (0.08) Balanophyllia (Balanophyllia) cellulosa (0.11) Calyptrophora josephinae (0.15) Caryophyllia (Caryophyllia) cyathus (0.19)	Aglaophenia tubulifera (0.03) Anomocora fecunda (0.05) Balanophyllia (Balanophyllia) cellulosa (0.08) Calyptrophora josephinae (0.11) Caryophyllia (Caryophyllia) cyathus (0.14)
Cluster 6	---	---	---	---	---	---	Desmophyllum dianthus (0.05) Geodia atlantica (0.09) Acanella arbuscula (0.13) Chrysogorgia agassizii (0.17) Pennatula phosphorea (0.20)

2.4.2 Biogeographical classification of VME indicator taxa in the deep North Atlantic

Our results showed 56 statistically significant ($p < 0.05$) groups for deep-water VME indicator taxa (Figure 69). The distribution of the majority of the 56 clusters follow mostly topographic features and are present on either side of the Mid-Atlantic Ridge. Besides this primary structure, some latitudinal effect seems to exist on the distribution of the clusters as they change in accordance along the eastern and western continental shelves. This is particularly noticeable on the western Atlantic. The most consistent bioregion is found in the northern North Atlantic (cluster 7 in Figure 69) which mainly starts north of the UK, although there are some grid cells in the northern continental shelf of Spain and south of Ireland. The rest of the clusters are mostly found in discrete areas. In general, a mix of the same clusters are observed in the eastern continental shelf of the Atlantic and the northern part of the Mid-Atlantic Ridge. The areas surrounding the Azores are quite heterogeneous in cluster composition, but it still shares most of its clusters with the eastern Atlantic. The western Atlantic seems to be divided in more discrete regions. The Labrador Sea harbours up to four clusters only found in those northern latitudes. The Flemish Cap belongs to one main cluster. From Nova Scotia down to Florida, the coast holds several clusters latitudinally stratified with New England and Corner Seamounts sharing one group. The Gulf of Mexico has two main unique clusters and shares some distinct communities found in the northern Mid-Atlantic Ridge and eastern North Atlantic. The Caribbean Sea is a mix of distinctive clusters, nevertheless there is one cluster spread all around this sea. The southern axis of the Mid-Atlantic Ridge seems to be ecologically isolated with just one unique group.

At $p < 0.01$ there were 49 significant clusters found in the data (Figure 70). The structure is similar to the resulting clusters from the SIMPROF analysis at $p < 0.05$, with the main differences being some cluster assimilation in the Caribbean Sea and in the Azores. Cutting the dendrogram from the hierarchical cluster analysis at 10% dissimilarity produced 36 clusters (Figure 71). At this level, the western Atlantic becomes one homogeneous cluster from latitude 35° N to the Labrador Sea. The Gulf of Mexico and Caribbean Sea are also similar in composition, but there are still some distinct clusters in the area. The Azores and the northern Mid-Atlantic Ridge continue to show heterogeneity in cluster composition. There is a clear cluster north of the UK towards the Arctic region. In the southern limit of this cluster starts another distinct cluster area that reaches the south of Spain. The area corresponding to the outflow of the Mediterranean water shares clusters with the Azores and the eastern Atlantic cluster. Around Cape Verde two distinct clusters are observed. The southern area of the Mid-Atlantic Ridge shares the same cluster as the south-west of the Azores.

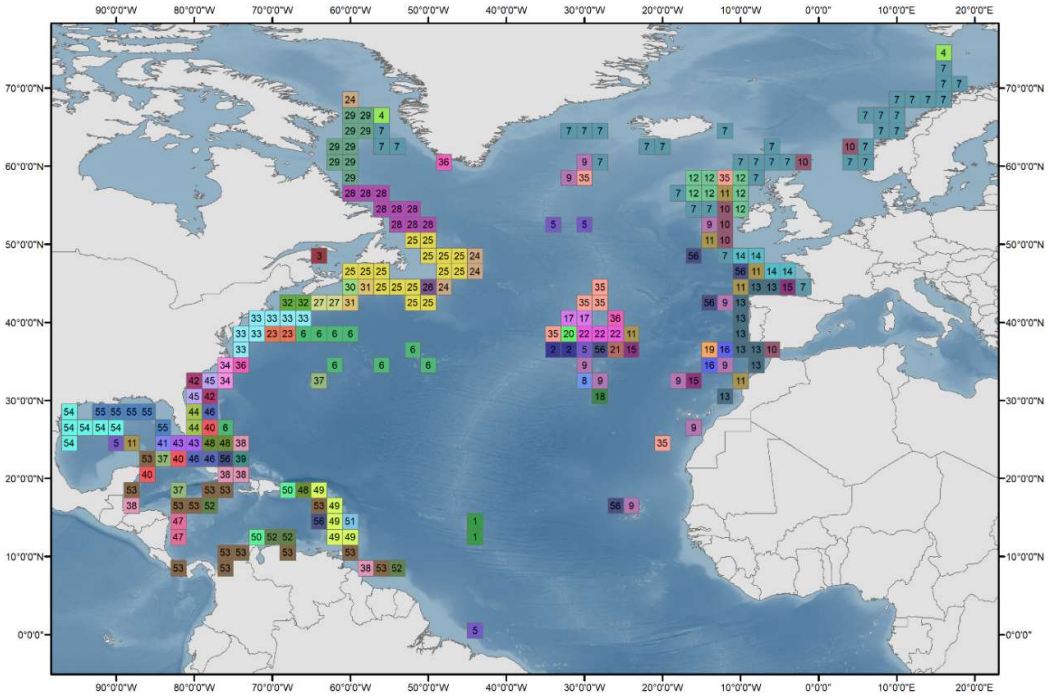

Figure 69. Biogeographical partitioning of the deep North Atlantic based on species level. Data comprise occurrences of 528 species of higher taxa (azooxanthellate corals, sponges, bivalves, decapods, echinoderms and xenophyophores). The partition is based on species groups ($p < 0.05$) in the North Atlantic identified from a similarity profile test (SIMPROF) analysis. Numbers and colours on cells indicate bioregion category.

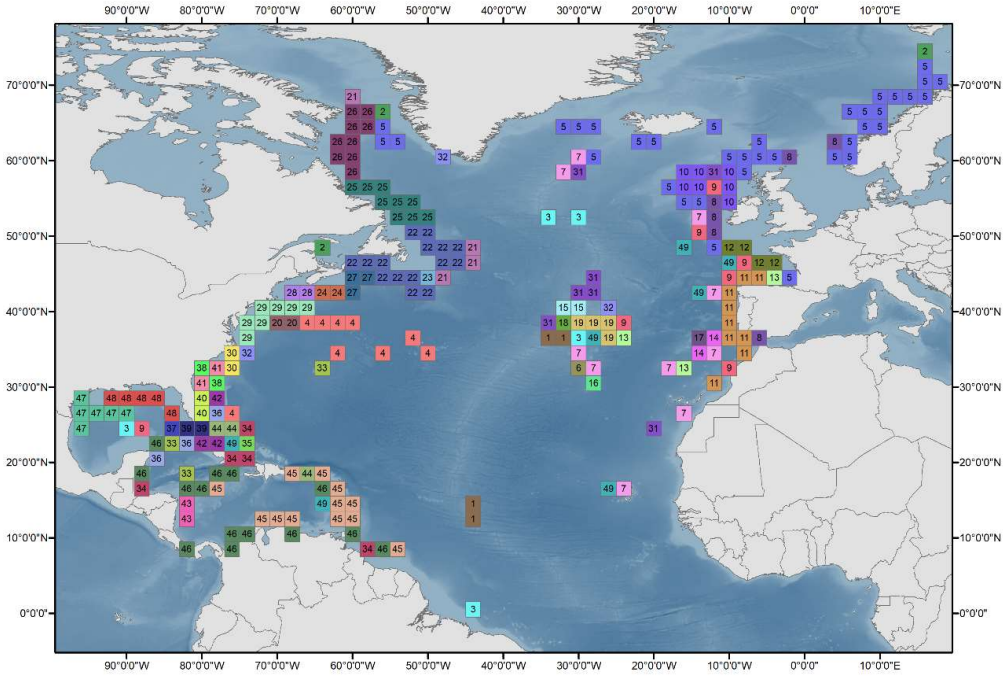

Figure 70. Biogeographical partitioning of the deep North Atlantic based on species level. Data comprise occurrences of 528 species of higher taxa (azooxanthellate corals, sponges, bivalves, decapods, echinoderms and xenophyophores). The partition is based on species groups ($p < 0.01$) in the North Atlantic identified from a similarity profile test (SIMPROF) analysis. Numbers and colours on cells indicate bioregion category.

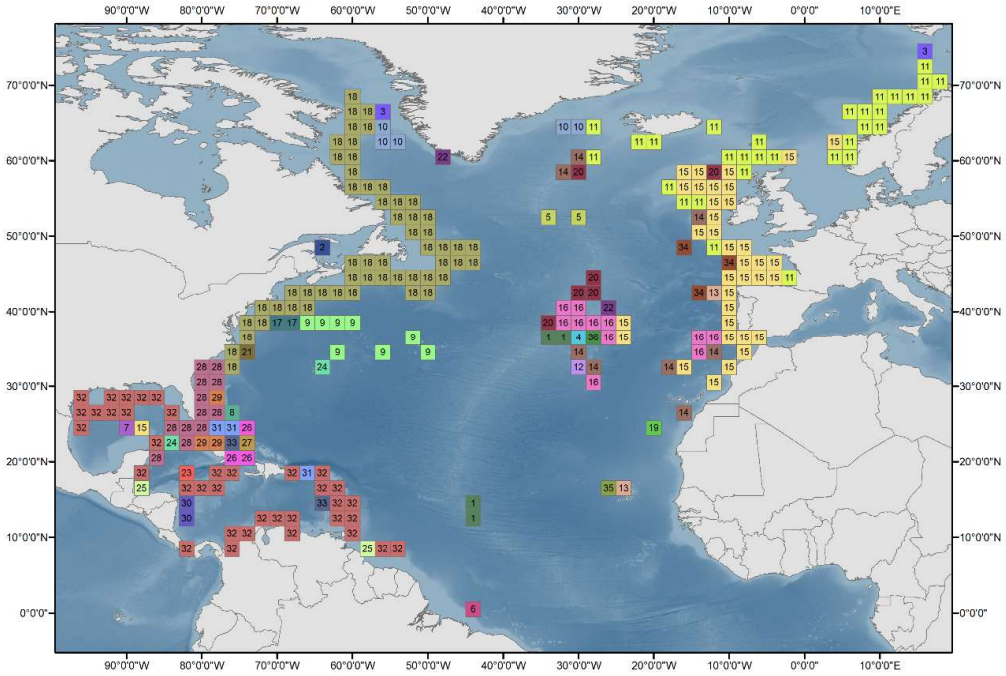

Figure 71. Biogeographical partitioning of the deep North Atlantic based on species level. Data comprise occurrences of 528 species of higher taxa (azooxanthellate corals, sponges, bivalves, decapods, echinoderms and xenophyophores). The partition is based on hierarchical clustering cut at 10% dissimilarity. Numbers and colours on cells indicate bioregion category.

The RDA model captured 5% of the sites variability within the deep North Atlantic. Although the level of variability explained by the RDA model is low, it is important to consider the size of the study area, the number of species included as well as the resolution of the environmental variables. In the ordination plot (Figure 72), sites (i.e. grid cells) form a horseshoe figure resulting from the unimodal response of species to environmental variables that the RDA cannot capture as it assumes a linear relationship between the species and the covariates. Nevertheless, the ordination plot suggests a single dominant gradient or direction of variation with latitude and an eastern and western separation. Overall, the strongest variables driving diversity among the sites were exported particulate carbon and maximum current speed. Slope has some effect on the species composition of sites, particularly for cluster 18 (from Labrador Sea up to latitude 30° N). Silicate and direction of currents appear to be correlated with each other. Some spatial strong patterns are observed in relation to the clusters. Clusters 28 and 32 (around Florida, Gulf of Mexico and the Caribbean Sea) are driven by currents. The eastern Atlantic (mainly clusters 11 and 15) groups together with no strong variable effect. The Azores, comprised of a heterogenous mix of clusters sharing some commonalities with the northern Mid-Atlantic Ridge and the area of the Mediterranean Outflow waters does not have a strong influence either, by any of the predictor variables. Clusters present in the Gulf of Mexico and Caribbean region seem to group close with the eastern Atlantic, while cluster 18 is isolated. Clusters 17 and 27 seem to be in a transitional zone.

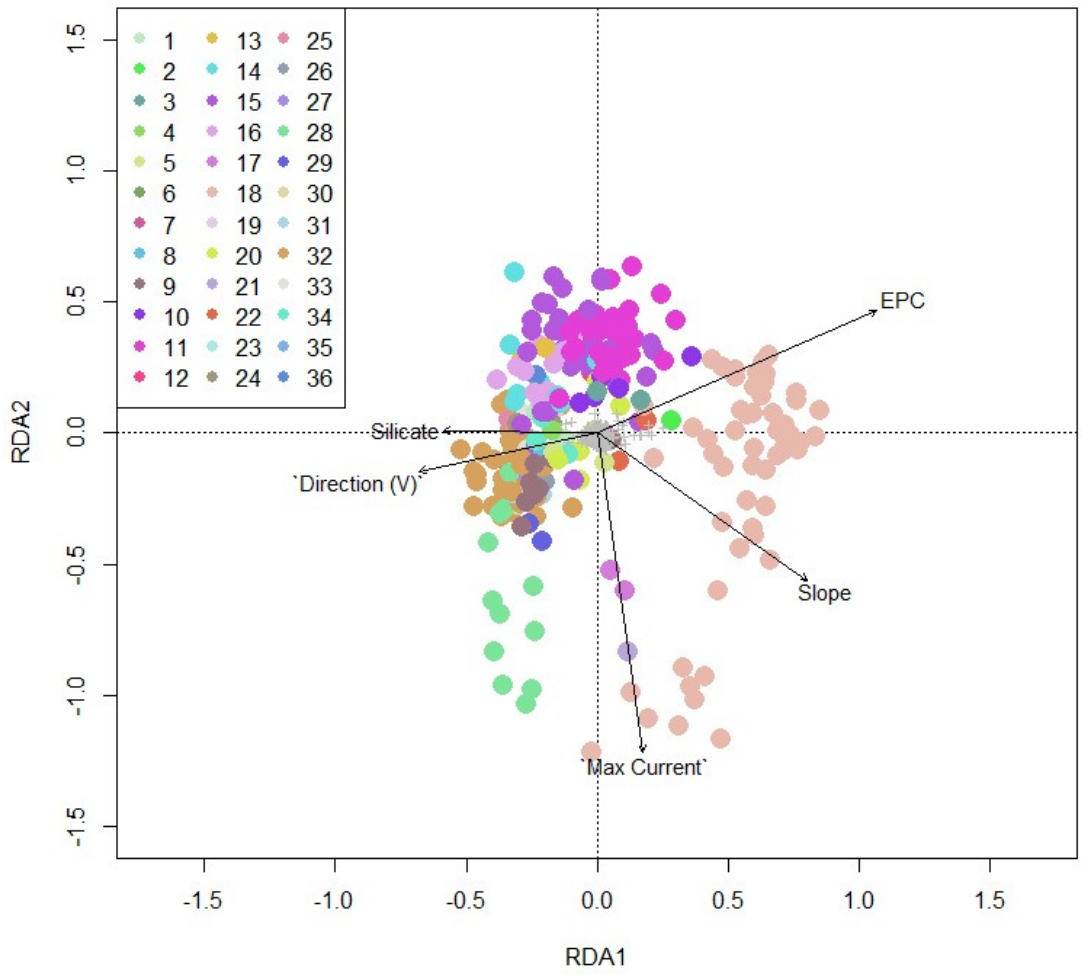

Figure 72. Biplot of redundancy analysis (RDA). Environmental determination of benthic bioregions via the association of abiotic parameters. Points indicate geographical cells. Bioregion changes are most prominent along the exported particulate carbon vector.

The fifteen species most influenced by the environmental variables are observed in Figure 73. The stony coral *Lophelia pertusa* and the chemosynthetic *Munidopsis curvirostra* are most impacted by exported particulate carbon, while *Solenosmilia variabilis* and *Madrepora oculata* are driven by other factors. These species are found in the western (cluster 18 in Figure 71) and eastern (mainly clusters 11 and 15) North Atlantic clusters. The solitary coral *Caryophyllia (Caryophyllia) ambrosia caribbeana* found mainly in the Caribbean Sea is mostly affected by the direction of currents and might drive the differences with other clusters. The gorgonians *Acanthogorgia armata*, *Gersemia rubiformis*, *Acanella arbuscula*, *Paragorgia arborea*, *Primnoa resedaeformis, Keratoisis grayi* and the sea pens *Pennatula aculeata* and *Pennatula grandis* were also driven by exported particulate carbon and by slope, which coincides with the main cluster they belong to (cluster 18 in Figure 71).

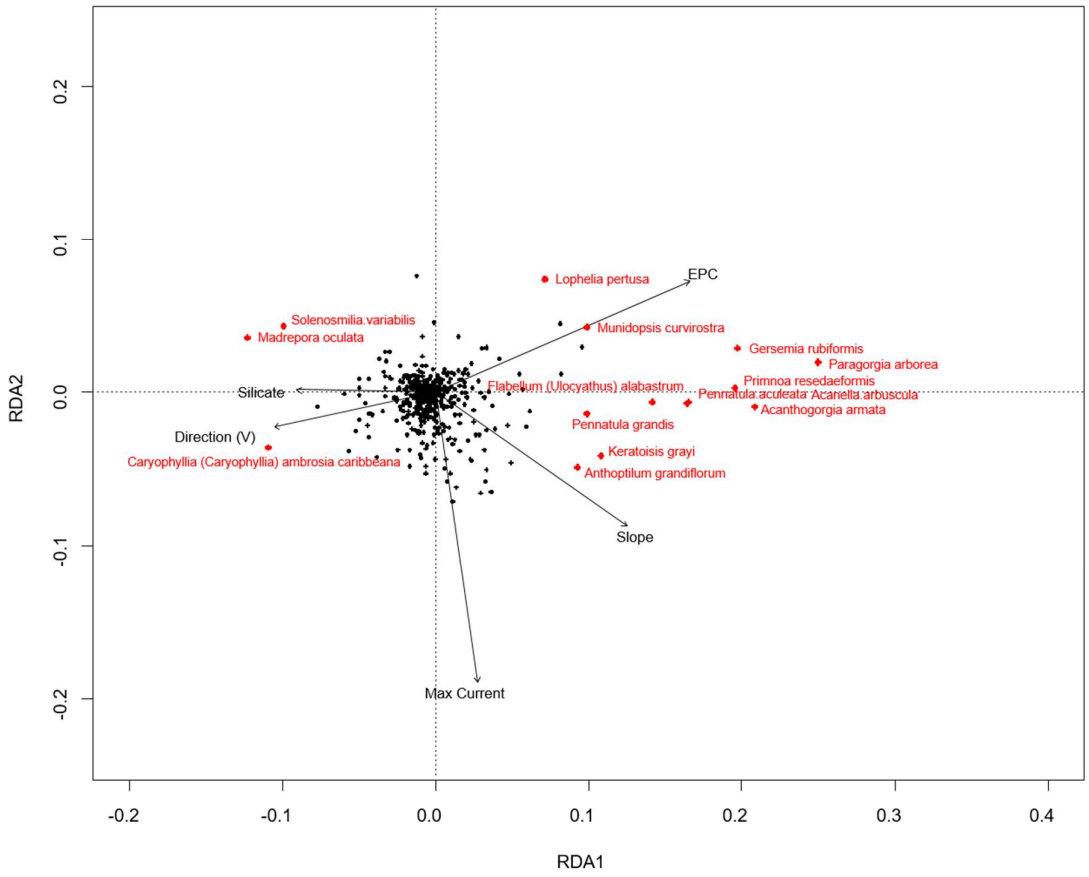

Figure 73. Biplot of redundancy analysis (RDA). Environmental determination of benthic bioregions via the association of abiotic parameters. Points indicate species. In red the fifteen most influential species in driving differences between bioregions.

2.5 Discussion

The distribution of VME records in the North Atlantic was heterogeneous with some areas aggregating most of the records, which particularly coincided with seafloor reliefs. The use of data present only in the high seas further reduced the species dataset considerably. Here, we rejected the hypothesis that these classifications are suitable to explain the distribution of VME indicator taxa in the deep North Atlantic or its different indicator groups separately. Nevertheless, according to our results, it is likely that the GOODS classification system could result in a valuable management tool after further validation in the future with inclusion of more species records. This work was based on the availability of existent data records at species level that hinders to some extent our ability to understand biogeography because of both the bias associated to sampling and the time lag and knowledge gap in species identification. Attempting to reduce sampling bias from the analysis removed unique or rare

species that might drive and define the biogeography of a region. While we might be losing on biodiversity or species richness with this procedure, it is thought that endemic and rare species help to further divide and refine boundaries rather than delineate new bioregions (Costello et al., 2017).

The hierarchical biogeographic analysis at 2° latitude-longitude grid cells produced 36 clusters encompassing areas in the continental shelves and the Mid-Atlantic Ridge. The spatial scale of our analysis at 2° latitude-longitude cells may have driven differences between the proposed clusters, while a larger scale might have homogenised areas. This compromise between losing species records and resolution is unavoidable with the current availability of data and required assumptions in analysis. The outlined bioregions resemble the coastal biogeography described by Costello et al. (2017) and Kocsis et al. (2018), but differences include a more distinct latitudinal pattern in congruence with past biogeographical analyses (Cairns & Chapman, 2001; Watling & Auster, 2005). We also identified the main environmental predictors driving the differences between clusters. Some of the predictor variables retained in the analysis are difficult to interpret in terms of their impact and discrimination in the distribution of species, as they correspond to physical variables. For instance, slope was one of the main variables having an effect in discriminating clusters. Most VMEs included in this study are filter feeders known to prefer areas with certain slope to favour the capture of food. In the present study, the environmental variables were derived from different models that originally had higher resolutions, but it was necessary to match the resolution to that of the species occurrences therefore missing detailed information for particular areas. With these analyses we aim to advance knowledge of deep-sea species biogeography that can facilitate the management of the deep North Atlantic.

2.5.1 North Atlantic biogeography

The distribution of species in the deep ocean is the result of the interplay of extrinsic (environmental), intrinsic (biological) and historic (glacial cycles and physical barriers) factors that create broad-scale patterns (McClain & Hardy, 2010). Bathymetric gradients can, however, restrain species distributions (McClain & Hardy, 2010) and many taxon-specific patterns require historical context (e.g. Henry et al., 2014). Likewise, many taxa show population structure suggesting that extrinsic factors may limit dispersal potential (Baco et al., 2016). Most of the studies on deep-sea biogeography have been conducted on small groups of well-known species of soft-bottom groups such as molluscs and crustaceans that are easily collected with grabs or dredges. Complex habitats such as cold-water corals, however, are often associated with underwater features such as seamounts, canyons and

elevated areas that add complexity to the environment. This additional complexity makes it challenging to understand their drivers of distribution and extrapolate the results to other areas.

In the Atlantic, biogeography is influenced by a bimodal latitudinal gradient that shows a dip in species richness at the equator (Chaudhary et al., 2016). While the bimodality in species richness with latitude is not present in all taxa, temperature is the main factor creating this latitudinal gradient and therefore the main predictor of species distribution (Chaudhary et al., 2017). In our biogeographical analysis temperature was not one of the significant predictor variables explaining the distribution of biogeographic clusters. However, the effect of temperature can actually be observed in the spatial distribution of the clusters in the RDA (Figure 10). There is a latitudinal separation in the clusters resulting directly from the difference in temperature from the equator towards higher latitudes. The model explained only 5% of the variability in the data, which also highlights that other factors not included in the model determine the distribution of the clusters. It is suggested that, at the working resolution of the variables, temperature was not as fundamental as other variables whose ranges resulted more informative. Nevertheless, the impact of temperature in the distribution of deep-sea biodiversity in the North Atlantic is unquestionable. Recently, the coastal biogeography of the North Atlantic was shown to originate from the configuration of the land masses and a latitudinal temperature gradient (Kocsis et al., 2018). Kocsis et al. (2018) found four bioregions based on species-level data from zooxanthellate scleractinians, bryozoans, brachiopods, bivalves, gastropods, echinoderms and decapods. The western North Atlantic presented two distinct bioregions that separated at approximately latitude 45° N, and the eastern Atlantic had a tropical eastern bioregion up to latitude 15° N and a main European bioregion up to latitude 60° N. This biogeographic partitioning of the North Atlantic is similar to that found by Costello et al. (2017). Including both nekton and benthos in their analysis, Costello et al. (2017) divided the North Atlantic in eight provinces, coinciding the coastal ones largely with those by Kocsis et al. (2018). The High Seas area was separated latitudinally at 30° N in two large provinces. Despite considering the whole water column, the work by Costello et al. (2017) represents the first global biogeographic map that extends the work of previous classifications combining efforts to a unified consensus of biogeographic provinces in the ocean for spatial management.

The biogeography of deep-sea VME indicator taxa was also influenced by exported particulate carbon and the speed of currents. Cluster 18 in the western Atlantic (from the Labrador Sea down to latitude 35 N) was particularly driven by these variables delineating the largest cluster. That western area of the North Atlantic has high levels of particulate organic carbon flux to the seafloor and important strong currents that drive these nutrients down to the seabed. The Gulf of Mexico and Caribbean Sea were also mainly influenced by the direction and speed of currents. This location is quite unique in its

influx of ocean currents and as a result the species composition will reflect this oceanographic system. Our results also point to a distinct eastern and western biogeographical separation. Clusters in the eastern or western Atlantic are only found on either side of the basin. Cairns & Chapman (2001) distinguished three superclusters in their biogeography of deep-sea scleractinians corals in the North Atlantic: the cold temperate North Atlantic, the western Atlantic and the eastern Atlantic, each supercluster divided in subclusters across the North Atlantic. Our clusters are very similar to those subclusters found by Cairns & Chapman (2001). In 2005, Watling & Auster (2005) investigating the distribution of deep-water Alcyonacea in the western Atlantic based on fishing records, further confirmed the regions defined by Cairns & Chapman (2001) with slight modifications. The question of an eastern and western biogeography on each side of the MAR was also explored studying deep-sea coral distributions on seafloor reliefs both sides of the North Atlantic. Hall-Spencer et al. (2007) found that species on offshore seamounts and islands of the northeast Atlantic are different from those occurring in the continental slope. Furthermore, Molodstova (2006) noted that several species of antipatharians occur only in the open ocean of this side of the Atlantic accumulating more evidence for an east and west separation.

The GOODS classification system divides the North Atlantic longitudinally along the Mid-Atlantic Ridge (MAR), with the ridge forming a province on its own with the continental shelves. The MAR has been subject to studies attempting to investigate whether this ocean feature constitutes a dispersal barrier. While Watling et al. (2013) supported the idea of a further division of the abyssal and bathyal GOODS provinces in the North Atlantic, studies on biogeography and species composition are inconclusive and taxon-specific. For instance, a study on molluscan composition of the abyssal zone at the Vema Fracture Zone found the composition to be similar at both sides of the ridge, although abundance was higher in the eastern side (Linse & Schwabe, 2018). Similarly, studies on the distribution of abyssal crustaceans found the MAR to be a dispersal barrier for non-swimming species of the families Macrostylidae and Desmosomatidae, but for swimming species of the family Munnopsidae there was unrestricted gene flow across the MAR (Bober et al., 2018). When looking at megafauna such as deep-sea corals and sponges, Bell et al. (2016) found that differences in species composition in the rocky cliffs of the Charlie Gibbs Fracture Zone were larger between north and south stations than at either side of the ridge. Alt et al. (2019) further studied the megafaunal assemblages of the flat terraces (0-2° slope) and the gentle slopes (10° slope) in the Charlie Gibbs Fracture Zone (CGFZ). The northern sites presented distinct differences in composition, while the southern sites were more similar, even being located on opposite sides of the ridge. The study suggested that, on this area of the MAR to the north of the CGFZ and the Subpolar Front, there is an ecological barrier for megafaunal assemblages. Gebruk et al. (2010) further suggested a biogeographic boundary on the bathyal benthic megafauna

on the MAR between the Azores and the southern end of the Reykjanes Ridge, with differences in species composition also east and west of the ridge. Although the study highlights under sampling as a cause for the differences found, results suggested some turnover in bathyal benthic fauna along that section of the ridge and an east and west differentiation. Our results indicate that the Reykjanes Ridge shares similar species composition with the Azores; however, at latitude 52 N (Charlie Gibbs Fracture Zone) there is a unique cluster not found anywhere else in the North Atlantic. The area of the Mid-Atlantic Ridge just south of the Azores shares the same cluster as that found at latitude 13 N in the ridge. Patterns along the length of the ridge and individual segments of the ridge might have different roles in structuring megafauna and more sampling is needed to disentangle the effects of sampling bias (Alt et al., 2019). As seamounts and elevated summits such as mid-ocean ridges are important habitats often harbouring a high biodiversity, considering them as VME candidates (Watling & Auster, 2017) could be a first step towards spatial management of the deep sea.

2.5.2 GOODS and EMUs validation

The similarity profile analysis found significant structure in the species data in the GOODS and EMUs datasets, however this was in contrast to the lack of significant differences in the distribution of all VME species grouped by GOODS and EMUs provinces. The significance of the GOODS analysis might be questioned (Table 8), as results suggest that including more species in the analysis could drive these results as significant. The differences in the development of the GOODS and EMUs provinces might have driven our results. While GOODS takes into account the depth realms where species turnover might take place, EMUs is an algorithm-driven classification that only takes into account certain environmental variables. Environmental variables certainly drive species distributions, but bathymetric ranges play a key role in species turnover that environmental predictors alone could not detect. Therefore, expert knowledge in the development of biogeographic classifications is decisive in order to fully understand the marine environment.

The lack of significance in explaining species distribution could also be a consequence of very heterogeneous data not yet adequate for validation of biogeographic classifications in the deep sea for complex habitats. Although a measure of progress towards marine regionalisation for management purposes, the availability of species distributional data is still limited to define well-represented biogeographical units in the deep sea. Data compilation for this study highlighted that the majority of data records in the public databases are classified up to the genus level. Together with the shortage of physical samples and taxonomic expertise, existing species-level records are relatively

poor for conducting biogeographical analyses in the deep sea, an important issue to address when information at species level is what drives differences in biogeographic ranges.

The lack of comprehensive understanding about species distribution and high-resolution environmental data, makes species-driven approaches meaningful in helping to produce biogeographical classifications. The biogeographical provinces generated in this work are similar in space to other recent classifications (e.g. Kocsis et al., 2018; Costello et al., 2017) and a comparison of these classifications may provide clear insights into delineating a new deep-sea biogeographic classification. This combination of expert opinions and clustering algorithms will lay the path to a biogeographic classification that is representative and accurate to the best of knowledge. Here, further to the spatial and bathymetric structure of GOODS, our results suggest that there is an eastern and western bathyal province differentiation that should be included in the GOODS classification, partitioning province BY4 into at least four branches: eastern, western, and a northern and southern mid-Atlantic Ridge. Our analysis also suggests that the bathyal zone of the Gulf of Mexico and Caribbean Sea behaves as a separate unit too. Coupling this information with GOODS is a first step towards a more integrated approach to understanding patterns in the deep sea.

2.6 Conclusions

The GOODS and EMUs biogeographic classifications are based on physical proxies and expert-based opinion dividing the deep ocean in provinces that aim to reflect species biogeography. Our work failed to highlight differences between the species composition of provinces, indicating that either the VME dataset used did not have sufficient representative data or that the distribution of species was not explained by these classifications. Our biogeographical analysis together with past studies support an eastern and western division of the bathyal North Atlantic that is not contemplated in GOODS. The lack of validation of the GOODS and EMUs classifications prevents their full use for the spatial management of the deep sea; however, it highlights important considerations to take into account in future spatial management decisions, such as the need to include expert opinion in the process. For instance, expert knowledge input such as ecological information of the limit where species turnover might occur in the deep sea provides essential information to couple with environmental predictors to better understand the existence of ecological zones that otherwise clustering algorithms might overlook. The usefulness of biogeographic classifications to management planning depends on continuous update of these tools with new data and our work provides more evidence to update the GOODS classification.

2.7 References

Alt, C. H., Kremenetskaia, A., Gebruk, A. V., Gooday, A. J. & Jones, D. O. (2019). Bathyal benthic megafauna from the Mid-Atlantic Ridge in the region of the Charlie-Gibbs fracture zone based on remotely operated vehicle observations. *Deep Sea Research Part I: Oceanographic Research Papers*, *145*, 1-12.

Assis, J., Tyberghein, L., Bosch, S., Verbruggen, H., Serrão, E. A. & De Clerck, O. (2018). Bio-ORACLE v2. 0: Extending marine data layers for bioclimatic modelling. *Global Ecology and Biogeography*, *27*(3), 277-284.

Bachraty, C., Legendre, P. & Desbruyères, D. (2009). Biogeographic relationships among deep-sea hydrothermal vent faunas at global scale. *Deep Sea Research Part I: Oceanographic Research Papers*, *56*(8), 1371-1378.

Baco, A. R., Etter, R. J., Ribeiro, P. A., Von der Heyden, S., Beerli, P. & Kinlan, B. P. (2016). A synthesis of genetic connectivity in deep-sea fauna and implications for marine reserve design. *Molecular Ecology*, *25*(14), 3276-3298.

Beliaev, G. M. (1989). Deep sea ocean trenches and their fauna. Nauka, Moscow, 255p (in Russian, translation courtesy of Scripps Institution of Oceanography Library).

Bell, J. B., Alt, C. H. & Jones, D. O. (2016). Benthic megafauna on steep slopes at the Northern Mid-Atlantic Ridge. *Marine Ecology*, *37*(6), 1290-1302.

Bober, S., Brix, S., Riehl, T., Schwentner, M. & Brandt, A. (2018). Does the Mid-Atlantic Ridge affect the distribution of abyssal benthic crustaceans across the Atlantic Ocean? *Deep Sea Research Part II: Topical Studies in Oceanography*, *148*, 91-104.

Borcard, D., Gillet, F. & Legendre, P. (2018). *Numerical ecology with R*. Springer.

Briggs, J. C. & Bowen, B. W. (2012). A realignment of marine biogeographic provinces with particular reference to fish distributions. *Journal of Biogeography*, *39*(1), 12-30.

Cairns, S. D. (2006). Studies on western Atlantic Octocorallia (Coelenterata: Anthozoa). Part 6: The genera Primnoella Gray, 1858; Thouarella Gray, 1870; Dasystenella Versluys, 1906. *Proceedings of the Biological Society of Washington*, *119*(2), 161-195.

Cairns, S. D. (2007). Deep-water corals: an overview with special reference to diversity and distribution of deep-water scleractinian corals. *Bulletin of marine Science*, *81*(3), 311-322.

Cairns, S. D. & Bayer, F. M. (2003). Studies on western Atlantic Octocorallia (Coelenterata: Anthozoa). Part 3. The genus Narella Gray, 1870. *Proceedings of the Biological Society of Washington*.

Cairns, S. D. & Chapman, R. E. (2001). Biogeographic affinities of the North Atlantic deep-water Scleractinia. In *Proceedings of the First International Symposium on Deep-Sea Corals, Ecology Action Centre and Nova Scotia Museum, Halifax, Nova Scotia, Canada*.

Cárdenas, P. & Moore, J. A. (2017). First records of Geodia demosponges from the New England seamounts, an opportunity to test the use of DNA mini-barcodes on museum specimens. *Marine Biodiversity*, 1-12.

Carvalho, F. C., Pomponi, S. A. & Xavier, J. R. (2015). Lithistid sponges of the upper bathyal of Madeira, Selvagens and Canary Islands, with description of a new species of Isabella. *Journal of the Marine Biological Association of the United Kingdom*, *95*(7), 1287-1296.

Chaudhary, C., Saeedi, H. & Costello, M. J. (2016). Bimodality of latitudinal gradients in marine species richness. *Trends in ecology & evolution*, *31*(9), 670-676.

Chaudhary, C., Saeedi, H. & Costello, M. J. (2017). Marine species richness is bimodal with latitude: A reply to Fernandez and Marques. *Trends in ecology & evolution*, *32*(4), 234-237.

Costello, M. J., Tsai, P., Wong, P. S., Cheung, A. K. L., Basher, Z. & Chaudhary, C. (2017). Marine biogeographic realms and species endemicity. *Nature communications*, *8*(1), 1057.

Gebruk, A. V., Budaeva, N. E. & King, N. J. (2010). Bathyal benthic fauna of the Mid-Atlantic Ridge between the Azores and the Reykjanes Ridge. *Journal of the Marine Biological Association of the United Kingdom*, *90*(1), 1-14.

Gregr, E. J., Ahrens, A. L. & Perry, R. I. (2012). Reconciling classifications of ecologically and biologically significant areas in the world's oceans. *Marine Policy*, *36*(3), 716-726.

Hall-Spencer, J., Rogers, A., Davies, J. & Foggo, A. (2007). Deep-sea coral distribution on seamounts, oceanic islands, and continental slopes in the Northeast Atlantic. *Bulletin of Marine Science*, *81*(3), 135-146.

Henderiks, J. (2001). *Coccolith studies in the Canary Basin: glacial-interglacial paleoceanography of the Eastern Boundary Current System* (Doctoral dissertation, ETH Zurich).

Henry, L. A., Frank, N., Hebbeln, D., Wienberg, C., Robinson, L., van de Flierdt, T., ... & Rogers, A. D. (2014). Global ocean conveyor lowers extinction risk in the deep sea. *Deep Sea Research Part I: Oceanographic Research Papers*, *88*, 8-16.

Hestetun, J. T., Fourt, M., Vacelet, J., Boury-Esnault, N. & Rapp, H. T. (2015). Cladorhizidae (Porifera, Demospongiae, Poecilosclerida) of the deep Atlantic collected during Ifremer cruises, with a biogeographic overview of the Atlantic species. *Journal of the Marine Biological Association of the United Kingdom*, *95*(7), 1311-1342.

Howell, K. L., Piechaud, N., Downie, A. L. & Kenny, A. (2016). The distribution of deep-sea sponge aggregations in the North Atlantic and implications for their effective spatial management. *Deep Sea Research Part I: Oceanographic Research Papers*, *115*, 309-320.

Kocsis, Á. T., Reddin, C. J. & Kiessling, W. (2018). The stability of coastal benthic biogeography over the last 10 million years. *Global ecology and biogeography*, *27*(9), 1106-1120.

Kussakin, O. G. (1973). Peculiarities of the geographical and vertical distribution of marine isopods and the problem of deep-sea fauna origin. *Marine Biology*, *23*(1), 19-34.

Legendre, P. & Gallagher, E. D. (2001). Ecologically meaningful transformations for ordination of species data. *Oecologia*, *129*(2), 271-280.

Levin, L. A. (2005). Ecology of cold seep sediments: interactions of fauna with flow, chemistry and microbes. In *Oceanography and Marine Biology* (pp. 11-56). CRC Press.

Linse, K., Griffiths, H. J., Barnes, D. K. & Clarke, A. (2006). Biodiversity and biogeography of Antarctic and sub-Antarctic mollusca. *Deep sea research Part II: Topical studies in oceanography*, *53*(8-10), 985-1008.

Linse, K. & Schwabe, E. (2018). Diversity of macrofaunal Mollusca of the abyssal Vema Fracture Zone and hadal Puerto Rico Trench, Tropical North Atlantic. *Deep Sea Research Part II: Topical Studies in Oceanography*, *148*, 45-53.

Lutz, M. J., Caldeira, K., Dunbar, R. B. & Behrenfeld, M. J. (2007). Seasonal rhythms of net primary production and particulate organic carbon flux to depth describe the efficiency of biological pump in the global ocean. *Journal of Geophysical Research: Oceans*, *112*(C10).

Martin, J. H., Knauer, G. A., Karl, D. M. & Broenkow, W. W. (1987). VERTEX: carbon cycling in the northeast Pacific. *Deep Sea Research Part A. Oceanographic Research Papers*, *34*(2), 267-285.

McClain, C. R., Lundsten, L., Ream, M., Barry, J. & DeVogelaere, A. (2009). Endemicity, biogeography, composition, and community structure on a Northeast Pacific seamount. *PLoS One*, *4*(1), e4141.

McClain, C. R. & Hardy, S. M. (2010). The dynamics of biogeographic ranges in the deep sea. *Proceedings of the Royal Society B: Biological Sciences*, *277*(1700), 3533-3546.

McClain, C. R. & Schlacher, T. A. (2015). On some hypotheses of diversity of animal life at great depths on the sea floor. *Marine Ecology*, *36*(4), 849-872.

Menzies, R. J., George, R. Y. & Rowe, G. T. (1973). Abyssal environment and ecology of the world oceans.

Mironov, A. N., Gebruk, A. V. & Southward, A. J. (2006). Biogeography of the Reykjanes Ridge, the northern Atlantic. *Biogeography of the North Atlantic seamounts*, 6-21.

Mironov, A. N. & Krylova, E. M. (2006). Origin of the fauna of the Meteor Seamounts, north-eastern Atlantic. *Biogeography of the North Atlantic seamounts*, 22-57.

Molodtsova, T. N. (2006). Black corals (Antipatharia: Anthozoa: Cnidaria) of the north-eastern Atlantic. *Biogeography of the Atlantic Seamounts, edited by: Mironov, AN, Gebruk, AV, and Southward, AJ, KMK Scientific Press, Moscow*, 141-151.

Molodtsova, T. N. (2011). A new species of Leiopathes (Anthozoa: Antipatharia) from the Great Meteor seamount (North Atlantic). *Zootaxa*, *3138*(1), 51-64.

Molodtsova, T. N., Sanamyan, N. P. & Keller, N. B. (2008). Anthozoa from the northern Mid-Atlantic Ridge and Charlie-Gibbs fracture zone. *Marine Biology Research*, *4*(1-2), 112-130.

Monniot, F. (1979). Faunal affinities among abyssal Atlantic basins. *Sarsia*, *64*(1-2), 93-95.

Oksanen, J., Blanchet, F. G., Kindt, R., Legendre, P., O'hara, R. B., Simpson, G. L., ... & Wagner, H. (2010). Vegan: community ecology package. R package version 1.17-4. *http://cran. r-project. org>. Acesso em*, *23*, 2010.

Pante, E. & Watling, L. (2012). Chrysogorgia from the New England and Corner Seamounts: Atlantic–Pacific connections. *Journal of the Marine Biological Association of the United Kingdom*, *92*(5), 911-927.

Parin, N. V., Mironov, A. N. & Nesis, K. N. (1997). Biology of the Nazca and Sala y Gomez submarine ridges, an outpost of the Indo-West Pacific fauna in the eastern Pacific Ocean: composition and distribution of the fauna, its communities and history. In *Advances in Marine Biology* (Vol. 32, pp. 145-242). Academic Press.

R Core Development Team (2018). R: A language and environment for statistical computing. R Foundation for Statistical Computing, Vienna, Austria. URL http://www.R-project.org/.

Ramirez-Llodra, E., Tyler, P. A., Baker, M. C., Bergstad, O. A., Clark, M. R., Escobar, E. & Van Dover, C. L. (2011). Man and the last great wilderness: human impact on the deep sea. *PLoS one*, *6*(8), e22588.

Ramiro Sanchez, B., Gonzalez Irusta, J. M., Henry, L. A., Cleland, J., Yeo, I., Xavier, J., ... & Messing, C. (2019). Characterization and mapping of a deep-sea sponge ground on the Tropic Seamount (Northeast tropical Atlantic): implications for spatial management in the High Seas. *Frontiers in Marine Science*, *6*, 278.

Rice, J., Gjerde, K. M., Ardron, J., Arico, S., Cresswell, I., Escobar, E., ... & Vierros, M. (2011). Policy relevance of biogeographic classification for conservation and management of marine biodiversity beyond national jurisdiction, and the GOODS biogeographic classification. *Ocean & coastal management*, *54*(2), 110-122.

Sayre, R. G., Wright, D. J., Breyer, S. P., Butler, K. A., Van Graafeiland, K., Costello, M. J., ... & Kavanaugh, M. T. (2017). A three-dimensional mapping of the ocean based on environmental data. *Oceanography*, *30*(1), 90-103.

Sibuet, M. (1979). Distribution and diversity of asteroids in Atlantic abyssal basins. *Sarsia*, *64*(1-2), 85-91.

Sibuet, M. & Olu, K. (1998). Biogeography, biodiversity and fluid dependence of deep-sea cold-seep communities at active and passive margins. *Deep Sea Research Part II: Topical Studies in Oceanography*, *45*(1-3), 517-567.

Simpson, A. & Watling, L. (2011). Precious corals (Coralliidae) from north-western Atlantic Seamounts. *Journal of the Marine Biological Association of the United Kingdom*, *91*(2), 369-382.

Spalding, M. D., Agostini, V. N., Rice, J. & Grant, S. M. (2012). Pelagic provinces of the world: a biogeographic classification of the world's surface pelagic waters. *Ocean & Coastal Management*, *60*, 19-30.

Sweetman, A. K., Thurber, A. R., Smith, C. R., Levin, L. A., Mora, C., Wei, C. L., ... & Ingels, J. (2017). Major impacts of climate change on deep-sea benthic ecosystems. *Elementa: Science of the Anthropocene*, *5*, Art-No.

Tabachnick, K. R. & Menshenina, L. L. (2002). Family Pheronematidae Gray, 1870. In *Systema Porifera* (pp. 1267-1280). Springer, Boston, MA.

Tabachnick, K. R. & Collins, A. G. (2008). Glass sponges (Porifera, Hexactinellida) of the northern Mid-Atlantic Ridge. *Marine Biology Research*, *4*(1-2), 25-47.

Tyberghein, L., Verbruggen, H., Pauly, K., Troupin, C., Mineur, F. & De Clerck, O. (2012). Bio-ORACLE: a global environmental dataset for marine species distribution modelling. *Global ecology and biogeography*, *21*(2), 272-281.

UNESCO (2009). Global Open Oceans and Deep Seabed (GOODS) – Biogeographic Classification. Paris, UNESCO-IOC. (IOC Technical Series, 84.)

Van Dover, C. (2000). *The ecology of deep-sea hydrothermal vents*. Princeton University Press.

Vinogradova, N. G. (1979). The geographical distribution of the abyssal and hadal (ultra-abyssal) fauna in relation to the vertical zonation of the ocean. *Sarsia*, *64*(1-2), 41-50.

Wang, Z., Brickman, D., Greenan, B. J. & Yashayaev, I. (2016). An abrupt shift in the Labrador Current System in relation to winter NAO events. *Journal of Geophysical Research: Oceans*, *121*(7), 5338-5349.

Watling, L. (2015). A new genus of bamboo coral (Octocorallia: Isididae) from the Bahamas. *Zootaxa*, *3918*(2), 239-249.

Watling, L., Guinotte, J., Clark, M. R. & Smith, C. R. (2013). A proposed biogeography of the deep ocean floor. *Progress in Oceanography*, *111*, 91-112.

Wei, T. & Simko, V. (2017). R package 'corrplot': visualization of a correlation matrix (version 0.84). *R Found. Stat. Comput., Vienna. https://github. com/taiyun/corrplot*.

Watling, L. & Auster, P. J. (2005). Distribution of deep-water Alcyonacea off the Northeast Coast of the United States. In *Cold-water corals and ecosystems* (pp. 279-296). Springer, Berlin, Heidelberg.

Watling, L. & Auster, P. J. (2017). Seamounts on the high seas should be managed as vulnerable marine ecosystems. *Frontiers in Marine Science*, *4*, 14.

Whitaker, D. & Christman, M. (2014). clustsig: Significant Cluster Analysis. R package version 1.1. https://CRAN.R-project.org/package=clustsig

Xavier, J. R., Tojeira, I. & Van Soest, R. W. (2015). On a hexactinellid sponge aggregation at the Great Meteor seamount (North-east Atlantic). *Journal of the Marine Biological Association of the United Kingdom*, *95*(7), 1389-1394.

Zezina, O. N. (1997). Biogeography of the bathyal zone. In *Advances in Marine Biology* (Vol. 32, pp. 389-426). Academic Press.

Zuur, A., Ieno, E. N. & Smith, G. M. (2007). *Analyzing ecological data*. Springer Science & Business Media..

CHAPTER 3 - Predicted spatial distribution of biodiversity in the deep North Atlantic under current environmental conditions

Project acronym:	ATLAS
Grant Agreement:	678760
Deliverable number:	D3.3
Deliverable title:	WP3
Work Package:	31st May 2019
Date of completion:	D3.3 Biodiversity, biogeography and GOODS classification system under current climate conditions and future IPCC scenarios
Author:	See next page

This project has received funding from the European Union's Horizon 2020 research and innovation programme under grant agreement No 678760 (ATLAS). This output reflects only the author's view and the European Union cannot be held responsible for any use that may be made of the information contained therein.

3 Chapter 3: Predicted spatial distribution of biodiversity in the deep North Atlantic under current environmental conditions

Telmo Morato[1,2], José-Manuel González-Irusta[1,2], Carlos Dominguez-Carrió[1,2], Chih-Lin Wei[3], Andrew Davies[4], Andrew K. Sweetman[5], Gerald H. Taranto[1,2], Lindsay Beazley[6], Ana García-Alegre[7], Anthony Grehan[8], Pascal Laffargue[9], F. Javier Murillo[6], Mar Sacau[7], Sandrine Vaz[10], Ellen Kenchington[6], Sophie Arnaud-Haond[10], Oisin Callery[8], Giovanni Chimienti[11,12], Erik Cordes[13], Hronn Egilsdottir[14]; André Freiwald[15], Ryan Gasbarro[13], Matt Gianni[16]; Kent Gilkinson[17], Vonda E. Wareham Hayes[17], Dierk Hebbeln[18], Kevin Hedges[19], Lea-Anne Henry[20], Georgios Kazanidis[20], Mariano Koen-Alonso[17], Cam Lirette[6], Francesco Mastrototaro[11,12], Lénaick Menot[9], Tina Molodtsova[21], Pablo Durán Muñoz[7], Bramley Murton[22], Covadonga Orejas[23], Maria Grazia Pennino[7], Patricia Puerta[23], Stefán Á. Ragnarsson[14], Berta Ramiro-Sánchez[20], Jake Rice[24], Jesús Rivera[25], Murray Roberts[20], Luis Rodrigues[1,2], Steve W. Ross[26], José L. Rueda[27], Paul Snelgrove[28], David Stirling[29], Margaret Treble[19], Javier Urra[27], Johanne Vad[20], Les Watling[30], Wojciech Walkusz[19], Claudia Wienberg[18], Mathieu Woillez[9], Lisa A. Levin[31], Francis Neat[29], Diya Das[1,2], Laurence Fauconnet[1,2], Claudia Viegas[1,2], Pedro Afonso[1,2], Gui Menezes[1,2,32], Mario Rui Pinho[1,2,32], Helder Silva[1,2,32], Alexandra Rosa[1,2], Diana Catarino[1,2], Eva Giacomello[1,2], Javi Guijarro[6], Jason Cleland[20], Isobel Yeo[33], Joana R. Xavier[34,35], Íris Sampaio[2,36], Jeremy Spearman[37], Lissette Victorero[33,38,39,40], Charles G. Messing[41], Sébastien Rochette[42], Christopher K. Pham[1,2], Marina Carreiro-Silva[1,2]

1- Okeanos Research Centre, Universidade dos Açores, Horta, Portugal
2- IMAR Instituto do Mar, Universidade dos Açores, Horta, Portugal
3- Institute of Oceanography, National Taiwan University, Taipei, Taiwan
4- Department of Biological Sciences, University of Rhode Island, Kingston, Rhode Island, USA
5- Marine Benthic Ecology, Biogeochemistry and In situ Technology Research Group, The Lyell Centre for Earth and Marine Science and Technology, Heriot-Watt University, Edinburgh, United Kingdom
6- Bedford Institute of Oceanography, Fisheries and Oceans Canada, Dartmouth, NS, Canada
7- Instituto Español de Oceanografía (IEO), Centro Oceanográfico de Vigo, Vigo, Pontevedra, Spain.
8- Earth and Ocean Sciences, NUI Galway, Ireland
9- IFREMER, Centre Atlantique, Nantes, France
10- MARBEC, IFREMER, Univ. Montpellier, IRD, CNRS, France
11- Department of Biology, University of Bari Aldo Moro, Bari, Italy
12- CoNISMa, Rome, Italy
13- Department of Biology, Temple University, Philadelphia, USA
14- Marine and Freshwater Research Institute, Reykjavík, Iceland
15- Senckenberg am Meer, Marine Research Department, Wilhelmshaven, Germany
16- Gianni Consultancy, Amsterdam, Netherlands
17- Northwest Atlantic Fisheries Centre, Fisheries and Ocean Canada, St. John's, NL, Canada
18- MARUM - Center for Marine Environmental Sciences, University of Bremen, Germany
19- Fisheries and Oceans Canada, Winnipeg, MB, Canada
20- School of GeoSciences, Grant Institute, University of Edinburgh, United Kingdom
21- P.P. Shirshov Institute of Oceanology, Moscow, Russia
22- National Oceanography Centre, Southampton, United Kingdom
23- Instituto Español de Oceanografía, Centro Oceanográfico de Baleares, Palma, Spain
24- Fisheries and Ocean Canada, Ottawa, ON, Canada
25- Instituto Español de Oceanografía, Madrid, Spain
26- Center for Marine Science, University of North Carolina at Wilmington, Wilmington, NC, USA
27- Instituto Español de Oceanografía, Centro Oceanográfico de Málaga, Málaga, Spain

28- Department of Ocean Sciences, Memorial University, St Johns, Newfoundland, Canada
29- Marine Laboratory, Marine Scotland Science, Aberdeen, Scotland, UK
30- School of Marine Sciences, University of Maine, Orono, Maine, USA
31- Center for Marine Biodiversity and Conservation and Integrative Oceanography Division, Scripps Institution of Oceanography, UC San Diego, La Jolla, CA, USA
32- Universidade dos Açores, Departamento de Oceanografia e Pescas, 9901-862 Horta, Portugal
33- National Oceanography Centre, Southampton SO14 3ZH, United Kingdom
34- CIIMAR – Interdisciplinary Centre of Marine and Environmental Research of the University of Porto, Matosinhos, Portugal
35- University of Bergen, Department of Biological Sciences and KG Jebsen Centre for Deep-Sea Research, Bergen, Norway
36- Senckenberg am Meer, Abteilung Meeresforschung, Wilhelmshaven, Germany
37- HR Wallingford Ltd, Wallingford OX10 8BA, United Kingdom
38- Institut de Systématique, Évolution, Biodiversité (ISYEB), CNRS, Muséum National d'Histoire Naturelle, Sorbonne Université, École Pratique des Hautes Études, Paris, France
39- Biologie des Organismes et Ecosystèmes Aquatiques (BOREA), CNRS, Muséum national d'Histoire naturelle, Sorbonne Université, Université de Caen Normandie, Université des Antilles, IRD, Paris, France
40- Centre d'Écologie et des Sciences de la Conservation (CESCO), CNRS, Muséum national d'Histoire naturelle, Sorbonne Université, Paris, France
41- Nova Southeastern University, Department of Marine and Environmental Sciences, Dania Beach, Florida, United States
42- IFREMER, Centre de Bretagne, Brest, France

Contents

3.1 Executive summary

More than any other biome on earth existing knowledge of deep-sea ecosystems advances slowly leaving many biological and ecological questions unanswered (Danovaro et al., 2017). Namely, *in situ* observations are still sparsely collected and data on faunal biodiversity distributions remains limited. ATLAS WP3, has significantly contributed to the increased knowledge on the biodiversity (Chapter 1) and biogeography (Chapter 2) of the North Atlantic but large areas of this ocean-basin still remain poorly sampled and known. The vast expanse and high cost and difficulty of directly observing the deep-sea floor over large areas means that we will rarely be able to document the full distribution of species; making habitat suitability modelling tools of paramount importance for evaluating the distribution of deep-water species. Environmental niche modelling, also called species distribution models (SDMs), habitat suitability models (HSM) or climate envelope models (CEM), are powerful tools to predict the distribution of species along wide geographical areas and forecast changes under future climatic scenarios (Pearson & Dawson, 2003; Hijmans & Graham, 2006; Wiens et al., 2009; Hattab et al., 2014).

The use of species distribution modeling has grown enormously in recent years with the accumulation of appropriate response and predictor data sets often global in scope. At the same time, exploitation of the deep sea is increasing and diversifying both within and beyond national jurisdictions while knowledge of the actual distribution of deep-sea biodiversity is still poor due to the limited spatial footprint of sampling to date. Therefore, there is now a great need for robust species distribution modelling that can inform decision making and anticipate global change. In particular, to support spatial planning and implementation of EU and other international directives such as the Voluntary Specific Workplan on Biodiversity in Cold-water Areas within the Jurisdictional Scope of the Convention on Biological Diversity, as adopted at CBD COP13 (EEC, 1992; EC, 2008; 2014; FAO, 2009; CBD 2013). In this chapter, ATLAS used the best available information along with knowledge developments made by WP1 and WP2 and a combination of modelling techniques to improve our understanding on the distribution of sensitive deep-water ecosystems and deep-sea fish, to predict the regional and basin scale occurrence of quality assured VME indicator taxa and deep-sea fish species, and inform analyses of the biogeographic patterns in the North Atlantic.

Habitat suitability models of vulnerable marine ecosystem indicator taxa and commercially important deep-sea fish were developed at the ocean-basin scale and in 9 ATLAS case studies across the North Atlantic (**Figure 2**); from the Florida-Haterras slopes, Flemish cap, and Davis Strait in the western

Atlantic, to the Icelandic and Azores water in the central Atlantic, and to the Rockall Bank, Porcupine Seabight, the Bay of Biscay, and the Tropic Seamount in the Eastern Atlantic.

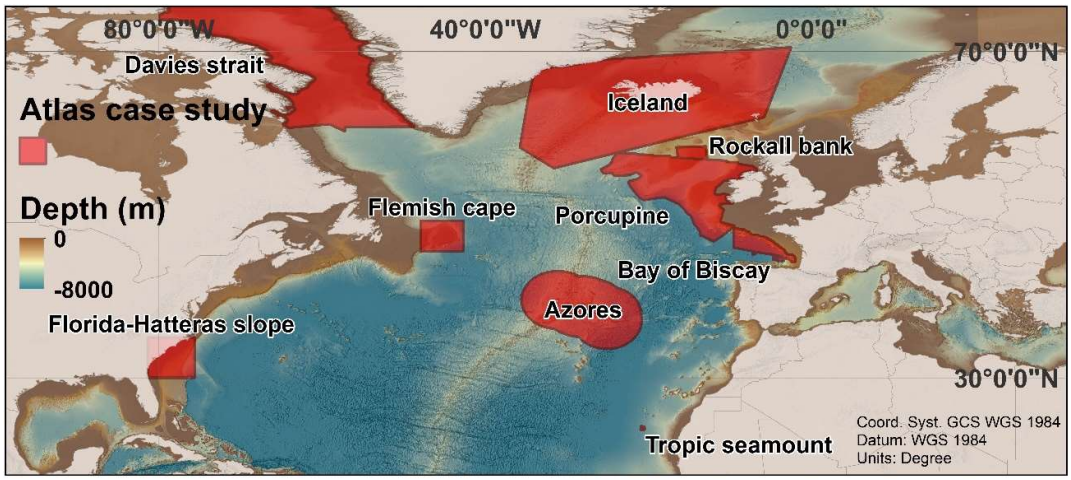

Figure 74. Habitat suitability models were developed at regional case study and ocean-basin scales.

Ocean-basin scale habitat suitability models have proved to be valuable tools for evaluating the potential distribution of deep-sea benthic species at large scale, and to identify broad areas of conservation (Ardron et al., 2014; Reiss et al., 2014) or blue growth importance. However, our results also demonstrated that after identifying those broad areas in the North Atlantic, regional habitat suitability models with higher spatial resolution will help the implementation of area based management tools at a finer scale. This is well illustrated in a comparison of the outputs of the ocean-basin scale model with the regional model outputs for *Lophelia pertusa* (Figure 75).

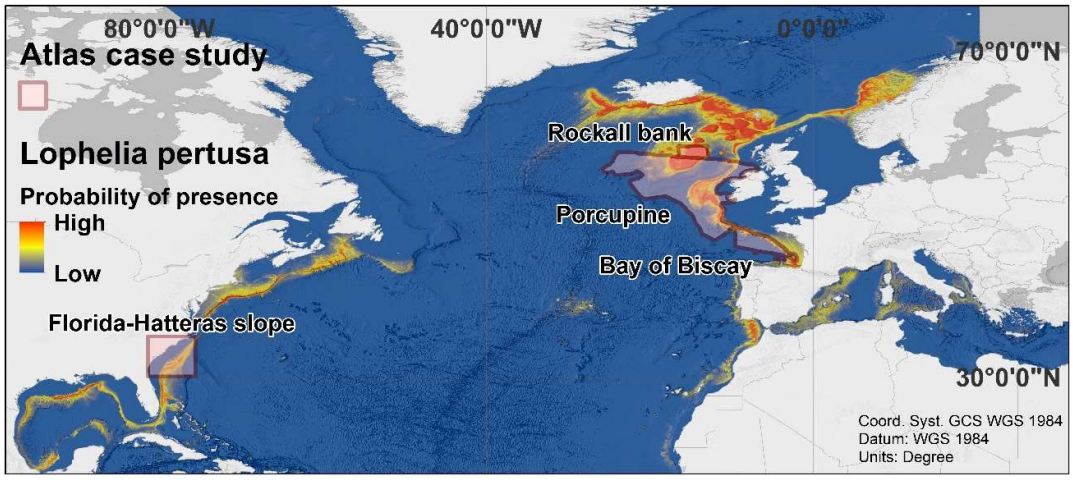

Figure 75. Outputs of the habitat suitability model for Lophelia pertusa *at different spatial scales; ocean-basin scale and four regional scales (Bay of Biscay), Porcupine bank, Rockall bank and the Florida-Hatteras slope.*

For example, the *L. pertusa* ocean-basin scale model, successfully identifies canyons in the Bay of Biscay as the most suitable area for this species. However, the regional model is actually able to identify what specific canyons in that region seemed to be the most suitable for *L. pertusa* (Figure 76). In the Florida-Hatteras of the NW Atlantic case study, the habitat suitability index of *L. pertusa* seemed to be similar between the regional and the ocean-basin scale models, but the ocean-basin scale model seemed to produce more plausible results (Figure 77); highlighting the importance of having a good spatial coverage of the species occurrence data. On the contrary, both in the Porcupine Bank in the Irish shelf (Figure 78) and in the Rockall Bank (Figure 79), the ocean-basin scale model significantly over-predict the suitable habitat of *L. pertusa* when compared to the regional models.

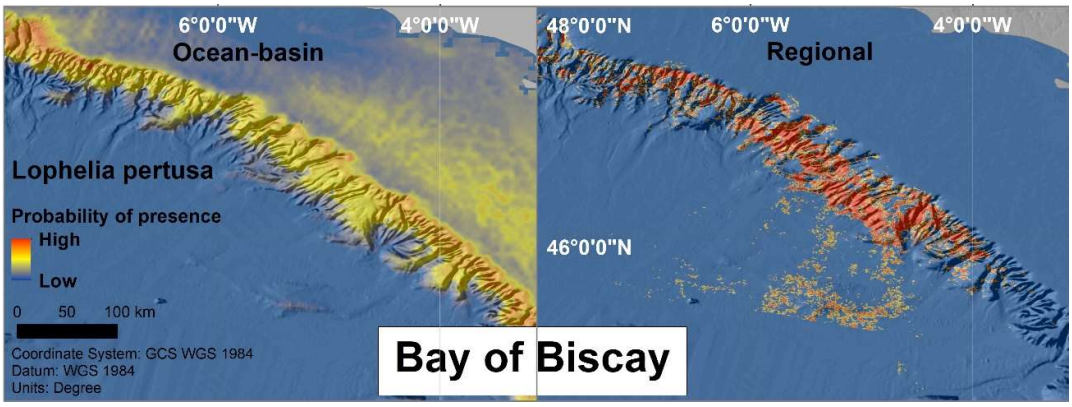

Figure 76. Outputs of the habitat suitability model for Lophelia pertusa at different spatial scales; ocean-basin scale and regional scale in the Bay of Biscay.

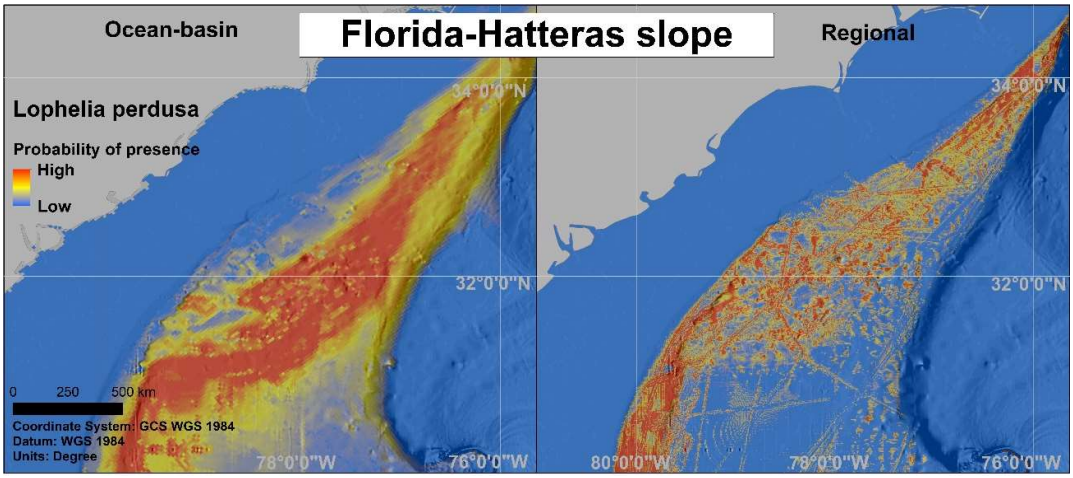

Figure 77. Outputs of the habitat suitability model for Lophelia pertusa *at different spatial scales; ocean-basin scale and regional scale in the Florida-Hatteras slope.*

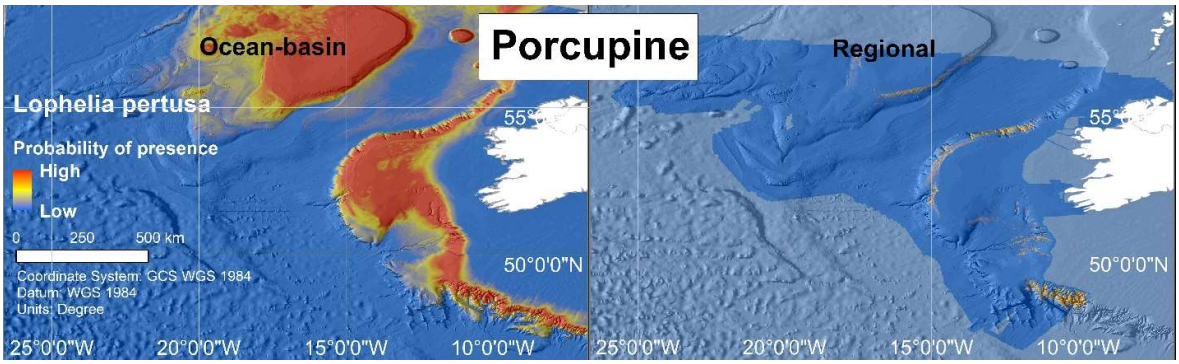

Figure 78. Outputs of the habitat suitability model for Lophelia pertusa *at different spatial scales; ocean-basin scale and the regional scale in the Porcupine bank.*

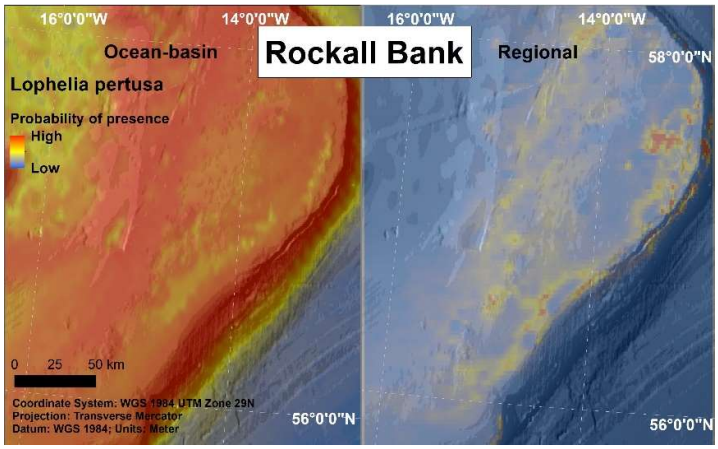

Figure 79. Outputs of the habitat suitability model for Lophelia pertusa *at different spatial scales; ocean-basin scale and the regional scale in the Rockall bank.*

There are multiples reasons for the inconsistencies between models at different scales including the spatial resolution and quality of the terrain and environmental data, the volume, the quality and the spatial coverage of the occurrence data, the availability of absence records, model selection, assumptions and parametrization, among others (Robinson et al., 2017). The ocean-basin scale model suffers from a number of common and well-known limitations that may be more pronounced when modelling deep-sea taxa. It is known that cold-water coral distributions respond to small-scale fluctuations of different terrain attributes, such as substrate type and seabed rugosity (De Clippele et al., 2017), and oceanographic conditions (Bennecke & Metaxas, 2017). However, both terrain and environmental information was derived from global datasets and not from detailed deep-sea in situ measurements which does not discriminate between areas with high small-scale heterogeneity. Furthermore, regional scale models are constrained to the regional distribution of presence records and therefore are able to account for changes in species distribution caused by anthropogenic

disturbances, something especially relevant in areas exposed to high levels of trawling such as the NE Atlantic (Eigaard et al., 2017).

The quantity and the spatial distribution of available occurrence data, and to some degree of uncertainty on deep-sea species identification (mostly for VME indicator taxa) and geo-location of occurrence data, also generates increased uncertainty in the model outputs. Finally, the use of presence-only records (as opposed to abundance data) with no true absence data, also generates increased uncertainty and usually over predict habitat suitability (Zaniewski et al., 2002). The deep sea is still one of the least studied and sampled areas on the planet and therefore many species are still unknown or the taxonomy still has to be resolved and the real spatial distribution is also undetermined (mostly for VME indicator taxa). This source of uncertainty will only be reduced with extensive exploration of the deep-sea environment.

Habitat suitability projections as those presented here, can be used to develop research agendas that confirm and advance the model outputs and clarify the roles of predictor variables in determining distributions. Incorporating these needs into global observing efforts (e.g., Deep Ocean Observing Strategy) can help identify data gaps, designate spatial locations for collection of physical and biogeochemical data from moorings, floats, ship tracks, or observatories, and advance technologies such as imaging and eDNA that can improve species detection.

Once habitat suitability models are sufficiently ground truthed they can become a valuable tool to inform environmental management and conservation policy (Robinson et al., 2017), including taking climate change into consideration. Protected areas in the deep sea take the form of Vulnerable Marine Ecosystem designation by the Regional Fisheries Management Organizations and Arrangements to regulate fishing, Areas of Particular Environmental Interest by the International Seabed Authority (ISA) to regulate seabed mining, Ecologically and Biologically Significant Areas (EBSAs) by the contracting parties to the Convention on Biological Diversity to highlight biodiversity, National Marine Monuments by the USA, etc. Similar protections are under discussion at the UN as part of a new biodiversity treaty to apply to areas beyond national jurisdiction. Each of these area-based management tools can benefit from the habitat suitability modeling approaches developed here. Within the fishing industries, accurate knowledge of VME distributions in relation to climate change parameters can be used to regulate fishing gear, locations and timing both within and beyond national jurisdiction.

Summary of the main model results

Ocean-basin scale habitat suitability models of cold-water corals and commercially important deep-sea fish in the North Atlantic under current environmental conditions

Making use of the best available curated species occurrence data obtained from multiple public and restricted sources and during the ATLAS project, and a set of static and dynamic environmental parameters, we modelled the habitat suitability for six cold-water coral (three scleractinian corals forming aragonitic skeletons, and three gorgonians forming calcitic skeletons; two groups that are expected to respond differently to future conditions of water mass properties) and six deep-sea fish species under current conditions for the whole northern Atlantic Ocean-basin (from 18°N to 76°N and 36E° to 98W), using an ensemble modelling approach.

The uncertainty associated with the habitat suitability model predictions was in general low for both cold-water corals and deep-sea fish. Temperature and depth were important predictors in determining the habitat suitability for CWC and deep-sea fish species, respectively. Food availability measured as POC flux to the seafloor was also an important predictor for most species suitable habitat. Although these modelling approaches come with some caveats, we showed that habitat suitability models are useful tools for predicting potential distribution of deep-water species in the north Atlantic and may inform management decisions within RFMOs.

Case study 3: Habitat suitability models of Lophelia pertusa and two sea pen species under current environmental conditions in Rockall Bank, NE Atlantic

Habitat suitability models were developed for *Lophelia pertusa*, and for 2 sea pen species (*Funiculina quadrangularis* and *Ptilella greyi*) in Rockall bank, in the eastern margin of the North Atlantic Ocean. Presence records were taken from the ICES VME and OSPAR habitats databases for *L. pertusa* and *F. quadrangularis*. These records arise from various sources including fisheries surveys, imaging, scientific surveys. Data for *P. greyi* was also collected during fisheries surveys. A point process modelling (PPM) framework was used to jointly model both the location and number of presence points as a function of the environmental variables for each species, with the response being the intensity of points per unit area. Some advantages of using PPMs for presence only SDMs include; clarity over what is being modelled in the response, unambiguous criteria for selecting background points / pseudo-absences, and a suite of diagnostic tools that can be used to check model assumptions.

In general, the models appear to fit the presence data well according to the diagnostic plots and performed well according to both the AUC and TSS scores. The most prominent variable for *L. pertusa* is observer bias, suggesting an overlap between fished areas and locations of reported occurrences of *L. pertusa*. The second most prominent variable is the cross between minimum salinity and minimum temperature, with the most suitable conditions for *L. pertusa* suggested by the model being found between 200 – 300, which are in keeping with the understood environmental tolerances of *L. pertusa*, where reefs most often occur at full oceanic salinities (34 – 36 ppt) and temperatures of 6 – 7 ˚C. For both sea pen species, the quadratic of percentage mud was the most important variable in the model, which is in keeping with their life-history as sea pens, which are the only octocorals adapted for life in entirely soft sediments.

The predictive layers generated from these modelling efforts will help inform conservation efforts on Rockall Bank. When the models (particularly those for *L. pertusa* and *F. quadrangularis*) were used to predict to the wider environment beyond Rockall Bank, some interesting patterns are evident. The predicted areas align with other records from the area as well as predicting new areas of occurrence, which will help direct survey efforts in this area of the Northeast Atlantic. The predictions also predict areas for which there are only unconfirmed records in the OSPAR habitat database.

Case study 5: Predictive Habitat suitability models for* Lophelia pertusa *under current environmental conditions in Porcupine

Habitat suitability models were developed for *Lophelia pertusa* in Porcupine Bank, in the eastern margin of the North Atlantic Ocean. *L. pertusa* was selected because of the availability of existing distribution data and the species importance as the primary framework constructing coral providing habitat for a large associated and biodiverse fauna. A two-step modelling approach was used to predict *L. pertusa* suitable habitat.

In general, the model outputs indicate that habitat suitability for *L. pertusa* increases with increased bathymetry complexity. Temperature, mean seabed current velocity, and aragonite concentration were the most important explanatory variables. The temperature response curve shows an upper limit of approximately 10.5°C, which is lower than the upper tolerable temperature threshold for *Lophelia* of 12-14°C reported in literature. The aragonite concentration response curve indicates that increases in aragonite concentration are associated with decreases in habitat suitability, that could be due to decreased coral calcification, however it is difficult to draw conclusions as, though well documented, the specifics of this issue are still poorly understood.

The Porcupine Bank, Porcupine Seabight and Rockall Bank host to some of the largest *L. pertusa* and *M. oculata* cold-water coral reefs in NE Atlantic. Living reefs are found at or near the summits of carbonate mounds, rising up to 350 m in height in waters between 500 and 1200m depth. The mounds themselves occur clustered together to form several distinct mound provinces off the west coast of Ireland. Habitat suitability models as those developed here help pointed toward likely locations of unknown cold-water coral reefs.

Case study 6: Present day predictive models for CWC in the Bay of Biscay

Habitat suitability models were developed for *Lophelia pertusa* and *Madrepora oculuta* in the Bay of Biscay, in the eastern North Atlantic Ocean. The continental margin of the Bay of Biscay is incised by over a hundred submarine canyons, which topographical and hydrological complexity, coupled with high substratum heterogeneity, make them ideal environments for CWC habitats. Twenty-four of these canyons were surveyed using a Remotely Operated Vehicle (ROV) or a towed camera system. This information was the main basis to predict the distribution of habitats formed by aggregations of the two reef-buidling corals *Lophelia pertusa* and *Madrepora oculuta*, living in syntopy in the Bay of Biscay and hardly distinguishable from landscape images, and which aggregations are dominant among CWC habitats.

Random Forests (RF) and Gradient boosting (GB) models were used to pre-select variables for the development of GAM and GLM models. The model outputs suggest that suspended organic matter concentrations (summer mean, and annual mean) are among the key drivers of the distribution of cold-coral reefs in the Bay of Biscay. Coral reefs have been observed in the north but not in the south of the Bay of Biscay, likely due to higher sediment supply and higher sedimentation rates in the southern Bay of Biscay where the continental shelf narrows down, what is accurately predicted by the model. The two other key predictors are chlorophyll a concentration (summer mean) and terrain ruggedness (VRM). The resolution of the model appears low to predict beyond the potential niche for coral reefs, resolution that has been constrained by the high level of spatial autocorrelation in the dataset. Spatial autocorrelation is partly due to the sampling design, based on non-random video surveys, and partly due to the biology of coral reefs, which grow asexually. Methods explicitly modelling spatial autocorrelation might improve the resolution of the model.

Case study 8a: Predictive habitat suitability models for key CWC species under current environmental conditions in the Azores

Habitat suitability models were developed for 13 vulnerable marine ecosystems indicator taxa in the Azores EEZ, the central North Atlantic Ocean. Presence data were compiled from: *i)* bycatch data obtained from regional demersal surveys; *ii)* observer programs on fishing vessels that reported coral bycatch; *iii)* video annotation of underwater images shot by ROV, drop and tow camera systems. A preliminary set of 19 environmental layers potentially affecting CWCs distributions were selected, but due to collinearity only 10 were included in the final selection. GAMs, and MAXENT were used to predict the distribution of CWCs.

Overall model performances were similar for MAXENT and GAMs, with MAXENT scoring better for seven out of the 13 modelled taxa both according to AUC and TSS scores. AUC and TSS scores for both GAM and MAXENT models were good for all species except for *Leiopathes spp.* and *Paracalyptrophora josephinae*. As expected, the predicted distribution of CWC taxa showed a strong association with areas of local relief, being them island shelves or slopes, ridges or seamounts. However, even among areas of similar depths, models discriminated between suitable and unsuitable zones showing that model outputs were not exclusively driven by depth correlated changes in environmental predictors. Overall the three most important variables for GAM were oxygen saturation, temperature and BPI coarse while the three most important variables for MAXENT were oxygen saturation, pH and temperature. Models built with a higher number of presence records and at a finer taxonomic resolution appeared to more consistently identify zones of suitable habitat, suggesting that an increase in presence records and taxonomic resolution would benefit model performance. As the number of presence records increased, response curves became more consistent among model methods and more sound biologically.

A further refinement of the environmental variables used to build such models, such as using finer resolution oceanographic model for currents, and at a temporal scale that allows to take account of periodic current bursts, using a combination of fine and coarse BPI able to more accurately synthetize geomorphological information across scales, and the inclusion of variables of sediment types and proxy variables for food export to the seafloor that are not available yet at the sufficient/suitable resolution, may also increase prediction accuracy. Current model predictions were found useful to identify areas of particular importance for management and investigation.

Case study 8b: Habitat suitability models under current environmental conditions of deep-sea sharks in Azores

Habitat suitability models were developed for 6 species of vulnerable deep-water sharks in the Azores EEZ, the central North Atlantic Ocean. Using species occurrence data collected from fishery-independent surveys and on-board fishery observers, the probability of presence (Pp) of fifteen elasmobranchs species was modelled in the Azores EEZ using GAMs. For the 6 species most frequently caught, abundance models were developed using a delta model approach, combining a binomial GAM to model the probability of presence, and a negative binomial GAM to model abundance. Depth was found to be the main driver for habitat suitability for most of the 15 selected species, followed by fishing effort (number of hooks). Contrary to the presence absence models, variables such fishing effort and year explained most of the variance observed in abundance models. The importance of other predictors varied among species, but the main predictors for both presence and abundance models, included BPI, slope, bottom currents, and aspect.

This work deepens our knowledge on little-known data-poor deep-sea elasmobranch populations and their suitable habitats. A better understanding of those species ecology and habitat is very important for their conservation and effective management of the fisheries that unintentionally but still occasionally catch them. As those species are recognized to be particularly vulnerable to fishing and are currently under a fishing prohibition in the European Union, this work is an important step forward relevant both for conservation and for fisheries management at the regional and international scales. It can help inform spatial planning and identify conservation objectives of this vulnerable species group.

***Case study 9: Habitat suitability models under current environmental conditions in Iceland. Predictive models for* Helicolenus dactylopterus**

Habitat suitability models were developed for the fish species *Helicolenus dactylopterus* in the Icelandic EEZ, the central North Atlantic Ocean. *Helicolenus dactylopterus* was selected for this study as the northern distribution limit for this widespread species is currently south of Iceland, but at the time when the trawl surveys were established this species was considered rare in this region. The earlier period was relatively colder than the latter period so the HSM may inform if the significant observed increase in abundances and detection rate of this species south of Iceland could be a result of warming sea water temperatures. GAM and MAXENT models were developed based on trawl survey data and based on average temperature and currents for that whole period and other static

environmental parameters. The results of the models were predicted for two separate time periods: 1989 - 1998 and 1999 - 2009.

Both MAXENT and GAM models performed well. The response curves of both models suggest that temperature is a major environmental driver affecting the occurrence and distribution of this species in the study region. Both models suggest a higher habitat suitability index for *Helicolenus dactylopterus* in the second, warmer, period. A large quantity of information on presence and absences was enough to develop well performing models. It would also be informative to develop models to estimate abundances. Model caveats are mainly related to the limited information on the environmental parameters. This work was able to show how rising temperatures in the marine environment in the North Atlantic contribute to a northward expansion of the distribution limits of a deep-sea fish species.

Case study 10: Habitat suitability models under current environmental conditions in Davis Strait, Eastern Arctic. Random Forest models for key CWC VME indicator taxa and archetypes models for sponges

Habitat suitability models were developed for sea pens, large gorgonian corals, and small gorgonian corals in the in Davis Strait, the western North Atlantic Ocean. Random forest was used to predict the probability of occurrence and range distribution of the 3 coral functional groups. Catch data were collected between 1999 and 2014 from a combination of DFO research vessel trawl surveys. Fifty-eight environmental variables, derived from long-term oceanographic or remote-sensing data, were used as predictor variables.

For all three CWC functional group models, temperature or salinity were amongst the most important variables. These likely do not reflect physiological tolerance limits but characterize the water masses in the region. The distribution of the corals is more likely closely governed by the currents, and in particular the Irminger Current seems suitable for the small and large gorgonian corals, while Polar and Atlantic waters seem to have more influence on the sea pen distribution. Predictive models of sponge communities were also developed using species archetype GLMs modelling, that are derived from a single finite mixture model and represent one or many species with similar ecological tolerances, to predict their probability of occurrence distribution in the Eastern Arctic.

Collectively these predictive models will be used to assess management options in the marine spatial planning scenarios for this Case Study. SDMs are already being used to determine closed areas to protect vulnerable marine ecosystems both in Canada and in international waters. Of the 34 marine

refugia that Canada has identified 24 have directly drawn on kernel density analysis (KDE) refined with SDM results.

Case study 11: Present day models for several sea-pens species or genus in Flemish cap

Habitat suitability models were developed for three sea pens (*Anthoptilum grandiflorum, Funiculina quadrangularis* and *Pennatula aculeata)* and the deep-sea bamboo coral (*Acanella arbuscula)* in the Flemish Cap and Flemish Pass areas, the western North Atlantic Ocean. A 11-year period (2007-2017) of data from two bottom-trawl groundfish surveys was used. Three modelling techniques (GAM, Random Forest, and MAXENT) were implemented and an ensemble of all models was estimated. Twelve environmental and explanatory variables were included.

Depth was the most important variable for all models for *Anthoptilum grandiflorum*, *Funiculina quadrangularis* and *Acanella arbuscula*, while for *Pennatula aculeata* the mixed layer depth was the most important variable. According to the species and models, other variables were also significant, the most frequent being bottom current speed, sediment texture and/or gravel factors, bottom temperature, and aspect (Eastness/Northness). All models were proved capable of successfully predicting the species distribution. According to AUC values, the most accurate model for the four species was GAM together with Random Forest for *Anthoptilum grandiflorum*. On the other hand, MAXENT obtained greater values in the other four evaluation statistics in most cases. Performing the ensemble predictions of all models is a way of reducing uncertainty allowing to obtain a more accurate map.

These outputs will be used to improve the understanding of habitat requirements of those four species in the Flemish Cap and Flemish Pass areas. In order to increase the accuracy of predictions, new explanatory variables could be included and different resolutions could be tested. Biomass data could also be included in order to produce models that could be more suitable for management for a better conservation of those vulnerable species.

Case study 12: Habitat suitability models for Lophelia pertusa in the Florida-Hatteras slope

Habitat suitability models were developed for *Lophelia pertusa* in the Florida-Hatteras slope off the southeastern coast of the United States, the western North Atlantic Ocean. The deep-sea scleractinian coral *L. pertusa* is a common species on continental slopes of south-western US margins, providing important structural habitat for fish and other megafauna communities. However, the distribution of

this VME indicator species is not very well resolved in this region. Occurrence data was downloaded from NOAA's Deep-Sea Coral Research and Technology (DSCRT) data portal and obtained from three submersible dives on the R/V Atlantis (dives AL4962, AL4963) and the NOAA Ship Okeanos Explorer (dive EX1806-7).

The MAXENT model achieved good performance and were able to define suitable habitats better than random with the terrain variables slope, aspect (sine), ruggedness, and fine bpi providing the highest contributions to the predictive model outputs. The predicted suitable habitat for *L. pertusa* was higher in the continental slopes between 200 and 800m depth. However, the predicted distribution seems to be highly related with the quality of the bathymetry data.

Case study 13: Small scale predictive model a sponge species in a Tropic seamount under current environmental conditions

Small scale habitat suitability models were developed for the sponge species *Poliopogon amadou,* in the Tropic seamount, eastern North Atlantic Ocean. *Poliopogon amadou* occurs on extensive monospecific grounds in a tropic seamount, located in an Area Beyond National Jurisdiction (ABNJ) of the subtropical North Atlantic. MAXENT, GAMs, and RF models, and an ensemble approach were produced to improve the understanding of the potential extent of these sponge grounds and inform spatial management. The selection of the variables in the model construction was the main driver of the differences found among the models, namely on the areas where data were not available. RF was built using only two variables (depth and maximum current speed), whereas GAM and MAXENT also included other environmental variables (backscatter, fine-scale BPI, slope, eastness and northness). The inclusion of these other variables in the model construction of GAM and MAXENT allowed us to take into account microscale effects related to the geomorphology of the seabed.

Those results contributed towards understanding the environmental drivers and biogeography of the species in the Atlantic. Furthermore, a case towards designating the Tropic Seamount as an Ecologically or Biologically Significant marine Area (EBSA) as a contribution to address biodiversity conservation in ABNJ was presented, as the Tropic Seamount in spite of being far from the impact of deep-sea fishing by being located at depths beyond current fishing in this area; might nevertheless be vulnerable to other types of deep-water exploitation.

3.2 Ocean-basin scale habitat suitability models of cold-water corals and commercially important deep-sea fish in the North Atlantic under current environmental conditions

Telmo Morato[1,2], José-Manuel González-Irusta[1,2], Carlos Dominguez-Carrió[1,2], Chih-Lin Wei[3], Andrew Davies[4], Andrew K. Sweetman[5], Gerald H. Taranto[1,2], Lindsay Beazley[6], Ana García-Alegre[7], Anthony Grehan[8], Pascal Laffargue[9], F. Javier Murillo[6], Mar Sacau[7], Sandrine Vaz[10], Ellen Kenchington[6], Sophie Arnaud-Haond[10], Oisin Callery[8], Giovanni Chimienti[11,12], Erik Cordes[13], Hronn Egilsdottir[14], André Freiwald[15], Ryan Gasbarro[13], Matt Gianni[16], Kent Gilkinson[17], Vonda E. Wareham Hayes[17], Dierk Hebbeln[18], Kevin Hedges[19], Lea-Anne Henry[20], Mariano Koen-Alonso[17], Cam Lirette[6], Francesco Mastrototaro[11,12], Lénaick Menot[9], Tina Molodtsova[21], Pablo Durán Muñoz[7], Bramley Murton[22], Covadonga Orejas[23], Maria Grazia Pennino[7], Patricia Puerta[23], Stefán Á. Ragnarsson[14], Berta Ramiro-Sánchez[20], Jake Rice[24], Jesús Rivera[25], Murray Roberts[20], Luís Rodrigues[1,2], Steve W. Ross[26], José L. Rueda[27], Tim Siferd[19], Paul Snelgrove[28], David Stirling[29], Margaret Treble[19], Javier Urra[27], Johanne Vad[20], Les Watling[30], Wojciech Walkusz[19], Claudia Wienberg[18], Mathieu Woillez[9], Lisa A. Levin[31], Marina Carreiro-Silva[1,2]

1- Okeanos Research Centre, Universidade dos Açores, Horta, Portugal
2- IMAR Instituto do Mar, Universidade dos Açores, Horta, Portugal
3- Institute of Oceanography, National Taiwan University, Taipei, Taiwan
4- Department of Biological Sciences, University of Rhode Island, Kingston, Rhode Island, USA
5- Marine Benthic Ecology, Biogeochemistry and In situ Technology Research Group, The Lyell Centre for Earth and Marine Science and Technology, Heriot-Watt University, Edinburgh, United Kingdom
6- Bedford Institute of Oceanography, Fisheries and Oceans Canada, Dartmouth, NS, Canada
7- Instituto Español de Oceanografía (IEO), Centro Oceanográfico de Vigo, Vigo, Pontevedra, Spain.
8- Earth and Ocean Sciences, NUI Galway, Ireland
9- IFREMER, Centre Atlantique, Nantes, France
10- MARBEC, IFREMER, Univ. Montpellier, IRD, CNRS, France
11- Department of Biology, University of Bari Aldo Moro, Bari, Italy
12- CoNISMa, Rome, Italy
13- Department of Biology, Temple University, Philadelphia, USA
14- Marine and Freshwater Research Institute, Reykjavík, Iceland
15- Senckenberg am Meer, Marine Research Department, Wilhelmshaven, Germany
16- Gianni Consultancy, Amsterdam, Netherlands
17- Northwest Atlantic Fisheries Centre, Fisheries and Ocean Canada, St. John's, NL, Canada
18- MARUM - Center for Marine Environmental Sciences, University of Bremen, Germany
19- Fisheries and Oceans Canada, Winnipeg, MB, Canada
20- School of GeoSciences, Grant Institute, University of Edinburgh, United Kingdom
21- P.P. Shirshov Institute of Oceanology, Moscow, Russia
22- National Oceanography Centre, Southampton, United Kingdom
23- Instituto Español de Oceanografía, Centro Oceanográfico de Baleares, Palma, Spain
24- Fisheries and Ocean Canada, Ottawa, ON, Canada
25- Instituto Español de Oceanografía, Madrid, Spain
26- Center for Marine Science, University of North Carolina at Wilmington, Wilmington, NC, USA
27- Instituto Español de Oceanografía, Centro Oceanográfico de Málaga, Málaga, Spain
28- Department of Ocean Sciences, Memorial University, St Johns, Newfoundland, Canada
29- Marine Laboratory, Marine Scotland Science, Aberdeen, Scotland, UK
30- School of Marine Sciences, University of Maine, Orono, Maine, USA
31- Center for Marine Biodiversity and Conservation and Integrative Oceanography Division, Scripps Institution of Oceanography, UC San Diego, La Jolla, CA, USA

3.2.1 Ocean-basin scale description

Habitat suitability models of VME indicator taxa and commercially important deep-sea fish species were developed for the deep waters of the North-Atlantic basin, from 18°N to 76°N and 36°E to 98°W. This area was selected for the present study because it is one of the best studied deep-water regions in the world with respects to both species distribution and environmental conditions, as well as an emerging understanding of how many deep-sea species respond to environmental variability. Additionally, the North Atlantic Ocean contains well established Regional Fisheries Management Organisations making these analyses extremely relevant for deep-sea fish stocks and VMEs management purposes. This basin-scale study area also leads to more focussed model performance since it accounts for the range of environmental variability and species ecological niches.

3.2.2 Species selection

Six VME indicator taxa and six commercially important deep-sea fish species representative of both the East and West North Atlantic deep-sea habitats were selected based on their ecological significance or fisheries catch relevance, and on the availability and spatial coverage of existing occurrence records. The VME indicator taxa selected included three scleractinian corals forming aragonitic skeletons (*Lophelia pertusa*[1], *Madrepora oculata*, and *Desmophyllum dianthus*), and three gorgonians forming calcitic skeletons (*Acanella arbuscula*, *Acanthogorgia armata*, and *Paragorgia arborea*). These two groups of VME indicators are expected to respond differently to future conditions of water mass properties. The six deep-sea fish species selected were the roundnose grenadier (*Coryphaenoides rupestris*), Atlantic cod (*Gadus morhua*), bluemouth rockfish (*Helicolenus dactylopterus*), American plaice (*Hippoglossoides platessoides*), Greenland halibut (*Reinhardtius hippoglossoides*), and beaked redfish (*Sebastes mentella*).

3.2.3 Species occurrence data sources

Georeferenced presence-only records were obtained for all twelve species from institutional databases of partners participating this work as well as from public databases (Table 10) such as the Ocean Biogeographic Information System portal[2] (OBIS), the NOAA Deep Sea Coral Data Portal[3], and the ICES Vulnerable Marine Ecosystems (VMEs) data portal[4]. In order to reduce potential errors in the spatial position of the records, the depth associated to the OBIS and NOAA's presence records were

[1] recently synonymised to *Desmophyllum pertusum*, Addamo et al., 2016
[2] https://obis.org/
[3] https://deepseacoraldata.noaa.gov/
[4] http://www.ices.dk/marine-data/data-portals/Pages/vulnerable-marine-ecosystems.aspx

compared with the depth value extracted from the depth raster layer. Data points with no depth information or with differences in depth values greater than 30% and more than 50 m in absolute depth were excluded. In the case of the ICES VMEs database, those records with a position accuracy lower than 5000 m were excluded. Data directly provide from the partners were considered accurate. Maps of the presence records used in the models are presented as supporting information (Supplementary Figure S1).

Table 10. ***Number of grid cells with occurrence data obtained from multiple sources*** *for the six species of Vulnerable Marine Ecosystem indicators and six deep-sea fish used to model the suitable habitat in the North Atlantic. Depth ranges of occurrence records, and mean and standard deviation (±) for slope, Bathymetric Position Index (BPI), temperature at seafloor (Temp), POC flux to seafloor, and Aragonite (Ωar) and Calcite (Ωcal) saturation state at seafloor are also shown. Depth ranges for scleractinian corals and gorgonians are shown (in italics) for reference purposes only since depth was not considered for these species.*

Group	Species	N. cells	Depth range (m)	Slope (°)	BPI	Temp (°C)	POC flux (mg C·m^{-2}·d^{-1})	Ωar	Ωcal
Scleractinian corals	*Lophelia pertusa*	1,311	20-2,840	1.55±2.01	0.73±1.06	8.24±2.57	14.78±8.31	1.99±0.30	-
	Madrepora oculata	418	100-2,120	2.23±2.41	0.88±1.79	9.41±2.93	9.94±6.48	1.96±0.45	-
	Desmophyllum dianthus	312	50-3,250	3.67±3.32	0.80±1.79	8.28±3.17	9.18±5.84	1.81±0.49	-
Gorgonians	*Acanthogorgia armata*	324	30-2,600	2.81±2.18	0.78±0.99	4.92±2.21	15.24±6.17	-	2.59±0.30
	Acanella arbuscula	852	50-4,810	2.52±2.41	0.75±1.44	4.71±1.99	12.00±5.54	-	2.54±0.28
	Paragorgia arborea	434	40-2,170	1.26±1.78	0.52±0.71	3.87±2.26	21.35±8.36	-	2.69±0.21
Deep-water fish	*Helicolenus dactylopterus*	4,508	20-1,790	1.49±2.23	1.08±1.19	8.59±1.79	24.08±16.35	-	-
	Sebastes mentella	15,476	10-1,630	0.80±1.15	0.44±0.74	3.71±1.70	21.08±7.08	-	-
	Gadus morhua	52,463	10-990	0.29±0.57	0.22±0.52	5.64±2.75	34.12±14.97	-	-
	Hippoglossoides platessoides	56,734	10-1,490	0.34±0.63	0.23±0.54	5.21±2.69	32.19±14.66	-	-
	Reinhardtius hippoglossoides	23,491	10-1,690	0.74±1.09	0.30±0.67	3.58±1.89	23.43±9.84	-	-
	Coryphaenoides rupestris	3,009	70-1,800	2.23±1.60	0.44±0.88	4.55±1.53	15.16±5.73	-	-

3.2.4 Environmental data layers

A set of terrain and environmental variables were used in this study as candidate predictors of present-day (1951-2000) distribution. All predictor variables were rescaled to a final grid cell resolution of approximately 3x3 km comprising about 3.8 million cells. Terrain variable depth was extracted from a bathymetry grid built from two data sources: the EMODnet Digital Bathymetry portal (EMODnet, 2016) and the General Bathymetric Chart of the Oceans (GEBCO 2014; Weatherall et al., 2015). The original resolution from EMODnet (0.002°) was up-scaled to the GEBCO resolution (0.008°) using a bilinear interpolation. The bathymetry layers were merged by using EMODnet data when available and completing it with GEBCO 2014, and rescaled to the final resolution of 3x3 km using bilinear interpolation. Slope (in degrees) was derived from the final bathymetry grid using the package *raster* of the R environment (Hijmans, 2016) and the Bathymetric Position Index (BPI) was computed using the Benthic Terrain Model 3.0 tool in ArcGIS 10.1 (ESRI, 2015) with an inner radius of 3 and an outer radius of 25. In order to avoid extreme values, BPI was standardized using the scale function from the *raster* package.

Environmental variables of present-day conditions, including particulate organic carbon (POC) flux at 100-m depth (*epc100*, mg $C \cdot m^{-2} \cdot d^{-1}$), dissolved oxygen concentration at seafloor ($mL \cdot L^{-1}$), pH at seafloor, and potential temperature at seafloor (°C) were downloaded from the Earth System Grid Federation (ESGF) Peer-to-Peer (P2P) enterprise system[5]. The *epc100* was converted to export POC flux at the seafloor using the Martin curve (Martin et al., 1987) following the equation: $epc = epc100*(water\ depth/export\ depth)^{-0.858}$, where the export depth was set to 100 m. Aragonite (Ωar) and calcite (Ωcal) saturation state at seafloor were used as candidate predictors for habitat suitability of cold-water coral species. These saturation states were computed by dividing the carbonate ion concentration ($mol \cdot m^{-3}$) at seafloor by the carbonate ion concentration ($mol \cdot m^{-3}$) for seawater in equilibrium with pure aragonite and calcite at seafloor. Yearly means of these parameters were calculated for the period 1951-2000 (historical simulation) using the average values obtained from the Geophysical Fluid Dynamics Laboratory's ESM 2G model (GFDL-ESM-2G; Dunne et al., 2012), the Institut Pierre Simon Laplace's CM6-MR model (IPSL-CM5A-MR; Dufresne et al., 2013) and Max Planck Institute's ESM-MR model (MPI-ESM-MR; Giorgetta et al., 2013) within the Coupled Models Intercomparison Project Phase 5 (CMIP5). Environmental variables were available at a 0.5° resolution and re-scaled to match the 3x3km cell size using universal kriging and depth as covariate. Maps of environmental predictors for present-day conditions are provided as Supplementary Figure S2.

[5] https://esgf-node.llnl.gov

3.2.5 Modelling approaches

Here, we used an ensemble modelling approach to predict the habitat suitability under present-day (1951-2000) conditions. We employed three widely used modelling methods (González-Irusta et al., 2015) capable of dealing with presence-only data using pseudo-absences: the maximum entropy model (Maxent, Phillips et al., 2006; 2017), Generalized Additive Models (GAMs, Hastie & Tibshirani, 1986) and the Random Forest machine learning algorithms (Breiman, 2001). Maxent models were developed using the function *maxent* from the R package *dismo* (Hijmans et al., 2017), with prevalence set as the proportion of presences over the pseudo-absences generated. GAMs were fitted with the function *gam* from the R package mgcv (Wood, 2018) using a binomial error distribution with logit function and constrained the smooth curves to 4 knots to avoid overfitting; 3 for temperature and aragonite in the cold-water coral models. Finally, Random Forest models were computed using the function *randomForest* from the package with the same name (Liaw & Wiener, 2002).

The variable selection in GAMs was performed using the Akaike Information Criteria (AIC) and the function *dredge* from the package 'MuMIn' (Barton, 2018) whereas the other two models (Maxent and Random Forest) were fitted with the original set of variables. To assess the contribution for each variable in the final predictions, we used a randomisation procedure adapted from Thuiller et al. (2009) which allows to estimate the importance of each variable independently of the modelling technique, enabling direct comparisons between models. This methodology computes the Pearson correlation between the original predictions and predictions where the variable under evaluation has been randomly permutated. This operation was repeated 10 times for each combination of model, variable and species. In order to have intuitive values of variable importance, we computed 1-Pearson correlation where high values equal to high variable importance. The relationship between the environmental predictors and the predicted habitat suitability was analysed using response curves produced using the same methodology described by Elith et al. (2006).

Ensemble outputs were computed for all species by computing the average HSI by cell after weighting the model outputs with the evaluation metrics AUC and TSS, using the same approach applied by Rowden et al. (2017). The importance of each predictor variable to the ensemble habitat suitability model predictions was estimated as the average of the variable importance in the individual models weighted by the models evaluation metrics.

3.2.6 Model outputs

Scleractinian corals under present day conditions showed a higher suitability in the Eastern North Atlantic and the Mid-Atlantic Ridge including the Azores, but also in the Gulf of Mexico and the Mediterranean Sea, whilst gorgonian showed higher suitability in the Western North Atlantic and south of Greenland (Figure 80). Most deep-sea fish species modelled showed a wide distribution range, with suitable habitats on the shelf and slope of both sides of the North Atlantic and along the coast of Iceland and Greenland (Figure 81). However, *Helicolenus dactylopterus* displayed a smaller suitable habitat limited to areas south of the Flemish Cap, south of Iceland, the Azores, and around the British Isles, while *Coryphaenoides rupestris* suitable habitat was limited to deeper areas along the continental slope of both sides of the Atlantic.

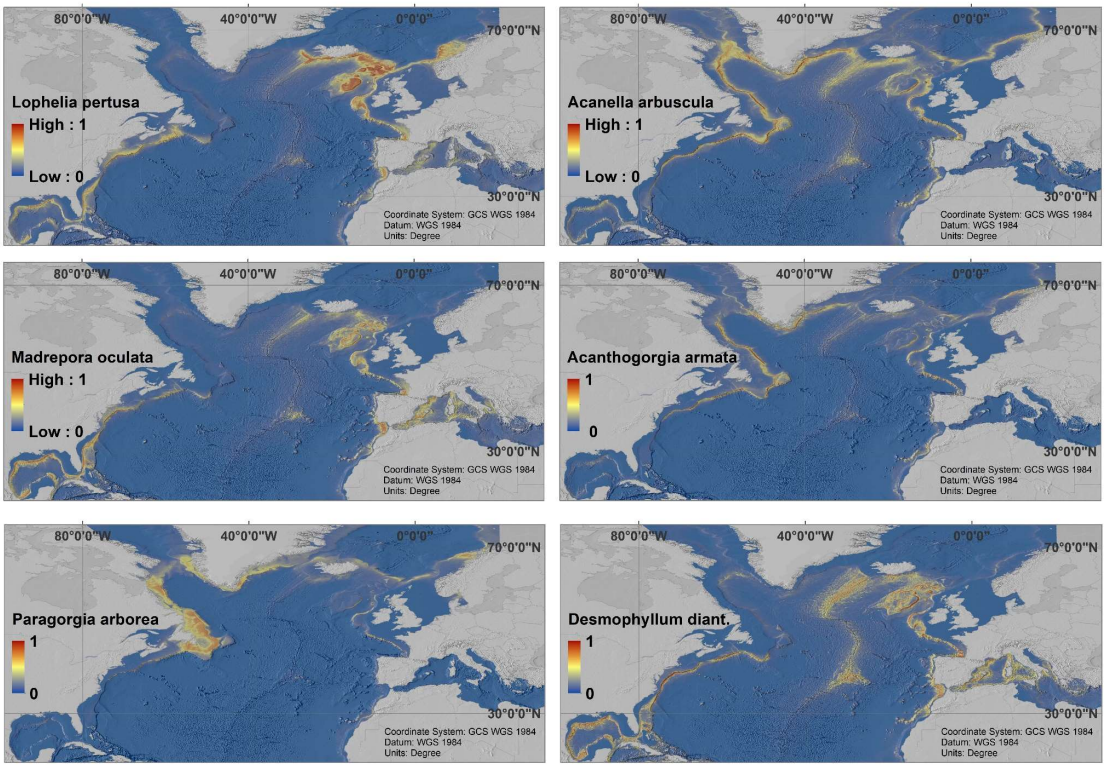

Figure 80. Predicted habitat suitability index under present-day (1951-2000) environmental conditions for cold-water corals in the North Atlantic Ocean using an ensemble modelling approach.

In general, the three modelling approaches (Supplementary Table S1) and the ensemble model (Table 11) predictions achieved good accuracy for most species (AUC> 0.80 and TSS> 0.60) with a reasonable match with the known species occurrences (Sensitivity> 0.80). Ensemble models for all cold-water corals species achieved good accuracy, although models for scleractinian corals performed slightly better than those for gorgonian species. The predicted distribution of *Desmophyllum dianthus* (AUC= 0.95; TSS> 0.74) and *Paragorgia arborea* (AUC= 0.95; TSS> 0.76) displayed the highest accuracy among

all corals, with *Acanella arbuscula* showing the lowest accuracy values (AUC= 0.88; TSS< 0.67). Deep-sea fish model predictions accuracy was slightly better when compared to cold-water corals but showed an inverse relation with sample size (Table 11). The predicted distribution of *Coryphaenoides rupestris* (AUC= 0.99; TSS> 0.88; n= 3,009) and *Helicolenus dactylopterus* (AUC= 0.97; TSS> 0.81; n= 4,508) displayed the highest accuracy among all fishes, whilst *Gadus morhua* (AUC= 0.94; TSS< 0.81; n= 52,463) and *Hippoglossoides platessoides* (AUC= 0.93; TSS< 0.81, n= 54,725) displayed lower values. The lowest accuracy was obtained for the *Reinhardtius hippoglossoides* (AUC= 0.87; TSS< 0.61, n= 23,491). The uncertainty associated with the ensemble habitat suitability model predictions under present-day conditions was in general low for both cold-water corals and deep-sea fish (Figure 82).

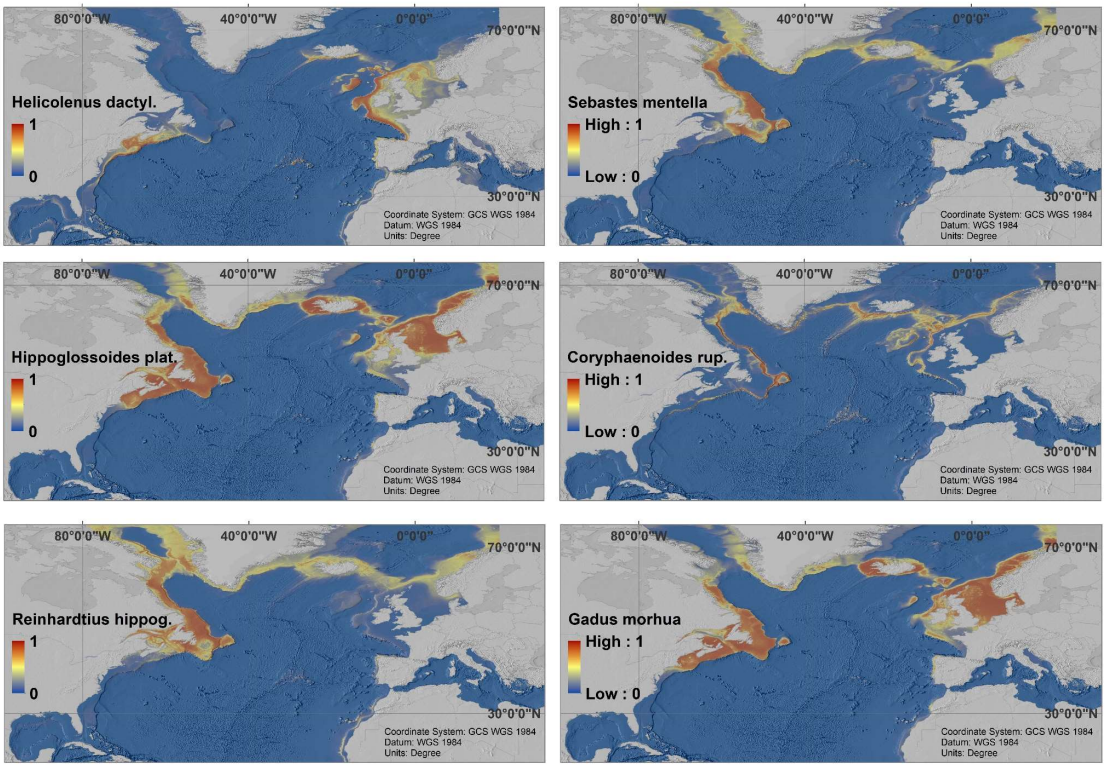

Figure 81. Predicted habitat suitability index under present-day (1951-2000) environmental conditions for commercially important deep-sea fish in the North Atlantic Ocean, using an ensemble modelling approach.

The habitat suitability models developed here included seven different predictors which provided different levels of contribution for the different modelled species (Table 12). In general, POC flux to the seafloor, seafloor temperature, and aragonite or calcite saturation were the most important predictors for scleractinian and gorgonians, while depth, POC flux, and temperature were the most important predictors for deep-sea fish (Table 12). It should be noted, however, that slope was also an important predictor for *Desmophyllum dianthus*, *Acanthogorgia armata*, and *Madrepora oculata*. The response curves derived from all modelling approaches are shown as Supplementary Figure S3 and Supplementary Figure S4.

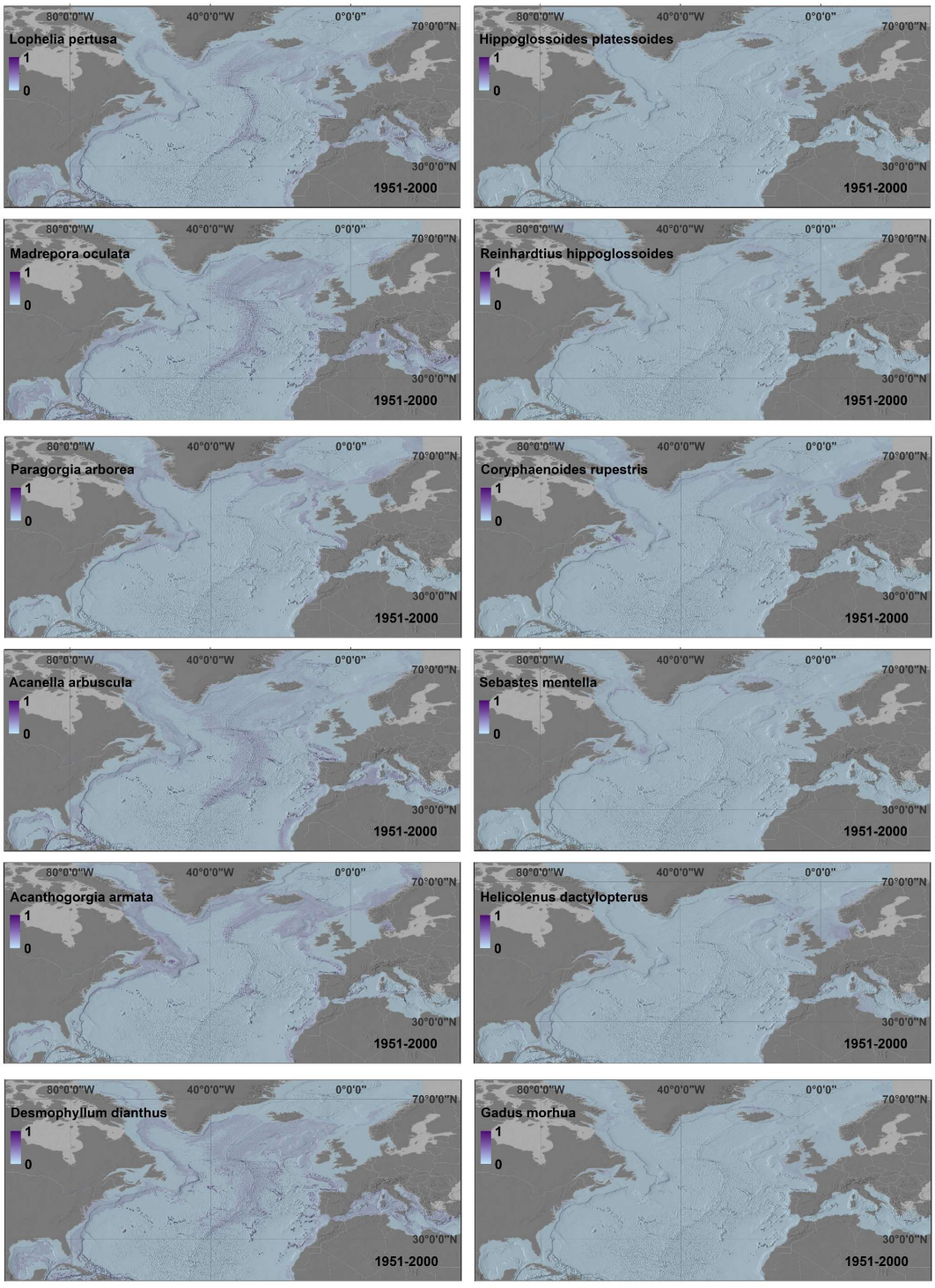

Figure 82. Uncertainty associated to the habitat suitability model predictions under present-day (1951-2000) environmental conditions for cold-water corals (left) and commercially important deep-sea fish (right) in the North Atlantic Ocean using an ensemble modelling approach.

Table 11. ***Model performance statistics*** *generated using an ensemble modelling approach. The ability of the training data to predict the probability of presence was tested with different statistical metrics: area under the curve (AUC) of the receiver operating characteristic, kappa statistic, sensitivity (% true positives), specificity (% true negatives), and True Skill Statistic (TSS). Statistics were calculated using two thresholds: 10-percentile training presence logistic threshold (10th) and maximum sensitivity and specificity (MSS).*

Group	Species	AUC	Kappa		Sensitivity		Specificity		TSS		Thresholds	
			10th	*MSS*	*10th*	*MSS*	*10th*	*MSS*	*10th*	*MSS*	*10th*	*MSS*
Scleractinian corals	*Lophelia pertusa*	0.91±0.08	0.51±0.31	0.57±0.25	0.90	0.88±0.06	0.78±0.18	0.85±0.11	0.68±0.18	0.72±0.17	0.34	0.24
	Madrepora oculata	0.92±0.06	0.31±0.22	0.41±0.19	0.90	0.88±0.09	0.77±0.16	0.87±0.07	0.66±0.16	0.75±0.14	0.31	0.20
	Desmophyllum dianthus	0.95±0.03	0.34±0.14	0.39±0.16	0.90	0.92±0.07	0.85±0.08	0.86±0.09	0.74±0.08	0.79±0.08	0.33	0.22
Gorgonians	*Acanthogorgia armata*	0.92±0.05	0.35±0.29	0.43±0.21	0.90	0.88±0.06	0.77±0.20	0.89±0.07	0.66±0.20	0.77±0.12	0.26	0.18
	Acanella arbuscula	0.88±0.03	0.22±0.20	0.49±0.20	0.90	0.81±0.07	0.60±0.15	0.86±0.10	0.50±0.15	0.67±0.10	0.32	0.19
	Paragorgia arborea	0.95±0.05	0.44±0.18	0.50±0.17	0.90	0.90±0.06	0.86±0.13	0.90±0.09	0.76±0.13	0.79±0.12	0.36	0.23
Deep-water fish	*Helicolenus dactylopterus*	0.97±0.03	0.81±0.08	0.84±0.08	0.90	0.96±0.02	0.91±0.08	0.88±0.08	0.81±0.08	0.84±0.08	0.54	0.33
	Sebastes mentella	0.94±0.06	0.68±0.22	0.67±0.21	0.90	0.95±0.03	0.85±0.15	0.82±0.15	0.75±0.15	0.78±0.13	0.63	0.50
	Gadus morhua	0.94±0.02	0.75±0.01	0.79±0.01	0.90	0.99±0.01	0.86±0.01	0.82±0.02	0.76±0.01	0.81±0.01	0.74	0.60
	Hippoglossoides platessoides	0.93±0.01	0.75±0.00	0.80±0.03	0.90	0.97±0.04	0.86±0.00	0.84±0.01	0.76±0.00	0.81±0.04	0.73	0.59
	Reinhardtius hippoglossoides	0.87±0.01	0.48±0.05	0.52±0.01	0.90	0.90±0.08	0.68±0.05	0.71±0.06	0.58±0.05	0.61±0.02	0.61	0.54
	Coryphaenoides rupestris	0.99±0.01	0.88±0.01	0.93±0.03	0.90	0.97±0.02	0.98±0.01	0.96±0.01	0.88±0.01	0.93±0.03	0.63	0.26

Table 12. ***Importance of each predictor variable to the habitat suitability model predictions****, measured as 1-Pearson correlation, for six species of Vulnerable Marine Ecosystem indicators and six deep-sea fish in the North Atlantic Ocean. Predictor variable were depth, slope, Bathymetric Position Index (BPI), temperature at seafloor (Temp), particulate organic carbon flux to seafloor (POC), Aragonite (Ωar) and Calcite (Ωcal) saturation state at seafloor, and dissolved oxygen (DO) concentration at seafloor.*

Group	Species	Relative importance							
		Depth	***Slope***	***BPI***	***Temp***	***POC***	***Ωar***	***Ωcal***	***DO***
Scleractinian corals	*Lophelia pertusa*	-	0.06±0.04	0.05±0.06	0.41±0.13	0.26±0.10	0.36±0.04	-	
	Madrepora oculata	-	0.16±0.09	0.07±0.05	0.47±0.14	0.40±0.06	0.14±0.09	-	
	Desmophyllum dianthus	-	0.27±0.13	0.05±0.04	0.44±0.15	0.48±0.20	0.11±0.13	-	
Gorgonians	*Acanthogorgia armata*	-	0.19±0.12	0.05±0.05	0.15±0.05	0.29±0.20	-	0.35±0.12	
	Acanella arbuscula	-	0.09±0.06	0.03±0.04	0.17±0.08	0.21±0.15	-	0.41±0.06	
	Paragorgia arborea	-	0.06±0.05	0.08±0.05	0.15±0.09	0.35±0.27	-	0.58±0.05	
Deep-water fish	*Helicolenus dactylopterus*	0.64±0.26	0.17±0.22	0.19±0.21	0.45±0.03	0.24±0.17	-	-	0.16±0.16
	Sebastes mentella	0.67±0.22	0.17±0.23	0.17±0.22	0.38±0.11	0.43±0.17	-	-	0.13±0.16
	Gadus morhua	0.70±0.15	0.15±0.17	0.14±0.17	0.27±0.13	0.40±0.09	-	-	0.31±0.25
	Hippoglossoides platessoides	0.64±0.11	0.12±0.14	0.11±0.13	0.29±0.12	0.41±0.12	-	-	0.35±0.13
	Reinhardtius hippoglossoides	0.64±0.26	0.22±0.30	0.23±0.30	0.48±0.14	0.50±0.16	-	-	0.27±0.17
	Coryphaenoides rupestris	0.67±0.16	0.21±0.19	0.16±0.22	0.20±0.20	0.41±0.10	-	-	0.25±0.17

3.2.7 Model interpretation, caveats and future directions

Some of the general distribution patterns identified here have been suggested for both cold-water corals and deep-sea fish. Therefore, this study highlights the appropriateness of environmental niche modelling in evaluating changes in the suitable habitat of deep-sea species at large spatial scales. However, the reliability of such models and the usefulness for management purposes depend on many aspects (Robinson et al., 2017) including the spatial resolution and quality of the terrain and environmental data, the volume, the quality and the spatial coverage of the occurrence data, the availability of absence records, model selection, assumptions and parametrization, among others. Our models suffer from a number of common and well-known limitations that may be more pronounced when modelling deep-sea taxa. It is known that cold-water coral distributions respond to small-scale fluctuations of different terrain attributes, such as substrate type and seabed rugosity (De Clippele et al., 2017), and oceanographic conditions (Bennecke & Metaxas, 2017). However, both terrain and environmental information was derived from global datasets and not from detailed deep-sea *in situ* measurements which does not discriminate between areas with high small-scale heterogeneity. Since we aim to evaluate the habitat suitability at large spatial scales, the data and grid size used in the models performed in this study can be considered adequate.

There are other sources of uncertainty including the quantity and the spatial distribution of available occurrence data, to some degree of uncertainty on deep-sea species identification (mostly for VME indicator taxa) and geo-location of data obtained from OBIS. Also, the use of presence-only records (as opposed to abundance data) with no true absence data generates increased uncertainty. The deep sea is still one of the least studied and sampled areas on the planet and therefore many species are still unknown or the taxonomy still has to be resolved and the real spatial distribution is also undetermined (mostly for VME indicator taxa). This source of uncertainty will only be reduced with extensive exploration of the deep-sea environment.

In summary, we showed that although improvements in the modelling approach may be required, species distribution or habitat suitability models are useful tools for predicting potential distribution of deep-water species in the north Atlantic and may inform management decisions within RFMOs.

Supplementary Material

Supplementary Table S1. Model performance statistics for the different modelling approaches. The ability of the training data to predict the probability of presence was tested with different statistical metrics using the maximum sensitivity and specificity (MSS) threshold. The weighting factor (Wf) used to produce the ensemble model outputs are also shown.

Species	Modelling approach	Relative importance AUC	TSS	W_f
Lophelia pertusa	GAM	0.86±0.10	0.64±0.18	0.32
	Maxent	0.89±0.06	0.69±0.13	0.34
	RF	0.90±0.07	0.66±0.14	0.33
Madrepora oculata	GAM	0.88±0.07	0.70±0.15	0.33
	Maxent	0.90±0.06	0.71±0.13	0.34
	RF	0.90±0.06	0.70±0.13	0.33
Desmophyllum dianthus	GAM	0.90±0.06	0.70±0.13	0.32
	Maxent	0.93±0.04	0.76±0.09	0.34
	RF	0.94±0.02	0.79±0.05	0.32
Acanthogorgia armata	GAM	0.92±0.06	0.77±0.10	0.34
	Maxent	0.93±0.05	0.78±0.12	0.34
	RF	0.91±0.06	0.73±0.15	0.34
Acanella arbuscula	GAM	0.86±0.05	0.63±0.11	0.32
	Maxent	0.88±0.04	0.66±0.13	0.33
	RF	0.90±0.05	0.69±0.12	0.33
Paragorgia arborea	GAM	0.89±0.10	0.68±0.22	0.32
	Maxent	0.93±0.08	0.75±0.17	0.34
	RF	0.90±0.12	0.73±0.19	0.33
Helicolenus dactylopterus	GAM	0.97±0.02	0.85±0.05	0.33
	Maxent	0.98±0.01	0.87±0.04	0.34
	RF	0.97±0.02	0.82±0.04	0.33
Sebastes mentella	GAM	0.98±0.01	0.85±0.03	0.34
	Maxent	0.97±0.01	0.84±0.01	0.33
	RF	0.97±0.01	0.84±0.01	0.33
Gadus morhua	GAM	0.95±0.02	0.81±0.03	0.34
	Maxent	0.94±0.02	0.79±0.01	0.33
	RF	0.95±0.03	0.78±0.14	0.34
Hippoglossoides platessoides	GAM	0.94±0.02	0.79±0.06	0.34
	Maxent	0.93±0.01	0.80±0.03	0.34
	RF	0.94±0.04	0.71±0.16	0.34
Reinhardtius hippoglossoides	GAM	0.87±0.01	0.61±0.02	0.33
	Maxent	0.87±0.01	0.62±0.02	0.33
	RF	0.87±0.01	0.62±0.02	0.33
Coryphaenoides rupestris	GAM	0.99±0.01	0.92±0.02	0.33
	Maxent	0.99±0.00	0.92±0.02	0.33
	RF	0.99±0.01	0.91±0.04	0.33

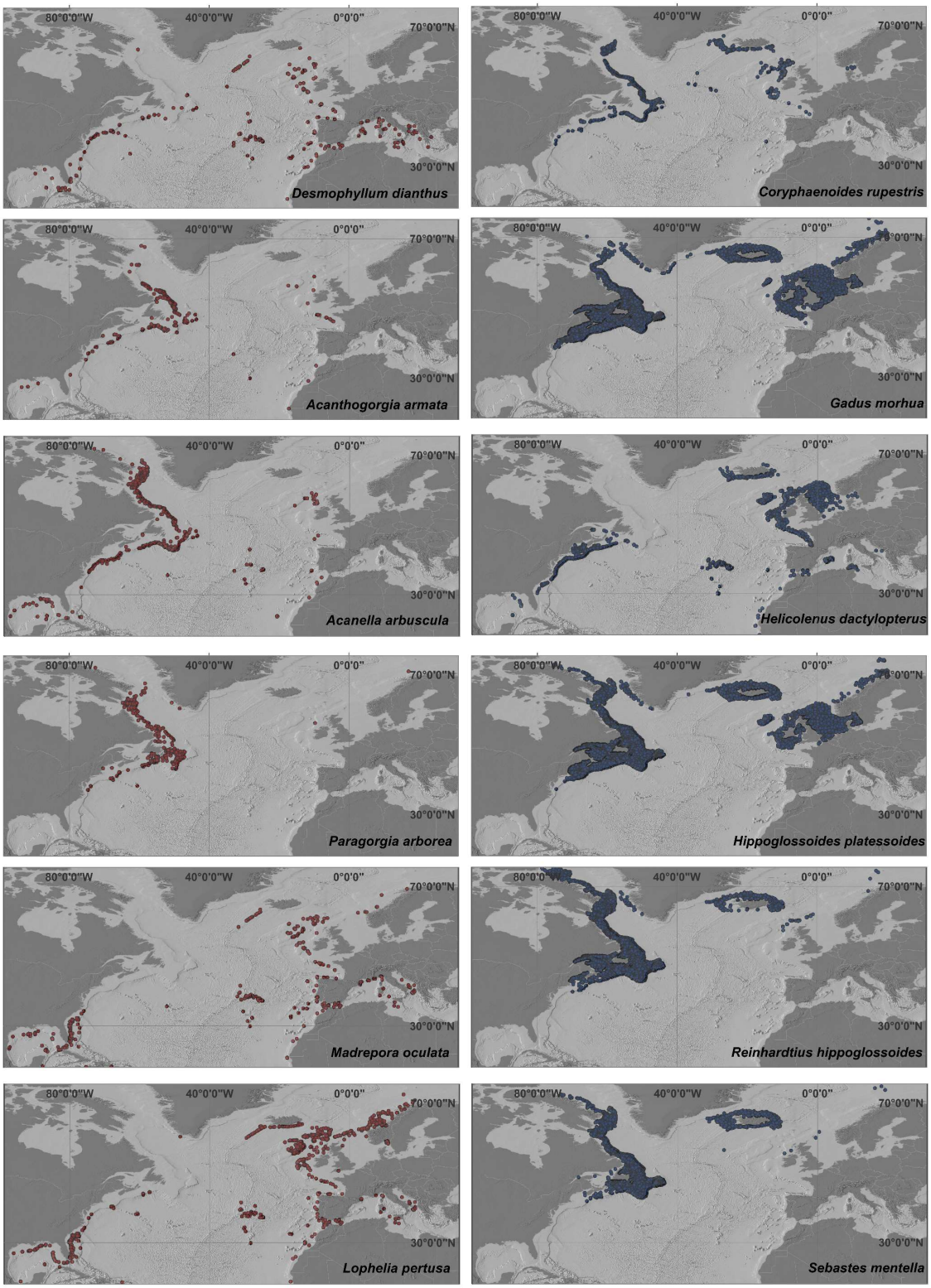

Supplementary Figure S1. Occurrences of the 6 species of cold-water corals (left) and 6 species of deep-sea fish (right) studied at the ocean-basin scale

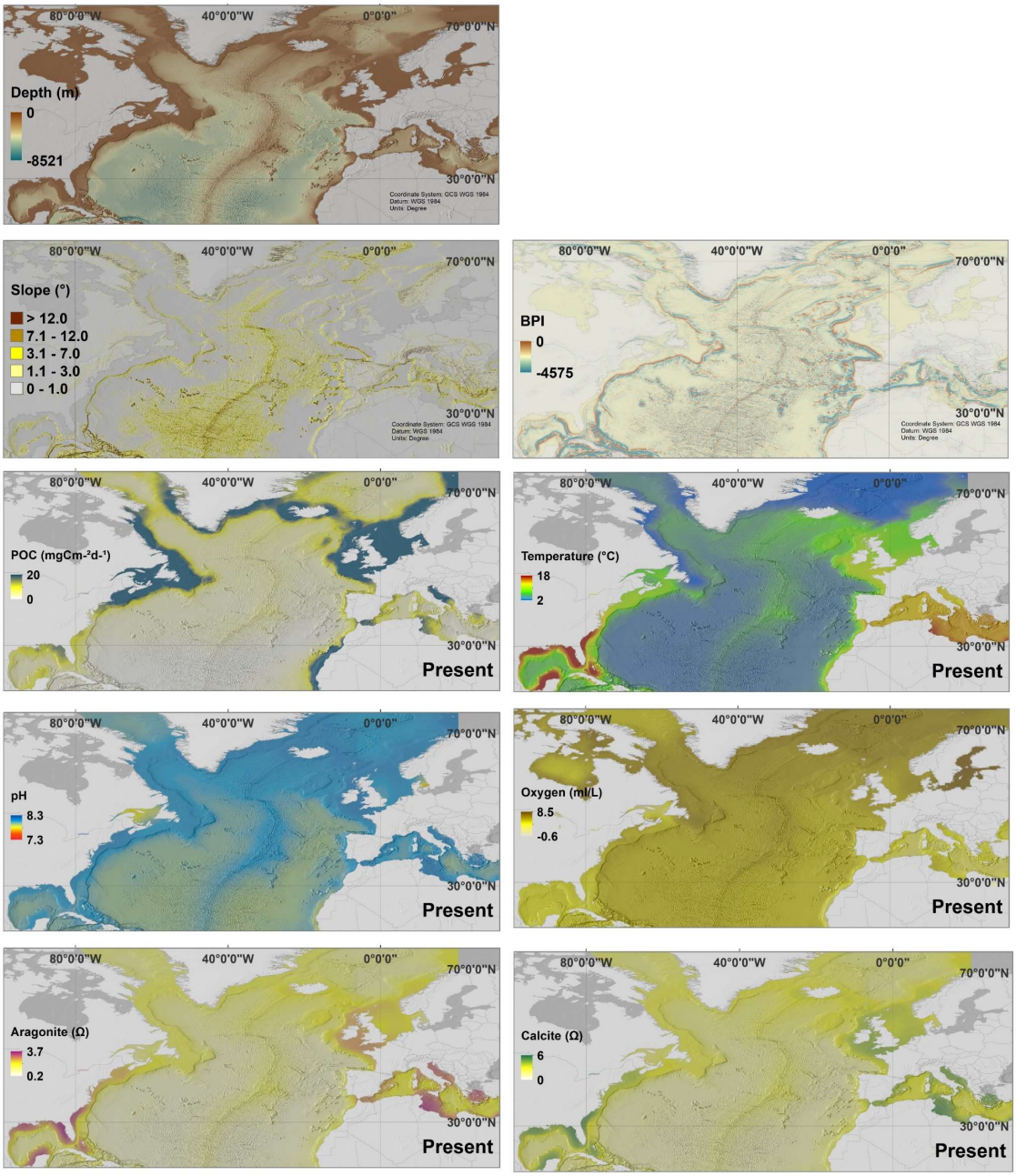

Supplementary Figure S2. Environmental predictors used to develop environmental niche models for present-day conditions in the northeast Atlantic Ocean.

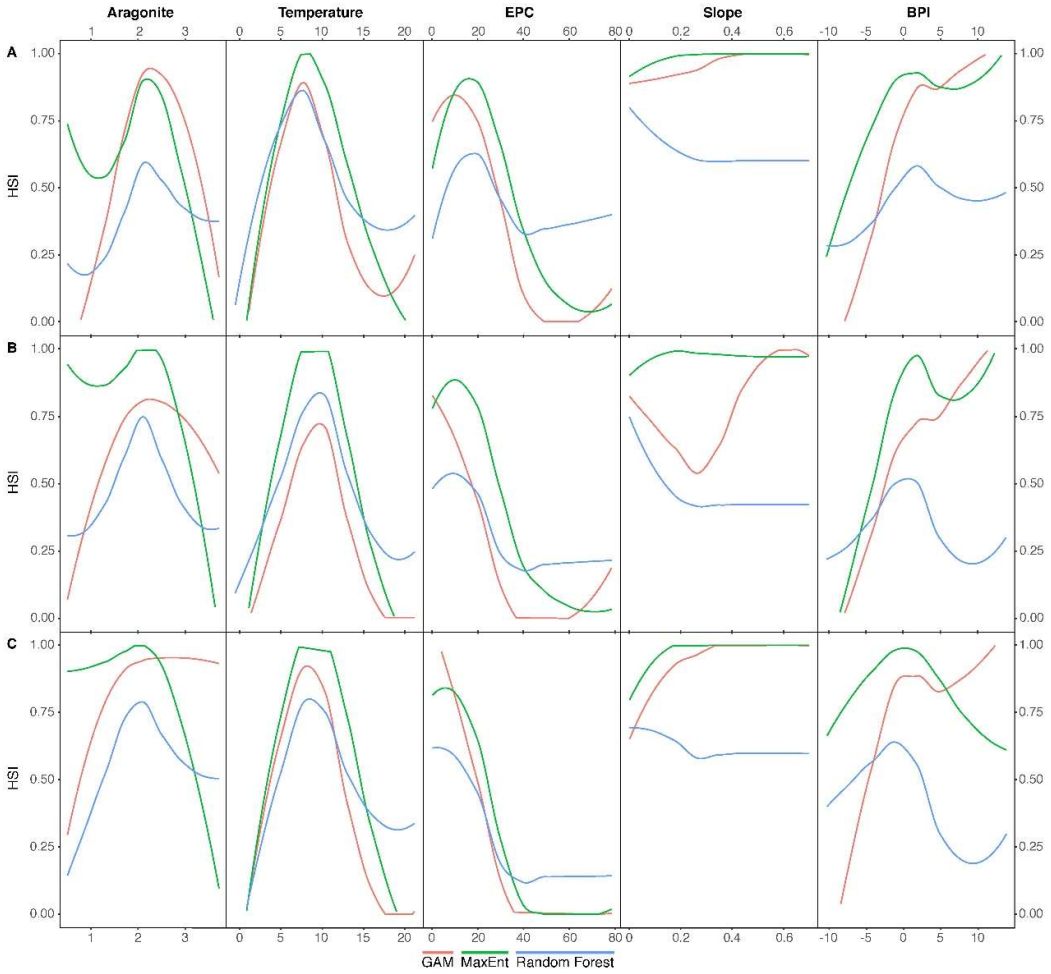

Supplementary Figure S3a. Response curves for predictor variables for scleractinian cold-water corals as determined by the three different modelling approaches: Generalized Additive Model (GAM), maximum entropy model (Maxent), and Random Forest (RF). A) Lophelia pertusa*; B)* Madrepora oculata; *C)* Desmophyllum dianthus. *Predictor variables included aragonite saturation state at seafloor, temperature at seafloor (°C), particulate organic carbon flux at the seafloor (EPC, mg C·m-2·d-1), slope (in radians) and standardized Bathymetric Position Index (BPI).*

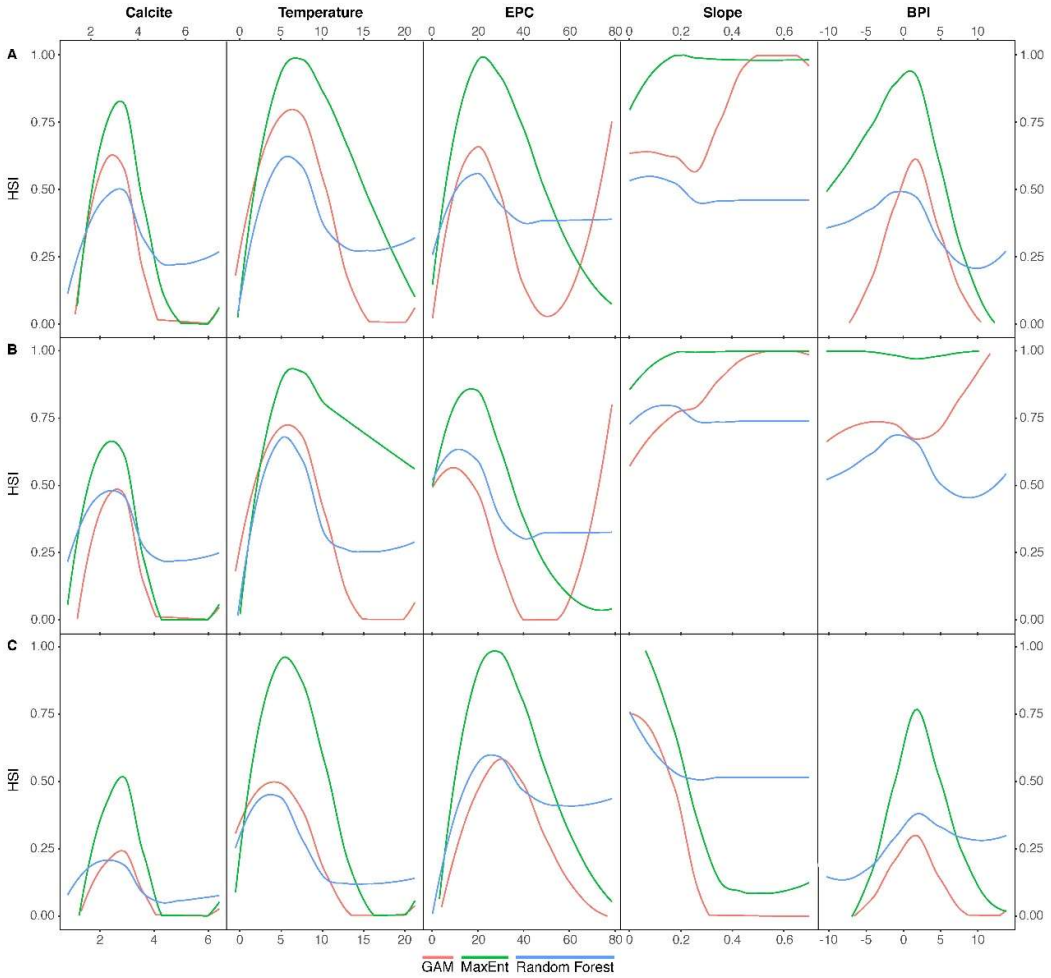

Supplementary Figure S3b. Response curves for predictor variables for gorgonian corals as determined by the three different modelling approaches: Generalized Additive Model (GAM), maximum entropy model (Maxent), and Random Forest (RF). A) Acanthogorgia armata*; B)* Acanella arbuscula*; C)* Paragorgia arborea*. Predictor variables included calcite saturation state at seafloor, temperature at seafloor (°C), particulate organic carbon flux at the seafloor (EPC, mg C·m-2·d-1), slope (radians) and standardized Bathymetric Position Index (BPI).*

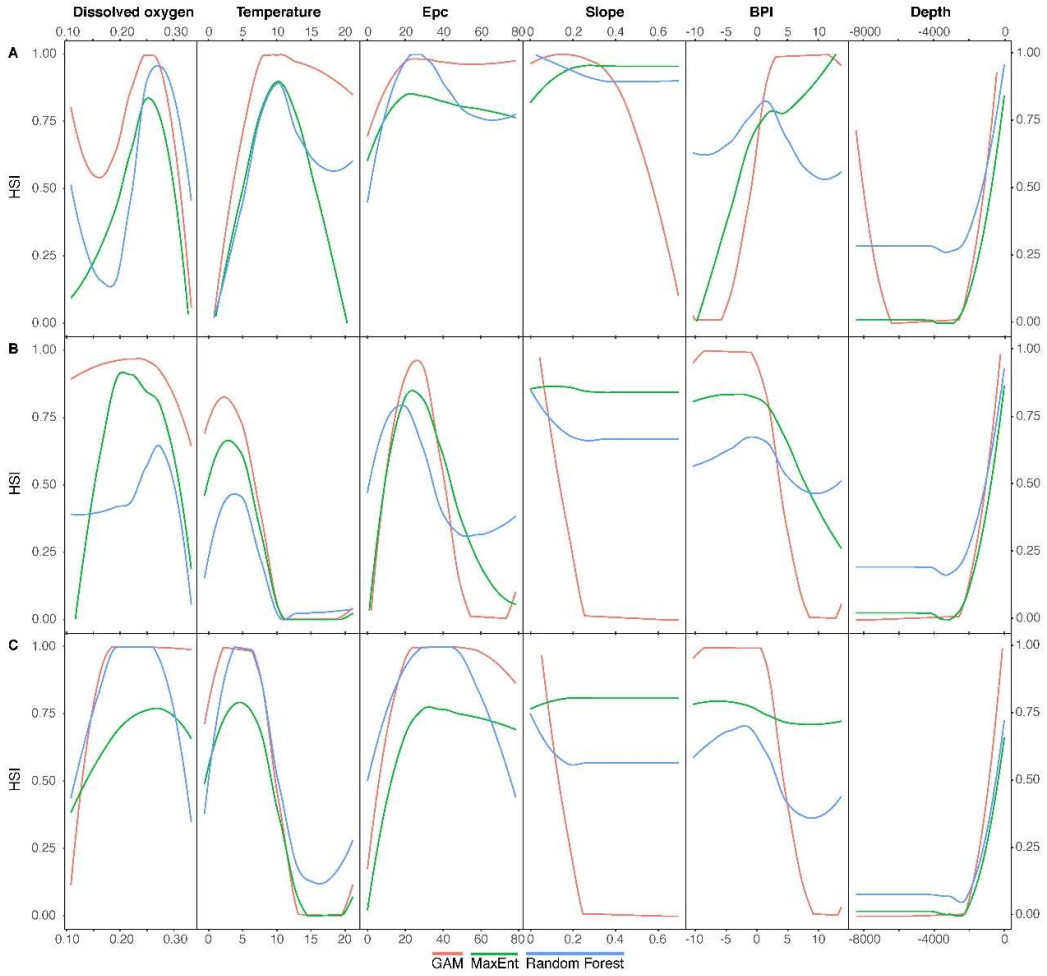

Supplementary Figure S4a. Response curves for predictor variables for commercially important deep-sea fish as determined by the three different modelling approaches: Generalized Additive Model (GAM), maximum entropy model (Maxent), and Random Forest (RF). A) Helicolenus dactylopterus*; B)* Sebastes mentella*; C)* Gadus morhua*. Predictor variables included dissolved oxygen concentration at seafloor (mL·L-1), temperature at seafloor (°C), particulate organic carbon flux at the seafloor (EPC, mg C·m-2·d-1), slope (in radians), standardized Bathymetric Position Index (BPI), and depth (m).*

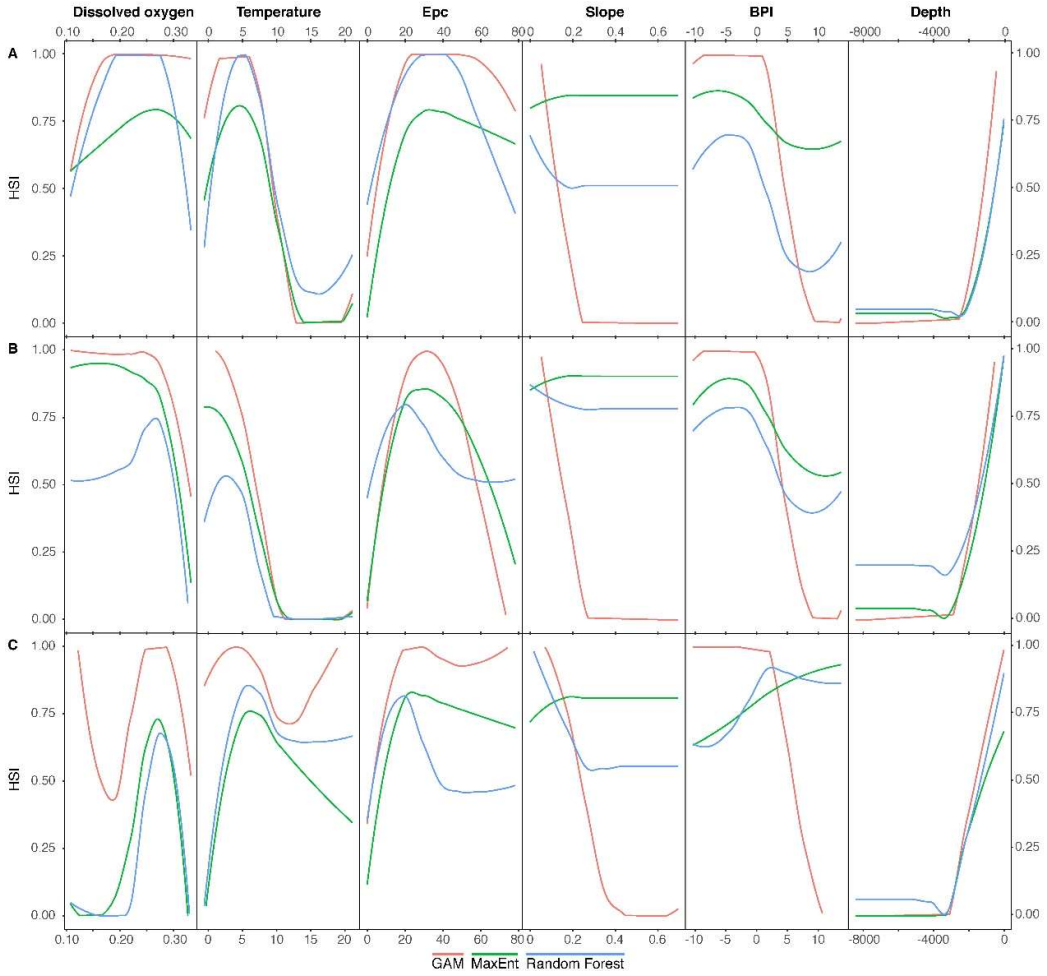

Supplementary Figure S4b. Response curves for predictor variables for commercially important deep-sea fish as determined by the three different modelling approaches: Generalized Additive Model (GAM), maximum entropy model (Maxent), and Random Forest (RF). A) Hippoglossoides platessoides*; B)* Reinhardtius hippoglossoides*; C)* Coryphaenoides rupestris*. Predictor variables included dissolved oxygen concentration at seafloor (mL·L-1), temperature at seafloor (°C), particulate organic carbon flux at the seafloor (EPC, mg C·m-2·d-1), slope (in radians), standardized Bathymetric Position Index (BPI), and depth (m).*

3.3 Case study 3: Habitat suitability models of *Lophelia pertusa* and two sea pen species under current environmental conditions in Rockall Bank, NE Atlantic

David Stirling[1], Francis Neat[1]

1- Marine Scotland Science, Marine Laboratory, Aberdeen, Scotland

3.3.1 Case study description

Rockall Bank lies to the eastern margin of the North Atlantic Ocean. It is the largest and shallowest of several banks that form the Faroese-Rockall Plateau (Figure 83). It rises from Rockall Trough (> 2000 m) in the east and breaks the surface towards the northern end of the bank. To the west it rises from the Hatton – Rockall Basin and depths of around 1 km. It is situated at the boundary between two counter rotating gyres; the subtropical and subpolar gyres of the North Atlantic (McGrath et al., 2012). The oceanography of Rockall Bank is dominated by the dynamics of the subpolar gyre (SPG), where changes in the strength and extent of the SPG dictate the marine climate (Hátún et al., 2009; Berx & Payne, 2017). During strong SPG conditions the North Atlantic Current predominantly flows to the east of the plateau bathing it in subarctic water, while during weak SPG conditions it predominantly flows to the west, exposing Rockall Bank to warmer, saltier Modified North Atlantic Water.

Rockall Bank has a long history of exploitation and exploration supporting a fishery for more than 200 years (Newton et al., 2008) as well as being the subject of hydrographic, oceanographic and fisheries surveys for many years (Johnson et al., 2019). There have been no oil and gas developments in the region and, until recently, the general view of petroleum exploration has been negative. However, with the acquisition and analysis of new seismic data and the granting of frontier exploration licenses in the recent licensing rounds, there has been increased interest in exploring Rockall Bank and the surrounding area (Schofield et al., 2018; N. Schofield, pers. comm.).

The diverse offshore habitats found on Rockall Bank support rich aggregations of benthic invertebrates, including long-lived and fragile cold-water coral reef ecosystems and sponge aggregations, as well as a diverse fish assemblage (Roberts et al., 2008; Neat & Campbell, 2011). Areas that constitute vulnerable marine ecosystems (VMEs) (FAO, 2009) are found on Rockall Bank (Figure 84). The recognition and protection of these has contributed to a complex arrangement of management areas in the region (reviewed by Johnson et al., 2019).

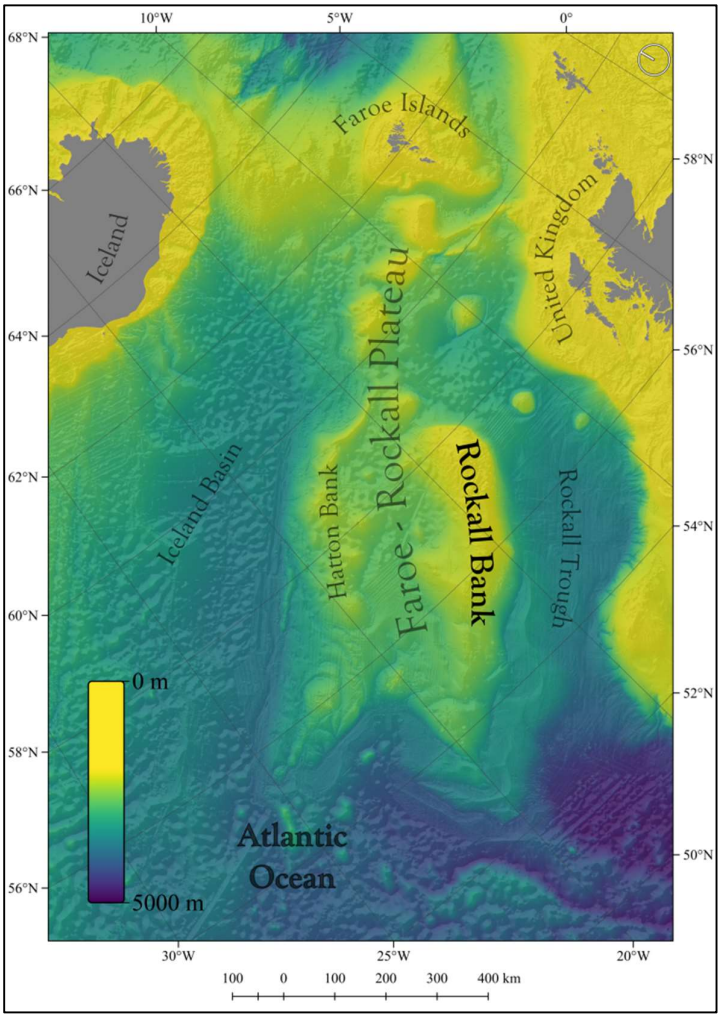

Figure 83. Rockall Bank and surrounding area (adapted from Johnson et al., 2019)

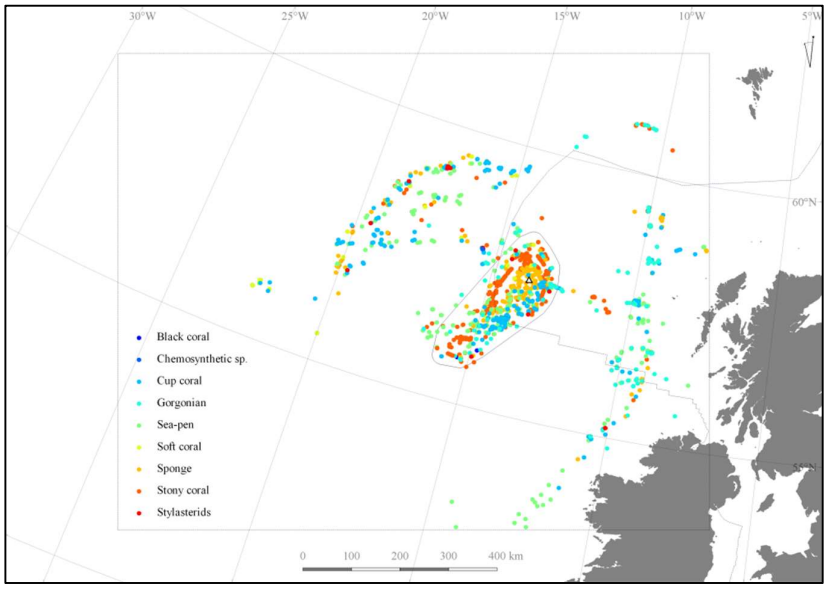

Figure 84. The distribution of ICES VME indicator groups on and around Rockall Bank.

3.3.2 Species selection

Modelling efforts for Rockall Bank have focused on benthic invertebrates and coral species in particular; *Lophelia pertusa* and two sea pen species (*Funiculina quadrangularis* and *Ptilella greyi*). *L. pertusa* is a reef forming cold-water coral species that provides habitat for other benthic invertebrates as well as fish species. *L. pertusa* and the reefs it forms are vulnerable to the effects of bottom contact fishing gears and are of key conservation importance (Hall-Spencer & Stehfest, 2009). Sea pens are the only octocorals adapted for life on soft muddy or sandy substrata making an important contribution to the overall structural complexity of soft-bottom communities and may act as good indicators of quality in these habitats as they are sensitive to demersal fishing activity (Malecha & Stone, 2009; Greathead et al., 2014). The tall sea pen, *F. quadrangularis*, is a large 'whip like' sea pen with a preference for fine mud sediments and has been reported from depths greater than 2000 m (Manuel, 1988; Edwards & Moore, 2009). *P. greyi* is a newly described species of sea pen, for which the genus *Ptilella* has been resurrected, that has been collected from Rockall Bank. It is a large sea pen that can exceed one metre in height and is a more robust form than *F. quadrangularis* (García-Cárdenas et al., 2019, in review).

3.3.3 Species occurrence data sources

Presence records were taken from the ICES VME and OSPAR habitats databases for *L. pertusa* and *F. quadrangularis* (Figure 85). These records arise from various sources including fisheries surveys, imaging, scientific surveys. Data for *P. greyi* was also collected during fisheries surveys but have only been described recently, so records were supplied by Jim Drewery of Marine Scotland Science.

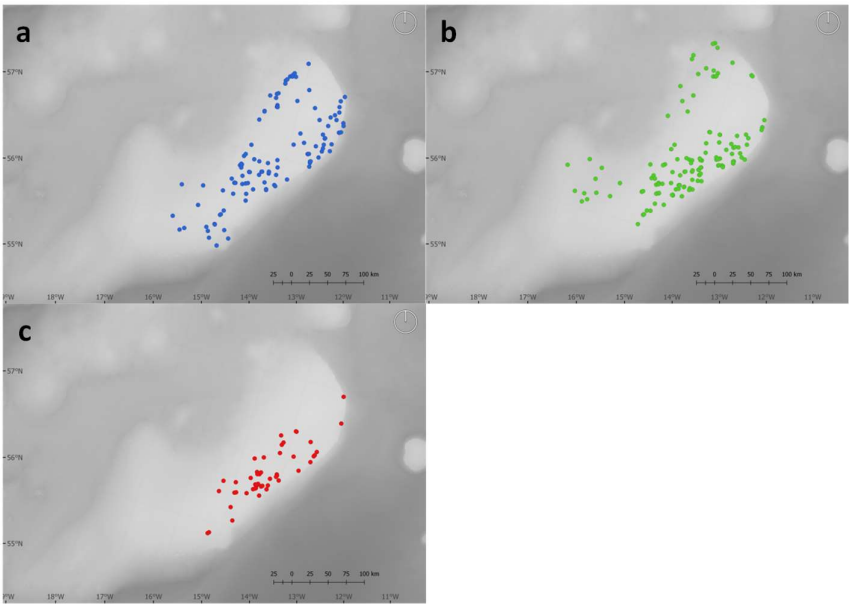

Figure 85. Lophelia pertusa *(A),* Funiculina quadrangularis *(B) and* Ptilella greyi *(C) records on Rockall Bank.*

3.3.4 Environmental data layers

EMODnet bathymetry was used to produce the depth derived layers: benthic position index (BPI) and slope. Bathymetry itself was not used in the models as it is highly correlated with other variables such as temperature. The VIKING20 hydrodynamic model was used to describe the physical oceanographic conditions on Rockall Bank: temperature (min, max), salinity (min, max) and current velocities (min, max) were derived from the near bottom values of the model and across the entire temporal domain (1958 – 2009). Sediment layers were interpolated (via regression kriging) using all available PSA grab data in the area, converted to % sand, mud and gravel. Thresholds used were: Mud = > 0.02 < 62.5 µm; Sand = > 62.5 < 2000 µm; Gravel > 2000 < 8000 µm. Surface productivity (min and max) were derived from ocean colour layers (chlorophyll) obtained from the EU's Copernicus data archive. Surface productivity can influence the supply of food to the benthic layer based on phenomenon such as Ekman transport and may potentially play a role in determining the distribution of benthic species. Observer bias layers were used to condition the models by taking the distance from raster cells that were that had non-zero fishing activity, the models were then predicted with this variable set to a common value. The Global Fishing Watch AIS layers were used to define fishing activity; these were then converted to a binary layer that was used to calculate distance to fished cells. All layers were resampled to a resolution of 1320 m * 2300 m (x, y), which represented a middle ground between the coarser physical layers (~ 4 km^2) and the finer resolution variables such as bathymetric derived variables.

For environmental layers that were correlated at > 0.7, one of the correlated variables pair was removed. First order polynomials were used and all variables apart from the observer bias layers were crossed at this level. Second order polynomials were also included to capture non-linear relationships; these were not crossed with other variables. The above method yielded 68 environmental variables. Naming conventions: A '2' suffix denotes a second order polynomial (e.g. temp.min2, is the second order polynomial of minimum temperature) and where variables have been crossed, both variables are included in the name and separated by a full stop '.'; e.g.; 'mud.surf.prod.max' is the cross between % mud and maximum surface productivity (derived from the ocean colour layer).

3.3.5 Variable selection methodology

Prediction was the principle driver of the modelling work undertaken here (see Shmueli, 2010), with the aim of identifying potentially unknown areas of species occurrence. As such, variables were selected based on an *a priori* understanding of the species-environment relationship and availability of data layers. Models were run with the full suite of variables included as outlined above. However, by default Maxent uses a least absolute shrinkage and selection penalty, which performs both variable selection and regularisation in order to enhance predictive accuracy.

3.3.6 Modelling approaches

A point process modelling (PPM) framework was used to jointly model both the location and number of presence points as a function of the environmental variables for each of the three species of interest, with the response being the intensity of points per unit area. The model domain for each of the species was derived from the extent of the presence records. PPMs are related to other regression based approaches that are used to model presence only data, including Maxent and some implementations of logistic regression (Renner et al., 2015). Some advantages of using PPMs for presence only SDMs include; clarity over what is being modelled in the response, unambiguous criteria for selecting background points / pseudo-absences (termed quadrature points in PPM literature), and a suite of diagnostic tools that can be used to check model assumptions (Renner et al., 2015). After testing the point data for inter-point dependence, inhomogeneous Poisson PPMs (IPPPM) were fitted for all three species. Analyses were performed in R using the 'spatstat' package (Version 1.59-0.023) (Baddeley & Turner, 2005; Baddeley et al., 2015).

The final models were constructed using all available presence points for each species. For *L. pertusa* and *P. greyi*, predictions were based on environmental layers where the observer bias variable was

set to a common level (0) across the study site, allowing predictions of species occurrence without the influence of observer bias (Warton et al., 2013). Maxent (Phillips et al., 2006) has been shown to be equivalent to a Poisson regression model (Aarts et al., 2012; Renner & Warton, 2013).

By adapting Maxent's default settings (Renner et al., 2015), the same IPPM model at the same spatial scale with the same number of quadrature points as in the spatstat models were fitted in Maxent in order to obtain partial response plots for the variables and a measure of variable importance. Maxent response plots are derived by holding the other variables at their mean values across the range of the presence points. Variable importance was derived from the built-in Maxent function, where the contribution for each variable is determined by randomly permuting the values of that variable among the training points (both presence and background) and measuring the resulting decrease in training AUC. These analyses were implemented in R using Maxent version 3.4.0 (Phillips et al., 2011) within the 'dismo' package (Hijmans et al., 2014).

The goodness of fit of the models was assessed by checking two key assumptions of IPPMs:

1. Independence points, conditional on the environmental and observer bias variables was assessed by plotting the global inhomogeneous K-function from 2002 randomly generated realizations of the fitted model against that expected from a Poisson point process using simulation envelopes (Diggle, 2003).
2. Accurate modelling of the intensity function as a function of the environmental variables was checked by constructing a spatially smoothed map of Pearson residuals (which should be approximately standardised and less than an absolute value of 2) and plotting the model residuals against the Cartesian coordinates (Baddeley, 2010).

The predictive performances of the models were evaluated using 10-fold cross-validation. The presence data was randomly partitioned into 10 groups. Nine of the groups were used to construct a model and its ability to predict the 'unseen' presence group and 10,000 points randomly sampled from the quadrature scheme used as absences. This was repeated for each partition for each species and reported via the area under the receiver operating characteristic curve (AUC) and True Skill Statistic (TSS). AUC is a threshold independent measure of model accuracy that is commonly used to assess presence only models (Jiménez-Valverde, 2012). It varies between 0 and 1, with values <0.7 indicating poor prediction, between 0.7 and 0.9 good prediction and those >0.9 very good prediction (Hosmer *et al.*, 2013). TSS is a threshold dependent model evaluation metric, and the threshold where both sensitivity and specificity were maximised was chosen (Allouche et al., 2006). TSS ranges from -1 to +1, with strength of agreement values < 0 being poor, 0 – 0.2 slight, 0.21 – 0.4 fair, 0.41 – 0.6 moderate, 0.61 – 0.8 substantial and > 0.81 almost perfect (Landis & Koch, 1977).

3.3.7 Model outputs

Lophelia pertusa

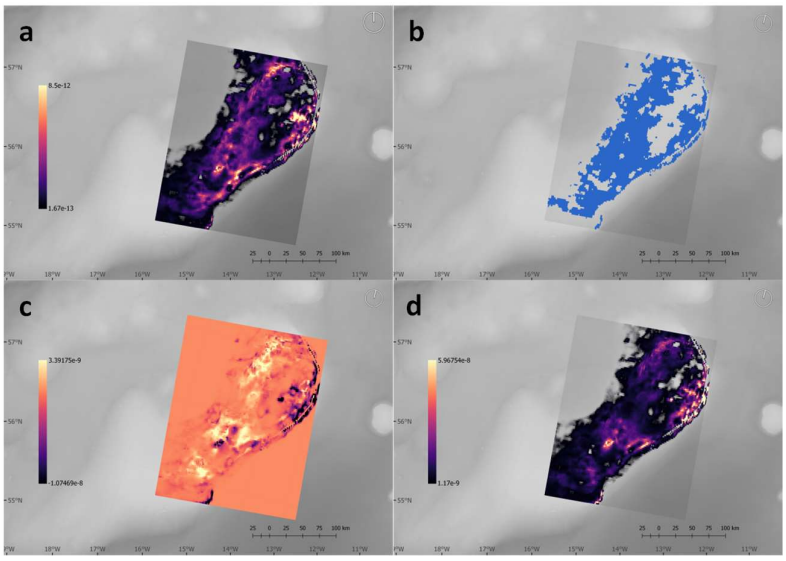

Figure 86. Lophelia pertusa *predicted intensity surface (A), binary surface converted at the threshold where sensitivity and specificity was maximised (B) and the 95% confidence intervals (C [2.5%] and D [97.5%])*

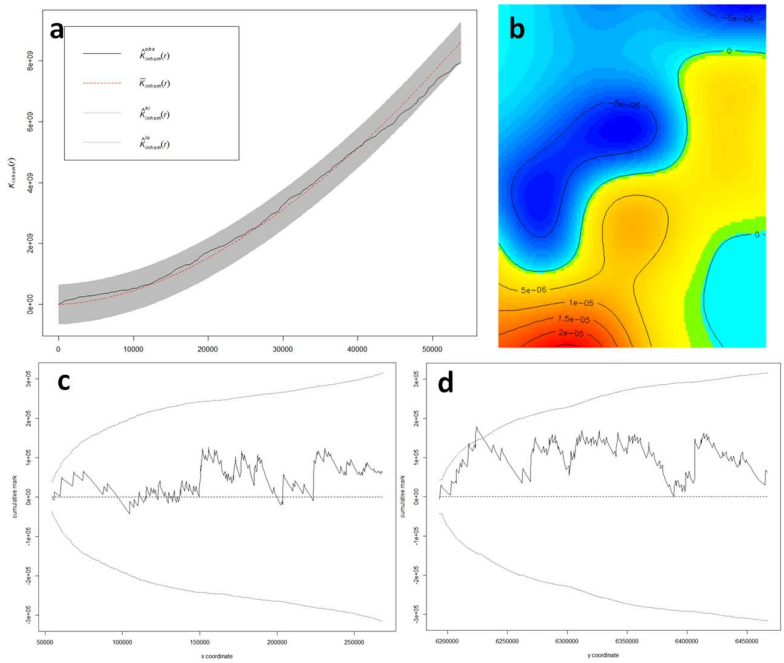

Figure 87. Goodness of fit tests for the L. pertusa *model: simulation envelopes for the fitted model at alpha = 0.025 (A); smoothed Pearson residuals that shows some pattern but has absolute values much smaller than 2 (B); lurking variable plots where the residuals are plotted against the x (C) and y (D) coordinates.*

Table 13. Lophelia pertusa *evaluation metrics from the 10-fold cross validation along with the min, mean, max and standard error of the mean. AUC = Area under the receiver operator curve characteristic; TSS = true skill statistic; MSS Threshold = the threshold at which sensitivity and specificity are maximised.*

	AUC	Sensitivity	Specificity	TSS	MSS Threshold
Min	0.826	0.583	0.576	0.493	3.70E-13
Mean	0.877	0.856	0.772	0.629	1.59E-12
Max	0.916	1	0.922	0.749	2.96E-12
SE	0.012	0.04	0.037	0.032	2.92E-13

Figure 88. Variable importance for the 20 most influential variables in the L. pertusa *model*

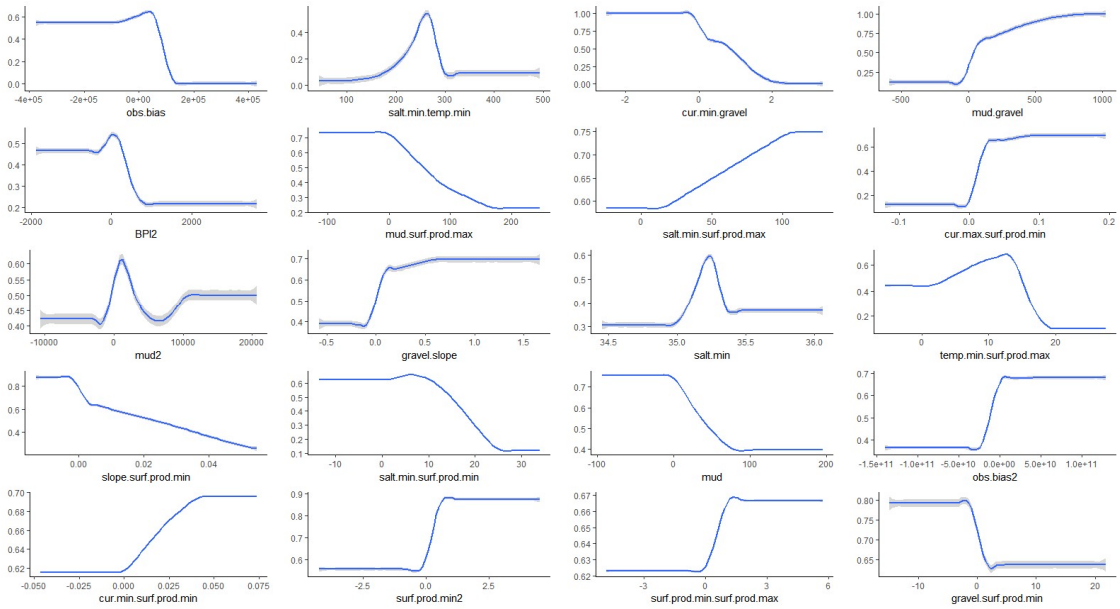

Figure 89. Response plots for the 20 most influential variables for the L. pertusa *model.*

Funiculina quadrangularis

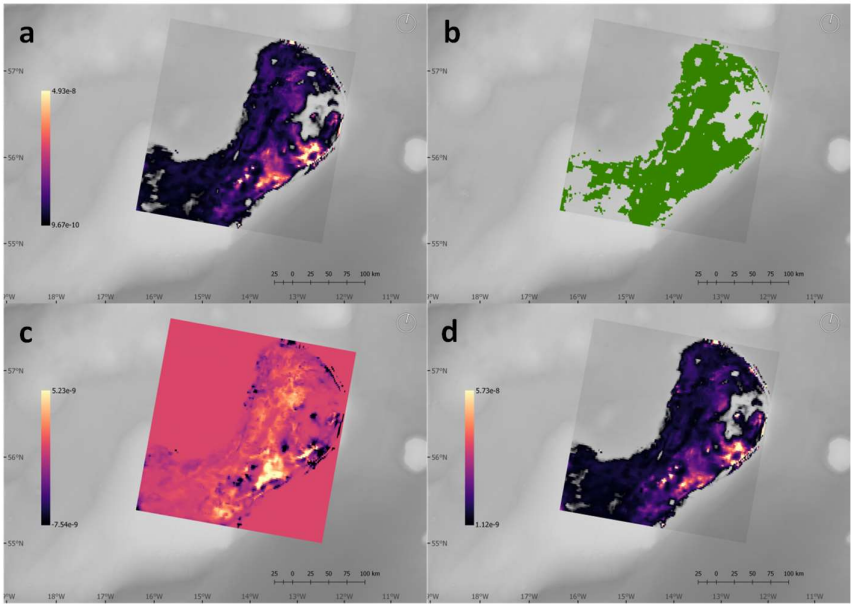

Figure 90. Funiculina quadrangularis *predicted intensity surface (A), binary surface converted at the threshold where sensitivity and specificity was maximised (B) and the 95% confidence intervals (C [2.5%] and D [97.5%])*

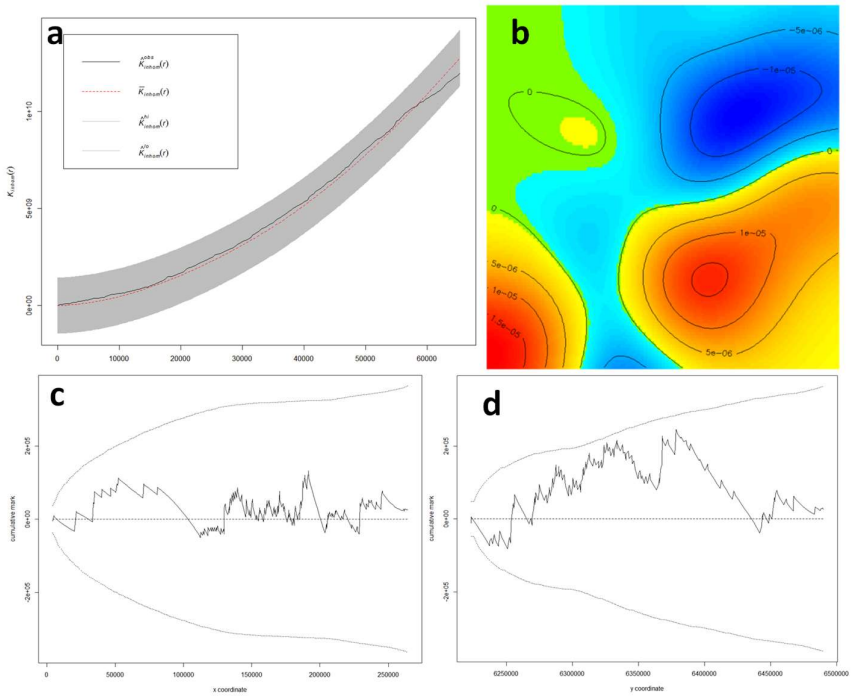

Figure 91. Goodness of fit tests for the F. quadrangularis *model: simulation envelopes for the fitted model at alpha = 0.025 (A); smoothed Pearson residuals that shows some pattern but has absolute values much smaller than 2 (B); lurking variable plots where the residuals are plotted against the x (C) and y (D) coordinates.*

Table 14. Funiculina quadrangularis *evaluation metrics from the 10-fold cross validation along with the min, mean, max and standard error of the mean. AUC = Area under the receiver operator curve characteristic; TSS = true skill statistic; MSS Threshold = the threshold at which sensitivity and specificity are maximised.*

	AUC	Sensitivity	Specificity	TSS	MSS Threshold
Min	0.746	0.5	0.55	0.371	3.49E-10
Mean	0.826	0.886	0.675	0.561	2.77E-09
Max	0.911	1	0.901	0.687	8.25E-09
SE	0.016	0.053	0.043	0.027	8.88E-10

Figure 92. Variable importance for the 20 most influential variables in the F. quadrangularis *model.*

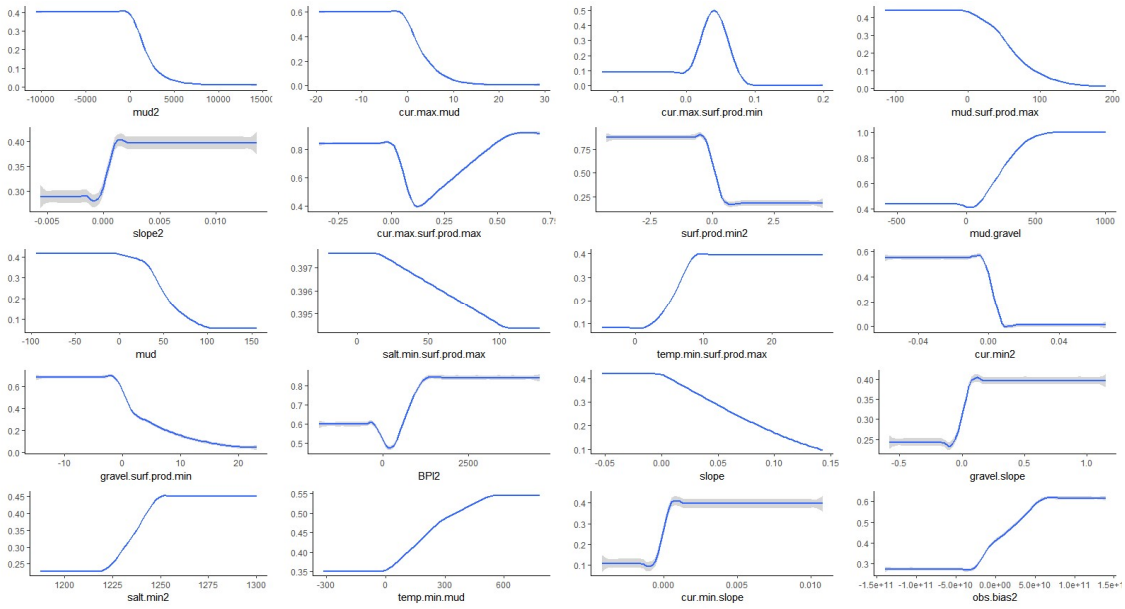

Figure 93. Response plots for the 20 most influential variables for the F. quadrangularis *model.*

Ptilella greyi

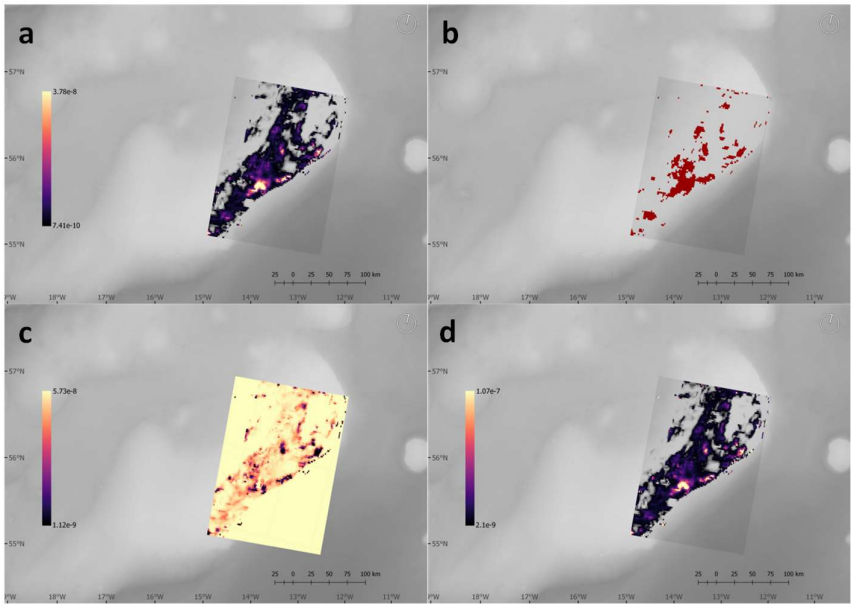

Figure 94. Ptilella greyi *predicted intensity surface (A), binary surface converted at the threshold where sensitivity and specificity was maximised (B) and 95% confidence intervals (C [2.5%] and D [97.5%]).*

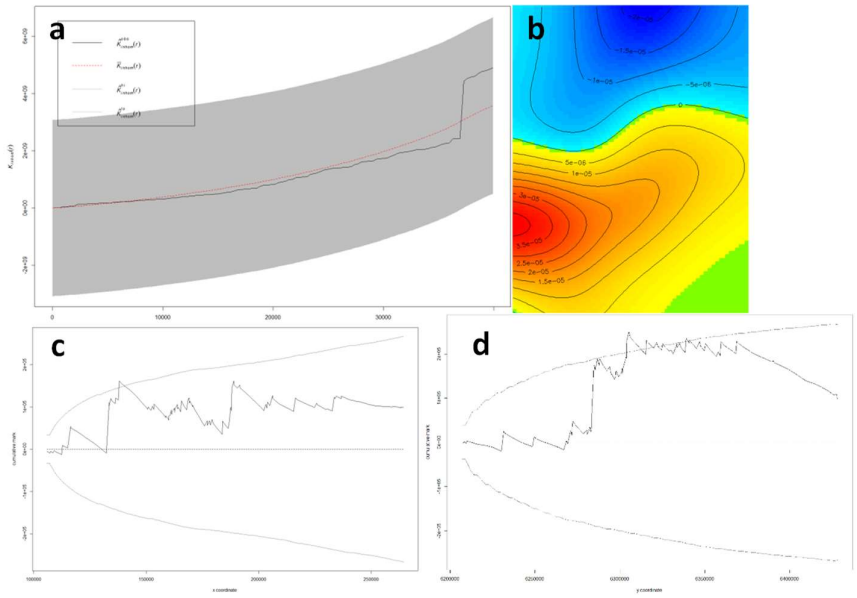

Figure 95. Goodness of fit tests for the Ptilella greyi *model: simulation envelopes for the fitted model at alpha = 0.025 (A); smoothed Pearson residuals that shows some pattern but has absolute values much smaller than 2 (B); lurking variable plots where the residuals are plotted against the x (C) and y (D) coordinates.*

Table 15. Ptilella greyi *evaluation metrics from the 10-fold cross validation along with the min, mean, max and standard error of the mean. AUC = Area under the receiver operator curve characteristic; TSS = true skill statistic; MSS Threshold = the threshold at which sensitivity and specificity are maximised.*

	AUC	Sensitivity	Specificity	TSS	MSS Threshold
Min	0.712	0.5	0.713	0.321	2.98E-10
Mean	0.831	0.717	0.841	0.558	4.65E-09
Max	0.965	1	0.988	0.928	1.90E-08
SE	0.024	0.063	0.032	0.062	2.19E-09

Figure 96. Variable importance for the 20 most influential variables in the P. greyi *model.*

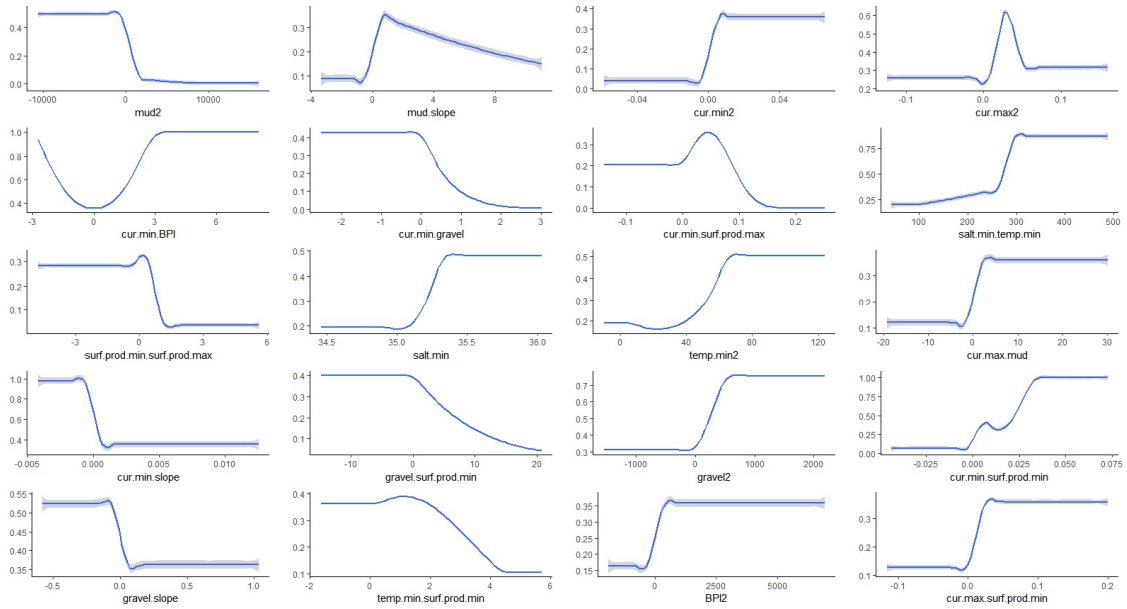

Figure 97. Response plots for the 20 most influential variables for the P. greyi *model.*

3.3.8 Model interpretation, caveats and future directions

The models presented here were constructed using incidental, presence only records (trawl bycatch) as well as records collected from imaging methods. In general, they appear to fit the presence data well according to the diagnostic plots. When the predictive accuracy was assessed using cross-validation, they performed reasonably well according to both AUC (all models were > 0.83) and TSS (all models were > 0.56).

There were no deviations from the global simulation envelopes for the *L. pertusa* model (Figure 87 A), suggesting the model fits the data well, and while the plot of smoothed Pearson's residuals (Figure 87 B) suggests some patterning in the residuals, with higher values occurring to the south of the domain, the magnitude of the values are small. This slight patterning may be reflected in the slight deviation from the two-standard-deviation error limits at low values of the y coordinate (Figure 87 D), though the residuals fall within the error limits at all other values of y. The evaluation metrics for *L. pertusa*, (AUC = 0.856 ± 0.012; TSS = 0.629 ± 0.032) suggest the model performs reasonably well in predicting new cases when assessed using 10-fold cross-validation (Table 13). Assessing variable importance suggests the most prominent variable for *L. pertusa* is observer bias (Figure 88). The observer bias variable was constructed using the Euclidean distance from fished areas as characterised by the Global Fishing Watch data. It was included in an effort to account for spatial patterning in reported presence locations due to the behaviour of fishers rather than the environmental tolerances of the study species. Predictions were then made at a common level, allowing the distribution of *L. pertusa* to be

mapped while controlling for observer bias. The prominence of this variable suggests an overlap between fished areas and locations of reported occurrences of *L. pertusa*. The second most prominent variable is the cross between minimum salinity and minimum temperature. Salinity and temperature are aspects of the chemical and physical properties of the water to which *L. pertusa* is exposed. The most suitable conditions for *L. pertusa* suggested by the model are found between 200 – 300 (Figure 89), which are in keeping with the understood environmental tolerances of *L. pertusa*, where reefs most often occur at full oceanic salinities (34 – 36 ppt) and temperatures of 6 – 7 ˚C (i.e.: 35 ppt * 6.5 ˚C = 228) (Davies et al., 2008). Other important variables include: current velocity, which is an important variable in delivering food to *L. pertusa*; sediment type (percentage gravel and mud), which may be important in providing hard substrate for colonisation (% gravel); Benthic Position Index, which relates to the elevation of a grid cell in relation to its neighbours and may interact with other variables to increase food delivery (e.g. current velocity); surface production is also thought to be important in delivering food to *L. pertusa* through passive sinking, active diurnal movement of planktonic organisms, or bentho-pelagic coupling via other oceanographic phenomena (e.g. Ekman transport).

For the *F. quadrangularis* model, no deviations were observed from the simulation envelope at any value of r (Figure 91 A), and the moderate pattern in the smoothed Pearson's residual plot (Figure 91 B) are at low absolute values. This, along with the residuals falling within the error limits of the lurking variable plots for the x and y coordinates, suggests that the model fits the data well. The evaluation metrics for *F. quadrangularis*, (AUC = 0.826 ± 0.016; TSS = 0.561 ± 0.027) suggest the models perform reasonably well in predicting new cases when assessed using 10-fold cross-validation (Table 14). In terms of the most important variables in determining the distribution of *F. quadrangularis* across Rockall Bank, the second order polynomial of percentage mud is the most prominent (Figure 92). The prominence of mud in the model is in keeping with the life-history of *F. quadrangularis* as a sea pen, which are the only octocorals adapted for life in entirely soft sediments (Edwards & Moore, 2009). The plot for 'mud2' in Figure 93, however, seems to tail off at higher percentages of mud. This is explained by the distribution of values in the interpolated percentage mud layer across the model domain for *F. quadrangularis*, where on Rockall Bank the maximum values of percentage mud are much lower than in the deeper areas within Rockall Trough and the Rockall-Hatton Basin, to the east and west of the bank respectively. No records of *F. quadrangularis* arose from these off-bank areas, so the model is characterising the species environmental relationship based on what it 'sees' in the lower percentage mud values from Rockall Bank. The second most prominent variable is that of the cross between current velocity (max) and percentage mud. The importance of current velocity can be understood as important for *F. quadrangularis* in terms of food delivery as it is passive suspension feeder. The shape of the response plot for this variable suggests, however, that there is an optimal

current speed for *F. quadrangularis* as the relationship tapers off at higher values. This relationship is complex as both percentage mud and current velocity interact (i.e., it is unlikely that sediments with a high percentage of mud co-occur in areas of strong current velocity). Other important variables include: surface production, which can be understood in a similar way to its importance for *L. pertusa*; seabed terrain (slope second order polynomial) is a measure of the gradient of the seabed in relation to its surroundings. The shape of the response in Figure 93 is difficult to explain in terms of the life-history of *F. quadrangularis* as soft sediments tend to occur in areas of relatively flat seabed and may be an artefact in the data. The physical and chemical properties of the water on Rockall Bank do not feature as prominently in the model for *F. quadrangularis* distribution on Rockall Bank as they do for *L. pertusa*.

For *P. greyi*, the simulation envelope (Figure 95 A) is respected at all values of r, but is wider than those for the other two species considered here. The smoothed Pearson's residuals are at low absolute values and the error limits are respected in the lurking variable plots for the x and y coordinates for all values except a small deviation for each (Figure 95 B-D). The evaluation metrics for *P. greyi*, (AUC = 0.831 ± 0.024; TSS = 0.558 ± 0.062) suggest the models perform reasonably well in predicting new cases when assessed using 10-fold cross-validation (Table 15). Similar to *F. quadrangularis*, the quadratic of percentage mud was the most important variable in the model for *P. greyi* (Figure 96). Other important variables included quadratic min and max current velocities, slope, sediment type and surface production. The reason for the importance of these variables is presumably similar to those for *F. quadrangularis*, though as the species has only recently been described there is no information on its environmental preferences or tolerances.

3.4 Case study 5: Predictive Habitat suitability models for *Lophelia pertusa* under current environmental conditions in Porcupine

Oisín Callery[1], Telmo Morato[2,3], José-Manuel González-Irusta[2,3], Anthony Grehan[1]

1- NUIG Earth and Ocean Sciences, NUI Galway, Ireland
2- Okeanos Research Centre, Universidade dos Açores, Horta, Portugal
3- IMAR Instituto do Mar, Universidade dos Açores, Horta, Portugal

3.4.1 Case study description

Ireland plays host to some of the best developed cold-water coral reefs in NE Europe. Reefs are formed principally by the frame-working constructing corals *Lophelia pertusa* and *Madrepora oculata*. The best developed living reefs are found at or near the summits of giant carbonate mounds, rising up to 350 m in height in waters between 500 and 1200 m depth. The mounds themselves occur clustered together to form several distinct mound provinces off the west coast of Ireland in the Porcupine Bank, Porcupine Seabight and Rockall Bank (Wheeler et al., 2007).

Porcupine Seabight mounds are conical (single or in elongated clusters) found between 700 to 1000m water depth. Mounds have exposed steep western seaward flanks and sedimentary, buried eastern landward flanks. Mounds are between 70 and 190 m high. Bottom temperatures are typically between 8.5-9.5°C. Bottom currents vary locally. Mostly exceeding 15 cm s^{-1} for only 7-15% of the time but locally 49% of the measured time. Residual current direction variable but locally along-slope and poleward. Reef building corals (*Lophelia pertusa* and *Madrepora oculata*) and associated fauna (sponges, bryozoans, octocorals) occur on the seaward but not on landward flanks.

Porcupine Bank mounds are mainly singular with a few clustered mounds of 1-2 km's diameter. Mounds are 50-100m high and separated by wide channels with less strong currents. Average bottom temperatures are 9.5°C with semi-diurnal fluctuation of ~1°C. Bottom currents on mound summits attain a maximum speed of 30 cm s^{-1} with an average between 10-20 cm s^{-1}. The residual current moves poleward. The summit of the mounds (650 m depth) is covered with a relatively open (live and dead) coral framework.

Rockall Bank mounds are clustered (and isolated) high mounds of several km's length located between 600-1000 m water depth. Mounds are found up to 380 m high. Mound clusters are intersected by current swept cross-slope channels. Mounds are composed of coral debris and foraminiferal mud. Average bottom temperature is about 9°C with a diurnal temperature fluctuation of 2°C. Bottom currents on mound summits attain a maximum of ~30 cm s^{-1} with a median of ~10 cm s^{-1}. The residual current on the summit is directed to the SE. The summit of the mounds (800 m depth) is covered with

a very dense and extensive coverage of (live and dead) coral framework ca 0.5-1 m high. Flanks of the mounds have no coral.

3.4.2 Species selection

Lophelia pertusa was selected because of the availability of existing distribution data and the species importance as the primary framework constructing coral providing habitat for a large associated and biodiverse fauna.

3.4.3 Species occurrence data sources

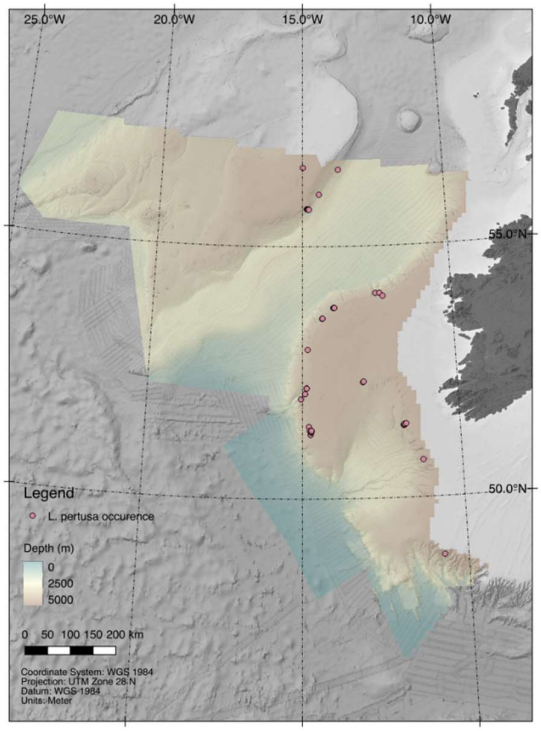

Figure 98. Locations of samples of Lophelia pertusa *used for model training.*

3.4.4 Environmental data layers

Layers of static variables (i.e. layers produced using bathymetric data) were derived from Infomar survey data (https://www.infomar.ie). The layers used to train the Maxent model were (i) depth, (ii) standard deviation of seabed slope, and (iii) bathymetric position index (BPI). The latter two of these

variables were derived from the first using the moving window terrain analysis approach described by Wilson et al. (2007); a window size of 5x5 grid squares was used for this analysis.

Layers of climate affected data were based on average values obtained from the Geophysical Fluid Dynamics Laboratory's ESM 2G model (GFDL-ESM-2G; Dunne et al., 2012), the Institut Pierre Simon Laplace's CM6-MR model (IPSL-CM5A-MR; Dufresne et al., 2013), and Max Planck Institute's ESM-MR model (MPI-ESM-MR; Giorgetta et al., 2013) within the Coupled Models Intercomparison Project Phase 5 (CMIP5); these data were downloaded from the Earth System Grid Federation Peer-to-Peer (P2P) enterprise system (ESGF, 2019). Mean values calculated for each of the three periods of interest: (i) a historical simulation for the period 1951-2000, and two future scenarios for the periods (ii) 2041-2060 and (iii) 2081-2100. All data for future scenarios were based on the RCP8.5 (business-as-usual) greenhouse gas concentration trajectory scenario (IPCC, 2014).

Static variable layers were derived from a bathymetry raster with a spatial resolution of 0.002°. Layers of dynamic variables (i.e. those affected by climate change) are upscaled from the climate affected data described above (these have a resolution of 0.5°) using the regression-kriging approach described by Hengl et al. (2007). This was achieved by using the *fit.gstatmodel* function of the Global Soil Information Facilities (GSIF; Hengl et al., 2017) R package to perform regression analyses of the relationships (using Generalized Linear Models (GLMs)) between each dynamic variable and four independent variables - (i) depth, (ii) latitude, (iii) longitude, and (iv) distance to coast (as calculated using the *distance* function of the Raster R package (Hijmans et al., 2015) – with kriging of the regression residuals.

In initial attempts to model the distribution of suitable *L. pertusa* habitat using the climate-affected data, the bathymetry derived data were dominating the Maxent model so completely that the climate-affected variables had very little impact on the model outputs. For this reason, it was decided to create two models; the first model (A) attempted to predict *L. pertusa* habitat based solely on "static" physical habitat variables (see below) that would remain constant with climate change, while the second model (B) attempted to predict *L. pertusa* habitat based on "dynamic" variables (see below) that would transform with climate change. It was reasoned that *L. pertusa* would be found within the envelope where optimal environmental conditions and suitable physical habitat overlap – this envelope (C) could be found by simply calculating the product of the outputs from the two models mentioned above: C = A x B.

Before calculating the aforementioned product, C, the model of suitable physical habitat (A) was first reduced to a binary prediction, i.e. one representing suitable or unsuitable physical habitats with '1's and '0's respectively, by defining all grid cells with a habitat suitability score above Maxent's 10th

percentile (training presence value) threshold as suitable, and everything below this threshold as unsuitable. This threshold results in a model which omits approximately 10% of the evaluation localities (i.e. training data) and it is therefore considered to be a relatively strict threshold (i.e. one resulting in a more constrained prediction in terms of areal extent) compared to other possible thresholds, e.g. the lowest presence threshold (Radosavljevic & Anderson, 2014). A matrix of pairwise Pearson correlation coefficients was developed for all predictor variables, and many were observed to be highly correlated. For physical habitat, the only two derivatives of bathymetry which were not significantly correlated with one another (or with depth) were BPI and the standard deviation of the slope (both calculated from a moving 5x5 pixel window as described above); for this reason, these two layers, along with depth, were used to develop model A. The least strongly correlated layers were selected for model B in a similar fashion; these were (i) average aragonite concentration, (ii) average calcite concentration, (iii) average temperature, (iv) average oxygen concentration, and (v) Viking20 current speed (Behrens, 2013). There is evidence that the Atlantic Meridional Overturning Circulation (AMOC) has been weakening in recent years (Thornalley et al., 2018), and this is very likely to impact cold water corals in Irish waters (Johnson et al., 2018). To simulate a weakening of the AMOC, the Viking20 output for 1992 (i.e., a strong AMOC) was used to train Model B and produce model predictions of current *L. pertusa* distribution, and the output for 1978 (i.e., a weak AMOC) was used for future predictions.

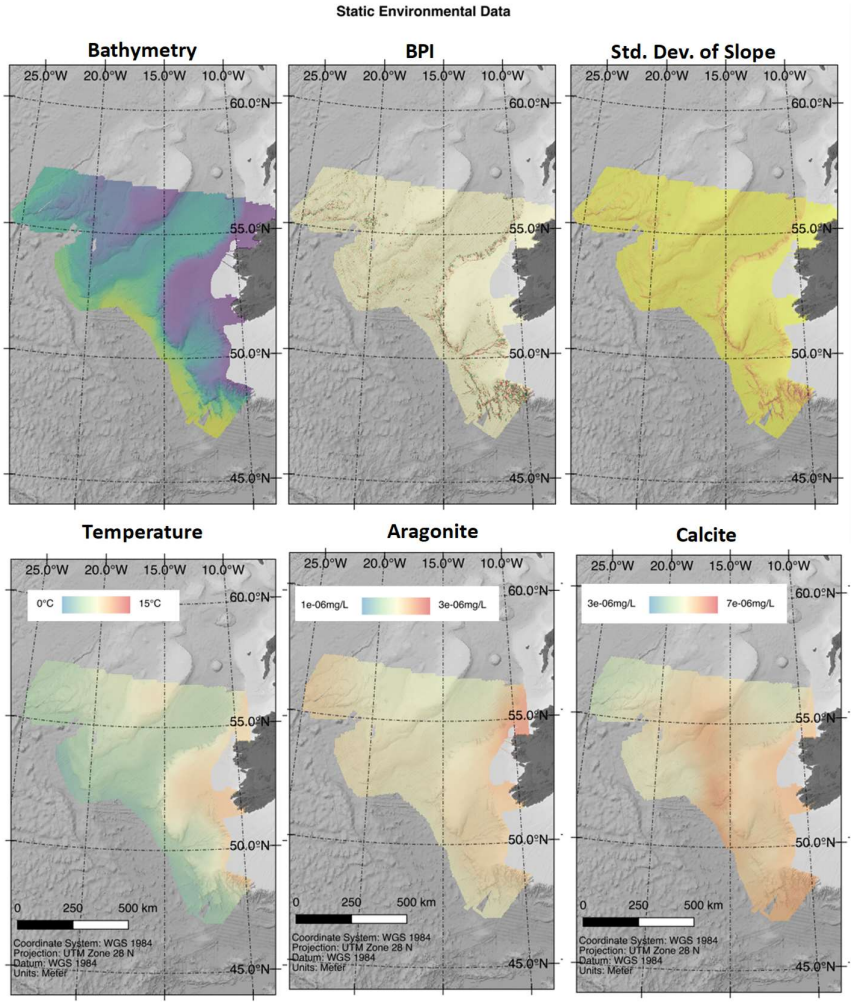

Figure 99. Environmental variables used in the model: static environmental data (bathymetry, BPI, standard deviation of slope) and dynamic environmental data for the period 1951-2000 (temperature, aragonite, calcite, oxygen, mean monthly current velocity at bed, that corresponds to a strong AMOC based on 1992).

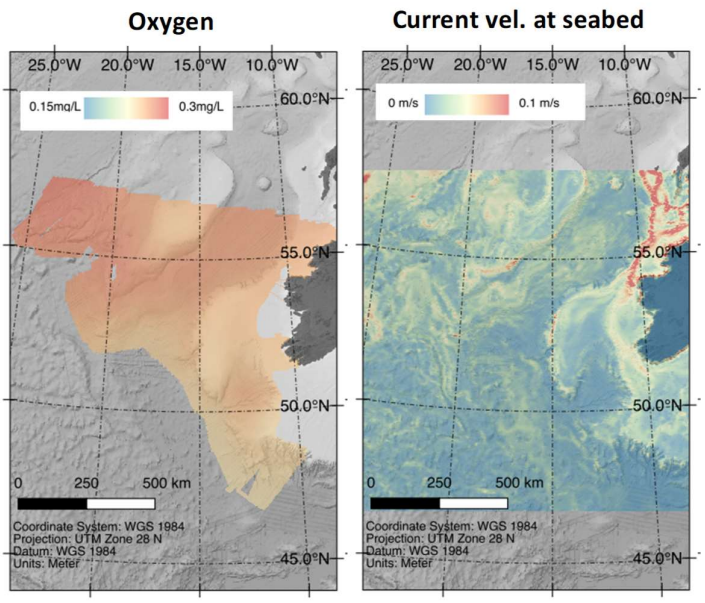

Figure 100. Dynamic environmental variables used in the model for the period 1951-2000 (oxygen, mean monthly current velocity at seabed, that corresponds to a strong AMOC based on 1992).

3.4.5 Modelling approaches

Two habitat suitability models were produced, using Maxent (run in R), following the approach described by Rengstorf et al. (2013): (i) a model describing the response of *L. pertusa* to physical variables (the aforementioned 'Model A'), and (ii) a model describing the response of *L. pertusa* to dynamic variables, which are subject to the effects of climate change (the aforementioned 'Model B'). The outputs from Models A and B may be are shown in Figure 101 and Figure 102 respectively. Using these two models, three model outputs providing predicted habitat suitably indices for *L. pertusa* were obtained, as described above, by finding the product of the outputs of models A and B (the output of model A being a single binary output of suitable/unsuitable *L. pertusa* habitat, and the outputs of model B being three maps of predicted distribution for the three time periods: 1951-2000, 2041-2060, and 2081-2100). The outputs of this combined model are shown in Figure 107.

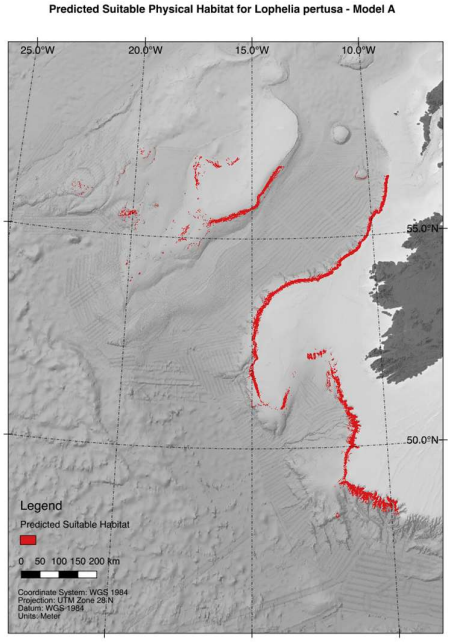

Figure 101. Binary output of Model A, showing the predicted extents of suitable Lophelia *habitat based solely on physical environmental variables which are unaffected by climate change.*

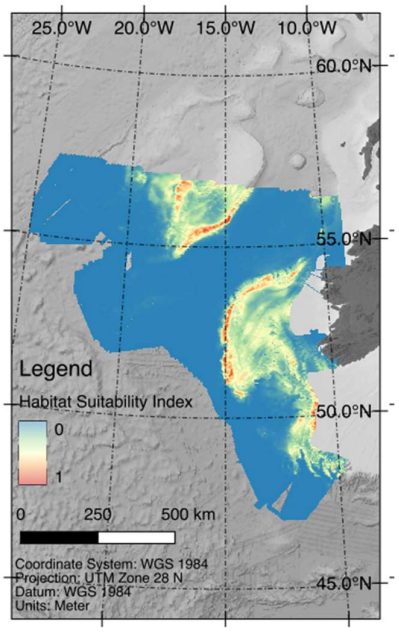

Figure 102. Outputs of Model B, showing the predicted extents of suitable Lophelia *habitat based solely on environmental variables which are affected by climate change for the period 1951-2000.*

3.4.6 Model outputs

Responses curves

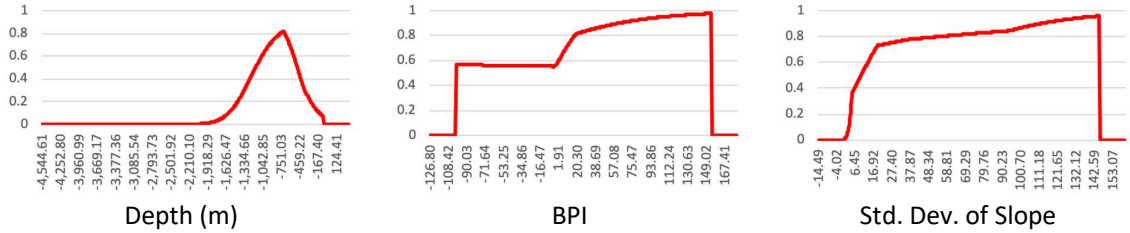

Figure 103. Response curves showing how each static (physical) environmental variable affects the Maxent prediction of L. pertusa *made by Model A.*

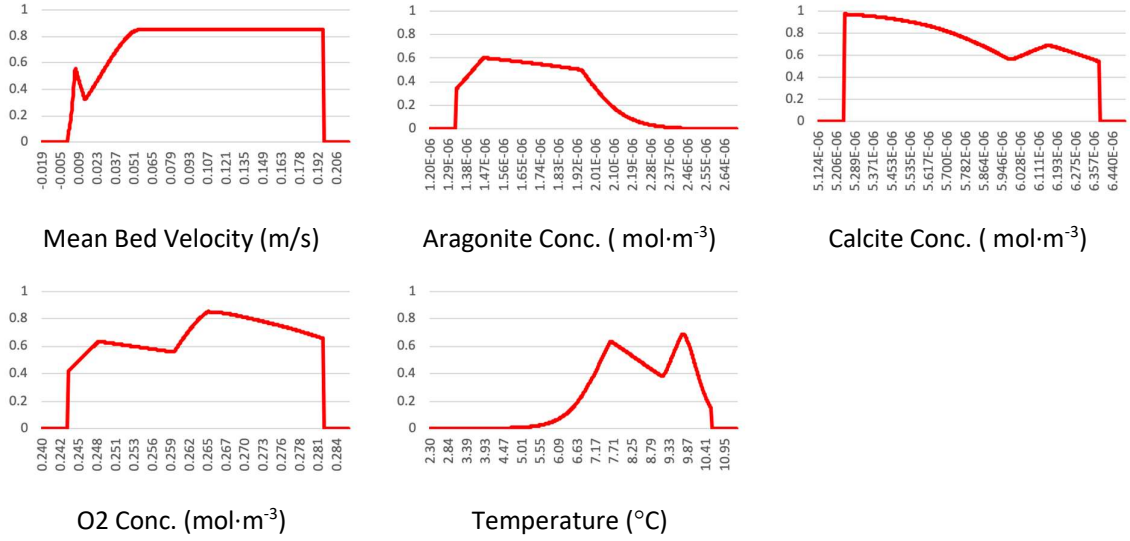

Figure 104. Response curves showing how each dynamic environmental variable affects the Maxent prediction of L. pertusa *made by Model B.*

Evaluation metrics /statistics

The receiver operating characteristic curves (i.e., plots of model sensitivity vs 1-model specificity - the true positive rate vs the false positive rate - across a range of thresholds) for Models A and B may be seen in Figure 105 and Figure 106.

Analysis of omission/commission for Model A

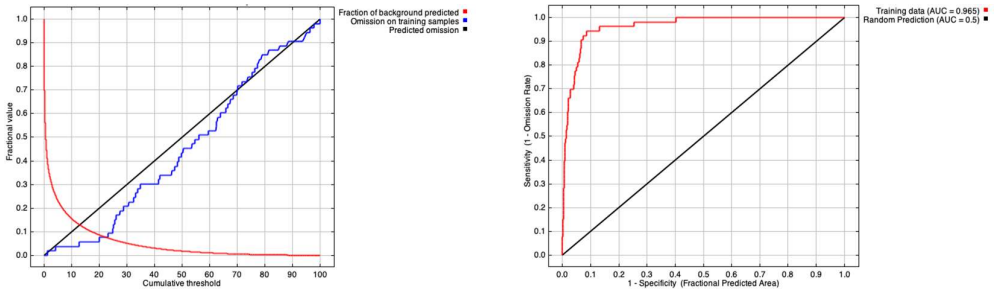

Omission and Predicted Area Sensitivity vs 1-Specificity

Figure 105. Omission rate and predicted area as a function of the cumulative threshold and receiver operating characteristic curve for Model A.

Analysis of omission/commission for Model B

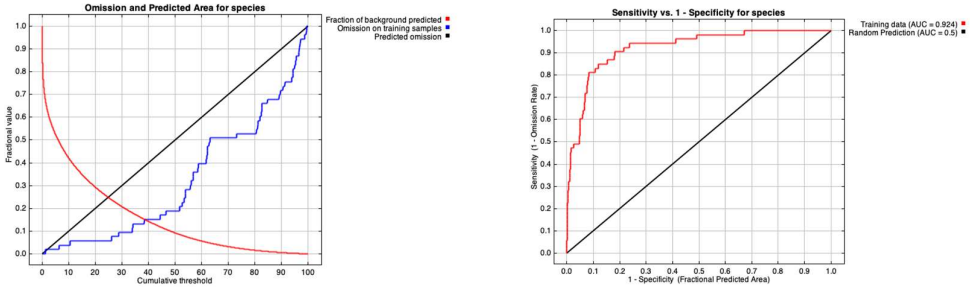

Omission and Predicted Area Sensitivity vs 1- Specificity

Figure 106. Omission rate and predicted area as a function of the cumulative threshold and receiver operating characteristic curve for Model B.

Maps of presence/absence

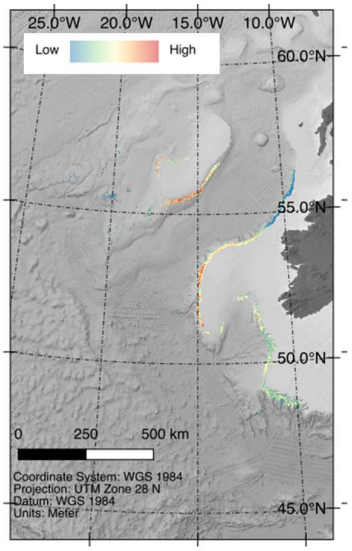

Figure 107. Extents and predicted suitability of L. pertusa *habitat for the period 1951-2000 based on the product of the outputs from model A and model B.*

3.4.7 Model interpretation, caveats and future directions

The effect of each static variable on Maxent predictions of suitable habitat made by Model A can be seen in Figure 103 above. In general, the response curves indicate that habitat suitability for *L. pertusa* increases with increased bathymetry complexity (as indicated by BPI and the standard deviation of the slope of the seabed).

The effect of each dynamic variable on Maxent predictions of suitable habitat made by Model B can be seen in Figure 104 above. Some of these responses would appear to somewhat anomalous; for instance, there are notable concavities or "dips" in the middle of the response curves for temperature and oxygen concentrations, making them resemble a bimodal distribution, whereas previous studies have found the response curves to closer resemble a normal distribution (e.g., Rengstorf et al., 2013) which would seem more intuitive.

Temperature, mean bed velocity, and aragonite concentration were the most important variables, contributing 49.6%, 19.1%, and 16.8% respectively to the Maxent model. The temperature response curve shows an upper limit of approximately 10.5°C, which is considerably lower than the upper tolerable temperature threshold for *L. pertusa* of 12-14°C reported in literature (Brooke et al., 2013), however, this is unsurprising given that the occurrence data used to train the Maxent model was primarily obtained from areas with a temperature range of 6.5-9°C.

The aragonite saturation state was calculated, but because it was found to be above 1 (i.e. fully saturated) for all areas of interest, and because earlier experimental models indicated that aragonite concentration was a better predictive variable, the latter was used in the final model. The aragonite concentration response curve indicates that increases in aragonite concentration are associated with decreases in habitat suitability. One interpretation of this could be that increased aragonite concentrations in the water are likely associated with increased dissolution of aragonite. This would, in turn, be associated with decreased coral calcification, however it is difficult to draw conclusions from this as, though well documented, the specifics of this issue (i.e. chemical thresholds, timing etc.) are poorly understood (Andersson & Gledhill, 2013).

Oxygen made a 12.3% relative contribution to the Maxent model. The response curve for oxygen concentration suggests that increased oxygen concentrations result in decreased habitat suitability for *L. pertusa*. This may be explained by the fact that, as noted by Freiwald (2002), the distribution of

L. pertusa in the northeastern Atlantic coincides with the Oxygen Minimum Zone (OMZ) which is located between depths of 500-1600m. Because the occurrence data used to train the Maxent model was largely collected in the depth range associated with the OMZ (Figure 108), the Maxent model would consequently associate lower oxygen levels with higher habitat suitability. This should be interpreted with caution, however, as it has been observed that *L. pertusa* survival is negatively impacted by very low oxygen concentrations (Lunden et al., 2014).

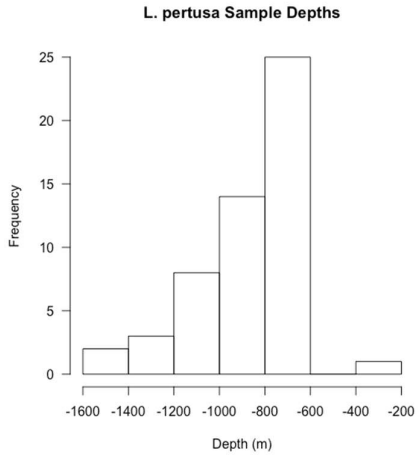

Figure 108. Histogram of depths from which L. pertusa *samples used for model training were collected.*

3.5 Case study 6: Present day predictive models for CWC in the Bay of Biscay

Sébastien Rochette[1], Sophie Arnaud-Haond[2], Pascal Laffargue[3], Sandrine Vaz[2], Mathieu Woillez[4], Lenaick Menot[5]

1- IFREMER - Centre de Bretagne, Unité DYNamiques des Ecosystèmes Côtiers (Dyneco), Brest, France
2- IFREMER Sète, Université de Montpellier, IRD, CNRS, Marine Biodiversity Exploitation and Conservation (MARBEC), Sète, France
3- IFREMER - Centre de Nantes, Département Ressources Biologiques et Environnement (RBE), Unité Ecologie et Modèles pour l'Halieutique (EMH), Nantes, France
4- IFREMER - Centre de Bretagne, Département Ressources Biologiques et Environnement (RBE), Unité Sciences et Technologies Halieutiques (STH), Brest, France
5- IFREMER - Centre de Bretagne, Département Ressources physiques et Écosystèmes de fond de Mer, Unité Etudes des Ecosystèmes Profonds (EEP), Brest, France

3.5.1 Case study description

The continental margin of the Bay of Biscay is incised by over a hundred canyons. The topographical and hydrological complexity of these submarine canyons, coupled with high substratum heterogeneity, make them ideal environments for cold-water coral (CWC) habitats. Twenty-four of these canyons were surveyed using a Remotely Operated Vehicle (ROV) or a towed camera system. Acquired images were annotated for habitat type (using the CoralFISH classification system). Eleven coral habitats, formed by 62 morphotypes of scleractinians, gorgonians, antipatharians and sea pens, inhabiting hard and/or soft substrates, were observed (van den Beld et al., 2017).

3.5.2 Species selection

The aim was to predict the distribution of habitats formed by aggregations of the two reef-buidling corals *Lophelia pertusa* and *Madrepora oculuta*. These two species are living in syntopy in the Bay of Biscay (Arnaud-Haon et al., 2017) and can hardly be distinguished from landscape images. These aggregations were dominant among CWC habitats. The 11 coral habitats mapped in the Bay of Biscay totalized a linear of 46 kilometres, off which *Lophelia pertusa*/*Madrepora oculata* reefs and rubbles contributed for 58% (van den Beld et al., 2017). The coral rubbles had a much larger bathymetric range than coral reefs, especially towards shallower depth. The shallower rubbles could be fossil reefs, which are no longer within the potential niche of the reef-building species in the Bay of Biscay. Predictions were thus limited to the occurrences of living *L. pertusa* and *M. oculata*. The presence/absence data are mapped on (Figure 109).

3.5.3 Species occurrence data sources

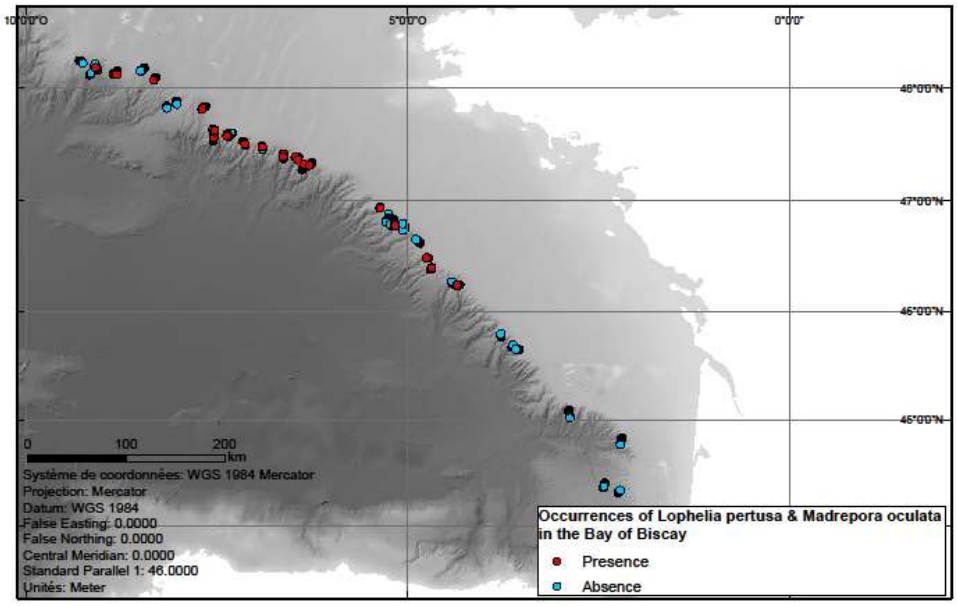

Figure 109. Map of the known distribution of presence and absence of coral reefs along ROV and towed camera transects in 24 canyons of the Bay of Biscay.

3.5.4 Environmental data layers

Data sources

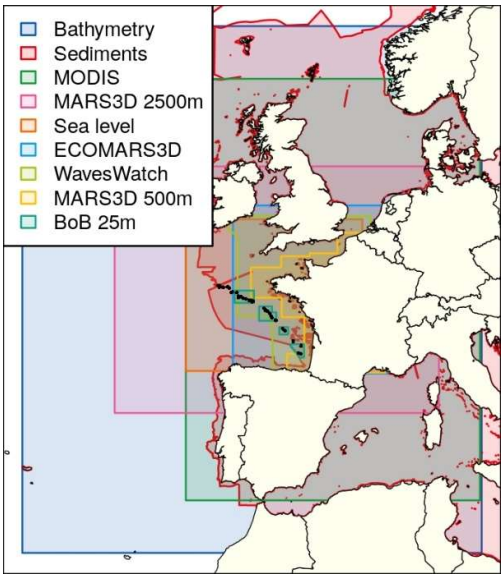

Figure 110. Map of coverage of the data sources for environmental data layers

Oceanographic covariates were retrieved from the PREVIMER project (Lecornu and De Roeck, 2009). Covariates such as kinetic energy of sea currents, sea level and water temperature originated from 5-year averages (2010-2014) of hind-cast archives predicted hourly by the MARS3D hydrodynamical model with a 2500 m regular grid resolution. Where available, some covariates were issued from MARS3D 500m resolution (2010-2015) hind-casts (Cailleau et al., 2016).

Covariates such as waves kinetic energy were averaged from the 2008-2012 period predicted by the WaveWatch wave model, which had a non-regular grid with increased precision towards the coast (Ardhuin et al., 2012). Water composition covariates such as suspended matter or Chlorophyll-a concentration were derived from MODIS satellite images with resolution of 2500*2000m averaged over the 2003-2010 period (Gohin et al., 2002). Covariates derived from the bathymetry were based on the EMODnet 470m resolution bathymetry (EMODnet Bathymetry Consortium, 2016). Where available, a 100m resolution bathymetry was used. Sediment repartition was the 7-class Folk sediment classification issued from the compiled EMODnet map of bottom sediment (EMODnet Geology project funded by the European Commission Directorate General for Maritime Affairs and Fisheries).

Spatial resolution used

The spatial resolution was constrained by the need to limit autocorrelation in the response variable. Indeed, the distribution of observations in space potentially induces spatial-auto-correlation that may interfere with modelling. In order to limit spatial auto-correlation, occurrence data are aggregated. The scale of aggregation is defined according to the scales of autocorrelation, which are explored through correlograms.

A visual inspection of the distribution of distances between observations suggest distances for calculating correlograms (Figure 111). The smallest distance (5km) is used as a reference to find local spatial auto-correlation. The biggest distance (10km) is to find larger scale spatial auto-correlation.

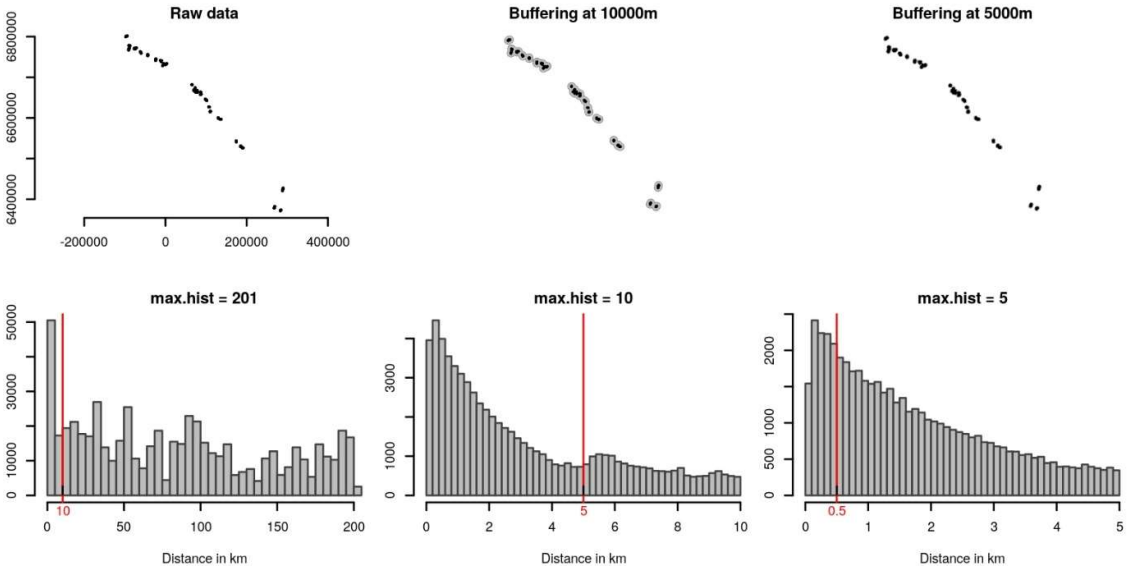

Figure 111. Distribution of distances among observations of raw data, data aggregated at a 5-km scale and data aggregated at a 10-km scale.

Two correlograms are calculated on the dataset based on these reference values. Correlograms help find a threshold in correlation in the dataset to be used for resampling in a regular grid (Figure 112). Correlograms suggested two threshold values to build the regular grid: 5650 and 825 m. The regular grid resolution finally selected was ~2000m.

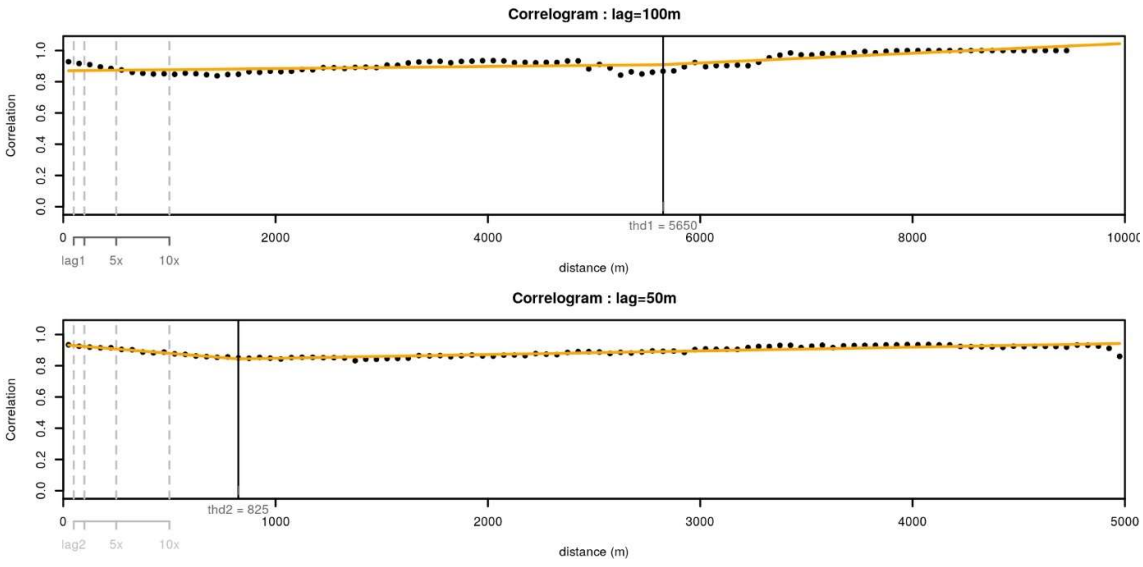

Figure 112. Correlograms

Variable selection methodology

Random Forests (RF) and Gradient boosting (GB) models were used to pre-select variables for the development of GAM/GLM models (Figure 113, Figure 114). A first selection was done according to importance of covariates in RF and GB models with all possible covariates. Correlated covariates (spearman >=0.9) were then ranked according to their importance in the models. Only the most important covariate of a group of correlated ones was retained. Models were run again on the remaining covariates. Covariates with a scaled importance higher than 0.05 were retained. The set of covariates issued from both methods was used for the classical GAM/GLM model selection. This resulted in the pre-selection of 52 variables.

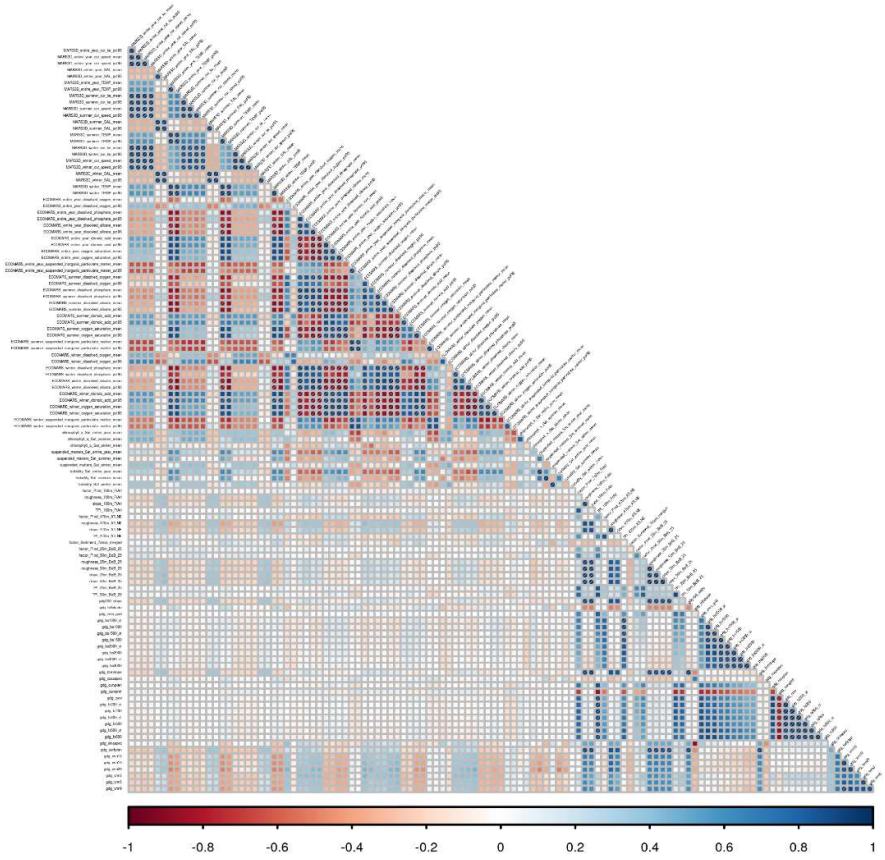

Figure 113. The selection of covariates using Random Forest and Gradient Boosting models: Correlation matrix among all covariates, the scale bar shows Spearman correlation coefficients.

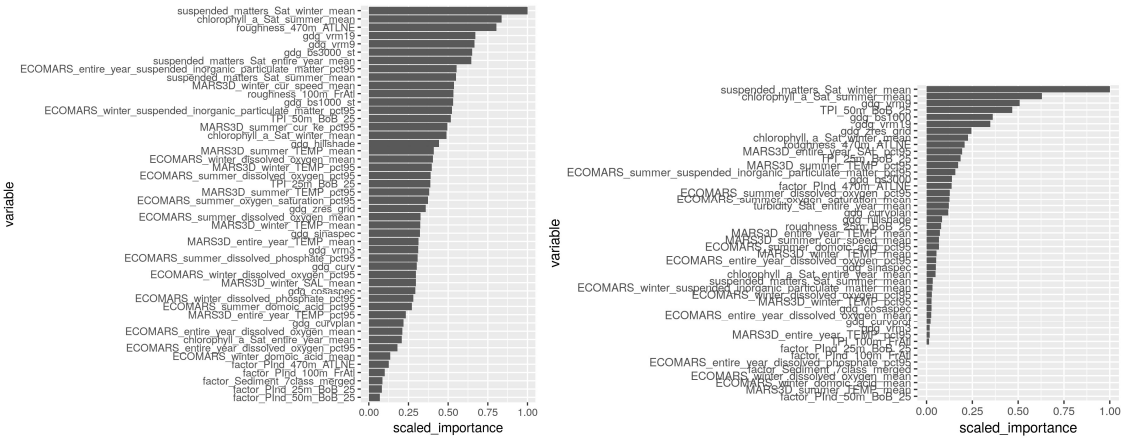

Figure 114. The selection of covariates using Random Forest and Gradient Boosting models: Uncorrelated covariates ranked by scaled importance in RF model (left),and Uncorrelated covariates ranked by scaled importance in GB model (right).

Maps of environmental layers

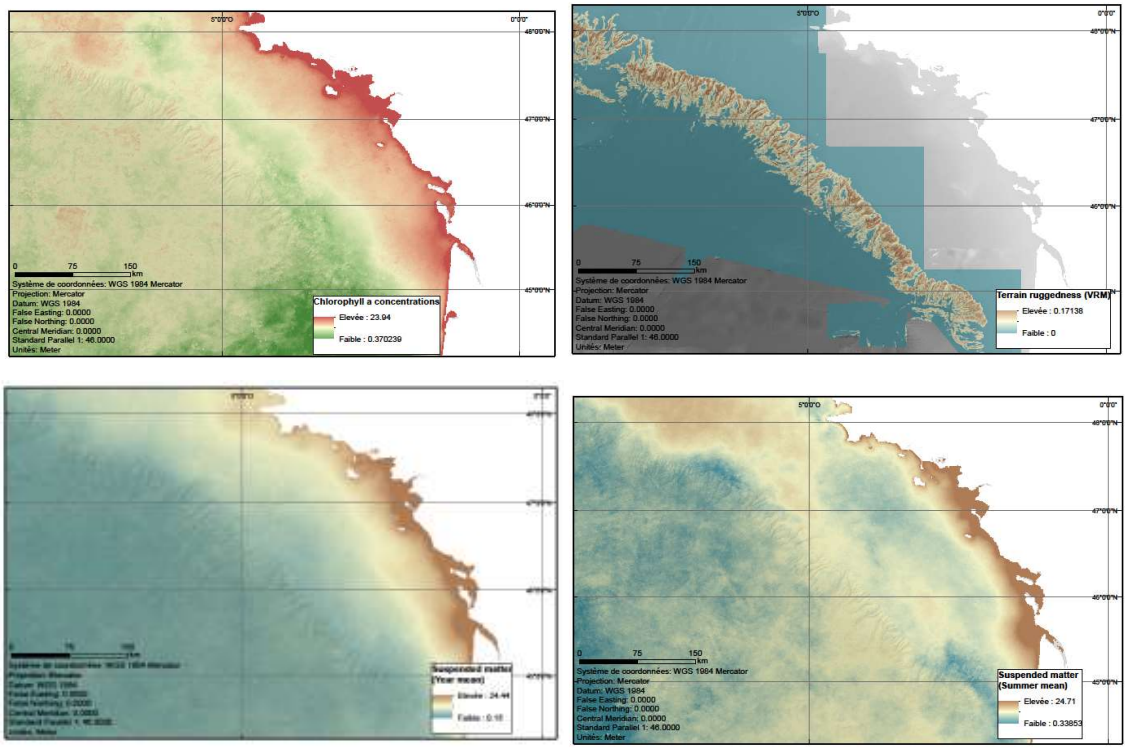

Figure 115. Maps of the four covariates that better explain the distribution of coral reefs in the Bay of Biscay.

3.5.5 Modelling approaches

Different combinations of covariates were tested and compared as well as different model structures. Generalized additive models (GAM) and (polynomial or natural splines) generalized linear models (GLM) using different residual distributions (Gaussian, Log-normal, Gamma, Tweedie) were compared. All computations were performed with R, using the SDMselect package (Rochette, 2018). For families not allowing zero values, data were transformed as Y + 1. Selection procedure was a forward step-wise procedure with model comparison based on a 10-times repeated 10-fold cross-validation. The Root of the Mean Squared Error (RMSE) of predictions against validation datasets was used as the index of comparison between all the modelling methods to choose the best predictive model. Cross-validation procedure is the recommended procedure for model selection, in particular for predictive modelling purposes. Here, the forward step-wise procedure is first processed for each model type (GAM or GLM + distribution) separately. Covariates are added one by one at each step while keeping only the best sets of covariates of the previous step.

The first best set of (same number of) covariates of a step is the one with the lowest average validation RMSE. The other sets of covariates are ordered with averaged RMSE and distributions of RMSE (10*10 RMSE for each set of covariates) are compared statistically with the best one. All sets of covariates with distribution of RMSE not statistically different than the best one are retained for the next step. When the step-wise procedure has been run for all model types, all sets of covariates of all model types are compared all together to define the model having the best prediction ability overall, based on the validation RMSE.

3.5.6 Model outputs

The k-fold cross-validation procedure allowed to select the model with the best quality of prediction. In the present case, this model was written as:

dataY ~ ns(chlorophyll_a_Sat_summer_mean, df=3) + ns(gdg_vrm19, df=4) + ns(suspended_matters_Sat_summer_mean, df=4) + ns(suspended_matters_Sat_entire_year_mean, df=4)

Characteristics of the model chosen for predictions were explored in a variance analysis, where covariates were added sequentially according to the order provided by the cross-validation procedure. The gain in deviance explained as well as the gain in the cross-validated RMSE were estimated. This allowed to assess the importance of each covariate in the model (Table 16).

In parallel, a classical residual analysis was performed to test for the assumptions on the distribution of observations values, with regards to covariates effects. This included scatterplots of residuals against predictions and standardized residuals analyses (Figure 116).

Table 16. Deviance explained by each covariate when added sequentially in the order specified by the cross-validation procedure. "%Exp.Dev" stands for percentage of explained deviance. "RMSE" is the root mean squared error on the validation datasets as issued from the cross-validation procedure. AUC is the mean Area under the curve as issued from the cross-validation procedure. ">Diff" is the difference of cross-validated AUC with the model above.

Contribution of factors

	Resid. Df	Resid. Dev	Df	Deviance	p	%Exp.Dev	AUC	>Diff
dataY ~ 1	103	121.16					*0.5*	*0*
dataY ~ ns(chlorophyll_a_Sat_summer_mean, df=3)	100	99.81	3	21.35	p<0.0001	17.62	*0.7*	*0.2*
ns(gdg_vrm19, df=4)	96	76.81	4	23	p<0.001	18.98	*0.81*	*0.11*
ns(suspended_matters_Sat_summer_mean, df=4)	92	64.12	4	12.69	p<0.05	10.47	*0.84*	*0.03*
ns(suspended_matters_Sat_entire_year_mean, df=4)	88	49.46	4	14.67	p<0.01	12.11	*0.88*	*0.04*
Residuals				*49.46*		*40.82*		

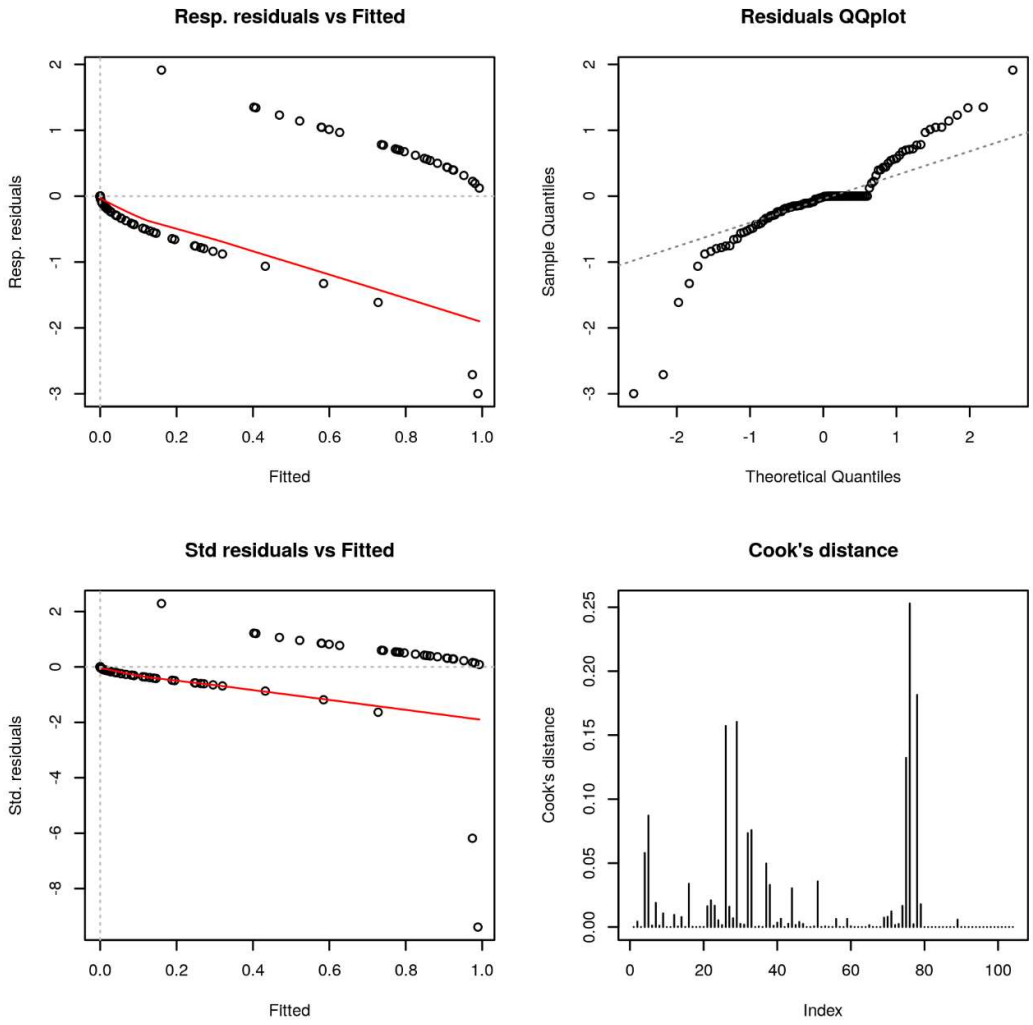

Figure 116. Residual analysis of the best model (natural spline GLM).

Marginal effects of retained covariates were also calculated to get the variations induced by each covariate along its range. Here are presented simplified marginal effects of each covariate in the range of observations. All covariates values except one have been fixed so that their combination give a prediction of the probability of presence close to 0.5. These simplified marginal figures are to be read for their relative effect and not for their absolute prediction (Figure 117).

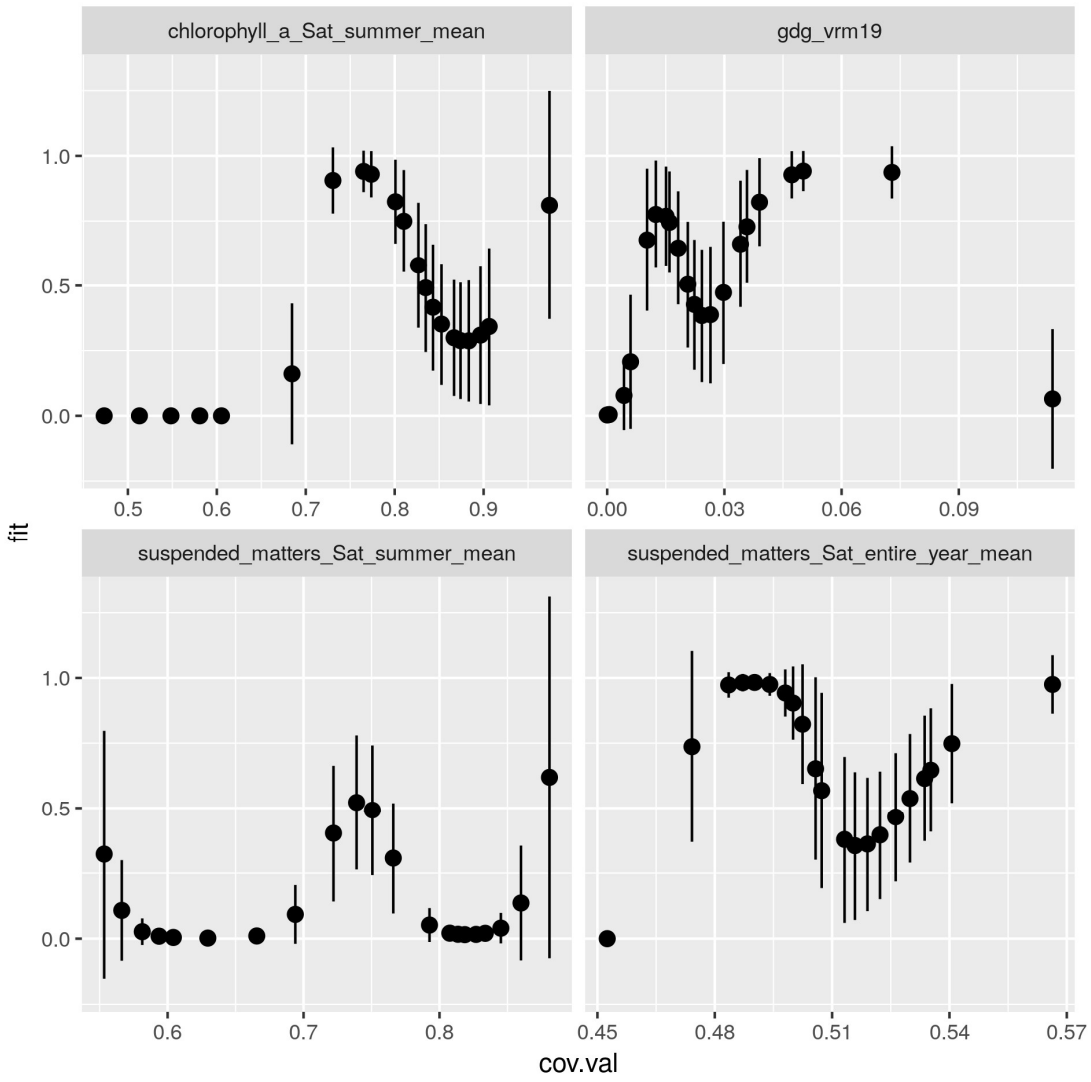

Figure 117. Simplified marginal effect of each covariate. All covariates values but one are fixed to be used for model prediction.

In models allowing the calculation of probability of presence, comparison of predicted presences with observed presences, with regards to thresholds calculated during the cross-validation procedure is also a good indicator of the quality of prediction of the model (Figure 118). Three thresholds are provided: Best THD, MaxZero and MinUn. The best THD is the best threshold value to separate presences from absences considering quality of prediction of the model. Indeed, the cross-validation built 10 times 10-fold cross-validation models, thus 100 validations. For each of the 100 models, the best threshold is the value that equilibrates selectivity and sensitivity of the predictions. The best THD on Figure 118 is the average of the 100 cross-validation thresholds. MaxZero is the average of 100 cross-validation threshold calculated as the threshold below which 95% of absence are correctly

classified as absences. MinUn is the average of 100 cross-validation threshold calculated as the threshold above which 95% of presences are correctly classified as presences.

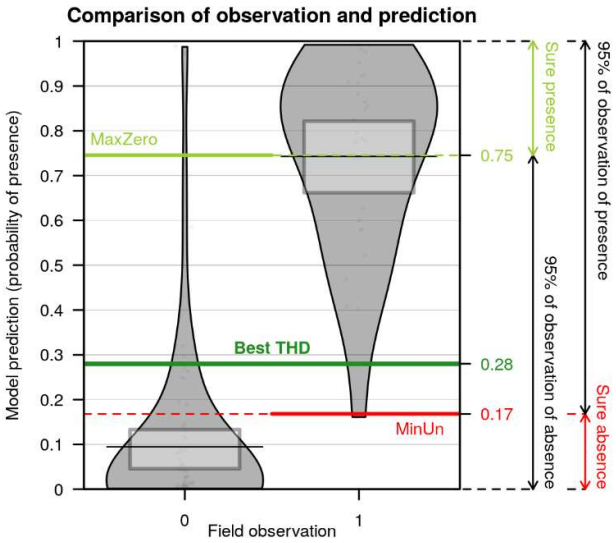

Figure 118. Pirat plot of the distributions of probability of presence according to true presence and true absence. The Bean plot is a smoothed density plot of probabilities of presence, the line shows the mean of the distribution and the boxplot represents the 95% Bayesian Highest Density Intervals of the mean.

Based on a threshold analysis, maps can be drawn of the potential occurrences of coral reefs within the niche envelope of the two reef-building corals *Lophelia pertusa* and *Madrepora oculata* in the Bay of Biscay (Figure 119).

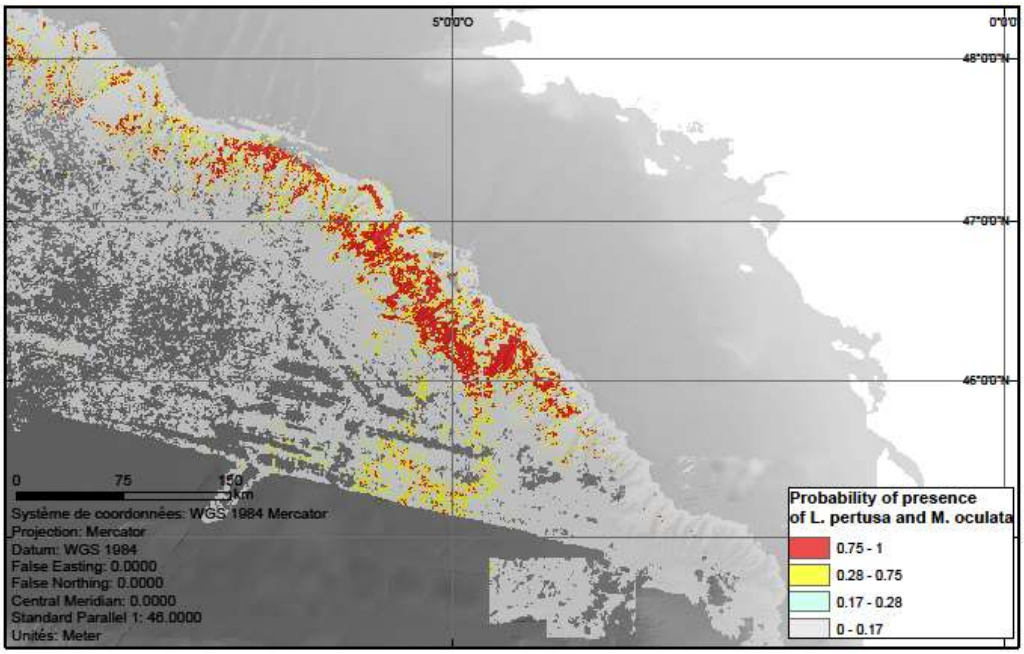

Figure 119. Map of the probabilities of presence of coral reefs in the Bay of Biscay, p > 0.28 is the best trade-off maximising true predictions of presence and true predictions of absence, p > 0.75 maximises the true predictions of presence.

3.5.7 Model interpretation, caveats and future directions

Coral reefs have been observed in the north but not in the south of the Bay of Biscay. The reason for this is likely due to higher sediment supply and higher sedimentation rates in the southern Bay of Biscay where the continental shelf narrows down. The pattern is accurately predicted by the model, which predicts that suspended matter concentrations are among the key drivers of the distribution of coral reefs. The response of coral reef occurrence to the suspended matter concentrations is however plurimodal, which is difficult to interpret from a biological point of view. Similarly, the response curves of the other two key predictors, chlorophyll a concentration and terrain ruggedness (VRM) are multimodal. Although the ecological processes behind the influence of chlorophyll a -as a proxy for food input - and terrain ruggedness - as a proxy for heterogeneous topography- are straightforward. The multimodal response of reef occurrences to these two variables is more difficult to explain. These multimodal responses may hide some unexplored interactions among covariables.

The resolution of the model is 2 km, while the median linear size of reefs in the Bay of Biscay is 65 m (van den Beld et al., 2017). The resolution of the model is thus too low to predict beyond the potential niche for coral reefs. In many models the resolution is limited by the resolution of the environmental covariates, in our model however the resolution has been constrained by the high level of spatial autocorrelation in our dataset. Spatial autocorrelation is partly due to the sampling design, based on non-random video surveys, and partly due to the biology of coral reefs, which grow asexually. Methods explicitly modelling spatial autocorrelation might improve the resolution of the model (e.g. Ovaskainen et al., 2017).

3.6 Case study 8a: Predictive habitat suitability models for key CWC species under current environmental conditions in the Azores

Gerald H. Taranto[1,2], José-Manuel González-Irusta[1,2], Carlos Dominguez-Carrió[1,2], Christopher K. Pham[1,2], Fernando Tempera[1,2,3], Marina Carreiro-Silva[1,2], Telmo Morato[1,2]

1- Okeanos Research Centre, Universidade dos Açores, Departamento de Oceanografia e Pesca, Horta, Portugal
2- IMAR Instituto do Mar, Universidade dos Açores, Departamento de Oceanografia e Pesca, Horta, Portugal
3- Laboratoire Environnement Profond, IFREMER, France

3.6.1 Case study description

Spanning over some of the most remote areas of the northern Mid-Atlantic Ridge, the Azores region (~1 million km^2) hosts a range of seascapes unique to European waters (Figure 120). Harsh bathymetric variations over short distances shape volcanic geomorphologies rising from plains well below 5000m deep and provide a great heterogeneity of deep-sea habitats. Such concentrations of habitat diversity have been suggested to constitute priority targets for global conservation actions (Costello & Chaudhary, 2017).

Oceanography in the region is influenced by two eastward currents branching from the Gulf Stream, the North Atlantic Current in the north and the Azores Current to the south (Klein & Siedler, 1989). Mediterranean water eddies (meddies) are also an important feature in the region, present as distinct lenses of warm and salty Mediterranean water at 800-1200 m deep (Bashmachnikov et al., 2009). In general, productivity is low, but localized upwelling associated with island slopes and seamounts can enhance local production (Bashmachnikov et al., 2004; Morato et al., 2008). The water current patterns result in a complex circulation, high salinity and temperature, and a low nutrient regime that typifies the Azores (Santos et al., 1995; Bashmachnikov et al., 2004; Palma et al., 2012).

The seafloor that surrounds the archipelago comprises a variety of open ocean deep-sea habitats, from island slopes and numerous seamounts to hydrothermal vents at various depths and abyssal plains exceeding 5,000m depth (Tempera et al., 2012). Among the organisms inhabiting the seafloor, the Azores region may represent a hotspot of cold-water coral (CWC) diversity (Braga-Henriques et al., 2013) especially within the subclass *Octocorallia* (Sampaio et al., 2019). Biogeographic studies indicate that coral species in the Azores show mixed zoographic affinities with a greater affinity to the Lusitanian-Mediterranean biogeographic region and to a lesser extent to the western North Atlantic (Braga-Henriques et al., 2013). Although the underlying reasons for the observed affinities are unknown, it is suggested that the pathway of the Mediterranean water from the Mediterranean into

the Atlantic Ocean may help explain the CWC biodiversity/biogeography patterns in the Azores and North Atlantic. The development of spatial models to describe the distribution of these prominent organisms in the region might help increasing our understanding of deep sea ecosystem in the case study area. Here we developed a set of HSMs for habitat-structuring CWC species known to form aggregations and likely to constitute Vulnerable Marine Ecosystems (VMEs) (FAO, 2009) in the Azores region.

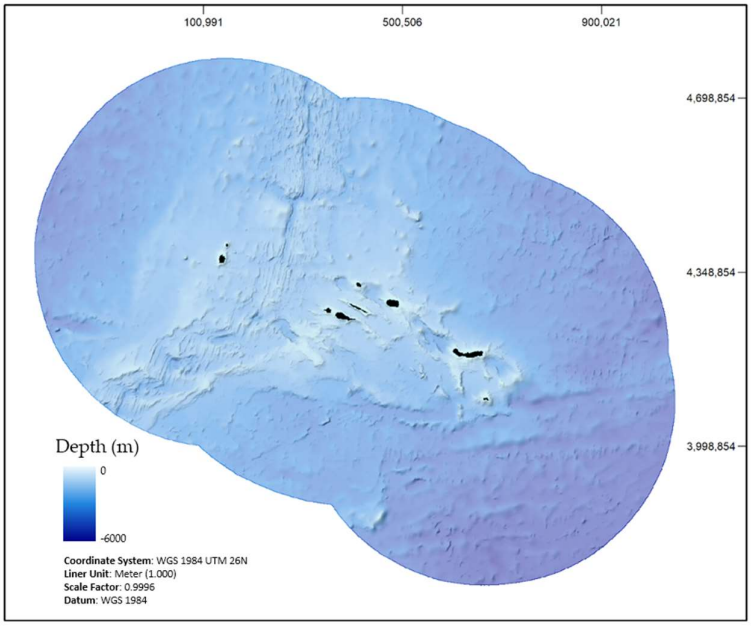

Figure 120. Azores economic exclusive zone (EEZ).

3.6.2 Species selection

Specific criteria determined the set of CWC taxa included in the present study: *i)* coral taxa known to form dense aggregation and/or conspicuous three-dimensional structures in the study region; *ii)* coral taxa known to grow to sizes sufficiently large to be easily detected in underwater images or taken as bycatch using longlines or handlines in the study region; *iii*) coral taxa known to have a sufficient geographic extent to ensure the development of sound HSMs at the scale of the Azores exclusive economic zone. The confidence of taxonomic identification constrained the resolution at which coral groups could be modelled without compromising model performance (Aubry et al., 2017; Araújo et al., 2019). The final list of CWC taxa was: *Acanella arbuscula, Acanthogorgiidae, Callogorgia verticillata, Coralliidae, Dentomuricea cf. meteor, Errina dabneyi, Leiopathes spp., Madrepora oculata, Narella spp., Narella versluysi*, *Paracalyptrophora josephinae, Solenosmilia variabilis* and *Viminella flagellum.* Their reported occurrences are presented in Figure 121.

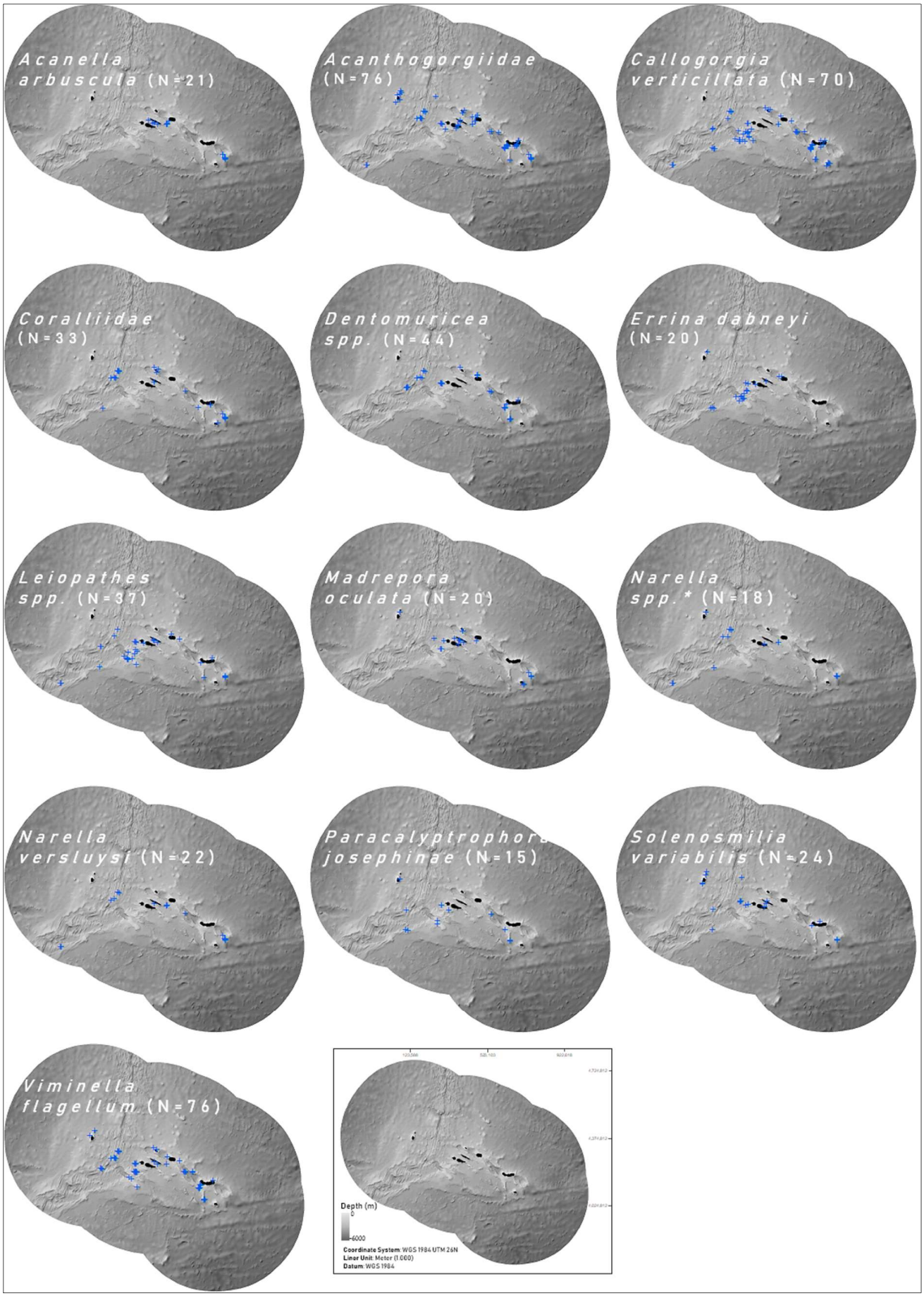

Figure 121. Presence records of the modelled CWC taxa within the Azores EEZ. In parenthesis the number of presence points once they have been aggregated on a 1x1 km grid. *Narella spp. *does not include* Narella versluysi.

3.6.3 Species occurrence, data sources and data tidying

Presence data for the species of interest were compiled from three main sources: *i)* bycatch data obtained from regional demersal surveys on-board the research vessel "Arquipélago"; *ii)* observer programs on fishing vessels that reported coral bycatch; *iii)* video annotation of underwater images shot by ROV, drop and tow camera systems. Data from historical datasets were excluded to avoid, as much as possible, uncertainties in georeferences and associated locational errors that may reduce models performance and complicate the interpretability of results (Osborne & Leitão 2009; Araújo et al., 2019). Two further steps helped increasing georeference reliability. First, the removal of all coordinates with associated location errors higher than 1.5 km so that potential errors were comparable to the resolution of environmental predictors (that were resampled to 1x1 km); given the strong spatial autocorrelation of environmental parameters this lessened detrimental effects on HSMs outputs (Osborne & Leitão, 2009; Naimi et al., 2011; Araújo et al., 2019). Second, the removal of bycatch records that did not have an associated depth or with a reported depth mismatching bathymetric data on the same location for more than 200m. Presence records were finally aggregated on a 1x1 km grid and duplicated records were filtered out. Only species present in at least 15 locations of the grid were retained and modelled (Figure 121).

Most HSMs require absence data to infer the relationship between the occurrence of species and environmental parameters. The use of presence-absence models when only presence data is available requires the generation of artificial absence data, generally called pseudo-absences. The geographical background from which pseudo-absences are drawn greatly affects HSMs estimates (Iturbide et al., 2015; 2018). In order to account for this effect, we estimated the sampling effort within the Azores EEZ (Figure 122) considering: sampling area of regional scientific surveys (both in cases of bycatch and no bycatch), extent of video transects and bycatch events from observer data (it was not possible to retrieve observers position when no bycatch occurred). As discussed in the next sections, the estimated sampling effort was then used to shape the geographical background from which pseudo-absences were sampled.

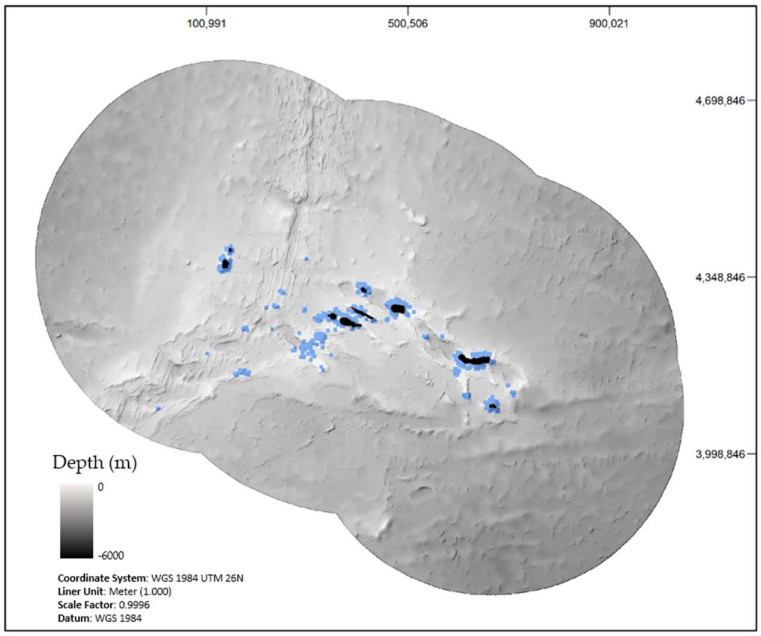

Figure 122. Estimated sampled area within the Azores EEZ.

3.6.4 Environmental data layers

A preliminary set of 19 environmental layers potentially affecting CWCs distributions were selected. Depth was downloaded from the EMODNET portal (EMODNET, 2018), while depth derivate layers were calculated using benthic terrain modeller (Walbridge et al., 2018) and focal statistic algorithms in ArcMap and included: coarse (30 km radius) and fine (3km radius) BPI, slope, standard deviation of slope (7x7 window), ruggedness, eastness and northness. Aragonite, calcite, nitrates, phosphates and silicates concentration near bottom (µmol l^{-1}), dissolved oxygen near bottom (ml l^{-3}), percentage of oxygen saturation near bottom (µmol l^{-1}), pH, salinity and temperature were extracted from Amorim et al. (2017); near-bottom current speed (m s^{-1}) were extracted from the oceanographic model MOHID. Depth derived layers were up-scaled, while the other environmental layers were down-scaled to a 1x1 km grid using bilinear interpolation and projected to UTM 26N.

To avoid prediction artifacts due to collinearity, the initial set of environmental predictors was screened using Pearson correlation and only layers showing coefficients lower than 0.7 (as discussed in Dormann et al., 2013) were included in the final selection (Figure 123).

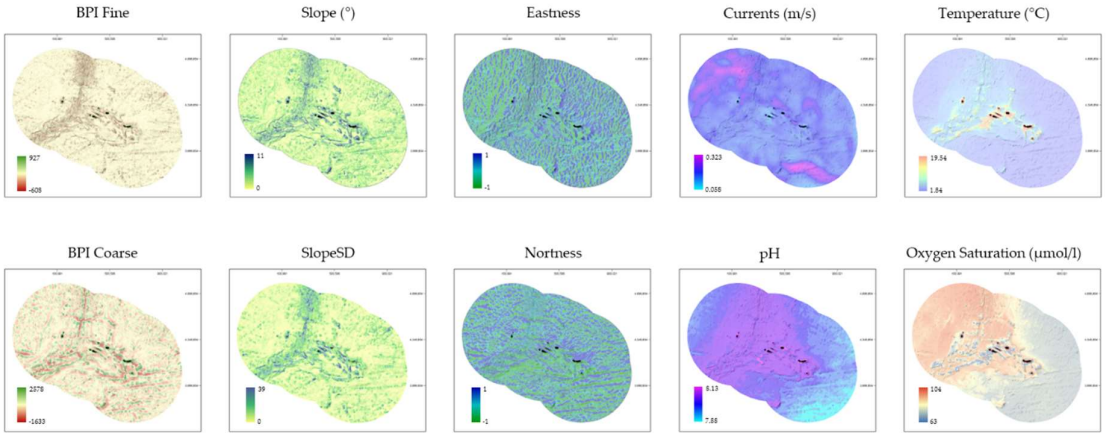

Figure 123. Final selection of environmental layers used as explanatory variables

3.6.5 Modelling approaches

Generalized Additive Models (GAMs, Hastie & Tibshirani, 1990), maximum entropy models (Maxent, Phillips et al., 2006; 2017) and Random Forest (RF, Breiman, 2001) were initially selected to predict the distribution of CWCs. During preliminary analysis, RF seemed to be highly affected by the low number of presence records and by biased sampling efforts (as shown in Freeman et al. 2012). It was therefore decided to exclude RF from further analyses and to focus on the other two modelling approaches.

Both Maxent and GAMs require pseudo-absence data. The way pseudo-absences are defined deeply influence the reliability of model predictions (McPherson et al., 2004; Phillips & Dudik, 2008; Barbet-Massin el al., 2012). Exploratory analysis to evaluate model performance under variable numbers of pseudo-absences showed that as they increase in number model outputs and response curves became more stable and of higher quality. The number of pseudo-absences used to build Maxent and GAMs was then set to 10 000, following Phillips & Dudik (2008) and Barbet-Massin el al. (2012). The geographical background from which pseudo-absences are generated also affect model performance (Kramer-Schadt et al., 2013; Iturbide et al. 2015; 2018). To limit detrimental effects on the HSMs pseudo-absences were generated from depth shallower than 2000m, as no sampling occurred below 2000m. Furthermore, environmental profiling helped defining the environmental range from which pseudo-absences were sampled by dividing the background area into suitable/unsuitable (Iturbide et al., 2018). Finally, to account for sampling bias, pseudo-absences were randomly selected within the profiled background following the depth distribution of the estimated sampling effort.

The environmental variables included in GAM were selected using the Akaike Information Criteria (Symonds & Moussalli, 2010) while Maxent was fitted using the whole set of environmental

predictors. To assess the contribution of each variable to final predictions, each variable at turn was randomly shuffled and new predictions were made. The degree of correlation between the predictions with permutations and the original prediction gives an estimate of the variable importance (Thuiller et al., 2009). Response curves were built following Elith et al. (2005), where changes in habitat suitability predictions are related to the variation of a single variable across its range while all other predictors are kept to a constant value.

Estimates of model performance were obtained using a 5-fold cross-validation (see Anderson et al., 2016) and measured using two statistical methods: area under the curve (AUC) and true skill statistics (TSS). According to these statistics, models can be scored as good (AUC >0.8; TSS>0.6), fair (0.7≤AUC≤0.8; 0.2≤TSS≤0.6) or poor (AUC<0.7; TSS<0.2) (Allouche et al., 2006; Mandrekar, 2010). Final models were built using the entire dataset while a bootstrap process (n = 30) was employed to determine the spatial confidence of predictions over the background area. Each iteration started sampling with replacement presences and pseudo-absences from the originals pools, continued fitting the final models and concluded predicting the suitability indices for the background area. Since the coefficient of variation tended to highlight variations in areas with suitability indices close to zero, prediction variability was measured as the frequency individual raster cell would be classified as suitable when the suitability index was transformed into a binary index using the sensitivity-specificity sum maximization (MSS) threshold (see Liu et al., 2005; Jiménez-Valverde & Lobo, 2007). Binary maps were then used to build maps of species richness; i.e. the number of species that were predicted to be present in a certain grid cell.

3.6.6 Model outputs

In general, AUC and TSS scores for both GAM and Maxent models were good for all species except for *Leiopathes spp.* and *Paracalyptrophora josephinae* (Table 17). Overall model performances were similar for Maxent and GAMs, with Maxent scoring better for seven out of the 13 modelled taxa both according to AUC and TSS scores. The predicted suitable habitats and the confidence level for individual CWC taxa are shown in Figure 124. As expected the predicted distribution of CWC taxa showed a strong association with areas of local relief, being them island shelves or slopes, ridges or seamounts. However, even among areas of similar depths, models discriminated between suitable and unsuitable zones showing that model outputs were not exclusively driven by depth correlated changes in environmental predictors. Most of the suitable area available for the modelled groups was located at lower latitudes than the northernmost island of the archipelago (Corvo) while suitable habitats were predicted to occur on both sides of the Mid-Atlantic Ridge with no group showing

marked longitudinal gradients. Models built with a higher number of presence records and at a finer taxonomic resolution appeared to more consistently identify zones of suitable habitat (high confidence predictions, Figure 124). The number of species for which each raster cell was predicted as suitable by GAM and Maxent outputs considering only high confidence predictions is shown in Figure 125. The relative importance of each explanatory is showed in Figure 126. Overall the three most important variables for GAM were oxygen saturation, temperature and BPI coarse while the three most important variables for Maxent were oxygen saturation, pH and temperature. Considering only the subclass *Octocorallia,* the three most important variables were temperature, pH and oxygen saturation for both GAM and Maxent (even though they did not rank in the same order). Within the subclass *Scleractinia* relative variable importance differed more markedly with GAMs having only oxygen saturation and BPI coarse as relevant explanatory variables and Maxent models having pH, slope and oxygen saturation as the three most important explanatory variables. The response curves of those variables whose relative importance when permuted was greater than the 20% are shown in Figure 127. Note that for comparison reason whenever a variable ranked above the 20% either in GAMs or Maxent models, we also reported the response curve of the other model even if it did not rank above the 20%. Response curves did not show clear patterns among taxonomic groups. Temperature oxygen saturation and pH were the most consistent variables of all, showing similar responses both in GAM and Maxent.

*Table 17. AUC and TSS scores of GAM and Maxent predictions using a 5-fold cross-validation process. * PR is presence records and it represents the number of grid cells containing a certain taxon. AUC is the area under the curve; TSS is true skill statistics; GAM is Generalized Additive Models.*

CWC TAXA	PR*	AUC GAM	AUC Maxent	TSS GAM	TSS Maxent
Acanella arbuscula	21	0.826	0.915	0.706	0.814
Acanthogorgiidae	76	0.864	0.883	0.634	0.645
Callogorgia verticillata	70	0.852	0.853	0.642	0.628
Coralliidae	33	0.854	0.847	0.694	0.673
Dentomuricea spp.	44	0.941	0.936	0.821	0.819
Errina dabneyi	20	0.819	0.821	0.651	0.635
Leiopathes spp.	37	0.692	0.745	0.460	0.516
Madrepora oculata	20	0.921	0.909	0.836	0.837
Narella spp.	18	0.894	0.900	0.780	0.783
Narella versluysi	22	0.895	0.882	0.779	0.759
Paracalyptrophora josephinae	15	0.784	0.683	0.622	0.486
Solenosmilia variabilis	24	0.863	0.849	0.695	0.700
Viminella flagellum	76	0.899	0.916	0.721	0.750

GAM

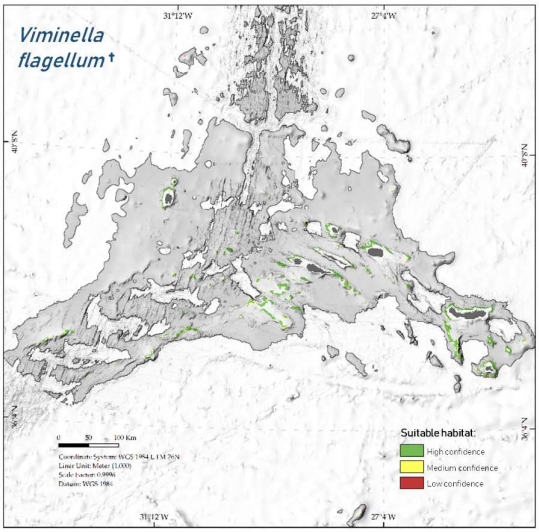
Viminella flagellum†
Suitable habitat:
High confidence
Medium confidence
Low confidence

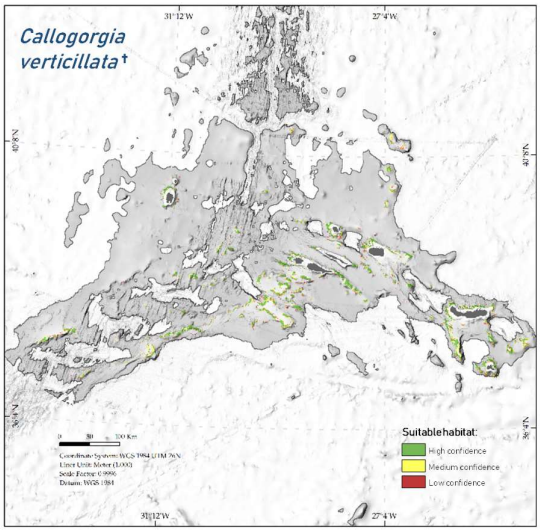
Callogorgia verticillata†
Suitable habitat:
High confidence
Medium confidence
Low confidence

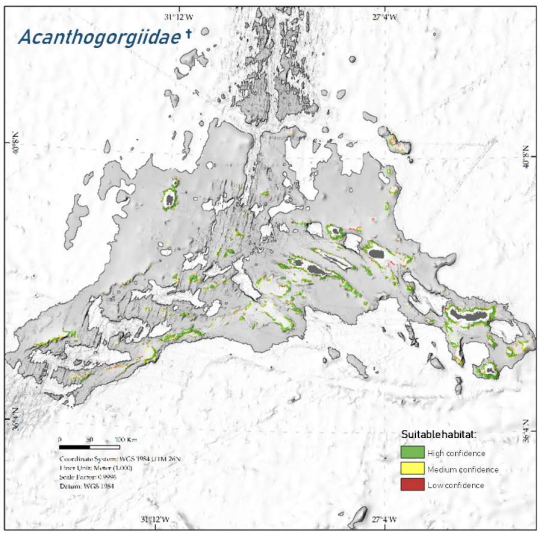
Acanthogorgiidae†
Suitable habitat:
High confidence
Medium confidence
Low confidence

MAXENT

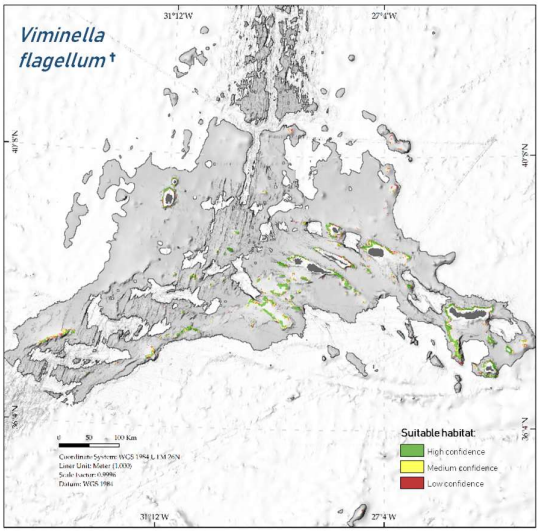
Viminella flagellum†
Suitable habitat:
High confidence
Medium confidence
Low confidence

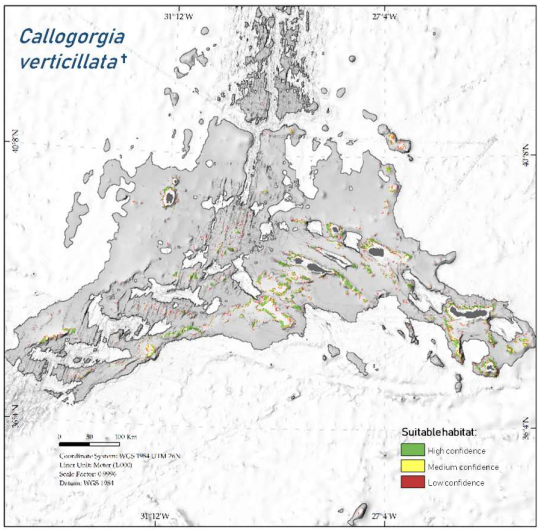
Callogorgia verticillata†
Suitable habitat:
High confidence
Medium confidence
Low confidence

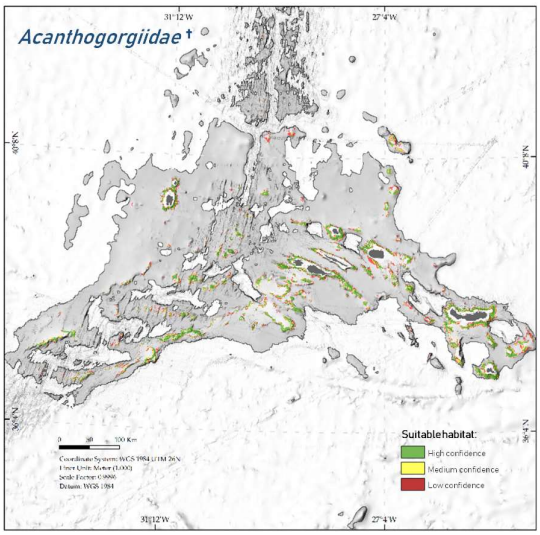
Acanthogorgiidae†
Suitable habitat:
High confidence
Medium confidence
Low confidence

GAM

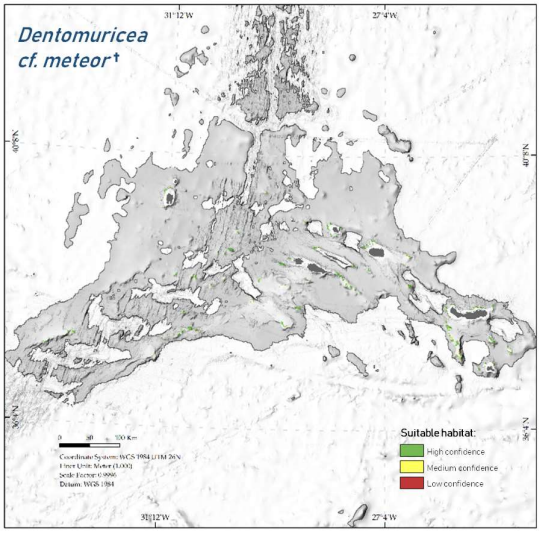
Dentomuricea cf. meteor†
Suitable habitat:
High confidence
Medium confidence
Low confidence

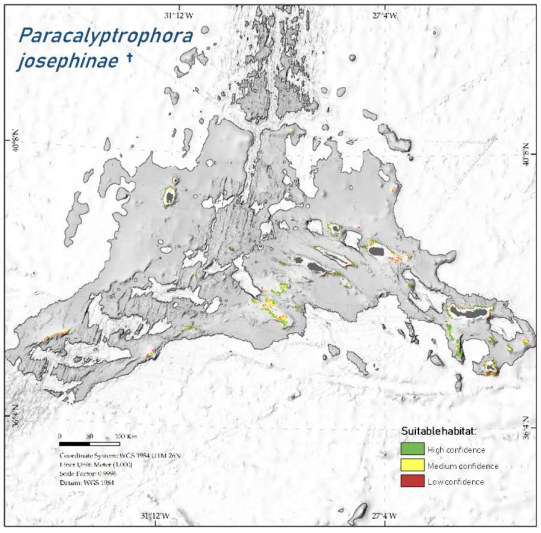
Paracalyptrophora josephinae †
Suitable habitat:
High confidence
Medium confidence
Low confidence

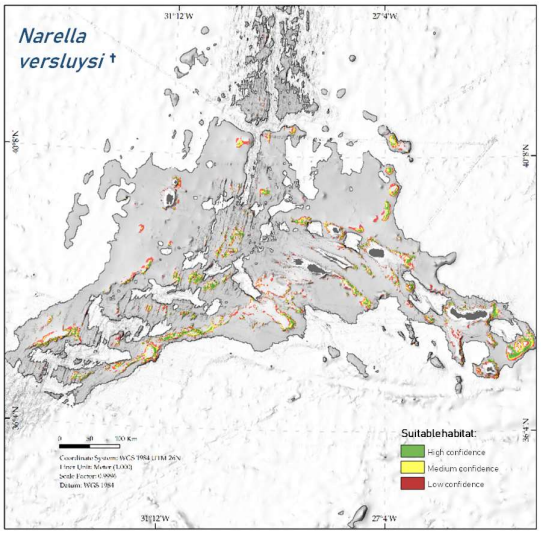
Narella versluysi †
Suitable habitat:
High confidence
Medium confidence
Low confidence

MAXENT

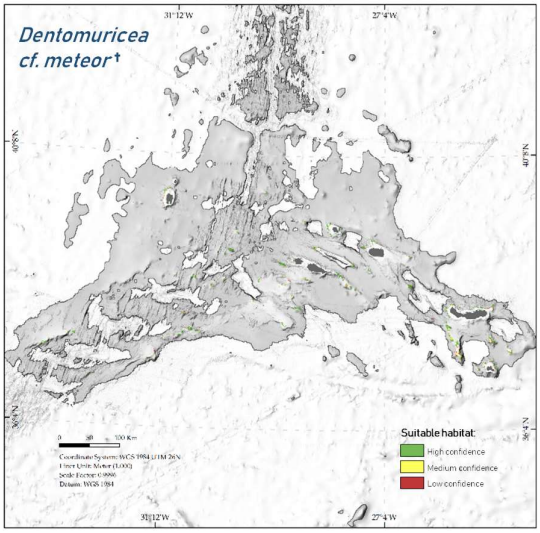
Dentomuricea cf. meteor†
Suitable habitat:
High confidence
Medium confidence
Low confidence

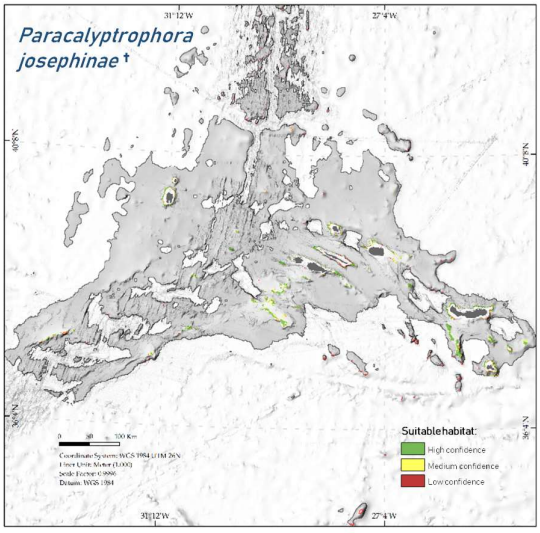
Paracalyptrophora josephinae †
Suitable habitat:
High confidence
Medium confidence
Low confidence

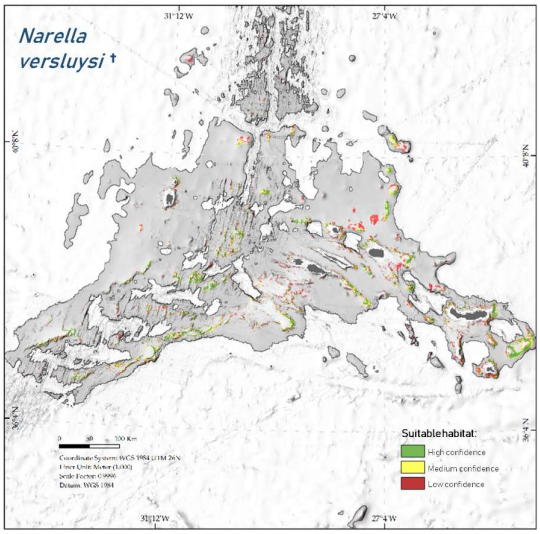
Narella versluysi †
Suitable habitat:
High confidence
Medium confidence
Low confidence

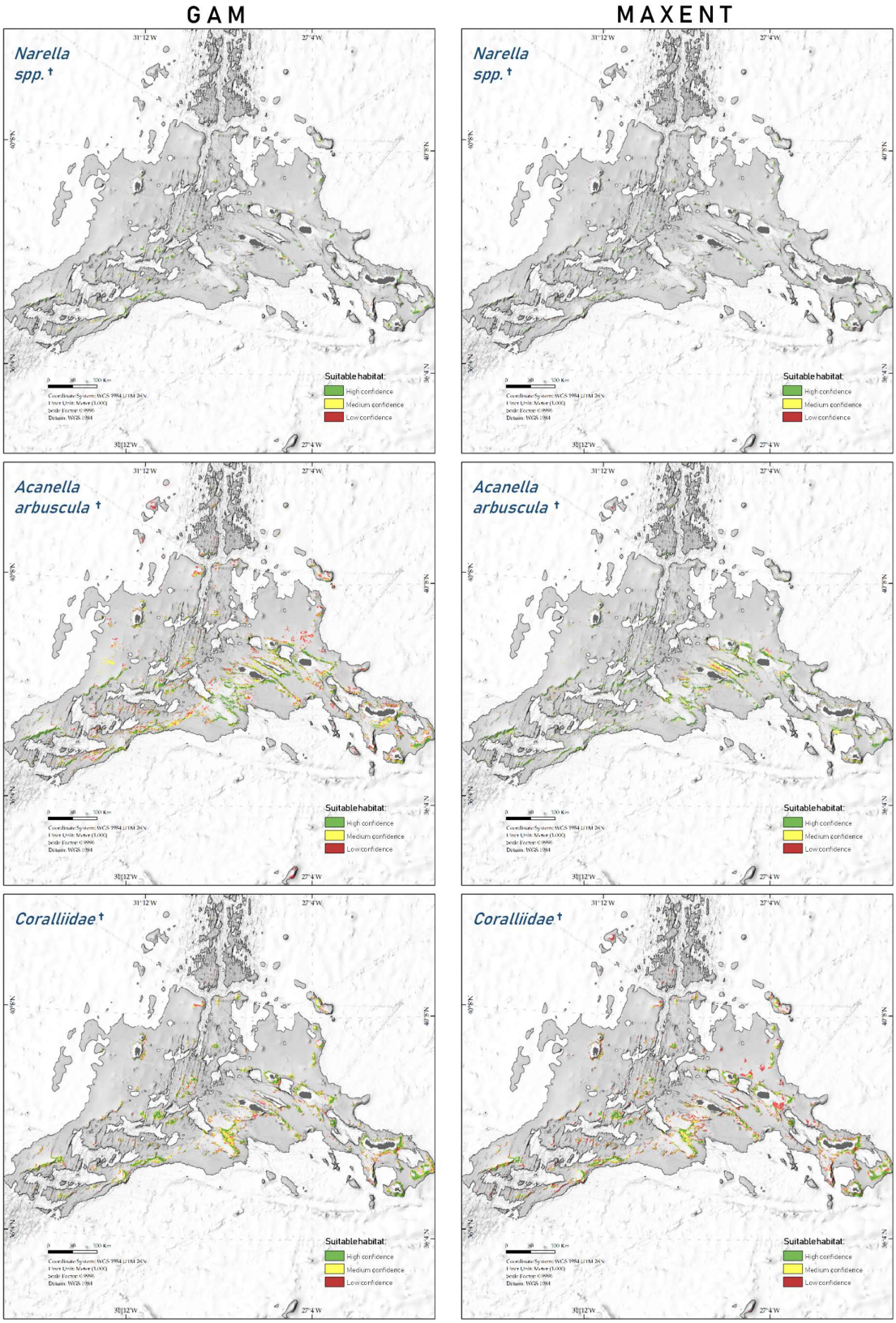
GAM
MAXENT
Narella spp.†
Acanella arbuscula †
Coralliidae †
Suitable habitat:
High confidence
Medium confidence
Low confidence

GAM MAXENT

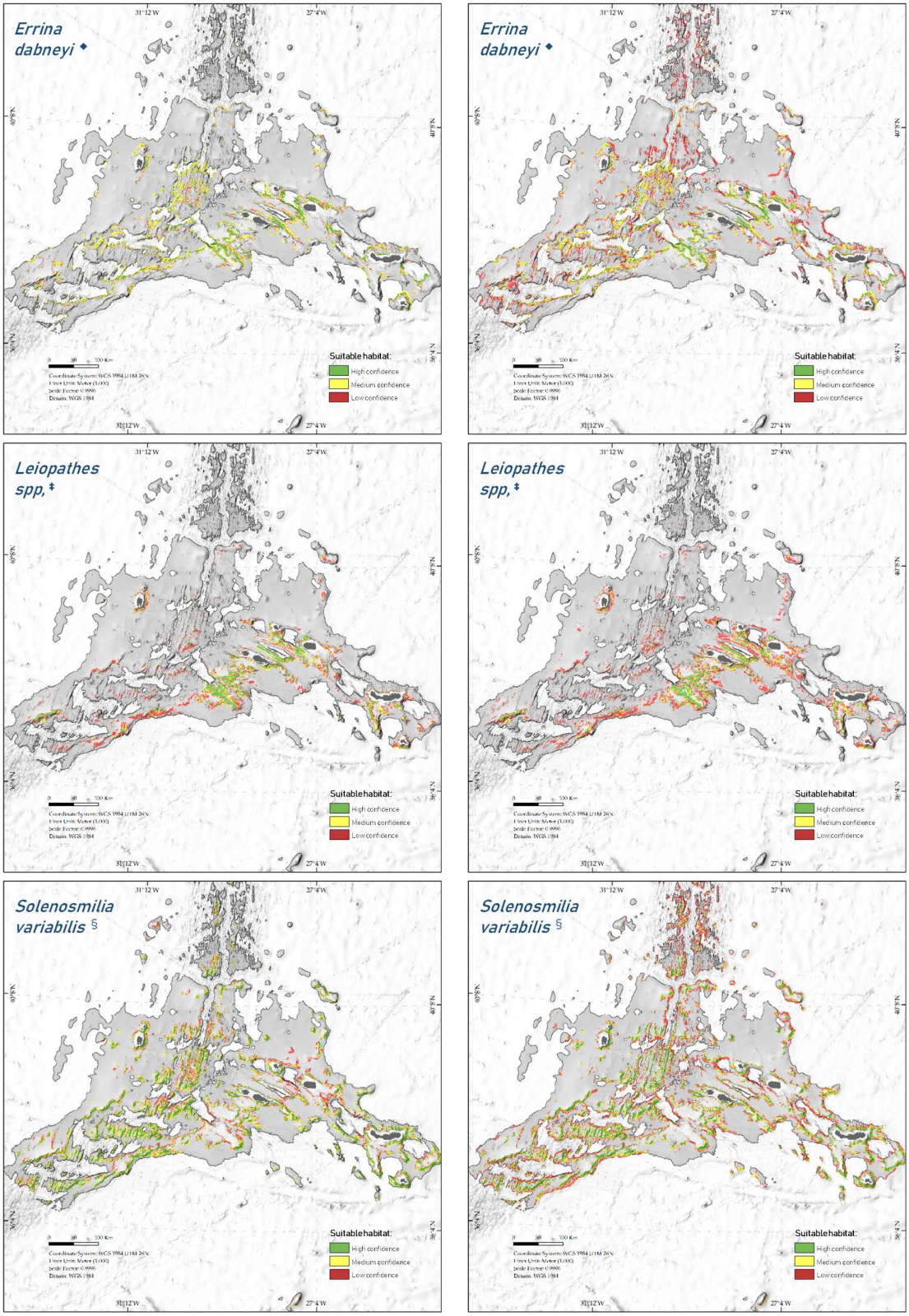
Errina dabneyi ◆
Leiopathes spp, ‡
Solenosmilia variabilis §
Suitable habitat:
High confidence
Medium confidence
Low confidence

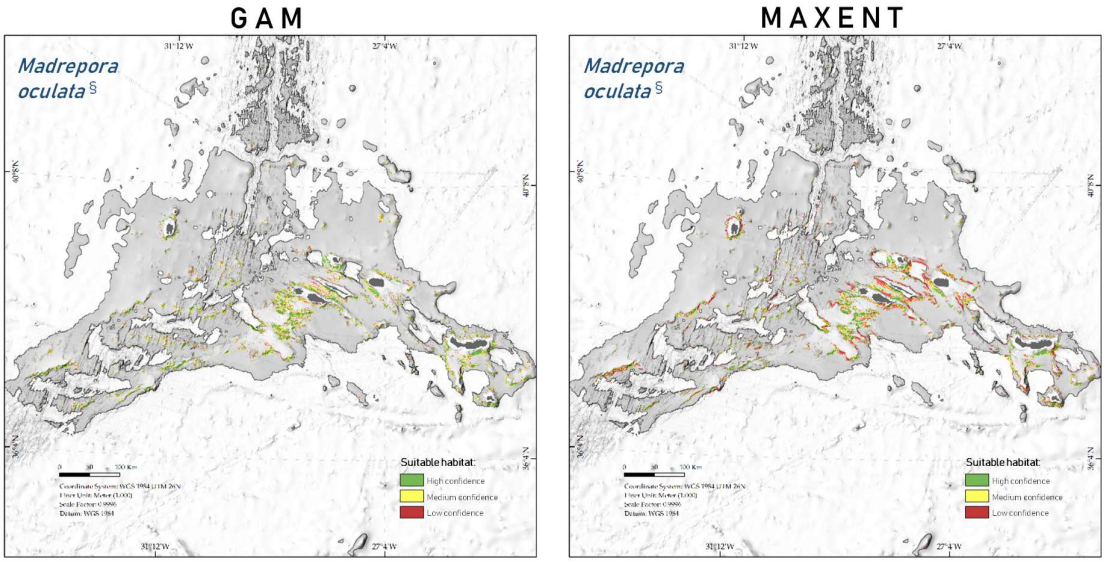

Figure 124- Suitable habitat after converting the predictions of GAM and Maxent into binary maps. Confidence levels reflect the frequency each raster cell is classified as a suitable habitat (above the MSS threshold) when presence and pseudo-absence records are permuted. † Octocorallia; ◆ Stylasteridae; ‡ Antipatharia; § Scleractinia.

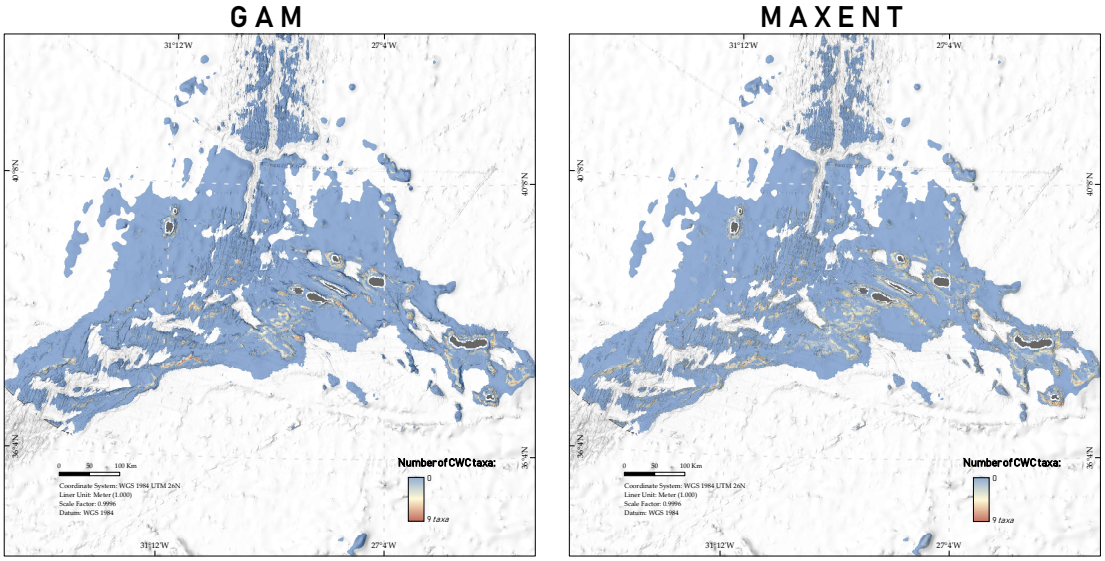

Figure 125- Number of species for which each raster cell was predicted as suitable by GAM and Maxent; only high confidence prediction from individual models were considered.

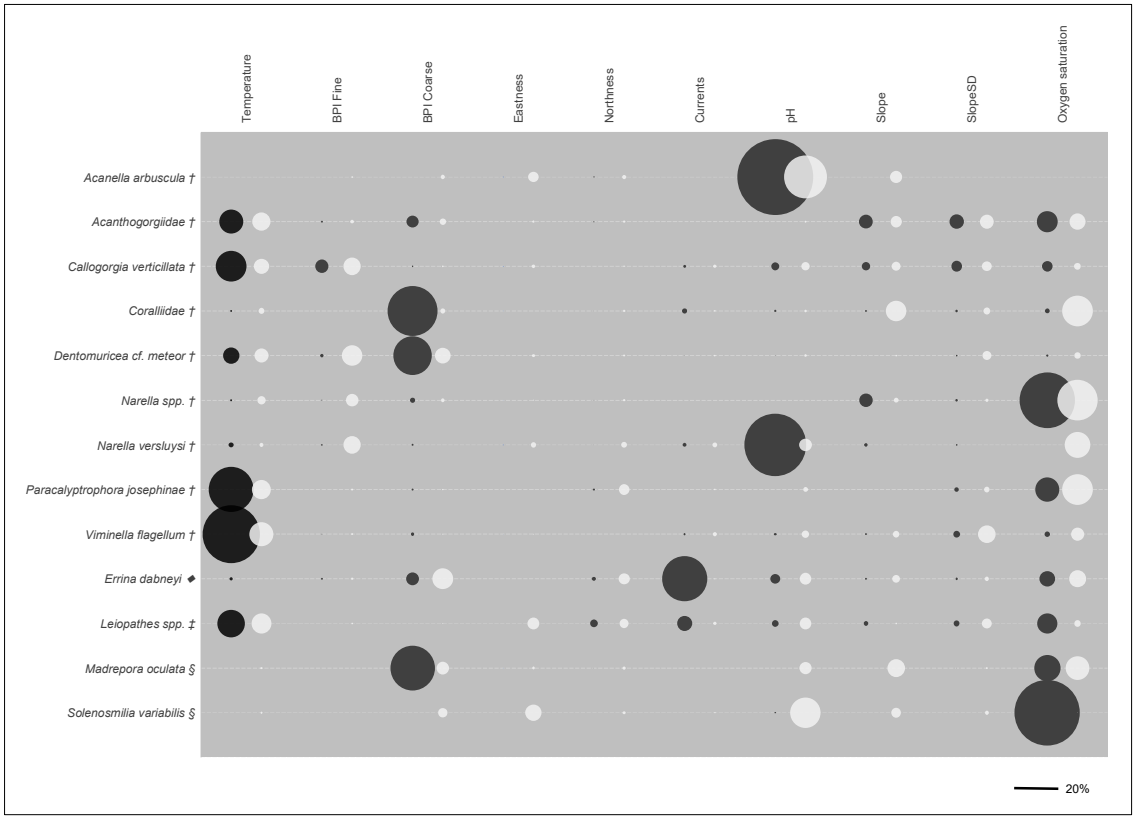

Figure 126. Relative variable importance for each CWC taxa. In black GAM models, in clear grey Maxent models. † Octocorallia; ◆ Stylasteridae; ‡ Antipatharia; § Scleractinia.

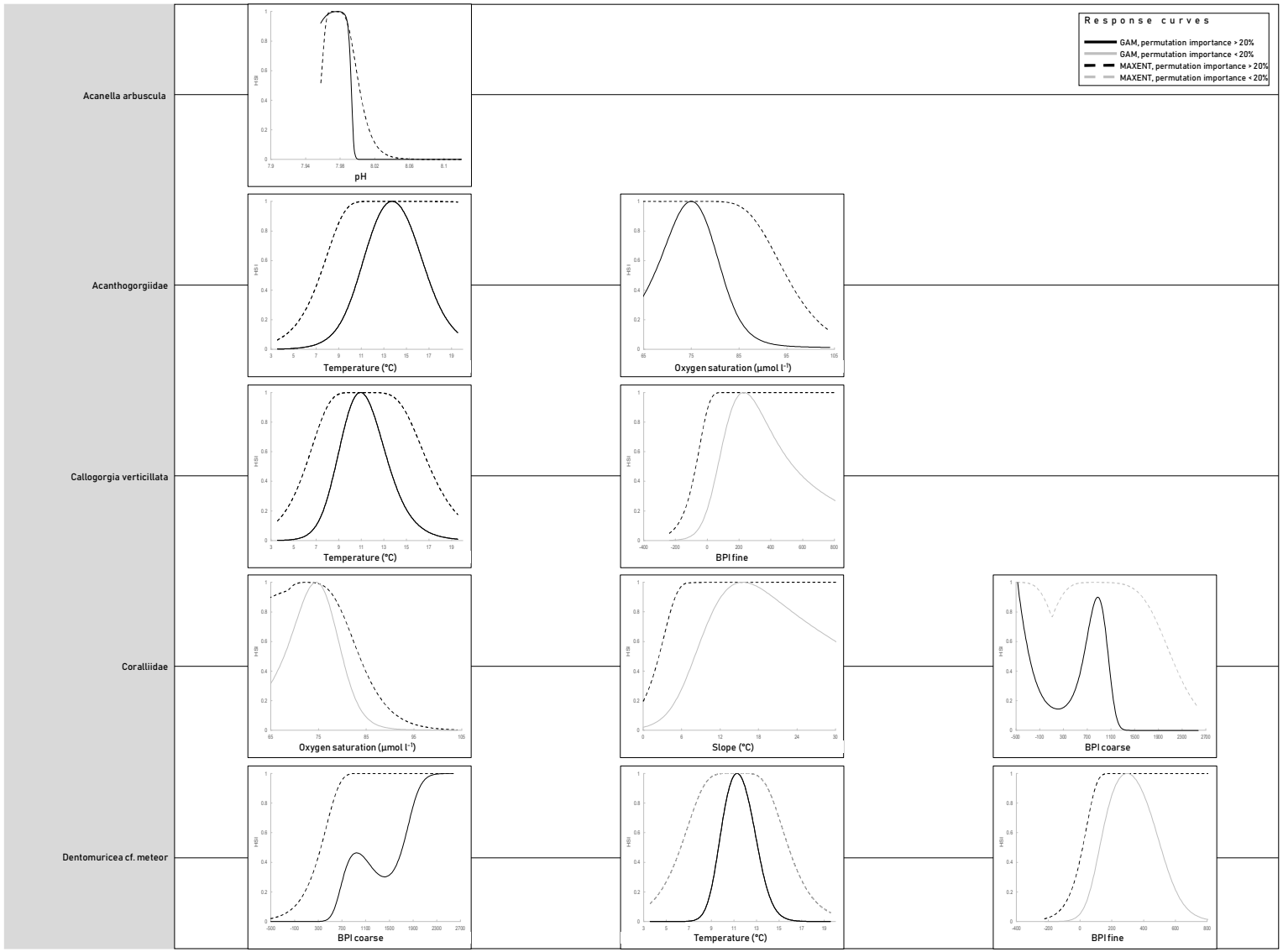
Response curves
GAM, permutation importance > 20%
GAM, permutation importance < 20%
MAXENT, permutation importance > 20%
MAXENT, permutation importance < 20%
Acanella arbuscula
Acanthogorgiidae
Callogorgia verticillata
Coralliidae
Dentomuricea cf. meteor
pH
Temperature (°C)
Oxygen saturation (µmol l⁻¹)
BPI fine
Slope (°C)
BPI coarse
HSI

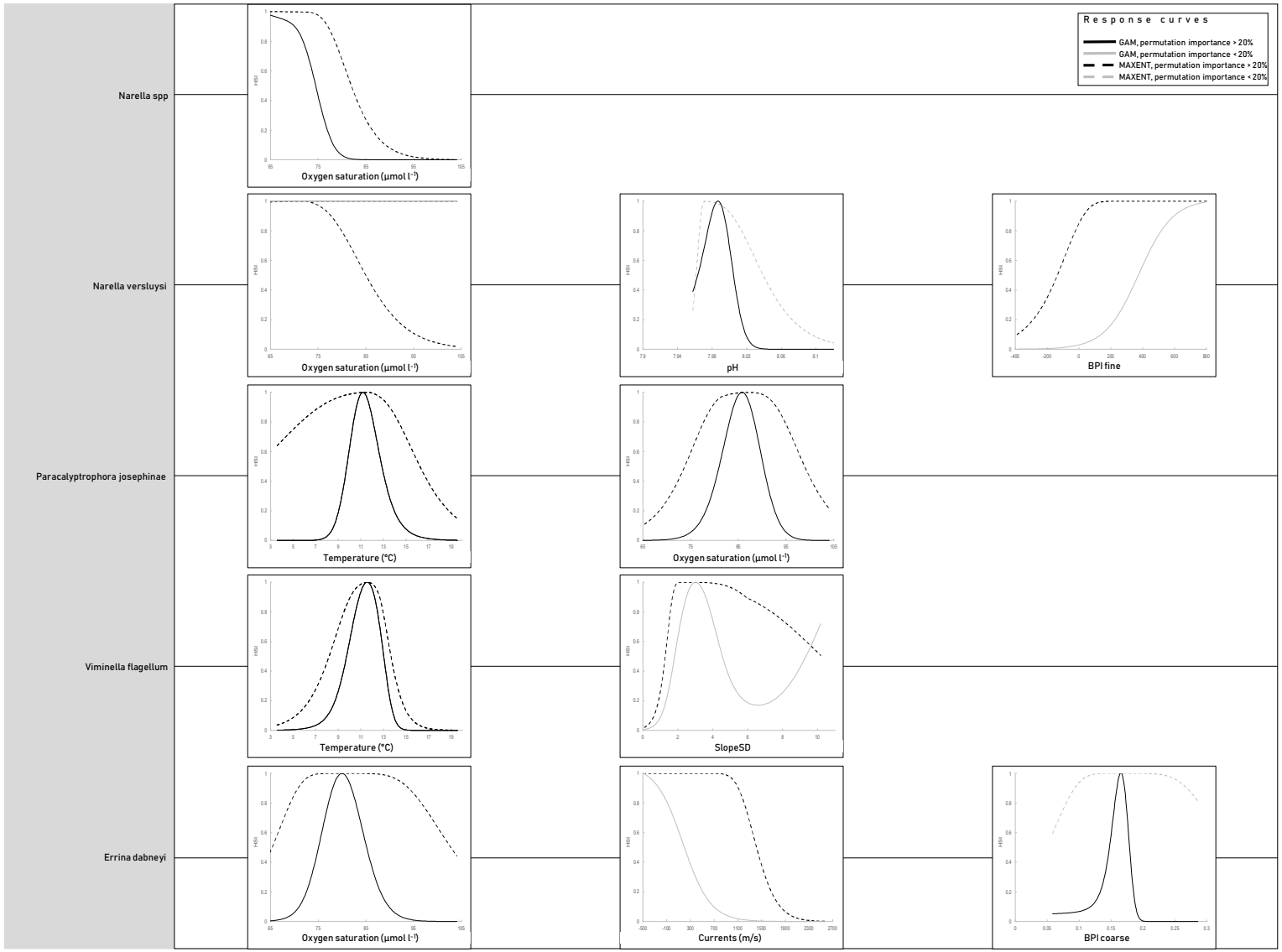
Response curves
GAM, permutation importance > 20%
GAM, permutation importance < 20%
MAXENT, permutation importance > 20%
MAXENT, permutation importance < 20%
Narella spp
Narella versluysi
Paracalyptrophora josephinae
Viminella flagellum
Errina dabneyi
Oxygen saturation (µmol l-1)
pH
BPI fine
Temperature (°C)
SlopeSD
Currents (m/s)
BPI coarse
HSI

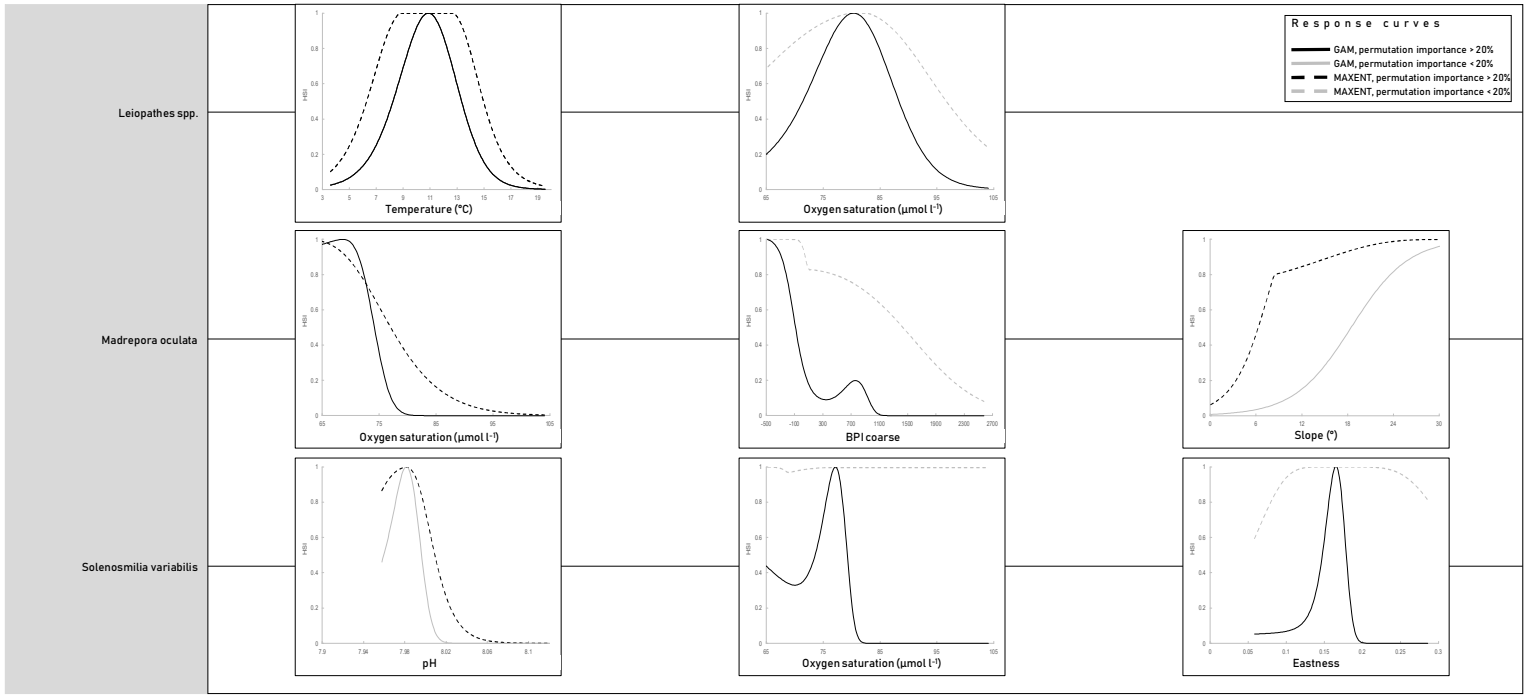

Figure 127. Response curves of the environmental explanatory variable whose permuted importance was above 20%.

3.6.7 Model interpretation, caveats and future directions

Current model predictions are useful to identify areas of particular importance for management and investigation. Most of the suitable area available for the modelled groups was located at lower latitudes than the northernmost island of the archipelago (Corvo) while suitable habitats were predicted to occur on both sides of the Mid-Atlantic Ridge with no group showing marked longitudinal gradients. As expected the predicted distribution of CWC taxa showed a strong association with areas of local relief, being them island shelves or slopes, ridges or seamounts. However, even among areas of similar depths, models discriminated between suitable and unsuitable zones showing that model outputs were not exclusively driven by depth correlated changes in environmental predictors. Models built with a higher number of presence records and at a finer taxonomic resolution appeared to more consistently identify zones of suitable habitat (high confidence predictions), suggesting that an increase in presence records and taxonomic resolution would benefit model performance. The richest shelf areas appeared to be north and south of Flores, on the south-eastern continuation of the Pico-Faial shelf, at the eastern and western tips of São Jorge, on the deepest slopes around Graciosa, west of São Miguel, south of Santa Maria and on the southern area of Formigas. Among seamounts and ridges, of particular importance appeared to be the Gigante Complex (between Flores and Faial), several shallower peaks on the south-western portion of the Mid-Atlantic Ridge, two isolated peaks between Terceira and São Miguel and some banks and seamounts south-west of Pico and Faial. These overall spatial patterns were confirmed by a good agreement of the suitable habitat predicted with high confidence by both GAM and Maxent, even in the worse performing models (*Leiopathes* spp. and *Paracalyptrophora josephinae*). Lower confidence predictions of suitable habitat showed stronger differences among GAMs and Maxents.

As the number of presence records increased, response curves became more consistent among model methods and more sound biologically. On the contrary, response curves of species with a lower number of records (< 25) tended to show stranger patterns in their response – e.g., negative relation of *Acanella arbuscula* (21), *Paracalyptrophora josephinae* (15) and *Narella versluysi* (22) to pH increase. It might be useful to rethink the minimum number of species occurrences to build HSMs at the scale of the Azores EEZ. At the moment, great efforts are in place to improve the overall habitat mapping of the Azores EEZ. In particular low cost monitory programmes and opportunistic scientific survey are expected to provide new video data on VMEs occurrence. Video surveys should improve our capacity to detect and map CWC, reducing the dependence of models on bycatch data.

A further refinement of the environmental variables used to build the model may also increase prediction accuracy. In particular, eastness and northness appeared to have very limited importance

in model predictions. The actual current layer also showed very limited explanatory importance, contrary to what was expected for CWC since their feeding capacity has been linked to current speeds. We believe that the resolution of the oceanographic model used to build the currents layer may have been too coarse to resolve small scale oceanographic patterns that influence CWCs distribution. Another possible issue may be related with use of average current values instead of other metrics capturing its variability. Most likely, CWCs do not depend on these average values, but rather they might be influenced by periodic current bursts that in the Azores region have been shown to associate with tides even at seamount depths. Moreover, a combination of fine and coarse BPI able to more accurately synthetize geomorphological information across scales (e.g., peak on plain, peak on peak, valley on peak, etc.) might simplify and improve models outputs. A better refined list of predictors could improve models performance since the inclusion of variables with little explanatory power tend to create prediction artifacts, especially when only small training sets are available. Also the inclusion of variables of sediment types and proxy variables for food export to the seafloor could be important to better describe CWC distributions; unfortunately, such layers of information were not available at a resolution sufficient to improve current model predictions. Information on food export to the seafloor might become available in the near future.

3.7 Case study 8b: Habitat suitability models under current environmental conditions of deep-sea sharks in Azores

Diya Das[1,2], José Gonzalez-Irusta[1,2], Telmo Morato[1,2], Laurence Fauconnet[1,2], Claudia Viegas[1,2], Pedro Afonso[1,2], Gui Menezes[1,2,3], Mario Rui Pinho[1,2,3], Helder Silva[1,2,3], Alexandra Rosa[1,2], Diana Catarino[1,2], Eva Giacomello[1,2]

1- Okeanos Research Centre, Universidade dos Açores, Departamento de Oceanografia e Pesca, Horta, Portugal
2- IMAR Instituto do Mar, Universidade dos Açores, Departamento de Oceanografia e Pesca, Horta, Portugal
3- Universidade dos Açores, Departamento de Oceanografia e Pescas, 9901-862 Horta, Portugal

3.7.1 Case study description

The Azores (Figure 128) is an oceanic archipelago in the mid North Atlantic Ocean, located between the continental Europe and North America and with an EEZ of more than 1 million km^2, most of it being a deep-sea habitat. The local fishery is typically artisanal and essentially composed of small (< 15m) vessels using hooks and lines (bottom longlines, handlines, pole-and-line) (Pinho & Menezes, 2009; Carvalho et al., 2011; Morato, 2012). With the absence of a continental shelf and surrounding great depths, fishing occurs around the island slopes and the many seamounts present in the area (Morato et al., 2008; Silva & Pinho, 2007) exposing non-target species with higher vulnerability to fisheries pressure (Morato et al., 2006). The marine region around the Azores is rich in VMEs (Morato et al., 2018; Abecasis et al., 2015) and possible essential fish habitats for deep water fish including elasmobranchs (Das & Afonso, 2017).

The sluggish life-history traits (slow-growing, long-lived, low productivity) of species inhabiting the deep-sea (Cheung, 2007; Morato et al., 2006; Devine, 2006) puts them at a disadvantage to cope with high exploitation pressure. Among deep sea fauna, elasmobranchs tend to lie on the extreme end of the susceptibility scale (Watling et al., 2011), being considerably more vulnerable than co-spatial teleosts (Rigby & Simpfendorfer, 2015; Garcia et al., 2007). As a result of the deep-sea shark vulnerability, a TAC 0 was implemented by the EU for over 15 species of deep-sea sharks since 2010 (EC. Reg. 1359/2008).

The bottom longline and handline fishery is by far the most valuable in terms of landed value with an average annual landed value of 18-29 million Euros, representing about 76% of all landed value in the Azores (Carvalho et al., 2011). It is also the main fishery in the region in terms of number of boats and jobs, and relies essentially on fresh export. Bycatch and discards of this fishery (Pham et al., 2013) includes many deep-water sharks listed in the IUCN red list of endangered species.

In this work, we aim to inform spatial planning objectives through modelling the distribution (using Distribution Models) of little-known but regularly caught deep-sea elasmobranch species, using the best scientific information available. Using species occurrence data collected from fishery-independent surveys and on-board fishery observers, we modelled suitable habitat of these elasmobranchs in the Mid-Atlantic Ridge around the Azores archipelago.

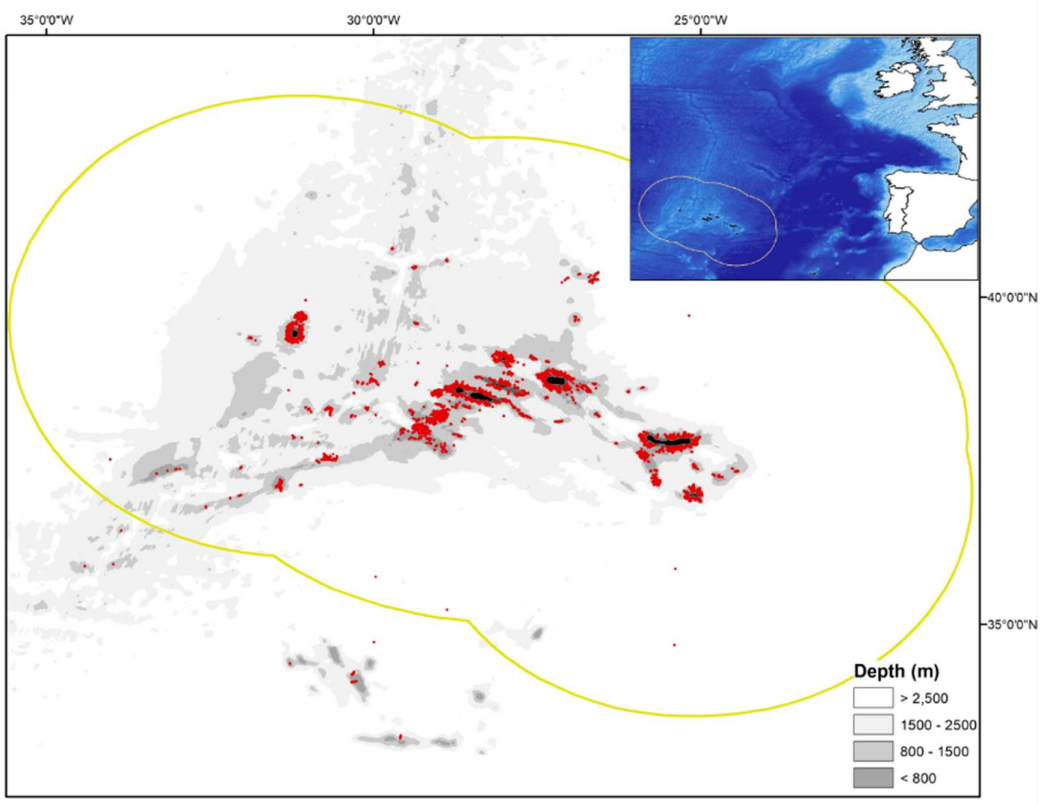

Figure 128. Distribution of available fishing sampling effort (red dots) in Azores EEZ (yellow line)

3.7.2 Species selection

Rather than focusing on any one species based on its vulnerability or legal status, we opted for a multi-specific assemblage (for a multi-specific problem), selecting all species of deep-water sharks and rays with “sufficient” information in either the survey or the observer catch data (Table 18).

Table 18. Number of presence records by species and survey type (n), total number of individuals by species (N) and depth range by species. (*) species for which abundance models were developed.

Species	n (Survey)	n (Observer)	n (Total)	N	Mean depth (m)	Depth range (m)
**Etmopterus spinax*	991	52	1043	3229	543.46	99 – 1155
**Deania profundorum*	1002	10	1012	2946	723.81	121 – 1396
**Raja clavata*	508	70	578	2768	154.53	1 – 567
**Deania calcea*	612	13	625	1392	1003.19	171 – 1597
**Etmopterus pusillus*	843	43	886	1345	684.84	68 – 1692
**Galeorhinus galeus*	307	19	326	1143	149.75	1 – 604
Centroselachus crepidater	207	0	207	285	1105.55	198 – 1651
Dipturus batis	105	40	145	249	423.76	47 – 801
Dalatias licha	96	35	131	217	574.04	56 – 1300
Etmopterus princeps	63	0	63	215	1409.94	823 – 2466
Centrophorus squamosus	75	0	75	112	1209.82	97 – 2191
Centroscymnus coelolepis	63	0	63	88	1369.62	905 – 2466
Squaliolus laticaudus	47	0	47	51	580.41	153 – 1053
Leucoraja fullonica	18	12	30	50	410.16	251 – 607
Centroscymnus owstonii	35	0	35	38	1179.84	222 – 1692

3.7.3 Species occurrence data sources

The species occurrences were extracted mainly from fisheries monitoring surveys, performed from 1996 to 2017 onboard the research vessel “Arquipélago” and completed with data from fishing observers (Figure 129).

Survey data

The fisheries monitoring surveys followed a standardized methodology to monitor demersal and deep-sea fish species abundance. In total, 666 bottom longline sets were used in the analyses. Most of these sets were completed in spring (n =548) with a few opportunistic sets performed in summer (n=48) and autumn (n=70). The fishing gear was like the one used by the Azorean commercial fishery,

known as stone/buoy bottom longline (LLA), with some deeper sets undertaken with a slightly different longline design (LLB -with larger hooks and a different setup of the mainline, details and schematic representation in Menezes et al., 2009). The fishing sets were randomly located around an island or seamount and deployed till 2000 meters of depth, but most commonly up to 1200 m (Figure 129).

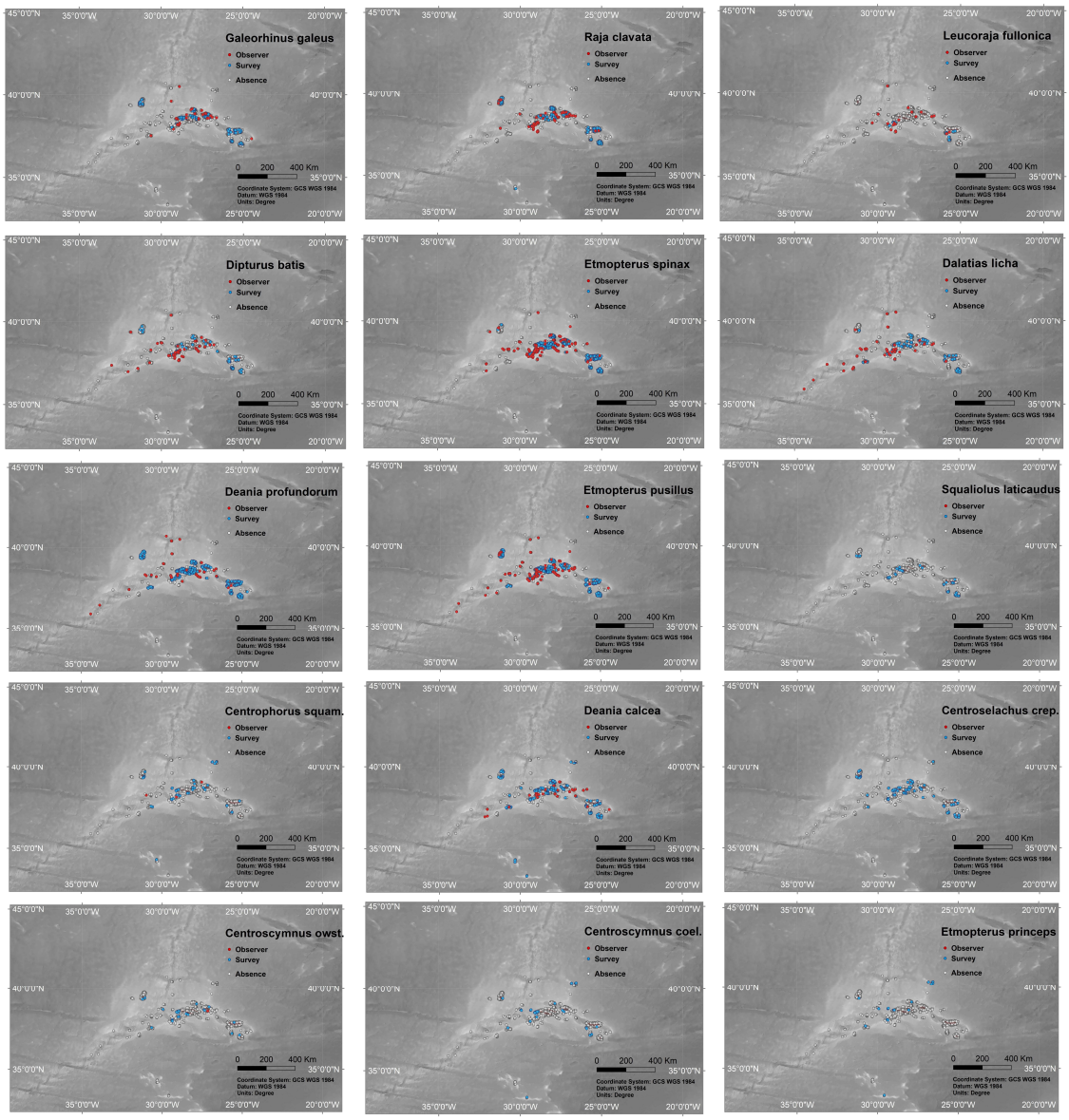

Figure 129. Maps of presences in survey data (blue dots), and observer data (red dots) and absences (white dots) by species

Each longline section was composed of about 25/30 hooks for LLA and 10 hooks for LLB (hook size no.9 for LLA, no.6 for LLB), approximately 40/45m long, and baited with chopped salted sardine. Each section of the longline was allocated to a 50m depth stratum. Geographic coordinates were recorded for each “event” (e.g., stone or buoy) during gear deployment, as well as the corresponding depth stratum. During hauling, the total number of each species of fish caught and the number of hooks

deployed were recorded by depth strata. Hence, each depth stratum of each fishing set was considered a sampling unit. All details of the surveys can be found in Menezes et al. (2006; 2009).

Observer data

A database of observer programmes within the scope of a national observer programme for discards (2004-2012 and 2016) and the project Discardless (2017-18) was also used. The catch data was collected by trained and independent observers aboard commercial fishing vessels. Commercial fishing operation using bottom longlines and handlines, and local variations were covered under these programmes. An artisanal vertical longline "gorazeira", with elasmobranch catches comparable to bottom longlines was included as a separate gear type, while commercial fishing sets using drifting longlines were removed due to significantly different catch rates of deep-sea elasmobranchs.

Catch data from 1249 sets (from 420 fishing trips) over the period of 12 years (hereafter called "observer dataset") was used in the modelling exercise. Catch of each species (number of individuals) and effort (number of hooks) were recorded at the level of each fishing set. Hence, the observer dataset had a considerably lower resolution as compared to the survey data, requiring a separate set of rules for processing catch data. Sets with at least one pair of coordinates were retained in the observer database. Wherever possible, the coordinates spatially between the beginning and end of the fishing set were used to allocate catch.

Data preparation

The survey dataset used intervals of 50m depth, called a stratum, as a sampling unit. Spatial coordinates were extracted for the beginning and end of each depth stratum within each fishing set. Fish catch was then allocated to the spatial middle point of the stratum. In the observer dataset, catch was allocated to coordinates for the mid-point between the beginning and end of the fishing set for bottom longlines, and to the single coordinates available for handlines. The survey and observer datasets were joined for further data cleaning. Since catches from a given length of fishing line were restricted to a single coordinate location, any survey depth stratum or observer fishing set > 3 km in length was removed from the final data to limit the location error to ±1.5 km. This length corresponded approximately to the grid-size of 1120x1120 m of the environmental rasters used in the modelling exercise.

Subsets of presence-absence data were used to model each species separately. Observer data was removed if less than 5 presence records were available for the species being modelled. If no records were found for a species in a given year or gear type, that year/gear type was removed from subsequent analysis.

3.7.4 Environmental data layers

An initial set of 12 environmental variables were compiled to model the distribution of the elasmobranchs, joining data from different databases. Depth was computing by merging multibeam data with EMODNET data (EMODNET, 2018) bathymetry (keeping always the multibeam data when available) and rescaling to a final resolution of 1120x1120 m using bilinear interpolation. Depth derivates, including slope, aspect and BPI, were computed using the function terrain in the R package raster (Hijmans, 2017) after rescaling depth.

Nitrates, phosphates and silicates concentration near bottom (µmol/l), dissolved oxygen near bottom (ml/l^3) and percentage of oxygen saturation near bottom (µmol/l) were extracted from Amorim et al. (2017). The layers were projected and rescaled (using bilinear interpolation) to the same resolution as depth (from an original resolution of 0.0083 degrees) using the R function projectRaster (Hijmans, 2017). Variables near-bottom temperature (°C) and near-bottom current speed (m/s) were extracted from the oceanographic model VIKING20 (Böning et al., 2016) and used to compute the average temperature and current values for the period 1989-2009. The data (with an original resolution of 5000x5000 m) were rescaled to resolution of 1120 m using bilinear interpolation.

Besides the environmental variables, other variables were included in the analysis: year, fishing effort and gear type. Year was included as a variable in order to compute possible inter-annual differences in deep-sea elasmobranch abundance. Only years which at least one catch were included in the analysis of each species. Fishing effort (measured as the number of hooks by sampling gear) has a significant effect in longline catchability and was therefore included in the model. Most of the data was associated to typical LLA longline configuration. Other gear types (LLB and “gorazeira”, previously described) were included to have the maximum number of presence records. To account for possible differences in catchability arising due to difference in gear type, gear type was included as a factor in the models.

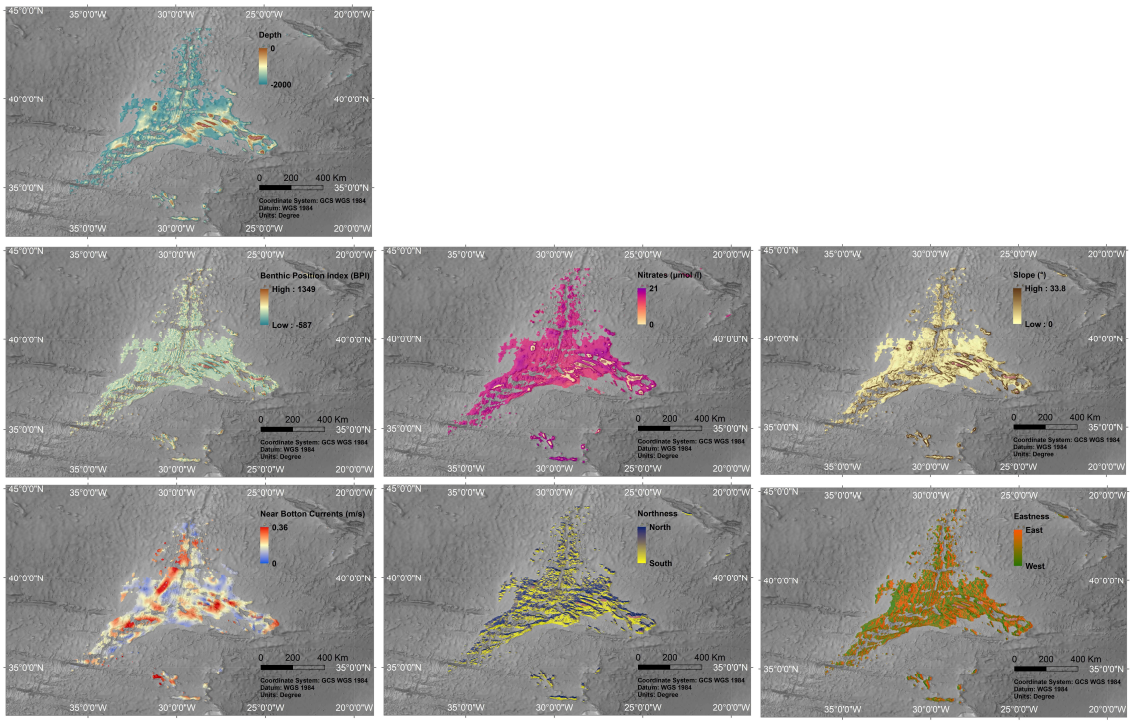

Figure 130. Environmental layers finally included in the full models (from top to bottom, left to right: depth, BPI, nitrates, slope, near bottom currents, northness and eastness).

A double approach using the Spearman coefficient of correlation and Variation Inflation Factors (VIFs) was applied to avoid predictor collinearity (Zuur et al., 2009). A set of 10 of the initial 15 variables were retained for analysis, 7 of them with spatial variation: current intensity near bottom, nitrates concentration near bottom, depth, aspect (eastness and northness), slope, BPI (Figure 130) and another three without spatial variation: fishing effort, year and gear.

3.7.5 Modelling approaches

The probability of presence (Pp) of the 15 species of deep-sea elasmobranchs was modelled using General Additive Models (GAMs) through the implementation gam in the package mgcv (Wood, 2015). A subset of 6 frequently caught (therefore, with a larger number of available data) species (*Deania profundorum, Etmopterus spinax, Etmopterus pusillus, Deania calcea*, *Raja clavata* and *Galeorhinus galeus*) were modelled for abundance (Ab) using a two-step approach (Barry & Welsh, 2002). A delta model approach was used which is recommended for modelling abundance of zero inflated data (Zuur et al., 2009). This method has been successfully used for fish or eggs abundance models (e.g. ,Lelièvre et al., 2014; González-Irusta & Wright, 2016a,b, 2017; Parra et al., 2016; Grüss et al., 2018). The first step of this approach involves modelling the probability of presence of the species using a binomial GAM, common to all 15 species. In the second step, the abundance of the subset of six species was

modelled using a negative binomial GAM. Logit and log were used as link functions for the binomial and negative binomial GAM. Finally, the binomial and negative binomial GAMs were combined resulting in a delta GAM. To avoid overfitting all the smoothers were constrained to 4 knots.

The full binomial model for the 15 species was:

$$P_p = \beta_1 + s(BPI) + s(depth) + s(fishingeffort) + s(nitratesconcentration) + s(moon) + s(eastness) + s(northness) + s(current\ intensity) + s(slope) + f(year) + f(gear) + \varepsilon_1$$

where P_p is the probability of presence of the species, β_1 is the intercept, s is an isotropic smoothing function (specific for each variable and model), f indicates the variables which were included as factors in the formula and ε1 is the error term.

The predicted abundance (P_a) was modelled using the same explanatory variables included in the full binomial model (equation 1) but using negative binomial GAMs.

The 15 binomial GAMs and the six negative binomial GAMs fitted for each species were used to generate distribution maps with P_p and P_a values respectively. The predictive maps were computed for the typical small-gape longline (LLA) with an effort of 1000 hooks, hence, the maps show the catch predicted from a typical commercial longline operating within the study area. The maps were always built for the year with a coefficient value of 0 (1996 in most of the cases). For the subset species for which abundance was modelled, Pp maps were then multiplied with the Pa maps to produce the final delta models for the final predicted abundance (P_a).

The accuracy of the models was tested using cross-validation. In order to avoid problems related with the spatial structure of the sampling method described by Fourcade et al. (2018), a random separation of training and evaluation data was performed using the get.block function from the EnMEVAL package (Muscarella et al., 2014) . This function finds the latitude and longitude that divide the occurrence localities into four groups of (insofar as possible) equal numbers. From the 4 groups, one is selected as evaluation data and the other as training data. The ability of the training data to predict the probability of presence was tested using the evaluation data and five different statistical metrics: i) the area under the curve (AUC) of the receiver operating characteristic (ROC) ii) the kappa statistic iii) the specificity, iv) the sensitivity and v) the True Skill Statistic (TSS). A more complete description of these statistics can be found in Fielding & Bell (1997). This operation was repeated 10 times with a random selection of evaluation and training groups each time and the values were used to compute a mean and standard error value for each metric. The same methodology was repeated to evaluate the abundance and delta models using the spearman coefficient (rho).

3.7.6 Model outputs, binomial (presence/absence) GAMs

Evaluation metrics

The explained deviance of the 15 binomial GAMs showed important differences between species with values ranged from 10.97 to 51.31% (Table 19).

Table 19. Deviance explained (Dev. Expl.), diagnostics (AUC and Kappa ± standard deviation SD) and GAM formula of the presence-absence models for the 15 selected species of deep-sea elasmobranches ranked by depth preferences (from shallowest to deepest).

Species	Dev. Expl.	AUC ± SD	Kappa ± SD	GAM Formula
Galeorhinus galeus	30.85	0.86 ± 0.05	0.61 ± 0.09	Pp12 = β12 + f(Gear type) + f(Year) + s(BPI (fine)) + s(Eastness) + s(Bottom currents) + s(Northness) + s(Slope) + 1 + s(Depth) + s(Effort)
Raja clavata	36.59	0.9 ± 0.03	0.69 ± 0.05	Pp14 = β14 + f(Gear type) + f(Year) + s(BPI (fine)) + s(Bottom currents) + s(Nitrates) + s(Northness) + s(Slope) + 1 + s(Depth) + s(Effort)
Leucoraja fullonica	31.59	0.87 ± 0.1	0.73 ± 0.16	Pp13 = β13 + s(BPI (fine)) + s(Northness) + s(Slope) + 1 + s(Depth) + s(Effort)
Dipturus batis	18.81	0.78 ± 0.11	0.54 ± 0.16	Pp8 = β8 + f(Year) + s(Slope) + 1 + s(Depth) + s(Effort)
Etmopterus spinax	19.25	0.77 ± 0.03	0.46 ± 0.06	Pp11 = β11 + f(Year) + s(BPI (fine)) + s(Eastness) + s(Bottom currents) + s(Nitrates) + s(Northness) + s(Slope) + 1 + s(Depth) + s(Effort)
Dalatias licha	14.59	0.66 ± 0.16	0.4 ± 0.21	Pp5 = β5 + s(Bottom currents) + s(Slope) + 1 + s(Depth) + s(Effort)
Deania profundorum	24.44	0.76 ± 0.03	0.46 ± 0.07	Pp7 = β7 + f(Year) + s(BPI (fine)) + s(Eastness) + s(Bottom currents) + s(Nitrates) + s(Northness) + s(Slope) + 1 + s(Depth) + s(Effort)
Etmopterus pusillus	10.97	0.66 ± 0.05	0.29 ± 0.05	Pp10 = β10 + f(Gear type) + f(Year) + s(BPI (fine)) + s(Bottom currents) + s(Nitrates) + s(Northness) + s(Slope) + 1 + s(Depth) + s(Effort)
Squaliolus laticaudus	20.02	0.54 ± 0.11	0.18 ± 0.22	Pp15 = β15 + f(Year) + s(Bottom currents) + s(Nitrates) + s(Northness) + s(Slope) + 1 + s(Depth) + s(Effort)
Centrophorus squamosus	30.59	0.84 ± 0.09	0.64 ± 0.24	Pp1 = β1 + f(Gear type) + s(Eastness) + s(Northness) + 1 + s(Depth) + s(Effort)
Deania calcea	38.61	0.87 ± 0.03	0.69 ± 0.05	Pp6 = β6 + f(Gear type) + f(Year) + s(BPI (fine)) + s(Eastness) + s(Bottom currents) + s(Northness) + s(Slope) + 1 + s(Depth) + s(Effort)
Centroselachus crepidater	33.56	0.91 ± 0.04	0.77 ± 0.08	Pp4 = β4 + f(Gear type) + s(BPI (fine)) + 1 + s(Depth) + s(Effort)
Centroscymnus owstonii	20.63	0.81 ± 0.16	0.66 ± 0.24	Pp3 = β3 + s(BPI (fine)) + s(Depth, k = 3) + s(Eastness) + s(Bottom currents) + s(Nitrates) + 1 + s(Effort)
Centroscymnus coelolepis	43.10	0.88 ± 0.1	0.81 ± 0.19	Pp2 = β2 + s(Eastness) + s(Bottom currents) + 1 + s(Depth) + s(Effort)
Etmopterus princeps	51.31	0.96 ± 0.04	0.83 ± 0.1	Pp9 = β9 + s(BPI (fine)) + s(Slope) + 1 + s(Depth) + s(Effort)

Responses curves

From the 10 predictor variables, depth was the only one which had a significant effect in the probability of presence of the 15 deep sea shark species and the only one which was included in all

the models, being the most important explanatory variable in 12 of the 15 studied species (Table 20). After depth, fishing effort (for *Raja clavata* and *Etmopterus pusillus*) and the year (for *Squaliolus laticaudus*) were the only variables which also showed the highest delta deviance value in at least one species. In fact, fishing effort was the second most important variable after depth, being included in all the models except for *Etmopterus princeps.* Year was only significant in 7 models but was among the most important variables for those models (2nd most important factor in 4 models). Slope, BPI, bottom currents, and northness had a significant effect on the P_p in around half of the models whereas the gear type, eastness and nitrates were the less important variables respectively.

The depth range of the 15 species is shown in Figure 131. *Galeorhinus galeus* and *Raja clavata* showed the shallowest depth niche, with the highest probability of presence in shallow waters. *Leucoraja fullonica, Dipturus batis* and *Etmopterus spinax* showed a peak in the probability of presence around 500 m, followed by *Dalatias licha* (600 m), *Deania profundorum* and *Etmopterus pusillus* (700 m*), Squaliolus laticaudus* (800 m), *Centrophorus squamosus* (1000 m), *Deania calcea* (1100 m) and *Centroselachus crepidater* (1200 m). Finally, the probability of presence of *Centroscymnus owstonii*, *Centroscymnus coelolepis* and *Etmopterus princeps* showed a positive relationship with depth, being maximum in the deepest part of the study area.

The Benthic Position Index (BPI) had a negative effect in 5 (*E. princeps, D. calcea*, *C. crepidater*, *E. spinax*, and *R. clavata*) of the seven species in which had a significant effect in the P_p (Figure 131), with higher values in the probability of presence in the low BPI values (cells deeper than the cells around). *Galeorhinus galeus* seems to prefer flat areas (areas with zero BPI) whereas *D. profundorum* showed a more complex relationship with BPI, with higher values of Pp in the lowest and highest values of BPI. Slope had a negative effect in four of the eight species for which had a significant in the P_p., and a positive effect in the four remaining species with *D. profundorum, D. calcea, G. galeus,* and *R. clavata* showing a small preference for areas with high values of slope whereas *D. batis, E. spinax, E. princeps* and *L. fullonica* seems to prefer flat areas.

The effect of the near bottom currents in the probability of presence was species dependent, with five of the seven species showing a negative effect in its values of Pp with currents, while *L. squaliolus* was showing a positive trend, and *D. calcea* was no showing clear trend. The nitrates concentration near bottom showed a positive relationship with the probability of presence of the 4 species for which was selected. Finally, aspect (northness and eastness) did not show clear trends, with northness, significant for 7 models, but showing very different and small effect depending of the species, and eastness included in only four of the fifteen species analysed with a positive effect, suggesting a preference for eastern flanks.

*Table 20. Variable importance (the number in brackets is the delta deviance for this variable) of the binomial GAM for each species. ** indicates the variables that are significant.*

Species	Variable Importance								
Centrophorus squamosus	**Depth (101.47)	**Gear type (51.49)	**Effort (40.28)	Northness (2.85)	**Eastness (2.84)				
Centroscymnus coelolepis	**Depth (140.28)	**Eastness (19.82)	**Effort (8.23)	Currents (2.97)					
Centroscymnus owstonii	**Depth (20.45)	BPI (fine) (9.84)	Currents (7.09)	**Effort (6.11)	Nitrates (3.63)	Eastness (3.36)			
Centroselachus crepidater	**Depth (278.2)	**Effort (30.42)	**BPI (fine) (13.5)	Gear type (2.02)					
Dalatias licha	**Depth (55.64)	Slope (11.35)	**Effort (7.08)	Currents (7.08)					
Deania calcea	**Depth (703.84)	**Year (115.8)	**Effort (66.92)	**Slope (15.45)	**Gear type (13.49)	**Currents (13.47)	**BPI (fine) (7.48)	Eastness (5.94)	**Northness (5.21)
Deania profundorum	**Depth (346.98)	**Year (223.62)	**Effort (42.94)	**BPI (fine) (85.63)	**Currents (41.58)	**Slope (40.43)	**Eastness (12.21)	**Nitrates (7.21)	**Northness (6.3)
Dipturus batis	**Depth (68.36)	**Slope (48.04)	**Effort (29.44)	**Year (29.31)					
Etmopterus princeps	**Depth (191.17)	**Slope (22.69)	**BPI (fine) (22.56)	Effort (1.76)					
Etmopterus pusillus	**Effort (85.44)	**Year (82.52)	**Depth (44.26)	**Nitrates (26.39)	**Currents (16.72)	**Northness (7.90)	**Gear type (1.23)		
Etmopterus spinax	**Depth (252.09)	**Year (141.64)	**BPI (fine) (112.61)	**Nitrates (65.82)	**Effort (44)	**Currents (23.39)	**Slope (21.01)	**Northness (7.87)	**Eastness (4.63)
Galeorhinus galeus	**Depth (243.92)	**Effort (56.31)	**BPI (fine) (54.44)	**Year (40.79)	**Northness (29.35)	**Slope (13.03)	**Gear type (12.89)	**Currents (11.91)	Eastness (7.63)
Leucoraja fullonica	**Depth (29.39)	**Effort (16.66)	**Slope (15.32)	BPI (fine) (7.35)	Northness (4.32)				
Raja clavata	**Effort (156.18)	**Depth (149.33)	**Year (92.58)	**BPI (fine) (88.96)	**Nitrates (23.43)	**Currents (18.31)	**Gear type (16.85)	**Northness (12.84)	**Slope (9.24)
Squaliolus laticaudus	**Year (47.09)	**Depth (18.19)	**Currents (12.46)	Nitrates (12.43)	**Effort (9.61)	Slope (7.64)	**Northness (4.13)		

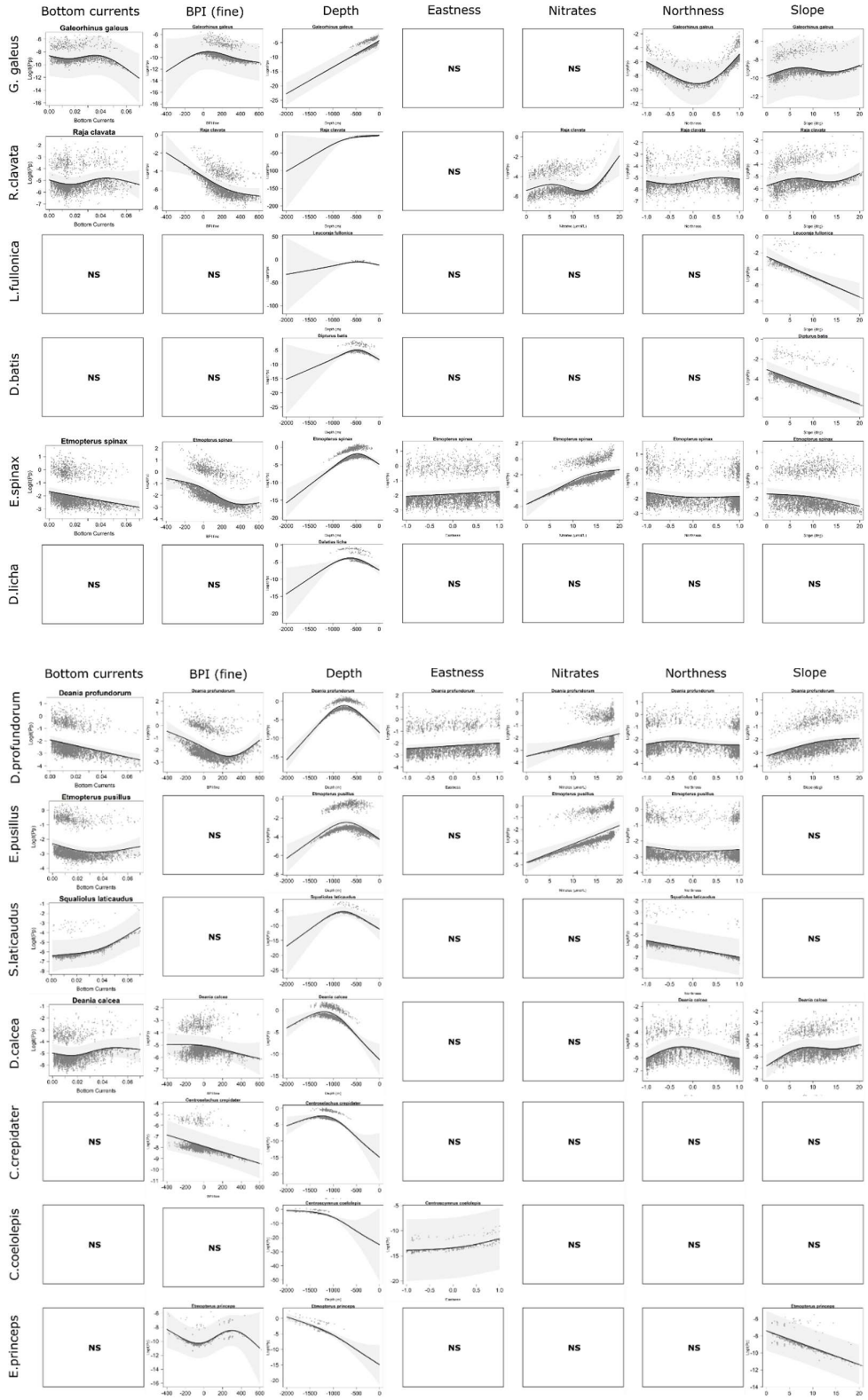

Figure 131. Environmental variables, with a significant effect on the predicted probability of presence (Pp) of DWS species. NS stands for Non-Significant.

Maps of presence / absence

The depth stratification by species which observed in Figure 131 and is also obvious in the maps showing the probability of presence (Figure 132). The distribution of the species included in the analysis ranges from shallow waters (a very narrow line around the islands) for species such as *G. galeus* or *R. clavata* to extent areas of the abyssal grounds for species such as *C. coelolepis* or *E. princeps*. Between these two extremes, the species show a wide range of different distributions but always restricted by its bathymetrical range because of the pronounced depth gradient existent in the area.

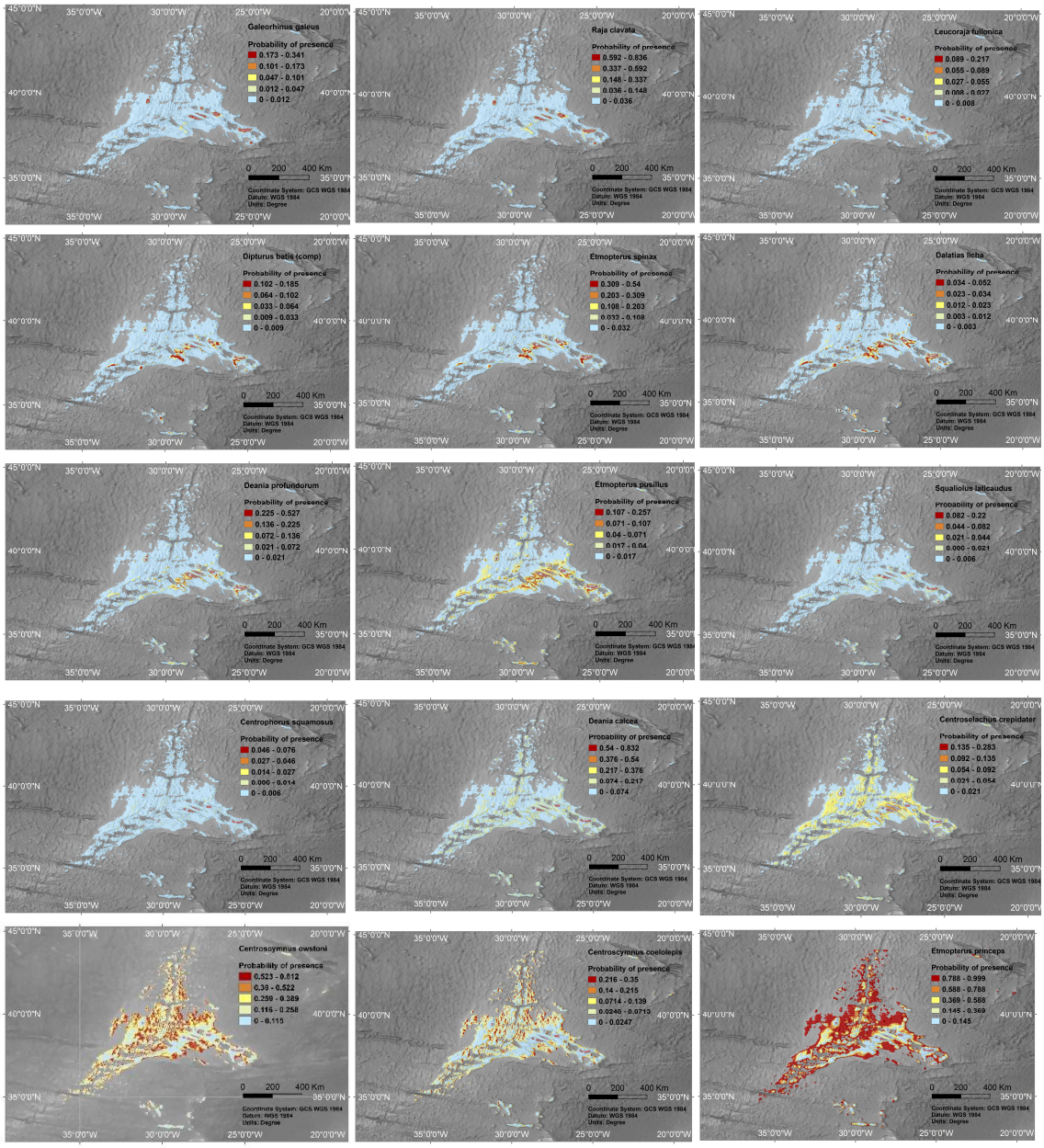

Figure 132. Distribution of the predicted probability of presence (Pp) in the study area.

It is important to highlight that although the maps show a similar colour pallet, the values of this pallet is very different between species since the prevalence of these species (total number of presences/total number of presences and absences) is also very different between species (Figure 129).

3.7.7 Model outputs, negative binomial (abundance) GAMs models

Evaluation metrics

The explained deviance of the 6 negative binomial GAMs ranged from 20.51% to 49.83% (Table 21).

Table 21. Negative binomial GAMs summary, including explaining deviance (Dev. Expl.), spearman coefficient (rho) for the negative binomial (Ab. stands for abundance) and delta models and final GAM formula.

Species	Dev. Expl.	Rho (Ab. Model)	Rho (Delta Model)	GAM Formula
Galeorhinus galeus	49.83%	0.43 ± 0.03	0.73 ± 0.05	Pp5 = β5 + f(Gear type) + f(Year) + s(Eastness) + s(Bottom currents) + s(Nitrates) + 1 + s(Depth) + s(Effort)
Raja clavata	45.45%	0.42 ± 0.12	0.71 ± 0.04	Pp6 = β6 + f(Gear type) + f(Year) + s(BPI (fine)) + s(Eastness) + s(Bottom currents) + s(Nitrates) + s(Northness) + s(Slope) + 1 + s(Depth) + s(Effort)
Etmopterus spinax	41.76%	0.4 ± 0.05	0.55 ± 0.06	Pp4 = β4 + f(Gear type) + f(Year) + s(BPI (fine)) + s(Eastness) + s(Nitrates) + s(Northness) + s(Slope) + 1 + s(Depth) + s(Effort)
Deania profundorum	28.77%	0.4 ± 0.1	0.6 ± 0.04	Pp2 = β2 + f(Year) + s(BPI (fine)) + s(Bottom currents) + s(Slope) + 1 + s(Depth) + s(Effort)
Etmopterus pusillus	34.64%	0.32 ± 0.04	0.45 ± 0.14	Pp3 = β3 + s(BPI (fine)) + s(Eastness) + s(Nitrates) + s(Northness) + s(Slope) + 1 + s(Depth) + s(Effort)
Deania calcea	20.51%	0.3 ± 0.11	0.71 ± 0.09	Pp1 = β1 + f(Year) + s(BPI (fine)) + s(Eastness) + s(Slope) + 1 + s(Depth) + s(Effort)

Responses curves

In contrast with the binomial GAMs, in the abundance models, depth was not the most important variable, although if we exclude variables which did not content spatial information about environmental conditions (such as fishing effort or year) depth still was one of the most important factors explaining deep-sea sharks abundance in the Azores (Table 22).

*Table 22. Variable importance (the number in brackets is the delta deviance for this variable; decreasing importance from left to right) of the negative binomial GAMs (abundance models).** identifies the variables that are significant*

Species	Variable Importance									
Galeorhinus galeus	**Year (33.15)	** Effort (14.77)	** Depth (6.86)	** Eastness (3.14)	Nitrates (2.22)	**Gear type (2.22)	** Currents (1.63)			
Raja clavata	** Effort (30.49)	**Year (17.65)	** Depth (11.36)	**Slope (10.06)	**BPI (fine) (5.57)	**Currents (5.31)	** Eastness (4.41)	** Nitrates (3.65)	** Gear type (3.17)	Northness (3.14)
Etmopterus spinax	**Year (45.35)	** Effort (36.55)	**BPI (fine) (3.85)	** Depth (3.75)	Northness (3.43)	Eastness (3.3)	Gear type (2.55)	** Slope (2.49)	Nitrates (1.49)	
Deania profundorum	**Year (25.4)	**BPI (fine) (10.21)	** Effort (8.82)	** Depth (5.69)	** Currents (2.99)	**Slope (0.07)				
Etmopterus pusillus	** Effort (76.24)	Slope (7.83)	** Nitrates (6.58)	**Northness (3.44)	Eastness (2.83)	BPI (fine) (2.37)	**Depth (2.35)			
Deania calcea	**Year (115.8)	**Effort (66.92)	Slope (15.45)	** Eastness (5.94)	**BPI (fine) (5.52)	Depth (2.5)				

The fishing effort was the only variable which had a significant effect in the P_a of the six species, following by depth (significant effect in the P_a of all the species except *D. calcea*), and year (significant effect in the P_a of all the species except *E. pusillus,* and most important variable for 4 out of 6 abundance models). Variables with lower importance included BPI (significant effect in the P_a of four of the six species), slope, eastness and bottom currents (each has significant effect in the P_a of three of the six species analysed but with weak explanatory power), gear type and nitrates (significant effect in the P_a of two species each) and finally northness (significant effect in the P_a of only one species).

The effect of depth in the P_a was very similar to the effect of this variable in the probability of presence (P_p). The abundance of *G. galeus* and *R. clavata* showed a negative relationship with depth, showing the highest abundance values in shallow waters, *D. profundorum* and *E. spinax* showed a peak in abundance at depths of 750 m and 500 m respectively (Figure 133, Figure 134). The only exception

being P_a of *E. pusillus* which showed a negative and linear relationship with depth, while its peak of presence occurs around 700m deep.

The BPI had a negative effect on the P_a in the four species which included this variable in their models (*R. clavata, D. calcea*, *E. pusillus* and *E. spinax*). Species had different relationships between slope and P_a: *R. clavata* abundance showed a linear and positive relationship with slope whereas *E. spinax* and *D. profundorum* seems to prefer flat grounds. *E. pusillus* prefers seabed areas with high nitrates concentration values, more pronounced than for *R. clavata*, whereas current speed seems to have a negative effect in the P_a values for *G. galeus* and *D. profundorum*. *R. clavata* did not have a clear relationship between currents and P_a values. Finally, eastness had a significant effect on the P_a of *G. galeus* which seems to prefer slopes with western orientation.

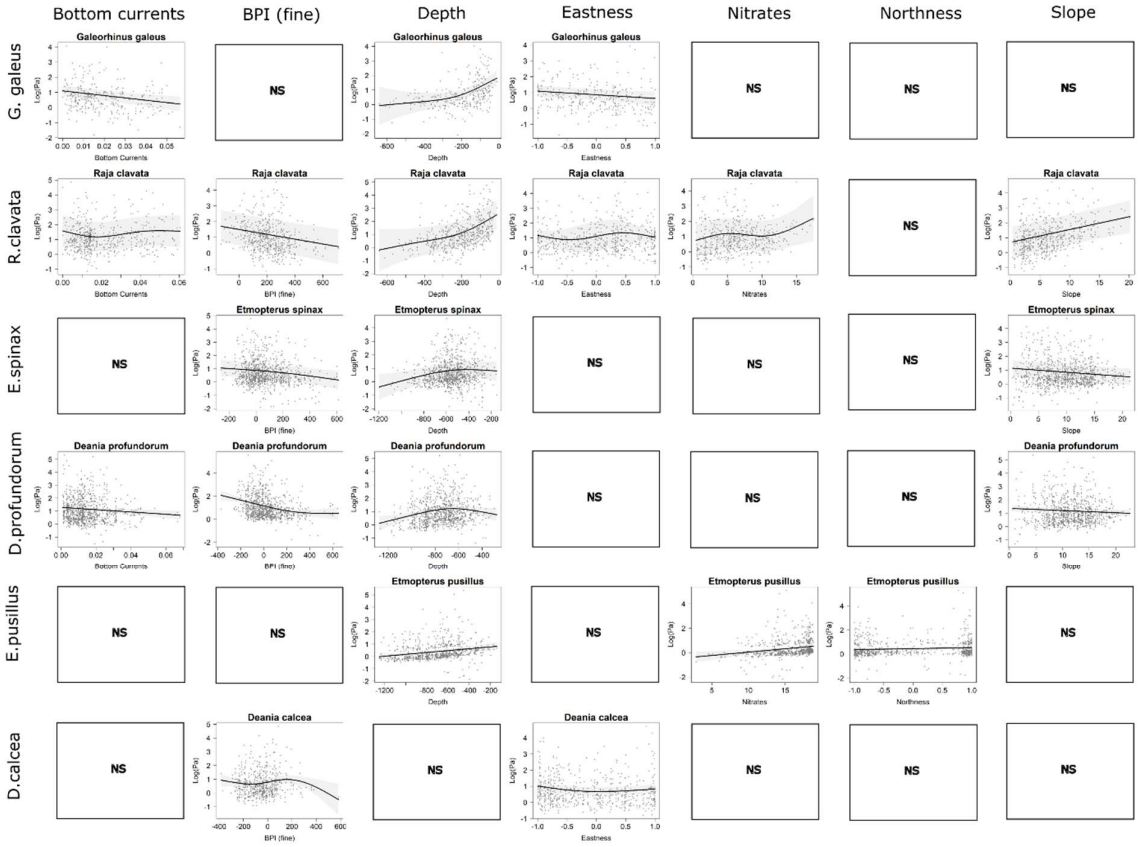

Figure 133. Effect of the environmental explanatory variables (only significant) on the predicted abundance (Pa) of DWS species.

Maps of abundance

The predicted maps of abundance of the 6 species are displayed in Figure 134.

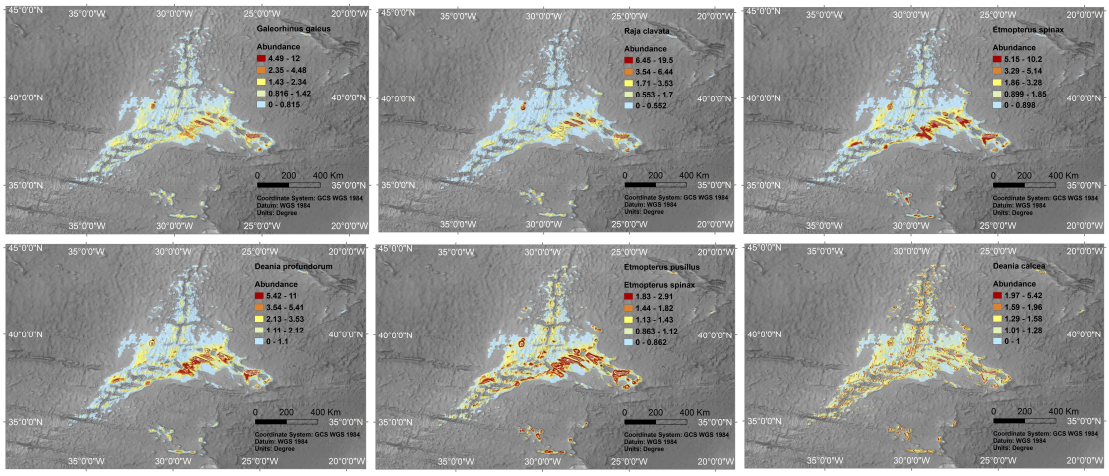

Figure 134. Distribution of the predicted abundance in the study area.

3.7.8 Model interpretation, caveats and future directions

The binomial GAMs showed a good or moderate performance for 12 of the 15 species analysed with mean AUC values higher than 0.7 and mean TSS values higher than 0.2 (Mandrekar, 2010; Jones et al., 2010) and with values of explained deviance in the range of values observed in previous works (e.g. Lelièvre et al., 2014; Parra et al., 2016; González-Irusta & Wright, 2016a,b; 2017). The only exceptions were the models for *Etmopterus pusillus, Dalatias licha,* and *Squaliolus laticaudus* which showed a poor performance according to its AUC and TSS values and which were also among the three models with lowest explained deviance (10.97, 14.59, and 20.02% respectively). All three species are worldwide distributed sharks (Coelho & Erzini, 2007; Navarro et al., 2014) with a certain plasticity in their feeding behaviour which allow them to feed in several parts of the water column, not being exclusively dependent on benthic resources (Xavier et al., 2012; Navarro et al., 2014). In this work, those species share a wide depth range and a poor explicative power of this variable in their models which could be linked with a broader niche of these species compared with others. The lower performance of species with broad niches has been previously described since these species might not be limited by any of the environmental variables analysed (Brotons et al., 2004; González-Irusta et al., 2015). Abundance and delta models also showed a good or moderate performance, with Spearman correlation coefficients between the predicted and observed values ranged from 0.3 to 0.73 similar to previous works (e.g. Parra et al., 2016; González-Irusta & Wright, 2016a,b; 2017).

The two main drivers for habitat suitability of the 15 species of deep-water sharks and rays included in this study were depth and fishing effort (number of hooks), while the importance of other predictors varied among species. Fishing effort was included in the model since it is expected to influence catch rates, and only for one species – *E. princeps* – it was not significant in the final model. The importance

of depth as predictor variable for all modelled species is not surprising, since it has been largely demonstrated its importance as structuring factor of demersal fishes (i.e., Menezes et al., 2006; Williams et al., 2001; Parra et al., 2014). Depth zoning (stratification by depth) of ichthyofauna is a well-known phenomenon, also in deep-sea communities, also because it is correlated with other environmental variables such as light, or temperature (Parra et al., 2014).

In addition to depth and fishing effort the main predictors of elasmobranch habitats included year, BPI, slope, bottom currents, and aspect, and for fewer species, gear type and nitrates. The importance of seafloor morphology has been already suggested as an important factor influencing elasmobranch habitats (Lauria et al., 2015), and our models (binomial GAMs) suggest BPI as an important predictor for 7 out of 15 species inhabiting different depth strata.

Contrary to the presence absence models, variables such fishing effort and year explained most of the variance observed in abundance models. However, these variables do not offer information about the spatial distribution of sharks and therefore depth still was one of the most important factors explaining deep sea elasmobranchs abundance in the Azores (except *D. calcea*).

This work deepens our knowledge on little-known data-poor deep-sea elasmobranch populations and their suitable habitats. A better understanding of those species ecology and habitat is very important for their conservation and effective management of the fisheries that unintentionally but still occasionally catch them. As those species are recognized to be highly vulnerable (Simpfendorfer & Kyne, 2009; Garcia et al., 2008) and are under a fishing prohibition in the European Union, this work is an important step forward relevant both for conservation and for fisheries management at the regional and international scales. It can help inform spatial planning and identify conservation objectives of this threatened species group.

3.8 Case study 9: Habitat suitability models under current environmental conditions in Iceland. Predictive models for *Helicolenus dactylopterus*

Hrönn Egilsdottir[1], José-Manuel González-Irusta[2,3], Telmo Morato[2,3], Stefán Aki Ragnarsson[1]

1- MFRI: Marine and Freshwater Research Institute, Reykjavík, Iceland
2- OKEANOS Center, Faculty of Science and Technology, University of the Azores, Horta, Portugal
3- Instituto do Mar, Marine and Environmental Sciences Centre, Universidade dos Açores, Portugal

3.8.1 Case study description

This work covers the shelf and slope of Iceland and therefore includes the Reykjanes Ridge which is case study 9 in the ATLAS project. The habitat suitability model (HSM) products encompass the Icelandic shelf and slope where two annual trawl surveys have taken place since 1986 (spring survey) and 1995 (autumn survey). Instead of focusing on the Reykjanes Ridge only, the larger spatial coverage of the HSMs resulted in a greater range of environmental variables included in the model, aiming for an enhanced understand environmental drivers affecting the distribution of the study species, *Helicolenus dactylopterus*.

Models were developed based on trawl survey data (e.g., Stefansdottir et al., 2010) collected in the years 1989 – 2009 and based on average temperature and currents for that whole period and other environmental parameters that are not assumed to change with time (depth and derived parameters). The results of the models were predicted for two separate time periods: A) 1989 - 1998 and B) 1999 - 2009. The occurrence (and abundance) of the study species increased considerably throughout the whole study period. The earlier period was relatively colder than the latter period so the HSM may inform if temperature changes are a likely driver explaining the observed changes in the occurrence of the study species.

3.8.2 Species selection

Helicolenus dactylopterus was selected for this study as the northern distribution limit for this widespread species is currently south of Iceland, but at the time when the trawl surveys were established, *H. dactylopterus* was considered rare in this region. The significant observed increase in abundances and detection rate of this species south of Iceland could be a result of warming sea water temperatures within the trawl-survey period. HSMs are a useful tool to investigate this hypothesis (Guisan et al., 2017).

3.8.3 Species occurrence data sources

The occurrences of *Helicolentus dactylopterus* individuals in Icelandic trawl surveys are displayed per year in Figure 135. Note that the data from the autumn and spring surveys are pooled together and the year 2011 was excluded from the HSMs due to a disruption in the sampling effort that year.

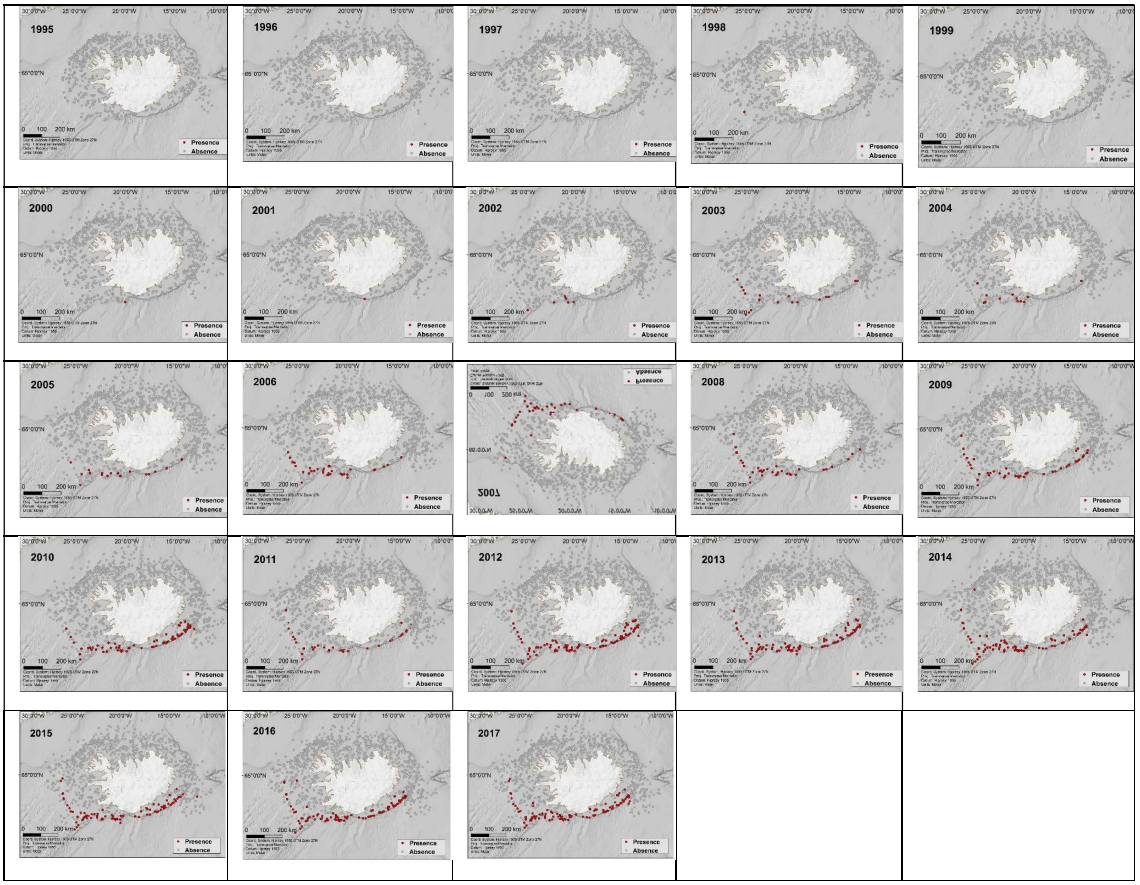

Figure 135. Annual occurrences (presences in red, absences in grey) of Helicolenus dactylopterus *individuals in Icelandic trawl surveys.*

3.8.4 Environmental data layers

Data sources, oceanographic models, etc

Table 23. Environmental variables used in this study.

Data	Source	Derived variables
Depth	EMODnet	Slope, Aspect, Roughness, BPI, Eastness, Northness
Temperature	VIKING20 model	-
Currents	VIKING20 model	-
Bottom temperature at time of sampling *(not incl. in models).*	MRFI fish database	-

Spatial resolution used

A spatial resolution of 3000 m was used.

Variable selection methodology

Environmental variables were investigated with respect to collinearity: linear model was used identify the variation inflation factors which were required to be lower than 3. Roughness was not included in the modelling due to a high correlation with Slope.

Environmental variables used in the HSMs were: Temperature, Currents, Depth, Slope, Bathymetric Position Index (BPI), Eastness and Northness (Figure 136).

GAM: HSMs using all possible combinations of the environmental layers noted above were compared based on their Akaike information criterion (AIC). The R package *MuMIn* was used to perform this comparison automatically and the best model chosen based on the lowest AIC score achieved. The final model included all the available environmental variables listed above (Temperature, Currents, Depth, Slope, Bathymetric Position Index (BPI), Eastness and Northness).

Maxent: The Maxent models also included all the environmental variables listed above (Temperature, Currents, Depth, Slope, Bathymetric Position Index (BPI), Eastness and Northness).

Maps of environmental layers

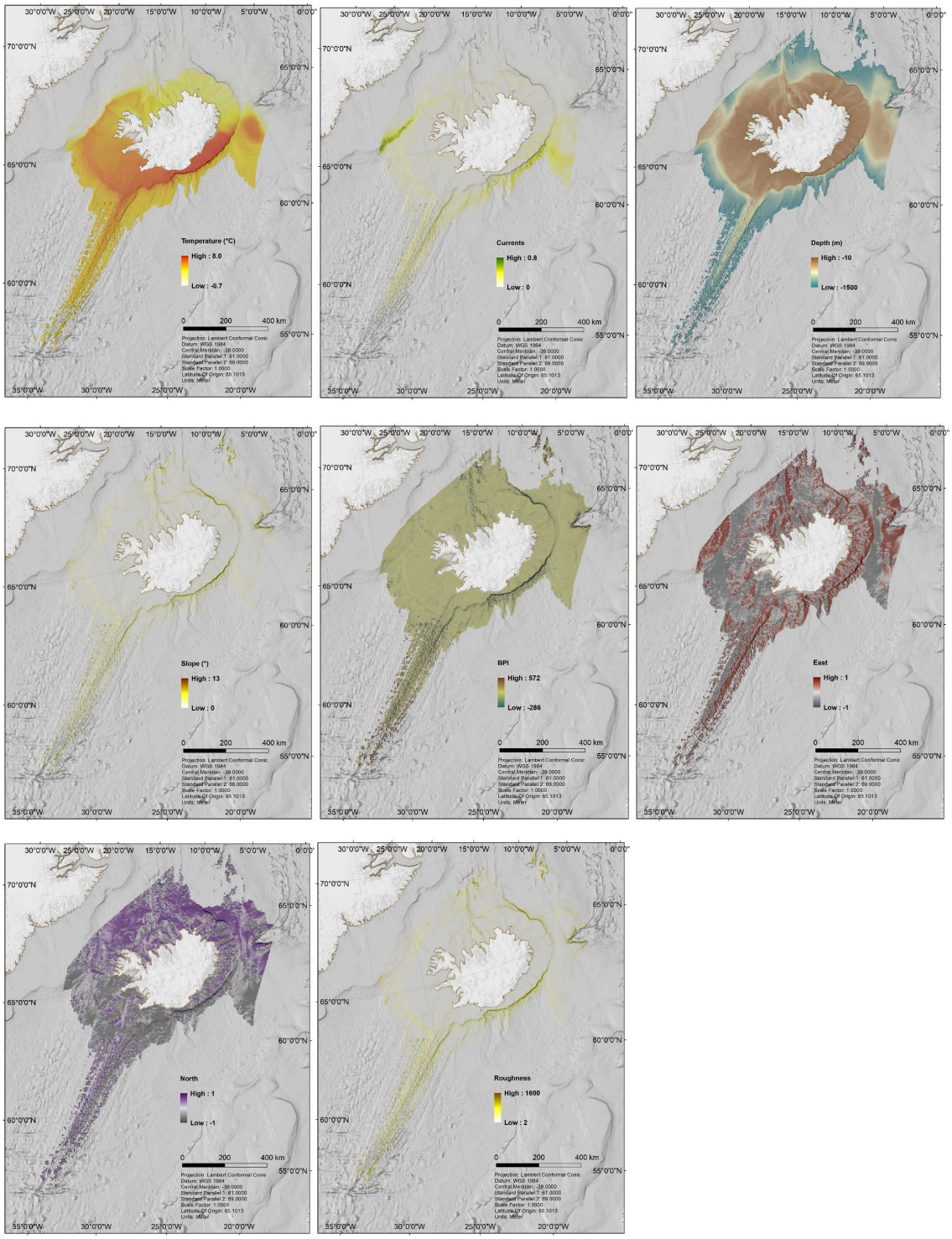

Figure 136. Environmental layers included in the models (from top left to bottom right: temperature, currents, depth, slope, BPI, eastness, northness, Roughness).

3.8.5 Modelling approaches

Two different modelling techniques were implemented: Generalised Additive Models (GAM) and Maxent. All models were constructed in R, version 3.5.2 (RStudio-Team, 2015; R-Core-Team, 2018).

GAM: The *mgcv* package (Wood & Wood, 2015) was used for running GAM's and *MuMIn* package (Barton, 2009) for selecting best model (model with lowest AIC score). The smoothing curves were set to a maximum of four (k = 4) for each environmental parameter.

Maxent: To run Maxent in R, the package *dismo* (Hijmans et al., 2017) was used (which runs a "behind the scenes" java version of the Maxent program).

MODEL EVALUATION: The GAM and Maxent models were evaluated by dividing species presence/absence data into training data (66% of the data) and data used to evaluate the models (33% of the data). Data division and subsequent model evaluation was repeated ten times. Evaluation parameters investigated were AUC (Area Under Curve) and Kappa and are given as means ± standard deviation.

3.8.6 Model outputs

GAM - Responses curves

Response curves are plotted with residuals (Figure 137).

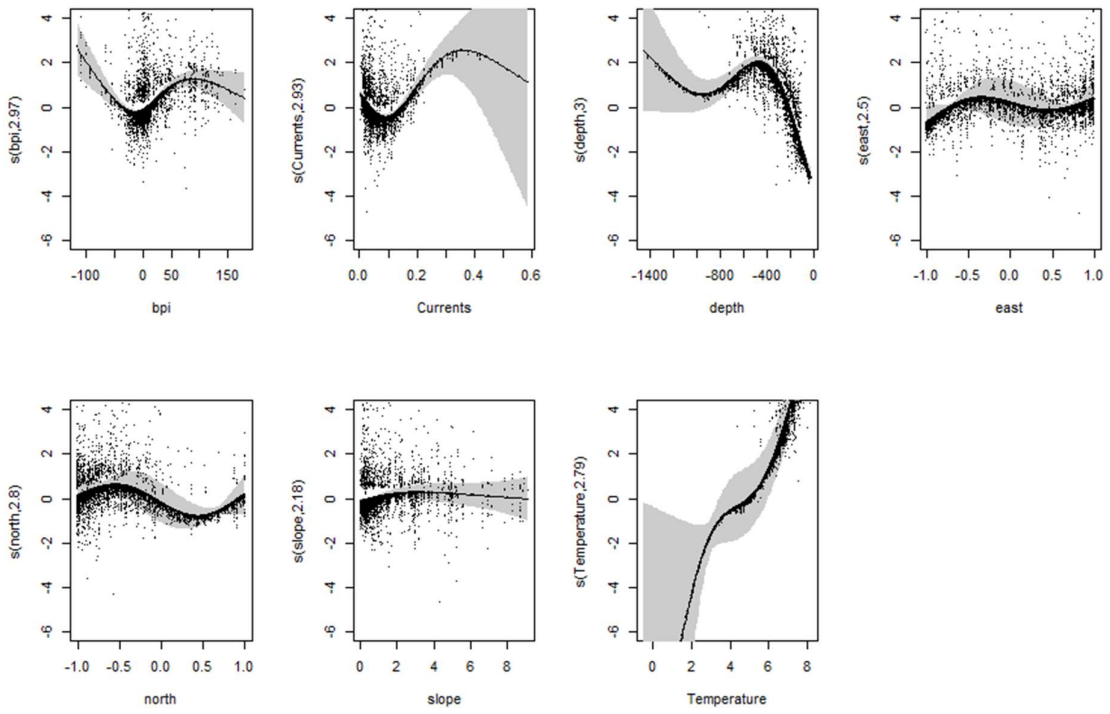

Figure 137. Response curves of the GAM model

GAM - Evaluation metrics /statistics

AUC and Kappa are given as means ± standard deviation based on 10 evaluations where data was split into training data (66% of data) and data used for evaluation (33% of data).

AUC = 0.94 ± 0.00

Kappa = 0.43 ± 0.01

GAM - Maps of presence/absence

GAM model was developed based on the whole period 1989-2009 (Figure 138, left panel). When predicted to the first period (1989-1998) the predicted occurrence is lower than that predicted for the second period (1999-2009; Figure 138). The model indicates that the increase in occurrence of *Helicolenus dactylopterus* from the first period to the second could be strongly related to the temperature increase occurring between the periods. Figure 139 shows the change in occurrence based on the GAM model between first and second time periods.

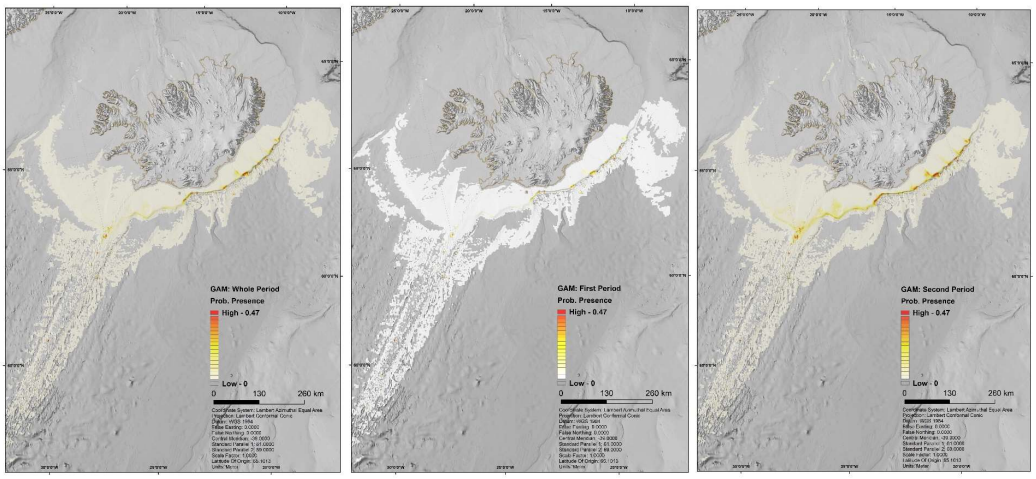

Figure 138. Maps of the probability of presence of Helicolenus dactylopterus *from the GAM models for the whole period (1989-2009 ; left), the first period (1989-1998; middle), and the second period (1999-2009; right).*

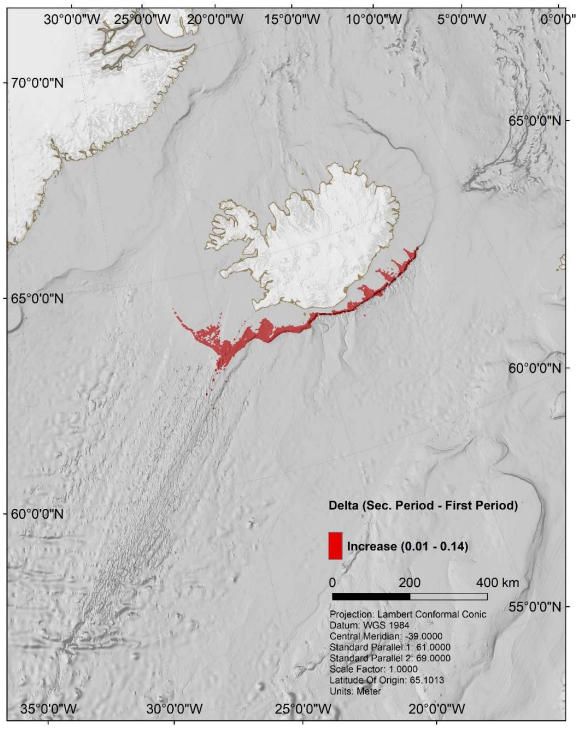

Figure 139. Change in occurrence based on the GAM model between first and second time periods

Maxent - Responses curves

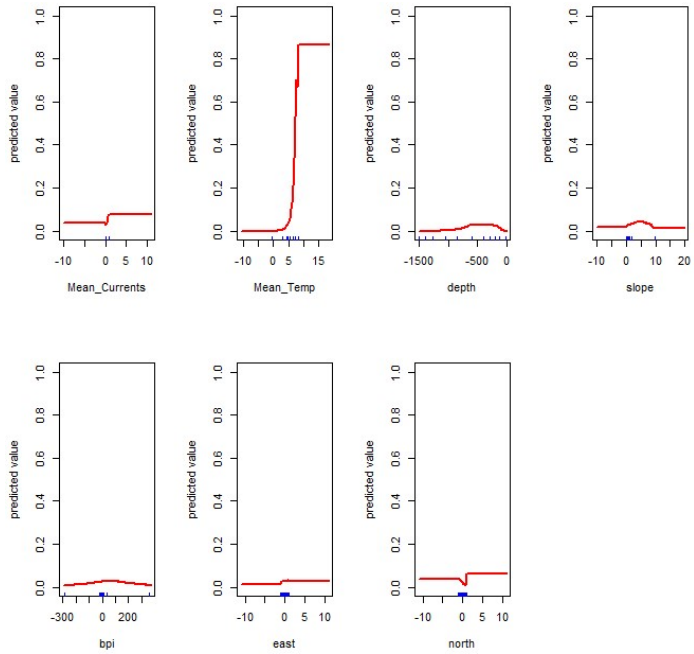

Figure 140. Response curves of the Maxent model

Maxent - Evaluation metrics /statistics

AUC and Kappa are given as means ± standard deviation based on 10 evaluations where data was split into training data (66% of data) and data used for evaluation (33% of data).

AUC = 0.94 ± 0.00

Kappa = 0.39 ± 0.01

Maxent - Maps of presence/absence

The model was developed for the whole time period 1989-2009 and predicted to that period, as well as to the period 1989-1998 and to a second, relatively warmer, period 1999-2009 (Figure 141). The model suggests a better habitat suitability for *Helicolenus dactylopterus* in the warmer second period.

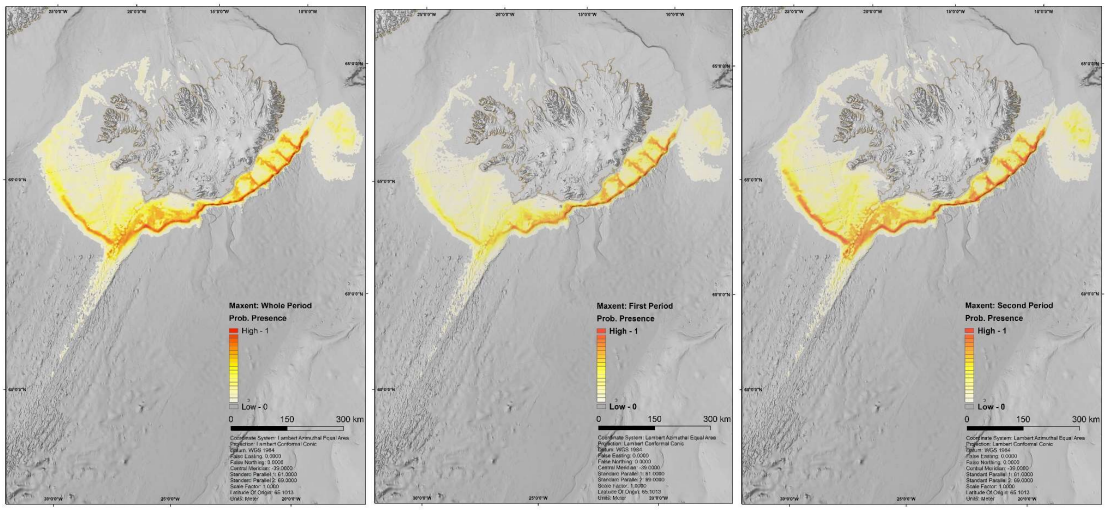

Figure 141. Maps of the probability of presence of Helicolenus dactylopterus *from the Maxent model for the whole period (1989-2009; left), the first period (1989-1998; middle), and the second period (1999-2009; right).*

3.8.7 Model interpretation, caveats and future directions

This work shows how rising temperatures in the marine environment in the North Atlantic contribute to a northward expansion of the distribution limits of a deep-sea fish species.

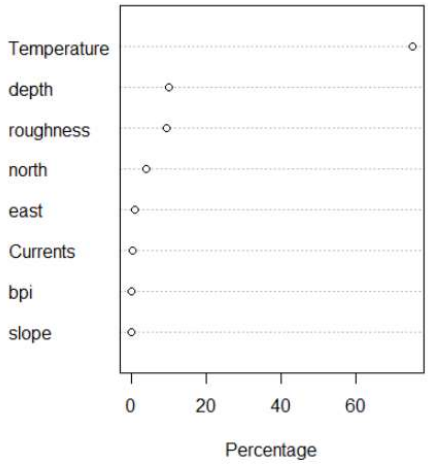

Figure 142. Variable importance in Maxent model developed for H. dactylopterus *in Icelandic waters*

Both Maxent and GAM models developed to predict the occurrence of *Helicolenus dactylopterus* performed well. An AUC greater than 0.90 indicates a good degree of discrimination between locations where the species was present and absent. The response curves of both models suggest that temperature is a major environmental driver affecting the occurrence and distribution of this species in the study region (Figure 137, Figure 140, Figure 142). This species does not occur north of Iceland where seawater temperatures are >3°C colder than south of Iceland. Models for the whole study period indicate that seawater temperature is the limiting factor, hindering the distribution of this species to the cool waters north of Iceland. This species was rarely observed south of Icelandic up until the year 2000, after which there was a rise in seawater temperature in the region (Valdimarsson et al., 2012). Since the year 2000 this species has become increasingly more common. When the Maxent model results were predicted to two study periods that differ in their mean temperature (the period 1989-1998 and the period from 1999-2009) it indicates an increase in suitable habitat for *H. dactylopterus* between the periods. Thus, it can be inferred that the rise in temperature occurring in the North-Atlantic, is going to lead to a northward expansion of the distribution limits of this deep-water fish species.

There are no major caveats to mention in the models but there is room for model improvements. A large quantity of information on presence and absences of this species was enough to develop well performing models. Model caveats are mainly related to the limited information on the environmental parameters. The temperature layers used for developing the models are averages for long time periods (9-10 years) but it would be more informative to develop the models based on annual temperatures as the species data was collected annually. Also, it would be informative to develop models to estimate abundances under different environmental settings, in addition to the models developed based on presence/absence of the species.

3.9 Case study 10: Habitat suitability models under current environmental conditions in Davis Strait, Eastern Arctic. Random Forest models for key CWC VME indicator taxa and archetypes models for sponges

Ellen Kenchington[1], Lindsay Beazley[1], F. Javier Murillo[1], Cam Lirette[1], Javi Guijarro[1]

1- Bedford Institute of Oceanography, Fisheries and Oceans Canada, Dartmouth, N.S., Canada

3.9.1 Case study description

Davis Strait joins two oceanic basins, Baffin Bay and the Labrador Sea, and separates western Greenland and Baffin Island. It connects to the Arctic Ocean in the north via Baffin Bay and to the Atlantic Ocean in the south via the Labrador Sea. It is considered the world's largest strait and is renowned for exceptionally strong tides, ranging from 9 to 18 m, and complex hydrography. The shelves extending from both Canada and Greenland typically range between 20 and 100 m in depth and are traversed by deep troughs. At its narrowest point, a ridge or sill up to approximately 600 m depth extends between Greenland (at Holsteinborg, Sisimiut) and Baffin Island (at Cape Dyer). The slopes along the Labrador Sea flank of this ridge and farther south along the Labrador and West Greenland shelves drop to 2500 m or more. On these slopes coral and sponge have been found, including the only known *Lophelia pertusa* reef in Greenlandic waters. South of Davis Strait the waters off west Greenland support intense phytoplankton blooms in April, which progress northward into Baffin Bay in May as the seasonal ice-cover retreats. These blooms are characterised by high phytoplankton biomass and a community of grazers dominated by large copepods, i.e. *Calanus*. Within the study region *Calanus* provide an important food source for higher trophic levels (e.g., fish, seabirds, whales). In addition, however, they play a key ecological role in supplying the benthic communities with high quality food via the production of large and fast-sinking faecal pellets. Baffin Bay and Davis Strait have the only large-scale commercial fisheries in Canada's Arctic.

The study extent (Figure 143) for the generation of environmental predictor and modelled presence probability surfaces was based on a combination of the ATLAS Baffin Bay-Davis Strait Spatial Planning Areas and the boundary of DFO's Eastern Arctic Biogeographic Region. The ATLAS Baffin Bay-Davis Strait Spatial Planning Areas span across both Canadian and Greenlandic Waters. The spatial planning areas were clipped to exclude areas within 20 km of land, and the boundary was extended in the southwest to match that of DFO's Eastern Arctic Biogeographic Region to ensure that all available catch data from the trawl surveys conducted in the region were included in the modelling extent.

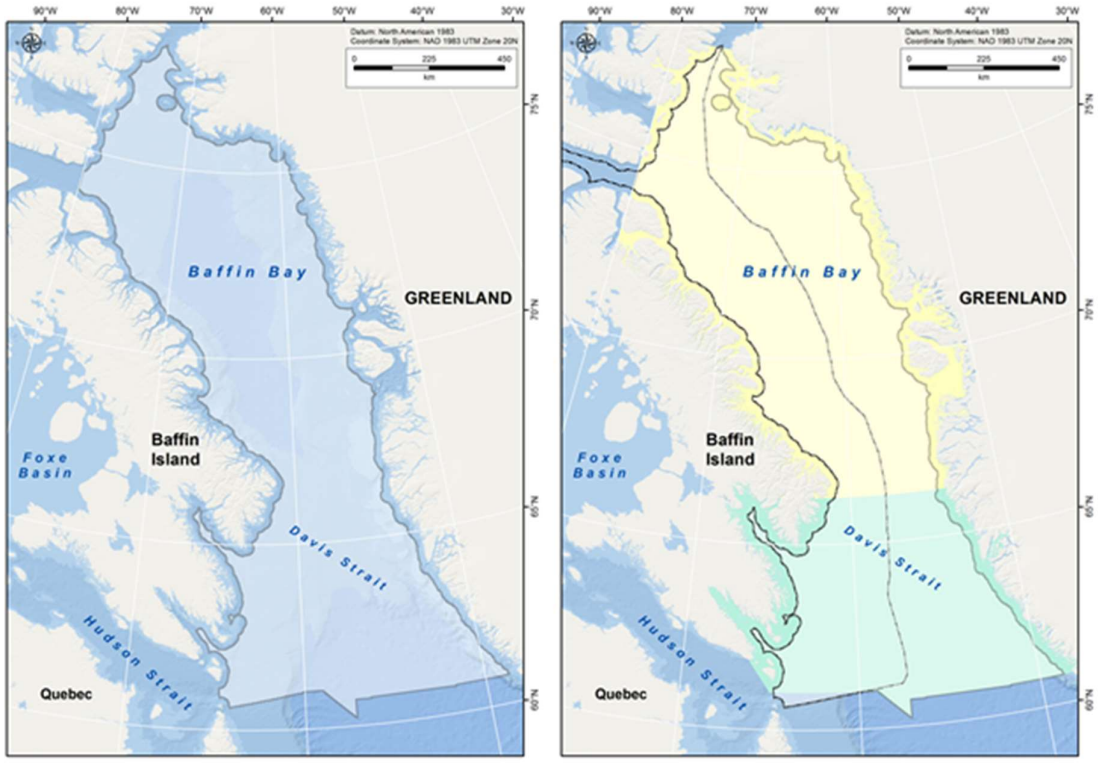

Figure 143. Left panel: study extent for Random Forest modelling of coral functional groups in Baffin Bay and Davis Strait. Right panel: depiction of the ATLAS Baffin Bay (yellow) and Davis (green) Strait Spatial Planning Areas, and DFO's Eastern Arctic Biogeographic Zone (grey dashed polygon on the western part of the spatial extent) for which the response data were extracted.

3.9.2 Species selection

Habitat suitability models were performed on cold-water coral taxa. Given the low occurrences of individual coral species (see Table 24) in DFO's Eastern Arctic Biogeographic Region, catch data were aggregated into coral functional groups (sea pens, large gorgonian corals, and small gorgonian corals). The composition of species in each functional group can be found in Table 24. Note that the gorgonian corals are no longer recognized as a taxonomic group and both large and small representatives are considered Alcyonacea.

3.9.3 Species occurrence data sources

Catch data were collected between 1999 and 2014 from a combination of DFO research vessel trawl surveys: DFO/industry Greenland Halibut/shrimp trawl surveys conducted on the fishing vessel

Paamuit using Alfredo and Cosmo trawl gear, and DFO northern shrimp surveys conducted on the *Cape Ballard*, *Aqviq*, and *Kinguk* using Campelen trawl gear. All surveys were stratified-random (by depth). Absence records were created from null (zero) catches that occurred in the same surveys. The presence/absence records were then filtered so that only one presence or absence occurred within a single environmental grid cell, with presence records taking precedence over absence when both occurred in the same cell (Table 24).

Table 24. Species composition within the sea pen, large gorgonian coral, and small gorgonian coral functional groups from trawl catch data collected in DFO's Eastern Arctic Biogeographic Region. Also shown are the number of tows that recorded each species/taxon, prior to filtering the data to 1 presence record per grid cell (i.e., these values are reduced prior to RF modelling).

Taxonomic Group	Species/Taxon	Number of Tows Recorded
Sea Pens (Pennatulacea)	Pennatulacea O.	12
	Anthoptilum grandiflorum	54
	Halipteris finmarchica	41
	Pennatula grandis	44
	Pennatula sp.	4
	Umbellula sp.	216
	Sea pen sp.	95
Large Gorgonian Corals	*Acanthogorgia armata*	6
	Keratoisis ornata	1
	Paragorgia arborea	92
	Paramuricea sp.	10
	Paramuricea placomus [28S-b]	1
	Primnoa resedaeformis	72
Small Gorgonian Corals	*Acanella arbuscula*	177
	Anthothela cf. *grandiflora*	3
	Radicipes gracilis	2

Sea Pens

Sea pen catch data (Table 25) consisting of 420 presences and 1962 absences collected between 1999 and 2014 were derived from *Paamuit* surveys conducted using Alfredo (302 presences and 451 absences) and Cosmos trawl gear (52 presences and 134 absences), and *Cape Ballard*, *Aqviq*, and *Kinguk* surveys conducted using Campelen trawl gear (66 presences and 1377 absences). DFO trawl survey records using Alfredo gear had the widest spatial distribution in the study extent (Figure 144).

Campelen records were restricted to lower Baffin Bay and Davis Strait, while Cosmos records were distributed along the Baffin Island Shelf and in Davis Strait in Canadian waters.

Table 25. Number of presence and absence records of sea pens recorded from DFO trawl surveys conducted between 1999 and 2014. Data are shown by year and trawl gear type.

	Alfredo		Campelen		Cosmos	
Year	**Presences**	**Absences**	**Presences**	**Absences**	**Presences**	**Absences**
1999	6	-	-	-	-	-
2000	6	-	-	-	-	-
2005	-	-	8	142	-	-
2006	31	30	12	130	15	60
2007	-	-	4	129	0	12
2008	38	45	9	134	28	38
2009	0	17	7	138	-	-
2010	73	48	5	139	8	14
2011	23	61	5	146	-	-
2012	71	87	4	147	1	10
2013	19	67	9	142	-	-
2014	35	96	3	130	-	-
TOTAL	**302**	**451**	**66**	**1377**	**52**	**134**

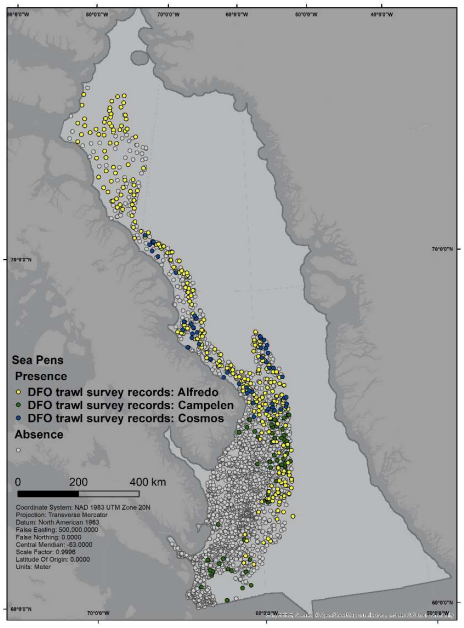

Figure 144. Sea pen catch data (presences and absences) collected in DFO's Eastern Arctic Biogeographic Region from DFO trawl surveys conducted between 1999 and 2014. Red dashed line represents the Canadian and Greenland exclusive economic zones. Presence records are colour-coded by trawl gear type.

Large Gorgonian Corals

Large gorgonian catch data (Table 26) consisting of 155 presences and 2211 absences collected between 1999 and 2014 were derived from *Paamuit* surveys conducted using Alfredo (39 presences and 698 absences) and Cosmos trawl gear (1 presence and 184 absences), and surveys conducted on the *Cape Ballard*, *Aqviq*, and *Kinguk* using Campelen trawl gear (115 presences and 1329 absences). DFO trawl survey records using Alfredo gear had the widest spatial distribution in the study extent (Figure 145). Campelen records were restricted to the Davis Strait, while Cosmos records were distributed along the Baffin Island Shelf, in southern Baffin Bay, and in Davis Strait in Canadian waters.

Table 26. Number of presence and absence records of large gorgonian corals recorded from DFO trawl surveys conducted between 1999 and 2014. Data are shown by year and trawl gear type.

	Alfredo		Campelen		Cosmos	
Year	**Presences**	**Absences**	**Presences**	**Absences**	**Presences**	**Absences**
1999	1	-	-	-	-	-
2000	-	-	-	-	-	-
2001	-	-	-	-	-	-
2005	-	-	6	145	-	-
2006	-	60	27	115	-	75
2007	-	-	5	128	-	12
2008	2	77	7	136	-	65
2009	-	17	4	140	-	-
2010	5	111	11	134	-	22
2011	6	76	20	130	-	-
2012	1	160	21	129	1	10
2013	18	67	11	140	-	-
2014	6	130	3	132	-	-
TOTAL	**39**	**698**	**115**	**1329**	**1**	**184**

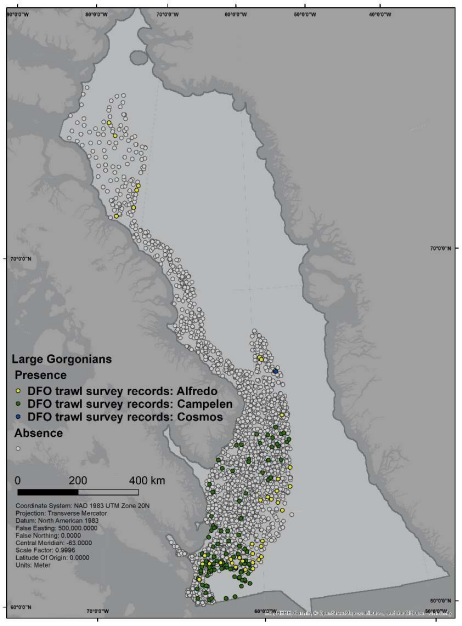

Figure 145. Large gorgonian catch data (presences and absences) collected in DFO's Eastern Arctic Biogeographic Region from DFO trawl surveys conducted between 1999 and 2014. Red dashed line represents the Canadian and Greenland exclusive economic zones. Presence records are colour-coded by trawl gear type.

Small Gorgonian Corals

Small gorgonian catch data (Table 27) consisting of 179 presences and 2188 absences collected between 2005 and 2014 were derived from *Paamuit* surveys conducted using Alfredo (85 presences and 655 absences) and Cosmos trawl gear (4 presence and 180 absences), and *Cape Ballard*, *Aqviq*, and *Kinguk* surveys using Campelen trawl gear (90 presences and 1353 absences). DFO trawl survey records using Alfredo gear had the widest spatial distribution in the study extent (Figure 146). Campelen records were restricted to the Davis Strait, while Cosmos records were distributed along the Baffin Island Shelf, in lower Baffin Bay, and in Davis Strait in Canadian waters.

Table 27. Number of presence and absence records of small gorgonian corals recorded from DFO trawl surveys conducted between 2005 and 2014. Data are shown by year and trawl gear type.

	Alfredo		Campelen		Cosmos	
Year	**Presences**	**Absences**	**Presences**	**Absences**	**Presences**	**Absences**
2005	-	-	7	143	-	-
2006	2	58	16	126	2	73
2007	-	-	15	118	0	12
2008	0	79	16	127	2	62
2009	1	16	4	140	-	-
2010	1	116	10	134	0	22
2011	32	51	4	148	-	-
2012	0	161	8	143	0	11
2013	25	61	10	141	-	-
2014	24	113	0	133	-	-
TOTAL	**85**	**655**	**90**	**1353**	**4**	**180**

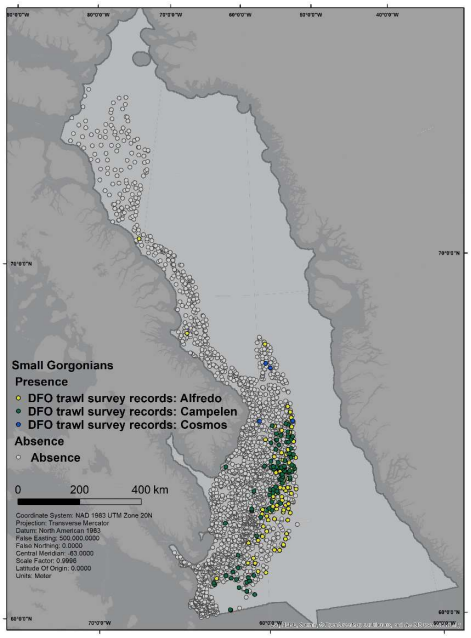

Figure 146. Small gorgonian coral catch data (presences and absences) collected in DFO's Eastern Arctic Biogeographic Region from DFO trawl surveys conducted between 2005 and 2014. Red dashed line represents the Canadian and Greenland exclusive economic zones. Presence records are colour-coded by trawl gear type.

Environmental data layers

Fifty-eight environmental variables derived from various sources and native spatial resolutions were used as predictor variables in Random Forest (see Table 28). Variables were derived from long-term oceanographic or remote-sensing data. Where possible, minimum, maximum, mean, and range (maximum-minimum) metrics were derived for each variable type (e.g., Bottom Temperature Minimum) in order to assess the impact of both average and extreme climate. The point data was spatially interpolated using ordinary kriging in ArcMap version 10.4 to create continuous surfaces with a ~0.013˚ grid size (approximately equal to 1 km horizontal resolution at 75˚N, approximately at the centre of the study extent). Details of the data sources for these variables and the methods used for their spatial interpolation are found in Beazley et al. (2018) and deposited in Mendeley (Beazley et al., 2019). All interpolated predictor layers were displayed in raster format with geographic coordinates using the WGS 1984 datum.

Bathymetry was derived from the General Bathymetric Chart of the Oceans (GEBCO; http://www.gebco.net/data_and_products/gridded_bathymetry_data/). This data is the highest resolution bathymetry available for the entire study area. The data are resolved to 30 arc-seconds which is equivalent to approximately 500 m at 75°N. Using the 'Slope' tool in ArcMap's Spatial Analyst

Toolbox, slope in degrees was derived from depth projected with the NAD 1983 Zone 20N coordinate system (in metres), and both depth and slope were re-projected using a WGS 1984 datum and resampled to the 0.013˚ grid size using the nearest neighbour technique.

Table 28. Summary of the 58 environmental layers used as predictor variables in Random Forest. N/A= Not applicable.

Variable	Data Source	Temporal Range	Unit	Native Resolution
Depth	GEBCO	N/A	metres	30 arc-sec.
Slope	GEBCO	N/A	degrees	30 arc-sec.
Bottom Salinity Mean	GLORYS2V1	1993 - 2011	N/A	¼ º
Bottom Salinity Minimum	GLORYS2V1	1993 - 2011	N/A	¼ º
Bottom Salinity Maximum	GLORYS2V1	1993 - 2011	N/A	¼ º
Bottom Salinity Range	GLORYS2V1	1993 - 2011	N/A	¼ º
Bottom Temperature Mean	GLORYS2V1	1993 - 2011	ºC	¼ º
Bottom Temperature Minimum	GLORYS2V1	1993 - 2011	ºC	¼ º
Bottom Temperature Maximum	GLORYS2V1	1993 - 2011	ºC	¼ º
Bottom Temperature Range	GLORYS2V1	1993 - 2011	ºC	¼ º
Bottom Current Speed Mean	GLORYS2V1	1993 - 2011	m s^{-1}	¼ º
Bottom Current Speed Minimum	GLORYS2V1	1993 - 2011	m s^{-1}	¼ º
Bottom Current Speed Maximum	GLORYS2V1	1993 - 2011	m s^{-1}	¼ º
Bottom Current Speed Range	GLORYS2V1	1993 - 2011	m s^{-1}	¼ º
Bottom Shear Mean	GLORYS2V1	1993 - 2011	Pa	¼ º
Bottom Shear Minimum	GLORYS2V1	1993 - 2011	Pa	¼ º
Bottom Shear Maximum	GLORYS2V1	1993 - 2011	Pa	¼ º
Bottom Shear Range	GLORYS2V1	1993 - 2011	Pa	¼ º
Surface Salinity Mean	GLORYS2V1	1993 - 2011	N/A	¼ º
Surface Salinity Minimum	GLORYS2V1	1993 - 2011	N/A	¼ º
Surface Salinity Maximum	GLORYS2V1	1993 - 2011	N/A	¼ º
Surface Salinity Range	GLORYS2V1	1993 - 2011	N/A	¼ º
Surface Temperature Mean	GLORYS2V1	1993 - 2011	ºC	¼ º
Surface Temperature Minimum	GLORYS2V1	1993 - 2011	ºC	¼ º
Surface Temperature Maximum	GLORYS2V1	1993 - 2011	ºC	¼ º
Surface Temperature Range	GLORYS2V1	1993 - 2011	ºC	¼ º
Surface Current Speed Mean	GLORYS2V1	1993 - 2011	m s^{-1}	¼ º
Surface Current Speed Minimum	GLORYS2V1	1993 - 2011	m s^{-1}	¼ º
Surface Current Speed Maximum	GLORYS2V1	1993 - 2011	m s^{-1}	¼ º
Surface Current Speed Range	GLORYS2V1	1993 - 2011	m s^{-1}	¼ º
Maximum Fall Mixed Layer Depth	GLORYS2V1	1993 - 2011	metres	¼ º
Maximum Winter Mixed Layer Depth	GLORYS2V1	1993 - 2011	metres	¼ º
Maximum Spring Mixed Layer Depth	GLORYS2V1	1993 - 2011	metres	¼ º
Maximum Summer Mixed Layer Depth	GLORYS2V1	1993 - 2011	metres	¼ º
Summer Chlorophyll *a* Mean	SeaWiFS Level-3, NASA's OceanColor	2001 - 2010	mg m^{-3}	9 km
Summer Chlorophyll *a* Minimum	SeaWiFS Level-3, NASA's OceanColor	2001 - 2010	mg m^{-3}	9 km
Annual Chlorophyll *a* Mean	SeaWiFS Level-3, NASA's OceanColor	2001 - 2010	mg m^{-3}	9 km
Annual Chlorophyll *a* Minimum	SeaWiFS Level-3, NASA's OceanColor	2001 - 2010	mg m^{-3}	9 km

Variable	Data Source	Temporal Range	Unit	Native Resolution
Summer Primary Production Mean	SeaWiFS Level-3 with other input parameters	2006 - 2010	mg C m^{-2} day^{-1}	9 km
Summer Primary Production Minimum	SeaWiFS Level-3 with other input parameters	2006 - 2010	mg C m^{-2} day^{-1}	9 km
Summer Primary Production Maximum	SeaWiFS Level-3 with other input parameters	2006 - 2010	mg C m^{-2} day^{-1}	9 km
Summer Primary Production Range	SeaWiFS Level-3 with other input parameters	2006 - 2010	mg C m^{-2} day^{-1}	9 km
Annual Primary Production Mean	SeaWiFS Level-3 with other input parameters	2006 - 2010	mg C m^{-2} day^{-1}	9 km
Annual Primary Production Minimum	SeaWiFS Level-3 with other input parameters	2006 - 2010	mg C m^{-2} day^{-1}	9 km
Annual Primary Production Maximum	SeaWiFS Level-3 with other input parameters	2006 - 2010	mg C m^{-2} day^{-1}	9 km
Annual Primary Production Range	SeaWiFS Level-3 with other input parameters	2006 - 2010	mg C m^{-2} day^{-1}	9 km
Spring Ice Cover Mean	HadISST	1993-2010	Percent (%)	1˚
Spring Ice Cover Minimum	HadISST	1993-2010	Percent (%)	1˚
Spring Ice Cover Maximum	HadISST	1993-2010	Percent (%)	1˚
Spring Ice Cover Range	HadISST	1993-2010	Percent (%)	1˚
Fall Ice Cover Mean	HadISST	1993-2010	Percent (%)	1˚
Fall Ice Cover Minimum	HadISST	1993-2010	Percent (%)	1˚
Fall Ice Cover Maximum	HadISST	1993-2010	Percent (%)	1˚
Fall Ice Cover Range	HadISST	1993-2010	Percent (%)	1˚
Winter Ice Cover Mean	HadISST	1993-2010	Percent (%)	1˚
Winter Ice Cover Minimum	HadISST	1993-2010	Percent (%)	1˚
Winter Ice Cover Maximum	HadISST	1993-2010	Percent (%)	1˚
Winter Ice Cover Range	HadISST	1993-2010	Percent (%)	1˚

3.9.4 Modelling approaches

Random Forest classification (Breiman et al., 2001) was used to predict the probability of occurrence and range distribution of sea pens, and large and small gorgonian corals. Random Forest is a non-parametric machine learning technique where multiple trees are built using random subsets of the response data. Each tree is fit to a bootstrap sample of these data, and the best predictor at each node is that which splits the response data so that maximum homogeneity in the child nodes is reached. Models were fitted using the 'randomForest' package (Liaw & Wiener, 2002) in the statistical software program R (version 3.5.1). Default parameters were used and 500 trees were constructed.

Model performance was assessed in R using 10-fold cross validation. In this process the response data are split into 10 folds of equal size, and a model is trained on a combination of 9 folds and validated on the remaining fold. The process is repeated 10 times, giving 10 repetitions for which accuracy measures are derived. Sensitivity (i.e., the proportion of accurately predicted presences) and specificity (the proportion of accurately predicted absences) were derived by summing the predicted outcomes across the 2 x 2 confusion matrices generated for each of the 10 model folds. Low sensitivity represents high omission error (i.e., false negative rate), while low specificity indicates high commission error (i.e., false positive rate). The response dataset for each of the three coral functional groups is characterized by a higher number of absences relative to presences (i.e., unbalanced species prevalence, where prevalence is the proportion of presences in relation to the total dataset). Classification accuracy in Random Forest is prone to bias when the categorical response variable is highly imbalanced (Chen et al., 2004; Evans et al., 2011). This is due to over-representation of the majority class in the bootstrap sample leading to a higher frequency in which the majority class is drawn, therefore skewing predictions in that favour. Given the highly imbalanced nature of the response dataset, a threshold defining above which a class probability is considered a presence is often used to convert the class probabilities into predicted outcomes that are then summarized in the 2 x 2 confusion matrix. We used prevalence, or the probability of presences in the training dataset, as the threshold defining when a species is considered present (Liu et al., 2005; Hanberry & He, 2013). The discrimination capacity of the training model was determined by calculating the average Area under the Receiver Operating Characteristic (ROC) Curve, or AUC, across all 10 model folds.

Using R's 'predict' function, a model trained on all the presence/absence data per functional group was used to predict the probability of presence across the entire study extent. The final outcome was a 1 km x 1 km grid raster surface of predicted presence probabilities. The probabilistic map was converted into a binary map showing areas of suitable versus unsuitable habitat using two different thresholds: 1) prevalence, or the observed presences in the data, and 2) true skill statistic. The true

skill statistic maximizes the sum of sensitivity and specificity and is considered to have all the advantages of the kappa statistic but is independent of prevalence (Allouche et al., 2006). TSS was generated for each model fold using the 'optimal.thresholds' function in R package 'Presence/Absence', and then averaged across all 10 folds.

3.9.5 Model outputs

Sea Pens

The accuracy measures of the Random Forest model generated on the 420 presences and 1962 absences are shown in Table 29. The cross validated AUC averaged across all 10 model folds was 0.8425 ± 0.0234 (± SD). The predicted presence probability surface is shown in Figure 147 and Figure 148, while Figure 149 and Figure 150 show the presence probability surface thresholded into a categorical map of suitable versus unsuitable habitat using prevalence and true skill statistic values. Figure 151 and Figure 152 show the importance of the predictor variables and response curves (partial dependence plots), respectively.

Table 29. Accuracy measures and confusion matrix from 10-fold cross validation of a Random Forest model of presence and absence of sea pens within the ATLAS Baffin Bay-Davis Strait case study area. AUC represents an average across all 10 model folds, while the confusion matrix, class error, sensitivity and specificity result from a summation of the predicted outcomes in the 2 x 2 confusion matrix generated for each of the 10 model folds. Prevalence (0.18) was used as the probability threshold. Observe. = Observations; Sensit. = Sensitivity, Specif. = Specificity.

Model Fold	AUC	Observ.	Predictions		Total n	Class error	Sensit.	Specif.
1	0.8746		**Absence**	**Presence**				
2	0.8502	**Absence**	1444	518	1962	0.2640	0.8143	0.7360
3	0.8362	**Presence**	78	342	420	0.1857		
4	0.8279							
5	0.8018							
6	0.8748							
7	0.8391							
8	0.8636							
9	0.8314							
10	0.8249							
Mean	**0.8425**							
SD	**0.0234**							

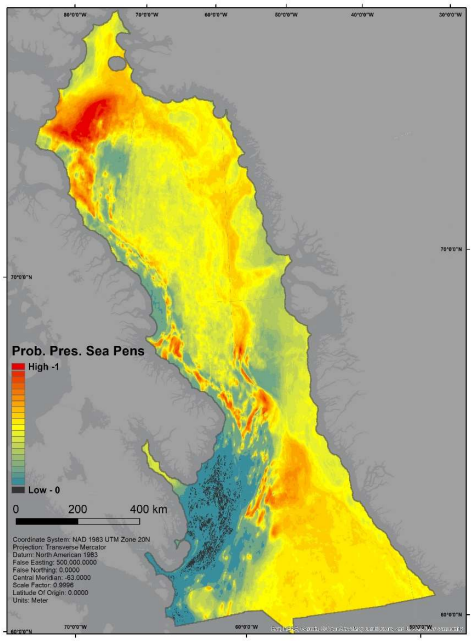

Figure 147. Presence probability (Pres. Prob.) of sea pens in the ATLAS Baffin Bay-Davis Strait case study area based on a Random Forest model on sea pen presence and absence data derived from DFO trawl surveys conducted in the DFO Eastern Arctic Biogeographic Region between 1999 and 2014.

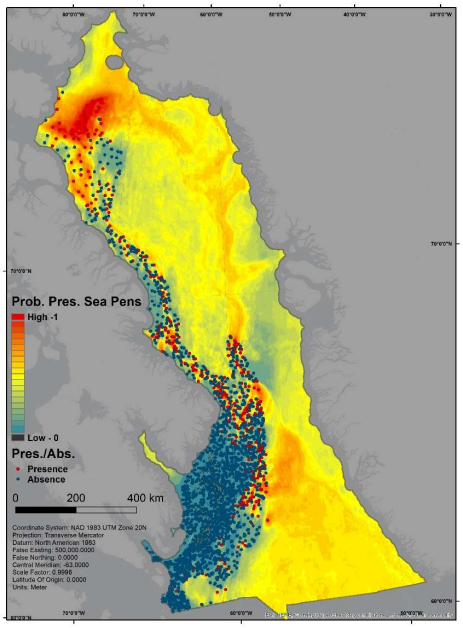

Figure 148. Presence probability (Pres. Prob.) of sea pens in the ATLAS Baffin Bay-Davis Strait case study area based on a Random Forest model on sea pen presence and absence data derived from DFO trawl surveys conducted in the DFO Eastern Arctic Biogeographic Region between 1999 and 2014. Also shown are the presences (red circles) and absences (blue circles) used in the model, and areas of model extrapolation.

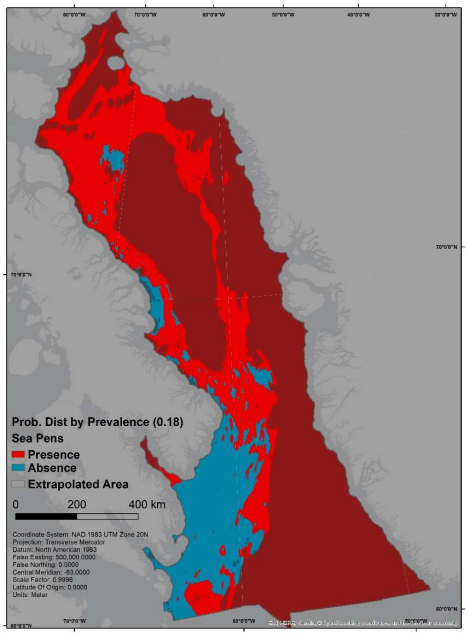

Figure 149. Predicted distribution of suitable (red) and unsuitable (blue) habitat for sea pens in the ATLAS Baffin Bay-Davis Strait case study area based on the prevalence threshold (0.18) applied to the predicted probabilities from Random Forest. Also shown are areas of model extrapolation (grey polygon may appear red or blue).

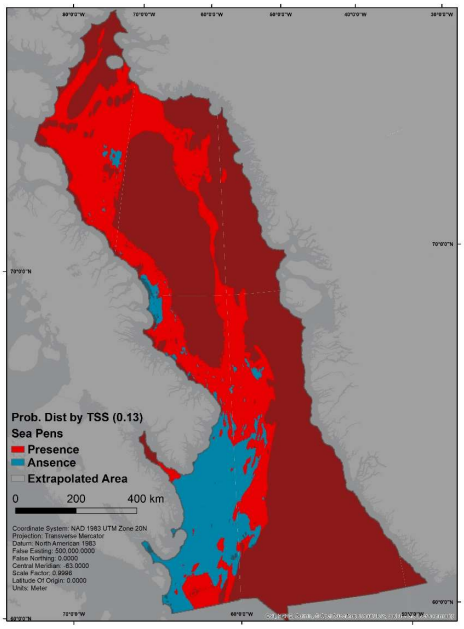

Figure 150. Predicted distribution of suitable (red) and unsuitable (blue) habitat for sea pens in the ATLAS Baffin Bay-Davis Strait case study area based on the true skill statistic (TSS) threshold (0.13) applied to the predicted probabilities from Random Forest. Also shown are areas of model extrapolation (grey polygon may appear red or blue).

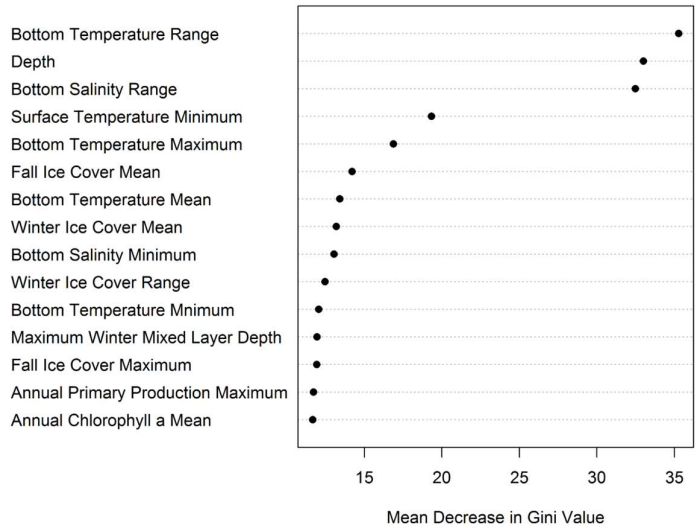

Figure 151. Importance of the top 15 predictor variables measured as the Mean Decrease in Gini value of the classification Random Forest model on sea pen presence and absence data. The higher the Mean Gini value the more important the variable is for predicting the response data.

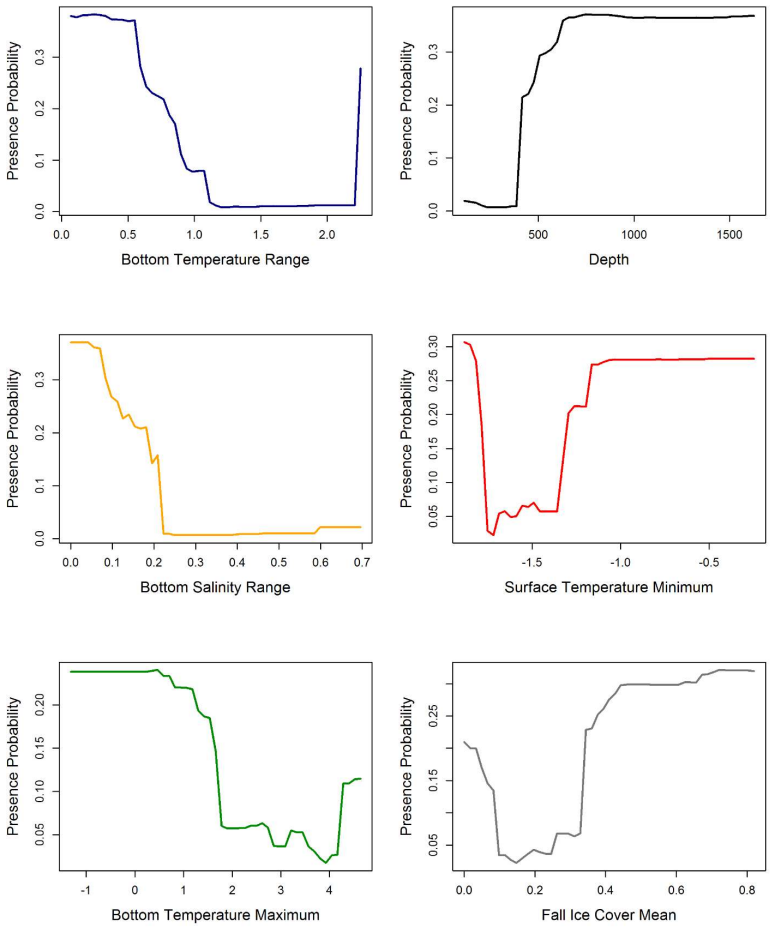

Figure 152. Partial dependence plots of the top six predictors from the classification Random Forest model on sea pen presence and absence data, ordered from left to right from the top. Presence probability is shown on the y-axis.

Large Gorgonian Corals

The accuracy measures of the Random Forest model generated on the 155 presences and 2211 absences are shown in Table 30. The cross validated AUC averaged across all 10 model folds was 0.7758 ± 0.0901. The predicted presence probability surface is shown in Figure 153 and Figure 154, while Figure 155 and Figure 156 show the presence probability surface thresholded into a categorical map of suitable versus unsuitable habitat using the prevalence and true skill statistic values. Figure 157 and Figure 158 show the importance of the predictor variables and response curves (partial dependence plots), respectively.

Table 30. Accuracy measures and confusion matrix from 10-fold cross validation of a Random Forest model of presence and absence of large gorgonians within the ATLAS Baffin Bay-Davis Strait case study area. AUC represents an average across all 10 model folds, while the confusion matrix, class error, sensitivity and specificity result from a summation of the predicted outcomes in the 2 x 2 confusion matrix generated for each of the 10 model folds. Prevalence (0.07) was used as the probability threshold. Observe. = Observations; Sensit. = Sensitivity, Specif. = Specificity.

Model Fold	AUC	Observ.	Predictions		Total n	Class error	Sensit.	Specif.
1	0.7896		**Absence**	**Presence**				
2	0.7576	**Absence**	1756	455	2211	0.2058	0.6194	0.7942
3	0.8944	**Presence**	59	96	155	0.3806		
4	0.6271							
5	0.8514							
6	0.7948							
7	0.7896							
8	0.6193							
9	0.8506							
10	0.7838							
Mean	**0.7758**							
SD	**0.0901**							

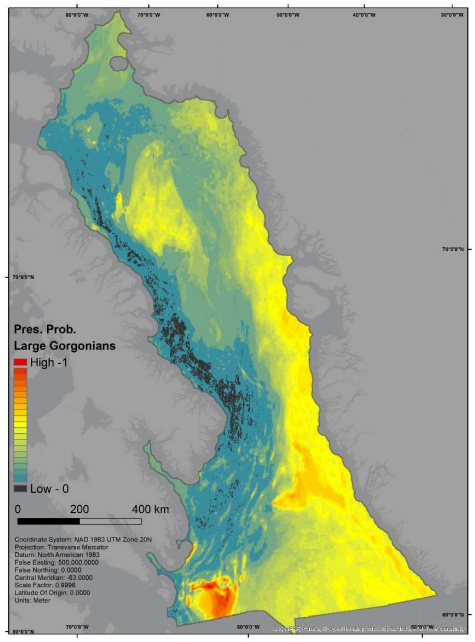

Figure 153. Presence probability (Pres. Prob.) of large gorgonian corals in the ATLAS Baffin Bay-Davis Strait case study area based on a Random Forest model on large gorgonian coral presence and absence data derived from DFO trawl surveys conducted in the DFO Eastern Arctic Biogeographic Region between 1999 and 2014.

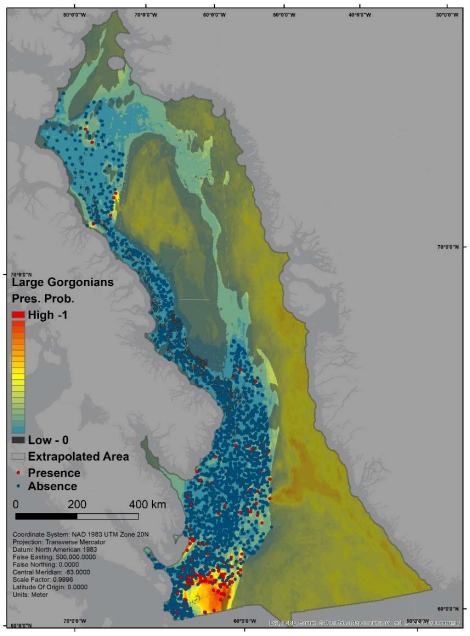

Figure 154. Presence probability (Pres. Prob.) of large gorgonian corals in the ATLAS Baffin Bay-Davis Strait case study area based on a Random Forest model on large gorgonian coral presence and absence data derived from DFO trawl surveys conducted in the DFO Eastern Arctic Biogeographic Region between 1999 and 2014. Also shown are the presences and absences used in the model, and areas of model extrapolation.

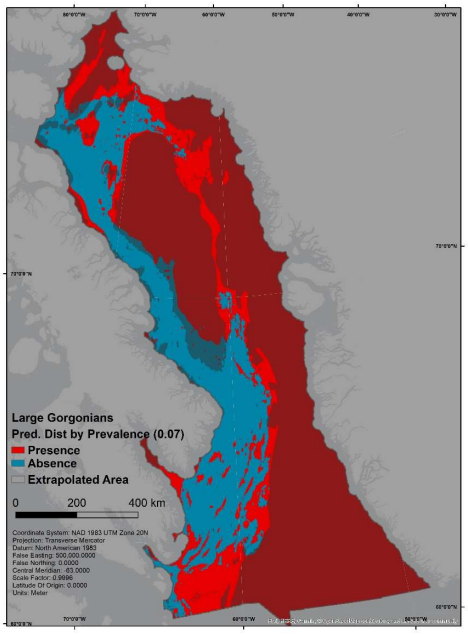

Figure 155. Predicted distribution of suitable (red) and unsuitable (blue) habitat for large gorgonians in the ATLAS Baffin Bay-Davis Strait case study area based on the prevalence threshold (0.07) applied to the predicted probabilities from Random Forest. Also shown are areas of model extrapolation (grey polygon may appear red or blue).

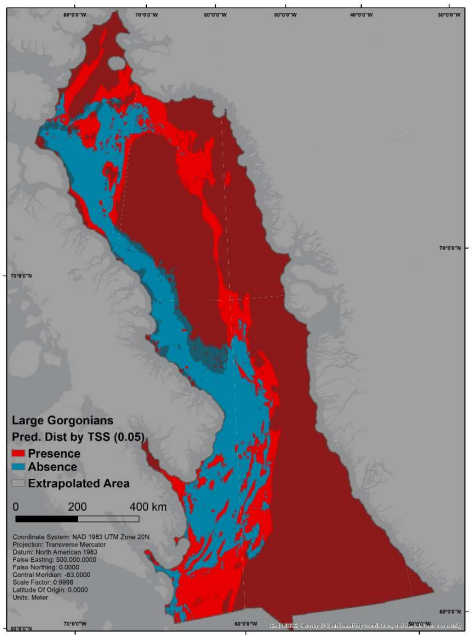

Figure 156. Predicted distribution of suitable (red) and unsuitable (blue) habitat for large gorgonians in the ATLAS Baffin Bay-Davis Strait case study area based on the true skill statistic (TSS) threshold (0.05) applied to the predicted probabilities from Random Forest. Also shown are areas of model extrapolation (grey polygon may appear red or blue).

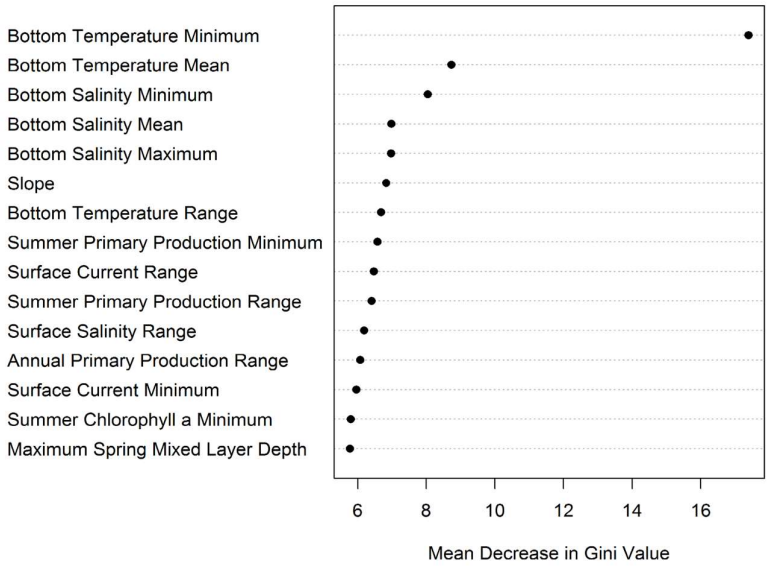

Figure 157. Importance of the top 15 predictor variables measured as the Mean Decrease in Gini value of the classification Random Forest model on large gorgonian presence and absence data. The higher the Mean Gini value the more important the variable is for predicting the response data.

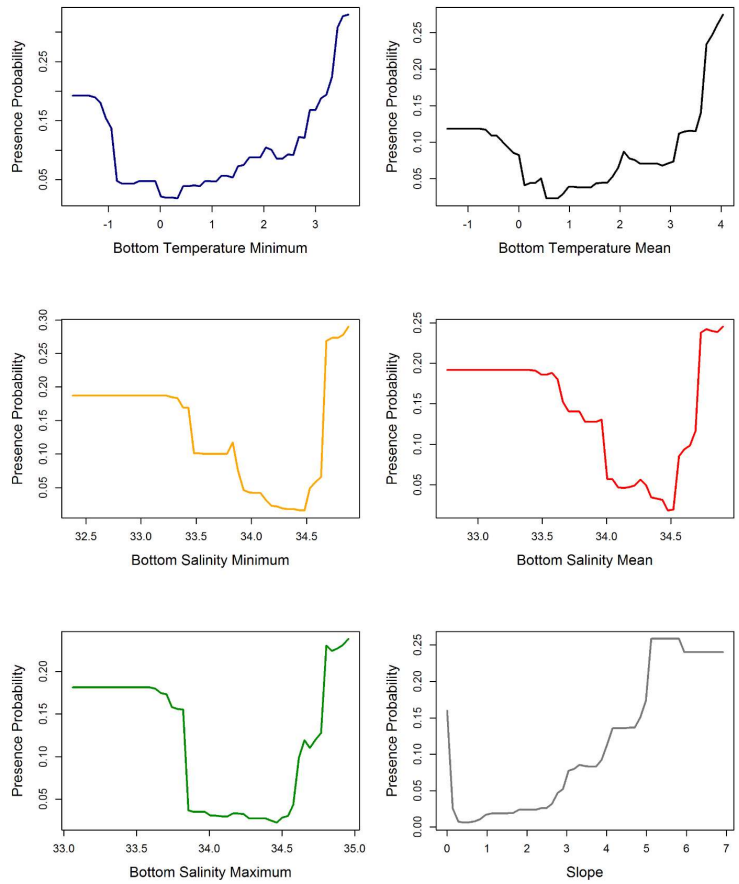

Figure 158. Partial dependence plots of the top six predictors from the classification Random Forest model on large gorgonian presence and absence data, ordered from left to right from the top. Presence probability is shown on the y-axis.

Small Gorgonian Corals

The accuracy measures of the Random Forest model generated on the 179 presences and 2188 absences are shown in Table 31. The cross validated AUC averaged across all 10 model folds was 0.8852 ± 0.0444 (SD). The predicted presence probability surface is shown in Figure 159 and Figure 160, while Figure 161 and Figure 162 show the presence probability surface thresholded into a categorical map of suitable versus unsuitable habitat using the prevalence and true skill statistic values. Figure 163 and Figure 164 show the importance of the predictor variables and response curves (partial dependence plots), respectively.

Table 31. Accuracy measures and confusion matrix from 10-fold cross validation of a Random Forest model of presence and absence of small gorgonians within the ATLAS Baffin Bay-Davis Strait case study area. AUC represents an average across all 10 model folds, while the confusion matrix, class error, sensitivity and specificity result from a summation of the predicted outcomes in the 2 x 2 confusion matrix generated for each of the 10 model folds. Prevalence (0.08) was used as the probability threshold. Observe. = Observations; Sensit. = Sensitivity, Specif. = Specificity.

Model Fold	AUC	Observ.	Predictions		Total n	Class error	Sensit.	Specif.
1	0.9128		**Absence**	**Presence**				
2	0.8361	**Absence**	1821	367	2188	0.1677	0.8156	0.8323
3	0.9009	**Presence**	33	146	179	0.1844		
4	0.8584							
5	0.9030							
6	0.9221							
7	0.9227							
8	0.8801							
9	0.9249							
10	0.7908							
Mean	**0.8852**							
SD	**0.0444**							

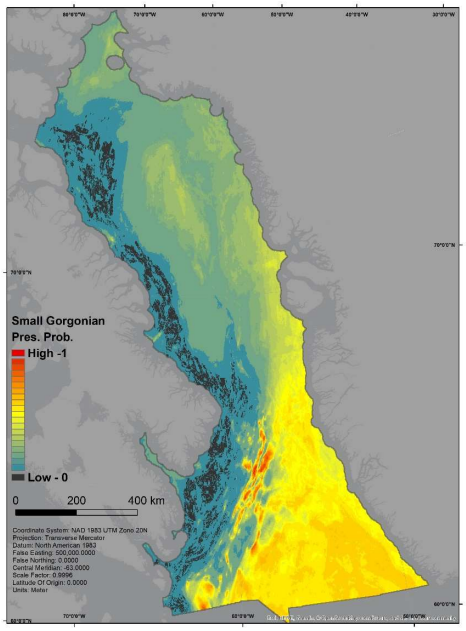

Figure 159. Presence probability (Pres. Prob.) of small gorgonian corals in the ATLAS Baffin Bay-Davis Strait case study area based on a Random Forest model on small gorgonian coral presence and absence data derived from DFO trawl surveys conducted in the DFO Eastern Arctic Biogeographic Region between 2005 and 2014.

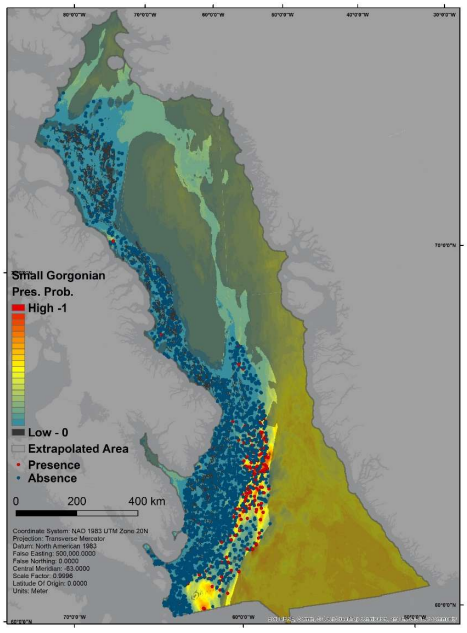

Figure 160. Presence probability (Pres. Prob.) of small gorgonian corals in the ATLAS Baffin Bay-Davis Strait case study area based on a Random Forest model on small gorgonian coral presence and absence data derived from DFO trawl surveys conducted in the DFO Eastern Arctic Biogeographic Region between 2005 and 2014. Also shown are the presences and absences used in the model, and areas of model extrapolation.

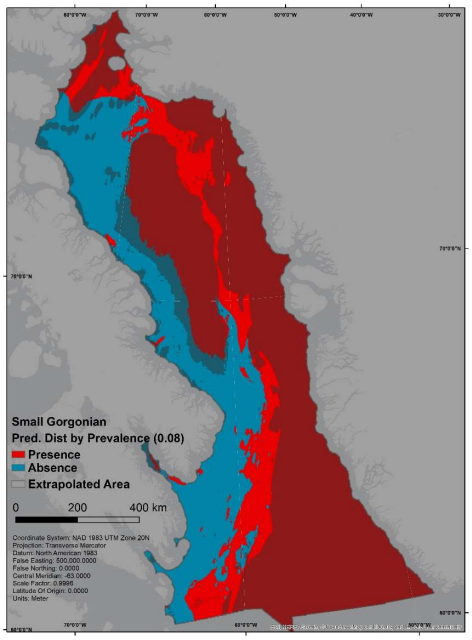

Figure 161. Predicted distribution of suitable (red) and unsuitable (blue) habitat for small gorgonians in the ATLAS Baffin Bay-Davis Strait case study area based on the prevalence threshold (0.08) applied to the predicted probabilities from Random Forest. Also shown are areas of model extrapolation (grey polygon may appear red or blue).

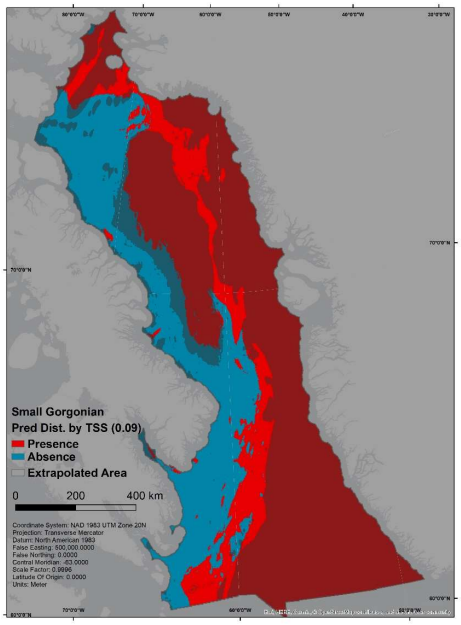

Figure 162. Predicted distribution of suitable (red) and unsuitable (blue) habitat for small gorgonians in the ATLAS Baffin Bay-Davis Strait case study area based on the true skill statistic (TSS) threshold (0.09) applied to the predicted probabilities from Random Forest. Also shown are areas of model extrapolation (grey polygon may appear red or blue).

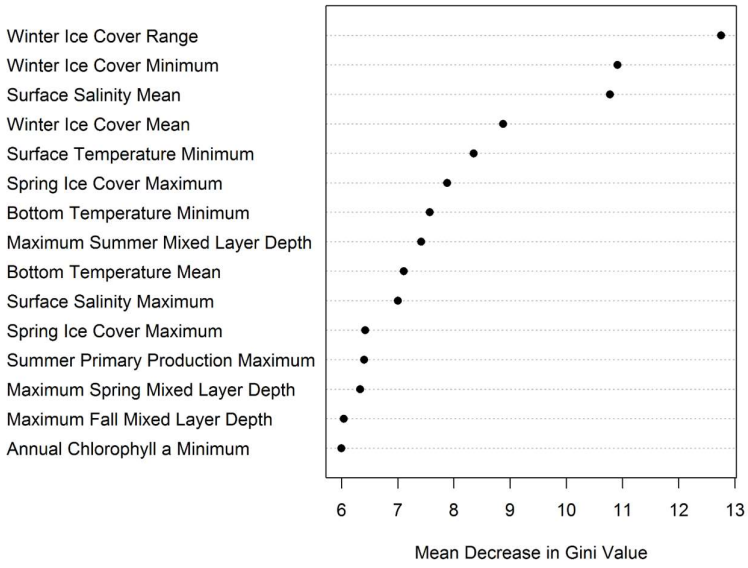

Figure 163. Importance of the top 15 predictor variables measured as the Mean Decrease in Gini value of the classification Random Forest model on small gorgonian coral presence and absence data. The higher the Mean Gini value the more important the variable is for predicting the response data.

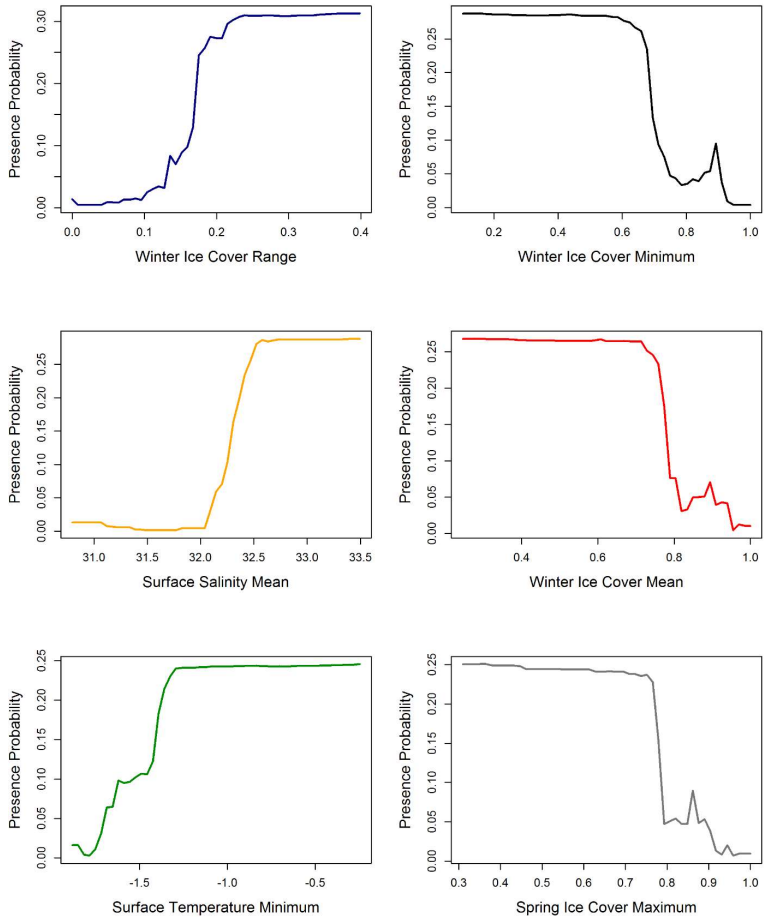

Figure 164. Partial dependence plots of the top six predictors from the classification Random Forest model on small gorgonian coral presence and absence data, ordered from left to right from the top. Presence probability is shown on the y-axis.

3.9.6 Model interpretation, caveats and future directions

Random Forest models of corals and sponges were produced for the Canadian portion of the study area in support of management decisions for the protection of sensitive benthic areas (DFO, 2017). The decision to use Random Forest models was made based on the large amount of validated null data that we had for the region from the surveys that we viewed as more valid than pseudo-absences generated in other approaches. We have compared the results from that work to the present study and found a good congruence of the predictions; however, model results could be independently validated with data on coral presence from Greenlandic waters. That should be done in future as data become available. Here we present the first models of cold-water corals for the entire Case Study area, as the previous work only predicted presence within the Canadian EEZ.

Model performance and top predictor variables were very similar to previously run models within the Canadian EEZ (Beazley et al., 2018). For all three CWC functional group models, temperature or salinity variables were amongst the most important. These likely do not reflect physiological tolerance limits as all of the species are widespread along the continental slopes of eastern Canada and are mainly boreal species. Temperature and salinity characterize the water masses in the region and the distribution of the corals is more likely closely governed by the currents. Areas of higher bottom temperature and surface salinity may correspond to the flow of the Irminger Current, which circulates cyclonically around the northern Labrador Sea and along the southern edge of Davis Strait, where it then turns southwest towards the Labrador Sea. This is where the highest probability for the small and large gorgonian corals were found. Polar Water is found close to the coast and Atlantic Water is found as a 500–800 m thick layer over the continental slope with a core at about 200–300 m depth. These waters seem to have more influence on the sea pen distribution.

Although we have not modelled the distribution of sponges in this Case Study area, a recent publication (Murillo et al., 2018) has provided predictive models of sponge communities that will be used for purposes of marine spatial planning in ATLAS. The sponge taxa of Hudson Strait, Ungava Bay, Western Davis Strait and Western Baffin Bay collected by Canadian research vessel trawl surveys have been recently described (Murillo et al., 2018) with 93 different taxa (79% identified to species) identified. A model-based clustering method developed (Dunstan et al., 2011) and referred to as species archetype modelling, or SAM, was used to predict the probability of occurrence distribution for sponge assemblages in the Eastern Arctic. This modelling method uses finite mixture models to cluster species based on their environmental responses. Species that have a similar response to environmental conditions are grouped together and represented by a single logistic generalized linear

model (GLM). These groups are referred to as species archetypes. The archetype GLMs are derived from a single finite mixture model and represent one or many species with similar ecological tolerances. This method also provides accurate predictions for rare species by borrowing strength from the most prevalent species classified into the same archetype (Hui et al., 2013). Five sponge species assemblages were identified (Murillo et al., 2018) spanning the case study area. Two of the Baffin Bay-Davis Strait assemblages were characterized by large structure-forming astrophorids; one, with arctic species, found at mid-water depths in Baffin Bay and the other, characterized by boreal species, was found deeper, south of Davis Strait. Another assemblage characterized by glass and carnivorous sponges was found along the continental slope of western Baffin Bay. Candidate target indicator species were provided for future sponge community monitoring (Murillo et al., 2018).

Collectively these predictive models will be used to assess management options in the marine spatial planning scenarios for this Case Study, however species distribution models (SDMs) also have been used to determine closed areas to protect vulnerable marine ecosystems both in Canada (DFO, 2017) and in international waters (NAFO, 2014). Canada has engaged in the identification and protection of sensitive benthic marine ecosystems under the Policy on Managing the Impacts of Fishing on Sensitive Benthic Areas, established in 2009. This policy was created in response to the United Nations General Assembly Resolution 61/105 which also drives the protection of VMEs in areas beyond national jurisdiction. The main tool used to identify significant concentrations of corals and sponges (and other VME indicator taxa) in both eastern Canada and the Northwest Atlantic Fisheries Organization (NAFO) is kernel density analysis (KDE) of research vessel catch data and an associated areal expansion approach (Kenchington et al., 2014) to identify significant concentrations of VME indicators (NAFO, 2014). KDE produces polygons encompassing high biomass concentrations. SDMs are then used to refine the boundaries of the KDE polygons (VMEs), which do not include any environmental data in their identification. This has been especially valuable when the polygons include both shelf and slope areas and the VME indicator occurs in one or other environment (NAFO, 2014). SDMs have the added characteristic in that they can more broadly interpolate and extrapolate predictions to areas not surveyed by the trawls but are within the environmental domain of the occurrence data. The ability to interpolate between trawl sets within polygons gave support to the polygon representing a VME, strengthening the scientific advice. Both KDE and SDM results have been independently validated using in situ imagery where more information is required to fine-tune boundaries or to convince managers and stakeholders of the results. To date there has been a high degree of consistency among these three approaches. Of the 34 marine refugia that Canada has identified (http://www.dfo-mpo.gc.ca/oceans/oeabcm-amcepz/refuges/index-eng.html) 24 have directly drawn on KDE/SDM results (Murillo et al., 2018). In the study area, Canada has identified two conservation areas, the 7485

km^2 Disko Fan Conservation Area and the 17298 km^2 Davis Strait Conservation Area which provide coral, sponge and sea pen protection based on KDE and SDM analyses.

3.10 Case study 11: Present day models for several sea-pens species or genera in Flemish Cap

Mar Sacau[1], Ana García-Alegre[1], Maria Grazia Pennino[1], Pablo Durán Muñoz[1]

1- Instituto Español de Oceanografía (IEO), Centro Oceanográfico de Vigo, Vigo, Pontevedra, Spain.

3.10.1 Case study description

The study area is located in the NW Atlantic, in an Area Beyond National Jurisdiction (ABNJ), within the Northwest Atlantic Fisheries Organization (NAFO) Regulatory Area (Figure 165). It is characterized by the Flemish Pass, the Flemish Cap and the NE part of the Grand Bank of Newfoundland including the "nose".

The Flemish Pass is a channel of ~1,200 m deep which separates Flemish Cap, an isolated plateau of approximately 200 km, and the Grand Banks of Newfoundland. The Cap has a minimum depth of 120m situated in the southeastern part and a maximum of 730 m in the north. This area is on the Canadian continental shelf and they stretch beyond 200 nautical miles (Canadian EEZ) off the coastline. It is within a transition zone between cold subpolar waters, influenced by fluctuations in the Labrador Current and in the North Atlantic Current (Gil et al., 2004). The Grand Banks shelf is separated from the Flemish Cap by the cold southward flow of the Labrador Current (Colbourne & Footek, 2000). Most part of the Flemish Cap substrata is constituted by unconsolidated substrata as muddy sand and sandy mud although in its centre a patch of sand is found, while stones are scattered in the entire area (Murillo et al., 2011).

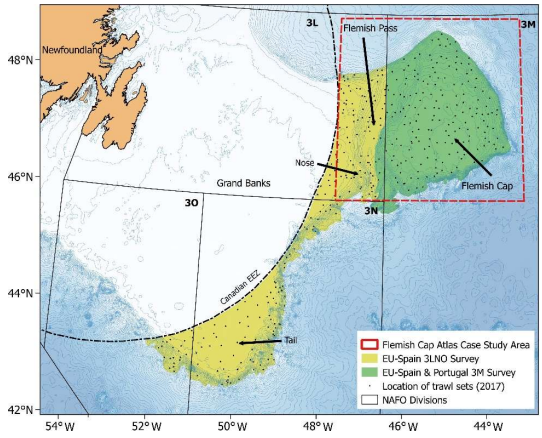

Figure 165. Flemish Cap Case Study area (Flemish Cap and Flemish Pass) is located in 3LM NAFO Divisions.

3.10.2 Species selection

We focused our study on deep-sea coral aggregations which represent important ecosystems in this area, where some areas have been closed to bottom fisheries by the Northwest Atlantic Fisheries Organization (NAFO)(Figure 166). Due to the aforementioned unconsolidated substrata which characteristic this area, soft corals and sea pens were the most common deep-sea corals in the area, followed by Gorgonians and black corals, all of them included in Octocorallia. Only solitary Scleractinea (Hexacorallia) were found in the area.

Species selected were four species of the subclass Octacorallia, which were the most dominant corals taxa observed in the study area and were included in the list of VMEs indicator species in NAFO (NAFO, 2019). Three sea pens (Order Pennatulacea): *Anthoptilum grandiflorum*, *Funiculina quadrangularis and Pennatula aculeata* and the deep-sea bamboo coral (Order Alcyonacea) *Acanella arbuscula.*

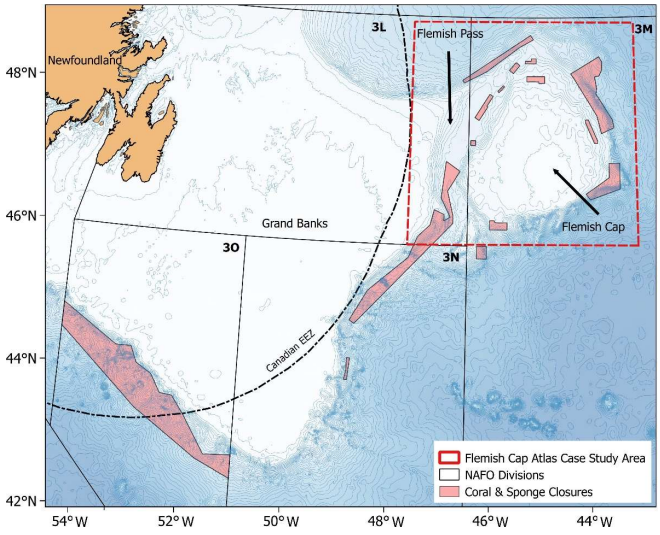

Figure 166. Coral and Sponge Closures to bottom fisheries by the Northwest Atlantic Fisheries Organization (NAFO) in the Flemish Cap Case Study area (Flemish Cap and Flemish Pass).

3.10.3 Species occurrence data sources

A 11-year period (2007-2017) data of two bottom-trawl groundfish surveys was used. These surveys are carried out every year during July and August according to a stratified random sampling design based on depth strata (Figure 165). They were carried out by the Instituto Español de Oceanografía (IEO) jointly with the European Union (EU): the EU Flemish Cap survey sampled all the Flemish Cap (NAFO Division 3M) and the Spanish 3L survey sampled the “Nose” of the Grand Banks of Newfoundland and the Flemish Pass (NAFO Division 3L).

The maps of species occurrences and number of presences for each species are displayed below (Figure 167):

- *Anthoptilum grandiflorum:* 886 presences
- *Funiculina quadrangularis:* 258 presences
- *Pennatula aculeata:* 127 presences
- *Acanella arbuscula:* 253 presences

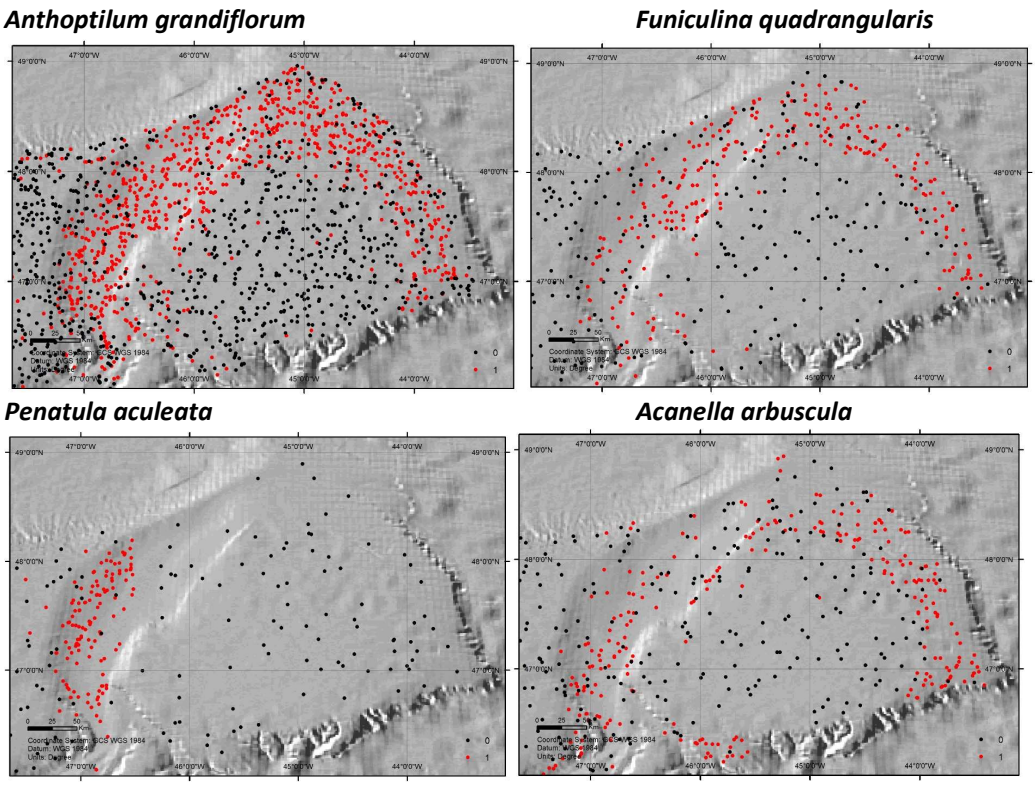

Figure 167. Maps of species presence (red dots) and absence (black dots) for the four species selected.

3.10.4 Environmental data layers

Data sources, oceanographic models, etc

Table 32 summarizes the environmental data layers used, showing the data sources, resolution, descriptor and units used. In particular, five oceanographic variables were used, such as Sea Bottom Temperature (SBT in C), Sea Bottom Salinity (SBS in PSU), Mixed Layer Depth (MLD in m), Bottom Current Speed (BCS in m/s) and Bottom Current Speed Components (U and V in m/s). SBT and SBS values were collected during the survey with a sounding CTD (conductivity, temperature and depth) in different sampling points of the study area. Monthly SBT and SBS maps of the entire area were

obtained for each year of the studied period with the RBF tool in ArcGIS 10.1. BCS and its components were extracted from Viking20 model (Breusing et al., 2016; Behrens et al., 2017).

Bathymetry was merged from the MARSPEC database (Sbrocco & Barber, 2013) (http://www.marspec.org) with a spatial resolution of ~1 km and the multibeam data obtained with the EM 302 multibeam echosounder on board R/V Miguel Oliver during the NEREIDA surveys (during 2009 and 2010), with a resolution of 75 m. For the merged bathymetric layer obtained (with a spatial resolution of ~1 km), three different variables were derived: slope (percentage in grades) and aspect of the seabed (North-South and East-West gradients) using the Benthic Terrain Modeller extension (Wright et al., 2005).

Table 32 Environmental data layers used for species modelling.

CONTINUOUS VARIABLES

Variable	Unit	Interpolated* Resolution	Descriptor	Data source
Sea Bottom Temperature	ºC	*1km	Temperature	SBE 25 Sealogger CTD
Sea Bottom Salinity	PSU	*1 km	Salinity	
Mixed Layer Depth	m	*1 km	Depth	Viking20 model
Bottom Current Speed and components (U and V)	m/s	*1 km	Current	
Bathymetry	m	*0.866 km 75 m	Bathymetry	http://www.marspec.org NEREIDA multibeam
Slope	Degrees	*0.866 km	Slope	
Aspect North/South and East/West	radians	*0.866 km	Orientation of the substrata	
Fishing effort 2008-2014	Hours/km^2	1.852 km	Fishing Effort average per km^2	NAFO

CATEGORICAL VARIABLES

Variable	Categories	Resolution	Descriptor	Data source
Sediment texture	2: Sand 3: Silty sand 4: Sandy silt 5:Silt 10:Clayed silt	*1 km	Typology of substrata	Murillo et al. (2016)
Gravel	0: 0-10% gravel content 1: 10-50% gravel content	*1km	Typology of substrata	Murillo et al. (2016)

Sediment texture and gravel data were extracted from Murillo et al. (2016) and introduced in the models to define the sediment substrata. The sediment texture map was constructed according to Shepard´s classification system (Shepard, 1954), following the methodology described in Jerosch

(Jerosch, 2013). To construct this map, all available data from the region were considered, including historical records from the Geological Survey of Canada (GSC) and from 317 box-corer samples collected from the area through the NEREIDA program (https://www.nafo.int/Science/Research).

Fishing effort layer was also included in the set of predictor variables used for species modeling. Following NAFO (2015), the VMS data from 2008–2014 were filtered to exclude records with vessel speed >5 knots, trawlers moving more slowly being assumed to be fishing, and mapped as annual average fishing effort (in vessel hours) per square kilometre, at the spatial resolution of the environmental layers and trimmed to the spatial extent of the latter. The resulting map (Figure 168) was used as a predictor layer in the models.

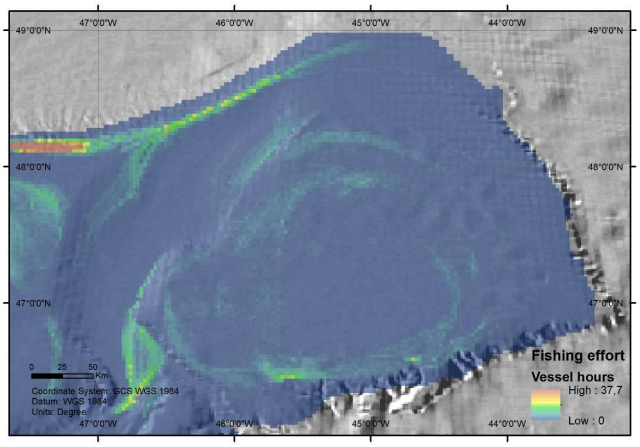

Figure 168. Representation of fishing activity based on 2008-2014 VMS data.

Spatial resolution used

Environmental data layers were incorporated with a 0.013 x 0.013 decimal degrees spatial resolution using the 'raster' package (Hijmans et al., 2016) in the R software (R Core team, 2017).

Variable selection methodology

All environmental data layers were tested for collinearity, correlation, outliers, and missing data before using them in the models following the procedure of Zuur et al. (2010). Then, we selected for the resultant variables not correlated and with a VIF values less than 3, the final variables for inclusion in the GAM through a stepwise forward and backward approach, based on optimizing the Akaike information criterion (AIC), variables significance and deviance explained (D2%). The GAM selected variables were then used in Random Forest and Maxent in order to be comparable.

Maps of environmental layers

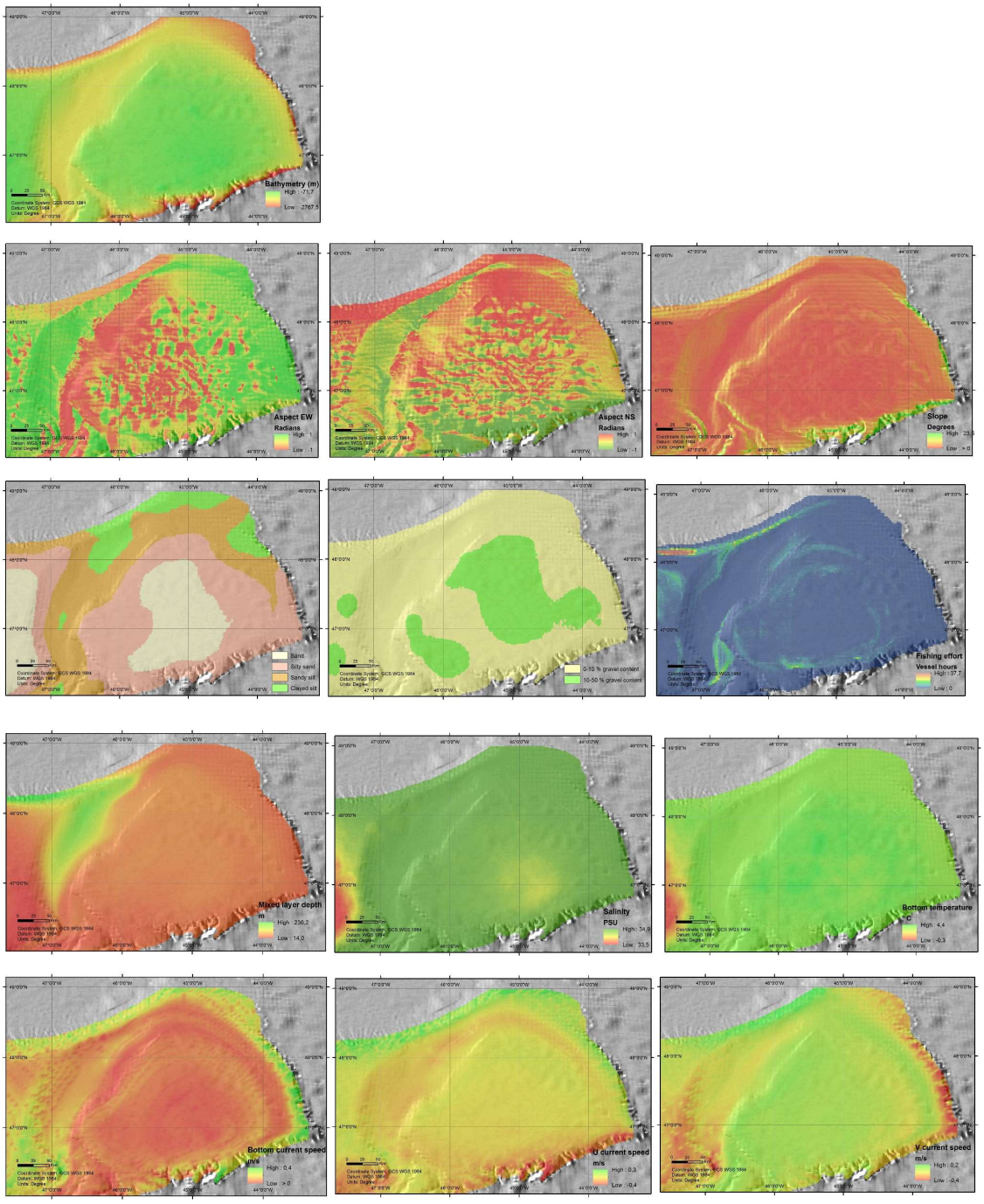

Figure 5. Maps of the environmental layers used (From top left to right: Depth, Aspect component E-W, Aspect component N-S, Slope, Sediment texture, Gravel, Fishing effort, Mixed layer depth, Bottom Salinity, Bottom Temperature, Bottom Current Speed, U Current Speed component and V Current Speed component).

3.10.5 Modelling approaches

- Three different modelling techniques were implemented: Generalised Additive Models (GAM; Hastie et al., 2001; Wood & Augustin, 2002), Random Forest (RF; Breiman, 2001; Cutler et al., 2007), and Maxent (Maximum Entropy model) (Elith et al., 2011; Phillips et al., 2006; Phillips & Dudik, 2008). All models were constructed in R 3.5.1 with the packages 'mgcv', 'randomForest', and 'dismo' interfaced with the standalone Maxent program v. 3.4.1e. (http://www.cs.prince-ton.edu/~schapire/maxent/).

  For GAM models, we used the default thin plate regression splines as the smoothing function (Wood, 2003), and we limited the smoothing to 4 degrees of freedom for each spline to avoid overfitting.

  For RFs, a sufficiently large number of trees (10, 000) were used, and different random seeds were applied to ensure stability in variable importance.

  While GAMs and RFs use the real occurrence dataset, Maxent is a presence-only modeling approach that uses background samples of the environment rather than absence locations to estimate environmental relationships. For this model we only used those grid cells that were surveyed in a given year as background data in order to be comparable with others models (Elith et al., 2011).

  We also estimated species probability of occurrence based on an ensemble of all models, as such predictions are often more robust than predictions derived from a single model (Thuiller et al., 2009). Ensemble predictions were calculated as averages of single-model predictions.

3.10.6 Model outputs

Response curves

Partial plots for the selected continuous and categorical variables for each species and model are shown in Figure 169 to Figure 172. Each plot represents the response variable shape, independent of the other variables, in relation to the probability of the species occurrence. Confidence intervals (95%) around the response curve are shaded in grey.

Anthoptilum grandiflorum

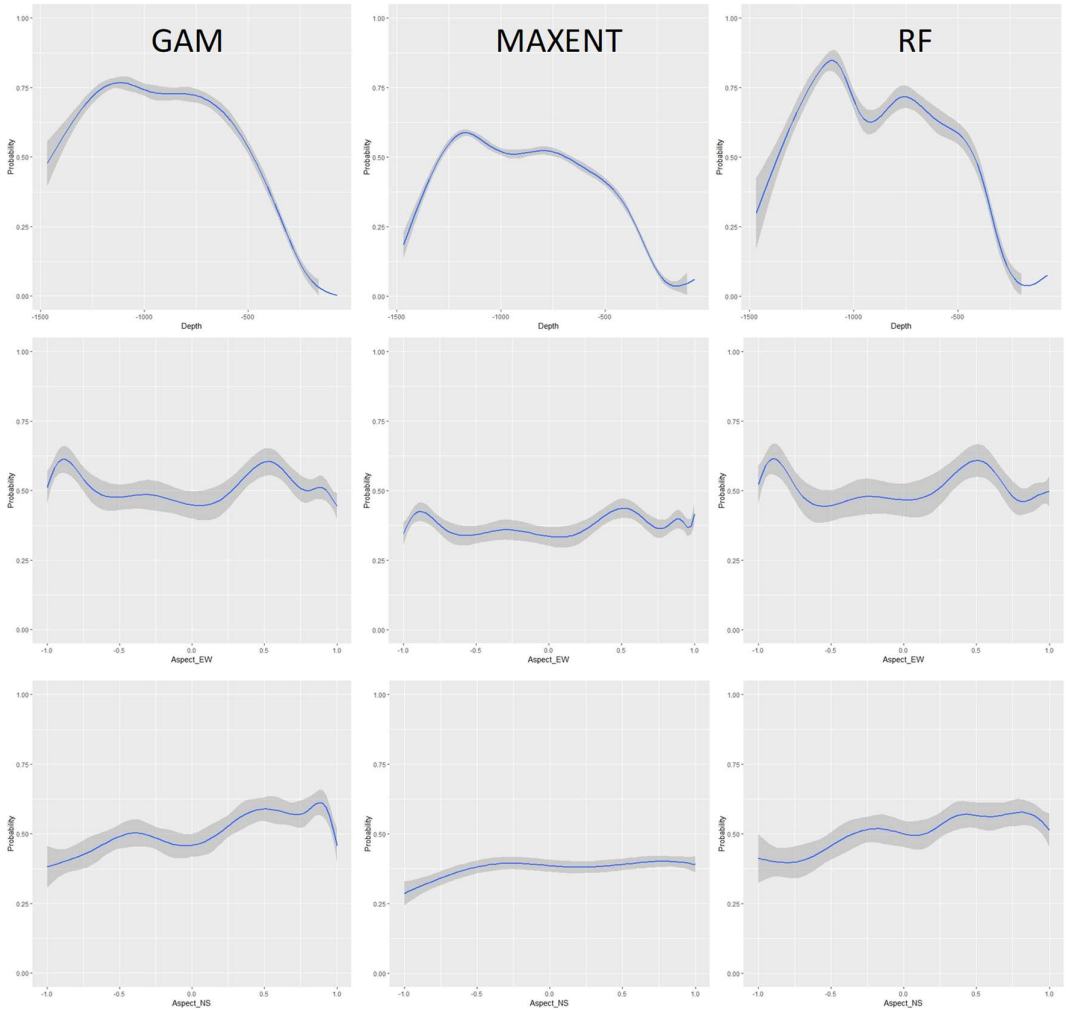

Figure 169. Partial GAM, Maxent and Random Forest (left, middle and right plots) for the selected continuous and categorical variables for Anthoptilum grandiflorum *(From top to bottom: Depth, Aspect component E-W, Aspect component N-S). Each plot represents the response variable shape, independent of the other variables, in relation to the probability of the species occurrence. Confidence intervals (95%) around the response curve are shaded in grey.*

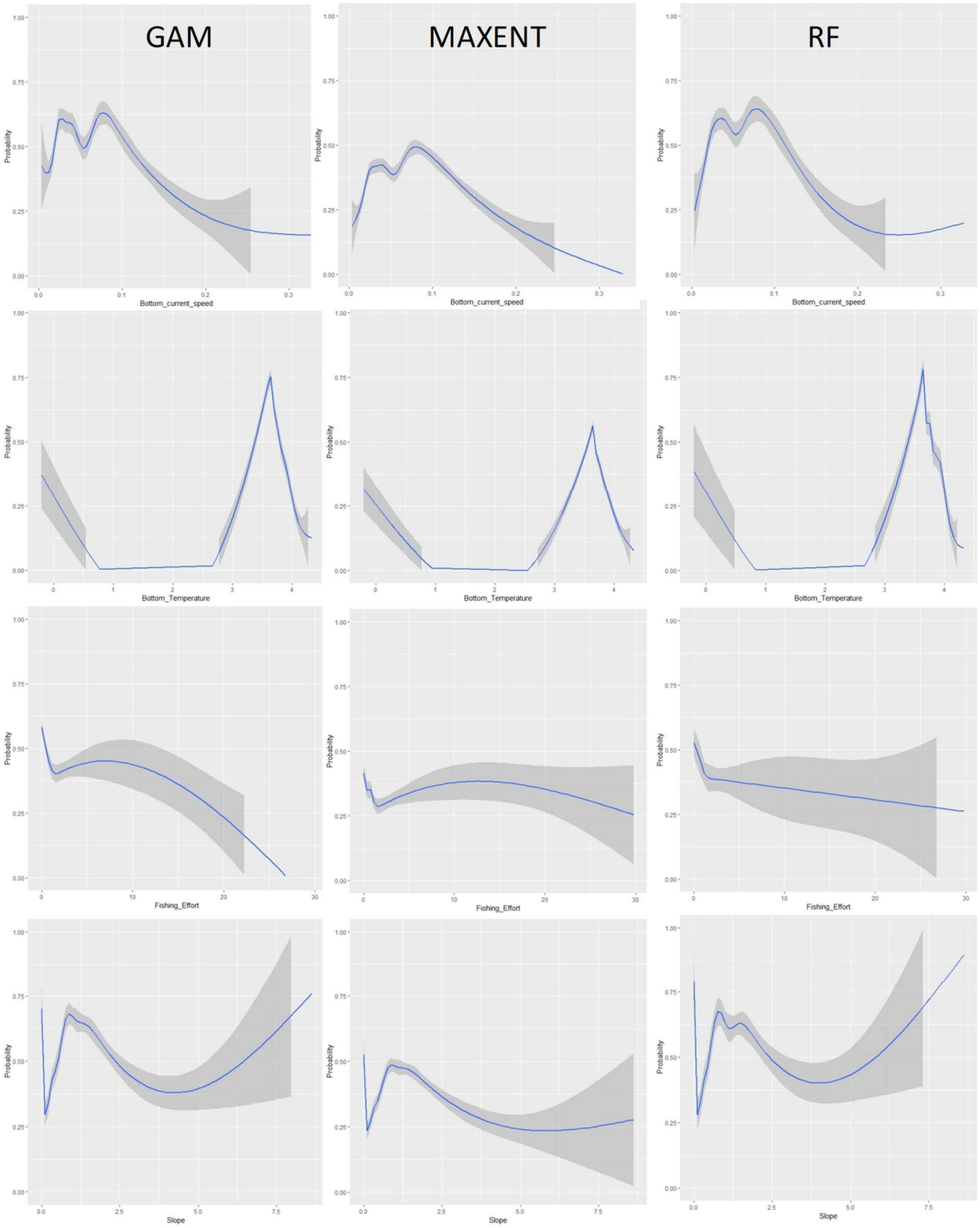

Figure 6 (cont.). Partial GAM, Maxent and Random Forest (left, middle and right plots) for the selected continuous and categorical variables for Anthoptilum grandiflorum *(From top to bottom: Bottom Current Speed, Bottom Temperature, Fishing Effort and Slope). Each plot represents the response variable shape, independent of the other variables, in relation to the probability of the species occurrence. Confidence intervals (95%) around the response curve are shaded in grey.*

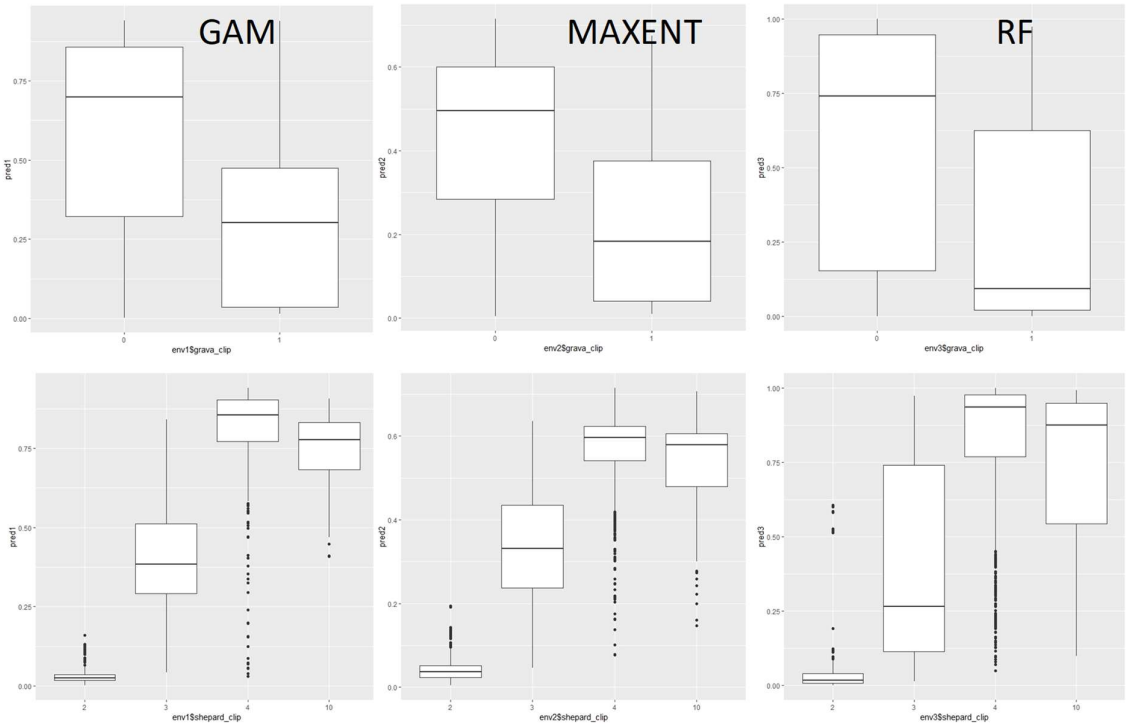

Figure 6 (cont.). Partial GAM, Maxent and Random Forest (left, middle and right plots) for the selected categorical variables for Anthoptilum grandiflorum *(From top to bottom: Gravel and Sediment texture).*

Funiculina quadrangularis

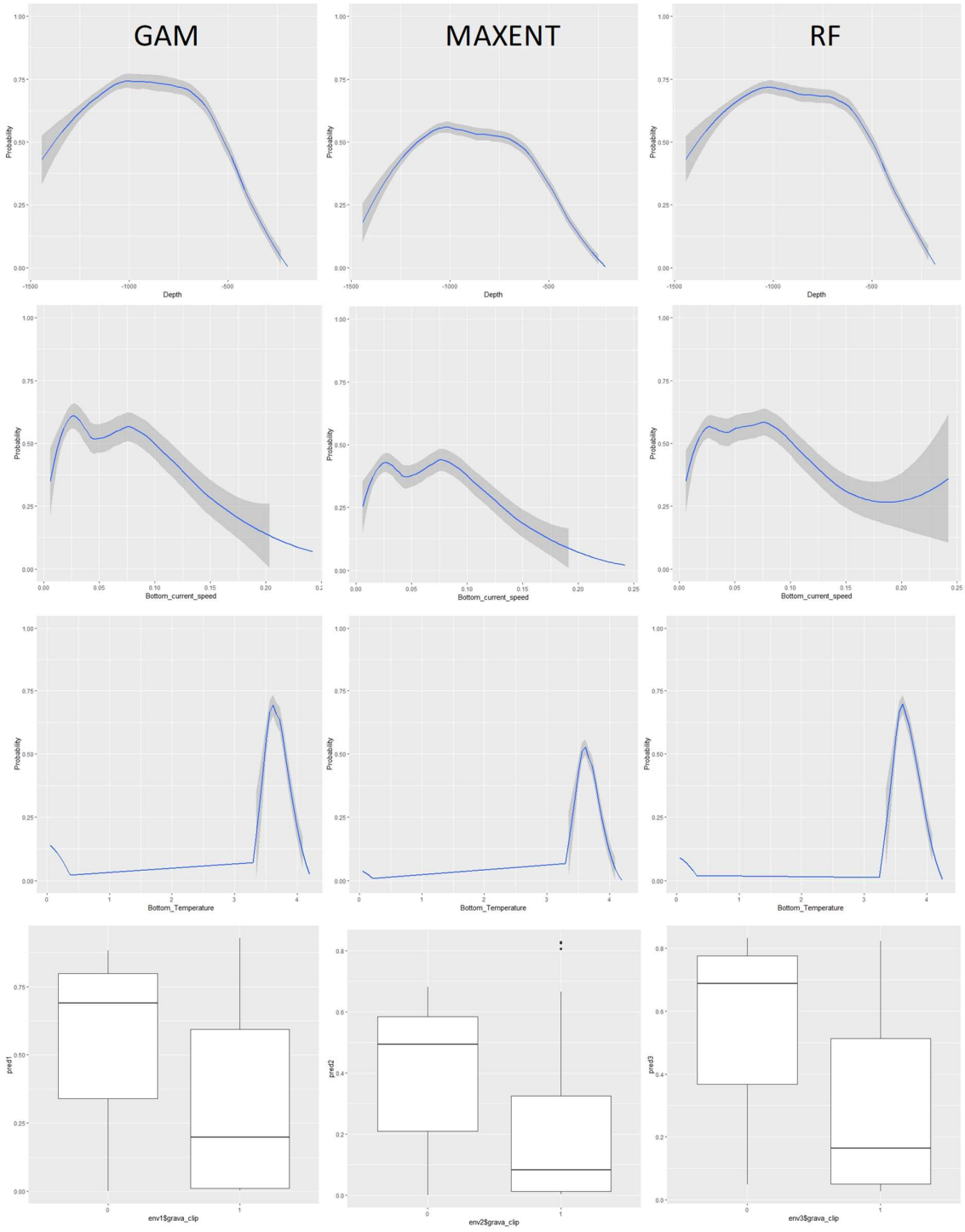

Figure 170. Partial GAM, Maxent and Random Forest (left, middle and right plots) for the selected continuous and categorical variables for Funiculina quadrangularis *(From top to bottom: Depth, Bottom Current Speed, Bottom Temperature and Gravel). Each plot represents the response variable shape, independent of the other variables, in relation to the probability of the species occurrence. Confidence intervals (95%) around the response curve are shaded in grey.*

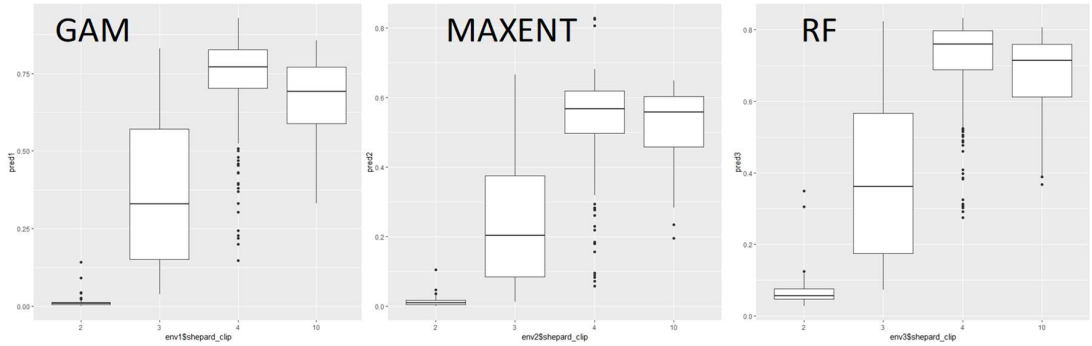

Figure 7 (cont.). Partial GAM, Maxent and Random Forest (left, middle and right plots) for the selected continuous and categorical variables for Funiculina quadrangularis *(Sediment texture).*

Pennatula aculeata

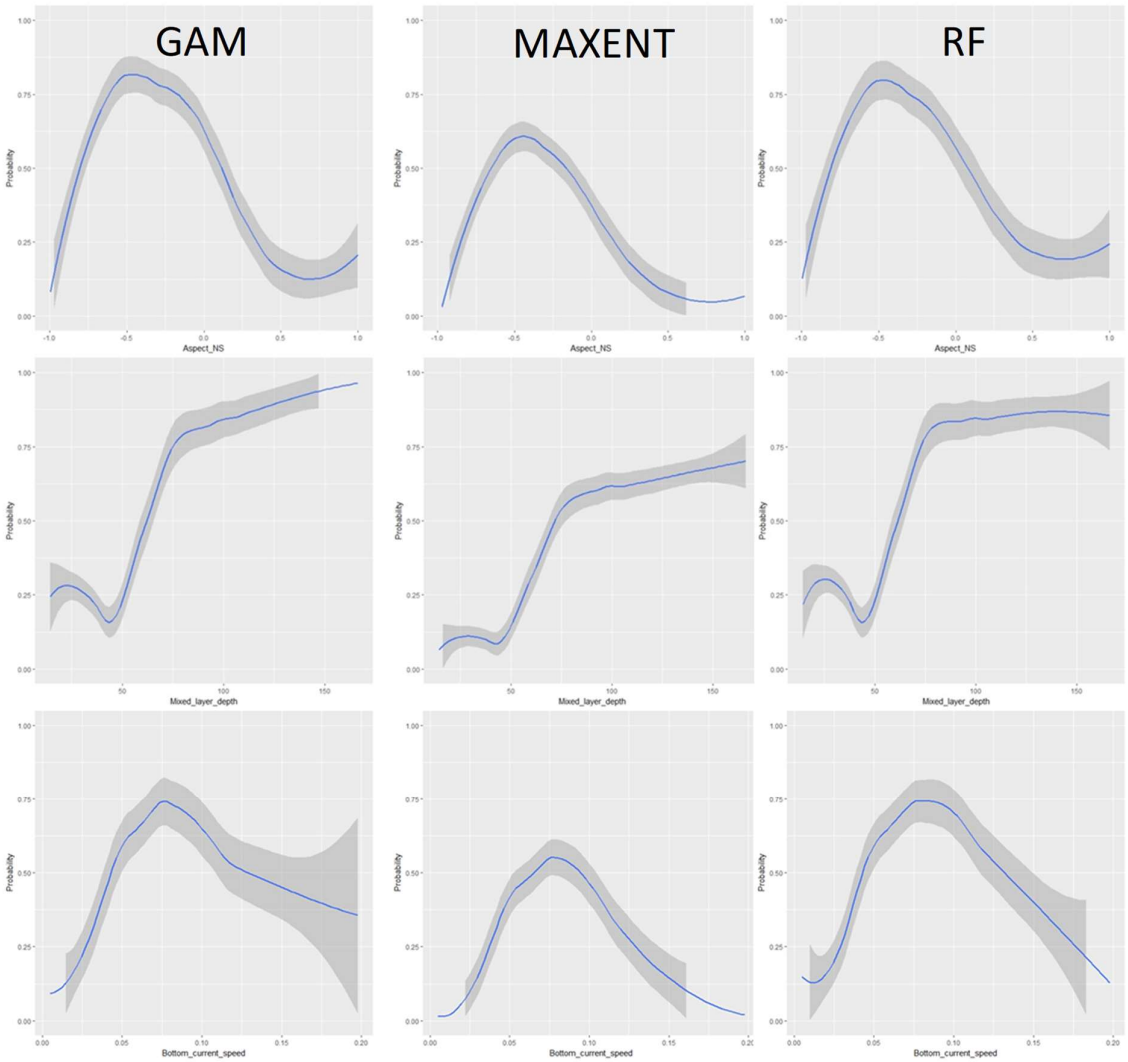

Figure 171. Partial GAM, Maxent and Random Forest (left, middle and right plots) for the selected continuous and categorical variables for Pennatula aculeata *(From top to bottom: Aspect component N-S, Mixed layer depth, Bottom current speed). Each plot represents the response variable shape, independent of the other variables, in relation to the probability of the species occurrence. Confidence intervals (95%) around the response curve are shaded in grey.*

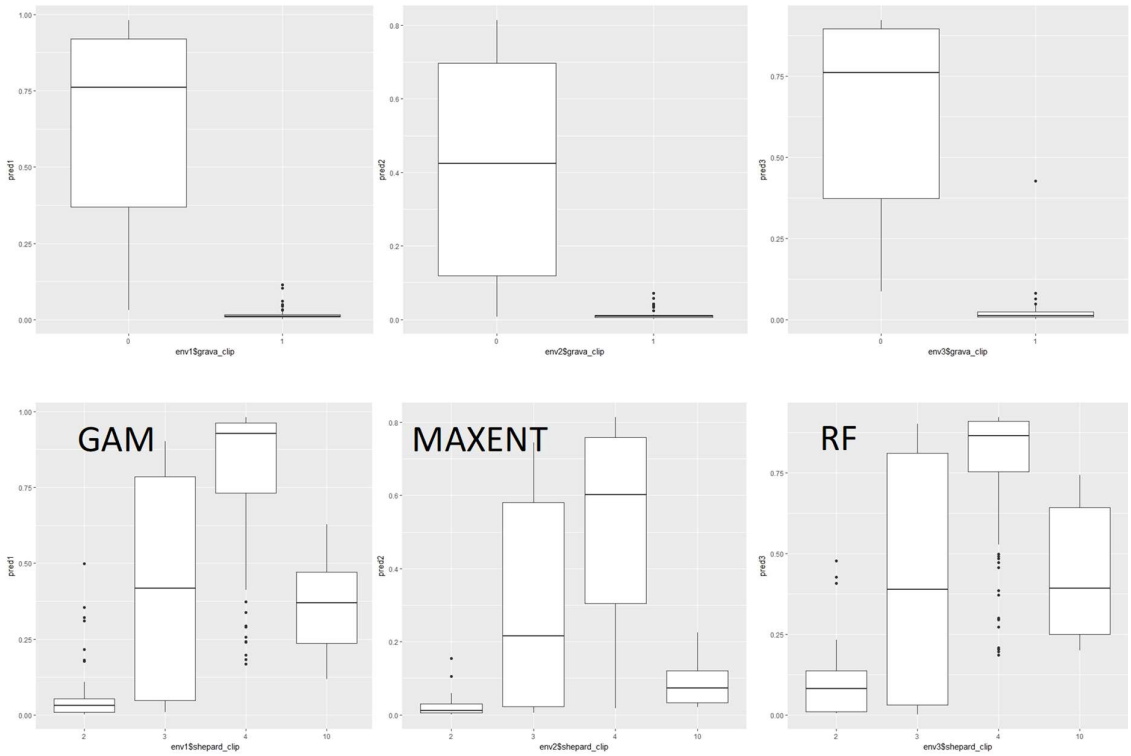

Figure 8 (cont.) Partial GAM, Maxent and Random Forest (left, middle and right plots) for the selected continuous and categorical variables for Pennatula aculeata *(Gravel and Sediment texture).*

Acanella arbuscula

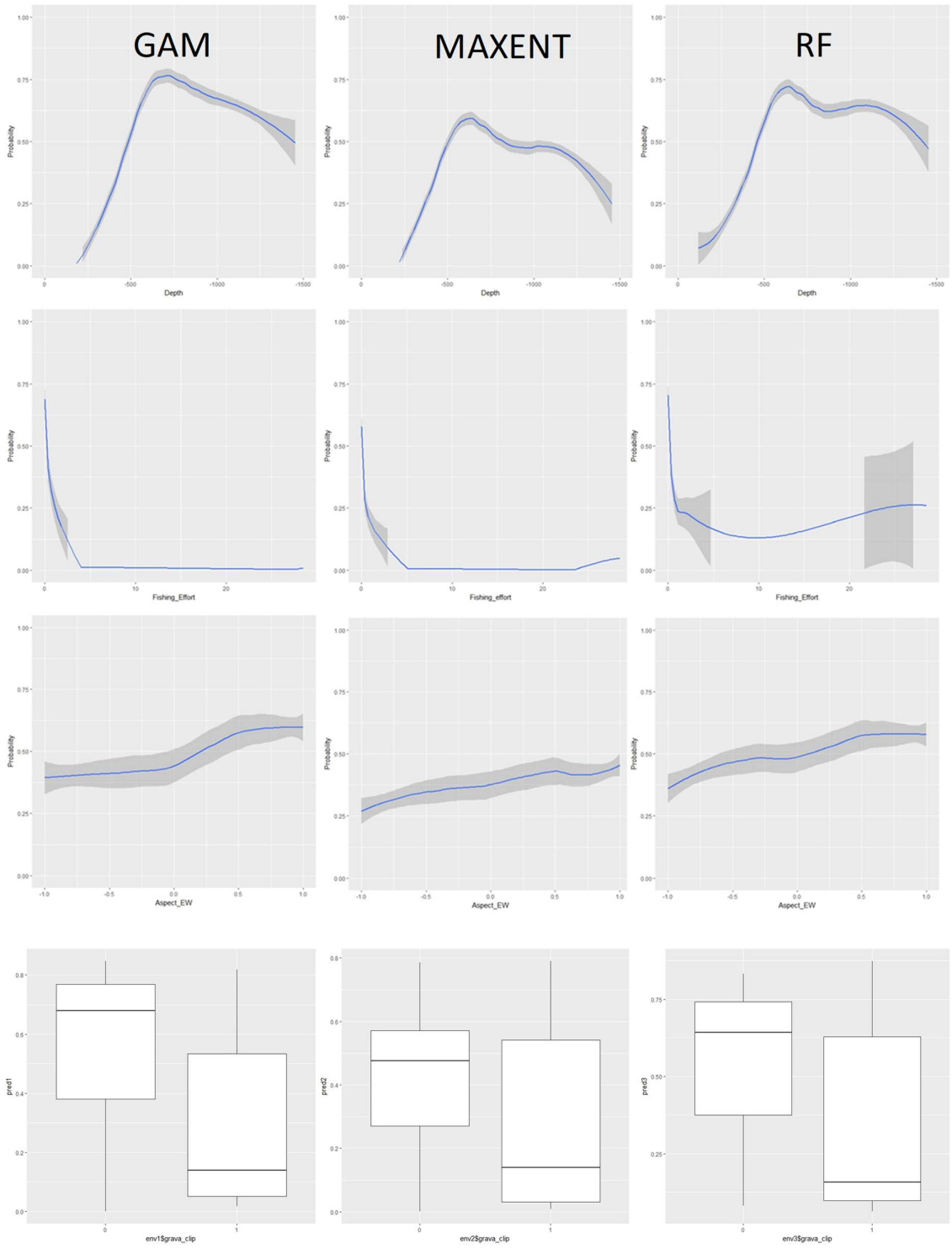

Figure 172. Partial GAM, Maxent and Random Forest (left, middle and right plots) for the selected continuous and categorical variables for Acanella arbuscula *(From top to bottom: Depth, Fishing effort, Aspect component E-W and Gravel). Each plot represents the response variable shape, independent of the other variables, in relation to the probability of the species occurrence. Confidence intervals (95%) around the response curve are shaded in grey.*

Evaluation metrics /statistics

The original dataset was randomly split into two main subsets: a training dataset including 80% of the total observations, and a validation dataset containing the remaining 20% of the data. The relationship between species and the environment was modeled by using the training dataset while the quality of predictions was then evaluated by using the validation dataset. We repeated this procedure 10 times for the best model for each species and results were then averaged over the different random subsets. In particular, five different statistics were used to evaluate the predictive models' performance, such as the receiver-operating characteristic curve (AUC) (Fielding & Bell, 1997), specificity, sensibility, the True Skill Statistic (TSS) (Allouche et al., 2006) and the Pearson's correlation (Table 33).

Table 33. Model prediction performance statistics of the different models assessed the four species. The statistics include the receiver-operating characteristic curve (AUC), specificity (TPR) and sensibility (TNR) proportion, the True Skill Statistic (TSS) and the Pearson's correlation r.

Anthoptilum grandiflorum					
	AUC	**TPR**	**TNR**	**TSS**	***r***
GAM	0.86	0.67	0.69	0.36	0.62
Maxent	0.78	0.95	0.62	0.56	0.66
Random Forest	0.86	0.67	0.69	0.36	0.62
Funiculina quadrangularis					
GAM	0.87	0.68	0.67	0.34	0.60
Maxent	0.80	0.92	0.61	0.53	0.64
Random Forest	0.84	0.67	0.66	0.33	0.61
Pennatula aculeata					
	AUC	**TPR**	**TNR**	**TSS**	***r***
GAM	0.95	0.72	0.69	0.41	0.73
Maxent	0.92	0.79	1	0.79	0.81
Random Forest	0.95	0.74	0.70	0.44	0.80
Acanella arbuscula					
GAM	0.86	0.69	0.66	0.36	0.51
Maxent	0.80	0.9	0.6	0.5	0.61
Random Forest	0.83	0.67	0.65	0.33	0.58

Maps of presence/absence and ensemble models

Anthoptilum grandiflorum

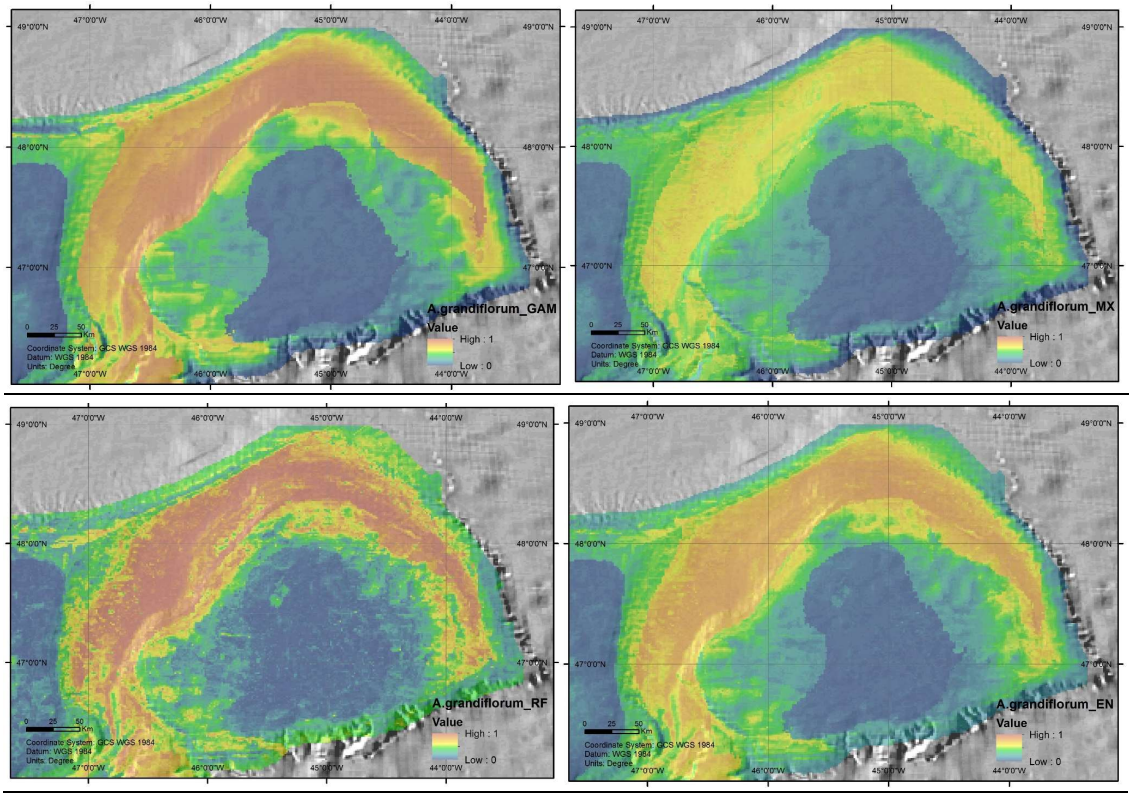

Figure 173. Habitat suitability maps for Anthoptilum grandiflorum *from GAM model (top left); Maxent (MX; top right); Random Forest (RF; bottom left); Ensemble (EN; bottom right).*

The deep-sea pennatulacean coral *Anthoptilum grandiflorum* exhibits a cosmopolitan distribution (Williams, 1990; 1995) and was recently determined to serve as habitat for other invertebrates and fish larvae in the northwest Atlantic (Baillon et al., 2014).

Figure 173 shows the probability of habitat suitability for *Anthoptilum grandiflorum* for the three fitted models and the ensemble one. The GAM selected for its best fit and the selection of variables for the other two models (based on the lowest AIC, higher D2 and significant variables) includes 9 of the 11 environmental variables considered (Depth, Bottom Temperature, Aspect components EW and NS, Slope, Bottom Current Speed, Fishing Effort, Sediment texture and Gravel factors). The resulting model explained 36.3 % of the deviance in *A. grandiflorum* occurrence.

Smooth functions for each of the selected continuous covariates indicated the relative occurrence of *A. grandiflorum* with respect to them (Figure 169). In particular, the species shows a bathymetry optimum between 750-1100 m and a temperature optimum of 3.7 ºC. According to Altuna & Murillo (2012), this species is present in a depth range from 200-1370 m indicating that this species is adapted to live in a wide range of depths.

The shape of the smoother of the Fishing effort highlights a decreasing pattern with respect to the species occurrence (Figure 169).

Gravel seabed was associated with higher estimated probability of occurrence than the reference level (0-10% gravel content). Results showed that category 4 and 10 (sandy silt and clayed silt) of the sediment texture factor were the ones with the highest estimated probability of occurrence for the species with respect to the reference level (category 2 = sand).

According to Maxent model (Figure 174) the environmental variable with highest gain when used in isolation is depth, which therefore appears to have the most useful information by itself. The environmental variable that decreases the gain the most when it is omitted is depth, which therefore appears to have the most information that is not present in the other variables.

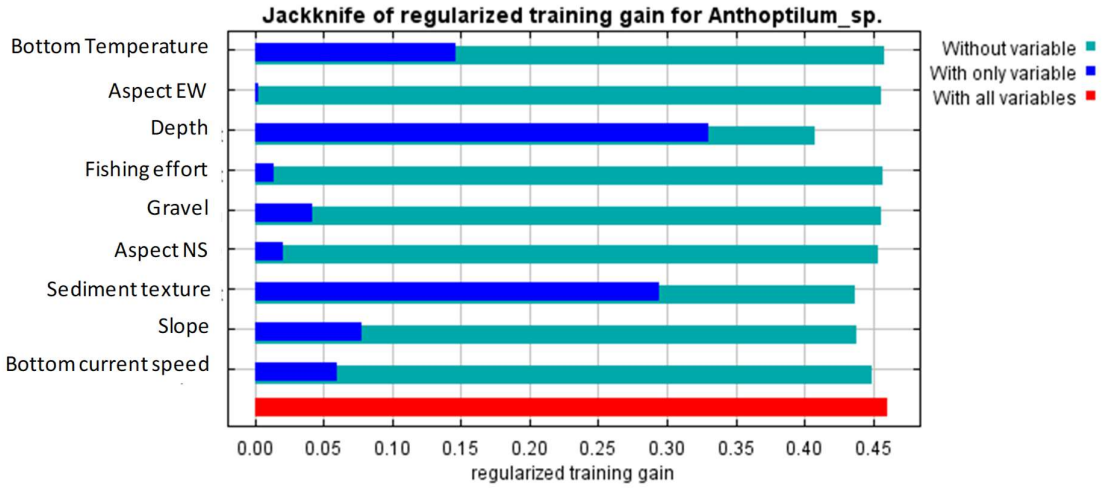

Figure 174. Results of the jackknife test of variable importance or each species training data in Maxent.

In accordance with Random Forest, depth is the most important variable followed by bottom current speed and sediment texture (Figure 175).

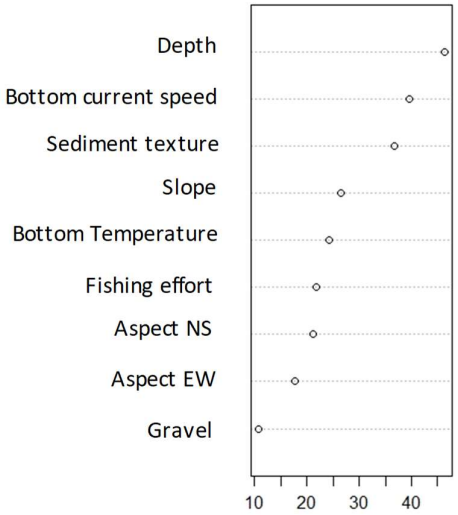

Figure 175. Variable importance in Random Forest, measured as the mean decrease in classification accuracy after permuting the considered variable over all trees.

Funiculina quadrangularis

- 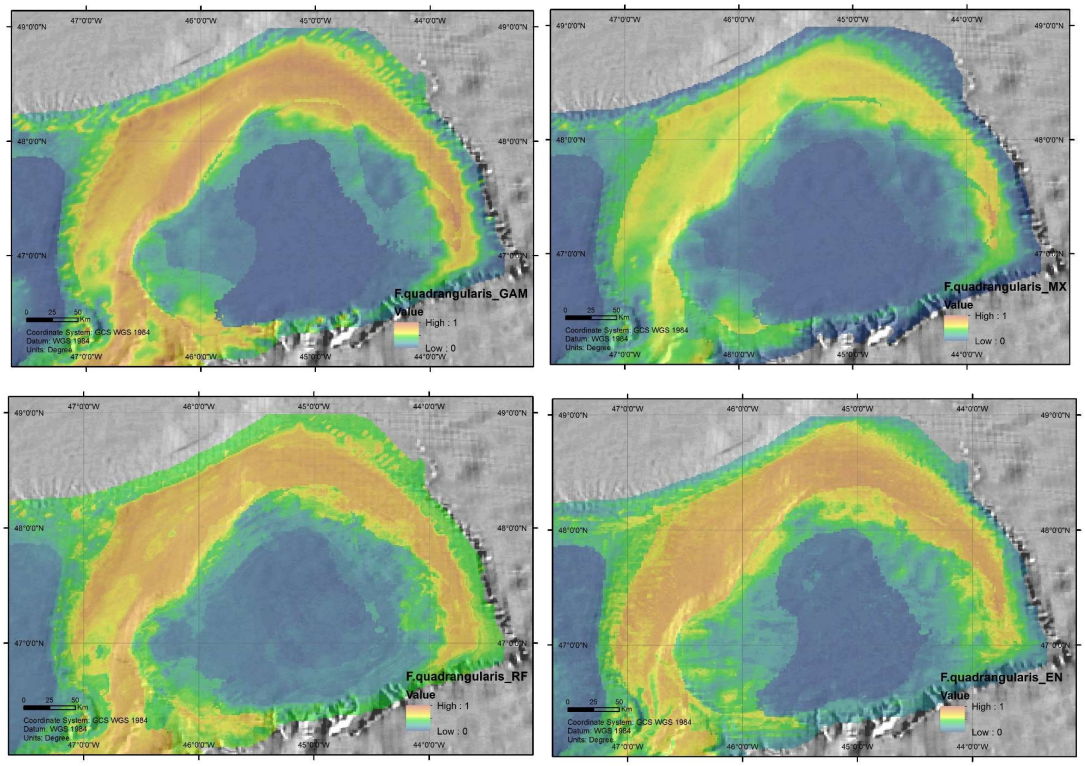

Figure 176. Habitat suitability maps for Funiculina quadrangularis *from GAM model (top left); Maxent (MX; top right); Random Forest (RF; bottom left); Ensemble (EN; bottom right).*

Funiculina quadrangularis has a worldwide range, being common throughout the North Atlantic and the Mediterranean Sea (Manuel, 1981; Gili & Pagès, 1987).

Figure 176 shows the probability of habitat suitability for *Funiculina quadrangularis* for the three fitted models and the ensemble one. The GAM selected for its best fit and the selection of variables for the other two models (based on the lowest AIC, higher D2 and significant variables) includes 5 of the 11 environmental variables considered (Depth, Bottom Temperature, Bottom Current Speed, Sediment texture and Gravel factors). The resulting model explained 33,6 % of the deviance in *Funiculina quadrangularis* occurrence.

Smooth functions for each of the selected continuous covariates indicated the relative occurrence of *F. quadrangularis* with respect to them (Figure 170). In particular, the species shows a bathymetry optimum between 800-1000 m and a temperature optimum of 3.7 ºC. The literature shows that this species appears on a wide bathymetric range from 20 m to depths of over 3000 m (Tixier-Durivault & d'Hondt, 1975; Manuel, 1981; López-González et al., 2001).

The shape of the smoother of the bottom current speed highlights a decreasing pattern with respect to the species occurrence (Figure 170).

Seabeds with the gravel content between 0-10% were associated with higher estimated probability of *F. quadrangularis* occurrence than the ones with gravel content between 10-50%. Among the sediment texture categories the level 4 (Sandy silt) was the one with the highest estimated probability of *F. quadrangularis* occurrence with respect to the reference level (category 2 = Sand). The other sediment texture categories, 3 (Silty sand) and 10 (Clayed silt), also showed higher estimated probabilities than the reference level.

According to Maxent model (Figure 177) the environmental variable with highest gain when used in isolation is Depth, which therefore appears to have the most useful information by itself. The environmental variable that decreases the gain the most when it is omitted is depth, which therefore appears to have the most information that is not present in the other variables.

Figure 177. Results of the jackknife test of variable importance or each species training data in Maxent.

In accordance with Random Forest, depth is the most important variable followed by bottom current speed and sediment texture (Figure 178).

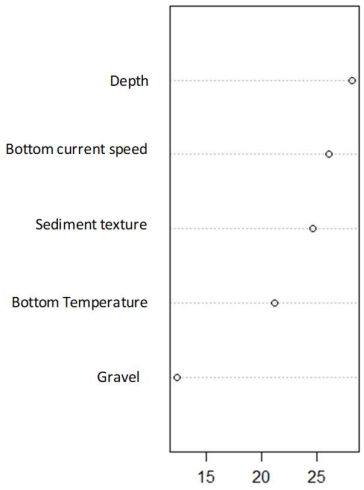

Figure 178. Variable importance in Random Forest, measured as the mean decrease in classification accuracy after permuting the considered variable over all trees.

Pennatula aculeata

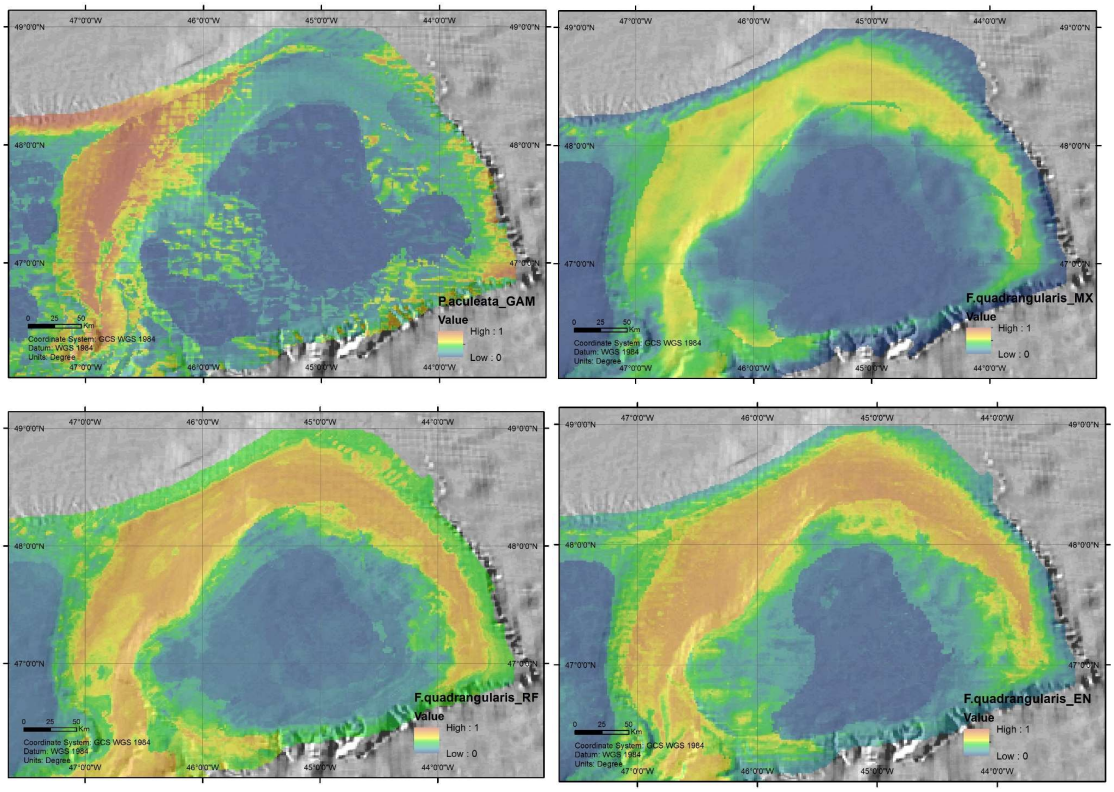

Figure 179. Habitat suitability maps for Pennatula aculeata *from GAM model (top left); Maxent (MX; top right); Random Forest (RF; bottom left); Ensemble (EN; bottom right).*

Figure 179 shows the probability of habitat suitability for *Pennatula aculeata* for the three fitted models and the ensemble one. The GAM selected for its best fit and the selection of variables for the other two models (based on the lowest AIC, higher D2 and significant variables) includes 5 of the 11 environmental variables considered (Mixed layer depth, Aspect N-S, Sediment texture and Gravel factors and Bottom current speed). The resulting model explained 49,9 % of the deviance in *P. aculeata* occurrence.

For *P. aculeata* mixed layer depth was the variable most significant for the three models in combination with bottom current speed in Maxent (Figure 180) and Random Forest (Figure 181) and with Aspect component N-S in the GAM model. The shape of the smoother of the Mixed layer depth highlights an increasing pattern with respect to the species occurrence. As for other pennatulanceans, this species requires a considerable bottom current for procuring food. The response curve for this variable shows this detail, showing an increase pattern until reaching an optimum value on approximately 0,75 m/s. The relationship with mixed layer depth and aspect need to be studied in more detail but it has a sense that these variables were important in their distribution pattern of this species as it is related to the circulation pattern and therefore in the food availability for a passive suspension feeder species.

Gravel seabed (category 1) was associated with lower estimated probability of occurrence than low values on gravel content (category 0: 0-10% gravel content). The sediment texture layer confirms it, where results showed that category 4 (sandy silt) of the sediment texture factor was the one with the highest estimated probability of occurrence for the species followed by the category 3 (Silty sand). These results corroborate their preference for muddy substrata as it was cited in previous studies (Ruiz-Pico et al., 2017).

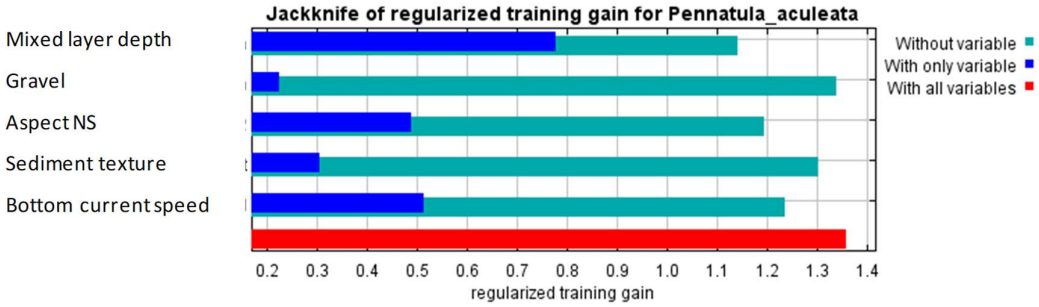

Figure 180. Results of the jackknife test of variable importance or each species training data in Maxent.

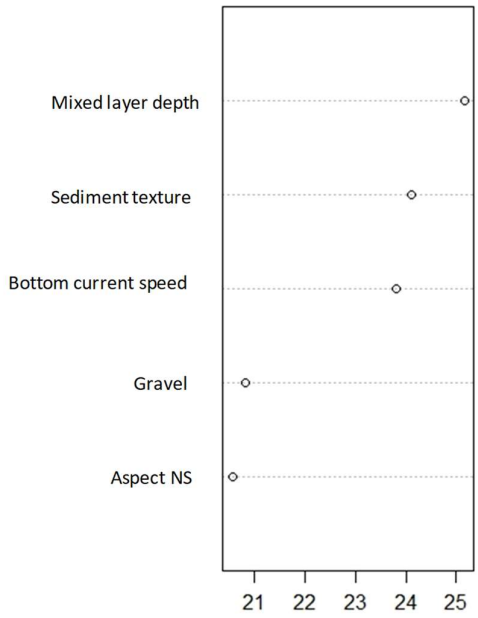

Figure 181. Variable importance in Random Forest, measured as the mean decrease in classification accuracy after permuting the considered variable over all trees.

Acanella arbuscula

Figure 182 shows the probability of habitat suitability for *Acanella arbuscula* for the three fitted models and the ensemble one. The GAM selected for its best fit and the selection of variables for the other two models (based on the lowest AIC, higher D2 and significant variables) includes 4 of the 11 environmental variables considered (bathymetry, aspect E-W, fishing effort and gravel factors). The resulting model explained 29,9 % of the deviance in *A. arbuscula* occurrence.

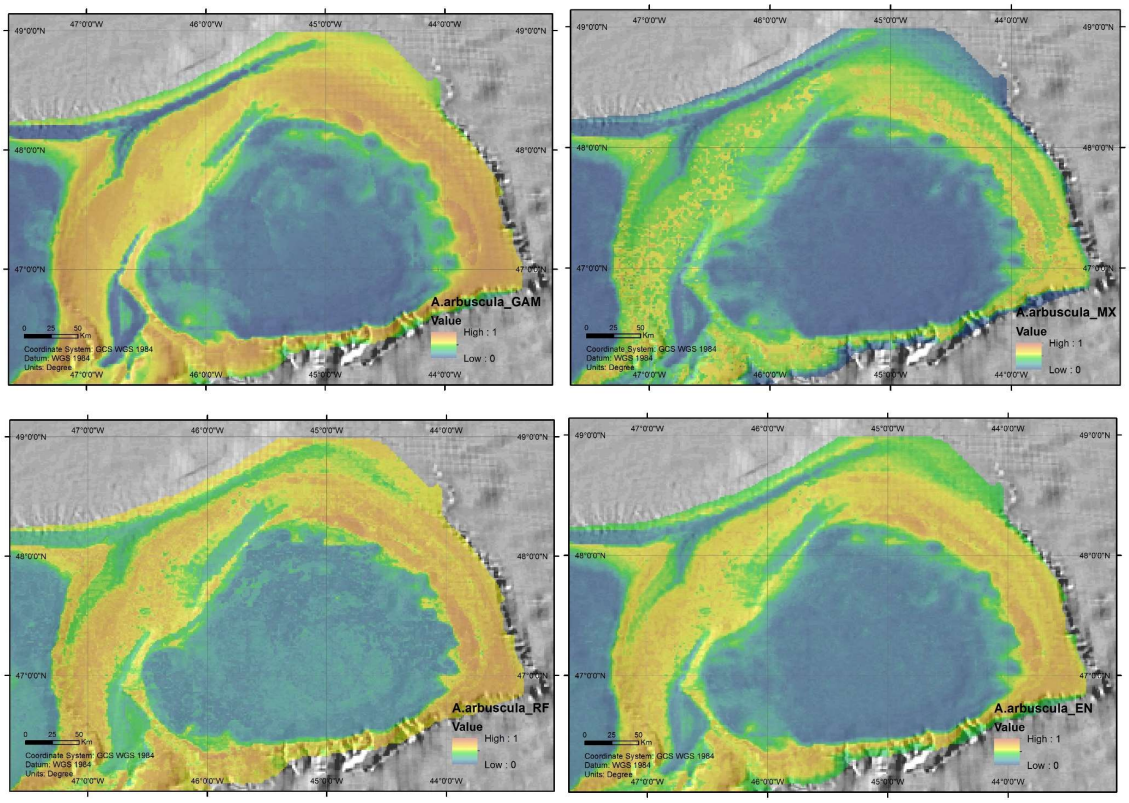

Figure 182. Habitat suitability maps for Acanella arbuscula *from GAM model (top left); Maxent (MX; top right); Random Forest (RF; bottom left); Ensemble (EN; bottom right).*

For *A. arbuscula,* depth was the variable most significant for the three models, following by the fishing effort layer (Figure 183, Figure 184). In particular, the species shows a bathymetry optimum between 600-700 m with a decreasing pattern with respect to the increase of the fishing effort (Figure 172). This small gorgonian with a stiff but delicate skeleton was cited before as vulnerable to bottom fishing gear (Beazley & Kenchington, 2012) and therefore the aforementioned negative effect of the fishing effort on their distribution corroborate it.

Gravel factor had also effect in their distribution and we have found a preference for a substrate with a major gravel content (category 1) as show the response curve of this variable in Figure 9. Thus, the species that had been previously described as having root-like holdfasts (Edinger et al., 2011) may can be fixed better to this type of substrate.

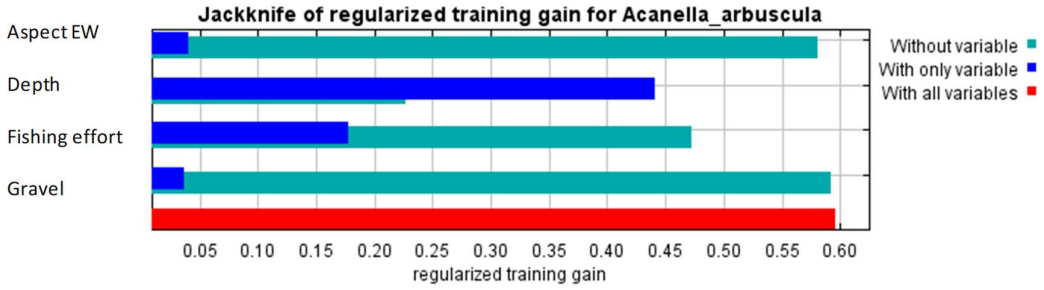

Figure 183. Results of the jackknife test of variable importance or each species training data in Maxent.

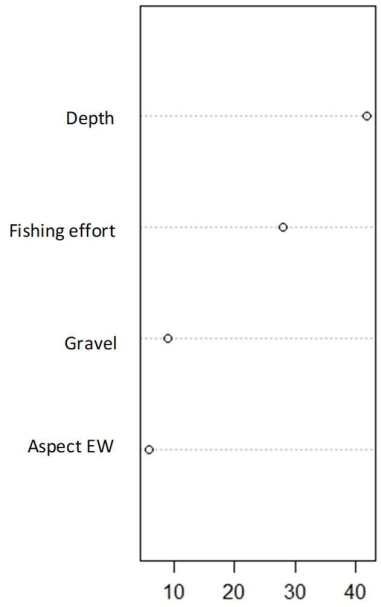

Figure 184. Variable importance for Random Forest, measured as the mean decrease in classification accuracy after permuting the considered variable over all trees.

3.10.7 Model interpretation, caveats and future directions

The present work attempted to provide a picture of four vulnerable marine species distribution in the Flemish Cap and Flemish Pass areas. This work should be considered as an approach for the creation of VME species maps and species distribution models. These outputs will be used to improve the understanding of habitat requirements of three different deep sea pen corals (*Anthoptilum grandiflorum*, *Funiculina quadrangularis* and *Pennatula aculeata*) and the deep-sea bamboo coral *Acanella arbuscula* in the Flemish Cap and Flemish Pass areas.

The work carried out demonstrated that all the algorithms developed proved capable of successfully predicting the species selected. All models, with the exception of Maxent for *A. grandiflorum*, achieved AUC values greater than 0.80, which indicates a good degree of discrimination between

those locations where sea pens are present and those where sea pens are absent. According to AUC values, the most accurate model for the four species was GAM together with Random Forest for *Anthoptilum grandiflorum*. On the other hand, Maxent obtained greater values in the other four statistics to evaluate the predictive models' performance in most cases (specificity, sensibility, TSS and the Pearson's correlation). Performing the ensemble predictions of all models is a way of reducing uncertainty in species distribution modelling allowing to obtain a more accurate map.

The predicted extents and the environmental variables contribution of the four species studied in this work were briefly explained above due to differences in their variables importance that can be linked to the autecology of each species.

The work sets a baseline for future analysis and mapping of different VMEs in this area. Each one of the models (GAM, Maxent and Random Forest) have different data requirements and mathematical algorithms. They can produce clearly different geographic predictions even when using the same data.

In order to increase the accuracy of habitat suitability models predictions, more detailed studies should be done including new explanatory variables and testing different resolutions to select the most appropriate for the different species. For example, the fishing effort layer used in this work was calculated using VMS data from 2008-2014. This could be improved by adding more VMS data years and also by creating fisheries-specific layers by linking VMS with logbook data.

Moreover, inclusion of biomass species data in the models could be implemented in order to produce abundance models that could be more suitable for management measures contributing to a better conservation of vulnerable species.

3.11 Case study 12: Habitat suitability models for the framework-forming deep-sea coral *Lophelia pertusa* in the Florida-Hatteras slope

Erik Cordes[1], Ryan Gasbarro[1]

1- Department of Biology, Temple University, Philadelphia, USA

3.11.1 Case study description

This model was developed to predict areas containing suitable habitat for the framework-forming deep-sea coral *Lophelia pertusa* off the southeastern coast of the United States (30-35° N; 75-81° W). Newly collected data from the summer of 2018 from three sites on a deep contiguous reef structure (Cordes et al., in prep) was combined with known *L. pertusa* occurrences retrieved from NOAA's Deep Sea Coral Research & Technology Program (DSCRTP) database. Suitable *L. pertusa* habitat was modelled using terrain variables derived from bathymetry and a Maximum Entropy (Maxent) approach.

3.11.2 Species selection

The deep-sea scleractinian coral *Lophelia pertusa* is a common species on continental slopes of south-western US margins (Reed et al., 2006; Brooke et al., 2013), providing important structural habitat for fish and other megafauna communities (Sulak et al., 2007; Lessard-Pilon et al., 2010). However, the distribution of this VME indicator species is not very well resolved in the Florida-Hatteras Slope region between Lookout (North Carolina) and the Cape Canaveral (Florida).

3.11.3 Species occurrence data sources

Lophelia pertusa presence data were downloaded from NOAA's Deep-Sea Coral Research & Technology (DSCRT) data portal. Points were excluded from analyses if location accuracy was greater than 1000 m; this generally excluded older, less reliable records that likely have lower fidelity to current distributions, and therefore, to gridded environmental data. The final dataset included 339 georeferenced records of *L. pertusa* presence. Additional *L. pertusa* presence points were generated per second of video from three submersible dives completed in the summer of 2018 on the R/V Atlantis (dives AL4962, AL4963) and the NOAA Ship Okeanos Explorer (dive EX1806-7). This created a dataset of 9854 presence points; this number was greatly reduced during the Maxent modeling

process, where only a maximum of one presence point is retained per grid cell to reduce spatial autocorrelation.

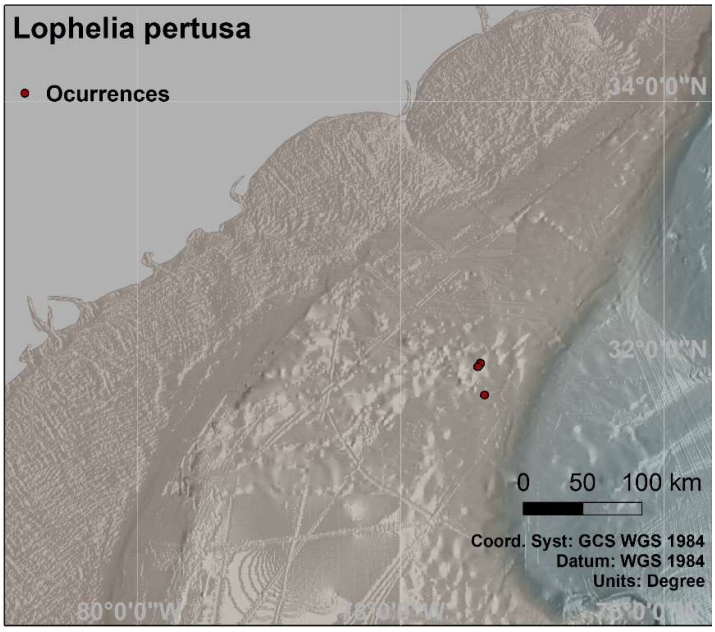

Figure 185. Map showing the location of the presence data records used in the Maxent species distribution model for Lophelia pertusa *in the Florida-Hatteras slope case study area*.

3.11.4 Environmental data layers

Predictions of suitable habitat for *L. pertusa* were based on a set of terrain variables. Terrain variables used were extracted or derived from the most recent version of the General Bathymetric Chart of the Oceans (GEBCO_2019), which provides a 15 arc-second global grid of elevations (cell size of 0.004°). Derived variables were computed from the bathymetric grid and included slope, statistical aspect (both north-south and east-west; i.e. sine and cosine), Terrain Ruggedness Index (TRI), broad and fine Benthic Position Index (BPI), curvature, plan curvature and profile curvature. Broad BPI was calculated with an inner radius of 3 and an outer radius of 25 while fine BPI was calculated with an inner radius of 2 and an outer radius of 4. The two BPI grids were standardized so their units are comparable using Benthic Terrain Modeler version 3.0. Terrain ruggedness was calculated using a neighbourhood size of 3.

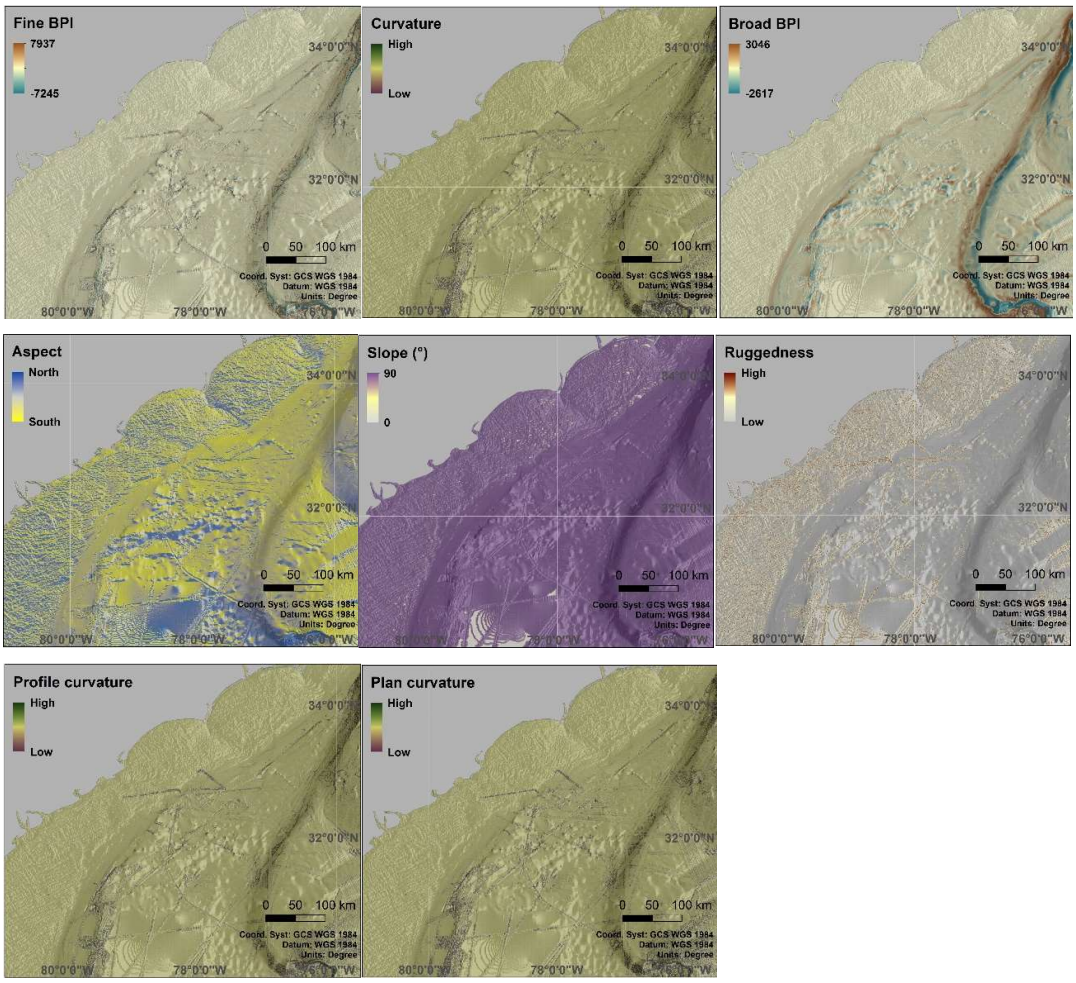

Figure 186. Terrain variable used to develop the Maxent species distribution model for Lophelia pertusa *in the Florida-Hatteras slope case study area.*

3.11.5 Modelling approaches

The maximum entropy model (Maxent version 3.4.0; Phillips et al., 2017) was used to predict the habitat suitability of *L. pertrusa* in the Florida-Hatteras Slope case study area. Maxent was selected as the modelling technique due to the nature of the data obtained; i.e. presence-only records. Maxent has been shown to be a reliable modelling tool for predicting changes in species distribution under climate change scenarios (Ashford et al., 2014; Beaumont et al., 2016; Morán-Ordóñez et al., 2017). Model outputs provided an estimate of probability of presence of each species between 0 and 1. Response curves for each predictor variable were generated together with jack-knife estimates of the relative contribution of each of the environmental predictors to the model output.

3.11.6 Model outputs

The Maxent model achieved good performance and was able to define suitable habitats better than random (AUC= 0.96). In general, terrain variables slope, aspect (sine), ruggedness, and fine BPI provided the highest contributions to the predictive models, broad BPI and aspect (cosine) were also relatively important. The response curves of these variables are shown in Figure 187. The predicted suitable habitat for *L. pertusa* was higher in the continental slopes between 200 and 800m depth. However, the predicted distribution seems to be highly related with the quality of the bathymetry data (Figure 188).

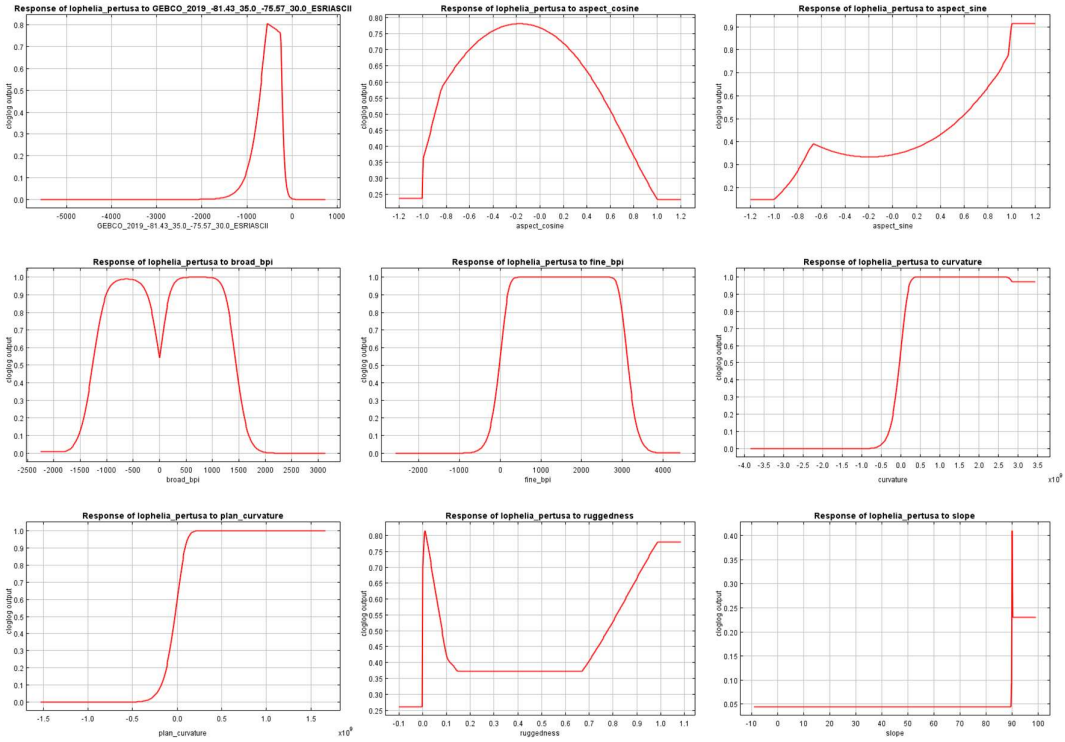

Figure 187. Responses curves of the most important predictors in the Maxent species distribution model for Lophelia pertusa *in the Florida-Hatteras slope case study area.*

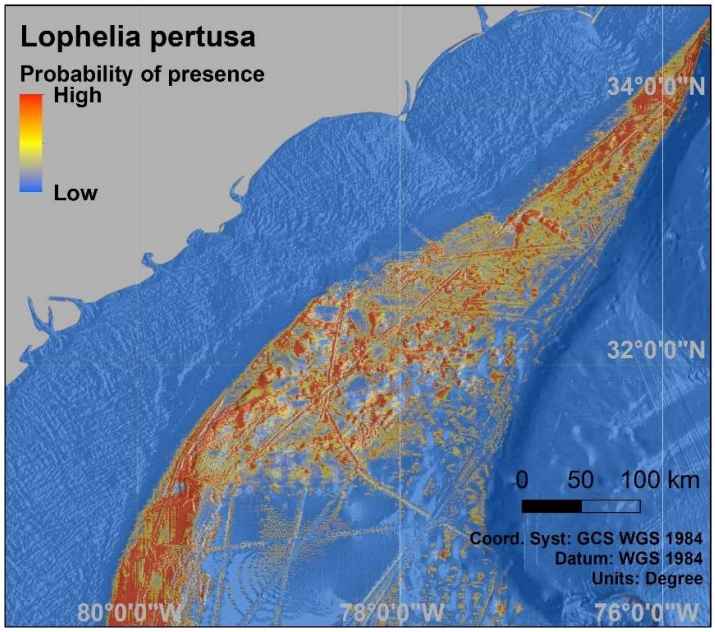

Figure 188. Habitat suitability index obtained from the Maxent species distribution model for Lophelia pertusa *in the Florida-Hatteras slope case study area.*

3.11.7 Model interpretation, caveats and future directions

Large expanses of suitable habitat were identified in this model, and the addition of new data from three submersible dives changes our perception of the realized niche of this abundant habitat-engineering species. However, the overall resolution of the bathymetry at large regional scales remains coarse; therefore, some habitat features (e.g. coral mounds, submarine canyons) potentially containing dense *L. pertusa* may have been overlooked by this model. In addition, some variables were likely correlated (e.g. terrain ruggedness and aspect/slope), but Maxent models are generally robust to predictor covariation. Incorporation of oceanographic variables (export carbon flux, dissolved oxygen, etc.) would help to improve predictions made by this model.

3.12 Case study 13: Small scale predictive model a sponge species in a Tropic Seamount under current environmental conditions

Berta Ramiro-Sánchez[1*], José Manuel González-Irusta[2,3], Lea-Anne Henry[1], Jason Cleland[1], Isobel Yeo[4], Joana R. Xavier[5,6], Marina Carreiro-Silva[2,3], Íris Sampaio[3,7], Jeremy Spearman[8], Lissette Victorero[4,9,10,11], Charles G. Messing[12], Georgios Kazanidis[1], J. Murray Roberts[1], Bramley Murton[4]

1- The University of Edinburgh, School of GeoSciences, Edinburgh EH9 3FE, United Kingdom
2- OKEANOS Center, Faculty of Science and Technology, University of the Azores, Horta, Portugal
3- Instituto do Mar, Marine and Environmental Sciences Centre, Universidade dos Açores, Portugal
4- National Oceanography Centre, Southampton SO14 3ZH, United Kingdom
5- CIIMAR – Interdisciplinary Centre of Marine and Environmental Research of the University of Porto, 4450-208 Matosinhos, Portugal
6- University of Bergen, Department of Biological Sciences and KG Jebsen Centre for Deep-Sea Research, 5006 Bergen, Norway
7- Senckenberg am Meer, Abteilung Meeresforschung, Südstrand 40, 26382, Wilhelmshaven, Germany
8- HR Wallingford Ltd, Wallingford OX10 8BA, United Kingdom
9- Institut de Systématique, Évolution, Biodiversité (ISYEB), CNRS, Muséum National d'Histoire Naturelle, Sorbonne Université, École Pratique des Hautes Études, 75005 Paris, France
10- Biologie des Organismes et Ecosystèmes Aquatiques (BOREA), CNRS, Muséum national d'Histoire naturelle, Sorbonne Université, Université de Caen Normandie, Université des Antilles, IRD, 75005 Paris, France
11- Centre d'Écologie et des Sciences de la Conservation (CESCO), CNRS, Muséum national d'Histoire naturelle, Sorbonne Université, 75005 Paris, France
12- Nova Southeastern University, Department of Marine and Environmental Sciences, Dania Beach, Florida 33004, United States

3.12.1 Case study description

Ferromanganese crusts occurring on seamounts are a potential resource for scarce elements such as cobalt, tellurium and rare earth elements that are critical for low-carbon technologies. Seamounts, however, frequently host Vulnerable Marine Ecosystems (VMEs), including cold-water coral gardens and sponge grounds, which means that spatial management is needed to address potential conflicts between mineral extraction and the conservation of deep-sea biodiversity. Exploration of the Tropic Seamount, located in an Area Beyond National Jurisdiction (ABNJ) in the subtropical North Atlantic, revealed large amounts of Rare Earth Elements, as well as numerous VMEs, including high-density octocoral gardens, *Solenosmilia variabilis* patch reefs, xenophyophores, crinoid fields and deep-sea sponge grounds.

This study focuses on the extensive monospecific grounds of the hexactinellid sponge *Poliopogon amadou* Thomson, 1878. Deep-sea sponge grounds provide structurally complex habitat for many seafloor ecosystems and augment local biodiversity. To understand the potential extent of these sponge grounds and inform spatial management, we produced the first ensemble species distribution

model and local habitat suitability maps for *P. amadou* in the Atlantic employing Maximum Entropy (Maxent), General Additive Models (GAMs), and Random Forest (RF). The lack of significant differences in model performance permitted to merge all predictions using an ensemble model approach. Our results contribute towards understanding the environmental drivers and biogeography of the species in the Atlantic. Furthermore, we present a case towards designating the Tropic Seamount as an Ecologically or Biologically Significant marine Area (EBSA) as a contribution to address biodiversity conservation in ABNJ.

3.12.2 Species selection

The Tropic Seamount revealed numerous VMEs, including high-density octocoral gardens, *Solenosmilia variabilis* patch reefs, xenophyophores, crinoid fields and deep-sea sponge grounds. The sponge *Poliopogon amadou* was one the most commonly observed habitat-forming VME indicator species in the study area, forming extensive monospecific sponge grounds and hence the focus of the study. Deep-sea sponge grounds provide structurally complex habitat for many seafloor ecosystems and augment local biodiversity and hence the focus of this study.

3.12.3 Species occurrence data sources

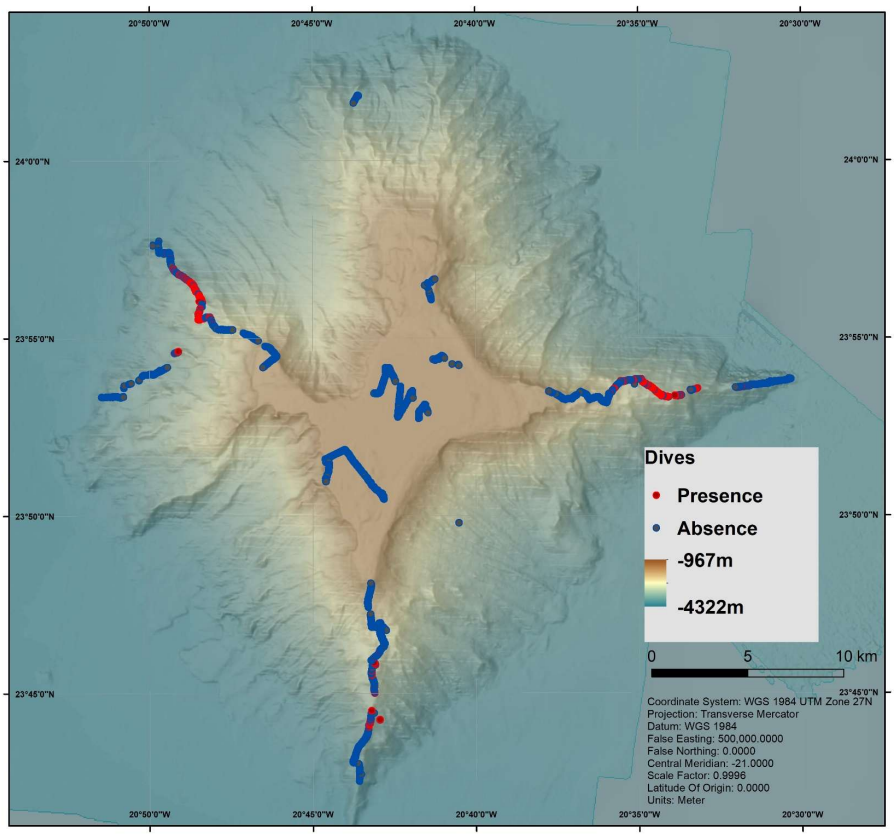

Figure 189. Map of species occurrence (presence / absence) and bathymetry (depth in m).

3.12.4 Environmental data layers

Data sources, oceanographic models, etc.

Multibeam echosounder and backscatter data were acquired using the ship mounted Kongsberg EM122. Processing was done using Caris HIPS and SIPS for the bathymetry and the QPS FM Geocoder Toolbox v7.6.3 for the backscatter. Final grids and mosaics were produced with a grid spacing of 50m. This resolution was applied in the distribution models after resampling (if needed) all the environmental variables used for the analysis. Acoustic backscatter strength measured the acoustic energy reflected back from the seafloor and is itself a function of slope, acoustic hardness and seafloor roughness. For flat seafloor, it can be considered a proxy for substrate type. High backscatter seafloor represents hard substratum while low reflectivity typically indicates soft-sediment. Substrate type influences the distribution of benthic organisms, and previous studies have related backscatter intensity to the distribution of sponges and other deep-sea species (e.g., González-Irusta et al., 2015; Rowden et al., 2017). A set of additional seafloor variables was derived from the bathymetric data, as quantitative seabed descriptors, using the terrain function in the R package 'raster' and the Benthic Terrain Model tool in ArcGIS 10.1 (ESRI, 2015). These variables were Aspect (measured in terms of northness and eastness), Slope, Roughness, and fine (3/25 radius) and broad-scale (25/250 radius) Bathymetric Position Index (BPI).

Mooring data together with CTD casts were used to produce a hydrodynamic model of the seamount(Cooper and Spearman, 2017). Model simulations were used to obtain the maximum near-bed velocity of currents (at 1 m above the bed) to include in the distribution models. The current information was derived at a variable resolution from 500 to 600 m, changing across the study area. The layer was then interpolated (using ordinary kriging) to the same resolution as the bathymetric data and rest of the variables using the function "krige" from the 'gstat' package(Pebesma, 2004).

Spatial resolution used

A 50 x 50 m cell resolution was used.

Variable selection methodology

Before starting data analysis, collinearity between variables was checked using Spearman's rank correlation coefficient and the Variance Inflation Factors (VIFs) (Zuur et al., 2009). Roughness and broad-scale BPI were highly correlated with slope and depth, respectively (Spearman's rank correlation values > 0.7 and VIFs > 3) and were removed from the analysis. Consequently, seven variables were retained for the construction of the models to explore the factors controlling the

distribution of P. *amadou*: water depth, slope, fine-scale BPI, eastness, northness, backscatter and maximum current speed (Figure 2).

The variable selection differed for each algorithm. Maxent was fitted using all the variables previously selected after checking for collinearity, whereas for GAMs the variable selection was performed using the Akaike Information Criteria (AIC) and the function “dredge” from the package ‘MuMIn’(Barton, 2018). For Random Forest the function “VSURF” from the package ‘VSURF’ (Genuer et al., 2010) was used to select the variables.

Maps of environmental layers

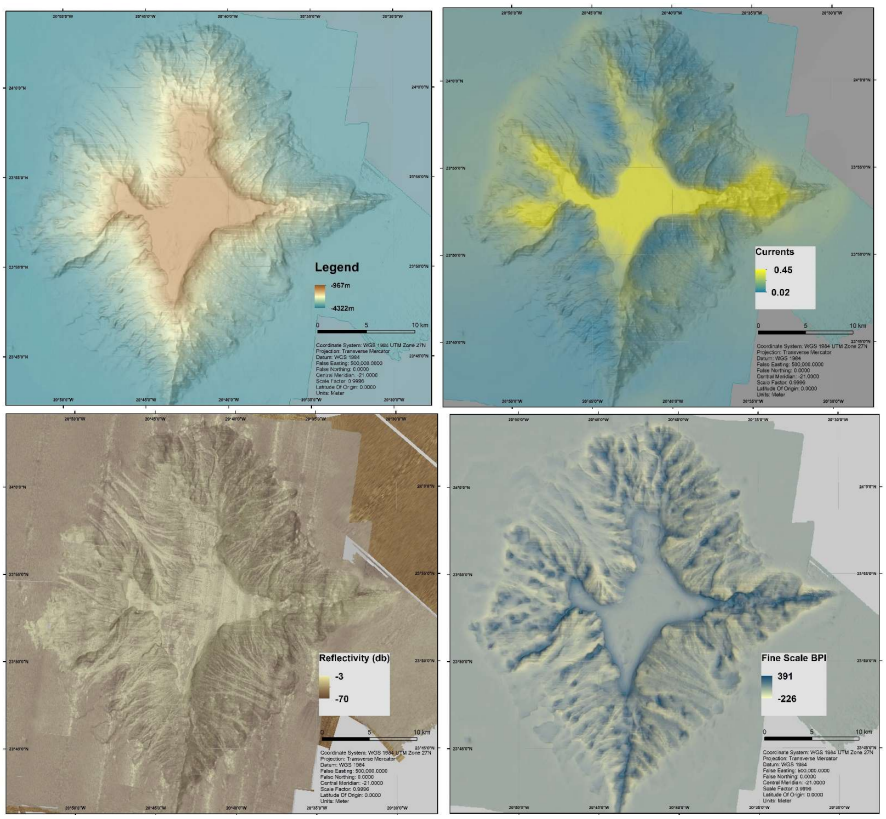

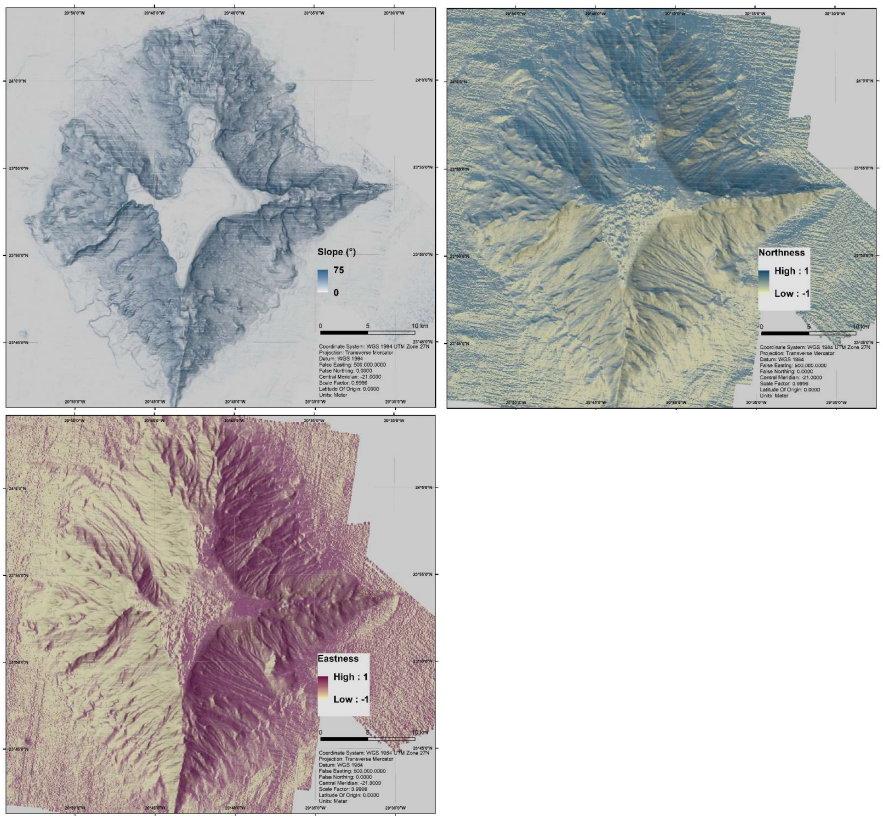

Figure 190. Maps of environmental variables used (left to right and top to bottom: depth, currents, reflectivity, fine BPI, slope, northness, and eastness)

3.12.5 Modelling approaches

The distribution of *P. amadou* at Tropic Seamount was modelled using three algorithms widely used in species distribution modelling (González-Irusta et al., 2015): Maxent(Phillips et al., 2006), GAMs (Hastie & Tibshirani, 1986) and Random Forest (Breiman, 2001) using R (R Development Core Team, 2018).

An ensemble of all models as the weighted average of the GAM, Maxent and RF models (after Oppel et al., 2012; Anderson et al., 2016; Rowden et al., 2017) was calculated, which integrated the spatial uncertainty of each of the three models in the estimation. Confidence levels for the prediction of each modelling approach were addressed using a bootstrap technique following Anderson et al. (2016) and Rowden et al. (2017).

3.12.6 Model outputs

Responses curves

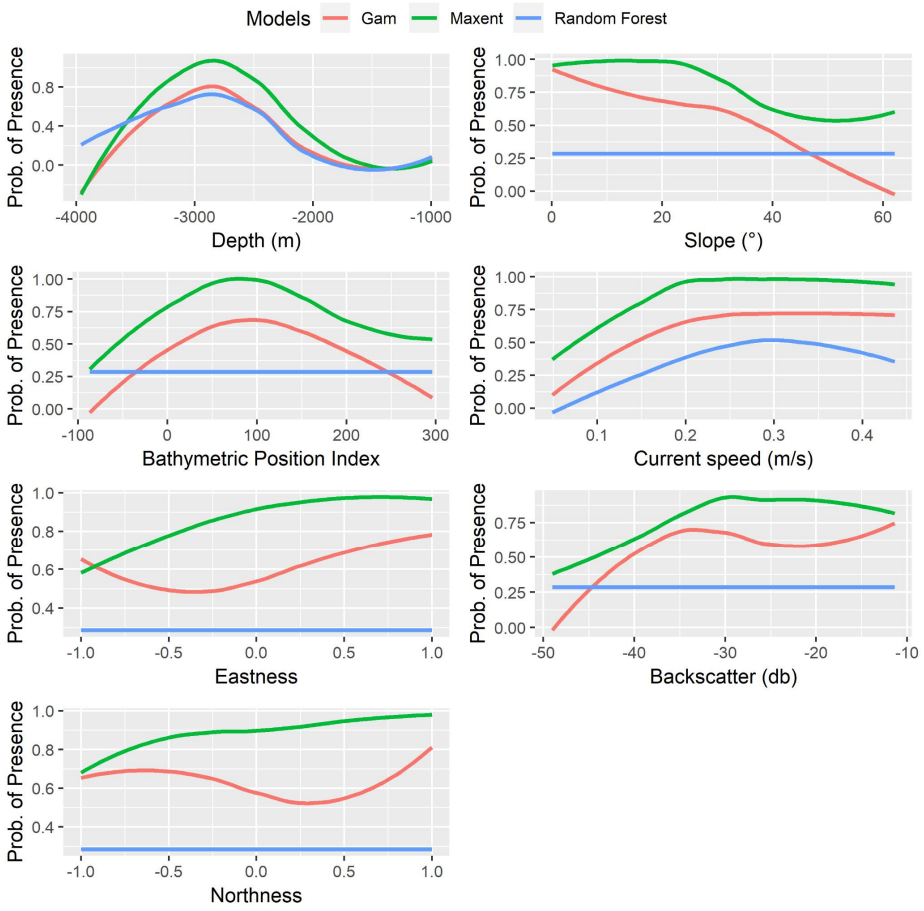

Figure 191. Response curves of the environmental variables from the different models

Evaluation metrics /statistics

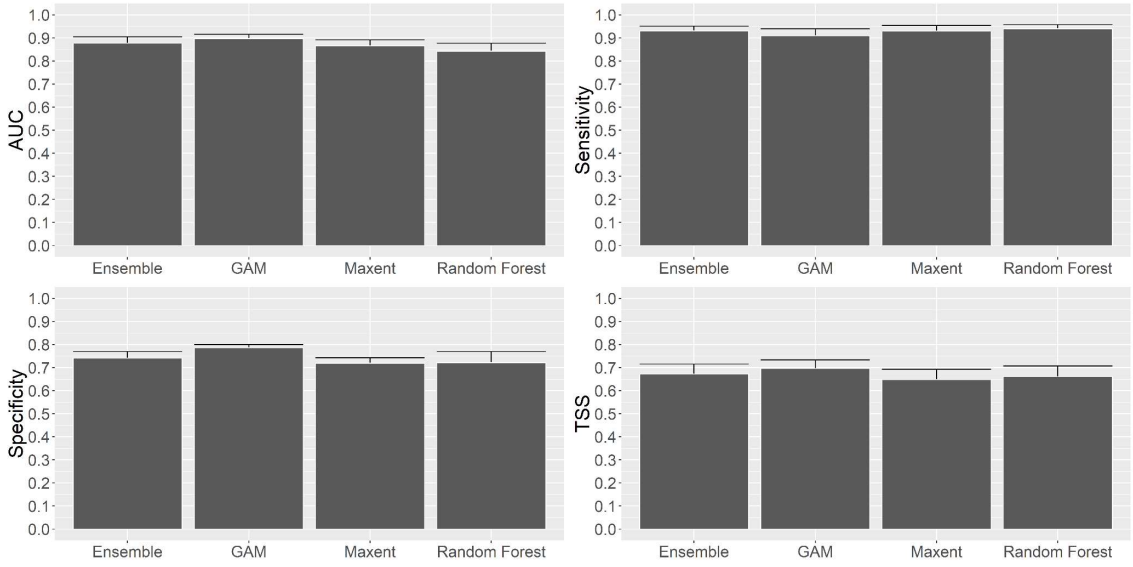

Figure 192. Evaluation metrics (AUC, sensitivity, specificity and TSS) of the different models.

Maps of presence/absence

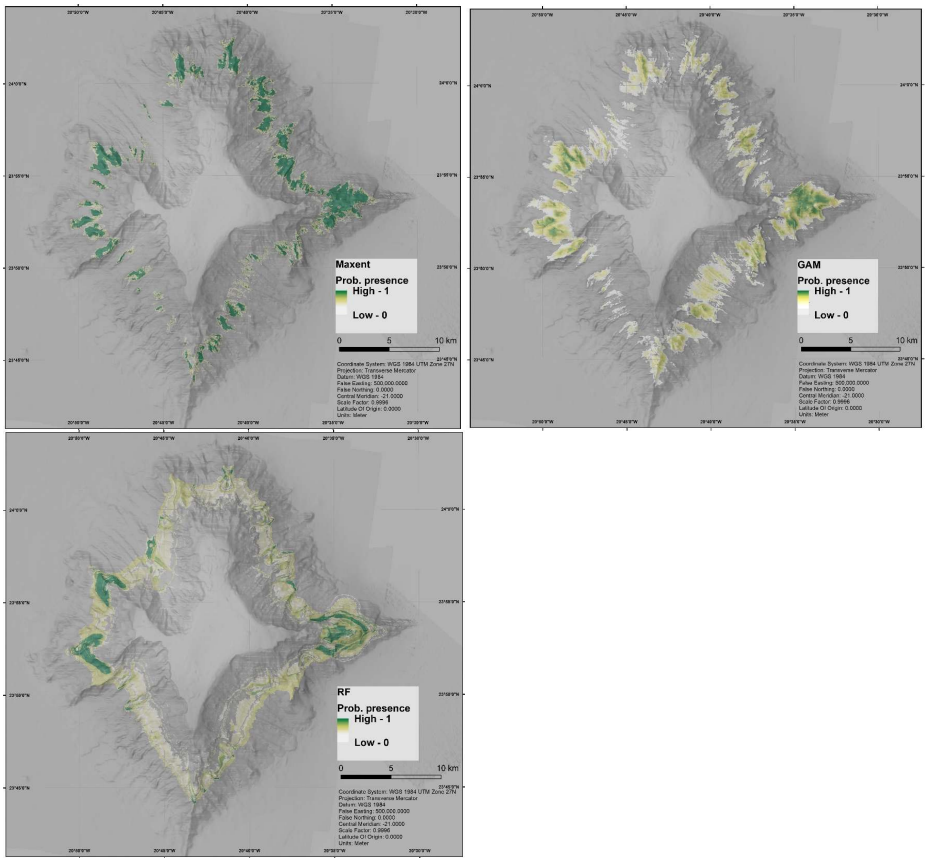

Figure 193. Maps of probability of presence from the Maxent model (top left), GAM model (top right), and Random Forest (RF) model (bottom left).

Maps of the ensemble model and model uncertainty

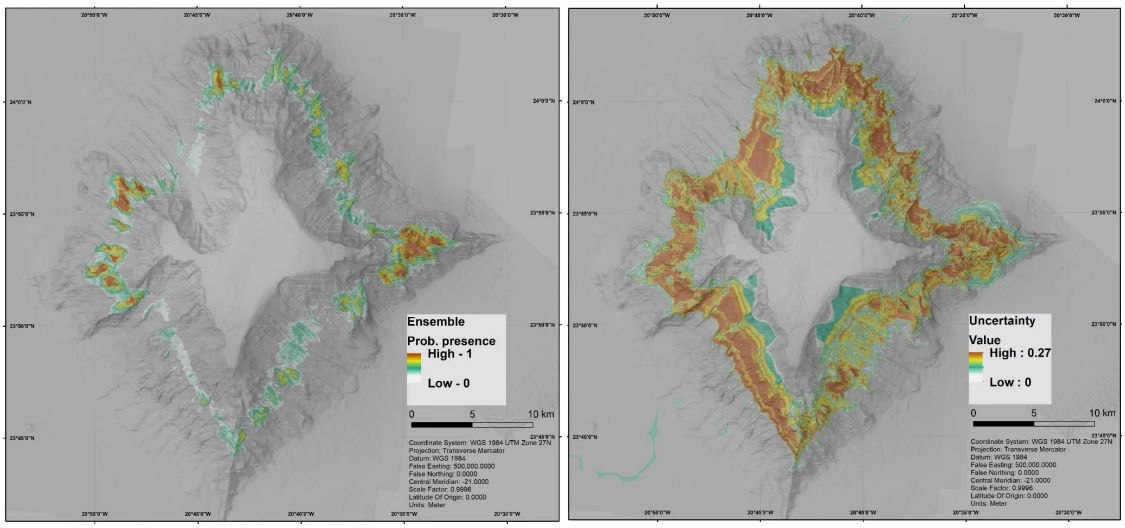

Figure 194. Map of the probability of presence from the ensemble model: mean (left), and standard deviation (right).

3.12.7 Model interpretation, caveats and future directions

The three models used to predict the distribution of *P. amadou* showed good performance, with no significant differences between them for any of the statistics analysed. The three models predicted the highest probability of presence of the sponge on the eastern and western ridges and certain patches on the northern spur. The selection of the variables in the model construction was the main driver of the differences found among the models, namely on the areas where data were not available. Random Forest was built using only two variables (depth and maximum current speed), whereas GAM and Maxent also included the rest of the environmental variables (backscatter, fine-scale BPI, slope, eastness and northness). The inclusion of these other variables in the model construction of GAM and Maxent allowed us to take into account microscale effects related to the geomorphology of the seabed. This resulted in less-broad predictions across the depth band suitable for *P. amadou* than the Random Forest probabilities. The differences are especially clear in the southwest slope of the seamount, mainly unsuitable for the GAM and Maxent prediction, but suitable for Random Forest. Despite the inclusion of these variables in the construction of the models, GAM and Maxent did not show statistically significant differences in any of the evaluation statistics and therefore the RF model was retained for the ensemble forecast, although its impact in the final ensemble model was weighted by the results of the evaluation process.

The library used in the variable selection for the RF model could have driven the main differences between the models. The library 'VSURF' for RF models selected only depth and currents as predictors, and this was reflected in the output of the RF model which displayed a continuous bathymetric belt of probability of presence for *P. amadou* on the seamount. Other methodologies for RF variable selection are available and it would be interesting to see how the selection process results would differ. This highlights the usefulness of ensemble models, which average all model outputs and so take into account uncertainties and performance of different algorithms. The resulting ensemble model is thought to provide a more robust predicted distribution of *P. amadou* than any of the individual models and thus have clearer value for spatial management measures. The ensemble model maintains areas of high probability of presence in the same areas predicted by the individual models. However, it also maintains high the probability of presence of *P. amadou* across its suitable bathymetric range regardless of slope orientation, which is an effect of the inclusion of Random Forest in the model.

The uncertainty of the ensemble model was higher along a bathymetric belt from approximately 2,000 to 2,800 m depth across the seamount, with a patch of lower uncertainty on the SE flank. This depth

is within the range where the highest probability of *P. amadou* occurring is predicted (2,500 – 3,000m) and where the maximum velocity of currents at the seabed is lowest. Model uncertainty is difficult to estimate, but the bootstrap procedures applied to the GAM, Maxent and RF models provided a measure of internal consistency across the models(Anderson et al., 2016). Uncertainty maps are a key resource when applying predictions of distribution models to management measures (Vierod et al., 2014), as they can incorporate some level of confidence to the predictions and management actions(Anderson et al., 2016). Sources of uncertainty not accounted for in our models might be other key driving factors of habitat suitability for the sponge including oceanographic variables such as silicate, phosphate and nitrate availability, and POC flux (Howell et al., 2016).

The Tropic Seamount seems to be far from the impact of deep-sea fishing by being located at depths beyond current fishing in this area; nevertheless, it might be vulnerable to other types of deep-water exploitation. The latest survey on the area (by NERC funded MarineE-Tech project) found deposits of ferromanganese crusts at all depths. Therefore, deep-sea biodiversity catalogued herein and associated biogeographic analysis are of utmost importance to contribute for considering the Tropic Seamount as an EBSA (CBD, 2008) or as a VME (Watling & Auster, 2017).

3.13 References

Aarts, G., Fieberg, J. & Matthiopoulos, J. (2012). Comparative interpretation of count, presence–absence and point methods for species distribution models. *Methods in Ecology and Evolution*, *3,* 177–187.

Abecasis, R.C., Afonso, P., Colaço, A., Longnecker, N., Clifton, J., Schmidt, L. & Santos, R.S. (2015). Marine conservation in the Azores: evaluating marine protected area development in a remote island context. *Frontiers in Marine Science*, *2*, 104.

Addamo, A. M., Vertino, A., Stolarski, J., García-Jiménez, R., Taviani, M. & Machordom, A. (2016). Merging scleractinian genera: the overwhelming genetic similarity between solitary *Desmophyllum* and colonial *Lophelia*. *BMC evolutionary biology, 16*(1), 108.

Allouche, O., Tsoar, A. & Kadmon, R. (2006). Assessing the accuracy of species distribution models: prevalence, kappa and the true skill statistic (TSS). *Journal of Applied Ecology*, 43, 1223–1232.

Altuna, A. & Murillo, F.J. (2012). Diversity and distribution of sea pens (Cnidaria: Anthozoa: Pennatulacea) of the Flemish Cap, Flemish Pass and Grand Banks of Newfoundland (Northwest Atlantic Ocean). *Revista de Investigación Marina*, *19* (6): 405 406 + póster.

Amorim, P., Perán, A.D., Pham, C.K., Juliano, M., Cardigos, F., Tempera, F. & Morato, T. (2017). Overview of the ocean climatology and its variability in the Azores region of the North Atlantic including environmental characteristics at the seabed. *Frontiers in Marine Science*, *4*, 56.

Anderson, O. F., Guinotte, J. M., Rowden, A. A., Tracey, D. M., Mackay, K. A. & Clark, M. R. (2016). Habitat suitability models for predicting the occurrence of vulnerable marine ecosystems in the seas around New Zealand. *Deep Sea Research Part I Oceanography Research Papers, 115*, 265–292.

Araújo, M. B., Anderson, R. P., Barbosa, A. M., Beale, C. M., Dormann, C. F., Early, R., ... & O'Hara, R. B. (2019). Standards for distribution models in biodiversity assessments. *Science advances*, *5*(1), eaat4858.

Ardhuin, F., Roland, A., Dumas, F., Bennis, A.-C., Sentchev, A., Forget, P., Wolf, J., Girard F., Osuna, P. & Benoit, M. (2012). Numerical Wave Modeling in Conditions with Strong Currents: Dissipation, Refraction, and Relative Wind. *Journal Of Physical Oceanography*, *42*(12), 2101-2120.

Arnaud-Haond, S., Van den Beld, I.M.J., Becheler, R., Orejas, C., Menot, L., Frank, N., Grehan, A. & Bourillet, J.F. (2017). Two "pillars" of cold-water coral reefs along Atlantic European margins:

Prevalent association of *Madrepora oculata* with *Lophelia pertusa*, from reef to colony scale. *Deep Sea Research Part II: Topical Studies in Oceanography*, *145*, 110-119.

Ashford, O.S., Davies, A.J. & Jones, D.O. (2014). Deep-sea benthic megafaunal habitat suitability modelling: a global-scale maximum entropy model for xenophyophores. *Deep Sea Research Part I: Oceanographic Research Papers, 94*, 31-44.

Aubry, K.B., Raley, C.M. & McKelvey, K.S. (2017). The importance of data quality for generating reliable distribution models for rare, elusive, andcryptic species. *PLoS ONE, 12*(6), e0179152.

Baddeley, A. & Turner, R. (2005). Spatstat: An R package for analyzing spatial point patterns. *Journal of Statistical Software*, *12*, 1–42.

Baddeley, A. (2010). Analysing spatial point patterns in R. Workshop notes. Version 4.1.

Baddeley, A., Rubak, E. & Turner, R. (2015). *Spatial Point Patterns: Methodology and Applications with R.* CRC Press Taylor & Francis Group, Boca Raton, Florida.

Baillon, S., Hamel, J.-F. & Mercier, A. (2014). Diversity, Distribution and Nature of Faunal Associations with Deep-Sea Pennatulacean Corals in the Northwest Atlantic. *PLoS ONE, 9*(11), e111519.

Barbet-Massin, M., Jiguet, F., Albert, C.H. & Thuiller, W. (2012). Selecting pseudo-absences for species distribution models: how, where and how many? *Methods in Ecology and Evolution*, *3*, 327– 338.

Barton, K. (2009). MuMIn: Multi-model inference. R package version 0.12. 2/r18. URL http://R-Forge. R-project. org/projects/mumin.

Barton, K. (2018). MuMIn: Multi-Model Inference. R package version 1.40.4. Available at: https://cran.r-project.org/web/packages/MuMIn/MuMIn.pdf [Accessed October 11 2018].

Bashmachnikov, I., Lafon, V. & Martins, A. (2004). SST stationary anomalies in the Azores region. *Proceedings Volume, 5569*, 148–155.

Bashmachnikov, I., Mohn, C., Pelegri, J.L., Martins, A., Jose, F., Machín, F. & White, M. (2009). Interaction of Mediterranean water eddies with Sedlo and Seine Seamounts, Subtropical Northeast Atlantic. *Deep-Sea Research Part II*, *56*(25):2, 593–2,605.

Beaumont, L.J., Graham, E., Duursma, D.E., Wilson, P.D., Cabrelli, A., Baumgartner, J.B., Hallgren, W., Esperón-Rodríguez, M., Nipperess, D.A., Warren, D.L. & Laffan, S.W. (2016). Which species distribution models are more (or less) likely to project broad-scale, climate-induced shifts in species ranges? *Ecological Modelling, 342*, 135-146.

Beazley, L. I. & Kenchington, E. L. (2012). Reproductive biology of the deep-water coral *Acanella arbuscula* (Phylum Cnidaria: class Anthozoa: Order Alcyonacea), northwest Atlantic. *Deep Sea Research Part I: Oceanographic Research Papers*, *68*, 92-104.

Beazley, L., Guijarro, J., Lirette, C., Wang, Z. & Kenchington, E. (2018). Characteristics of Environmental Data Layers for Use in Species Distribution Modelling in the Eastern Canadian Arctic and Sub-Arctic Regions. *Canadian Technical Report of Fisheries and Aquatic Sciences*; *3248*: vii + 488p.

Beazley, L., Guijarro-Sabaniel, J., Lirette, C., Wang, Z. & Kenchington, E. (2019). "Characteristics of Environmental Data Layers for Use in Species Distribution Modelling in the Eastern Canadian Arctic and Sub-Arctic Regions", Mendeley Data, v2; http://dx.doi.org/10.17632/zmwyjs222s.2).

Behrens, E. (2013). The oceanic response to Greenland melting: The effect of increasing model resolution (Doctoral dissertation, Christian-Albrechts-Universität).

Behrens, E., Våge, K., Harden, B., Biastoch, A. & Böning, C.W. (2017). Composition and variability of the Denmark Strait Overflow Water in a high-resolution numerical model hindcast simulation. *Journal of Geophysical Research: Oceans*, *122*.

Bennecke, S. & Metaxas, A. (2017). Is substrate composition a suitable predictor for deep-water coral occurrence on fine scales? *Deep Sea Research Part I: Oceanographic Research Papers, 124*, 55-65.

Berx, B. & Payne, M.R. (2017). The Sub-Polar Gyre Index – a community data set for application in fisheries and environment research. *Earth System Science Data*, *9*, 259–266.

Böning, C. W., Behrens, E., Biastoch, A., Getzlaff, K. & Bamber, J. L. (2016). Emerging impact of Greenland meltwater on deepwater formation in the North Atlantic Ocean. *Nature Geoscience*, *9*(7), 523.

Braga-Henriques, A., Porteiro, F. M., Ribeiro, P. A., Matos, V. D., Sampaio, Í., Ocaña, O. & Santos, R. S. (2013). Diversity, distribution and spatial structure of the cold-water coral fauna of the Azores (NE Atlantic). *Biogeosciences*, *10*(6), 4009-4036.

Breiman, L. (2001). Random Forests. *Machine Learning, 45*, 5–32.

Breusing, C., Biastoch, A., Drews, A., Metaxas, A., Jollivet, D., Vrijenhoek, R.C., Bayer, T., Melzner, F., Sayavedra, L., Petersen, J.M., Dubilier, N., Schilhabel, M.B., Rosenstiel, P. & Reusch, T.B.H. (2016). Biophysical and Population Genetic Models Predict the Presence of "Phantom" Stepping Stones Connecting Mid-Atlantic Ridge Vent Ecosystems. *Current Biology, 26*.

Brooke, S., Ross, S.W., Bane, J.M., Seim, H.E. & Young, C.M. (2013). Temperature tolerance of the deep-sea coral *Lophelia pertusa* from the southeastern United States. *Deep Sea Research Part II: Topical Studies in Oceanography*, *92*, 240-248.

Brotons, L., Thuiller, W., Araújo, M.B. & Hirzel, A.H. (2004). Presence-absence versus presence-only modelling methods for predicting bird habitat suitability. *Ecography*, *27*(4), 437-448.

Caillaud, M., Petton, S., Dumas, F., Rochette, S. & Vasquez, M. (2016). Rejeu hydrodynamique à 500 m de résolution avec le modèle MARS3D-AGRIF - Zone Manche-Gascogne. IFREMER. https://doi.org/10.12770/3edee80f-5a3e-42f4-9427-9684073c87f5

Carvalho, N., Edwards-Jones, G. & Isidro, E. (2011). Defining scale in fisheries: Small versus large-scale fishing operations in the Azores. *Fisheries Research*, *109*(2-3), 360-369.

Chen, C., Liaw, A. & Breiman, L. (2004). Using random forest to learn imbalanced data. Berkeley: University of California.

Cheung, W.W., Watson, R., Morato, T., Pitcher, T.J. & Pauly, D. (2007). Intrinsic vulnerability in the global fish catch. *Marine Ecology Progress Series*, *333*, 1-12.

Coelho, R. & Erzini, K. (2007). Population parameters of the smooth lantern shark, *Etmopterus pusillus*, in southern Portugal (NE Atlantic). *Fisheries Research*, *86*(1), 42-57.

Colbourne, E.B. & Foote, K, D. (2000). Variability of the stratification and circulation on the Flemish Cap during the decades of the 1950s–1990s. *Journal of Northwest Atlantic Fishery Science*, *26*, 103-122.

Cooper, A. J. & Spearman, J. (2017). Validation of a TELEMAC - 3D model of a seamount. in Proceedings of the TELEMAC-MASCARET user Conference, 17-20 October 2017 (Graz University of Technology, Austria, 29-34). Available at: https://henry.baw.de/bitstream/handle/20.500.11970/104505/03_Cooper_2017.pdf?sequence=1&isAllowed=y. Accessed 1 Nov 2018.

Costello, M.J. & Chaudhary, C. (2017). Marine Biodiversity, Biogeography, Deep-Sea Gradients, and Conservation. *Current Biology*, *27* (13), 2051.

Council Regulation (EC) No 1359/2008 of 28 November 2008 fixing for 2009 and 2010 the fishing opportunities for Community fishing vessels for certain deep-sea fish stocks

Cutler, D.R., Edwards, T.C., Beard, K.H., Cutler, A., Hess, K.T., Gibson, J. & Lawler, J.J. (2007). Random forests for classification in ecology. *Ecology, 88*, 2783–2792.

Da Silva, H.M. & Pinho, M.R. (2007). Small-scale fishing on seamounts. *In: Pitcher, TJ, Morato T, Hart PJB, Clark MR, Haggan N, Santos RS (eds.) Seamounts: Ecology Fisheries and Conservation, Fisheries and Aquatic Resource Series, Blackwell Scientific*, pp.335-360.

Das, D. & Afonso, P. (2017). Review of the diversity, ecology, and conservation of elasmobranchs in the Azores region, mid-north Atlantic. *Frontiers in Marine Science*, *4*, 354.

Davies, A.J. & Guinotte, J.M. (2011). Global Habitat Suitability for Framework-Forming Cold-Water Corals. *PLoS ONE, 6*(4), e18483.

Davies, A.J., Wisshak, M., Orr, J.C. & Murray, R.J. (2008). Predicting suitable habitat for the cold-water coral *Lophelia pertusa* (Scleractinia). *Deep Sea Research Part I: Oceanographic Research Papers*, *55*, 1048–1062.

De Clippele, L. H., Gafeira, J., Robert, K., Hennige, S., Lavaleye, M. S., Duineveld, G. C. A., ... & Roberts, J. M. (2017). Using novel acoustic and visual mapping tools to predict the small-scale spatial distribution of live biogenic reef framework in cold-water coral habitats. *Coral Reefs, 36*(1), 255-268.

Devine, J.A., Baker, K.D. & Haedrich, R.L. (2006). Fisheries: deep-sea fishes qualify as endangered. *Nature*, *439*(7072), 29.

DFO (2017). Delineation of Significant Areas of Coldwater Corals and Sponge-Dominated Communities in Canada's Atlantic and Eastern Arctic Marine Waters and their Overlap with Fishing Activity. DFO Canadian Science Advisory Secretariat Science Advisory Report 2017/007.

Diggle, P.J. (2003). *Statistical analysis of spatial point patterns.* Arnold, London.

Dormann, C. F., Elith, J., Bacher, S., Buchmann, C., Carl, G., Carré, G., ... & Münkemüller, T. (2013). Collinearity: a review of methods to deal with it and a simulation study evaluating their performance. *Ecography*, *36*(1), 27-46.

Dufresne, J. L., Foujols, M. A., Denvil, S., Caubel, A., Marti, O., Aumont, O., ... & Bony, S. (2013). Climate change projections using the IPSL-CM5 Earth System Model: from CMIP3 to CMIP5. *Climate Dynamics*, *40*(*9-10*), 2123-2165.

Dunne, J.P., John, J.G., Adcroft, A.J., Griffies, S.M., Hallberg, R.W., Shevliakova, E., Stouffer, R.J., Cooke, W., Dunne, K.A., Harrison, M.J., Krasting, J.P., Malyshev, S.L., Milly, P.C.D., Phillipps, P.J., Sentman, L.T., Samuels, B.L., Spelman, M.J., Winton, M., Wittenberg, A.T. & Zadeh, N. (2012). GFDL's ESM2 Global Coupled Climate–Carbon Earth System Models. Part I: Physical Formulation and Baseline Simulation Characteristics. *Journal of Climate*, *25*, 6646–6665.

Dunstan, P.K., Foster, S.D. & Darnell, R. (2011). Model based grouping of species across environmental gradients. *Ecological Modelling*; *222*, 955–963.

Edinger, E. N., Sherwood, O. A., Piper, D. J., Wareham, V. E., Baker, K. D., Gilkinson, K. D. & Scott, D. B. (2011). Geological features supporting deep-sea coral habitat in Atlantic Canada. *Continental Shelf Research*, *31*(2), S69-S84.

Edwards, D.C.B. & Moore, C.G. (2009). Reproduction in the sea pen *Funiculina quadrangularis* (Anthozoa: Pennatulacea) from the west coast of Scotland. *Estuarine, Coastal and Shelf Science*, *82*, 161–168.

Elith, J., Ferrier, S., Huettmann, F. & Leathwick, J.R. (2005). The evaluation strip: A new and robust method for plotting predicted responses from species distribution models. *Ecological Modelling, 186*(3), 280-289.

Elith, J., H. Graham, C., P. Anderson, R., Dudík, M., Ferrier, S., Guisan, A., ... & Li, J. (2006). Novel methods improve prediction of species' distributions from occurrence data. *Ecography, 29*(2), 129-151.

Elith, J. & Leathwick, J.R. (2009). Species distribution models: ecological explanation and prediction across space and time. *Annual Review of Ecology, Evolution, and Systematics*, *40*, 677–697.

Elith, J., Phillips, S.J., Hastie, T., Dudík, M., Chee, Y.E. & Yates, C.J. (2011). A statistical explanation of MAXENT for ecologists. *Diversity and Distributions, 17*, 43–57.

EMODnet (2018). EMODnet Bathymetry Digital Terrain Model (DTM) for the European Seas. 24 September 2018 European Marine Observation and Data Network (EMODnet Secretariat), Ostend. EMODnet Bathymetry Portal: www.emodnet-bathymetry.eu

EMODnet Bathymetry Consortium (2016) EMODnet Digital Bathymetry (DTM). Marine Information Service. https://doi.org/10.12770/c7b53704-999d-4721-b1a3-04ec60c87238.

EMODnet Bathymetry Consortium (2018). EMODnet Digital Bathymetry (DTM 2018). EMODnet Bathymetry Consortium. https://doi.org/10.12770/18ff0d48-b203-4a65-94a9-5fd8b0ec35f6.

ESGF (2019) https://esgf-node.llnl.gov/projects/esgf-llnl/ (accessed 15/4/19).

ESRI (Environmental Systems Research Institute) (2015). ArcGIS 10.3. 1 for desktop.

Evans, J.S., Murphy, M.A., Holden, Z.A. & Cushman, S.A. (2011). Modelling Species Distribution and change using Random Forests. In: Drew CA, Wiersma YF, Huettmann F, editors. Predictive Species and

Habitat Modelling in Landscape Ecology: Concepts and Applications. Springer, New York, 2011. pp. 139-159.

FAO (2009). *International Guidelines for the Management of Deep-sea Fisheries in the High Seas.* FAO, Rome.

Fielding, A. H., Bell, J. F. (1997). A review of methods for the assessment of prediction errors in conservation presence/absence models. *Environmental Conservation*, *24*(1), 38-49.

Fourcade, Y., Besnard, A. G. & Secondi, J. (2018). Paintings predict the distribution of species, or the challenge of selecting environmental predictors and evaluation statistics. *Global Ecology and Biogeography*, *27*, 245–256.

Freeman, E.A., Moisen, G.G. & Frescino, T.S. (2012). Evaluating effectiveness of down-sampling for stratified designs and unbalanced prevalence in Random Forest models of tree species distributions in Nevada. *Ecological Modelling*, *233* (0), 1-10.

Freiwald, A. (2002). Reef-Forming Cold-Water Corals. *Ocean Margin Systems*, 365–385.

García, V.B., Lucifora, L.O. & Myers, R.A. (2007). The importance of habitat and life history to extinction risk in sharks, skates, rays and chimaeras. *Proceedings of the Royal Society B: Biological Sciences*, *275*(1630), 83-89.

García-Cárdenas, F.J., Drewery, J. & López-González, P.J. (2019). Resurrection of the sea pen genus *Ptilella* Gray, 1870, and description of *Ptilella grayi* n. sp. from NE Atlantic (Octocorallia, Pennatulacea). *Molecular Ecology Resources*, in review.

Genuer, R., Poggi, J.-M. & Tuleau-Malot, C. (2010). Variable selection using random forests. *Pattern Recognition Letters, 31*, 2225–2236.

Gil, J., Sánchez, R., Cerviño, S. & Garabana, D. (2004). Geostrophic circulation and heat flux across the Flemish Cap, 1988-2000, *Journal of Northwest Atlantic Fishery Science*, *34*, 61-81.

Gili, J.M. & Pagès, F. (1987). Pennatuláceos (Cnidaria, Anthozoa) recolectados en la plataforma continental catalana (Mediterrá- neo occidental). *Miscellaneous Zoology, 11*, 25-39.

Giorgetta, M.A., Jungclaus, J., Reick, C.H., Legutke, S., Bader, J., Böttinger, M., Brovkin, V., Crueger, T., Esch, M., Fieg, K. & Glushak, K. (2013). Climate and carbon cycle changes from 1850 to 2100 in MPI-ESM simulations for the Coupled Model Intercomparison Project phase 5. *Journal of Advances in Modeling Earth Systems*, *5*(3), 572-597.

Gohin, F., Druon, J. & Lampert, L. (2002). A five channel chlorophyll concentration algorithm applied to SeaWiFS data processed by SeaDAS in coastal waters. *International Journal Of Remote Sensing*, *23*(8), 1639-1661.

González-Irusta, J. M., González-Porto, M., Sarralde, R., Arrese, B., Almón, B. & Martín-Sosa, P. (2015). Comparing species distribution models: A case study of four deep sea urchin species. *Hydrobiologia*, *745*, 43–57.

González-Irusta, J. M. & Wright, P. J. (2016a). Spawning grounds of Atlantic cod (*Gadus morhua*) in the North Sea. *ICES Journal of Marine Science*, *73*, 304–315.

González-Irusta, J. M. & Wright, P. J. (2016b). Spawning grounds of haddock (*Melanogrammus aeglefinus*) in the North Sea and West of Scotland. *Fisheries Research*, 183, 180-191.

González-Irusta, J. M. & Wright, P. J. (2017). Spawning grounds of whiting (*Merlangius merlangus*). *Fisheries Research*, *195*, 141–151.

Greathead, C., González-Irusta, J.M., Clarke, J., Boulcott, P., Blackadder, L., Weetman, A. & Wright, P.J. (2014). Environmental requirements for three sea pen species: relevance to distribution and conservation. *ICES Journal of Marine Science*, *72*, 576–586.

Grüss, A., Drexler, M. D., Ainsworth, C. H., Babcock, E. A., Tarnecki, J. H. & Love, M. S. (2018). Producing Distribution Maps for a Spatially-Explicit Ecosystem Model Using Large Monitoring and Environmental Databases and a Combination of Interpolation and Extrapolation. *Frontiers in Marine Science*, *5*, 1–20.

Guisan, A., Thuiller, W. & Zimmermann, N.E. (2017). Habitat suitability and distribution models: with applications in R. Cambridge University Press.

Hall-Spencer, J.M. & Stehfest, K.M. (2009). Background Document for *Lophelia pertusa* reefs.

Hanberry, B.B. & He, H.S. (2013). Prevalence, statistical thresholds, and accuracy assessment for species distribution models. *Web Ecology*, *13*, 13-19.

Hastie, T. & Tibshirani, R. (1986). Generalized Additive Models. *Statistical Science, 1*(3), 297–318. Available at: https://projecteuclid.org/download/pdf_1/euclid.ss/1177013604 [Accessed November 14, 2018].

Hastie, T. & Tibshirani, R. (1990). Generalised additive models. – Chapman & Hall.

Hastie, T., Tibshirani, R. & Friedman, J.H. (2001). The Elements of Statistical Learning: Data Mining, Inference, and Prediction. Springer, New York, NJ.

Hátún, H., Payne, M.R. & Jacobsen, J.A. (2009). The North Atlantic subpolar gyre regulates the spawning distribution of blue whiting (*Micromesistius poutassou*). *Canadian Journal of Fisheries and Aquatic Sciences*, *66*, 759–770.

Hengl, T., Heuvelink, G.B. & Rossiter, D.G. (2007). About regression-kriging: From equations to case studies. *Computers & geosciences*, *33*(10), 1301-1315.

Hengl, T., Kempen, B., Heuvelink, G., Malone, B. & Hannes, R. (2017). Package 'GSIF: Global soil information facilities'. *R package*. http://gsif.r-forge.r-project.org

Hijmans, R.J., Phillips, S., Leathwick, J. & Elith, J. (2014). *dismo: Species distribution modelling.* Version 1.0-5, Available at: http://cran.r-project.org/web/packages/dismo/index.html.

Hijmans, R.J., van Etten, J., Cheng, J., Mattiuzzi, M., Sumner, M., Greenberg, J.A., Lamigueiro, O.P., Bevan, A., Racine, E.B., Shortridge, A. & Hijmans, M.R.J. (2015). Package 'raster'. *R package*. https://cran.r-project.org/web/packages/raster/index.html

Hijmans, R. J., van Etten, J., Cheng, J., Mattiuzzi, M., Sumner, M., Greenberg, J. A., Perpinan Lamigueiro, O., et al. (2016). Package 'raster'. R package.

Hijmans, R.J. (2016) Introduction to the 'raster' package (version 2.5-8). 27 pp.

Hijmans, R.J., Phillips, S., Leathwick, J. & Elith, J. (2017). dismo: Species Distribution Modeling. R package version 1.1-4.

Hijmans, R.J., Phillips, S., Leathwick, J., Elith, J. & Hijmans, M.R.J. (2017). Package 'dismo'. *Circles*, *9*(1), 1-68.

Hosmer, D.W., Lemeshow, S. & Sturdivant, R.X. (2013). Assessing the Fit of the Model. *Applied Logistic Regression* pp. 153–225. John Wiley & Sons, Inc.,

Hui, F.K.C., Warton, D.I., Foster, S.C. & Dunstan, P.K. (2013). To mix or not to mix: comparing the predictive performance of mixture models vs. separate species distribution models. *Ecology*, *94*, 1913–1919.

ICES (2016). Report of the Workshop on the Vulnerable Marine Systems Database (WKVME), 10–11 December 2015, Peterborough: ICES.

Iturbide, M., Bedia, J., Herrera, S., Hierro, O., Pinto, M. & Gutiérrez, J.M. (2015). A framework for species distribution modelling with improved pseudo-absence generation. *Ecological. Modelling, 312*, 166– 174.

Iturbide, M., Bedia, J. & Gutiérrez, J. M. (2018). Background sampling and transferability of species distribution model ensembles under climate change. *Global and Planetary Change*, *166*, 19-29.

Jerosch, K. (2013). Geostatistical mapping and spatial variability of surficial sediment types on the Beaufort Shelf base don grain size. *Journal of Marine Systems*, *127*, 5-13.

Jiménez-Valverde, A. & Lobo, J. M. (2007). Threshold criteria for conversion of probability of species presence to either-or presence-absence. *Acta Oecologica, 31*(3), 361–369.

Jiménez-Valverde, A. (2012). Insights into the area under the receiver operating characteristic curve (AUC) as a discrimination measure in species distribution modelling. *Global Ecology and Biogeography*, *21*, 498–507.

Johnson, D., Adelaide Ferreira, M. & Kenchington, E. (2018). Climate change is likely to severely limit the effectiveness of deep-sea ABMTs in the North Atlantic. *Marine Policy, 87*, 111–122.

Johnson, D.E., Barrio Froján, C., Neat, F., Van Oevelen, D., Stirling, D., Gubbins, M.J. & Roberts, J.M. (2019). Rockall and Hatton: Resolving a Super Wicked Marine Governance Problem in the High Seas of the Northeast Atlantic Ocean. *Frontiers in Marine Science*, *6*.

Jones, D. O., Yool, A., Wei, C. L., Henson, S. A., Ruhl, H. A., Watson, R. A. & Gehlen, M. (2014). Global reductions in seafloor biomass in response to climate change. *Global Change Biology*, *20*(6), 1861-1872.

Kenchington, E., Murillo, F.J., Lirette, C., Sacau, M., Koen-Alonso, M., Kenny, A., Ollerhead, N., Wareham, V. & Beazley, L. (2014). Kernel density surface modelling as a means to identify significant concentrations of vulnerable marine ecosystem indicators. *PLoS ONE 10*(1), e0117752.

Klein, B. & Siedler, G. (1989). On the origin of the Azores current. *Journal of Geophysical Research*, *94*, 6159–6168.

Kramer-Schadt, S., Niedballa, J., Pilgrim, J. D., Schröder, B., Lindenborn, J., Reinfelder, V., ... & Cheyne, S. M. (2013). The importance of correcting for sampling bias in MAXENT species distribution models. *Diversity and Distributions*, *19*(11), 1366-1379.

Landis, J.R. & Koch, G.G. (1977). The Measurement of Observer Agreement for Categorical Data. *Biometrics*, *33*, 159–174.

Lauria, V., Gristina, M., Attrill, M.J., Fiorentino, F. & Garofalo, G. (2015). Predictive habitat suitability models to aid conservation of elasmobranch diversity in the central Mediterranean Sea. *Scientific reports*, *5*, 13245.

Lecornu, F. & De Roeck, Y.-H. (2009). PREVIMER - Observations & Prévisions Côtières. *La Houille Blanche, 1*, 60-63.

Lelièvre, S., Vaz, S., Martin, C. S. & Loots, C. (2014). Delineating recurrent fish spawning habitats in the North Sea. *Journal of Sea Research*, *91*, 1–14.

Lessard-Pilon, S. A., Podowski, E. L., Cordes, E. E. & Fisher, C. R. (2010). Megafauna community composition associated with *Lophelia pertusa* colonies in the Gulf of Mexico. *Deep Sea Research Part II: Topical Studies in Oceanography, 57*(21-23), 1882-1890.

Liaw, A. & Wiener, M. (2002). Classification and regression by randomForest. *R News*, *2*, 18-22.

Liu, C., Berry, P.M., Dawson, T.P. & Pearson, R.G. (2005). Selecting thresholds of occurrence in the prediction of species distributions. *Ecography, 28*, 385-393.

López-González, P.J., Gili, J.M. & Williams, G.C. (2001). New records of Pennatulacea (Anthozoa: Octocorallia) from the African Atlantic coast, with description of a new species and a zoogeographic analysis. *Scientia Marina*, *65*, 59-74.

Lunden, J.J., McNicholl, C.G., Sears, C.R., Morrison, C.L. & Cordes, E.E. (2014). Acute survivorship of the deep-sea coral *Lophelia pertusa* from the Gulf of Mexico under acidification, warming, and deoxygenation. *Frontiers in Marine Sciences*, *1*, 78.

Malecha, P.W. & Stone, R.P. (2009). Response of the sea whip *Halipteris willemoesi* to simulated trawl disturbance and its vulnerability to subsequent predation. *Marine Ecology Progress Series*, *388*, 197–206.

Mandrekar, J. N. (2010). Receiver operating characteristic curve in diagnostic test assessment. *Journal of Thoracic Oncology*, *5*(9), 1315-1316.

Manuel, R.L. (1981). British Anthozoa. Synopses of the British Fauna (New Series). No 18. Linnean Society Academic Press, London, 241 pp.

Manuel, R.L. (1988). *Synopses of the British Fauna: British Anthozoa.* Academic Press, London,

Martin, J. H., Knauer, G. A., Karl, D. M. & Broenkow, W. W. (1987). VERTEX: carbon cycling in the northeast Pacific. *Deep Sea Research Part A. Oceanographic Research Papers, 34*(2), 267-285.

Mateo, R.G., Croat, T.B., Felicisimo, A.M. & Munoz, J. (2010). Profile or group discriminative techniques? Generating reliable species distribution models using pseudo-absences and target-group absences from natural history collections. *Diversity and Distributions*, *16*, 84–94.

McGrath, T., Nolan, G. & McGovern, E. (2012). Chemical characteristics of water masses in the Rockall Trough. *Deep Sea Research Part I: Oceanographic Research Papers*, *61*, 57–73.

McPherson, J.M., Jetz, W. & Rogers, D.J. (2004). The effects of species' range sizes on the accuracy of distribution models: ecological phenomenon or statistical artefact? *Journal of Applied Ecology*, *41*, 811–823.

Menezes, G.M., Sigler, M.F., Silva, H.M. & Pinho, M.R. (2006). Structure and zonation of demersal fish assemblages off the Azores Archipelago (mid-Atlantic). *Marine Ecology Progress Series*, *324*, 241-260.

Menezes, G.M., Rosa, A., Melo, O. & Pinho, M.R. (2009). Demersal fish assemblages off the Seine and Sedlo seamounts (northeast Atlantic). *Deep Sea Research Part II: Topical Studies in Oceanography*, *56*(25), 2683-2704.

Morán-Ordóñez, A., Lahoz-Monfort, J.J., Elith, J. & Wintle, B.A. (2017). Evaluating 318 continental-scale species distribution models over a 60-year prediction horizon: what factors influence the reliability of predictions? *Global Ecology and Biogeography, 26*(3), 371-384.

Morato, T., Cheung W.W. & Pitcher T.J. (2006). Vulnerability of seamount fish to fishing: fuzzy analysis of life-history attributes. *Journal of Fish Biology 68*(1), 209-221.

Morato, T., Varkey, D.A., Damaso, C., Machete, M., Santos, M., Prieto, R., Santos, R.S. & Pitcher, T.J. (2008). Evidence of a seamount effect on aggregating visitors. *Marine Ecology Progress Series*, *357*, 23-32.

Morato, T. (2012). Description of environmental issues, fish stocks and fisheries in the EEZs around the Azores and Madeira. *Request for Services: Scientific, Technical and Economic Committee for Fisheries (STECF) Joint Research Centre (JRC)* 62p.

Morato, T., Pham, C.K., Pinto, C., Golding, N., Ardron, J.A., Muñoz, P.D. & Neat, F. (2018). A multi criteria assessment method for identifying Vulnerable Marine Ecosystems in the North-East Atlantic. *Frontiers in Marine Science*, 5*(*DEC).

Murillo, F. J., Durán Muñoz, P., Altuna, A. & Serrano, A. (2011). Distribution of deep-water corals of the Flemish Cap, Flemish Pass, and the Grand Banks of Newfoundland (Northwest Atlantic Ocean): interaction with fishing activities. *ICES Journal of Marine Science*, *68*, 319-332.

Murillo, F. J., Serrano, A., Kenchington, E. & Mora, J. (2016). Epibenthic assemblages of the Tail of the Grand Bank and Flemish Cap (northwest Atlantic) in relation to environmental parameters and trawling intensity. *Deep Sea Research Part I: Oceanographic Research Papers*, *109*, 99-122.

Murillo, F.J., Kenchington, E., Tompkins, G., Beazley, L., Baker, E., Knudby, A. & Walkusz, W. (2018). Sponge assemblages and predicted archetypes in the eastern Canadian Arctic. *Marine Ecology Progress Series*, *597*, 115-135.

Muscarella, R., Galante, P. J., Soley-Guardia, M., Boria, R. A., Kass, J. M., Uriarte, M. & Anderson, R. P. (2014). ENMeval: An R package for conducting spatially independent evaluations and estimating optimal model complexity for <scp>MAXENT</scp> ecological niche models. *Methods in Ecology and Evolution*, *5*, 1198–1205.

NAFO (2015). Report of the 8th Meeting of the NAFO Scientific Council Working Group on Ecosystem Science and Assessment (WGESA). NAFO SCS Doc. 15/19, Serial No.N6549, 176 pp.

NAFO (2019). NAFO Conservation and Enforcement Measures. Serial No. N6901, NAFO/COM Doc. 19-01.

Naimi, B., Skidmore, A. K., Groen, T. A. & Hamm, N. A. (2011). Spatial autocorrelation in predictors reduces the impact of positional uncertainty in occurrence data on species distribution modelling. *Journal of biogeography*, *38*(8), 1497-1509.

Navarro, J., López, L., Coll, M., Barría, C. & Sáez-Liante, R. (2014). Short-and long-term importance of small sharks in the diet of the rare deep-sea shark *Dalatias licha*. *Marine biology*, *161*(7), 1697-1707.

Neat, F. & Campbell, N. (2011). Demersal fish diversity of the isolated Rockall plateau compared with the adjacent west coast shelf of Scotland. *Biological journal of the Linnean Society*, *104*, 138–147.

Newton, A.W., Peach, K.J., Coull, K.A., Gault, M. & Needle, C.L. (2008). Rockall and the Scottish haddock fishery. *Fisheries Research*, *94*, 133–140.

Oppel, S., Meirinho, A., Ramírez, I., Gardner, B., O'Connell, A. F., Miller, P. I., et al. (2012). Comparison of five modelling techniques to predict the spatial distribution and abundance of seabirds. *Biological Conservation*, *156*, 94–104.

Osborne, P.E. & Leitão, P.J. (2009). Effects of species and habitat positional errors on the performance and interpretation of species distribution models. *Diversity and Distributions*, *15*, 671– 681.

Ovaskainen, O., Tikhonov, G., Norberg, A., Guillaume Blanchet, F., Duan, L., Dunson, D., Roslin, T. & Abrego, N. (2017). How to make more out of community data? A conceptual framework and its implementation as models and software. *Ecology Letters, 20* (5), 561-576.

Palma C., Lillebø A.I., Borges C., Souto M., Pereira E., Duarte A.C. & Abreu M.P. (2012). Water column characterisation on the Azores platform and at the seamounts south of the archipelago. *Marine Pollution Bulletin*, *64*, 1884–1894.

Parra, H. E., Pham, C. K., Menezes, G. M., Rosa, A., Tempera, F. & Morato, T. (2016). Predictive modeling of deep-sea fish distribution in the Azores. *Deep Sea Research Part II: Topical Studies in Oceanography*.

Pebesma, E. J. (2004). Multivariate geostatistics in S: the gstat package. *Computers & Geosciences, 30*, 683–691.

Pham, C.K., Canha, A., Diogo, H., Pereira, J.G., Prieto, R. & Morato, T. (2013). Total marine fishery catch for the Azores (1950–2010). *ICES Journal of Marine Science*, *70*(3), 564-577.

Phillips, S.J., Anderson, R.P. & Schapire, R.E. (2006). Maximum entropy modelling of species geographic distributions. *Ecological Modelling*, *190*, 231–259.

Phillips, S.J. & Dudik, M. (2008). Modelling of species distributions with MAXENT: new extensions and a comprehensive evaluation. *Ecography*, *31*, 161–175.

Phillips, S.J., Dudík, M. & Schapire, R. (2011). MAXENT Software. Version 3.3.3k, Available at: https://www.cs.princeton.edu/~schapire/MAXENT/ (May 2015).

Phillips, S. J., Anderson, R. P., Dudík, M., Schapire, R. E. & Blair, M. E. (2017). Opening the black box: an open-source release of MAXENT. *Ecography, 40*(7), 887-893.

Pinho, M.R. & Menezes, G. (2009). Pescarias de demersais nos Açores (Demersal fishery off the Azores) *Boletim do Núcleo Cultural da Horta* pp 85-102.

R Core Team (2017) R: A Language and Environment for Statistical Computing. https://www.R-project.org/

R Core Team (2018). R: A language and environment for statistical computing. R Foundation for Statistical Computing, Vienna, Austria. URL https://www.R-project.org/.

Radosavljevic, A. & Anderson, R.P. (2014). Making better MAXENT models of species distributions: complexity, overfitting and evaluation. *Journal of biogeography*, *41*(4), 629-643.

Reed, J. K., Weaver, D. C. & Pomponi, S. A. (2006). Habitat and fauna of deep-water *Lophelia pertusa* coral reefs off the southeastern US: Blake Plateau, Straits of Florida, and Gulf of Mexico. *Bulletin of Marine Science, 78*(2), 343-375.

Rengstorf, A.M., Yesson, C., Brown, C. & Grehan, A.J. (2013). High-resolution habitat suitability modelling can improve conservation of vulnerable marine ecosystems in the deep sea. *Journal of Biogeography*, *40*, 1702-1714.

Rengstorf, A.M., Mohn, C., Brown, C., Wisz, M.S. & Grehan, A.J. (2014). Predicting the distribution of deep-sea vulnerable marine ecosystems using high-resolution data: Considerations and novel approaches. *Deep-Sea Research Part I: Oceanographic Research Papers*, *93*, 72-82.

Renner, I.W. & Warton, D.I. (2013). Equivalence of MAXENT and Poisson point process models for species distribution modelling in ecology. *Biometrics*, *69*, 274–281.

Renner, I.W., Elith, J., Baddeley, A., Fithian, W., Hastie, T., Phillips, S.J., Popovic, G. & Warton, D.I. (2015). Point process models for presence-only analysis. *Methods in Ecology and Evolution*, *6*, 366–379.

Rigby, C. & Simpfendorfer, C.A. (2015). Patterns in life history traits of deep-water chondrichthyans. *Deep Sea Research Part II: Topical Studies in Oceanography*, *115*, 30-40.

Robert, J. Hijmans (2017). raster: Geographic Data Analysis and Modelling. R package version 2.6-7. https://CRAN.R-project.org/package=raster

Roberts, J.M., Henry, L.-A., Long, D. & Hartley, J.P. (2008). Cold-water coral reef frameworks, megafaunal communities and evidence for coral carbonate mounds on the Hatton Bank, north east Atlantic. *Facies*, *54*, 297–316.

Robinson, N. M., Nelson, W. A., Costello, M. J., Sutherland, J. E. & Lundquist, C. J. (2017). A Systematic Review of Marine-Based Species Distribution Models (SDMs) with Recommendations for Best Practice. *Frontiers in Marine Science, 4,* 421.

Rochette, S. (2018). SDMSelect: A R-package for cross-validation model selection and species distribution mapping (Version v0.1.4). Zenodo. http://doi.org/10.5281/zenodo.894344

Rowden, A. A., Anderson, O. F., Georgian, S. E., Bowden, D. A., Clark, M. R., Pallentin, A. & Miller, A. (2017). High-Resolution Habitat Suitability Models for the Conservation and Management of Vulnerable Marine Ecosystems on the Louisville Seamount Chain, South Pacific Ocean. *Frontiers in Marine Sciences, 4*, 335.

RStudio-Team (2015). "RStudio: Integrated Development for R. RStudio, Inc., Boston, MA URL http://www.rstudio.com/.".).

Ruiz-Pico, S., Serrano, A., Punzón, A., Altuna, Á., Fernández-Zapico, O. & Velasco, F. (2017). Sea pen (Pennatulacea) aggregations on the northern Spanish shelf: distribution and faunal assemblages. *Scientia Marina*, *81*(3), 413-423.

Sampaio, Í., Freiwald, A., Porteiro, F.M., Menezes, G. & Carreiro-Silva, M. (2019). Census of Octocorallia (Cnidaria: Anthozoa) of the Azores (NE Atlantic) with a nomenclature update. *Zootaxa*, *4550*(4), 451-498.

Santos, R.S., Hawkins, S., Monteiro, L.R., Alves, M. & Isidro, E.J. (1995). Marine research, resources and conservation in the Azores. *Aquatic Conservation: Marine and Freshwater Ecosystems*, *5*, 311–354.

Sbrocco, E. J. & Barber, P. H. (2013). MARSPEC: ocean climate layers for marine spatial ecology: Ecological Archives E094-086. *Ecology*, *94*(4), 979-979.

Schofield, N., Jolley, D., Holford, S., Archer, S., Watson, D., Hartley, A., Howell, J., Muirhead, D., Underhill, J. & Green, P. (2018). Challenges of future exploration within the UK Rockall Basin. *Geological Society, London, Petroleum Geology Conference series, 8*, 211–229.

Shepard, F.P. (1954). Nomenclature based on sand-silt-clay ratios: *Journal of Sedimentary Petrology, 24*, 151-158.

Shmueli, G. (2010). To explain or to predict? *Statistical science*, *25*, 289–310.

Simpfendorfer, C.A. & Kyne, P.M. (2009). Limited potential to recover from overfishing raises concerns for deep-sea sharks, rays and chimaeras. *Environmental Conservation*, *36*(2), 97-103.

Stefansdottir, L., Solmundsson, J., Marteinsdottir, G., Kristinsson, K. & Jonasson, J.P. (2010). Groundfish species diversity and assemblage structure in Icelandic waters during recent years of warming. *Fisheries Oceanography, 19*(1), 42-62.

Sulak, K. J., Brooks, R. A., Luke, K. E., Norem, A. D., Randall, M., Quaid, A. J., ... & Ross, S. W. (2007). Demersal fishes associated with *Lophelia pertusa* coral and hard-substrate biotopes on the continental slope, northern Gulf of Mexico. *Bulletin of Marine Science, 81*(3), 65-92.

Symonds, M.R.E. & Moussalli, A. (2010). A brief guide to model selection, multimodel inference and model averaging in behavioural ecology using Akaike's information criterion. *Behavioral Ecology and Sociobiology*, *65*, 13– 21.

Tempera, F., Pereira, J.N., Braga Henriques, A., Porteiro, F., Morato, T., Matos, V., Souto, M., Guillaumont, B. & Santos, R.S. (2012). Cataloguing deep-sea biological facies of the Azores. In:

Galparsoro, I. (Ed.), Using EUNIS habitat classification for benthic mapping in European seas, 19. Revista de Investigacion Marina, AZTI-Tecnalia, pp. 21–70.

Thornalley, D.J.R., Oppo, D.W., Ortega, P., Robson, J.I., Brierley, C.M., Davis, R., Hall, I.R., Moffa-Sanchez, P., Rose, N.L., Spooner, P.T., Yashayaev, I. & Keigwin, L.D. (2018). Anomalously weak Labrador Sea convection and Atlantic overturning during the past 150 years. *Nature, 556*, 227.

Thuiller, W., Lafourcade, B., Engler, R. & Araújo, M.B. (2009). BIOMOD – A platform for ensemble forecasting of species distributions. *Ecography*, *32*, 369– 373.

Tixier-Durivault, A. & d'Hondt M.J. (1975). Les Octocoralliaires de la campagne Biaçores. Bulletin du Muséum National d'Histoire Naturelle de Paris, *Zoology, 174*, 1361-1433.

Valdimarsson, H., Astthorsson, O.S. & Palsson, J. (2012). Hydrographic variability in Icelandic waters during recent decades and related changes in distribution of some fish species. *ICES Journal of Marine Science, 69*(5), 816-825.

van den Beld, I.M.J., Bourillet, J.-F., Arnaud-Haond, S., de Chambure, L., Davies, J.S., Guillaumont, B., Olu, K. & Menot, L. (2017). Cold-Water Coral Habitats in Submarine Canyons of the Bay of Biscay. *Frontiers in Marine Science, 4* (118).

Vierod, A., Guinotte, J. & Davies, A. (2014). Predicting the distribution of vulnerable marine ecosystems in the deep sea using presence-background models. *Deep Sea Research Part II Topical Studies in Oceanography*, *99*, 6–18.

Walbridge, S., Slocum, N., Pobuda, M. & Wright, D.J. (2018). Unified Geomorphological Analysis Workflows with Benthic Terrain Modeler. *Geosciences*, *8*, 94.

Warton, D.I., Renner, I.W. & Ramp, D. (2013). Model-Based Control of Observer Bias for the Analysis of Presence-Only Data in Ecology. *PLoS ONE*, *8*, e79168.

Watling, L., Haedrich, R.L., Devine, J., Drazen, J., Dunn, M.R., Gianni, M., Baker, K., Cailliet, G., Figueiredo, I., Kyne, P.M., Menezes, G., Neat, F., Orlov, A., Duran, P., Perez, J.A., Ardron, J.A., Bezaury, J., Revenga, C. & Nouvian, C. (2011). *Can ecosystem-based deep-sea fishing be sustained? Report of a workshop held 31 August-3 September 2010. Walpole, ME*: University of Maine, Darling Marine Center. Darling Marine Center Special Publication 11-1. 84p

Watling, L. & Auster, P. J. (2017). Seamounts on the High Seas Should Be Managed as Vulnerable Marine Ecosystems. *Frontiers in Marine Sciences*, *4*.

Weatherall, P., Marks, K.M., Jakobsson, M., Schmitt, T., Tani, S., Arndt, J.E., Rovere, M., Chayes, D., Ferrini, V. & Wigley, R. (2015). A new digital bathymetric model of the world's oceans. *Earth and Space Science, 2*(8): 331-345.

Wheeler, A. J., Beyer, A., Freiwald, A., de Haas, H., Huvenne, V. A. I., Kozachenko, M., Olu-Le Roy, K. & Opderbecke, J. (2007). Morphology and environment of cold-water coral carbonate mounds on the NW European margin. *International Journal of Earth Science*, *96*, 37–56.

Williams, G.C. (1990). The Pennatulacea of southern Africa (Coelenterata, Anthozoa). *Annals of the South African Museum*, *99*(4), 31–119. 7.

Williams, G.C. (1995). Living genera of sea pens (Coelenterata: Octocorallia: Pennatulacea) – illustrated key and synopses. *Zoological Journal of The Linnean Society, London, 113*(2), 93–140.

Williams, A., Koslow, J.A. & Last, P.R. (2001). Diversity, density and community structure of the demersal fish fauna of the continental slope off western Australia (20 to 35 S). *Marine Ecology Progress Series*, *212*, 247-263.

Wilson, M.F.J., O'Connell, B., Brown, C., Guinan, J.C. & Grehan, A.J. (2007) Multiscale terrain analysis of multibeam bathymetry data for habitat mapping on the continental slope. *Marine Geodesy*, *30*, 3–35.

Wood, S.N. & Augustin, N.H., (2002). GAMs with integrated model selection using penalized regression splines and applications to environmental modelling. *Ecological Modelling*, 157, 157–177.

Wood, S. N. (2003). Thin plate regression splines. *Journal of the Royal Statistical Society: Series B (Statistical Methodology)*, 65(1), 95-114.

Wood, S. & Wood, M.S. (2015). Package 'mgcv'. R package version, 1-7.

Wood, S. (2018) Mixed GAM Computation Vehicle with Automatic Smoothness Estimation (version 1.8-28). 302 pp.

Wright, D. J., E. R. Lundblad, E. M. Larkin, R. W. Rinehart, J. Murphy, L. Cary-Kothera & K. Draganov. (2005). ArcGIS Benthic Terrain Modeler. Corvallis, Oregón, Universidad Estatal de Oregón, Davey Jones Locker Seafloor Mapping/Marine GIS Laboratory y NOAA Coastal Services Center.

Xavier, J.C., Vieira, C., Assis, C., Cherel, Y., Hill, S., Costa, E., Borges, T.C. & Coelho, R. (2012). Feeding ecology of the deep-sea lanternshark *Etmopterus pusillus* (Elasmobranchii: Etmopteridae) in the northeast Atlantic. *Scientia Marina*, *76*(2), 301-310.

Zuur, A.F., Ieno, E.N., Walker, N.J., Saveliev, A.A. & Smith, G.M. (2009). Zero-truncated and zero-inflated models for count data. In *Mixed effects models and extensions in ecology with R* (pp. 261-293). Springer, New York, NY.

Zuur, A. F., Ieno, E. N. & Elphick, C. S. (2010). A protocol for data exploration to avoid common statistical problems. *Methods in ecology and evolution*, *1*(1), 3-14.

CHAPTER 4 - Changes in biodiversity, GOODS and GES under IPCC scenarios

Project acronym:	ATLAS
Grant Agreement:	678760
Deliverable number:	D3.3
Deliverable title:	WP3
Work Package:	31st May 2019
Date of completion:	D3.3 Biodiversity, biogeography and GOODS classification system under current climate conditions and future IPCC scenarios
Author:	See next page

This project has received funding from the European Union's Horizon 2020 research and innovation programme under grant agreement No 678760 (ATLAS). This output reflects only the author's view and the European Union cannot be held responsible for any use that may be made of the information contained therein.

4 Chapter 4: Changes in biodiversity, GOODS and GES under IPCC scenarios

Telmo Morato[1,2], José-Manuel González-Irusta[1,2], Carlos Dominguez-Carrió[1,2], Chih-Lin Wei[3], Andrew Davies[4], Andrew K. Sweetman[5], Gerald H. Taranto[1,2], Lindsay Beazley[6], Ana García-Alegre[7], Anthony Grehan[8], Pascal Laffargue[9], F. Javier Murillo[6], Mar Sacau[7], Sandrine Vaz[10], Ellen Kenchington[6], Sophie Arnaud-Haond[10], Oisin Callery[8], Giovanni Chimienti[11,12], Erik Cordes[13], Hronn Egilsdottir[14], André Freiwald[15], Ryan Gasbarro[13], Matt Gianni[16], Kent Gilkinson[17], Vonda E. Wareham Hayes[17], Dierk Hebbeln[18], Kevin Hedges[19], Lea-Anne Henry[20], David Johnson[21], Georgios Kazanidis[20], Mariano Koen-Alonso[17], Cam Lirette[6], Francesco Mastrototaro[11,12], Lénaick Menot[9], Tina Molodtsova[22], Pablo Durán Muñoz[7], Bramley Murton[23], Covadonga Orejas[24], Maria Grazia Pennino[7], Patricia Puerta[24], Stefán Á. Ragnarsson[14], Berta Ramiro-Sánchez[20], Jake Rice[25], Jesús Rivera[26], Murray Roberts[20], Luís Rodrigues[1,2], Steve W. Ross[27], José L. Rueda[28], Paul Snelgrove[29], David Stirling[30], Margaret Treble[19], Javier Urra[28], Johanne Vad[20], Les Watling[31], Wojciech Walkusz[19], Zeliang Wang[6], Claudia Wienberg[18], Mathieu Woillez[9], Lisa A. Levin[32], Marina Carreiro-Silva[1,2]

1- Okeanos Research Centre, Universidade dos Açores, Horta, Portugal
2- IMAR Instituto do Mar, Universidade dos Açores, Horta, Portugal
3- Institute of Oceanography, National Taiwan University, Taipei, Taiwan
4- Department of Biological Sciences, University of Rhode Island, Kingston, Rhode Island, USA
5- Marine Benthic Ecology, Biogeochemistry and In situ Technology Research Group, The Lyell Centre for Earth and Marine Science and Technology, Heriot-Watt University, Edinburgh, United Kingdom
6- Bedford Institute of Oceanography, Fisheries and Oceans Canada, Dartmouth, NS, Canada
7- Instituto Español de Oceanografía (IEO), Centro Oceanográfico de Vigo, Vigo, Pontevedra, Spain.
8- Earth and Ocean Sciences, NUI Galway, Ireland
9- IFREMER, Centre Atlantique, Nantes, France
10- MARBEC, IFREMER, Univ. Montpellier, IRD, CNRS, France
11- Department of Biology, University of Bari Aldo Moro, Bari, Italy
12- CoNISMa, Rome, Italy
13- Department of Biology, Temple University, Philadelphia, USA
14- Marine and Freshwater Research Institute, Reykjavík, Iceland
15- Senckenberg am Meer, Marine Research Department, Wilhelmshaven, Germany
16- Gianni Consultancy, Amsterdam, Netherlands
17- Northwest Atlantic Fisheries Centre, Fisheries and Ocean Canada, St. John's, NL, Canada
18- MARUM - Center for Marine Environmental Sciences, University of Bremen, Germany
19- Fisheries and Oceans Canada, Winnipeg, MB, Canada
20- School of GeoSciences, Grant Institute, University of Edinburgh, United Kingdom
21- Seascape Consultants Ltd, Romsey, United Kingdom
22- P.P. Shirshov Institute of Oceanology, Moscow, Russia
23- National Oceanography Centre, Southampton, United Kingdom
24- Instituto Español de Oceanografía, Centro Oceanográfico de Baleares, Palma, Spain
25- Fisheries and Ocean Canada, Ottawa, ON, Canada
26- Instituto Español de Oceanografía, Madrid, Spain
27- Center for Marine Science, University of North Carolina at Wilmington, Wilmington, NC, USA
28- Instituto Español de Oceanografía, Centro Oceanográfico de Málaga, Málaga, Spain
29- Department of Ocean Sciences, Memorial University, St Johns, Newfoundland, Canada
30- Marine Laboratory, Marine Scotland Science, Aberdeen, Scotland, UK
31- School of Marine Sciences, University of Maine, Orono, Maine, USA
32- Center for Marine Biodiversity and Conservation and Integrative Oceanography Division, Scripps Institution of Oceanography, UC San Diego, La Jolla, CA, USA

Contents

4.1 Executive summary

The deep sea plays a critical role in global climate regulation through uptake and storage of heat and carbon dioxide. But this uptake causes warming, acidification, and deoxygenation of deep waters, leading to decreased food availability. These changes and their forecasted projections are likely to severely affect productivity, biodiversity, and distributions of deep-sea fauna, especially Vulnerable Marine Ecosystems and their indicator species, and commercially important deep-sea fishes, thereby compromising key ecosystem services. Understanding how climate change can lead to shifts in deep-sea species distributions is critically important in developing management measures that consider such changes; especially those aimed to preserving refugia areas to aid conservation of cold-water corals or secure food, income and livelihoods from fisheries.

Climate-induced changes in deep-sea biodiversity distribution

We used environmental niche modelling along with the best available species occurrence data and a set of environmental parameters to model the habitat suitability for key cold-water coral and commercially important deep-sea fish species under present-day (1951-2000) environmental conditions and to forecast changes under future (2081-2100) climate projections (RCP8.5 or a business-as-usual scenario) for the entire North Atlantic Ocean. Our results show a marked decrease of 30% to 100% in suitable habitat for cold-water corals and a marked shift in the suitable habitat of deep-sea fishes from 2.0° to 9.9° towards higher latitudes. Our projections forecast the largest reductions in suitable habitat for the scleractinian coral *Lophelia pertusa* and the octocoral *Paragorgia arborea*, with declines of at least 79% and 99%, respectively. We predict expansion of suitable habitat by 2100 only for the fishes *Helicolenus dactylopterus* and *Sebastes mentella* by about 20 to 30%, mostly through northern latitudinal range expansion. Our modelling results forecasted limited climate refugia locations in the North Atlantic by 2100 for scleractinian corals (between 29% and 44% of North Atlantic present-day habitat), even smaller refugia locations for the octocorals *Acanella arbuscula* and *Acanthogorgia armata* (1.9-14.8% of present-day suitable habitat), and almost no refugia locations for *Paragorgia arborea*. Our results emphasize the need to understand how anticipated climate change will affect the distribution of deep-sea species, and highlight the importance to identify and preserve of climate refugia for Vulnerable Marine Ecosystems and commercially important deep-sea fishes.

Climate-induced changes in biogeography and biogeographic regions

With such forecasted changes in species suitable habitat, it is likely that species biogeography will change under future climate conditions. Our work also suggested that the existing Global Open Oceans and Deep Seabed (GOODS) provinces might change under future climate conditions. The bathyal province BY4 around the Mid-Atlantic Ridge will suffer environmental changes mostly related to decreased food supply that may affect the distribution of Vulnerable Marine Ecosystem indicator taxa. The cluster corresponding to the New England and Corner Seamounts is likely to be a refugia for some scleractinian species. The northern cluster coinciding with GOODS bathyal northern North Atlantic (BY2) will possibly suffer the strongest changes. Octocorals are forecast to lose habitat in an extensive measure in the Reykjanes Ridge, the continental shelf west of this ridge (Davis Strait and Labrador Sea), and east towards Rockall. This is likely the result of changes in temperature across a latitudinal gradient with this province probably moving northwards in the future. It is possible that this area will become available for other scleractinian taxa found at southern latitudes and hence GOODS bathyal province BY4 extending its limit up to the Davis Strait. Finally, GOODS suggests one homogeneous abyssal province for the North Atlantic. Even with inconclusive evidence of an eastern and western separation as results vary depending on taxa, future climate changes are unlikely to make any spatial differentiation or major latitudinal shift in this province.

Climate-induced changes in Good Environment Status

The remarkable reduction of scleractinian and octocoral suitable habitat predicted towards 2100, may imply the loss of an important part of the cold-water coral reefs and gardens. A decrease in the suitable habitat for cold-water corals, may produce a significant loss in biodiversity as well as negative effects in ecosystem functioning, and on the goods and services it provides. Therefore, the occurrence of Vulnerable Marine Ecosystems has been suggested as one indicator for assessing the Good Environmental Status (GES) in the deep sea (ATLAS D3.1 Deliverable). It can thus be anticipated that the reduction of the suitable habitat of some indicator taxa and, consequently, their associated fauna will have a negative effect in the GES of certain areas of the deep North Atlantic. The likely shifts of deep-water fish species towards higher latitudes may also have a direct impact on the GES of certain areas of the North Atlantic. Although, the ‘empty’ niche generated by the northward movement of one species may promote the replacement by another (usually southern) fish species. Therefore, without a broad understanding of the climate-induced changes in the distribution of deep-sea fishes, it will be difficult to predict and measure fish stock indicators of Good Environmental Status.

In summary, climate change will definitely affect the GES in the North Atlantic but predicting GES future trends will be challenging. Habitat suitability models may become a useful tool to produce

insights into the future GES; especially in the deep sea due to the difficulties to get access to this remote realm. Due to limited data availability (over space and time), difficulties in setting baselines, lack of standardizations (and a whole series of issues summarized in ATLAS Deliverable 3.1), makes the assessment of deep-sea GES under current and future environmental conditions a huge challenge. Knowledge gained in the ATLAS exercise of assessing GES in the deep-sea in combination with the outputs of the models in future climate scenarios, as well as the increasing knowledge on performance of key organisms under different environmental conditions, will be extremely useful tools for assessing environmental status of deep-sea ecosystems under the future climatic scenarios predicted by the IPCC, and for management purposes.

Conclusions

Habitat suitability models that are sufficiently ground-truthed, become a valuable tool to inform environmental management and conservation policy and provide a basis for taking climate change into consideration, as demonstrated here. However, more than any other biome on earth, the deep sea suffers from a lack of in situ observations and data on faunal biodiversity and distributions; which brings some additional uncertainties to modeling exercises. The vast expanse and high cost and difficulty of directly observing the deep-sea floor over large areas means that we will rarely be able to document the full distribution of species. This makes habitat suitability modelling tools of paramount importance for evaluating the distribution of data-poor deep-water species and to understand how current biogeography may alter. Habitat suitability projections under current and future climate scenarios, can be used to develop research agendas that confirm and advance the model outputs and clarify the roles of predictor variables in determining species distributions. Incorporating these needs into global observing efforts (e.g., the Deep Ocean Observing Strategy) can help fill data gaps, determine spatial locations for the collection of key physical and biogeochemical data using moorings, floats, ship tracks, or observatories, and advance technologies such as imaging and eDNA that can improve species detection. Further integration of species-level biogeochemical and physical data, as well as results of the ecophysiological performance of deep-sea organisms from *ex situ* experimental work, will improve suitability and distribution mapping, but additional mechanistic (experimentally derived) understanding is needed of how climate drivers elicit ecological responses. The United Nations' Decade for Ocean Science, the Global Ocean Observing System (GOOS) and the Regular Process for Global Reporting and Assessment of the State of the Marine Environment (a.k.a. World Ocean Assessment) are forward-looking international entities that can help set such science agendas.

In summary, we have showed that despite all the caveats, habitat suitability models are useful tools for predicting potential future changes in the distribution of deep-water species and may be used to

inform management decisions. This is especially the case when such dramatic changes as shown here are forecasted. Such models will improve in concert with climate change predictions. We hope the present study can provide a suitable template for and will stimulate similar analyses conducted for other taxa or regions.

4.2 Background

The deep sea represents at least 95% of the habitable ocean and plays a critical role in climate regulation through uptake and storage of heat and carbon dioxide (Sabine et al., 2004; Purkey & Johnson, 2010). But this is causing warming, acidification, and deoxygenation of deep waters, and decreasing food availability (Mora et al., 2013; Gehlen et al., 2014; Chen et al., 2017; Sweetman et al., 2017; Perez et al., 2018). Recent projections of deep water mass properties suggested that portions of the seafloor will experience an average increase in temperature of over 1°C, a decrease in pH greater than 0.3 units, a loss of dissolved oxygen up to 3.7%, and a 40-55% decrease in the flux of particulate organic matter to the seafloor by 2100 (Gehlen et al., 2014; Sweetman et al., 2017). These forecasted changes may severely affect productivity, biodiversity, and distribution of deep-sea fauna, especially Vulnerable Marine Ecosystems (VMEs) indicator species and commercially important deep-sea fish, compromising key ecosystem services (Jones et al., 2014; Thurber et al., 2014; Levin & Le Bris, 2015; Pecl et al., 2017).

Among deep-sea VMEs indicators, cold-water corals (CWC) that form important biogenic habitats are known to be vulnerable to anthropogenic climate change, particularly to Ocean Acidification (OA) (Guinotte et al., 2006; Roberts et al., 2016; Perez et al., 2018). This is because most CWC with carbonate skeletons are found in waters supersaturated in carbonate that promote the bio-calcification of their skeletons (Guinotte et al., 2006; Davies & Guinotte, 2011; Yesson et al., 2012). Although several experimental studies have shown reef-building scleractinian CWCs to be highly resilient to OA (Form & Riebesell, 2012; Maier et al., 2012; 2013; 2018; Hennige et al., 2014; 2015; Movilla et al., 2014; Büscher et al., 2017), other studies suggested a great susceptibility of the same CWC species to OA alone or in combination with warming and deoxygenation with decreased calcification rates, increased skeletal dissolution, and induced mortality (Kurman et al., 2017; Lunden et al., 2014; Georgian et al., 2016; Gomez et al., 2018; Brooke et al., 2013; Naumann et al., 2013). Notwithstanding the genotype variability in the responses to OA (Kurman et al., 2017), the long term survival of CWC reefs may be impaired by the chemical dissolution and biological erosion (bioerosion) of the tissue-unprotected skeleton exposed to corrosive waters (Thresher et al., 2011; Hennige et al., 2015; Schönberg et al., 2017). Thus, the predicted shoaling of the calcite and aragonite saturation horizon as a consequence of OA is expected to lead to the loss of suitable habitat (Davies & Guinotte, 2011; Yesson et al., 2012; Perez et al., 2018), and weakening of the reef framework that may result in their structural collapse of slow-growing scleractinian (Schönberg et al., 2017), and increased mortality of gorgonians forming coral gardens (e.g. Cerrano et al., 2013); resulting in the loss of biodiversity and ecosystem service provisioning associated to these ecosystems.

Along with climate regulation, provisioning of fish stocks is one of the most recognised ecosystem service that the deep sea provides (Thurber et al., 2014), with increasing importance in global food provision (Watson & Morato, 2013; Victorero et al., 2018). However, warming and deoxygenation will directly and synergistically affect fish condition by increasing metabolic rates and oxygen demand while limiting their capacity to supply oxygen to their tissues to meet the increased demand in deoxygenated environments (Holt & Jørgensen, 2015; Pörtner & Knust, 2007; Pörtner et al., 2017). Decreasing food availability will indirectly add to the stress imposed by enhanced temperature increasing metabolism (Woodworth-Jefcoats et al., 2017). Therefore, climate change is expected to reduce fish size and growth, abundance, survival, and shift the distribution of bottom fish and fisheries (Perry et al., 2005; Pörtner & Knust, 2007; Dulvy et al., 2008; Cheung et al., 2010; Baudron et al., 2014; Pecl et al., 2017; Bryndum-Buchholz et al., 2018). Nevertheless, there is still much to be understood regarding the underlying physiological mechanisms influencing potential responses of fishes to climate change (Lefevre et al., 2017).

Understanding how human-induced climatic change can lead to shifts in the distribution of deep-sea species is of paramount importance in developing management measures that take such changes into consideration, especially those that aim to preserve refugia areas and secure food resources from fisheries (Cheung et al., 2010; Thresher et al., 2015; Cheung et al., 2017; Gaines et al., 2018). Environmental niche modelling, also called species distribution models (SDMs), habitat suitability models (HSM) or climate envelope models (CEM), are powerful tools to predict the distribution of species along wide geographical areas and forecast changes under future climatic scenarios (Pearson & Dawson, 2003; Hijmans & Graham, 2006; Wiens et al., 2009; Hattab et al., 2014). Whilst not without limitations, for example, species genetic variability, phenotypic plasticity, evolutionary changes, and acclimation could limit the accuracy of such models (Pearson & Dawson, 2003; Elith & Leathwick, 2009; Austin & Van Niel, 2011; Fillinger & Richter, 2013; Sandblom et al., 2014; Kurman et al., 2017), these approaches have been widely applied to terrestrial species and habitats (e.g. Iverson & Prasad, 1998; Fordham et al., 2012) and marine (e.g., benthic macrofauna, Singer et al., 2018; seagrass, Chefaoui et al., 2018; and fish, Morley et al., 2018). However, due to the lack of reliable predictions of the future environmental conditions close to the seabed, forecasts of shifts in the distribution of deep-sea bottom dwelling species has remained unstudied.

The recent development of modelled scenarios of future seabed environmental conditions at a global scale (e.g., Sweetman et al., 2017) and the increased understanding of the ecology and distribution of key deep-sea benthic species (e.g., Priede, 2017; Rossi et al., 2017; Orejas & Jiménez, 2019), have enabled the ability to forecast changes in the distribution of such species. Making use of the best available curated species occurrence data obtained from multiple public and restricted sources and a

set of static (depth and derived variables) and dynamic environmental parameters (POC flux to seabed, pH, dissolved oxygen concentration, temperature at seafloor, and aragonite and calcite saturation state), we modelled the habitat suitability for six cold-water coral and six deep-sea fish species under current conditions and forecasted changes under future projected climate conditions for the whole northern Atlantic Ocean. With this work we aimed to provide insights on how projected climate change could affect the distribution of deep-sea species at an ocean-basin scale and may help in the identification of refugia areas for Vulnerable Marine Ecosystems and commercially important deep-sea fish. We will then use the outputs of these models to evaluate the climate-induced changes in biogeography and biogeographic provinces in the deep North Atlantic and discuss how climate change may affect measures of Good Environmental Status (GES).

4.3 Climate-induced changes in the habitat suitability of cold-water corals and commercially important deep-sea fishes in the North Atlantic

4.3.1 Methodology

Here, we used the habitat suitability models developed for VME indicator taxa and commercially important deep-sea fish species in the deep waters of the North-Atlantic basin (from 18°N to 76°N and 36E° to 98W) under present-day environmental conditions (see Chapter 3) and forecasted changes under future projected climate conditions. As in Chapter 3, the VME indicator taxa selected included three scleractinian corals forming aragonitic skeletons (*Lophelia pertusa*[6], *Madrepora oculata*, and *Desmophyllum dianthus*), and three gorgonians forming calcitic skeletons (*Acanella arbuscula*, *Acanthogorgia armata*, and *Paragorgia arborea*). These two groups of VME indicators are expected to respond differently to future conditions of water mass properties. The six deep-sea fish species selected were the roundnose grenadier (*Coryphaenoides rupestris*), Atlantic cod (*Gadus morhua*), bluemouth rockfish (*Helicolenus dactylopterus*), American plaice (*Hippoglossoides platessoides*), Greenland halibut (*Reinhardtius hippoglossoides*), and beaked redfish (*Sebastes mentella*).

Environmental variables of future conditions were calculated for the 2081-2100 (RCP8.5 or business-as-usual scenario) using the average values obtained from the Geophysical Fluid Dynamics Laboratory's ESM 2G model (GFDL-ESM-2G; Dunne et al., 2012), the Institut Pierre Simon Laplace's CM6-MR model (IPSL-CM5A-MR; Dufresne et al., 2013) and Max Planck Institute's ESM-MR model (MPI-ESM-MR; Giorgetta et al., 2013) within the Coupled Models Intercomparison Project Phase 5 (CMIP5). Environmental variables were available at a 0.5° resolution and re-scaled to match the 3x3km

[6] recently synonymised to *Desmophyllum pertusum*, Addamo et al., 2016

cell size using universal kriging and depth as covariate. Maps of environmental predictors for future climate scenarios are provided as Supplementary Figure S1.

Here, we used an ensemble modelling approach to forecast changes under future (2081-2100) climate projections (RCP8.5 or business-as-usual scenario). Each model was used to forecast the Habitat Suitability Index (HSI) for the period 2081-2100 by projecting the present-day niche onto the environmental layers of predicted future conditions. The ensemble outputs were computed for all species and for the two study periods by computing the average HSI by cell after weighting the model outputs with the evaluation metrics AUC and TSS, using the same approach applied by Rowden et al. (2017). Maps with continuous values of HSI were converted into binary maps of predicted suitable and unsuitable areas in both current and future scenarios using two thresholds: 10-percentile training presence logistic threshold and maximum sensitivity and specificity (MSS). Binary maps were used to calculate the suitable habitat area, and the median values of the latitudinal and depth distribution of all species in the North Atlantic; excluding the Mediterranean Sea. Refugia areas (*sensu* Keppel & Wardell-Johnson, 2012) for Vulnerable Marine Ecosystems and commercially important deep-sea fish in the North Atlantic Ocean were inferred from those areas predicted to be suitable both under present-day and future conditions.

4.3.2 Results

Changes in the suitable habitat under future climate conditions showed contrasting patterns for the different VME indicators (Figure 195) and deep-sea fish species evaluated (Figure 196). In general, the model outputs for scleractinian corals and gorgonians showed a marked decrease in the suitable habitat towards the 2100, while deep-sea fish showed a marked shift towards higher latitudes. According to the ensemble model outputs, the scleractinian coral *Lophelia pertusa* may face a major reduction in suitable habitat >79% (Figure 197), with no certain shift in the median latitudinal distribution by 2100 (Figure 198), but a shift in the median depth distribution towards deeper waters (Figure 199) due to habitat suitability loss at shallower depths. The other two scleractinian corals (*Madrepora oculata* and *Desmophyllum dianthus*) may face a moderate reduction in the suitable habitat of about 30% to 55% (Figure 197), with a northern shift in the median latitudinal distributions (ranging from 1.9° to 4.6° in latitude) (Figure 198) and a shift of *Madrepora oculata* median suitable depths towards deeper waters (Figure 199). The suitable habitat for all scleractinian corals was forecasted to increase in the Davis Strait and Labrador Sea and to decrease mostly in the south part of the North Atlantic from the Gulf of Mexico to the Flemish Cap, but also in the Mid-Atlantic Ridge (MAR), Bay of Biscay, and in the Rockall and Faroe Shetland areas (Figure 195). Forecasted climate

refugia for scleractinian corals were in average between 29% and 44% of North Atlantic present-day habitat, depending on the threshold considered (Table 34). However, refugia for *Lophelia pertusa* estimated with the 10th percentile threshold was only about 3% of the North Atlantic present day habitat (Table 34). Forecasted climate refugia for scleractinian corals are located in both sides of the North Atlantic (Figure 195).

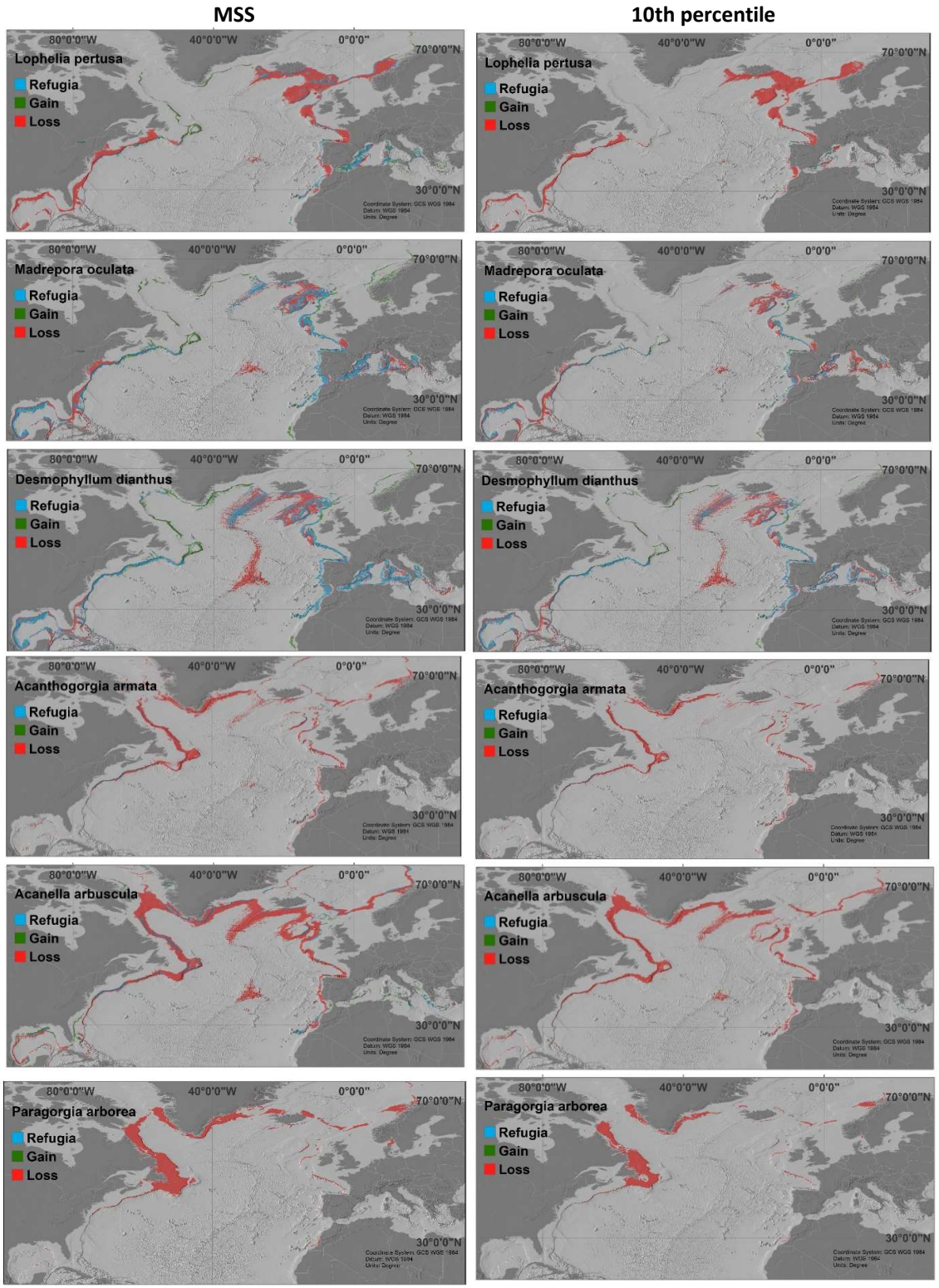

Figure 195. Forecasted present-day suitable habitat loss, gain, and acting as climate refugia areas (sensu Keppel & Wardell, 2012) under future (2081-2100; RCP8.5 or business-as-usual scenario) environmental conditions for cold-water corals fish in the North Atlantic Ocean. Areas were identified from binary maps built with an ensemble modeling approach and two thresholds: 10-percentile training presence logistic threshold (10th) and maximum sensitivity and specificity (MSS).

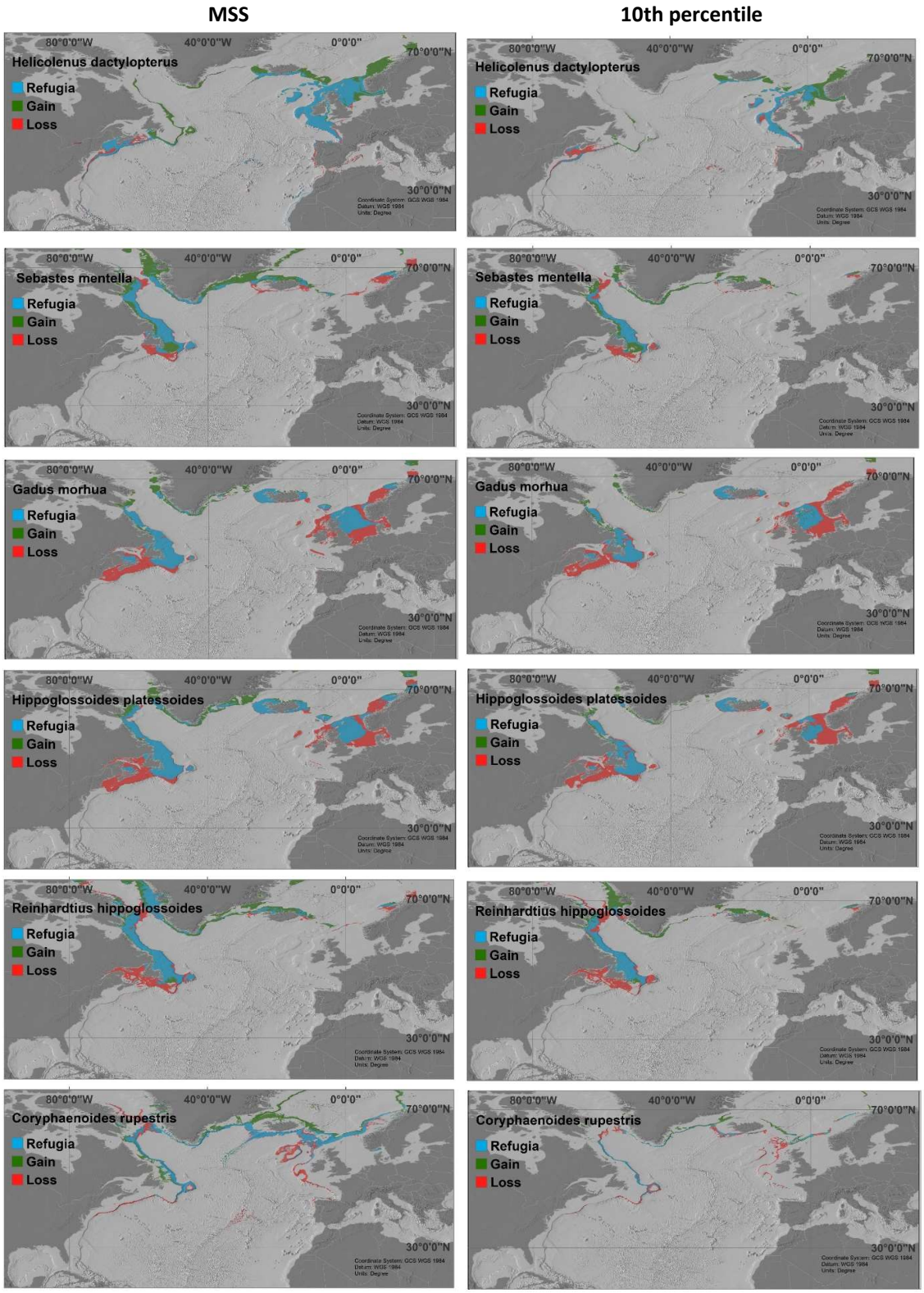

Figure 196. Forecasted present-day suitable habitat loss, gain, and acting as climate refugia areas (sensu Keppel & Wardell, 2012) under future (2081-2100; RCP8.5 or business-as-usual scenario) environmental conditions for commercially important deep-sea fish in the North Atlantic Ocean.

Table 34. Proportion of the present-day suitable habitat acting as refugia areas (Keppel & Wardell, 2012) under future (2081-2100; RCP8.5 or business-as-usual scenario) environmental conditions for Vulnerable Marine Ecosystems and commercially important deep-sea fish in the North Atlantic Ocean. Refugia areas were identified from binary maps built with an ensemble modeling approach and two thresholds: 10-percentile training presence logistic threshold (10th) and maximum sensitivity and specificity (MSS). Refugia areas estimated by the different models used to calculate the ensemble outputs are also shown: Generalized Additive Model (GAM), maximum entropy model (Maxent), and Random Forest (RF).

Group	**Species**	**Refugia areas** (% present day habitat)							
		Ensemble		**GAM**		**Maxent**		**RF**	
		10th	***MSS***	***10th***	***MSS***	***10th***	***MSS***	***10th***	***MSS***
Scleractinian corals	*Lophelia pertusa*	3.20	20.47	0.26	0.61	45.85	58.40	4.38	21.03
	Madrepora oculata	36.92	54.76	24.98	38.50	60.35	71.74	14.02	51.61
	Desmophyllum dianthus	47.77	57.01	43.74	44.39	63.39	70.73	25.67	46.33
Gorgonians	*Acanthogorgia armata*	4.02	8.13	9.16	12.07	4.99	7.46	4.96	12.67
	Acanella arbuscula	1.90	14.84	0.36	1.80	12.91	27.84	12.66	32.56
	Paragorgia arborea	0.00	0.00	0.00	0.00	0.14	0.39	0.00	9.99
Deep-water fish	*Helicolenus dactylopterus*	67.69	82.18	72.19	87.70	85.13	87.60	45.28	62.00
	Sebastes mentella	55.92	64.78	51.05	61.59	53.05	70.24	48.07	64.22
	Gadus morhua	42.62	51.73	52.10	56.45	12.33	45.84	39.77	47.96
	Hippoglossoides platessoides	42.61	55.79	54.97	59.75	13.83	53.70	37.84	48.22
	Reinhardtius hippoglossoides	51.54	60.86	50.68	55.68	50.76	57.79	43.81	50.20
	Coryphaenoides rupestris	43.48	62.45	52.55	59.63	44.47	68.65	28.52	57.88

All three gorgonians (*Acanella arbuscula*, *Acanthogorgia armata*, and *Paragorgia arborea*) may be endangered in the North Atlantic as a consequence of climate change. The ensemble model outputs suggested a substantial reduction in the suitable habitat greater than 80%, in all regions with no exception and regardless of the modelling approach or threshold used (Figure 197). The large reduction in the suitable habitat resulted in a forecasted marked southern shift of the median latitude (ranging from -11.3° to -27.8° in latitude) (Figure 198) and a shift toward shallower depths for *Acanella arbuscula* and *Acanthogorgia armata* (Figure 199). New suitable habitat was forecasted for these two species by 2100 in the shallower waters of the northern most part of the North Atlantic and Gulf of Mexico (Figure 195). Extremely small refugia areas may remain in the North Atlantic for gorgonians *Acanella arbuscula* and *Acanthogorgia armata* (1.9-14.8% of present-day suitable habitat) while for *Paragorgia arborea* the ensemble model forecasts no climate refugia will remain by 2100 (Table 34, Figure 195).

The suitable habitat for fish species was forecasted to be reduced by about 30 to 50% for *Gadus morhua* and *Hipoglossoides platessoides*, about 10 to 15% for *Reinhardtius hippoglossoides*, and up to about 2 to 25% for *Coryphaenoides rupestris,* mostly in their lower latitudinal range (Figure 197). The suitable habitat for *Gadus morhua* was forecasted to decrease in important fishing grounds such as the Georges Bank, the Irish Sea, the Norwegian Sea, and the south part of the North Sea (Figure 196). *Helicolenus dactylopterus* and *Sebastes mentella* were the only species for which the predicted total suitable habitat may increase by 2100 (by about 20 to 30%), mostly by expanding the northern latitudinal range (Figure 195). Therefore, a clear northern shift of the median latitude of fish suitable habitat by 2100 (ranging from 2.0° to 9.9° in latitude) was observed for most fish species (Figure 198), but there was no clear trend in terms of depth distribution (Figure 199). Predicted climate refugia for deep-water fish were in average large, between 51 and 63% of present-day habitat, depending on the threshold (Table 34). Forecasted climate refugia for deep-water fish are mostly located in both sides of the northern part of the North Atlantic (Figure 196).

The uncertainty associated with the habitat suitability model predictions under future environmental conditions was in general low for both cold-water corals and deep-sea fish (Supplementary Figure S2).

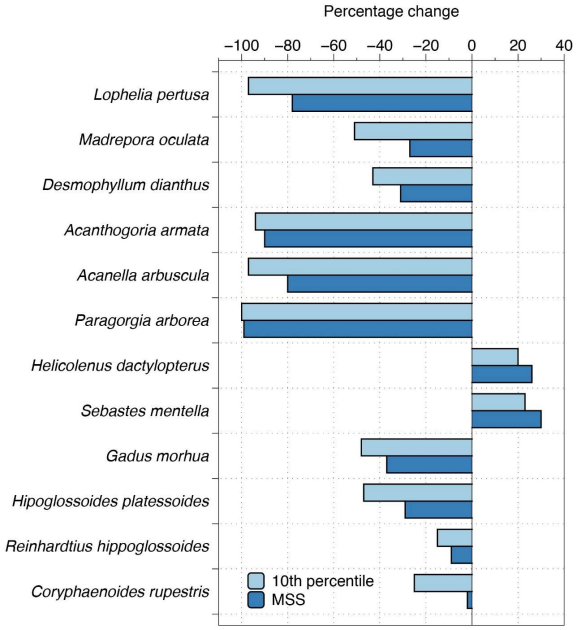

Figure 197. Climate induced changes (RCP8.5 or business-as-usual scenario) in the suitable habitat for cold water corals and deep-sea fish in North Atlantic Ocean forecasted with an ensemble modelling approach. The extension of the habitat was calculated from binary maps built with two thresholds: 10-percentile training presence logistic (10th percentile) and maximum sensitivity and specificity (MSS).

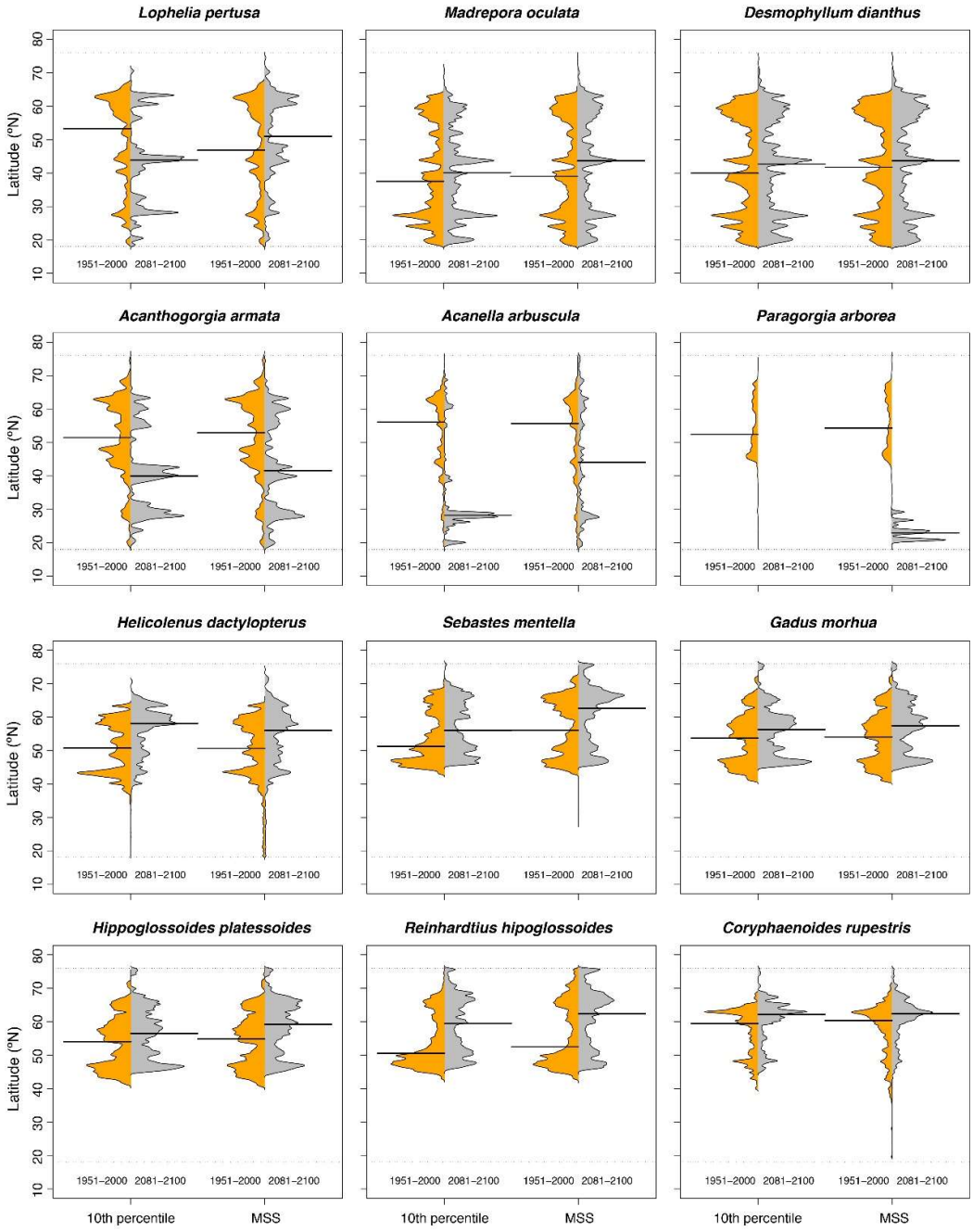

Figure 198. Climate induced changes (RCP8.5 or business-as-usual scenario) in the latitudinal distribution of cold water corals and deep-sea fish in North Atlantic Ocean forecasted with an ensemble modelling approach. The extension of the habitat was calculated from binary maps built with two thresholds: 10-percentile training presence logistic (10th percentile) and maximum sensitivity and specificity (MSS). The black line indicates the median latitudinal.

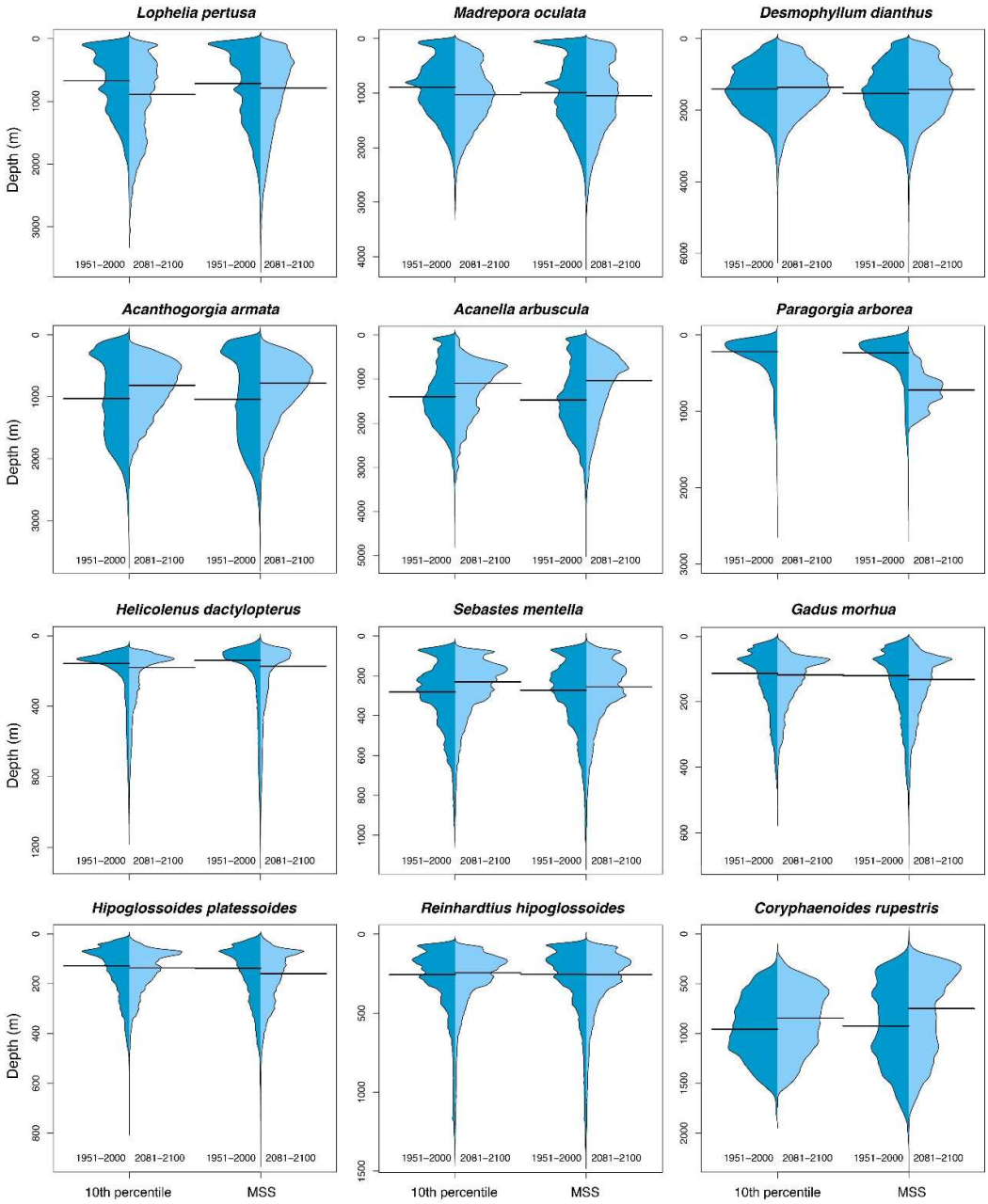

Figure 199. Climate induced changes (RCP8.5 or business-as-usual scenario) in the depth distribution of cold water corals and deep-sea fish in North Atlantic Ocean forecasted with an ensemble modelling approach. The extension of the habitat was calculated from binary maps built with two thresholds: 10-percentile training presence logistic (10th percentile) and maximum sensitivity and specificity (MSS). The black line indicates the median depth.

4.3.3 Discussion

Our model predictions and forecasts showed that studied deep-sea species could be facing a significant reduction in suitable habitat by 2100. Climate change is expected to reduce the suitable

habitat of scleractinian corals in their North Atlantic distribution range by more than 50%, and potentially endangering all three gorgonians studied (*Acanella arbuscula*, *Acanthogorgia armata*, and *Paragorgia arborea*). This reduction is particularly worrisome for *Acanthogorgia armata*, whose distribution is limited to the North Atlantic Ocean. The forecast produced also suggest a northward shift of the suitable habitat of many commercially important deep-sea fish, which agrees with the hypothesis of a poleward expansion in response to climate change (Perry et al., 2005; Jones et al., 2013; Poloczanska et al., 2013). We also predicted that climate change refugia for cold-water corals, mainly for gorgonians, may be limited to specific small areas, highlighting the need for accurate fine-scale climate grids and methodologies to properly identify those refugia (Ashcroft, 2010; Keppel et al., 2012; Kavousi & Keppel, 2018).

Some of the general changes in distribution patterns identified here have been suggested for both cold-water corals and deep-sea fish. Namely, the significant loss of suitable habitat for cold-water coral reefs globally (Guinotte et al., 2006; Zheng & Cao, 2014) or in the UK waters (Jackson et al., 2014) due to ocean acidification. Also, the loss of suitable habitat for Atlantic cod in the Georges Bank, and Celtic and Irish Seas, with a reduction in the southern North Sea and a northwards expansion along Greenland and the Davis Strait and the Arctic Ocean (Drinkwater et al., 2005; Fogarty, et al., 2008; Fossheim et al., 2015). Furthermore, some of the observed patterns are already being reported from field surveys, as for example the collapse of the Atlantic cod fisheries in the Gulf of Maine (Pershing, 2015) due to warming, the northward movement of bluemouth rockfish and Atlantic cod in the North Sea (Beare et al., 2004; Perry et al., 2005), the northward movement of bluemouth rockfish and the reduction in the suitable habitat for American plaice in the western North Atlantic (Nye et al., 2009), and the reduction in abundance of Greenland halibut in the Barents Sea (Fossheim et al., 2015). Therefore, this study highlights the appropriateness of environmental niche modelling in evaluating changes in the suitable habitat of deep-sea species under future climate scenarios and at large spatial scales.

Although these modelling approaches come with some caveats, our results showed that warming, acidification, and decreasing food availability, will act independently or synergistically and will affect the suitable habitat of deep-sea species. Marked loss of suitable habitat for cold-water corals were linked with the shoaling of the aragonite and calcite saturation horizon as a consequence of OA in the NE (the Rockall and Faroe Shetland areas) and SE regions of the North Atlantic, and that this will act synergistically with a strong decrease in food availability in the MAR. In the NW (Davis Strait and Labrador Sea) region of the North Atlantic, the shoaling of the calcite saturation horizon as a consequence of OA will likely produce a loss in the suitable habitat of gorgonians in the deeper waters. In the SW (from the Strait of Florida to the Georges Bank) region, loss of suitable habitat for

scleractinian corals was linked with a forecasted warming of the deeper waters, while for gorgonians was linked to the shoaling of the calcite saturation horizon. In the Gulf of Mexico, the forecasted decrease in suitable habitat was linked with a forecasted warming of the deeper waters. The marked loss of suitable habitat for deep-sea fish was associated with an increase in the water temperature in most regions of the North Atlantic and with a decrease in food availability in the MAR. On the contrary, gain in suitable habitat was linked with a warming of shallow waters in the Davis Strait and Labrador Sea and in the NE region for both corals and fish, and a warming of deeper waters in the lower latitudes of the North Atlantic for corals.

Temperature and depth were important predictors in determining the habitat suitability for CWC and deep-sea fish species, respectively. This is consistent with similar studies that have evaluated the distribution of other deep-sea corals (e.g., Davies & Guinotte, 2011; Guinotte & Davies, 2014; Georgian et al., 2014; Buhl-Mortensen et al., 2015; Lauria et al., 2017) and deep-sea fish (Gomez et al., 2015; Parra et al., 2017). However, since depth and temperature are auto-correlated and are correlated with other environmental and biological factors it is difficult to uncover which environmental parameters are primarily responsible for the observed patterns. It should, however, be noted that auto-correlation between depth and temperature was lower at ocean-basin scale than in most regional and local approaches. The importance of slope for some cold-water coral species could be linked to the higher suitability of some species in areas of high geomorphological relief that promote stronger near-bed currents and enhanced food supply (Genin et al., 1986).

Food availability measured as POC flux to the seafloor was also an important predictor for most cold-water corals and deep-sea fish species suitable habitat. This corroborates the fact that, for example, *Lophelia pertusa* have been generally described in areas with elevated POC flux, both in recent times (White et al., 2005; Davies et al., 2011) and since last glacial periods (Wienberg et al., 2010; Matos et al., 2015). Indeed, reduced food availability has been linked with reduced physiological performance (e.g., calcification and respiratory metabolism) and condition of cold-water corals (Naumann et al., 2011; Larsson et al., 2013; Büscher et al., 2017), and with their ability to cope with ocean change (Wood et al., 2008; Maier et al., 2016; Büscher et al., 2017; Gomez et al., 2018). On the contrary, the direct link between POC flux and deep-sea fish abundances have been proven hard to demonstrate (Bailey et al., 2006), but there is some evidence that increased surface production may fuel key prey taxa of such benthic invertebrate (Ruhl & Smith, 2004; Bailey et al., 2006). Therefore, the forecasted decrease in food availability by 2010 in the North Atlantic (Gehlen et al., 2014; Sweetman et al., 2017) may exacerbate the likely negative effects of other environmental changes.

Aragonite and calcite saturation states were shown to be important in determining cold-water coral habitat suitability (e.g., Davies & Guinotte, 2011; Yesson et al., 2012; Thresher et al., 2015). Some of

the present-day cold-water coral habitats in the North Atlantic are projected to become undersaturated in aragonite and calcite by 2100; which helps explaining the decrease in the suitable habitat area under future climate conditions. In fact, laboratory experiments have suggested that reduced aragonite and calcite saturation reduce calcification, growth, and metabolism of both scleractinian and gorgonians (e.g. Cerrano et al., 2013; Hennige et al., 2015; Carreiro-Silva, unpublished data). On the other hand, records of cold-water coral occurrences in undersaturated waters have been associated with areas of high productivity, leading to the hypothesis that increased food supply may compensate the extra necessary energy to survive under undersaturation conditions (Thresher et al., 2011; Baco et al., 2017). However, in an environment where food is permanently scarce the metabolic costs of calcifying in extremely low carbonate conditions may become prohibitively expensive compromising coral survival (Carreiro-Silva et al., 2014; Hennige et al., 2015; Maier et al., 2016).

It is challenging to infer the future capacity of deep-sea species, mostly corals, to adapt to changes in the water chemistry forecasted by climatic models. For example, it has been suggested from experimental (Keller & Os'kina, 2008) and paleoecological studies (Wienberg et al., 2010) that some *Madrepora oculata* populations can tolerate elevated seawater temperatures which may explain its prevalence at shallower depths (180-360 m) in the Mediterranean Sea (Freiwald et al., 2009; Gori et al., 2013). On the other hand, *Desmophylum dianthus*, which may also tolerate high temperatures (Naumann et al., 2013) and survive in aragonite undersaturated waters (Thresher et al., 2011; Jantzen et al., 2013; Rodolfo-Metalpa et al., 2015), may experience reduced metabolism compromising survival when exposed to the combined effects of increased temperature and reduced aragonite saturation (Gori et al., 2016). Additionally, scleractinian and gorgonians may be able calcify and grow under low or undersaturated conditions (Thresher et al., 2011; Form & Riebesell, 2012; Maier et al., 2012, 2013; Hennige et al., 2014, 2015; Movilla et al., 2014; Büscher et al., 2017); but it remains unclear whether calcification can be sustained indefinitely, as low carbonate has been shown to affect coral metabolism (Hennige et al., 2014) and increase energy demand to maintain pH homeostasis at the site of calcification (McCulloch et al., 2012; Raybaud et al., 2017). Despite all the uncertainties on how cold-water coral species may adapt to changes in climate conditions, along with the interspecific genetic variability (Kurman et al., 2017) and potential for local adaptation (Georgian et al., 2016) which alter their response to climate change, there is growing evidence supporting the limited adaptation ability under the long-term (e.g., Kurman et al., 2017) and multiple stressors.

More than any other biome on Earth, the deep sea suffers from a lack of *in situ* observations and data on faunal biodiversity and distributions; which brings some additionally uncertainty to modeling exercises. The vast expanse and high cost and difficulty of directly observing the deep-sea floor over

large areas means that we will rarely be able to document the full distribution of species; making habitat suitability modelling tools of paramount importance for evaluating the distribution of deep-water species. At the same time, the increasing human activities and pressures both within and beyond national jurisdictions and have created growing need to identify the distributions of sensitive species and habitats. Habitat suitability projections under current and future climate scenarios, can be used to develop research agendas that confirm and advance the model outputs and clarify the roles of predictor variables in determining distributions. Incorporating these needs into global observing efforts (e.g., Deep Ocean Observing Strategy) can help identify data gaps, designate spatial locations for collection of physical and biogeochemical data from moorings, floats, ship tracks, or observatories, and advance technologies such as imaging and eDNA that can improve species detection. Further integration of species-level biogeochemical and physical data will improve suitability and distribution mapping, but additional mechanistic (experimentally derived) understanding is needed of how climate drivers elicit ecological responses. Both the Decade for Ocean Science, the Global Ocean Observing System (GOOS) and the Regular Process (World Ocean Assessments) are forward-looking international entities that can help set such science agendas.

Once habitat suitability models are sufficiently ground-truthed, they can become a valuable tool to inform environmental management and conservation policy (Robinson et al., 2017) and provide a basis for taking climate change into consideration, as demonstrated here. The numbers and types of protected areas in the deep sea have grown in response to increasing regulation of activities in the marine environment and national and international commitments to protect marine biodiversity. Protected areas take many forms and include areas identified as Vulnerable Marine Ecosystems (VMEs) that are closed to bottom contact fishing by Regional Fisheries Management Organizations (RFMOs) in response to resolutions adopted by the UN General Assembly, or Areas of Particular Environmental Interest (APEI) designated by the International Seabed Authority (ISA) as ‘no-go’ areas for seabed mining, or other similar designations. Ecologically and Biologically Significant Areas (EBSAs) have been identified through mechanisms established under the Convention on Biological Diversity (CBD) to highlight biodiversity, but these do not have protected status. Additional mechanisms designed to establish Marine Protected Areas and facilitate the use of other area based management tools on the high seas are under discussion at the UN as part of the negotiation of a new treaty for the conservation of marine biodiversity in areas beyond national jurisdiction (BBNJ).

Each of these area-based management tools can benefit from the habitat suitability modeling approaches developed here. For the management of deep-sea fisheries, accurate knowledge of VME distributions in relation to climate change parameters can be used to regulate fishing gear, locations and timing both within and beyond national jurisdiction by RFMOs. The value of modeling to identify

areas where VMEs are known or likely to occur in fact has been recognized by the UN General Assembly in its resolution 71/123 adopted in 2016. In the same resolution, the General Assembly called on States and RFMOs to take into account the potential impacts of climate change in the management of deep-sea fisheries and the protection of VMEs (UNGA, 2016). Knowledge of changing species distribution can also inform UNFCCC climate policy, particularly adaptation scenarios. Knowledge of changing species distribution can also inform UNFCCC climate policy, particularly adaptation scenarios.

In summary, we have showed that despite all the caveats, habitat suitability models are useful tools for predicting potential future changes in the distribution of deep-water species and may be used to inform management decisions. This is especially the case when such dramatic changes as shown here are forecasted. Such models will improve in concert with climate change predictions. We hope the present study can provide a suitable template for and will stimulate similar analyses conducted for other taxa or regions.

4.4 Climate-induced change in the habitat suitability of *Lophelia pertusa* at regional spatial scale in the Porcupine Bank, Irish Shelf

(Contributors: Oisín Callery, Telmo Morato, José-Manuel González-Irusta, Anthony Grehan)

We used the habitat suitability models developed for *Lophelia pertusa* in the Porcupine Bank, Irish Shelf under present-day environmental conditions (see Chapter 3) and forecasted changes under future projected climate conditions at a regional scale. As in Chapter 3, the *Lophelia pertusa* was selected as a candidate species to test future climate change scenarios because of its keystone role in supporting cold-water coral reef habitat in Irish waters. In addition, we have already developed a high-resolution habitat suitability model for the species under current conditions (Rengstorf et al., 2013) that can be adapted to run with the future environmental conditions envisaged to occur under climate change scenarios (particularly weak AMOC conditions).

Environmental variables of future conditions were calculated for the 2081-2100 (RCP8.5 or business-as-usual scenario) using the average values obtained from the Geophysical Fluid Dynamics Laboratory's ESM 2G model (GFDL-ESM-2G; Dunne et al., 2012), the Institut Pierre Simon Laplace's CM6-MR model (IPSL-CM5A-MR; Dufresne et al., 2013), and Max Planck Institute's ESM-MR model (MPI-ESM-MR; Giorgetta et al., 2013) within the Coupled Models Intercomparison Project Phase 5 (CMIP5); these data were downloaded from the Earth System Grid Federation Peer-to-Peer (P2P)

enterprise system (ESGF, 2019). Mean values calculated for each of the three periods of interest: (i) a historical simulation for the period 1951-2000, and two future scenarios for the periods (ii) 2041-2060 and (iii) 2081-2100. All data for future scenarios were based on the RCP8.5 (business-as-usual) greenhouse gas concentration trajectory scenario (IPCC, 2014). Maps of environmental predictors for future climate scenarios are provided as Supplementary Figure S3.

As described in Chapter 3, two habitat suitability models were produced using Maxent: (i) a model describing the response of *Lophelia pertusa* to physical variables (the aforementioned 'Model A'), and (ii) a model describing the response of *Lophelia pertusa* to dynamic variables, which are subject to the effects of climate change (the aforementioned 'Model B'). Using these two models, three model outputs providing predicted habitat suitably indices for *Lophelia pertusa* were obtained, as described above, by multiplying the outputs of models A and B (the output of model A being a single binary output of suitable/unsuitable *Lophelia pertusa* habitat, and the outputs of model B being three maps of predicted distribution for the three time periods: 1951-2000, 2041-2060, and 2081-2100). The outputs of this combined model are shown in Figure 200 and the changes in the habitat suitability index are shown in Figure 201.

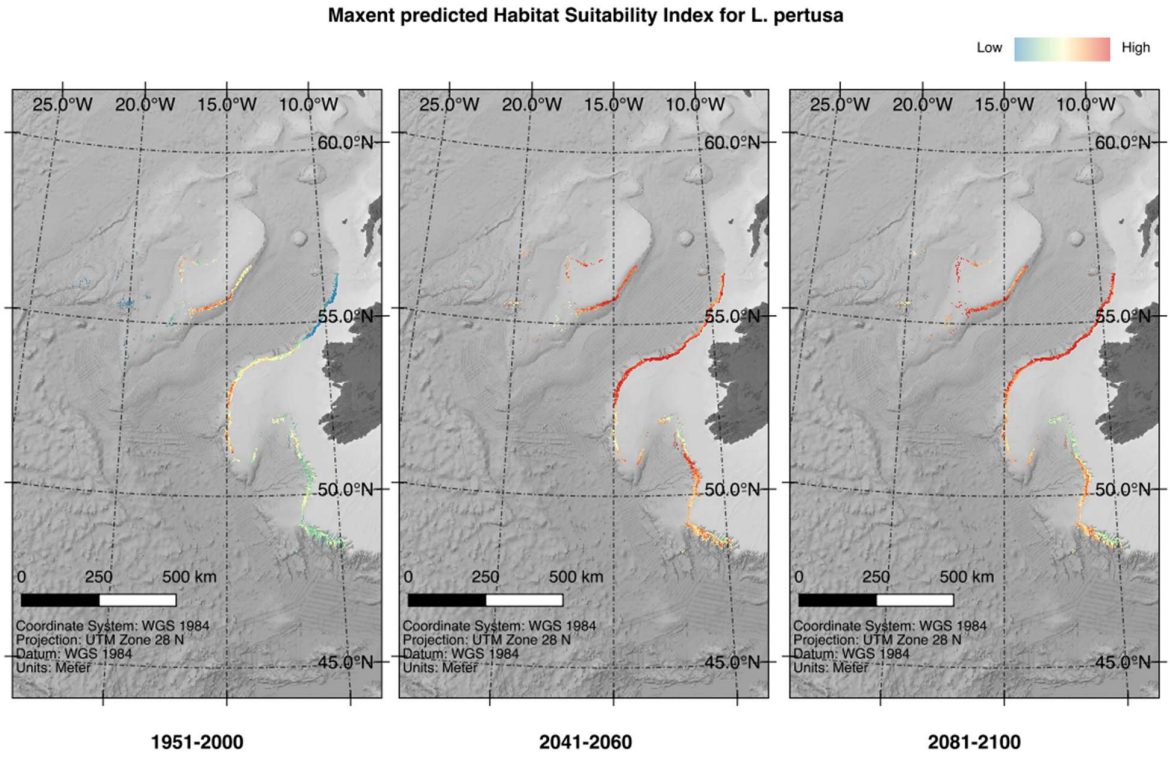

Figure 200. Extents and predicted suitability of Lophelia pertusa *habitat for three time periods (1951-2000, 2041-2060, and 2081-2100) based on the product of the outputs from model A and model B.*

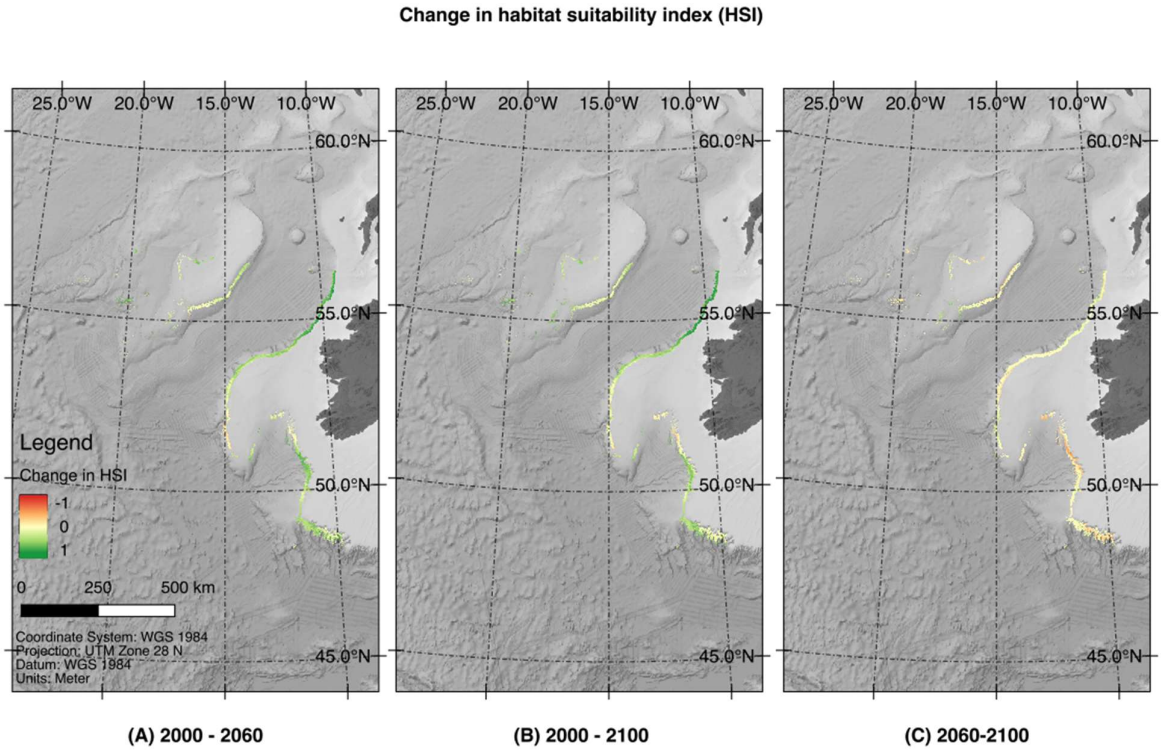

Figure 201. Comparative changes in the predicted suitability of Lophelia pertusa *habitat from (A) 2000-2060 (B) 2000-2100 and (C) 2060-2100.*

Using the climate change variables as inputs to the Maxent model initially predicts (in the period 2041-2060) a general expansion of suitable *Lophelia pertusa* habitat into the northern latitudes of the study area as well as a shift from shallower depths to deeper waters in the southern latitudes. Then, in the period 2081-2100, the habitat in the northern latitudes begins to follow the same pattern previously observed in the southern latitudes – i.e. a contraction of suitable habitat area in shallow depths coupled with a shift toward deeper waters. The "dynamic" Maxent model – i.e. the model which uses climate affected variables – is very strongly affected by temperature, which has a relative contribution of 49.6% to the prediction output. The temperature response curve also has a number of areas which are very steeply sloped – e.g., an increase from 6°C to 6.5°C results in a four-fold increase in predicted habitat suitability (with respect to temperature only) - and it seems likely that the sensitivity of the model to these minute changes is largely responsible for the shifts in distribution described above. The sensitivity of the model predictions to minute changes in temperature (and the effects of the shape of the temperature response curve) should be taken into consideration when interpreting model outputs, as should the coarse (0.5°) resolution and uncertain nature of the original model predicted layers from which these temperature data are derived.

When comparing the forecasted changes of the regional model with the ocean-basin scale model we noted that the areas forecasted to become suitable in the future in the regional model are those that

were considered as the refugia areas in the ocean-basin scale model. This shows that the ocean-basin scale model, as expected, may be over-predicting the suitable habitat for present-day environmental conditions but that the patterns of future habitat suitability are very similar; giving some extra confidence on the outputs of the ocean-basin scale model.

4.5 Climate-induced changes in biogeography, GOODS and EMUs under IPCC scenarios

(Contributors: same as in Chapter 2)

Using results from the biogeography analyses (Chapter 2), and the species distribution model (Section 4.3), we highlight how the biogeography and GOODS biogeographic provinces may change under future climate scenarios. It is likely that species biogeography will change under future climate conditions since oceanographic conditions are predicted to shift significantly by 2100 (Sweetman et al., 2017). In the biogeography analysis (Chapter 2), the most important environmental variables predicting biogeographical regions were exported particulate carbon to the seafloor and currents speed; however, the latitudinal pattern observed in the data suggested temperature as the main driver of distribution. Kocsis et al. (2018) found that coastal bioregions have not changed in the past 10 million years in response to environmental conditions, but these probably shifted latitudinally in response to changes in climate. Therefore, temperature, the main driver in structuring bioregionalization, will play a key component in climate change. The response of deep-sea fauna to increasing temperatures in the ocean is unknown and it is a difficult task to predict these changes in space. Predictive habitat suitability models provided new lines of evidence to help identify species that are likely to be sensitive to climate change and areas with interest for conservation that could act as climate refugia for certain deep-sea species. Given the difficulty in forecasting spatial changes in species biogeography and in biogeographic regions, the best way forward to address this is the analyses of the predicted species distribution based on environmental predictors projected in future scenarios.

We suggest how the GOODS provinces might change under future climate conditions based on our five main clusters found in the High Seas of the North Atlantic and the results from species distribution models of six VME scleractinian and octocoral species. The Mid-Atlantic Ridge south of the Azores, a province on its own in our results, is characterized by chemosynthetic megafauna. Corresponding to GOODS bathyal province BY4, this area and depth zone of the Mid-Atlantic Ridge will suffer changes in accordance to modifications in food supply. Chemosynthetic organisms may not be impacted as much due to their dependence on hydrothermal energy by-products, but it may impact other recorded organisms such as cold-water corals and sponges. Occurrences of other VMEs in this area are,

however, very limited and predictions are scarce for other organisms that rely on food export from surface waters.

The cluster corresponding to the New England and Corner Seamounts consistently identified throughout the analyses as a unique region. This area is likely to be a refugia for some scleractinian species as the SDMs for Section 4.3 show in their predictions, whereas octocorals may not be able to stand the shoaling of calcite as a result of rising temperatures. Currently part of GOODS bathyal province BY4, this area will likely reflect conditions from lower latitudes near the equator in the future. The northern cluster coinciding with GOODS bathyal northern North Atlantic (BY2) will possibly suffer the strongest changes.

Octocorals are forecasted to lose habitat in an extensive measure in the Reykjanes Ridge, the continental shelf west of this ridge (Davis Strait and Labrador Sea), and east towards Rockall. Scleractinians such as *Lophelia pertusa*, *Madrepora oculata* and *Desmophyllum dianthus* are predicted to lose habitat in the deeper parts of the Reykjanes Ridge and Rockall Bank, however, they are expected to gain habitat in the slope depths of the Labrador Sea and Davis Strait. This is likely the result of changes in temperature across a latitudinal gradient with this province probably moving northwards in the future. It is possible that this area will become available for other scleractinian taxa found at southern latitudes and hence GOODS bathyal province BY4 extending its limit up to the Davis Strait.

The bathyal depths of the cluster including the southern Azores Seamount Chain, the Tropic Seamount southwest off the Canary Islands, and the Condor Seamounts are considered part of the GOODS bathyal province BY4. Nevertheless, these geographic areas were clustered together indicating a different influence from other nearby bathyal regions. Both case study octocorals and scleractinians are predicted to lose habitat in the Azores region where a set of different surface currents converge. While the Condor Seamount may have a stronger influence from the Mediterranean Outflow Water, southern seamounts such as the Tropic Seamount (and therefore the Western Sahara Seamount Province), are not influenced as much by these saltier and warmer waters. Therefore even in projected warmer conditions, the latter may become a refugia for some octocorals due to the seasonally productive waters of the NW African coast (Henderiks, 2001).

Finally, GOODS suggests one homogeneous abyssal province for the North Atlantic. Even with inconclusive evidence of an eastern and western separation as results vary depending on taxa, future climate changes are unlikely to make any spatial differentiation or major latitudinal shift in this province.

4.6 Climate-induced changes in Good Environment Status

(Contributors: Georgios Kazanidis, Covadonga Orejas)

4.6.1 ATLAS work addressing Marine Strategy Framework Directive/Good Environmental Status in the deep sea

The Marine Strategy Framework Directive (MSFD) aims to protect more effectively the marine environment across Europe. The European Commission (EC) targets to the achievement of Good Environmental Status (GES) by 2020. However, current regional assessments have made little progress in developing or applying indicators for GES descriptors to deep-sea ecosystems despite the vast extension of waters beyond the continental shelf and the occurrence of Vulnerable Marine Ecosystems (VMEs). In ATLAS, a group of experts -on the ecology of deep North Atlantic and beyond- carried out an academic exercise on deep-sea GES focusing on 9 ATLAS case studies in the North-East Atlantic (ATLAS Deliverable 3.1 "Good Environmental Status and Biodiversity Assessments", currently under review by the EC).

ATLAS developed a new definition of GES (see ATLAS Deliverable D 3.1 "Good Environmental Status and Biodiversity Assessments"), which could be more suitable for the deep sea than the definition included in the MSFD. ATLAS, also, explored potential scientific indicators for Descriptors D1 "Biodiversity", D3 "Commercial Fish and shellfish", D6 "Seafloor integrity" and D10 "Marine litter", that could be measured and monitored in future to ensure an effective management, aiming to avoid or minimise destructive impacts of human activities. To address the 4 selected MSFD Descriptors, the "Nested Environmental status Assessment Tool" (NEAT) tool was selected. Details on NEAT can be found in ATLAS deliverable D 3.1 as well as in the following link: http://www.devotes-project.eu/neat/. A selection among the more than 500 scientific indicators included in the database of the NEAT software was conducted. In addition, new scientific indicators were proposed by ATLAS experts considering the specific constraints of working in the deep sea (e.g. remoteness, difficulties in conducting scientific surveys and sampling, lack of baseline data and long-term monitoring) and the main characteristics of these ecosystems (Table 35). As it can be seen in Table 35, many of these indicators refer to corals (e.g. "abundance of coral colonies alive", "density of biogenic reef-forming species", "VMEs and VME indicator taxa") and fish (e.g. "Body-length distribution of fish in the community") highlighting the importance that deep-sea experts attribute to these components for assessing the health status of deep-sea ecosystems.

Table 35. List of scientific indicators to assess GES in deep-sea ecosystems. In italic are highlighted the indicators generated within ATLAS.

D1	D3	D6	D10
Distributional range and pattern of selected (sensitive) non-commercial demersal fish species	Abundance ratio of mature individuals of selected fish species	Abundance of coral colonies alive	*Areal extent of litter*
Species richness of non-commercial fish	Age class structure of commercial fish	Areal extent of biogenic / vulnerable habitats	*Density of abandoned fishing gear*
Abundance of non-commercial demersal fish and cephalopods	Age-frequency distribution of fish	Areal extent of human affected area	*Colonisation on litter*
Abundance of non-commercial functional groups of fish	Biomass of demersal fish	Areal extent of protected sea areas	*Microplastics / Contaminants in sediments / organisms*
Species diversity (Shannon index) of non-commercial fish	Biomass of selected fish species	Density of biogenic reef forming species	*Number of organisms entangled in fishing lines or nets*
	Biomass of selected fish species (SSB-spawning stock biomass)	Distribution and condition of habitat forming species	
	Body length distribution of fish	*Areal extent of sedimentary seafloor / vulnerable habitats*	
	Body length distribution of fish in the community	Abundance and composition of functional groups in selected habitats	
	Fishing effort	Species richness of corals	
	Large fish indicator	*Ratio of live versus dead / overgrown coral cover*	
		VMEs and VME indicator taxa	
		Structural complexity	

As part of the ATLAS GES work, the case study leaders identified also the challenges and opportunities related to the achievement of GES in the deep sea. Some of the major challenges identified by ATLAS experts were: 1) the limited data availability on the occurrence and distribution of species and habitats and the almost complete lack of long term data series; 2) the difficulties to set up baseline values to be able to assess the current environmental status; 3) the difficulties to disentangle the effects of the natural variability and the variability originated due to the human activities, in shaping the structure and functionality of deep-sea ecosystems; and 4) the lack of methodology standardization. The opportunities identified to address those challenges were: 1) the current technological (e.g., autonomous underwater vehicles, new generations of remotely operated vehicles) and computational (e.g., environmental niche modelling, machine learning) development will highly contribute and

improve the situation of the current knowledge of deep-sea ecosystems, especially to overcome the problem of data scarcity; 2) the scientific community could highly be benefited from intersectoral collaborations (e.g., between industry and academia), as well as from increasing promotion of data sharing (e.g., archival in online data depositories) in order to improve the data acquisition; 3) comparison with pristine areas, use of historical data, modelling as well as expert judgement could address the difficulties on setting up baselines and disentangle natural variability from effects from human activities; and 4) development of video-processing protocols and species morphotype catalogues could improve the lack of standardization.

Regarding the assessment of GES in future scenarios, the use of historical data whenever possible, as well as the modelling tools will be fundamental elements which should contribute to simulate future scenarios under the predicted environmental conditions (see Sweetman et al., 2017; IPCC, 2018).

4.6.2 Current vs forecasted occurrence of scleractinian and gorgonian corals. Potential consequences for the Environmental Status of the deep sea

As part of research activities under Work Package 3 ("Biodiversity and Biogeography"), the ATLAS researchers used niche environmental modelling to record the habitat suitability for six cold-water coral and six deep-sea fish species under current and future environmental conditions for the whole northern Atlantic Ocean (see above). Specifically, habitat suitability was modelled for three scleractinian CWCs (*Lophelia pertusa*, *Madrepora oculata*, and *Desmophyllum dianthus*), three gorgonians (*Acanella arbuscula*, *Acanthogorgia armata*, and *Paragorgia arborea*) and six deep-sea fishes [the roundnose grenadier *Coryphaenoides rupestris*), Atlantic cod (*Gadus morhua*), bluemouth rockfish (*Helicolenus dactylopterus*), American plaice (*Hippoglossoides platessoides*), Greenland halibut (*Reinhardtius hippoglossoides*), and beaked redfish (*Sebastes mentella)*]. The distribution of CWCs and fishes was modelled using a set of static (depth and derived variables) and dynamic environmental parameters (POC flux to seabed, pH, temperature at seafloor, and aragonite and calcite saturation states). In overall, the model predictions for all species, achieved good accuracy for all species with a reasonable agreement between model outputs and known species occurrences.

Empirical data of the occurrence of scleractinian corals under present day conditions, showed a higher habitat suitability in the eastern North Atlantic and the Mid-Atlantic Ridge, as well as in the Gulf of Mexico and the Mediterranean Sea, whilst gorgonian showed higher suitability in the western North Atlantic and south of Greenland. In the predictive models described above, the overall model outputs for scleractinians and gorgonians revealed a marked decrease in the suitable habitat towards 2100.

Specifically, the scleractinian coral *L. pertusa* and the gorgonian *P. arborea* are the species that might face in the future the major reductions in suitable habitat.

The scleractinian and gorgonian species are VME indicators and form VME habitat in many areas of the North Atlantic. Vulnerable Marine Ecosystems (VMEs) may be regarded as habitats characterized by habitat forming species sensitive to anthropogenic activities (Buhl-Mortensen et al., 2019). Therefore, a considerable reduction of the suitable habitat of these species in the North Atlantic will probably have a direct influence in the number and extension of VMEs. Specifically, regarding the analysed scleractinians in the modelling work, for *L. pertusa* a habitat reduction of at least 68 %, and a southern shift towards deeper waters has been predicted by 2100, while an increase in habitat suitability has been predicted for the western Atlantic (Davis Strait and Labrador Sea). The forecasted habitat reduction will have most probably consequences for most of the *Lophelia* large coral reefs currently existent, as the ones in the Norwegian Margin, Porcupine, Rockall Bank, Logachev Mounds or Gulf of Mexico. A decrease in the area covered by these CWC reefs, will have associated a remarkable biodiversity loss as well as dramatic effects in ecosystem functioning, whose magnitude cannot be anticipated. We do not know which fauna will replace the cold-water coral (CWC) reefs if habitat suitability for them becomes smaller, as well as which will be the accompanying species in the potential scenario of its fading. The southern shift of the suitable habitats for *Lophelia,* as well as to deeper waters could have consequences difficult to forecast. However, a different environment with most probably different current regimes will also influence in the degree of connectivity among populations. These are aspects that the models do not include, and it is difficult to anticipate how this will influence the fate of the species. The same applies to the biological interactions with other species already inhabiting these locations, an aspect impossible to cover by the models, and how *Lophelia* will cope, for instance with competence with other species.

The occurrence of VMEs has been suggested as one of the scientific indicators for assessing Good Environmental Status (GES) in the deep sea (ATLAS D3.1 Deliverable). Therefore, it can be anticipated that the reduction of the distribution area of VMEs formed by *Lophelia,* and the associated fauna, will have consequences in the environmental status in the area; the current highly structured communities might be replaced by a more simplified community with more opportunistic/generalist species and less structuring organisms.

The outputs of the models for the other analyzed scleractinians *M. oculata* and *D. dianthus* revealed a potential moderate reduction of their habitats (ca. 30 to 55%) and no marked shifts in the latitudinal or depth distributions by 2100. These two CWC species are frequently associated to *Lophelia* reefs, indeed they are also bibliographic references that talk about the “coral triad” (Pérès & Piccard, 1964).

The apparently higher resilience of *M. oculata* and *D. dianthus* in front of future climate scenarios could lead to VMEs, where these two corals are more dominant than *L. pertusa*, leading to less structured reefs that will most probably harbour communities with an impoverished biodiversity; *Madrepora* rarely forms real frameworks as *Lophelia* does, and *Desmophyllum* is a solitary coral species. It is known, from fossil registers (e.g,. Wienberg et al., 2009) but also from *ex situ* experimental work (Naumann et al., 2014), that *Madrepora* displays a higher thermal tolerance for warmer temperatures than *Lophelia* (indeed *Madrepora* seems to be the most abundant and ubiquitous colonial CWC in the Mediterranean, Chimienti et al., in press). Aquaria studies conducted with *Desmophyllum* also reveal a high tolerance in this solitary coral in front warm temperatures (Naumann et al., 2013). However, this potential dominance of *Madrepora* and/or *Desmophyllum* will depend on the composition and species dominance of the original community.

As a general result from the model outputs, the suitable habitat for all scleractinian corals was forecasted to increase in the Davis Strait and Labrador Sea. This model prediction can be characterized as an indication that the deep-sea environmental status in these areas may improve, as potentially the area covered by VMEs will increase. Larger areas covered by scleractinian reefs will contribute to more complex three-dimensional habitats where, usually, diverse faunal communities establish (e.g., mainly suspension and filter feeders but also predators and grazers; Henry & Roberts, 2017; Kenchington et al., 2017; Buhl-Mortensen et al., 2017). This expansion of the habitat-forming species scleractinian corals may also attract commercially important fishes, as it is known from current areas where these highly structured ecosystems grow (Kutti et al., 2014).

The models outputs for the three analysed gorgonians (*A. arbuscula*, *A. armata*, and *P. arborea*), revealed that all three species may experience a reduction of the habitat greater than 77%. This large reduction might be closely related to climate change as the forecast indicates a marked southern shift of the median latitude (ranging from -11.6° to -26.5° in latitude) of all gorgonians suitable habitats, as well as a shift toward shallower depths for *A. armata* and towards deeper waters for *P. arborea*. *A. arbuscula* is documented as one of the currently most abundant and more widely distributed deep-sea gorgonians. The remarkable reduction of its habitat predicted towards 2100 will imply the loss of an important part of the deep-sea coral gardens, which are also included in the VME category. The future scenarios presented for *P. arborea* are also not very encouraging as the same great reduction of its habitat has been forecasted. Beside the gorgonian forest that *P. arborea* forms in the northwest Atlantic, *Paragorgia* is also one of the conspicuous species associated to *Lophelia* reefs in the northeast Atlantic (i.e. Norwegian reefs). The future unfavourable scenarios for *Lophelia* will also be associated to the loss of this gorgonian species. *Paragorgia* plays also an important role as biodiversity "attractor" and its habitat reduction will be, again, associated to a biodiversity loss. This reduction in

habitat of benthic structuring species implies the reduction and disappearance of VMEs, that will in turn lead to a less complex ecosystems and to negative effects in the future environmental status of the areas where these systems currently occur.

Model outputs showed that temperature is the most important predictor variable to determine the habitat suitability for CWC, agreeing with previous studies (e.g., Davies & Guinotte, 2011; Guinotte & Davies, 2014; Buhl-Mortensen et al., 2015; Lauria et al., 2017). Particulate organic carbon (POC) has also been identified in the modelling work as an important predictor for the occurrence of most of the CWCs investigated in the work. The availability of food (POC flux) has been linked with the physiological performance of calcareous fauna (e.g., calcification and respiratory metabolism, Naumann et al., 2011; Larsson et al., 2013) and their potential ability to cope with ocean change (Wood et al., 2008; Maier et al., 2016; Büscher et al., 2017). However, in an environment where food is permanently scarce, a shift in energy allocation might occur in favour of physiological functions other than calcification and growth and compromise the survival of corals (Hennige et al., 2015; Maier et al., 2016). These important physiological aspects are not currently taken into account in the modelling approach. Beside temperature and food availability, aragonite and calcite saturation state were also shown to be important predictors in determining CWC habitat suitability (e.g., Davies & Guinotte, 2011; Yesson et al., 2012; Thresher et al., 2015). Models predict that some areas of the global ocean will become undersaturated in aragonite and calcite by 2100, especially in deep-sea areas and higher latitudes (Orr et al., 2005). As a response, CWC habitats currently found in aragonite- and calcite-saturated waters will be exposed in undersaturated conditions in the future (Orr et al., 2005; Guinotte et al., 2006).

An important aspect to address when considering the assessment of the deep-sea status in future scenarios is the predicted scenario for “climate refugia” for deep-sea scleractinians and gorgonians. The model outputs predict a decrease in the refugia size of scleractinian corals by 2100. Specifically, this decrease will range from 29% to 44% compared to present-day refugia size. The forecasted climate refugia for scleractinian corals are located in both sides of the North Atlantic and in the Mediterranean Sea. Regarding the gorgonians, the climate refugias have been predicted as extremely small for the gorgonians *A. arbuscula* and *A. armata* (1.9-14.8% of present-day suitable habitat), and almost inexistent for *P. arborea*. The small areas for refugia anticipated for future scenarios highlight the need of accurate fine-scale climate grids and methodologies to properly identify those refugia (Ashcroft, 2010; Keppel et al., 2012; Kavousi & Keppel, 2018), and stress the importance and need, regarding GES assessment, of nesting different scales approached (from local to regional) for the obtainment of more realistic and accurate results.

Overall, when thinking in assess GES in future scenarios, the use of models could be very useful (especially in the deep sea due to the difficulties to get access to this remote realm), also regarding the set of thresholds values. The Article 13 of the Commission Decision from 2017 (Commission Decision EU 2017/848) highlight that "*threshold values should also be set on the basis of the precautionary principle, reflecting the potential risks to the marine environment. The setting of threshold values should accommodate the dynamic nature of marine ecosystems and their elements, which can change in space and time through hydrological and climatic*"; Therefore, models can be useful to set-up threshold values for the tested environmental and biological variables and parameters, considering the predicted future scenarios. Specifically, the models can be useful to respond to Criterion 4 for Descriptor 1: *"Primary for species covered by Annexes II, IV or V to Directive 92/43/EEC and secondary for other species: The species distributional range and, where relevant, pattern is in line with prevailing physiographic, geographic and climatic conditions. Member States shall establish threshold values for each species through regional or subregional cooperation..."*. Model outputs produced here can be helpful to establish the comparison between current and predicted species distributional ranges, and therefore to evaluate the potential environmental status in future scenarios. This will be also important for management purposes, which should consider future climate scenarios when planning long term management measures in these changing scenarios.

Concluding, it must be highlighted that predicting the environmental status of deep-sea ecosystems under future climate scenarios is very challenging as many aspects remain unknown and the deep sea is a vast, remote area with a very small part of it being studied by scientists, up to date. Due to limited data availability (over space and time), difficulties in setting baselines, lack of standardizations (and a whole series of issues summarized in ATLAS Deliverable 3.1) set the assessment of deep-sea environmental status a huge challenge even under current conditions, let alone under future scenarios. Knowledge gained in the ATLAS exercise of assessing GES in the deep sea in combination with the outputs of the models in future climate scenarios, as well as the increasing knowledge on performance of key organisms under different environmental conditions, will be extremely useful tools for assessing environmental status of deep-sea ecosystems under the future climatic scenarios predicted by the IPCC, and for management purposes.

4.7 References

Addamo, A. M., Vertino, A., Stolarski, J., García-Jiménez, R., Taviani, M. & Machordom, A. (2016). Merging scleractinian genera: the overwhelming genetic similarity between solitary *Desmophyllum* and colonial *Lophelia*. *BMC evolutionary biology, 16*(1), 108.

Ashcroft, M. B. (2010). Identifying refugia from climate change. *Journal of Biogeography, 37*(8), 1407-1413.

Austin, M. P. & Van Niel, K. P. (2011). Improving species distribution models for climate change studies: variable selection and scale. *Journal of Biogeography, 38*(1): 1-8.

Baco, A. R., Morgan, N., Roark, E. B., Silva, M., Shamberger, K. E. & Miller, K. (2017). Defying dissolution: discovery of deep-sea scleractinian coral reefs in the North Pacific. *Scientific reports, 7*(1), 5436.

Bailey, D. M., Ruhl, H. A. & Smith Jr, K. L. (2006). Long-term change in benthopelagic fish abundance in the abyssal northeast Pacific Ocean. *Ecology, 87*(3), 549-555.

Baudron, A. R., Needle, C. L., Rijnsdorp, A. D. & Tara Marshall, C. (2014). Warming temperatures and smaller body sizes: synchronous changes in growth of North Sea fishes. *Global change biology, 20*(4), 1023-1031.

Beare, D. J., Burns, F., Greig, A., Jones, E. G., Peach, K., Kienzle, M., ... & Reid, D. G. (2004). Long-term increases in prevalence of North Sea fishes having southern biogeographic affinities. *Marine Ecology Progress Series, 284*, 269-278.

Brooke, S., Ross, S. W., Bane, J. M., Seim, H. E. & Young, C. M. (2013). Temperature tolerance of the deep-sea coral *Lophelia pertusa* from the southeastern United States. *Deep Sea Research Part II: Topical Studies in Oceanography, 92*, 240-248.

Bryndum-Buchholz, A., Tittensor, D. P., Blanchard, J. L., Cheung, W. W., Coll, M., Galbraith, E. D., ... & Lotze, H. K. (2018). 21st century climate change impacts on marine animal biomass and ecosystem structure across ocean basins. *Global change biology*.

Buhl-Mortensen, L., Olafsdottir, S. H., Buhl-Mortensen, P., Burgos, J. M. & Ragnarsson, S. A. (2015). Distribution of nine cold-water coral species (Scleractinia and Gorgonacea) in the cold temperate North Atlantic: effects of bathymetry and hydrography. *Hydrobiologia, 759*(1), 39-61.

Buhl-Mortensen, P., Gordon Jr, D.C., Buhl-Mortensen, L. & Kulka, D.W. (2017) First description of a *Lophelia pertusa* reef complex in Atlantic Canada. *Deep-Sea Research I, 126*, 21-30.

Buhl-Mortensen, L., Burgos, J.M., Steingrund, P., Buhl-Mortensen, P., Ólafsdóttir, S.H. & Ragrnarsson, S.A. (2019) Vulnerable Marine Ecosystems (VMEs). Coral and sponges VMEs in Artic and sub-Arctic waters – Distribution and threats. Tema Nord 2019: 519. 146p.

Büscher, J. V., Form, A. U. & Riebesell, U. (2017). Interactive effects of ocean acidification and warming on growth, fitness and survival of the cold-water coral *Lophelia pertusa* under different food availabilities. *Frontiers in Marine Science, 4*, 101.

Carreiro-Silva, M., Cerqueira, T., Godinho, A., Caetano, M., Santos, R. S. & Bettencourt, R. (2014). Molecular mechanisms underlying the physiological responses of the cold-water coral *Desmophyllum dianthus* to ocean acidification. *Coral Reefs, 33*(2), 465-476.

Cerrano, C., Cardini, U., Bianchelli, S., Corinaldesi, C., Pusceddu, A. & Danovaro, R. (2013). Red coral extinction risk enhanced by ocean acidification. *Scientific reports, 3*, 1457.

Chefaoui, R.M., Duarte, C.M. & Serrão, E.A. (2018) Dramatic loss of seagrass habitat under projected climate change in the Mediterranean Sea. *Global change biology, 24*, 4919–4928.

Chen, C.-T.A., Lui, H.-K., Hsieh, C.-H., Yanagi, T., Kosugi, N., Ishii, M. & Gong, G.-C. (2017) Deep oceans may acidify faster than anticipated due to global warming. *Nature Climate Change*, *7*, 890–894.

Cheung, W. W., Lam, V. W., Sarmiento, J. L., Kearney, K., Watson, R. E. G., Zeller, D. & Pauly, D. (2010). Large-scale redistribution of maximum fisheries catch potential in the global ocean under climate change. *Global Change Biology, 16*(1), 24-35.

Cheung, W. W., Jones, M. C., Lam, V. W., D Miller, D., Ota, Y., Teh, L. & Sumaila, U. R. (2017). Transform high seas management to build climate resilience in marine seafood supply. *Fish and Fisheries, 18*(2), 254-263.

Chimienti G, Bo M, Taviani M, Mastrototaro F (in press) Occurrence and Biogeography of Mediterranean Cold-Water Corals. In: Mediterranean cold-water corals: past, present and future (Orejas C, Jimenez C eds), Coral Reefs of the World, Vol 9, 213-143, Springer, Cham.

Commission decision 2017/848/EU Laying down criteria and methodological standards on good environmental status of marine waters and specifications and standardised methods for monitoring and assessment, and repealing Decision 2010/477/EU (Text with EEA relevance).

Davies, A. J. & Guinotte, J. M. (2011). Global habitat suitability for framework-forming cold-water corals. *PloS one, 6*(4), e18483.

Drinkwater, K. F. (2005). The response of Atlantic cod (*Gadus morhua*) to future climate change. *ICES Journal of Marine Science, 62*(7), 1327-1337.

Dufresne, J. L., Foujols, M. A., Denvil, S., Caubel, A., Marti, O., Aumont, O., ... & Bony, S. (2013). Climate change projections using the IPSL-CM5 Earth System Model: from CMIP3 to CMIP5. *Climate Dynamics, 40*(9-10), 2123-2165.

Dulvy, N. K., Rogers, S. I., Jennings, S., Stelzenmüller, V., Dye, S. R. & Skjoldal, H. R. (2008). Climate change and deepening of the North Sea fish assemblage: a biotic indicator of warming seas. *Journal of Applied Ecology, 45*(4), 1029-1039.

Dunne, J. P., John, J. G., Adcroft, A. J., Griffies, S. M., Hallberg, R. W., Shevliakova, E., ... & Krasting, J. P. (2012). GFDL's ESM2 global coupled climate–carbon earth system models. Part I: Physical formulation and baseline simulation characteristics. *Journal of Climate, 25*(19), 6646-6665.

Elith, J. & Leathwick, J. R. (2009). Species distribution models: ecological explanation and prediction across space and time. *Annual Review of Ecology, Evolution, and Systematics, 40*, 677-697.

ESGF (2019) https://esgf-node.llnl.gov/projects/esgf-llnl/ (accessed 15/4/19).

Fillinger, L. & Richter, C. (2013). Vertical and horizontal distribution of *Desmophyllum dianthus* in Comau Fjord, Chile: a cold-water coral thriving at low pH. *PeerJ, 1*, e194.

Fogarty, M., Incze, L., Hayhoe, K., Mountain, D., & Manning, J. (2008). Potential climate change impacts on Atlantic cod (*Gadus morhua*) off the northeastern USA. *Mitigation and Adaptation Strategies for Global Change, 13*(5-6), 453-466.

Fordham, D.A., Resit Akçakaya, H., Araujo, M.B., Elith, J., Keith, D.A., Pearson, R., Auld, T.D., Mellin, C., Morgan, J.W., Regan, T.J., Tozer, M., Watts, M.J., White, M., Wintle, B.A., Yates, C. & Brook, B.W. (2012) Plant extinction risk under climate change: are forecast range shifts alone a good indicator of species vulnerability to global warming? *Global change biology, 18*, 1357–1371.

Form, A. U. & Riebesell, U. (2012). Acclimation to ocean acidification during long-term CO2 exposure in the cold-water coral *Lophelia pertusa*. *Global change biology, 18*(3), 843-853.

Fossheim, M., Primicerio, R., Johannesen, E., Ingvaldsen, R. B., Aschan, M. M., & Dolgov, A. V. (2015). Recent warming leads to a rapid borealization of fish communities in the Arctic. *Nature Climate Change, 5*(7), 673.

Freiwald, A., Beuck, L., Rüggeberg, A., Taviani, M., Hebbeln, D., & R/V Meteor Cruise M70-1 Participants. (2009). The white coral community in the central Mediterranean Sea revealed by ROV surveys. *Oceanography, 22*(1), 58-74.

Gaines, S.D., Costello, C., Owashi, B., Mangin, T., Bone, J., Molinos, J.G., Burden, M., Dennis, H., Halpern, B.S., Kappel, C.V., Kleisner, K.M. & Ovando, D. (2018) Improved fisheries management could offset many negative effects of climate change. *Science advances*, *4*, eaao1378.

Gehlen, M., Séférian, R., Jones, D. O., Roy, T., Roth, R., Barry, J. P., ... & Joos, F. (2014). Projected pH reductions by 2100 might put deep North Atlantic biodiversity at risk. *Biogeosciences, 11*, 6955-6967.

Genin, A., Dayton, P. K., Lonsdale, P. F. & Spiess, F. N. (1986). Corals on seamount peaks provide evidence of current acceleration over deep-sea topography. *Nature, 322*(6074), 59.

Georgian, S. E., Shedd, W. & Cordes, E. E. (2014). High-resolution ecological niche modelling of the cold-water coral *Lophelia pertusa* in the Gulf of Mexico. *Marine Ecology Progress Series, 506*, 145-161.

Georgian, S. E., Dupont, S., Kurman, M., Butler, A., Strömberg, S. M., Larsson, A. I. & Cordes, E. E. (2016). Biogeographic variability in the physiological response of the cold-water coral *Lophelia pertusa* to ocean acidification. *Marine ecology, 37*(6), 1345-1359.

Giorgetta, M. A., Jungclaus, J., Reick, C. H., Legutke, S., Bader, J., Böttinger, M., ... & Glushak, K. (2013). Climate and carbon cycle changes from 1850 to 2100 in MPI-ESM simulations for the Coupled Model Intercomparison Project phase 5. *Journal of Advances in Modeling Earth Systems, 5*(3), 572-597.

Gomez, C., Williams, A. J., Nicol, S. J., Mellin, C., Loeun, K. L., & Bradshaw, C. J. (2015). Species distribution models of tropical deep-sea snappers. *PloS-one, 10*(6), e0127395.

Gomez, C. E., Wickes, L., Deegan, D., Etnoyer, P. J. & Cordes, E. E. (2018). Growth and feeding of deep-sea coral *Lophelia pertusa* from the California margin under simulated ocean acidification conditions. *PeerJ, 6*, e5671.

Gori, A., Orejas, C., Madurell, T., Bramanti, L., Martins, M., Quintanilla, E., ... & Greenacre, M. (2013). Bathymetrical distribution and size structure of cold-water coral populations in the Cap de Creus and Lacaze-Duthiers canyons (northwestern Mediterranean). *Biogeosciences, 10*, 2049-2060.

Gori, A., Ferrier-Pagès, C., Hennige, S.J., Murray, F., Rottier, C., Wicks, L.C. & Roberts, J.M. (2016) Physiological response of the cold-water coral *Desmophyllum dianthus* to thermal stress and ocean acidification. *PeerJ, 4*, e1606.

Guinotte, J. M. & Davies, A. J. (2014). Predicted deep-sea coral habitat suitability for the US West Coast. *PloS one, 9*(4), e93918.

Guinotte, J. M., Orr, J., Cairns, S., Freiwald, A., Morgan, L. & George, R. (2006). Will human-induced changes in seawater chemistry alter the distribution of deesea scleractinian corals? *Frontiers in Ecology and the Environment, 4*(3), 141-146.

Hattab, T., Albouy, C., Lasram, F. B. R., Somot, S., Le Loc'h, F. & Leprieur, F. (2014). Towards a better understanding of potential impacts of climate change on marine species distribution: a multiscale modelling approach. *Global ecology and biogeography, 23*(12), 1417-1429.

Henderiks, J. (2001). Coccolith studies in the Canary Basin: glacial-interglacial paleoceanography of the Eastern Boundary Current System (Doctoral dissertation, ETH Zurich).

Hennige, S. J., Wicks, L. C., Kamenos, N. A., Bakker, D. C., Findlay, H. S., Dumousseaud, C. & Roberts, J. M. (2014). Short-term metabolic and growth responses of the cold-water coral *Lophelia pertusa* to ocean acidification. *Deep Sea Research Part II: Topical Studies in Oceanography, 99*, 27-35.

Hennige, S. J., Wicks, L. C., Kamenos, N. A., Perna, G., Findlay, H. S., & Roberts, J. M. (2015). Hidden impacts of ocean acidification to live and dead coral framework. *Proceedings of the Royal Society B: Biological Sciences*, *282*(1813), 20150990.

Henry, L-A. & Roberts, J.M. (2017) Global biodiversity in cold-water coral reef ecosystems. In Marine Animal Forests, eds. S. Rossi, L. Bramanti, A. Gori, C. Orejas (Springer), 235-256.

Hijmans, R. J. & Graham, C. H. (2006). The ability of climate envelope models to predict the effect of climate change on species distributions. *Global change biology, 12*(12), 2272-2281.

Holt, R. E. & Jørgensen, C. (2015). Climate change in fish: effects of respiratory constraints on optimal life history and behaviour. *Biology letters, 11*(2), 20141032.

IPCC (2018) An IPCC Special Report on the impacts of global warming of 1.5°C above pre-industrial levels and related global greenhouse gas emission pathways, in the context of strengthening the global response to the threat of climate change, sustainable development, and efforts to eradicate poverty [V. Masson-Delmotte, P. Zhai, H. O. Pörtner, D. Roberts, J. Skea, P. R. Shukla, A. Pirani, W. Moufouma-Okia, C. Péan, R. Pidcock, S. Connors, J. B. R. Matthews, Y. Chen, X. Zhou, M. I. Gomis, E. Lonnoy, T. Maycock, M. Tignor, T. Waterfield (eds.)]. World Meteorological Organization, Geneva, Switzerland, 32 pp.

Iverson, L. R. & Prasad, A. M. (1998). Predicting abundance of 80 tree species following climate change in the eastern United States. *Ecological Monographs, 68*(4), 465-485.

Jackson, E. L., Davies, A. J., Howell, K. L., Kershaw, P. J. & Hall-Spencer, J. M. (2014). Future-proofing marine protected area networks for cold water coral reefs. *ICES Journal of Marine Science, 71*(9), 2621-2629.

Jantzen, C., Häussermann, V., Försterra, G., Laudien, J., Ardelan, M., Maier, S. & Richter, C. (2013). Occurrence of a cold-water coral along natural pH gradients (Patagonia, Chile). *Marine Biology, 160*(10), 2597-2607.

Jones, M. C., Dye, S. R., Fernandes, J. A., Frölicher, T. L., Pinnegar, J. K., Warren, R. & Cheung, W. W. (2013). Predicting the impact of climate change on threatened species in UK waters. *PLoS One, 8*(1), e54216.

Jones, D. O., Yool, A., Wei, C. L., Henson, S. A., Ruhl, H. A., Watson, R. A. & Gehlen, M. (2014). Global reductions in seafloor biomass in response to climate change. *Global change biology, 20*(6), 1861-1872.

Kavousi, J. & Keppel, G. (2018). Clarifying the concept of climate change refugia for coral reefs. *ICES Journal of Marine Science, 75*(1), 43-49.

Keller, N. B. & Os'kina, N. S. (2008). Habitat temperature ranges of azooxantellate scleractinian corals in the world ocean. *Oceanology, 48*(1), 77-84.

Kenchington, E., Yashayaev, I., Tendal, O.S. & Jørgensbye, H. (2017). Water mass characteristics and associated fauna of a recently discovered *Lophelia pertusa* (Scleractinia, Anthozoa) reef in Greenlandic waters. *Polar Biology, 40,* 321-337.

Keppel, G. & Wardell-Johnson, G. W. (2012). Refugia: keys to climate change management. *Global Change Biology, 18*(8), 2389-2391.

Keppel, G., Van Niel, K. P., Wardell-Johnson, G. W., Yates, C. J., Byrne, M., Mucina, L., ... & Franklin, S. E. (2012). Refugia: identifying and understanding safe havens for biodiversity under climate change. *Global Ecology and Biogeography, 21*(4), 393-404.

Kocsis, Á. T., Reddin, C. J. & Kiessling, W. (2018). The stability of coastal benthic biogeography over the last 10 million years. *Global ecology and biogeography, 27*(9), 1106-1120.

Kurman, M. D., Gomez, C. E., Georgian, S. E., Lunden, J. J. & Cordes, E. E. (2017). Intra-specific variation reveals potential for adaptation to ocean acidification in a cold-water coral from the Gulf of Mexico. *Frontiers in Marine Science, 4*, 111.

Kutti, T., Bergstad, O.A., Fosså, J.H., Helle, K. (2014). Cold-water coral mounds and sponge-beds as habitats for demersal fish on the Norwegian shelf. *Deep-Sea Research II, 99*, 122-133.

Larsson, A. I., Lundälv, T. & van Oevelen, D. (2013). Skeletal growth, respiration rate and fatty acid composition in the cold-water coral *Lophelia pertusa* under varying food conditions. *Marine Ecology Progress Series, 483*, 169-184.

Lauria, V., Garofalo, G., Fiorentino, F., Massi, D., Milisenda, G., Piraino, S., ... & Gristina, M. (2017). Species distribution models of two critically endangered deep-sea octocorals reveal fishing impacts on vulnerable marine ecosystems in central Mediterranean Sea. *Scientific reports, 7*(1), 8049.

Lefevre, S., McKenzie, D. J. & Nilsson, G. E. (2017). Models projecting the fate of fish populations under climate change need to be based on valid physiological mechanisms. *Global change biology, 23*(9), 3449-3459.

Levin, L.A. & Le Bris, N. (2015) The deep ocean under climate change. *Science*, *350*, 766–768.

Lunden, J. J., McNicholl, C. G., Sears, C. R., Morrison, C. L. & Cordes, E. E. (2014). Acute survivorship of the deep-sea coral *Lophelia pertusa* from the Gulf of Mexico under acidification, warming, and deoxygenation. *Frontiers in Marine Science, 1*, 78.

Maier, C., Watremez, P., Taviani, M., Weinbauer, M. G. & Gattuso, J. P. (2012). Calcification rates and the effect of ocean acidification on Mediterranean cold-water corals. *Proceedings of the Royal Society B: Biological Sciences, 279*(1734), 1716-1723.

Maier, C., Schubert, A., Sànchez, M. M. B., Weinbauer, M. G., Watremez, P. & Gattuso, J. P. (2013). End of the century pCO2 levels do not impact calcification in Mediterranean cold-water corals. *PLoS One, 8*(4), e62655.

Maier, C., Popp, P., Sollfrank, N., Weinbauer, M. G., Wild, C. & Gattuso, J. P. (2016). Effects of elevated pCO2 and feeding on net calcification and energy budget of the Mediterranean cold-water coral *Madrepora oculata*. *Journal of Experimental Biology, 219*, 3208-3217.

Maier, C., Weinbauer, M.G. & Gattuso, J-P. (2018). Fate of Mediterranean cold-water corals as a result of global climate change. In C. Orejas & C. Jiménez, eds. Mediterranean Cold-Water Corals: Past, Present and Future. Springer (in press)

Matos, L., Mienis, F., Wienberg, C., Frank, N., Kwiatkowski, C., Groeneveld, J., ... & Hebbeln, D. (2015). Interglacial occurrence of cold-water corals off Cape Lookout (NW Atlantic): first evidence of the Gulf Stream influence. *Deep Sea Research Part I: Oceanographic Research Papers, 105,* 158-170.

McCulloch, M., Trotter, J., Montagna, P., Falter, J., Dunbar, R., Freiwald, A., ... & Taviani, M. (2012). Resilience of cold-water scleractinian corals to ocean acidification: Boron isotopic systematics of pH and saturation state up-regulation. *Geochimica et Cosmochimica Acta, 87*, 21-34.

Mora, C., Wei, C. L., Rollo, A., Amaro, T., Baco, A. R., Billett, D., ... & Gooday, A. J. (2013). Biotic and human vulnerability to projected changes in ocean biogeochemistry over the 21st century. *PLoS Biology, 11*(10), e1001682.

Morley, J.W., Selden, R.L., Latour, R.J., Frölicher, T.L., Seagraves, R.J. & Pinsky, M.L. (2018) Projecting shifts in thermal habitat for 686 species on the North American continental shelf. *PLoS One, 13*, e0196127.

Movilla, J., Gori, A., Calvo, E., Orejas, C., López-Sanz, À., Domínguez-Carrió, C., ... & Pelejero, C. (2014). Resistance of two Mediterranean cold-water coral species to low-pH conditions. *Water, 6*(1), 59-67.

Naumann, M. S., Orejas, C., Wild, C. & Ferrier-Pagès, C. (2011). First evidence for zooplankton feeding sustaining key physiological processes in a scleractinian cold-water coral. *Journal of Experimental Biology, 214*(21), 3570-3576.

Naumann, M. S., Orejas, C. & Ferrier-Pagès, C. (2013). High thermal tolerance of two Mediterranean cold-water coral species maintained in aquaria. *Coral Reefs, 32*(3), 749-754.

Naumann, M.S., Orejas, C. & Ferrier-Pagès, C. (2014). Species-specific physiological response by the cold-water corals *Lophelia pertusa* and *Madrepora oculata* to variations within their natural temperature range. *Deep Sea Research Part II: Topical Studies in Oceanography, 99*, 36-41.

Nye, J. A., Link, J. S., Hare, J. A. & Overholtz, W. J. (2009). Changing spatial distribution of fish stocks in relation to climate and population size on the Northeast United States continental shelf. *Marine Ecology Progress Series, 393*, 111-129.

Orejas, C. & Jiménez, C. (2019). Mediterranean Cold-Water Corals: Past, Present and Future. Understanding the Deep-Sea Realms of Coral. (pp1-862). Berlin: Springer International Publishing.

Orr, J. C., Fabry, V. J., Aumont, O., Bopp, L., Doney, S. C., Feely, R. A. & Key, R. M. (2005). Anthropogenic ocean acidification over the twenty-first century and its impact on calcifying organisms. *Nature, 437*(7059), 681.

Parra, H. E., Pham, C. K., Menezes, G. M., Rosa, A., Tempera, F. & Morato, T. (2017). Predictive modeling of deep-sea fish distribution in the Azores. *Deep Sea Research Part II: Topical Studies in Oceanography, 145*, 49-60.

Pearson, R. G. & Dawson, T. P. (2003). Predicting the impacts of climate change on the distribution of species: are bioclimate envelope models useful? *Global ecology and biogeography, 12*(5), 361-371.

Pecl, G. T., Araújo, M. B., Bell, J. D., Blanchard, J., Bonebrake, T. C., Chen, I. C., ... & Falconi, L. (2017). Biodiversity redistribution under climate change: Impacts on ecosystems and human well-being. *Science, 355*(6332), eaai9214.

Pérès, J. M. & Picard, J. (1964). Nouveau manuel de bionomie benthique de la Mer Mditerrane. *Recueil des Travaux de la Station Marine dEndoume Bulletin*, *31*(47), 5137.

Perez, F.F., Fontela, M., García-Ibáñez, M.I., Mercier, H., Velo, A., Lherminier, P., Zunino, P., la Paz, de, M., Alonso-Pérez, F., Guallart, E.F. & Padin, X.A. (2018) Meridional overturning circulation conveys fast acidification to the deep Atlantic Ocean. *Nature*, *554*, 515–518.

Perry, A. L., Low, P. J., Ellis, J. R. & Reynolds, J. D. (2005). Climate change and distribution shifts in marine fishes. *Science, 308*(5730), 1912-1915.

Pershing, A. J., Alexander, M. A., Hernandez, C. M., Kerr, L. A., Le Bris, A., Mills, K. E., ... & Sherwood, G. D. (2015). Slow adaptation in the face of rapid warming leads to collapse of the Gulf of Maine cod fishery. *Science, 350*(6262), 809-812.

Poloczanska, E. S., Brown, C. J., Sydeman, W. J., Kiessling, W., Schoeman, D. S., Moore, P. J., ... & Duarte, C. M. (2013). Global imprint of climate change on marine life. *Nature Climate Change, 3*(10), 919.

Pörtner, H. O. & Knust, R. (2007). Climate change affects marine fishes through the oxygen limitation of thermal tolerance. *Science, 315*(5808), 95-97.

Pörtner, H. O., Bock, C. & Mark, F. C. (2017). Oxygen-and capacity-limited thermal tolerance: bridging ecology and physiology. *Journal of Experimental Biology, 220*(15), 2685-2696.

Priede, I. (2017). Deep-Sea Fishes Biology, Diversity, Ecology and Fisheries. In Deep-Sea Fishes: Biology, Diversity, Ecology and Fisheries (pp. I-Ii). Cambridge: Cambridge University Press.

Purkey, S. G. & Johnson, G. C. (2010). Warming of global abyssal and deep Southern Ocean waters between the 1990s and 2000s: Contributions to global heat and sea level rise budgets. *Journal of Climate, 23*(23), 6336-6351.

Raybaud, V., Tambutté, S., Ferrier-Pagès, C., Reynaud, S., Venn, A. A., Tambutté, É., ... & Allemand, D. (2017). Computing the carbonate chemistry of the coral calcifying medium and its response to ocean acidification. *Journal of theoretical biology, 424*, 26-36.

Rengstorf, A.M., Yesson, C., Brown, C. & Grehan, A.J. (2013). High-resolution habitat suitability modelling can improve conservation of vulnerable marine ecosystems in the deep sea. *Journal of Biogeography, 40*, 1702-1714.

Roberts, J. M., Murray, F., Anagnostou, E., Hennige, S., Gori, A., Henry, L. A., ... & Foster, G. L. (2016). Cold-Water Corals in an Era of Rapid Global Change: Are These the Deep Ocean's Most Vulnerable Ecosystems? In The Cnidaria, Past, Present and Future (pp. 593-606). Springer, Cham.

Robinson, N. M., Nelson, W. A., Costello, M. J., Sutherland, J. E. & Lundquist, C. J. (2017). A Systematic Review of Marine-Based Species Distribution Models (SDMs) with Recommendations for Best Practice. *Frontiers in Marine Science, 4*, 421.

Rodolfo-Metalpa, R., Montagna, P., Aliani, S., Borghini, M., Canese, S., Hall-Spencer, J. M., ... & Houlbrèque, F. (2015). Calcification is not the Achilles' heel of cold-water corals in an acidifying ocean. *Global change biology, 21*(6), 2238-2248.

Rossi, S., Bramanti, L., Gori, A. & Orejas, C. (2017). Marine Animal Forests. The Ecology of Benthic Biodiversity Hotspots (pp1-1366). Berlin: Springer International Publishing.

Rowden, A. A., Anderson, O. F., Georgian, S. E., Bowden, D. A., Clark, M. R., Pallentin, A. & Miller, A. (2017). High-resolution habitat suitability models for the conservation and management of vulnerable marine ecosystems on the Louisville Seamount Chain, South Pacific Ocean. *Frontiers in Marine Science, 4*, 335.

Ruhl, H. A. & Smith, K. L. (2004). Shifts in deep-sea community structure linked to climate and food supply. *Science, 305*(5683), 513-515.

Sabine, C. L., Feely, R. A., Gruber, N., Key, R. M., Lee, K., Bullister, J. L., ... & Millero, F. J. (2004). The oceanic sink for anthropogenic CO2. *Science, 305*(5682), 367-371.

Sandblom, E., Gräns, A., Axelsson, M. & Seth, H. (2014). Temperature acclimation rate of aerobic scope and feeding metabolism in fishes: implications in a thermally extreme future. *Proceedings of the Royal Society of London B: Biological Sciences, 281*(1794), 20141490.

Schönberg, C. H., Fang, J. K., Carreiro-Silva, M., Tribollet, A. & Wisshak, M. (2017). Bioerosion: the other ocean acidification problem. *ICES Journal of Marine Science, 74*(4), 895-925.

Singer, A., Millat, G., Staneva, J. & Kroncke, I. (2017) Modelling benthic macrofauna and seagrass distribution patterns in a North Sea tidal basin in response to 2050 climatic and environmental scenarios. *Estuarine, Coastal and Shelf Science, 188*, 99–108.

Sweetman, A. K., Thurber, A. R., Smith, C. R., Levin, L. A., Mora, C., Wei, C. L., ... & Ingels, J. (2017). Major impacts of climate change on deep-sea benthic ecosystems. *Elementa: Science of the Anthropocene, 5*, 4.

Thresher, R. E., Tilbrook, B., Fallon, S., Wilson, N. C. & Adkins, J. (2011). Effects of chronic low carbonate saturation levels on the distribution, growth and skeletal chemistry of deep-sea corals and other seamount megabenthos. *Marine Ecology Progress Series, 442*, 87-99.

Thresher, R. E., Guinotte, J. M., Matear, R. J. & Hobday, A. J. (2015). Options for managing impacts of climate change on a deep-sea community. *Nature Climate Change, 5*(7), 635.

Thurber, A. R., Sweetman, A. K., Narayanaswamy, B. E., Jones, D. O. B., Ingels, J. & Hansman, R. L. (2014). Ecosystem function and services provided by the deep sea. *Biogeosciences, 11*(14), 3941-3963.

Victorero, L., Watling, L., Deng Palomares, M. L. & Nouvian, C. (2018). Out of sight, but within reach: A Global History of Bottom-Trawled Deep-Sea Fisheries from> 400 m depth. *Frontiers in Marine Science, 5*, 98.

Watson, R. A. & Morato, T. (2013). Fishing down the deep: Accounting for within-species changes in depth of fishing. *Fisheries Research, 140*, 63-65.

White, M., Mohn, C., de Stigter, H. & Mottram, G. (2005). Deep-water coral development as a function of hydrodynamics and surface productivity around the submarine banks of the Rockall Trough, NE Atlantic. In: Freiwald A., Roberts J.M. (eds), Cold-water corals and ecosystems (pp. 503-514). Berlin: Springer.

Wienberg, C., Hebbeln, D., Fink, H.G., Mienis, F., Dorschel, B., Vertino, A., Lopez Correa, M., & Freiwald, A. (2009). Scleractinian cold-water corals in the Gulf of Cadiz-First clues about their spatial and temporal distribution. *Deep-Sea Research I, 56*, 1873-1893.

Wienberg, C., Frank, N., Mertens, K. N., Stuut, J. B., Marchant, M., Fietzke, J., ... & Hebbeln, D. (2010). Glacial cold-water coral growth in the Gulf of Cádiz: Implications of increased palaeo-productivity. *Earth and Planetary Science Letters, 298*(3-4), 405-416.

Wiens, J. A., Stralberg, D., Jongsomjit, D., Howell, C. A. & Snyder, M. A. (2009). Niches, models, and climate change: assessing the assumptions and uncertainties. *Proceedings of the National Academy of Sciences, 106*(Supplement 2), 19729-19736.

Wood, H. L., Spicer, J. I. & Widdicombe, S. (2008). Ocean acidification may increase calcification rates, but at a cost. *Proceedings of the Royal Society B: Biological Sciences, 275*(1644), 1767-1773.

Woodworth-Jefcoats, P. A., Polovina, J. J. & Drazen, J. C. (2017). Climate change is projected to reduce carrying capacity and redistribute species richness in North Pacific pelagic marine ecosystems. *Global change biology, 23*(3), 1000-1008.

Yesson, C., Taylor, M. L., Tittensor, D. P., Davies, A. J., Guinotte, J., Baco, A., ... & Rogers, A. D. (2012). Global habitat suitability of cold-water octocorals. *Journal of Biogeography, 39*(7), 1278-1292.

Zheng, M. D. & Cao, L. (2014). Simulation of global ocean acidification and chemical habitats of shallow-and cold-water coral reefs. *Advances in Climate Change Research, 5*(4), 189-196.

Supplementary Material

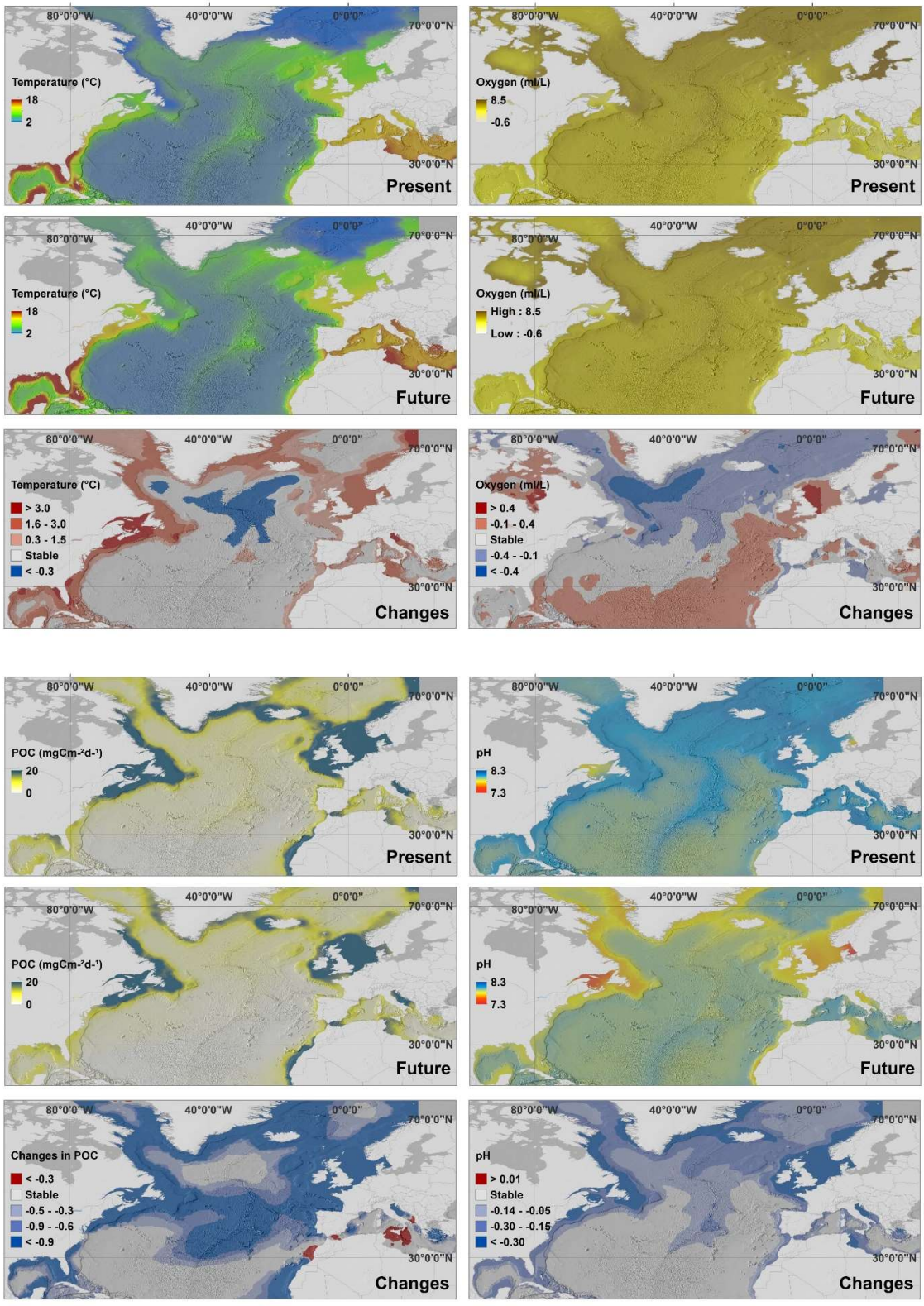

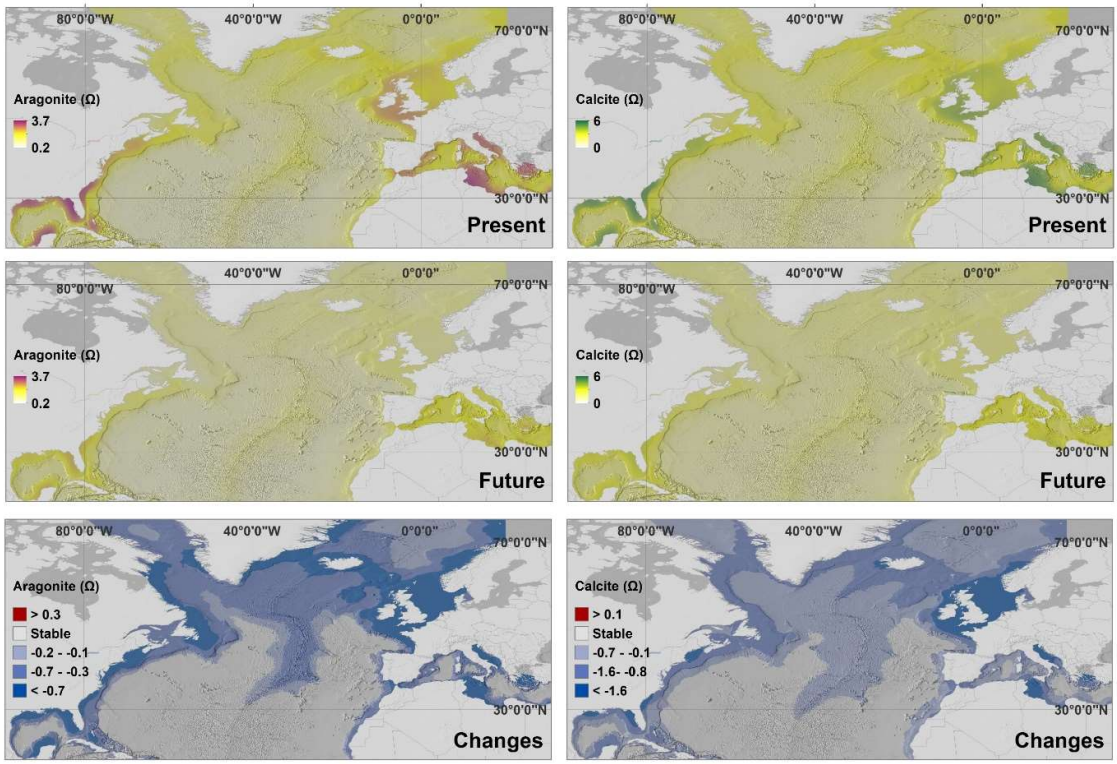

Supplementary Figure S1. *Environmental predictors used to develop environmental niche models for present-day conditions and forecast habitat suitability under future environmental conditions in the North Atlantic Ocean.*

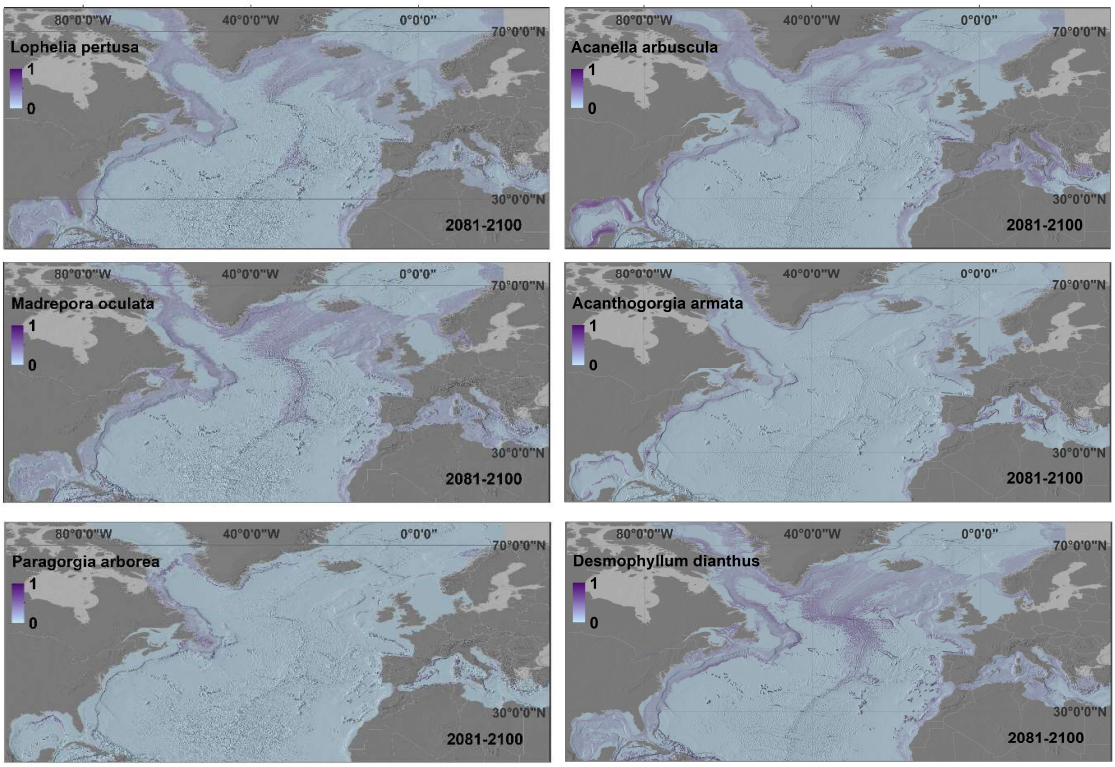

Supplementary Figure S2a. *Uncertainty associated to the habitat suitability model predictions under present-day (1951-2000) and future (2081-2100; RCP8.5 or business-as-usual scenario) environmental conditions for cold-water corals in the North Atlantic Ocean using an ensemble modelling approach.*

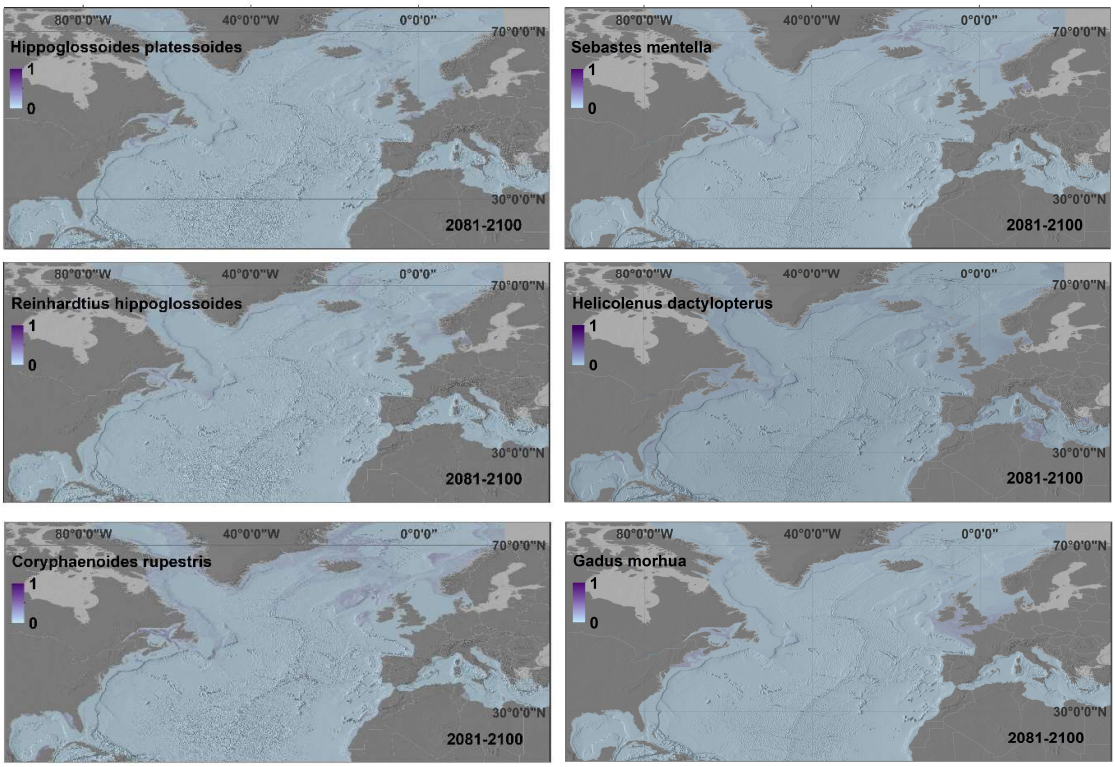

Supplementary Figure S2b. *Uncertainty associated to the habitat suitability model predictions under present-day (1951-2000) and future (2081-2100; RCP8.5 or business-as-usual scenario) environmental conditions for cold-water corals in the North Atlantic Ocean using an ensemble modelling approach*.

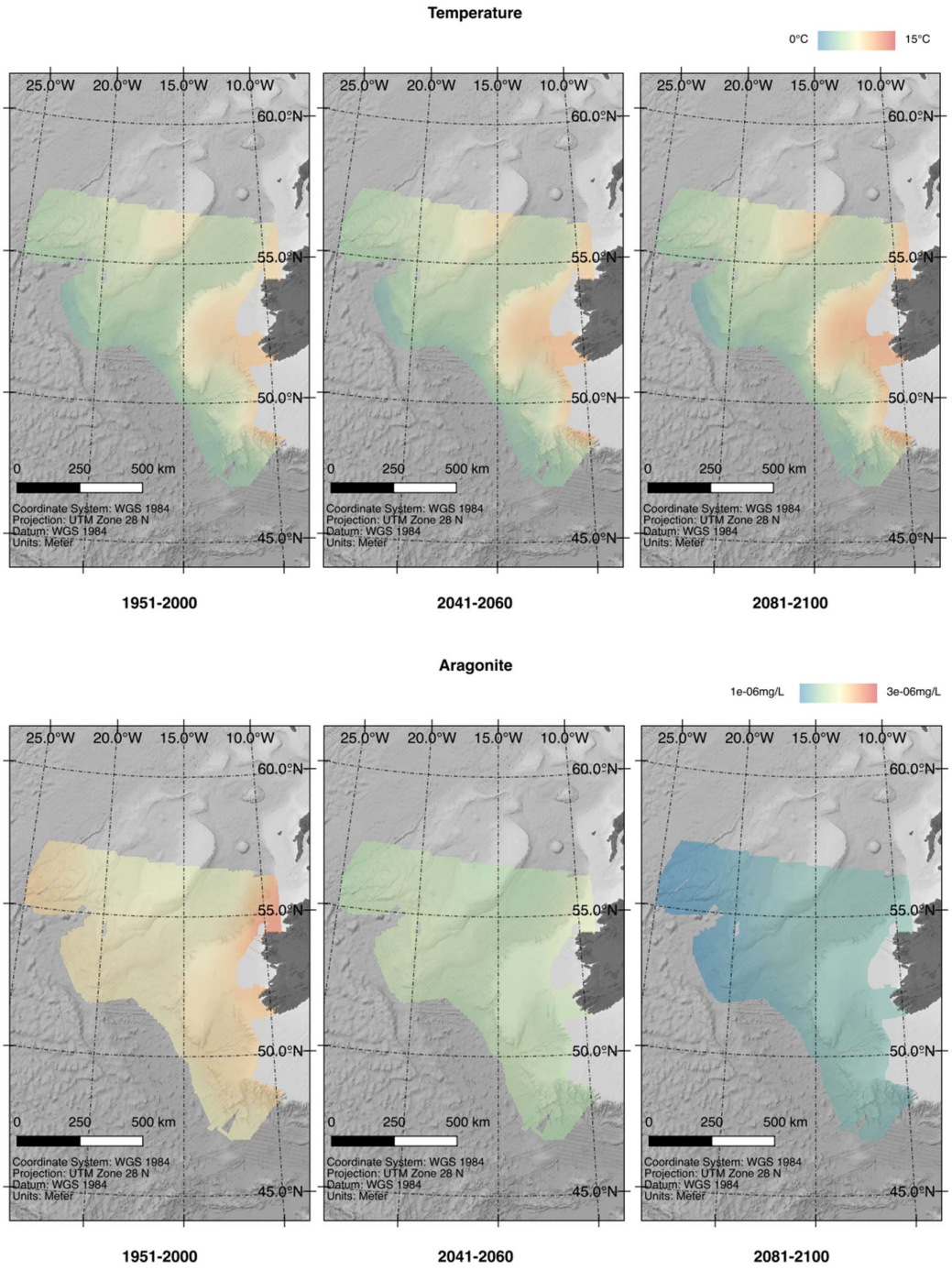

Supplementary Figure S3a. *Environmental predictors used to develop environmental niche models for present-day conditions and forecast habitat suitability under future environmental conditions in the Porcupine Bank, Irish Shelf.*

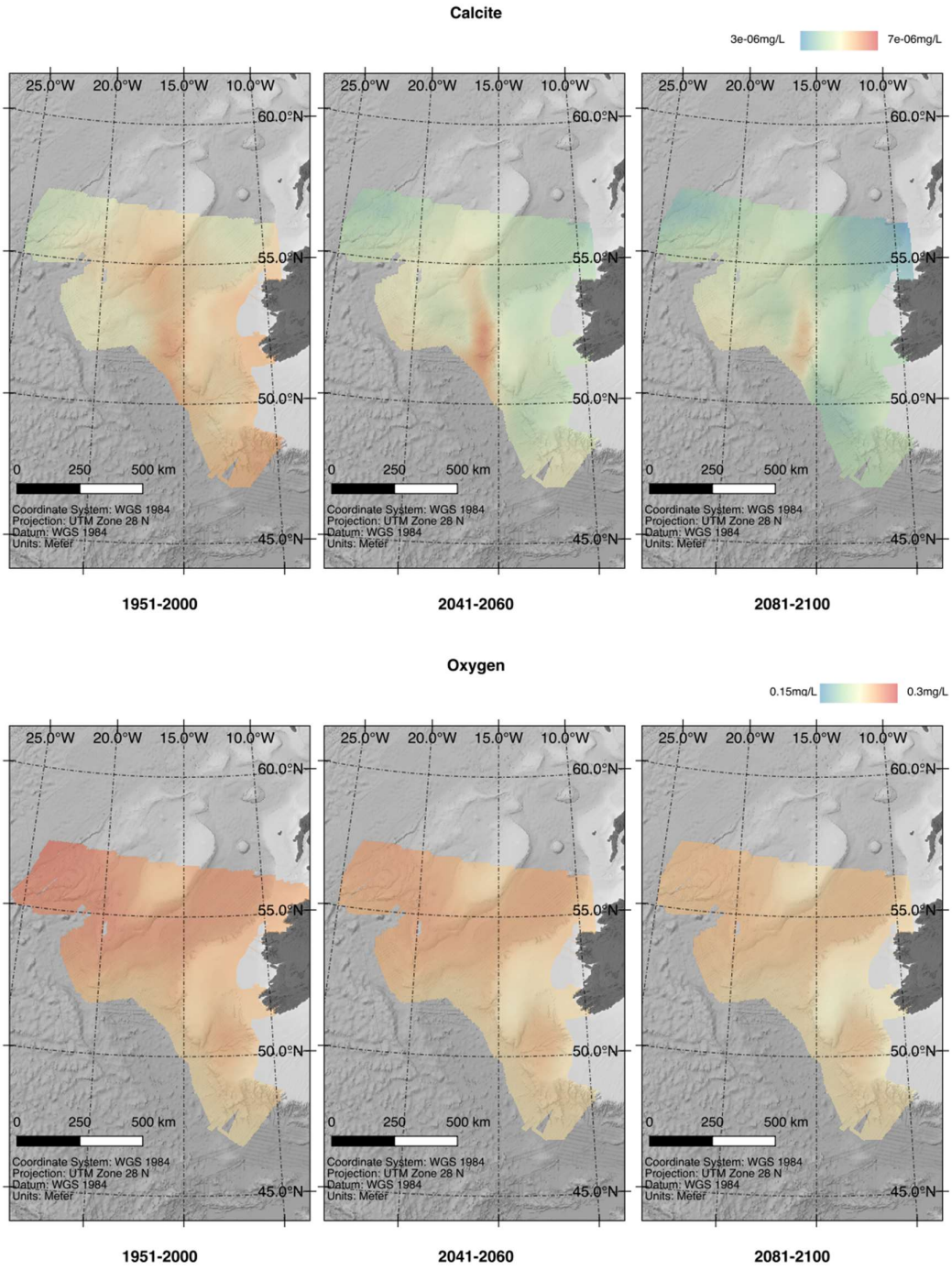

Supplementary Figure S3b. *Environmental predictors used to develop environmental niche models for present-day conditions and forecast habitat suitability under future environmental conditions in the Porcupine Bank, Irish Shelf.*

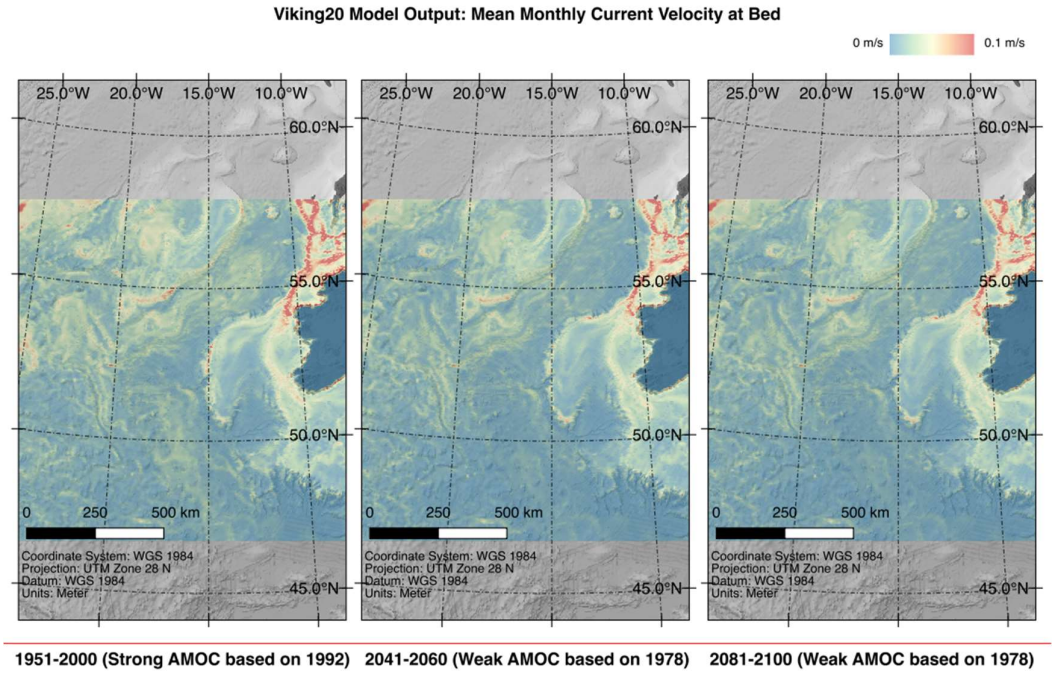

Supplementary Figure S3b. *Environmental predictors used to develop environmental niche models for present-day conditions and forecast habitat suitability under future environmental conditions in the Porcupine Bank, Irish Shelf.*

Document Information

EU Project N°	678760	**Acronym**	ATLAS
Full Title	A trans-Atlantic assessment and deep-water ecosystem-based spatial management plan for Europe		
Project website	www.eu-atlas.org		

Deliverable	**N°**	D3.3	**Title**	Biodiversity, biogeography and GOODS classification system under current climate conditions and future IPCC scenarios
Work Package	**N°**	WP3	**Title**	Biodiversity and Biogeography

Date of delivery	**Contractual**	31st May 2019	**Actual**	31st May 2019
Dissemination level	X	PU Public, fully open, e.g. web		
		CO Confidential restricted under conditions set out in Model Grant Agreement		
		CI Classified, information as referred to in Commission Decision 2001/844/EC		

Authors (Partner)				
Responsible Authors	**Name**		**Email**	

Version log			
Issue Date	**Revision N°**	**Author**	**Change**